



HAL
open science

Préparation de nouveaux polymères biosourcés et recyclables par des voies de synthèse durables et respectueuses de l'environnement

Hugo Fouilloux

► **To cite this version:**

Hugo Fouilloux. Préparation de nouveaux polymères biosourcés et recyclables par des voies de synthèse durables et respectueuses de l'environnement. Chimie organique. Université Paris sciences et lettres, 2021. Français. NNT : 2021UPSLC012 . tel-03956227

HAL Id: tel-03956227

<https://pastel.hal.science/tel-03956227>

Submitted on 25 Jan 2023

HAL is a multi-disciplinary open access archive for the deposit and dissemination of scientific research documents, whether they are published or not. The documents may come from teaching and research institutions in France or abroad, or from public or private research centers.

L'archive ouverte pluridisciplinaire **HAL**, est destinée au dépôt et à la diffusion de documents scientifiques de niveau recherche, publiés ou non, émanant des établissements d'enseignement et de recherche français ou étrangers, des laboratoires publics ou privés.



THÈSE DE DOCTORAT
DE L'UNIVERSITÉ PSL

Préparée à l'École Nationale Supérieure de Chimie de Paris

**Synthesis of biobased and recyclable polymers by
sustainable and eco-friendly methods**

Soutenue par

Hugo FOUILLOUX

Le 08 décembre 2021

Ecole doctorale n° 406

**École Doctorale de Chimie
moléculaire de Paris centre**

Spécialité

Chimie moléculaire

Composition du jury :

Anna, PROUST Prof., Sorbonne Université	<i>Présidente</i>
Karine, VIGIER DE OLIVEIRA Prof., Université de Poitiers	<i>Rapporteuse</i>
Simon, HARRISSON CR CNRS, Université de Bordeaux	<i>Rapporteur</i>
François, TOURNILHAC DR CNRS, ESPCI	<i>Examineur</i>
Estelle, RENARD Prof., Université Paris-Est Créteil	<i>Examinatrice</i>
Christophe, THOMAS Prof., Chimie Paristech - PSL	<i>Directeur de thèse</i>



ParisTech

Table of Contents

Remerciements.....	5
Résumé en français	9
General introduction	30
CHAPTER 1 - Production and polymerization of biobased acrylates and analogs.....	35
Abstract	36
1. Introduction	36
2. Production of Biobased Acrylates and Analogs.....	40
2.1. Acrylic Acid (AA).....	40
2.2. Methacrylic Acid (MAA).....	44
2.3. Itaconic Acid	52
2.4. α -Methylene- γ -butyrolactone and Analogs	56
2.5. Other Biobased Lactones.....	64
2.5.1. Methylene Lactide (MLA)	64
2.5.2. β -Angelica Lactone (β -AL).....	65
2.6. β -Substituted Acrylics	66
2.6.1. Cinnamic Acid.....	66
2.6.2. Fumaric Acid.....	67
2.6.3. Muconic Acid	69
2.6.4. Crotonic Acid	72
3. Polymerization of (Meth)Acrylic Monomers and Analogs.....	76
3.1. (Meth)Acrylates.....	77
3.1.1. Radical Polymerization	78
3.1.2. Anionic Polymerizations	84
3.2. Itaconic Acid Vinyl Polymerization.....	88
3.3. α -Methylene- γ -butyrolactone and Analogs	90
3.4. Other Biobased Lactones.....	98
3.4.1. Methylene Lactide.....	98
3.4.2. β -Angelica Lactone	100
3.5. β -Substituted Acrylics	102
3.5.1. Cinnamic Acid.....	102
3.5.2. Fumaric Acid.....	104
3.5.3. Muconic Acid	106
3.5.4. Crotonic Acid	107

4. Conclusion.....	109
References	113
CHAPTER 2 - Multicatalytic Transformation of (Meth)acrylic Acids: a One-Pot Approach to Biobased Poly(meth)acrylates	
Biobased Poly(meth)acrylates	134
Abstract	135
Introduction	135
Results and discussion.....	137
Monomer formation sequence.....	137
Formation of (meth)acrylic anhydrides.....	137
Acylation with anhydrides	139
Esterification of (meth)acrylic acids	141
Polymer Formation step	147
Conclusion.....	154
References	155
Supporting Information	158
CHAPTER 3 – Ambient Temperature Polymerization of MMA mediated by Ate Complexes.....	
Complexes.....	241
Abstract	242
Introduction	242
Results and discussion.....	244
Conclusion.....	255
Experimental section	255
References	258
Supporting Information	260
CHAPTER 4 - Highly Efficient Synthesis of Poly(silylether)s: Access to Degradable Polymers from Renewable Resources	
Renewable Resources	269
Abstract	270
Introduction	270
Results and discussion.....	273
Conclusion.....	287
References	288
Supporting Information	293
Conclusion and Perspectives.....	356

Remerciements

L'exercice des remerciements est paradoxalement à la fois convenu et attendu. Aussi, la pression est forte pour finalement faire... comme tout le monde, à sa manière. Ces quelques lignes viennent ponctuer trois années uniques pour obtenir un grade décerné à environ 15 000 personnes en France par an, soulignant encore un peu plus le caractère exceptionnel et banal de mon expérience.

Mes premiers remerciements vont naturellement à mon directeur de thèse **Christophe Thomas**. On dit souvent que pour qu'une thèse se passe bien, il faut que l'encadrant.e donne de l'autonomie au doctorant.e, tout en restant disponible et présent.e. J'ai conscience d'avoir pu bénéficier d'un tel équilibre, et pour cela, Christophe, je voulais te remercier. Merci également pour m'avoir transmis ta passion pour la synthèse des matériaux, ta rigueur exemplaire sur la bibliographie, ton expérience et ta connaissance du milieu académique. J'ai apprécié nos longues discussions scientifiques, ton honnêteté intellectuelle et tes digressions sur l'actualité, le sport, ou l'histoire de la catalyse de polymérisation.

Je ne serais sans doute pas le chimiste que je suis sans la passion et la patience de mes trois précédents encadrants de stage en recherche académique, **Carine Robert**, **Geoffroy Guillemot** et **Salvador Conejero**. Un immense merci pour m'avoir conduit dans vos laboratoires respectifs, m'avoir enseigné les subtilités expérimentales de la chimie, et surtout pour votre bienveillance et votre amitié. Je termine ce petit crochet par Séville en remerciant également **Pablo Ríos**, pour sa joie de vivre communicative et son amitié indéfectible donnée après 5 mois de synthèse de complexes de platine sur fond de musique rock dans le chaleureux « laboratorio nueva ».

Revenons à Paris, et à notre petite équipe de chimie organométallique et catalyse de polymérisation. En trois ans et quelques mois, j'ai eu la chance de croiser de nombreux permanents, étudiants, docteurs ou futurs docteurs. Merci donc à **Frédéric de Montigny**, **Pierre Haquette** et **Régis Gauvin** pour vos conseils et votre bienveillance. Merci à **Wei Qiang**, **Lucie Fournier**, **Dapeng**

Remerciements

Zhang, et **Jiraya Kiriratnikom**, pour m'avoir accueilli avec entrain à la fin de vos doctorats respectifs. **Nancy Soliman** et **Clément Ravet** ont partagé avec moi deux ans et demi de galères, de rigolade, de questionnements, bref, de thèse, et je les remercie pour avoir ouvert la voie devant moi. Votre expérience et votre honnêteté m'ont énormément aidé, les blagues de Clément et le rire de Nancy m'ont à coup sûr diverti et rassuré. Merci également à **Xuezhao Xu** pour m'avoir aidé à relativiser. **Zahra Mazloomi** et **Ondřej Železník** sont des collègues formidables, j'espère que nos routes se recroiseront à l'avenir. Merci à **Émilie Bertrand**, **Sami Fadlallah**, **Apichai Manaprasertsak**, **Najlaé Mahi**, **Simon Peyras**, **Suppajittra Yimthachote** alias « Bee » et **Kwanchanok Udomsasporn** alias « Kwan » pour avoir échangé avec moi vos idées, votre gentillesse. Merci **Bo Jiang** pour ta disponibilité et ton esprit d'équipe. Merci à **Malaury Simon** pour t'être cassé la tête avec moi sur la SPS, la GPC, ou toute autre machine qui décidait de se mettre en erreur fatale le vendredi à 17h. Merci **Pascal Matton** pour ta prévenance et l'envoi de ces fameux manuscrits de thèse ! Cette dernière année de thèse n'aurait pas été la même sans **João Antonio** et **Lucie Guillaume**, les « tauliers du labo ». Merci João pour ta curiosité et ta bonne humeur, merci Lucie pour tes expressions québécoises et tes conseils en chimie organique (et l'organisation de ces cadeaux de thèse, deadly !).

Je suis également très reconnaissant envers les stagiaires que j'ai eu l'occasion d'encadrer lors de ces années de thèse. Car on apprend autant en encadrant qu'en étant encadré. Merci donc à **Cyrine Saïd-Ali**, **Anthyme Dutriaux** et **Fiona Kamougue**.

Merci aux collègues permanents **Vincent Placet**, **Philippe Guégan**, **Gilles Gasser**, **Kévin Cariou** et **Guillaume Lefèvre**, avec qui j'ai pu collaborer, qui m'ont conseillé, ou que j'ai simplement croisé dans notre couloir animé du 1^{er} étage escalier G de Chimie Paris. Je veux aussi remercier tous mes collègues et surtout amis croisés dans les différents laboratoires de notre institut, la liste est longue mais chacun.e m'a marqué par un sourire, une blague ou un point de vue singulier. Merci donc à **Lidie Rousseau** (les discussion politiques !), **Pablo Chourreu**, **Maé Robin**, **Vincent Wowk**, **Johannes Karges**, **Anna Notaro**, **Joe Cowell**, **Capucine Mahé** (dab & drama), **Yan Lin**, **Robin Vinck**, **Marta**

Remerciements

Martinez Alonso, Sarah Keller, Yin Ching Ong, Marta Jakubszek, Patrick Felder, Cristina Mari, Marie Huynh, Francisca Figueiredo, Niovi-Giorgia Voutsara, Lisa Gourdon, Germain Niogret, James Ng, James Southwell, Albert Grandioso, Luke Mckenzie, Harley Betts, Kallol Purkait, Cillian O’Beirne (crazy dancer), Yiyi Zhang, Maria Dalla Pozza (crazy dancer bis), Ivanna Amarsy, Youchao Wang, Diana Melis, Siqi Zhang, Camille Evin, Christelle Chauffeton, Éloïse Lafitte-Houssat, Nao Harada, Ersan Gurbuz (à vous 4 pour les karaokés et raclettes !), Pierre Alexandre Royoux, Giovanni Mutton, Anne Westermeyer, Johanne Ling et Ricardo Molina-Betancourt. Je finis ce tour de Chimie Paris en remerciant **Nathalie Ouvry**, pour son aide en toute circonstance, **Didier Lecomte**, pour les blagues et le livre Métronome, et l’indéboulonnable Ali Eskandari, une véritable âme de cette école.

Enfin, je n’oublie pas toutes les personnes qui m’ont accompagné en dehors des heures de boulot, de près ou de loin, lors de ces années de thèse. Merci donc à tous mes coéquipier.ère.s de flag football, à mes potos du foot et des « five » **Fabien Perez, Marc Chachuat, Tom Seimandi, Thibaut Sauvage, Hadrien Hendrikx, Charles Boubert, Othman Lamdouar, Julien Maudet, Youssef Yacine, Olivier Rémy, Tristan Fulchiron, Félix Roy, Gabriel Follin-Arbelet, Alexis Geslin, Paul Welter**, à mes ami.e.s **Mathilde Boissier, Geoffroy Ransac, Fabien Cockenpot, Adrien Deschamps, Bertrand Marchand, Antonin Gallet, Agathe Maurin, Robin Bais, Caroline Desmurget, Bérénice Guiboud, Amélie Klein, Delphine Boursette, Grégory Gredat, Nina Chini et Steven Hearn.** À cette petite bande de « graus » qui s’est formée il y a maintenant dix ans, je vous aime **Fiona Le Coz, Georgina Beng, Aurélie Moron, Hélène Collomb, Arthur Auché et Ibrahim Ghalayini.** À cette colocation qui est devenue une deuxième famille, un immense merci **Solène Marie, Cyrille Pastour, Antoine Devulder, Emma Alluyn, Jean-Baptiste Lienhart, Nam Phan Van Song** et bien sûr **Isis le chat**, qui m’a rappelé régulièrement que je travaillais trop et que je pouvais tout aussi bien dormir et manger des croquettes en regardant les pigeons passer à travers la fenêtre. **Flocon le chien** figure également en bonne place des compagnons indispensables pour écrire un manuscrit de

Remerciements

thèse tout en gardant une humeur débonnaire. Viriville fut pour moi un repaire accueillant et agréable, grâce à mon adorable famille d'adoption **Sylvie, Hubert, Mathis et Dorian Renevier**. Mes derniers mots de remerciements iront bien sûr à ma sœur **Julie Fouilloux**, et à **Adrien Finance**, pour leur soutien « hardware » indispensable en cette fin de thèse, et surtout parce qu'ils sont adorables ; à mes parents **Jean-Michel et Pascale Fouilloux**, qui, grâce à leur amour et la tendresse de leur éducation, m'ont permis de faire les rencontres que j'énumère maintenant depuis quelques pages ; et à **Clémentine Renevier**, qui sait en tout temps me rassurer et me pousser à faire mieux, et, surtout, me combler, comme j'espère le faire avec toi.

Résumé en français

L'année 2020 a marqué le centième anniversaire de la première description d'une réaction dite de « polymérisation » par Herman Staudinger.^[1] Depuis, les polymères, et plus particulièrement les matières plastiques, ont envahi notre quotidien, qu'il s'agisse de l'emballage des denrées alimentaires ou des matériaux haute-performance utilisés dans la construction, les transports ou le domaine médical.^[2] Leur succès repose sur la facilité avec laquelle ils peuvent être préparés à partir de produits dérivés du pétrole (environ 4% de la production annuelle de pétrole est utilisée pour fabriquer du plastique),^[3] grâce notamment aux travaux fondateurs de Ziegler et Natta sur la catalyse de polymérisation, qui leur valut le prix Nobel de Chimie en 1963. Cependant, l'industrie des polymères traverse actuellement une crise matérialisée par deux défis d'importance : 1) le rejet incontrôlé de matières plastiques dans l'environnement représente une pollution particulièrement nocive pour les milieux naturels et la biodiversité qu'ils abritent ;^[4] 2) les ressources pétrolifères devront rester majoritairement inexploitées si les sociétés humaines espèrent contenir le dérèglement climatique, ce qui pousse l'industrie des polymères à extraire ses matières premières de manière renouvelable, par exemple à partir de biomasse.^[5]

La recherche en académie et en industrie s'est ainsi récemment efforcée de relever ces deux défis. Les différentes fins de vie possibles d'un matériaux polymère ont été théorisées dans le concept plus général d'économie circulaire (voir Schéma 1) :^[6,7] la réutilisation, les recyclages mécanique, puis chimique, et enfin la biodégradation dans l'environnement doivent être priorisés dans cet ordre. Comme certains produits ou objets ne peuvent être réutilisés indéfiniment, et comme le recyclage mécanique souffre de certains désavantages (perte de propriétés optiques ou mécaniques), le recyclage chimique a récemment attiré l'attention des chercheurs en tant que méthode efficace pour obtenir des matières premières chimiquement pures à partir de déchets.^[8-10] En outre, les polymères biodégradables ne devraient être utilisés que lorsque leur dépôt dans l'environnement ne peut être

évité.^[11] Plusieurs matières premières renouvelables ont par ailleurs été identifiées pour la synthèse de polymères biosourcés : les polysaccharides, la lignine,^[12,13] les protéines et différentes essences végétales comme les terpènes.^[5,14]

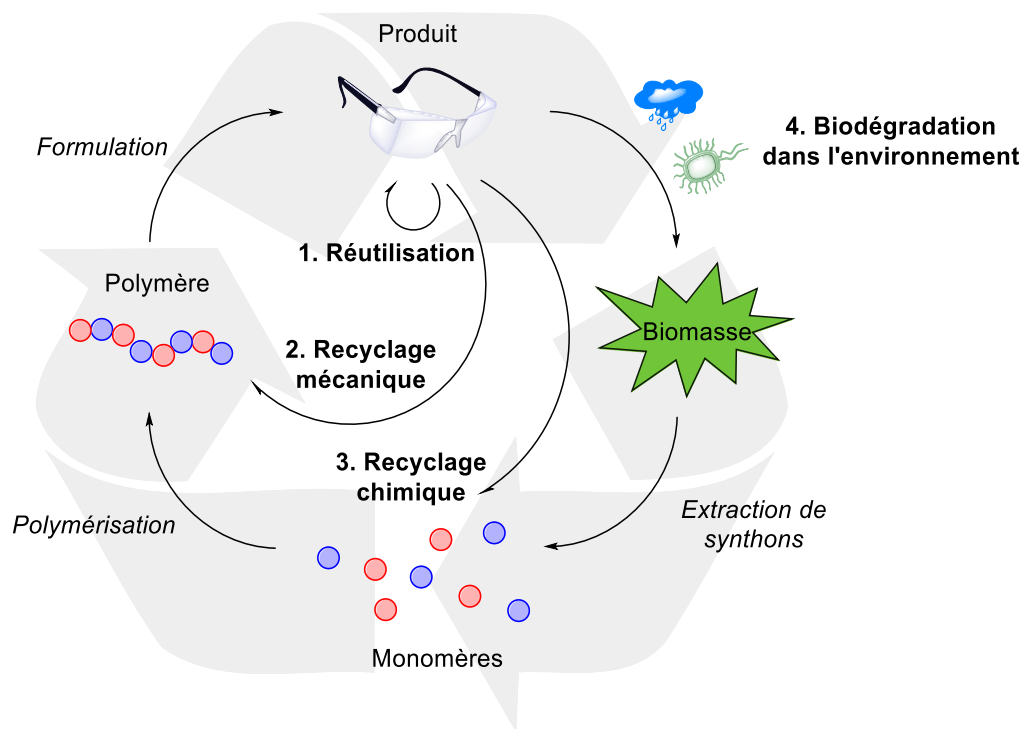


Schéma 1. Économie circulaire idéale des matériaux polymères, adapté de [6].

L'objectif du travail de thèse présenté ici fut de développer des méthodes innovantes de synthèse de polymères, capables de répondre à ces deux défis, et qui soient donc biosourcés et intrinsèquement recyclables. Ayant toujours à l'esprit les principes de la chimie verte,^[15] notre recherche s'est concentrée sur l'utilisation de catalyseurs efficaces, dans des conditions douces, tout en essayant de réduire la production de déchets tels que les solvants.

Le premier chapitre de ce travail de thèse est un état de l'art concernant la préparation et la polymérisation des (méth)acrylates et de leurs analogues. La production de plastiques biosourcés n'en est en effet encore qu'à ses prémices, et leur avènement annoncé se fait attendre : en 2014, la production mondiale de plastiques biosourcés s'élevait à 1.7 millions de tonnes, et était projetée à 7.8 millions pour l'année 2019.^[16] Cinq ans plus tard, ce chiffre ne s'est élevé qu'à 2.1 millions,^[17] soit

une augmentation de 15% égale à celle plus globale de la production de plastiques (de 311 à 359 millions de tonnes).^[18,19] Les plastiques biosourcés ne représentent donc aujourd'hui qu'1% de tous les plastiques produits annuellement. Cependant, de nombreuses recherches ont récemment été conduites afin de d'accélérer cette tendance.

Parmi la multitude de matériaux polymères disponibles, les dérivés acryliques et leurs analogues sont particulièrement prometteurs en raison de la grande variété de leurs structures chimiques, et des différentes propriétés qui peuvent donc être obtenues.^[20,21] Ces dérivés sont en effet utilisés pour la production de revêtements, de fibres optiques, ou d'adhésifs. La partie vinylique des monomères acryliques peut être obtenue à partir de biomasse de différentes manière (Figure 1).

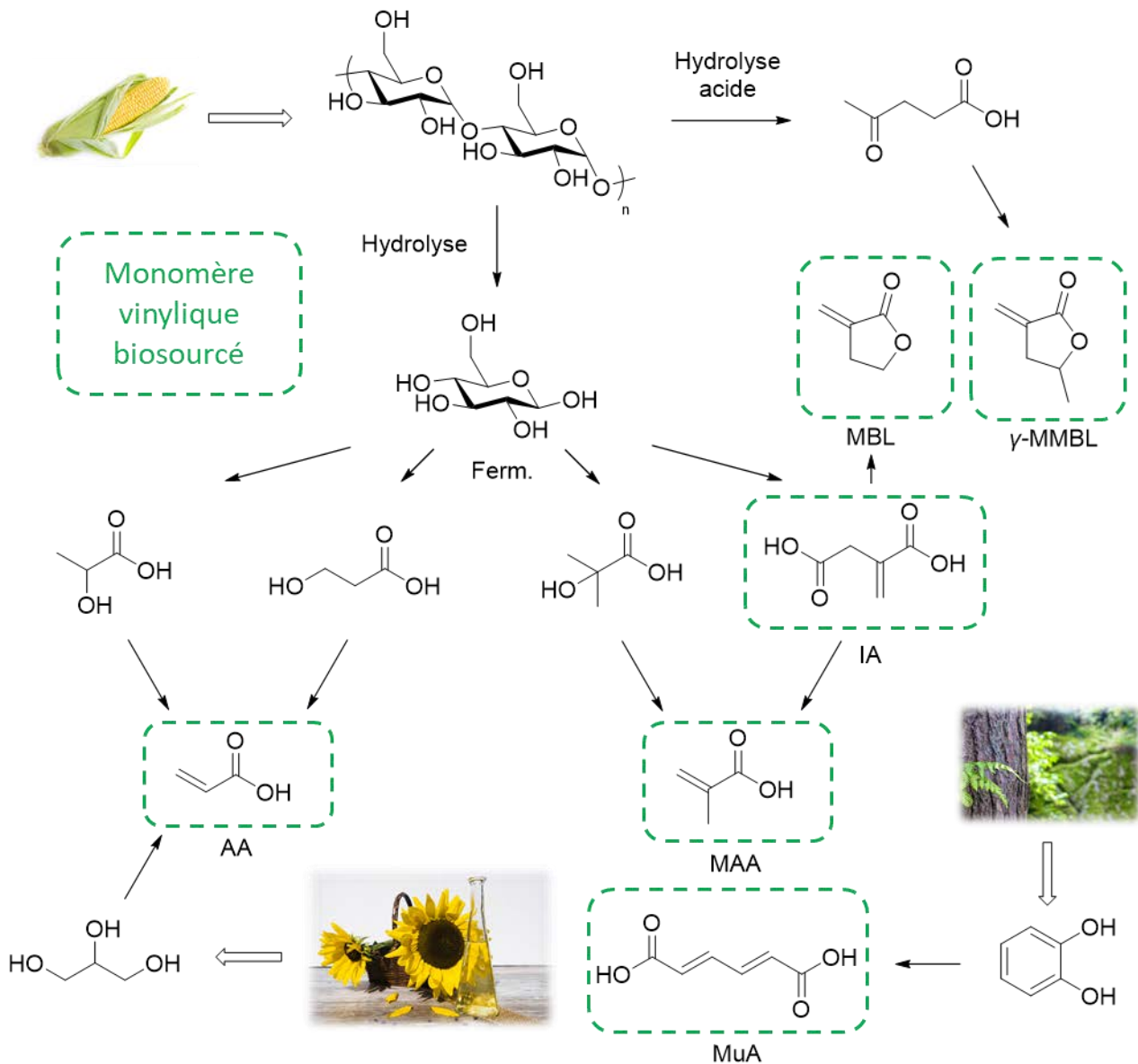


Figure 1. Les différents monomères vinyliques qu’il est possible d’obtenir à partir de synthons clés, eux-mêmes produits à partir de biomasse.

Le plus simple des monomères acryliques est l’acide acrylique (AA). En 2014, sa production s’élevait à 5.2 millions de tonnes.^[22] Il est principalement produit *via* l’oxydation en deux étapes du propène, un sous-produit de l’industrie pétrolière. Différentes voies de production à partir de synthons biosourcés comme le glycérol, l’acide lactique ou l’acide 3-hydroxypropanoïque ont cependant été étudiées.^[23] L’entreprise Cargill a récemment annoncé son intention de produire un AA commercial à partir de l’acide lactique.^[24] L’acide méthacrylique (MAA), dont l’ester correspondant, le méthacrylate

de méthyle (MMA), est produit à environ 4 millions de tonnes par an, constitue le deuxième plus important dérivé acrylique.^[25] Son obtention à partir de biomasse est sensiblement moins avancée que pour l'AA. Certaines voies prometteuses ont cependant été envisagées à partir des acides citrique ou itaconique.^[26] L'acide itaconique est lui-même un monomère vinylique possédant une double liaison polymérisable. Sa production actuelle se fait principalement par fermentation du glucose obtenu à partir de biomasse de première génération.^[27] Différentes butyrolactones vinyliques comme la α -méthylène- γ -butyrolactone (MBL) ou la γ -méthyl- α -méthylène- γ -butyrolactone (γ -MMBL) sont également des produits de départ prometteurs pour la production de matériaux haute-performance.^[28] Les acides itaconique, succinique et lévulinique ont été identifiés comme des intermédiaires clés permettant l'obtention de MBL ou de γ -MMBL. Enfin, l'acide muconique constitue un exemple original de monomère vinylique obtenu à partir de lignine, *via* la fermentation du catéchol.^[29]

Ainsi, suivant le dérivé acrylique considéré, la maturité de sa production à partir de biomasse, et son potentiel volume de production diffèrent (Figure 2). L'augmentation attendue de la part des plastiques biosourcés dans la production globale de plastique n'aura sans doute lieu que si ces matières deviennent plus compétitives économiquement. Cette compétitivité peut toutefois être orientée par des politiques publiques volontaires, tout en évitant de financer des procédés à partir de biomasse qui ne semblent pas soutenables sur le long terme, comme la production actuelle de polyéthylène biosourcé. Le défi qui se présente est donc bien de trouver des matières premières véritablement renouvelables, des voies de synthèses efficaces et rapides, et des applications soutenables.

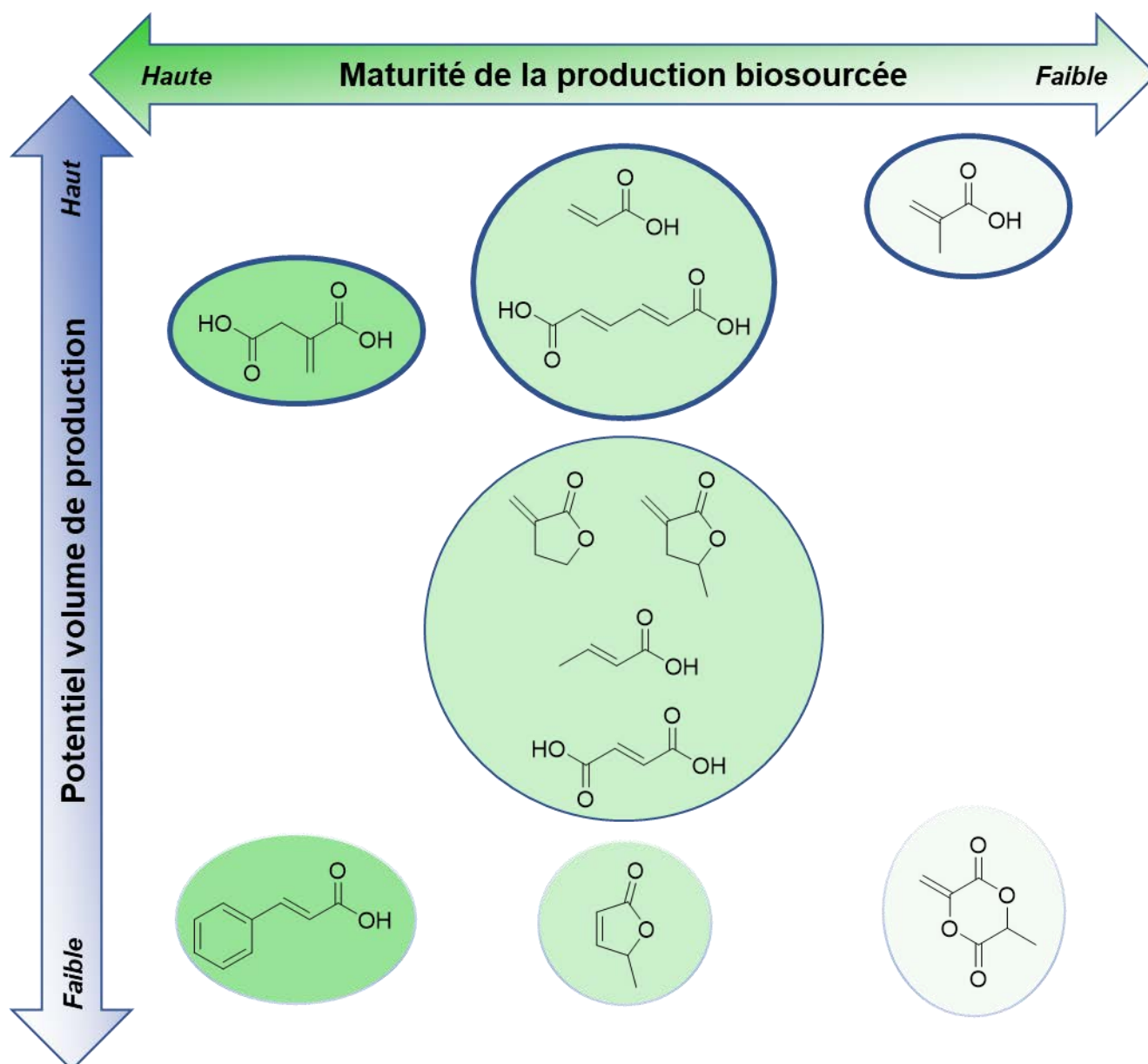


Figure 2. Statut actuel de la production de monomères biosourcés et leur potentiel volume de production.

Le deuxième chapitre de cette thèse a été l'occasion de développer une méthode de synthèse de poly(méth)acrylates biosourcés dite « one-pot » (c'est-à-dire sans étape de purification intermédiaire entre la synthèse du monomère et sa polymérisation). Cette méthode a permis d'obtenir de manière sélective différents monomères, et de les transformer en homopolymères, et copolymères statistiques ou blocs (Schéma 2).

Résumé en français

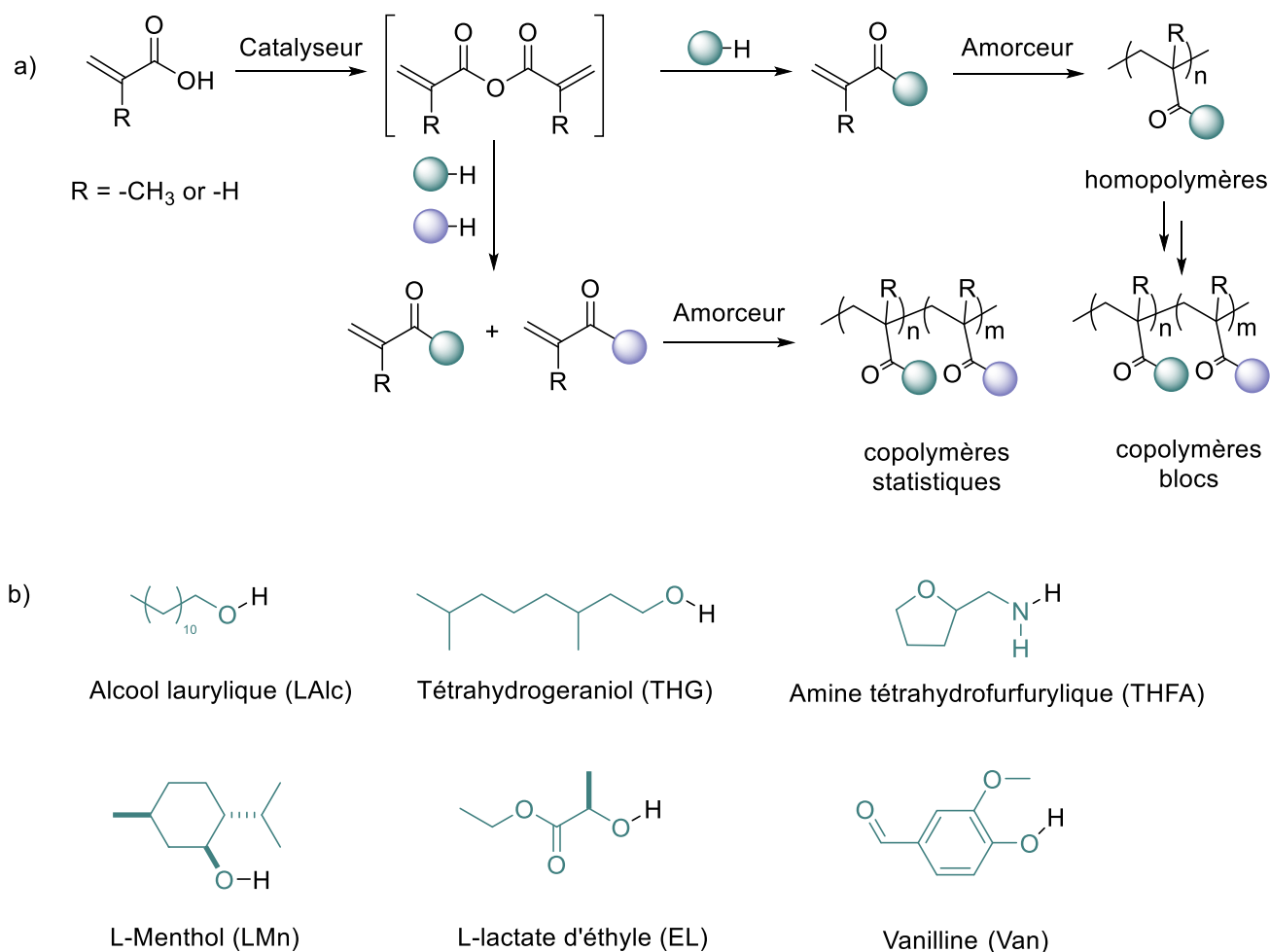


Schéma 2. a) Synthèse one-pot de co-poly(méth)acrylates à partir d'alcools biosourcés et d'acide (méth)acrylique. b) Inventaire des substituants biosourcés utilisés dans cette étude.

La première étape de ce travail a consisté en l'étude détaillée de la production des (méth)acrylates à partir des acides correspondants. Inspirés par les travaux de Bartoli et de ses collègues sur la synthèse d'anhydrides ou d'esters à partir d'acides, à l'aide de dicarbonates,^[30] nous avons d'abord cherché à produire l'anhydride (méth)acrylique de manière quantitative, dans des conditions douces (30 à 40°C). L'utilisation du chlorure de magnésium (MgCl₂) comme catalyseur de cette réaction a permis d'obtenir sélectivement l'anhydride désiré. Différents triflates de terres-rares ont également été testés, mais se sont révélés trop peu sélectifs pour cette réaction. Ensuite, l'acylation de différents alcools biosourcés à l'aide d'anhydride méthacrylique a pu être réalisée de manière quantitative, que ce soit avec MgCl₂, Sc(OTf)₃, Y(OTf)₃ ou La(OTf)₃. Enfin, l'estérification directe de

l'acide (méth)acrylique par différents alcools, à l'aide du dicarbonate de *tert*-butyle (Boc_2O), a permis d'obtenir des mélanges réactionnels contenant seulement le ou les synthon(s) polymérisable(s) souhaité(s). Cette sélectivité est cruciale afin d'obtenir le polymère cible lors de l'étape suivante. L'étude du mécanisme de cette transformation a permis de mettre en évidence les différents intermédiaires impliqués dans la production de l'ester, à savoir l'anhydride mixte (décrit pour la première fois) puis l'anhydride. Parmi les produits secondaires générés lors de cette étape, citons la formation de carbonates mixtes par addition-élimination de l'alcool sur le Boc_2O : ce carbonate n'est pas réactif dans la suite de la séquence réactionnelle, mais sa formation non voulue nécessite l'utilisation d'un léger excès d'alcool et de Boc_2O ($1.2 \times [\text{Acide}]$) afin d'atteindre une conversion complète de l'acide (méth)acrylique.

Cette étude s'est ensuite tournée vers l'étape de polymérisation. Une première preuve de concept a été produite par la polymérisation statistique des méthacrylates de méthyle et de lauryle (MMA et LMA), par simple ajout de 2,2'-azobis(2-méthylpropionitrile) (AIBN) et de toluène au mélange réactionnel (accompagné d'un chauffage à 70°C). L'efficacité de cette méthode a été illustrée par la copolymérisation de différents méthacrylates. De plus, deux agents de transfert de chaîne, le dodécyle mercaptan ou le dithiobenzoate de cyanopropyle (CPDB), ont permis de contrôler la masse molaire des matériaux obtenus. L'utilisation du CPDB rend par ailleurs possible l'obtention de copolymères blocs, sans étape de purification intermédiaire : après une première polymérisation, le milieu réactionnel est en effet ramené à une température suffisante pour une nouvelle étape d'estérification ($30\text{-}40^\circ\text{C}$), les réactifs désirés sont ajoutés, et une fois le nouveau monomère formé, l'ajout d'une faible quantité d'AIBN ainsi que le chauffage du réacteur à 70°C permettent de produire des copolymères blocs. Cette méthode a été illustrée avec différents monomères, ce qui a permis d'obtenir des matériaux aux propriétés thermiques variées (températures de transition vitreuse allant de -61 à 111°C).

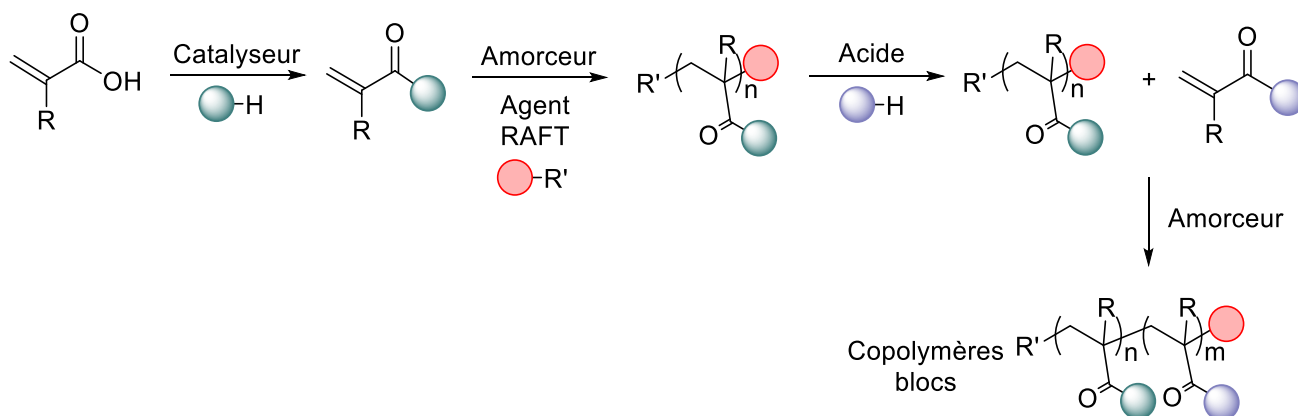


Schéma 3. Séquence réactionnelle pour la production de copolymères blocs.

L'impact environnemental de cette méthode de synthèse a enfin été évalué, en comparant la synthèse d'un copolymère bloc déjà rapportée avec celle du même matériau obtenu *via* notre méthode.^[31] Le facteur environnemental (soit la masse de tous les produits utilisés lors de la synthèse divisée par la masse du produit obtenu, moins 1) a ainsi pu être divisé par plus de 3 grâce à notre approche, passant de 500 à 150. La méthode développée lors de ce projet a ainsi prouvé son intérêt en termes d'efficacité, de facilité de mise en œuvre, et de réduction de production de déchets.

Dans un troisième chapitre, nous nous sommes intéressés au développement d'une méthode de polymérisation anionique des méthacrylates à température ambiante, à l'aide de complexes métalates formés *in situ* à partir de réactifs commerciaux. Les méthodes de polymérisation anionique sont généralement mises en œuvre à basse température (entre -40 et -78°C) et requièrent souvent la synthèse de catalyseurs en plusieurs étapes. Par ailleurs, les complexes métalates ou « ates » (sels associant une base et un acide de Lewis, dans lesquels la partie acide devient formellement anionique), isolés pour la première fois par Wanklyn en 1858,^[32] et développés principalement par Wittig,^[33] sont régulièrement utilisés pour l'activation des liaisons C-H des cycles aromatiques, et présentent une meilleure stabilité à température ambiante que leurs analogues organolithiens. De rares exemples d'utilisation de complexes « ates » pour la polymérisation du MMA font état de résultats prometteurs, qu'il s'agisse de magnésiates,^[34,35] d'yttriumate^[36] ou de cuprate.^[37]

Résumé en français

Notre attention s'est d'abord portée sur la synthèse du lithium-magnésiate $\text{LiMg}[\text{N}(\text{TMS})_2]_2n\text{Bu}$ à partir des produits commerciaux $\text{Mg}[\text{N}(\text{TMS})_2]_2$ et du $n\text{BuLi}$. Le complexe attendu est formé quantitativement dans le toluène, alors qu'un équilibre de Schlenk est observé dans le THF (voir Schéma 4). Cependant, les meilleurs résultats de polymérisation ont été obtenus dans le THF, solvant donneur qui stabilise sans doute plus efficacement la chaîne polymérique en propagation. Avec ce système, la polymérisation de 50, 100 ou 200 équivalents de MMA est en effet possible dans le THF, la conversion du monomère est importante (de 83 à 99%) et les masses molaires obtenues sont proches de celles attendues. Remarquablement, les expériences de contrôle, utilisant le $n\text{BuLi}$ ou le $\text{Mg}[\text{N}(\text{TMS})_2]_2$ seul pour amorcer la polymérisation, ont montré des conversions très faibles à température ambiante (de l'ordre de 1%), et ainsi illustré l'intérêt des complexes « ates ».

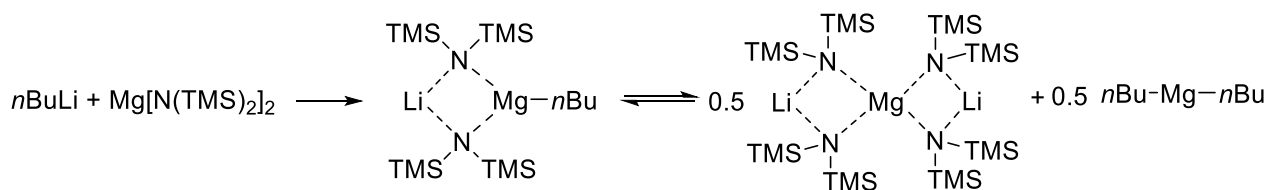


Schéma 4. Synthèse de $\text{LiMg}[\text{N}(\text{TMS})_2]_2n\text{Bu}$ et équilibre de Schlenk correspondant.

L'influence de plusieurs paramètres expérimentaux a ensuite été étudiée afin de déterminer les conditions optimales de polymérisation. L'utilisation du toluène comme solvant a conduit à l'obtention de distributions de masses multimodales pour les PMMA obtenus, suggérant une faible stabilité de la chaîne en croissance dans ce solvant. La réduction de la température de réaction à -30°C a réduit le contrôle sur les masses obtenues de manière surprenante. Cette observation a été attribuée à la lenteur de l'attaque nucléophile du groupe amidure $\text{N}(\text{TMS})_2$ sur le premier monomère de MMA à ces températures. Pour obtenir un bon contrôle sur le procédé de polymérisation, une étape d'amorçage suffisamment rapide par rapport à l'étape de propagation de la chaîne polymérique est en effet déterminante. L'influence du centre métallique a été également étudiée : en remplaçant l'atome de magnésium par un atome de calcium, une activité similaire en polymérisation du MMA a été obtenue.

Cependant, les complexes analogues à base de zinc ou de fer se sont révélés bien moins performants. Enfin, l'utilisation de différents ligands lithiés pour stabiliser le précurseur $\text{Mg}[\text{N}(\text{TMS})_2]_2$ a été proposée, mais ont donné des résultats similaires à ceux obtenus avec le système simple $\text{LiMg}[\text{N}(\text{TMS})_2]_2n\text{Bu}$.

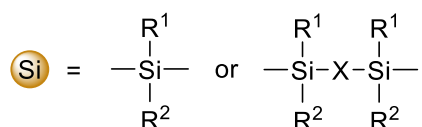
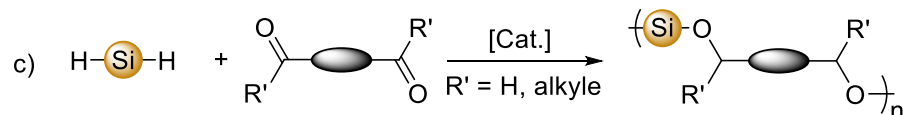
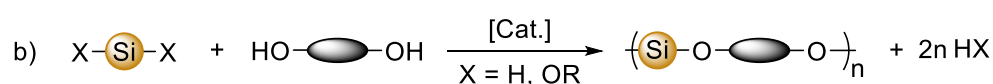
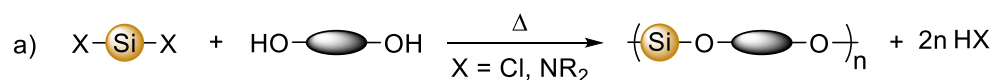
L'utilisation de $\text{LiMg}[\text{N}(\text{TMS})_2]_2n\text{Bu}$ pour la polymérisation du lactide racémique a enfin permis d'illustrer sa réactivité prometteuse. À température ambiante, dans le THF (0.5 mol/L), le catalyseur formé *in situ* peut convertir 88% de 100 équivalents de *rac*-lactide en poly(acide lactique) (PLA) en 5h. Une distribution monomodale des masses molaires obtenues, ainsi qu'une valeur de M_n qui augmente proportionnellement avec la conversion du monomère, confirment le contrôle de la polymérisation. Nous avons ensuite supposé que l'énolate formé lors de la polymérisation du MMA pourrait également amorcer la polymérisation par ouverture de cycle du *rac*-lactide. Nous avons donc réalisé la polymérisation de 50 équivalents de MMA avec $\text{LiMg}[\text{N}(\text{TMS})_2]_2n\text{Bu}$, dans le THF à température ambiante, puis ajouté 100 équivalents de *rac*-lactide et arrêté la réaction après 3h. L'obtention d'un copolymère bloc de PMMA et PLA a été confirmée par spectroscopie RMN et chromatographie d'exclusion stérique : la distribution monomodale des masses molaires du matériaux a en effet été décalée vers les plus hautes masses après addition du *rac*-lactide.

La méthode développée dans ce troisième chapitre présente ainsi des particularités prometteuses, comme la possibilité d'obtenir en quelques minutes des polymères variés, à température ambiante, en utilisant de simples réactifs commerciaux.

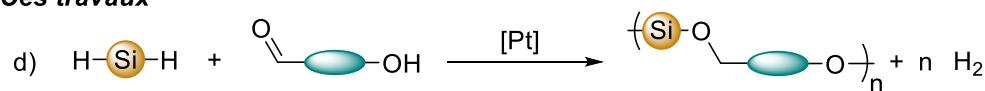
Enfin, le dernier chapitre de ce travail de thèse a été l'occasion d'étudier la synthèse des poly(silyléthers) (PSEs) (Figure 3). Ces polymères sont peu connus mais présentent des caractéristiques prometteuses conférées par leur liaison Si-O-C. Cette liaison est notamment sensible à l'hydrolyse ou l'alcoolyse en conditions acide ou basique.^[38-40] La synthèse des PSEs a principalement été étudiée à partir de diols et de différents monomères silylés tels que des dichloro-

ou diaminosilanes. Récemment, les dihydrosilanes se sont imposés comme des comonomères appropriés car leur couplage déshydrogénant avec des alcools produit du dihydrogène, un gaz qui s'échappe du milieu réactionnel, ce qui déplace donc l'équilibre vers de hautes conversions. De plus, l'hydrosilylation d'aldéhydes ou de cétones est possible avec des dihydrosilanes.^[41,42] Notre approche a donc été de coupler ces dihydrosilanes avec des hydroxyaldéhydes, comonomères issus de la biomasse en peu d'étapes, comme le 5-hydroxyméthyl furfural (HMF) ou la vanilline. L'utilisation de catalyseurs de platine très actifs a permis de réduire la charge catalytique (jusqu'à 500 ppm) et d'accéder à diverses structures polymériques.

Travaux précédents



Ces travaux



- ✓ **Complexes de platine actifs à faible charge catalytique**
- ✓ **Variété des dihydrosilanes et hydroxyaldéhydes utilisés**
- ✓ **Reyclage chimique via l'hydrolyse ou la méthanolyse en conditions acides**

Figure 3. Les différentes stratégies précédemment utilisées pour préparer des PSEs et les principaux points d'intérêt de notre méthodologie.

Nous nous sommes tout d'abord intéressés à l'obtention d'homopolymères à partir de HMF et de différents dihydrosilanes (MePhSiH_2 , Ph_2SiH_2 , Et_2SiH_2). Dans des conditions douces (20h à température ambiante puis 4h à 50°C), des PSEs de masses molaires prometteuses ont été obtenus (environ 15 kg/mol), et caractérisés par spectroscopies RMN et infrarouge. La capacité du catalyseur de platine à activer le diéthyle silane est particulièrement notable, les poly(silyléthers) généralement décrits dans la littérature étant plutôt obtenus à partir de MePhSiH_2 ou Ph_2SiH_2 , le noyau aromatique attracteur d'électrons exacerbant l'électrophilie de l'atome de silicium. Deux autres comonomères directement issus de la lignine ont ensuite retenu notre attention : la vanilline et le syringaldéhyde. Ces hydroxyaldéhydes ont également pu être copolymérisés avec différents dihydrosilanes, et l'étude de la régiosélectivité de cette polymérisation a pu être menée par RMN ^1H - ^{29}Si HMBC. Les polymères issus de vanilline ont présenté une distribution équilibrée d'enchaînements tête-à-queue, tête-à-tête et queue-à-queue, alors que ceux obtenus à partir de syringaldéhyde présentaient une plus forte proportion d'enchaînements tête-à-queue. Cette observation s'explique par la gêne stérique importante rencontrée lors d'un enchaînement tête-à-tête due aux deux groupements méthoxys du syringaldéhyde.

Plusieurs structures de copolymères ont ensuite été étudiées. Tout d'abord, un copolymère statistique à partir de 1 équivalent de HMF et de 0.5 équivalent de Et_2SiH_2 et 0.5 équivalent de MePhSiH_2 a pu être préparé. De manière surprenante, l'obtention de copolymères blocs n'a pas été possible dans nos conditions réactionnelles, a priori à cause de de réactions secondaires coupant les chaînes polymériques déjà formées (voir Schéma 5). Cette hypothèse est suggérée sur la base du résultat suivant : un premier homopolymère poly(HMF-*co*- Et_2SiH_2) a été préparé ($M_n = 24\,700$ g/mol, $D = 2.6$), puis l'ajout de HMF et de MePhSiH_2 pour constituer le second bloc a conduit à un copolymère de masse molaire inférieure ($M_n = 9\,000$ g/mol and $D = 2.0$). Le produit final a présenté des caractéristiques identiques au copolymère statistique poly(HMF-*co*- MePhSiH_2 -*r*- Et_2SiH_2) précédemment synthétisé. Enfin, des copolymères alternés ont pu être préparés par fonctionnalisation préalable de la vanilline ou du syringaldéhyde en bis-silyl éther (Schéma 6). La réaction de ces

hydroxyaldéhydes avec deux équivalents de dihydrosilane conduit en effet à l'obtention quantitative de monomères bifonctionnels pouvant être copolymérisés avec un nouvel hydroxyaldéhyde, comme le HMF.

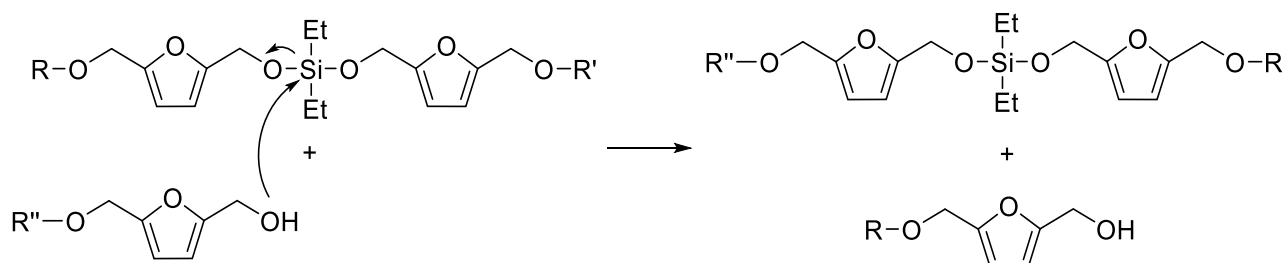


Schéma 5. Réaction secondaire suspectée de couper les chaînes polymériques préalablement formées.

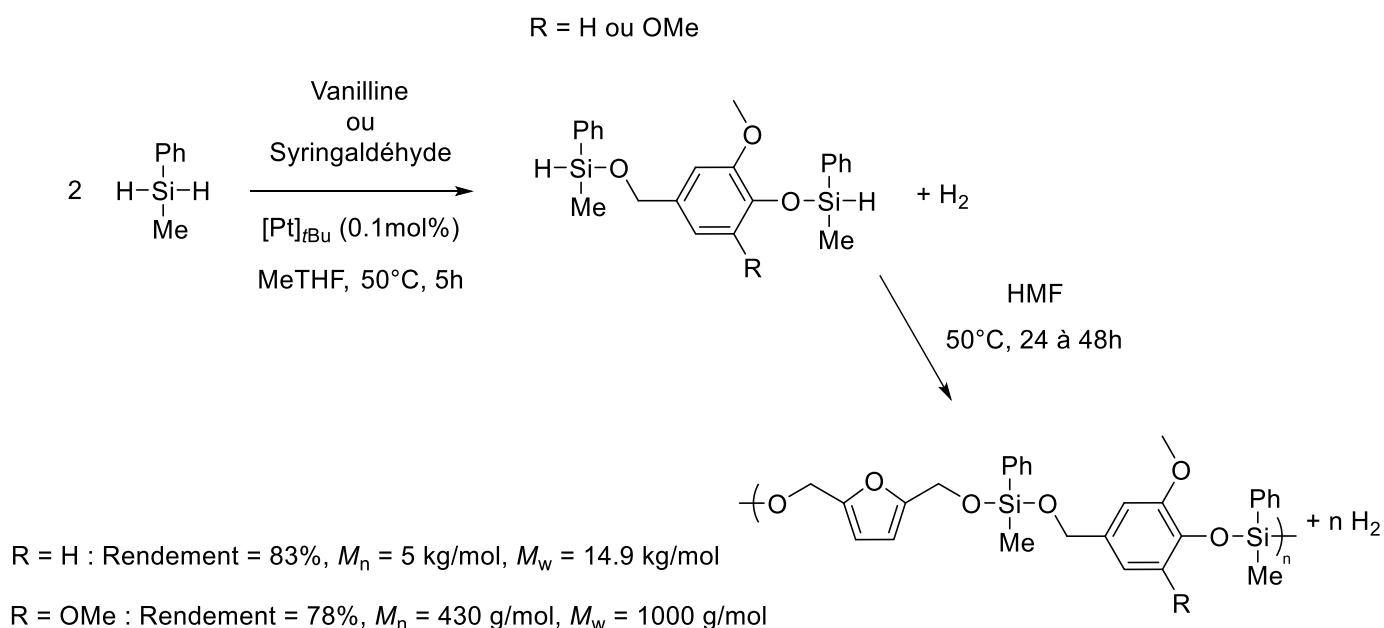


Schéma 6. Séquence réactionnelle donnant accès à des copolymères alternés.

Les poly(silyléthers) obtenus ont ensuite été caractérisés par calorimétrie différentielle à balayage et par analyse thermogravimétrique. Comme régulièrement observé dans la littérature, la température de transition vitreuse de nos matériaux dépend fortement de la nature du dihydrosilane utilisé ($T_g = 7^\circ\text{C}$ pour poly(HMF-co- Ph_2SiH_2) et $T_g = -60^\circ\text{C}$ pour poly(HMF-co- Et_2SiH_2)). L'impact de l'hydroxyaldéhyde utilisé s'est également vérifié, mais dans une moindre mesure.

Résumé en français

Enfin, une étude de dégradabilité et de recyclabilité de ces PSEs a été menée. L'expérience consiste à solubiliser le polymère dans un solvant organique (le THF), puis d'y ajouter un agent de dégradation (du méthanol ou de l'eau distillée, avec ou sans traces d'acide de Brønsted). L'évolution de la masse molaire du polymère permet de déterminer sa résistance ou sa dégradabilité dans les conditions choisies (Figure 4). Les PSEs préparés se sont montrés relativement stables en conditions de méthanolyse simple. L'utilisation d'acide de Brønsted a néanmoins permis de catalyser la dégradation quantitative de certains polymères à base de HMF ou de vanilline, restituant le diol correspondant. Le retour à l'état de monomère ouvre ainsi la voie à un potentiel recyclage chimique de ces matériaux (Schéma 7).

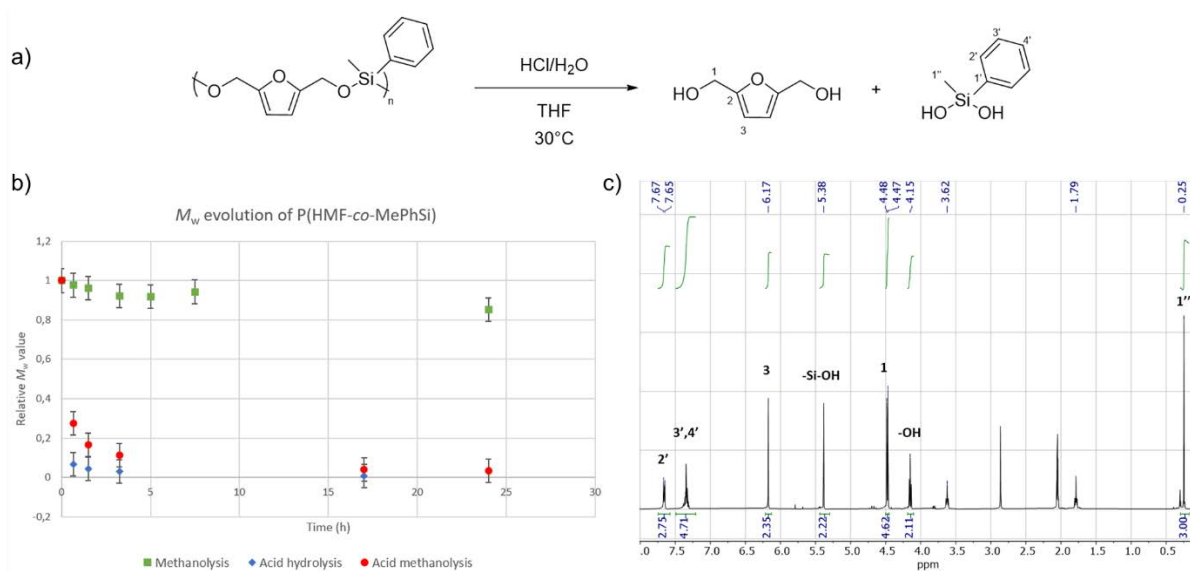


Figure 4. Étude de la dégradation du poly(HMF-co-MePhSiH₂) montrant les conditions réactionnelles (a), l'évolution relative du M_w du polymère avec le temps, suivant les conditions réactionnelles (b), et le spectre RMN ^1H du brut réactionnel de l'hydrolyse acide du poly(HMF-co-MePhSiH₂) après 17h (Acetone-*d*₆, 400 MHz) (c).

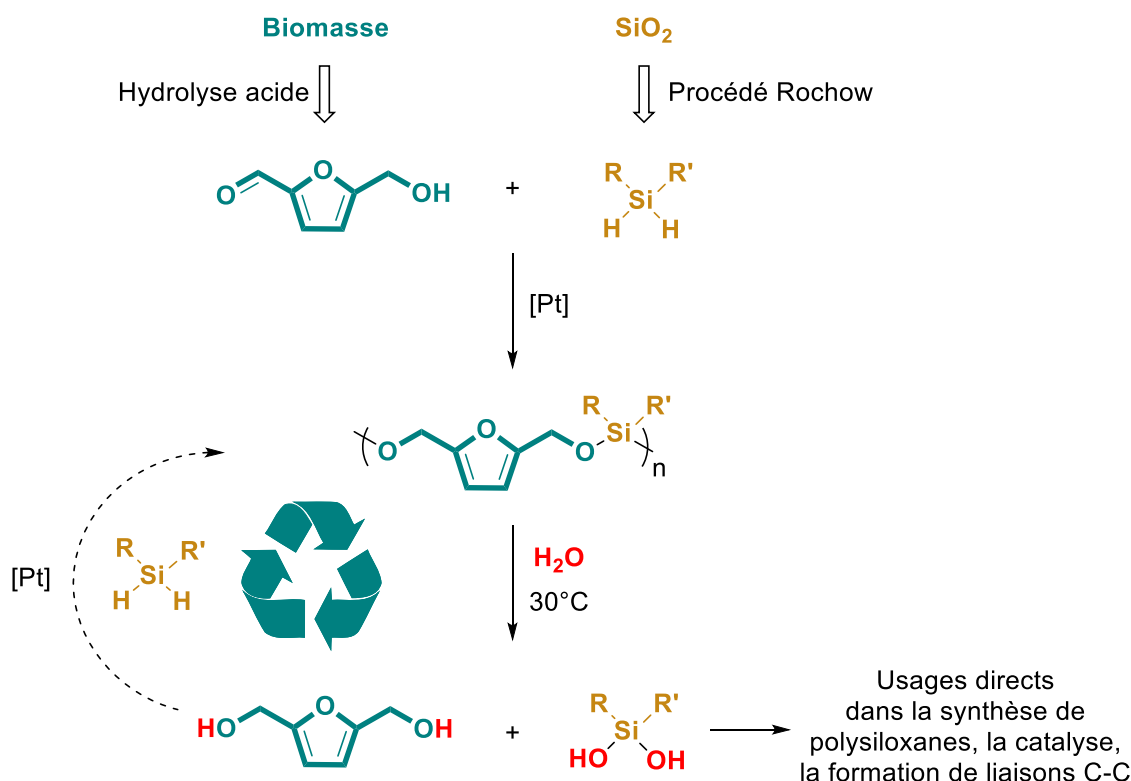


Schéma 7. Recyclage chimique des PSEs.

À partir d'hydroxyaldéhydes issus en peu d'étapes de ressources renouvelables, et en utilisant des complexes de platine actifs à faible charge catalytique, nous avons donc pu développer une synthèse efficace de poly(silyléthers). L'influence des comonomères sur les propriétés des polymères obtenus a pu être illustrée, et une méthode de recyclage chimique de certains de ces matériaux a pour la première fois été proposée.

En guise de conclusion, plusieurs perspectives ouvertes par ce travail de thèse sont soulignées. Le chapitre 1 de ce manuscrit a mis en évidence les efforts produits par les milieux académiques et industriels pour préparer les monomères acryliques à partir de ressources renouvelables. L'un des principaux représentants de cette classe de monomères, le MMA, est cependant toujours produit industriellement à partir de dérivés du pétrole. Jusqu'à maintenant, la voie de synthèse la plus prometteuse du MMA biosourcé consiste en la décarboxylation de l'acide itaconique, lui-même issu de la fermentation de sucres. L'intensification des efforts de recherche dans cette technologie semble

être la manière la plus simple d'obtenir du PMMA biosourcé. Cependant, dans le cas d'applications spécifiques où des propriétés originales et la provenance du matériau importent plus que son coût, il serait peut-être plus pertinent de développer de nouveaux polymères à base de butyrolactones ou d'acides itaconique ou crotonique. La récente publication de Miller, Allais et leurs collègues sur l'usage de différents alcools biosourcés pour l'obtention de poly(méth)acrylates originaux constitue un bon complément à notre état de l'art.^[43]

L'approche « one-pot » pour la synthèse de poly(méth)acrylates biosourcés que nous avons présentée dans le chapitre 2 offre une méthode efficace pour la synthèse durable de matériaux innovants. L'utilisation de catalyseurs commerciaux et bon marché comme $MgCl_2$, ainsi que la possibilité d'obtenir des copolymères blocs dans un seul et même réacteur, sont des caractéristiques particulièrement intéressantes pour des groupes de recherches travaillant dans le domaine de la caractérisation de nouveaux matériaux. En se limitant à une seule étape de purification, et en mettant à profit des réactions simples et robustes, cette méthode peut être utilisée par des chimistes inexpérimentés pour la synthèse et l'évaluation rapide de nouveaux matériaux. Bien que notre travail soit dédié à la chimie des acrylates et des méthacrylates, d'autres monomères pouvant être polymérisés par voie radicalaire devraient donner accès à des matériaux innovants *via* une méthode similaire. Coupler l'acide itaconique avec différents alcools biosourcés devrait être particulièrement intéressant, tandis que la β -hydroxy méthylène butyrolactone pourrait être combinée avec des monoacides biosourcés comme l'acide lévulinique pour produire une nouvelle collection de polymères (Schéma 8).

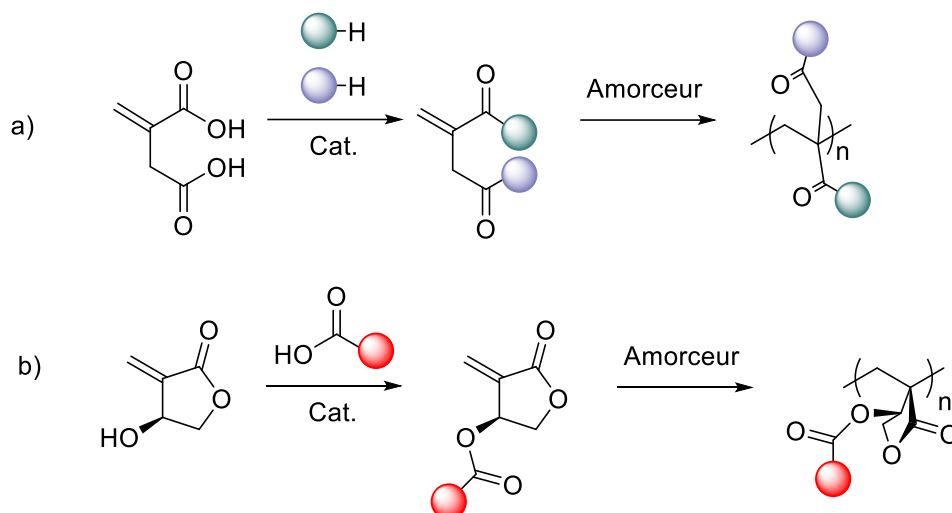


Schéma 8. Possible synthèse “one-pot” de (a) poly(itaconate)s ou de (b) polymères dérivés de β-hydroxy méthylène butyrolactone et d’acides biosourcés.

La préparation du PMMA par polymérisation anionique à température ambiante a montré des résultats prometteurs dans le chapitre 3. Le potentiel des complexes métalates en tant que catalyseurs pour des réactions de polymérisation dans des conditions douces est illustré. Cependant, le manque de contrôle sur la tacticité des polymères obtenus est préjudiciable, étant donné que la polymérisation anionique est souvent utilisée pour obtenir un contrôle sur la microstructure des matériaux désirés. La conception de ligands ayant une interaction suffisamment importante avec le centre métallique du catalyseur pourrait augmenter ce contrôle sur la tacticité. Notre méthode a également permis d’obtenir un copolymère bloc de PMMA et PLA. En s’appuyant sur la capacité de notre système à amorcer la polymérisation de monomères vinyliques et cycliques, une grande variété de nouveaux matériaux devrait être accessible de manière simple et efficace.

Enfin, la synthèse de poly(silyléthers) à partir de ressources renouvelables a permis de mettre en valeur cette classe de polymères relativement peu connue. Notre contribution illustre pour la première fois le potentiel recyclage chimique de ces matériaux. Le prochain défi pour ces polymères serait de réussir à séparer et réutiliser les monomères obtenus lors de leur hydrolyse ou méthanolyse acide. À cause du coût important des monomères silylés, et des faibles températures de transition

vitreuse des matériaux obtenus, l'utilisation de la liaison silyl éther serait sans doute plus appropriée dans la chaîne pendante d'un polymère ayant une haute T_g (Schéma 9).^[44] Cela permettrait de réticuler le matériau tout en permettant de le recycler et le remouler si nécessaire.

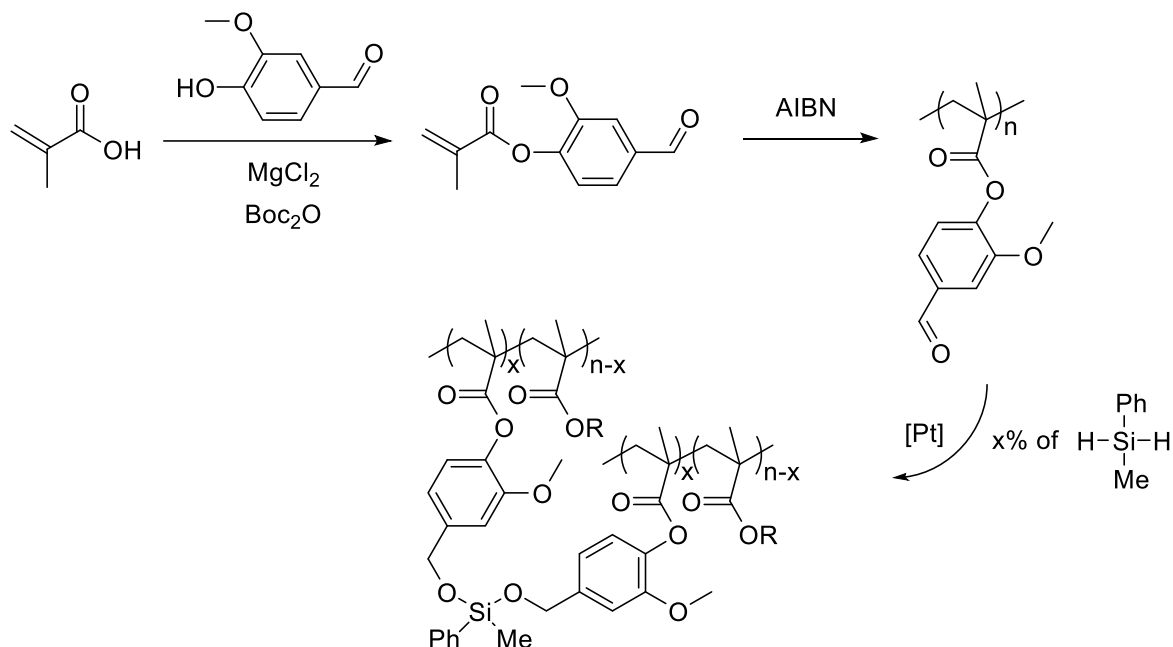


Schéma 9. Synthèse envisagée d'un polymère thermodurcissable et recyclable grâce aux liaisons silyl éthers.

Ainsi, de nouveaux polymères durables ont été préparés *via* des méthodes de synthèse innovantes et respectueuses de l'environnement, pouvant être utilisées pour découvrir les matériaux haute-performance de demain.

Références

- [1] H. Staudinger, *Ber. Dtsch. Chem. Ges.* **1920**, *53*, 1073–1085.
- [2] A. S. Abd-El-Aziz, M. Antonietti, C. Barner-Kowollik, W. H. Binder, A. Böker, C. Boyer, M. R. Buchmeiser, S. Z. D. Cheng, F. D'Agosto, G. Floudas, H. Frey, G. Galli, J. Genzer, L. Hartmann, R. Hoogenboom, T. Ishizone, D. L. Kaplan, M. Leclerc, A. Lendlein, B. Liu, T. E. Long, S. Ludwigs, J. Lutz, K. Matyjaszewski, M. A. R. Meier, K. Müllen, M. Müllner, B. Rieger, T. P. Russell, D. A. Savin,

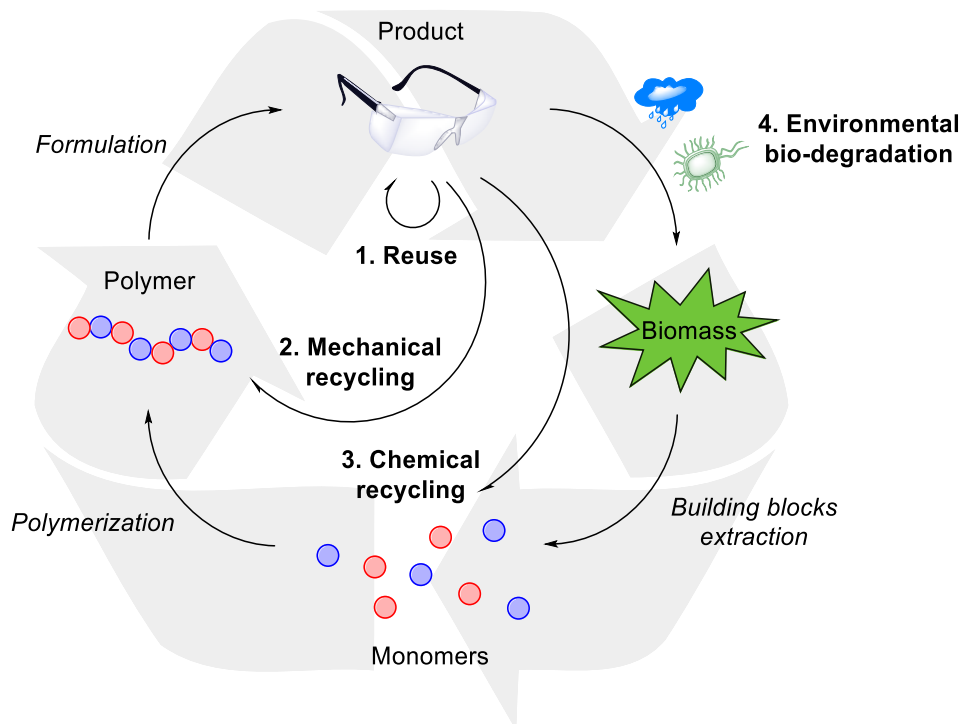
- A. D. Schlüter, U. S. Schubert, S. Seiffert, K. Severing, J. B. P. Soares, M. Staffilani, B. S. Sumerlin, Y. Sun, B. Z. Tang, C. Tang, P. Théato, N. Tirelli, O. K. C. Tsui, M. M. Unterlass, P. Vana, B. Voit, S. Vyazovkin, C. Weder, U. Wiesner, W. Wong, C. Wu, Y. Yagci, J. Yuan, G. Zhang, *Macromol. Chem. Phys.* **2020**, *221*, 2000216.
- [3] J. Hopewell, R. Dvorak, E. Kosior, *Phil. Trans. R. Soc. B* **2009**, *364*, 2115–2126.
- [4] R. Geyer, J. R. Jambeck, K. L. Law, *Sci. Adv.* **2017**, *3*, e1700782.
- [5] J. H. Clark, F. E. I. Deswarte, Eds., *Introduction to Chemicals from Biomass*, John Wiley & Sons, Ltd, The Atrium, Southern Gate, Chichester, West Sussex, United Kingdom, **2015**.
- [6] R. Hatti-Kaul, L. J. Nilsson, B. Zhang, N. Rehnberg, S. Lundmark, *Trends in Biotechnology* **2019**, *38*, 50–67.
- [7] X. Zhang, M. Fevre, G. O. Jones, R. M. Waymouth, *Chem. Rev.* **2018**, *118*, 839–885.
- [8] G. W. Coates, Y. D. Y. L. Getzler, *Nat. Rev. Mater.* **2020**, *5*, 501–516.
- [9] J. M. Garcia, M. L. Robertson, *Science* **2017**, *358*, 870–872.
- [10] M. Hong, E. Y.-X. Chen, *Green Chem.* **2017**, *19*, 3692–3706.
- [11] L. Filiciotto, G. Rothenberg, *ChemSusChem* **2021**, *14*, 56–72.
- [12] H. Kobayashi, A. Fukuoka, *Green Chem.* **2013**, *15*, 1740.
- [13] R. Palkovits, I. Delidovich, P. J. C. Hausoul, L. Deng, R. Pfützenreuter, M. Rose, *Chem. Rev.* **2016**, *116*, 1540–1599.
- [14] S. L. Kristufek, K. T. Wacker, Y.-Y. T. Tsao, L. Su, K. L. Wooley, *Nat. Prod. Rep.* **2017**, *34*, 433–459.
- [15] P. T. Anastas, J. C. Warner, *Green Chemistry: Theory and Practice*, **1998**.
- [16] European Bioplastics, *Bioplastics, Facts and Figures*, European Bioplastics, **2014**, <https://www.european-bioplastics.org/news/publications/> (consulté en avril 2020).
- [17] European Bioplastics, *Bioplastics, Facts and Figures*, **2019**, <https://www.european-bioplastics.org/news/publications/> (consulté en avril 2020).
- [18] PlasticsEurope, *Plastics, the Facts*, **2015**, <https://www.plasticseurope.org/en/resources/market-data/> (consulté en avril 2020).
- [19] PlasticsEurope, *Plastics, the Facts*, **2020**, <https://www.plasticseurope.org/en/resources/market-data/> (consulté en avril 2020).
- [20] R. V. Slone, *Encyclopedia of Polymer Science and Technology*, John Wiley & Sons, Inc., Hoboken, NJ **2001**. Methacrylic Ester Polymers 243.
- [21] P. F. Holmes, M. Bohrer, J. Kohn, *Prog. Polym. Sci.* **2008**, *33*, 787–796.
- [22] T. Ohara, T. Sato, N. Shimizu, G. Prescher, H. Schwind, O. Weiberg, K. Marten, H. Greim, T. D. Schaffer, P. Nandi, in *Ullmann's Encyclopedia of Industrial Chemistry*, Wiley, **2020**.

- [23] D. Sun, Y. Yamada, S. Sato, W. Ueda, *Green Chem.* **2017**, *19*, 3186–3213.
- [24] M. M. Bomgardner, *Chem. Eng. News* **2020**, *98*. <https://cen.acs.org/business/biobased-chemicals/Cargill-gives-biobased-acrylicacid/98/i20/> (consulté en avril 2020).
- [25] Looming Production Shutdowns and Second Dip in Operating Rates Challenge Global Methyl Methacrylate Market, IHS Markit Says, <https://www.businesswire.com/news/home/20180828005216/en/> (consulté en avril 2020).
- [26] M. Carlsson, C. Habenicht, L. C. Kam, M. J. Jr. Antal, N. Bian, R. J. Cunningham, M. Jr. Jones, *Ind. Eng. Chem. Res.* **1994**, *33*, 1989–1996.
- [27] M. Okabe, D. Lies, S. Kanamasa, E. Y. Park, *Appl. Microbiol. Biotechnol.* **2009**, *84*, 597.
- [28] A. L. Holmberg, K. H. Reno, R. P. Wool, T. H. Epps, III, *Soft Matter* **2014**, *10*, 7405–7424.
- [29] I. Khalil, G. Quintens, T. Junkers, M. Dusselier, *Green Chem.* **2020**, *22*, 1517–1541.
- [30] G. Bartoli, M. Bosco, A. Carlone, R. Dalpozzo, E. Marcantoni, P. Melchiorre, L. Sambri, *Synthesis* **2007**, *2007*, 3489–3496.
- [31] A. L. Holmberg, J. F. Stanzione, R. P. Wool, T. H. Epps, *ACS Sustainable Chem. Eng.* **2014**, *2*, 569–573.
- [32] J. A. Wanklyn, *Ann. Chem. Pharm.* **1858**, *108*, 67–79.
- [33] G. Wittig, F. J. Meyer, G. Lange, *Justus Liebigs Ann. Chem.* **1951**, *571*, 167–201.
- [34] C.-C. Lin, M.-L. Hsueh, B.-T. Ko, T. Athar, T.-M. Wu, S.-F. Hsu, *Organometallics* **2006**, *25*, 4144–4149.
- [35] G. W. Honeyman, A. R. Kennedy, R. E. Mulvey, D. C. Sherrington, *Organometallics* **2004**, *23*, 1197–1199.
- [36] E. Ihara, N. Omura, T. Itoh, K. Inoue, *J. Organomet. Chem.* **2007**, *692*, 698–704.
- [37] S. Kawaguchi, E. Nomura, K. Ito, *Polym. J.* **1998**, *30*, 546–551.
- [38] J. K. Paulasaari, W. P. Weber, *Macromolecules* **1998**, *31*, 7105–7107.
- [39] J. Cella, S. Rubinsztajn, *Macromolecules* **2008**, *41*, 6965–6971.
- [40] C. Cheng, A. Watts, M. A. Hillmyer, J. F. Hartwig, *Angew. Chem.* **2016**, *128*, 12051–12055.
- [41] C. S. Sample, S.-H. Lee, M. W. Bates, J. M. Ren, J. Lawrence, V. Lensch, J. A. Gerbec, C. M. Bates, S. Li, C. J. Hawker, *Macromolecules* **2019**, *52*, 1993–1999.
- [42] S. Vijjamari, S. Streed, E. M. Serum, M. P. Sibi, G. Du, *ACS Sustainable Chem. Eng.* **2018**, *6*, 2491–2497.
- [43] C. Veith, F. Diot-Néant, S. A. Miller, F. Allais, *Polym. Chem.* **2020**, *11*, 7452–7470.
- [44] S. Gao, *J. Mater. Chem. A* **2019**, *7*, 17498–17504.

General introduction

The year 2020 marked the 100th anniversary of Herman Staudinger's first description of a chemical process he called "polymerization".^[1] Since then, polymers, and especially plastics, have become ubiquitous in our daily life, from food packaging to high-performance materials in construction, mobility and healthcare.^[2] Their success has relied on their wide availability as cheap side-products of the petrochemical industry (around 4% of annual petroleum production is used to make plastics),^[3] thanks in part to the seminal work of Ziegler and Natta on polymerization catalysis, which earned them the 1963 Nobel Prize in Chemistry. However, the polymer industry nowadays faces two existential challenges: 1) plastic materials are responsible for some of the largest pollution on the planet, with life-threatening impacts on biodiversity;^[4] 2) petroleum resources are expected to remain largely unexploited if human societies plan to mitigate climate change, thus prompting the polymer industry to shift to renewable feedstocks extracted from biomass.^[5]

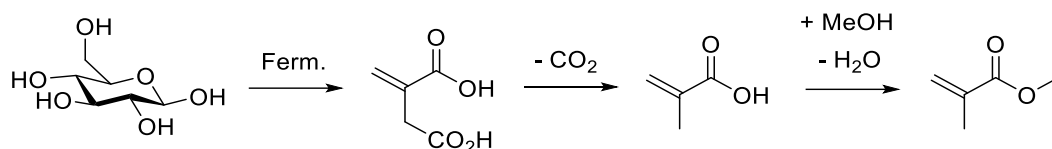
Research in academia and industry has therefore recently focused on solving these two challenges. End-of-life options for polymeric materials have been theorized within the broader framework of the circular economy (see Scheme 1):^[6,7] reuse, mechanical then chemical recycling, and eventually environmental biodegradation are to be prioritized in that specific order. Since products and goods cannot be reused indefinitely, and mechanical recycling suffers from limitations such as the loss of optical and mechanical properties, chemical recycling of polymers has recently gained attention as an efficient method to obtain virgin-like chemical building blocks from waste streams.^[8-10] Ultimately, biodegradable polymers should be used when their potential leakage in the environment cannot be excluded.^[11] In the meantime, various renewable feedstocks have been identified as potential sustainable resources for polymer synthesis, namely polysaccharides, lignin,^[12,13] proteins and extracts such as terpenes.^[5,14]



Scheme 1. Ideal circular economy of polymeric materials, adapted from [6]

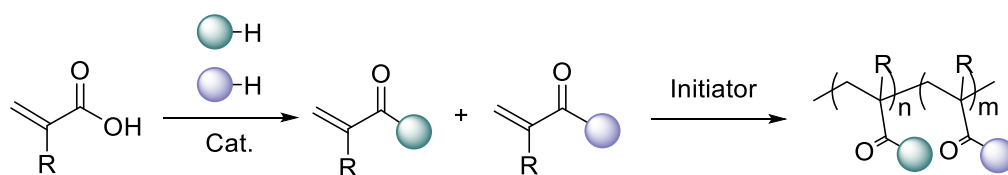
The objective of the present thesis work was to develop innovative methods for producing polymers able to meet these two main challenges, thus being biobased and intrinsically recyclable. In an effort to comply with the guiding principles of green chemistry,^[15] our research was driven by the use of catalytic reagents, under mild conditions, while trying to reduce waste production (*e.g.* solvent consumption).

The first chapter of this manuscript presents the state of the art in the production and polymerization methods of various acrylic monomers.^[16] Methyl methacrylate (MMA) and acrylic acid (AA) are the most widely used chemicals in this class of monomers. While AA biobased production is now reaching commercialization, MMA biosourcing still remains in its infancy, with itaconic acid decarboxylation being the most promising route to date (Scheme 2). Other more readily bioderived monomers, such as itaconic acid itself, or crotonic acid, have the potential to be innovative substitutes depending on the targeted polymer.



Scheme 2. Biobased route to MMA *via* itaconic acid.

In the second chapter, our work on the one-pot synthesis of various biobased poly(meth)acrylates is detailed.^[17] A simple and robust esterification method was developed, using MgCl_2 or triflate salts as catalysts, as well as a coupling agent. Quantitative yields and the absence of any polymerizable side-products allowed us to perform the one-pot synthesis of the corresponding polymeric material using radical initiators (Scheme 3). The possibility to obtain block copolymers by this method was particularly interesting, thereby significantly reducing the amount of waste produced during their synthesis.



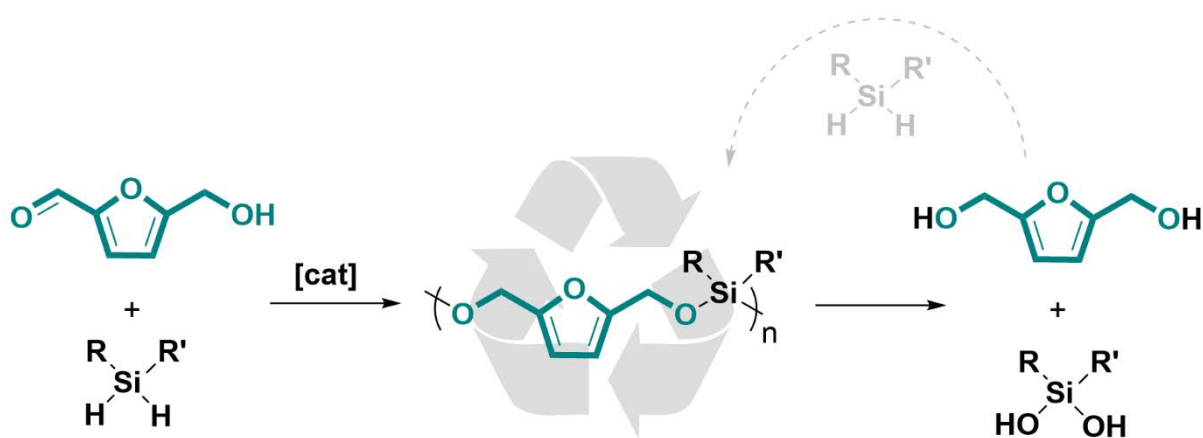
R = H or CH_3

Scheme 3. One-pot strategy for biobased poly(meth)acrylates synthesis.

Investigations on the room temperature anionic polymerization of MMA and other biobased methacrylates are described in chapter 3. Since PMMA is already a widely used polymer with excellent optical properties and good chemical recyclability *via* pyrolysis (up to 98% monomer recovery),^[18] its synthesis is of particular interest. The use of original metalate complexes enabled to achieve the challenging task of rapidly polymerizing MMA under mild conditions. The *in situ* formation of the catalyst from commercially available reagents drastically reduced the time required to obtain the material of interest.

Chapter 4 of this manuscript is devoted to the synthesis of poly(silylether)s (PSEs), which were found to have intrinsic chemical recyclability (Scheme 4). Platinum complexes active at low catalyst loadings permitted to obtain PSEs from renewable resources. Lignin derived monomers such as vanillin and syringaldehyde were used for the first time to prepare such polymers. The resulting materials were quite resistant to degradation, but their chemical recycling could be triggered by Brønsted acid-catalyzed hydrolysis or methanolysis.

Finally, the conclusion lists the notable perspectives highlighted by the present work.



Scheme 4. Example of a potentially recyclable poly(silylether).

References

- [1] H. Staudinger, *Ber. Dtsch. Chem. Ges.* **1920**, *53*, 1073–1085.
- [2] A. S. Abd-El-Aziz, M. Antonietti, C. Barner-Kowollik, W. H. Binder, A. Böker, C. Boyer, M. R. Buchmeiser, S. Z. D. Cheng, F. D’Agosto, G. Floudas, H. Frey, G. Galli, J. Genzer, L. Hartmann, R. Hoogenboom, T. Ishizone, D. L. Kaplan, M. Leclerc, A. Lendlein, B. Liu, T. E. Long, S. Ludwigs, J. Lutz, K. Matyjaszewski, M. A. R. Meier, K. Müllen, M. Müllner, B. Rieger, T. P. Russell, D. A. Savin, A. D. Schlüter, U. S. Schubert, S. Seiffert, K. Severing, J. B. P. Soares, M. Staffilani, B. S. Sumerlin, Y. Sun, B. Z. Tang, C. Tang, P. Théato, N. Tirelli, O. K. C. Tsui, M. M. Unterlass, P. Vana, B. Voit, S. Vyazovkin, C. Weder, U. Wiesner, W. Wong, C. Wu, Y. Yagci, J. Yuan, G. Zhang, *Macromol. Chem. Phys.* **2020**, *221*, 2000216.

- [3] J. Hopewell, R. Dvorak, E. Kosior, *Phil. Trans. R. Soc. B* **2009**, *364*, 2115–2126.
- [4] R. Geyer, J. R. Jambeck, K. L. Law, *Sci. Adv.* **2017**, *3*, e1700782.
- [5] J. H. Clark, F. E. I. Deswarte, Eds. , *Introduction to Chemicals from Biomass*, John Wiley & Sons, Ltd, The Atrium, Southern Gate, Chichester, West Sussex, United Kingdom, **2015**.
- [6] R. Hatti-Kaul, L. J. Nilsson, B. Zhang, N. Rehnberg, S. Lundmark, *Trends in Biotechnology* **2019**, *38*, 50–67.
- [7] X. Zhang, M. Fevre, G. O. Jones, R. M. Waymouth, *Chem. Rev.* **2018**, *118*, 839–885.
- [8] G. W. Coates, Y. D. Y. L. Getzler, *Nat. Rev. Mater.* **2020**, *5*, 501–516.
- [9] J. M. Garcia, M. L. Robertson, *Science* **2017**, *358*, 870–872.
- [10] M. Hong, E. Y.-X. Chen, *Green Chem.* **2017**, *19*, 3692–3706.
- [11] L. Filiciotto, G. Rothenberg, *ChemSusChem* **2021**, *14*, 56-72.
- [12] H. Kobayashi, A. Fukuoka, *Green Chem.* **2013**, *15*, 1740.
- [13] R. Palkovits, I. Delidovich, P. J. C. Hausoul, L. Deng, R. Pfützenreuter, M. Rose, *Chem. Rev.* **2016**, *116*, 1540–1599.
- [14] S. L. Kristufek, K. T. Wacker, Y.-Y. T. Tsao, L. Su, K. L. Wooley, *Nat. Prod. Rep.* **2017**, *34*, 433–459.
- [15] P. T. Anastas, J. C. Warner, *Green Chemistry: Theory and Practice*, **1998**.
- [16] H. Fouilloux, C. M. Thomas, *Macromol. Rapid Commun.* **2021**, *42*, 2000530.
- [17] H. Fouilloux, W. Qiang, C. Robert, V. Placet, C. M. Thomas, *Angew. Chem. Int. Ed.* **2021**, *60*, 19374–19382.
- [18] W. Kaminsky, M. Predel, A. Sadiki, *Polym. Degrad. Stabil.* **2004**, *85*, 1045–1050.

Chapter 1 – Production and polymerization of biobased acrylates and analogs

*Hugo Fouilloux and Christophe M. Thomas**

Chimie ParisTech, PSL University, CNRS, Institut de Recherche de Chimie Paris, 75005 Paris, France.

E-mail: christophe.thomas@chimie-paristech.fr

WWW: <https://www.ircp.cnrs.fr/la-recherche/equipe-cocp/>

This chapter has been published in *Macromolecular Rapid Communications*:

H. Fouilloux, C. M. Thomas, *Macromol. Rapid Commun.* **2021**, 42, 2000530.

Contributions to the publication:

Hugo Fouilloux made the literature survey and wrote the first draft of the review. Christophe M. Thomas supervised the work and helped write the final manuscript.

Hugo Fouilloux



30/12/2021

Christophe M. Thomas



Abstract

To prepare biobased polymers, particular attention must be paid to the obtention of the monomers from which they are derived. (Meth)acrylates and their analogs constitute such a class of monomers that have been extensively studied due to the wide range of polymers accessible from them. This review therefore aims to highlight the progresses made in the production and polymerization of (meth)acrylates and their analogs. Acrylic acid production from biomass is close to commercialization, as three different high-potential intermediates are identified: glycerol, lactic acid, and 3-hydroxypropionic acid. Biobased methacrylic acid is less common, but several promising options are available, such as the decarboxylation of itaconic acid or the dehydration of 2-hydroxyisobutyric acid. Itaconic acid is also a vinylic monomer of great interest, and polymers derived from it have already found commercial applications. Methylene butyrolactones are promising monomers, obtained from bioresources via three different intermediates: levulinic, succinic, or itaconic acid. Although expensive, methylene butyrolactones have a strong potential for the production of high-performance polymers. Finally, β -substituted acrylic monomers, such as cinnamic, fumaric, muconic, or crotonic acid, are also examined, as they provide an original access to biobased materials from various renewable raw materials, such as protein waste, lignin, or wastewater.

1. Introduction

Since the second half of the 19th century, the development of the chemical industry has been closely linked to the use of fossil raw materials, in the form of oil and gas. Today fossil feedstocks remain the most important raw materials for the chemical industry, accounting for more than 90%. However, the 1973–1974 oil crisis affected the world crude oil market and coincided with the emergence of alternative energy and raw materials sources such as biomass. Research in chemistry, both academic and industrial, has therefore recently been highlighted by the development of various

molecules and materials derived from biomass.^[1-7] This shift in focus from petrochemical resources to renewable resources is often advocated as an urging necessity due to the projected depletion of oil resources and the threat of global warming. There is no denying the importance of developing a sustainable chemical industry that should be based on renewable resources and produce benign molecules. This is a long-term goal that should remain the focus of research to meet the future challenges of the 21st century, as plant-derived small molecules (e.g., sugars, terpenes, and vegetable oils) and macromolecules (e.g., lignin, cellulose, and other polysaccharides) represent an almost inexhaustible source of renewable feedstocks.

Additionally, two short-term factors have been identified for green chemistry:^[3,8] 1) increased public awareness of the chemical industry's almost exclusive dependence on the petroleum industry and therefore the new demand for more sustainable and biobased products; 2) the innovations that may result from the multitude of molecules that are accessible from biobased building blocks, a consequence of the chemical variety of bioresources as opposed to that of the oil resource. However, despite these short- and long-term incentives, the development of the biobased chemical industry in the first two decades of the 21st century has not lived up to the high expectations it had raised. The example of the plastics sector is particularly telling: in 2014, biobased materials global production amounted to 1.7 million tons and was expected to increase to 7.8 million tons by 2019.^[9] Five years later, this figure only reached 2.1 million,^[10] a 15% increase following the same growth as global plastics production (from 311 to 359 million tons).^[11,12] Biobased plastics thus still account for less than 1% of the total plastics produced. Moreover, while about half of the biobased plastics produced today is composed of biodegradable materials (e.g., starch blends and poly(lactic acid) (PLA)), another half is made from petroleum-sourced commodity plastic analogs such as bio-poly(ethylene) (PE) and bio-poly(ethylene terephthalate) (PET).^[10] On the one hand, PE and PET made respectively from biobased ethylene and ethylene glycol are so-called "drop-in" chemicals, which do not perform better than their petroleum-sourced counterparts from an economic point of view. Their development is

mainly based on regulations that impose on suppliers a certain quantity of biobased plastics and they do not overcome the limitations of conventional PE and PET as the final products are strictly identical. Among these limitations, their widespread use and lack of biodegradability are of particular concern.^[13] This is probably the reason why the production of bio-PE and bio-PET has dropped by 44% and 30%, respectively, between 2014 and 2019.^[9,10] On the other hand, PLA is undoubtedly a very good example of the kind of developments expected from the chemical industry to produce safer and more sustainable materials.

Almost all current polymers can be prepared from renewable raw materials. Among the multitude of biobased polymers available, the class of acrylates and analogs is of particular interest due to the wide range of molecular structures available and the different properties that are obtained thereof.^[14,15] These materials have thus been used in the manufacture of chemicals such as coatings, optical fibers, and pressure-sensitive adhesives. The objective of the present review is therefore to provide an overview of the different methodologies and strategies that have been employed to synthesize acrylates and analogs from bioresources. In order to avoid duplicity with existing literature,^[16-25] herein, we will focus on the path from renewable feedstocks to the vinylic moiety of the biobased monomers (**Figure 1**) and the multiple molecular structures that have been obtained by different synthetic routes. We will also emphasize important advances in the polymerization of these monomers.

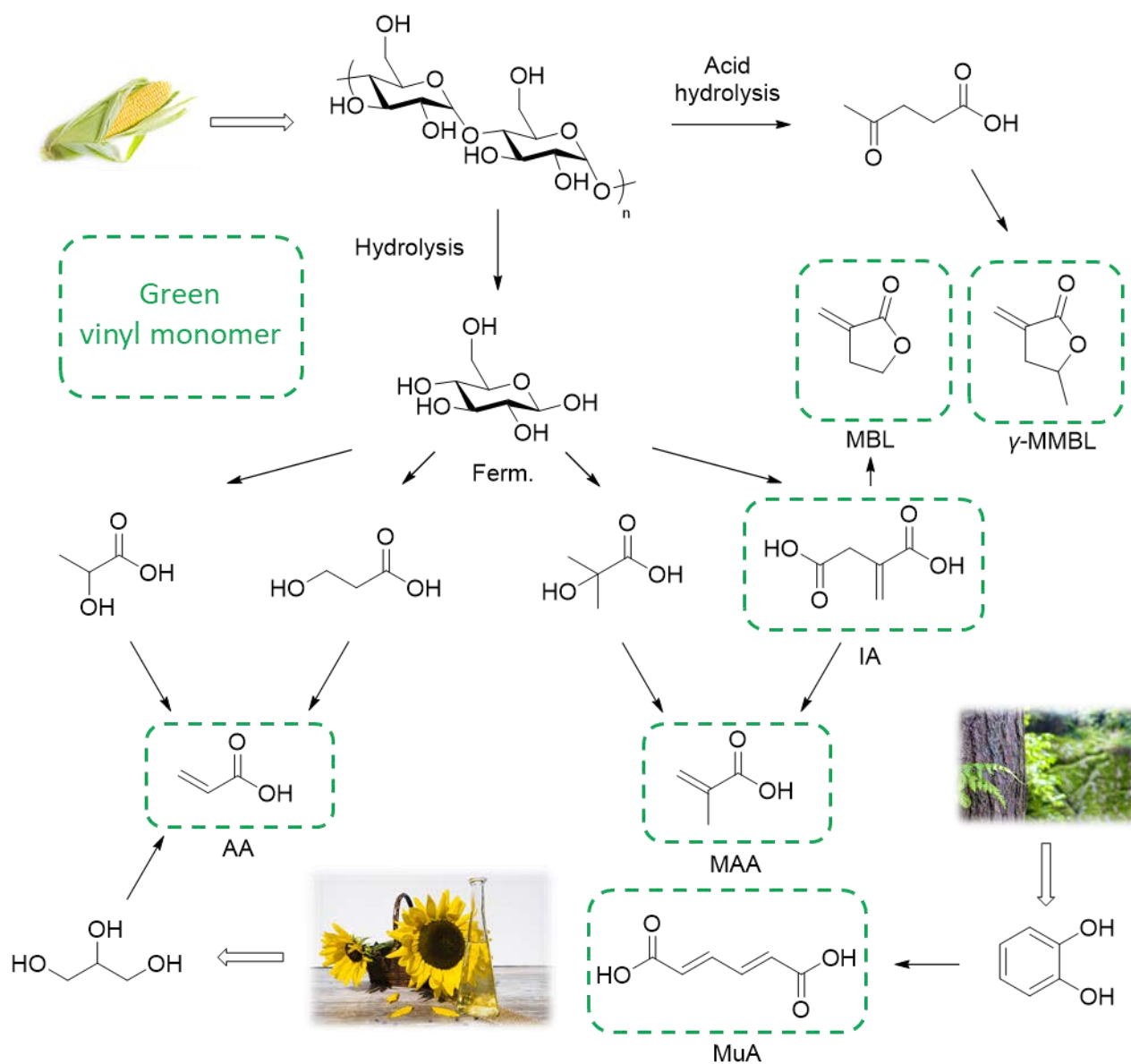


Figure 1. Most important biobased vinyl moieties available for polymerization, and the building blocks and bio-resources they can be derived from.

2. Production of Biobased Acrylates and Analogs

2.1. Acrylic Acid (AA)

In 2014, global production of AA amounted to 5.2 million tons.^[26] The main suppliers of AA are BASF, Nippon Shokubai, Dow, and Arkema. The most economically viable current process for producing acrylic acid is the two-step oxidation of petroleum-based propene (**Figure 2**). In the first step, propene is converted to acrolein over bismuth molybdate-based catalysts at temperatures ranging from 300 to 370 °C, while in the second step, the acrolein is oxidized to acrylic acid over vanadium–molybdenum catalysts between 260 and 300 °C, with an overall yield of 85–90%.^[27] Lately, research has focused on the production of acrylic acid from renewable feedstocks such as fermentable sugars and plant oils. Recent reviews cover these biobased routes from glycerol, lactic acid (LA), and 3-hydroxypropanoic acid (3-HPA) in depth.^[27–29] In this section, we will focus on selected examples, the advantages and drawbacks of each of these renewable pathways, as well as other interesting alternatives.

Until recently, the most promising route for the production of bioacrylic acid was from 3-HPA (Figure 2).^[30] Its dehydration to acrylic acid is indeed highly efficient, with several patents claiming yields close to 95%,^[31,32] using various heterogeneous catalysts and processing 3-HPA in gas phase fixed-bed reactors at temperatures ranging from 200 to 300 °C.^[28] Several industrial collaborations have been initiated to produce AA from sugars via 3-hydroxypropanoic acid, including joint developments by Dow and OPX Biotechnologies in 2011,^[30] or collaborative investigations of Novozymes, Cargill, and BASF.^[5] However, BASF withdrew from this collaboration in 2015,^[28] and no commercial application of this route has been reported to date. This might be explained by the difficulty in finding an efficient process for the fermentation of sugars to 3-HPA. Recent research has focused on the use of bioengineered microorganisms as well as on improving the recovery of 3-HPA from the fermentation broth.^[33,34] Alternatively, the direct fermentation of AA from glucose, using

biosynthetic pathways similar to the one of 3-HPA, has recently been reported and may spur more investigations, although obtained titers were at best lower than 0.25 g.L^{-1} of AA.^[35,36]

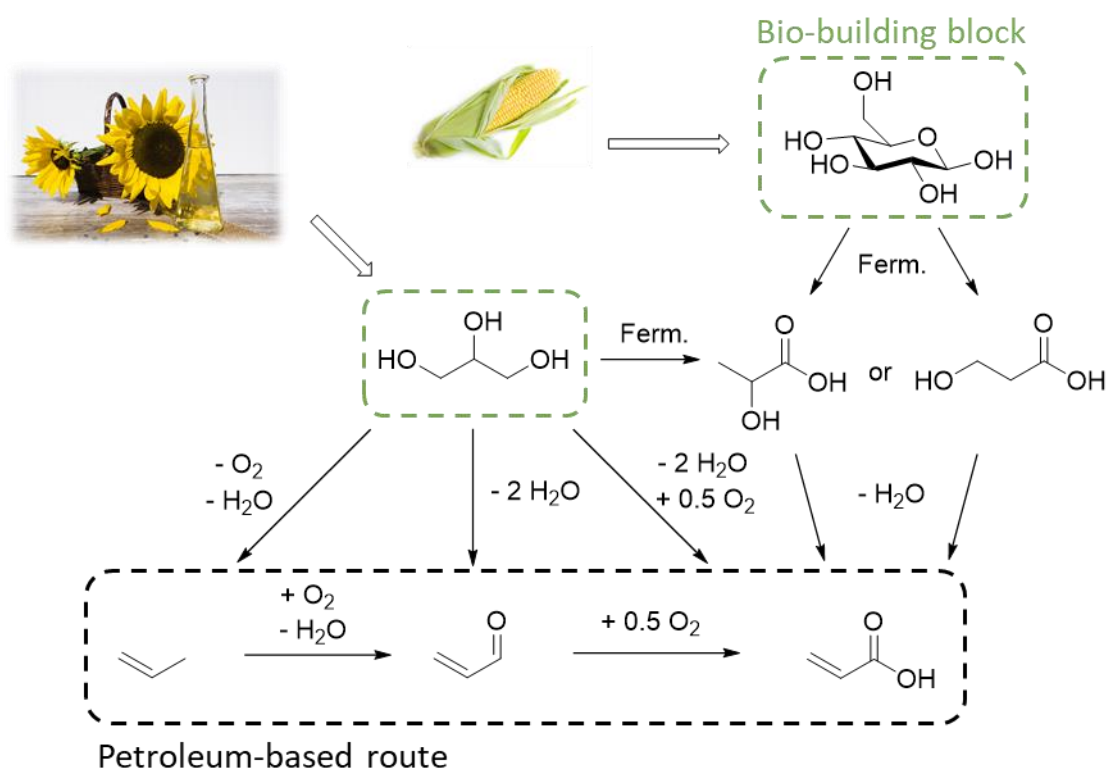


Figure 2. Different routes to produce acrylic acid.

As a structural isomer of 3-HPA, LA can also be dehydrated to acrylic acid (Figure 2). The advantage of this route is the well-known and already commercialized process of fermentation of sugars to lactic acid, with an annual commercial production of 300–400 ktons in 2012.^[37] The challenging aspect of this pathway, however, is the dehydration step, which is subject to side-reactions, such as decarboxylation, decarbonylation, and hydrogenation, and only modest yields (<70%) had been reported until recently.^[38] For this last step, three main types of catalysts were reported: bulk salts, supported salts, and zeolites. Promising catalysts have been identified in each group, with yields above 80% for some of them. For instance, Procter & Gamble recently patented the use of mixed potassium and barium phosphate salts to selectively convert lactic acid from an aqueous mixture into acrylic acid (up to 93% selectivity, 85% yield).^[39] In 2020, Cargill obtained an exclusive license to use

this technology to prepare biobased AA.^[40] However, several years of development are still required as these synthetic options are at the research state. Alternative routes have involved converting LA into various esters and then dehydrating them to produce acrylates directly.^[28]

Glycerol was also recommended as a promising precursor to acrylic acid. Triglycerides are the major components of vegetable oils and their transesterification to fatty esters for biodiesel production leaves glycerol as the main byproduct (i.e., 10 wt%; **Figure 3**). In 2017, 4.5 million tons of glycerol were thus produced worldwide, indicating its widespread availability.^[29] It can be converted to acrylic acid following various synthetic pathways (Figure 2). The simplest and most suitable route for the industry is the dehydration of glycerol to acrolein, a “drop-in” intermediate for the current petroleum-based process. This reaction is usually performed in the vapor-phase using flow reactors and solid Brønsted acid catalysts. Full conversions and high selectivities are regularly observed when starting from pure glycerol, but economically viable performance has yet to be described when using a feed of crude glycerol, due to strong catalyst deactivation. On the other hand, glycerol purification increases the overall cost of the process to uncompetitive levels. The direct conversion of glycerol to acrylic acid actually involves the same steps as the acrolein route, namely, dehydration and oxidation. Various approaches have been investigated, either by stacking two catalytic beds in the same reactor or by using a multifunctional catalyst with Brønsted acid sites for dehydration and Lewis acid sites for oxidation. In that case, it is however mandatory to use catalysts capable of operating under the same reaction conditions, and these approaches have the same limitations as the two-step process mentioned above.^[28] The conversion of glycerol to propene has also been investigated, but this method is less atom economical and not selective enough to make it viable.^[27] Arkema holds several patents on the production of acrylic acid from glycerol,^[41] but has reportedly put its interest in commercializing this route on hold since 2013.^[28]

Alternatively, glycerol can be converted to lactic acid or 3-hydroxypropanoic acid via bioprocesses (Figure 2).^[27] Although conversion of glycerol to lactic acid may not be useful for the

production of acrylic acid since the bottleneck in this route is the subsequent dehydration of lactic acid, the glycerol-3-HPA pathway may be more promising. In 2015, Dishisha et al. reported an integrated three-step process that converts glycerol to 3-HPA and 1,3-propanediol, oxidizes 1,3-propanediol to 3-HPA, and subsequently transforms 3-HPA to acrylic acid over TiO₂ in the gas phase with an overall yield of 95%.^[42] The first two steps were carried out in fed-batch and batch mode using various microorganisms. Expensive cultivation media and the use of pure glycerol were among the limitations of this work, which nevertheless highlights the potential of integrated processes.

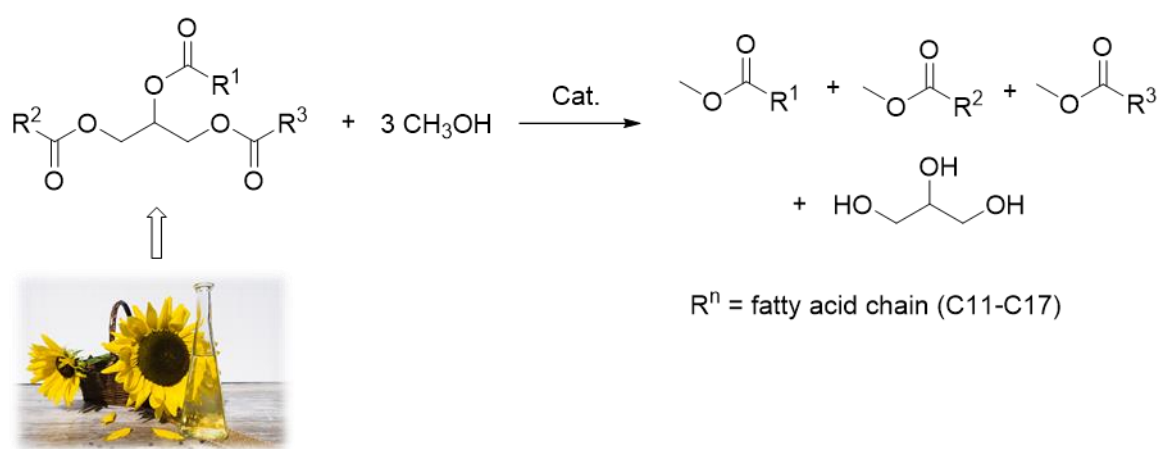


Figure 3. Bio-diesel production from vegetable oils.

Another approach consists in the synthesis of poly(3-hydroxypropionate) (P3HP), a solid, chemically stable, and easily transportable polymer, which can be pyrolyzed to acrylic acid on-site, without any by-product formation. This alternative could be chosen whenever the cost of transportation outweighs the cost of production. Novomer issued a patent in 2013 on the carbonylation of ethylene oxide to β -propiolactone and its subsequent polymerization to P3HP (**Figure 4**).^[43] BASF later claimed the use of tertiary amine catalysts to accelerate thermal degradation to acrylic acid.^[44] In 2016, Coates and coworkers investigated various catalysts for the Novomer route.^[45] Ethylene oxide and carbon monoxide can be derived from fossil resources or respectively from bioethanol and CO₂ or gasified biomass, making it virtually a biobased route. Similarly, poly(3-hydroxybutyrate) (PHB), biosynthesized by various microorganisms from wastewater, can be pyrolyzed to crotonic acid (CrA)

(see Section 2.5.4 for more details). Subsequent metathesis with ethylene (preferably biobased) yields propene and acrylic acid.^[46-48] Cinnamic acid (CMA), fumaric acid (FmA), and muconic acid (MuA), three β -substituted acrylics (see Sections 2.5.1 to 2.5.3), can also produce AA by metathesis with ethylene.^[47,49-52]

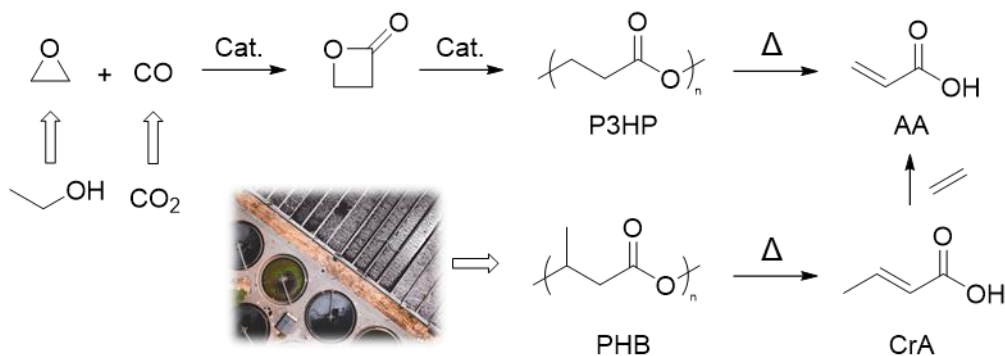


Figure 4. The poly(3-HPA) and crotonic acid routes to acrylic acid.

The production of bioacrylic acid is thus an area of intensive research in both academia and industry. Attempts to outperform the classical propene route have not yet been successful, mainly due to the lack of purity inherent in biomass streams compared to fossil-resource streams. The development of more robust catalytic systems, both inorganic and living organisms, and improved purification and recovery methods should make it possible to achieve commercial production of bioacrylic acid in the near future. The use of poly(acrylic acid) as a superabsorbent in diapers, a commercial product under public scrutiny, is probably an important driver for the development of such a biobased route.

2.2. Methacrylic Acid (MAA)

MAA is mainly used as an intermediate in the synthesis of its corresponding esters, of which methyl methacrylate (MMA) is the most widely produced, at around 4 million tons for a market price of roughly 3 \$.kg⁻¹.^[53] Patience and co-workers recently reviewed the multiple heterogeneously catalyzed routes to MAA and MMA,^[54] while Lynch and co-workers described the biotechnological production of various intermediates for MAA synthesis.^[55] This section will therefore broadly cover

the classical pathways to MAA and MMA and will more specifically review recent research on the production of these two important monomers from renewable resources via chemical transformations.

MMA was originally produced on an industrial scale via the acetone-cyanohydrin process, with the first commercial production dating back to 1933 (**Figure 5**).^[56] It is still the most prominent process for the production of MMA, although it has been criticized for its use of toxic raw materials and the production of large amounts of waste. Significant efforts were made by Mitsubishi and Evonik to avoid the use of H₂SO₄.^[54] Alternatively, the isobutene route was developed in the early 1980s by Mitsubishi.^[56] Similarly to the production of acrylic acid from propene, it consists of two successive oxidations (via methacrolein) on various heterogeneous catalysts to yield MAA, which can then be esterified to MMA (Figure 5). In 1990, BASF commissioned a plant that performs the hydrocarbonylation of ethylene to propanal, its subsequent condensation with formaldehyde to methacrolein, and final oxidation to MAA.^[56] Ethylene can also be hydroxycarbonylated to propionic acid before being converted to MAA (Eastman-Bechtel route; Figure 5). Lucite has extended this methodology and developed the Alpha process to produce MMA via the methoxycarbonylation of ethylene to methyl propionate and its final condensation with formaldehyde to MMA. In 2008, the company started a 100 000 tons.year⁻¹ production plant using this process.^[54]

The four routes presented above represent the bulk of MMA and MAA production at present. They are all based on fossil resources, although recent patents by Arkema have claimed a possible biosourcing of raw materials,^[57,58] in particular ethylene, carbon monoxide and methanol from bioethanol and biomass gasification, respectively.^[59] The obtention of these building blocks from renewable resources have been reviewed elsewhere.^[60–62] Herein, we will focus on three other routes for obtaining biobased MAA, namely, decarboxylation of citric acid (CA) or itaconic acid (IA), dehydration of 2-hydroxyisobutyric acid (2-HIBA), and production of bioisobutene.

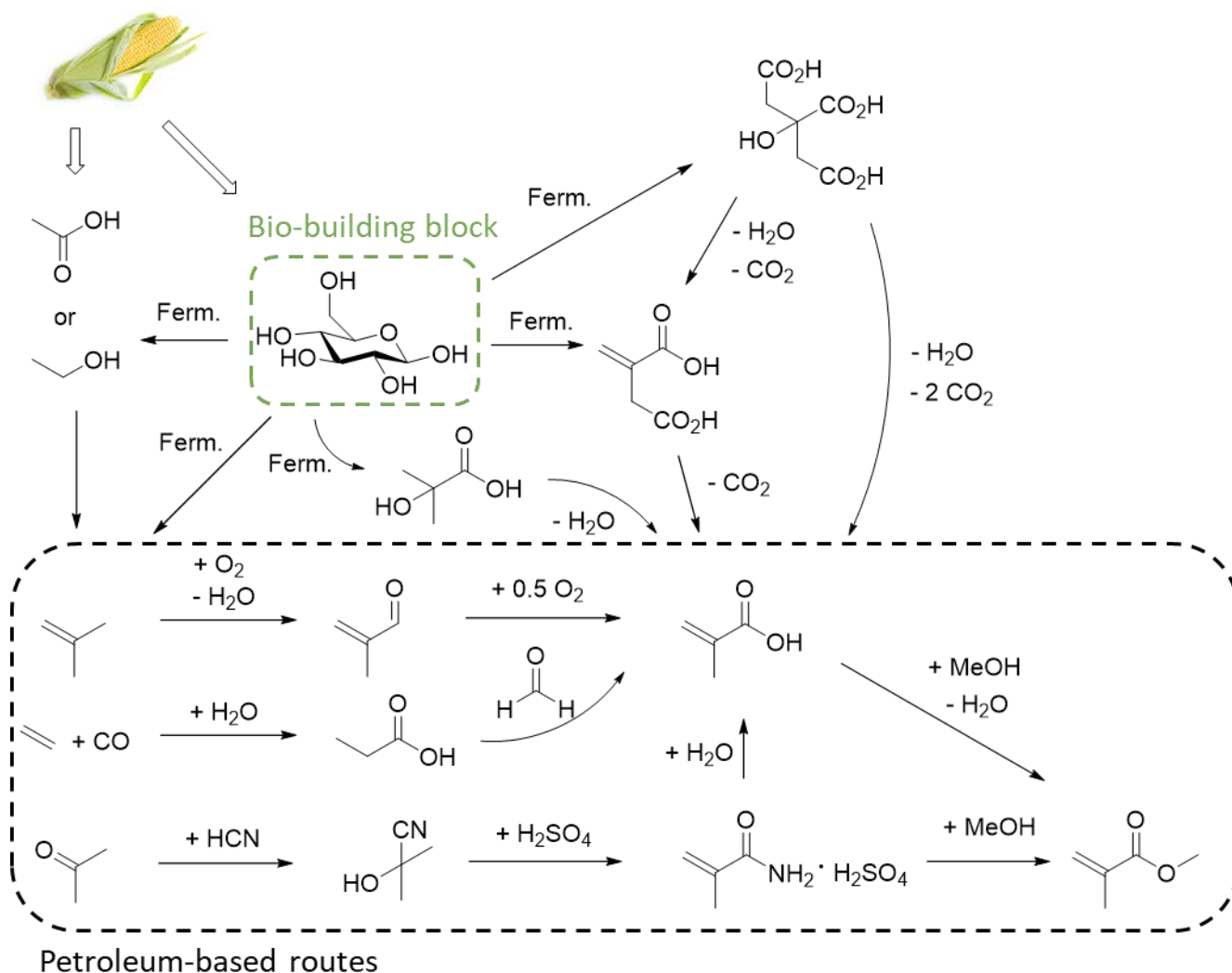


Figure 5. Different routes for the production of methacrylic acid.

Citric acid is the main organic acid produced in tonnage by fermentation, with around 2 million tons in 2015.^[63] Present at high concentrations in fruit juices, it is mainly produced by submerged fermentation, using cheap substrates such as sugar cane and beet molasses digested by the productive fungal strain *Aspergillus niger*.^[64] Due to the potential contamination of the fermentation broth with trace metals, pretreatment is required to remove these pollutants. Recent research has focused on solid state substrates that do not necessitate pretreatment. One of the main difficulties associated with fermentation processes is the recovery of the product from the fermentation broth. Citric acid is no exception to this rule as it is usually recovered by precipitation, by adding calcium hydroxide, which is then neutralized with sulfuric acid, generating large quantities of gypsum waste in the process (e.g.,

lactic acid). Citric acid can be pyrolyzed to itaconic anhydride (IANh), which is subsequently hydrolyzed to itaconic acid.^[65] The other main route for obtaining IA is its direct fermentation from glucose by the fungal strain *Aspergillus terreus*.^[66] It produced 40 000 tons of IA in 2018.^[67] Unlike CA, fermentative production of IA from cheaper substrates has been more challenging. Its recovery from the production medium is performed by filtrating, evaporating a certain amount of water, cooling, and crystallization. Purification techniques to achieve higher yields, such as reactive extraction or adsorption, are still in the research state.^[65] More details on IA production are available in Section 2.3 of this article.

The conversion of CA to IA, and subsequent decarboxylation to methacrylic acid was first reported by the group of Antal in 1994 (**Figure 6**).^[68] They pointed out that the separation of citric acid from its broth triples its cost (and produces waste as well), hence their suggestion that their reactions be carried out from a water-diluted medium that mimics the fermentation broth. Working under supercritical conditions ($P = 35$ MPa, $T = 250\text{--}360$ °C), with a stoichiometric amount of NaOH, they obtained yields of 70% for each step, 50% in total. Li and Brill then studied the kinetics of these reactions and their pH-dependence.^[69] In particular, they showed that the decarboxylation of the monoanion of itaconic acid is faster than that of the dianion or of free acid, which explains the need to use a base to control the pH of the medium. The use of water is beneficial because itaconic anhydride is also less reactive to decarboxylation.

In the early 2010's, a similar process was patented by Lucite International.^[70,71] By converting CA to IA or citramalic acid and then to MAA, they claimed higher selectivities (up to 90%) at lower temperatures (i.e., 125–180 °C) than Antal and co-workers, using a wide range of bases. In 2014, Scott and coworkers revisited the decarboxylation of IA to MAA using heterogeneous Pd, Pt, or Ru catalysts on various supports (i.e., activated C, Al₂O₃, and BaSO₄).^[72,73] This made it possible to avoid running the reaction under highly corrosive supercritical water conditions, as they obtained 84% selectivity and 50% isolated yield in basic aqueous solutions at 200–225 °C without external pressure (P increased

to 40 bars due to CO₂ release). Moser and co-workers later converted IA into MAA using a homogeneous ruthenium carbonyl propionate catalyst with a high selectivity (90%), at high concentration (5.5 M for increased throughput), moderate temperature, and pressure (200–225 °C and 30 bars), without the use of a base.^[74,75]

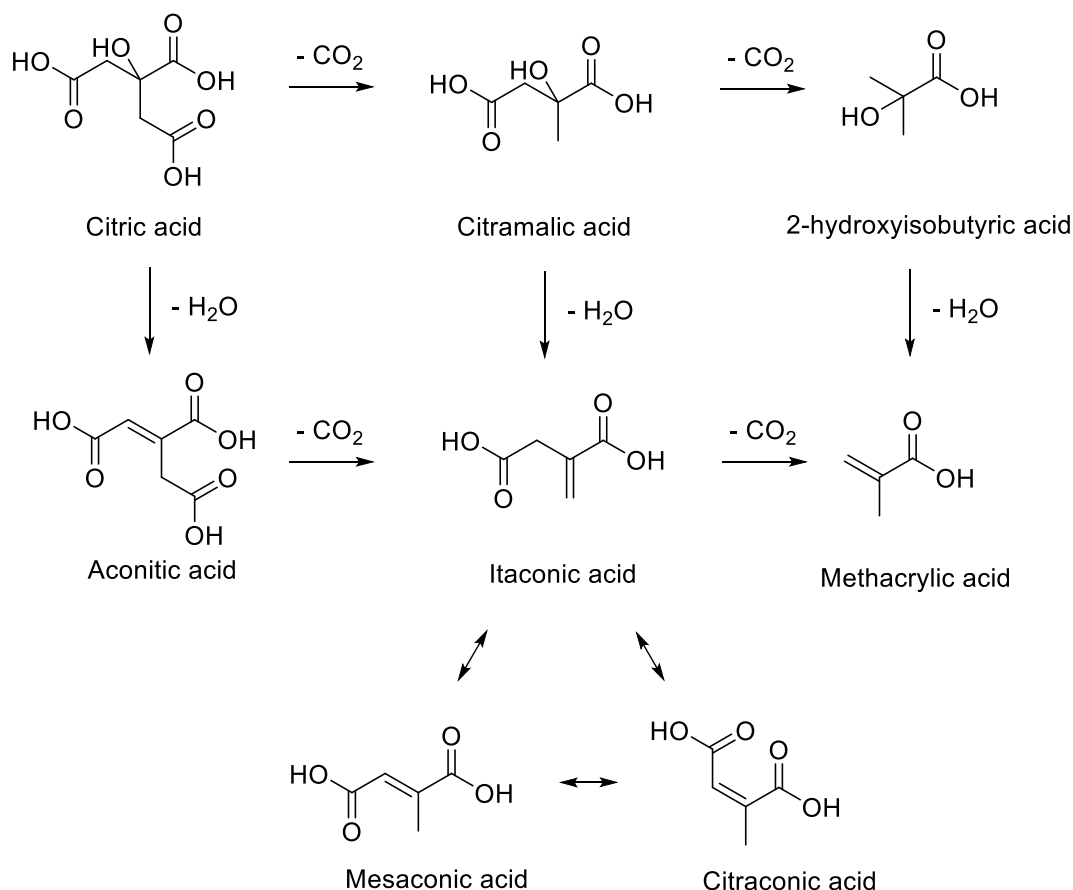


Figure 6. Reaction network of citric acid to methacrylic acid.

Pirmoradi and Kastner took a different approach using calcinated hydrotalcite, a cheap solid base catalyst composed of magnesium and aluminum oxides.^[76,77] They achieved modest yields (20–25%) at moderate temperatures (250 °C) in subcritical water, without pH neutralization or expensive catalysts. The multiple uses of the hydrotalcite increased yields, as did the addition of fermentation impurities (up to 30%), which would have resulted from unknown catalyst modifications. Recently, Likozar and co-workers also prepared various heterogeneous basic catalysts to convert CA or IA to MAA.^[78,79] Using barium hexa-aluminate, they obtained 50% yield with both raw materials after 3 h at 250 °C under 20 bar N₂ atmosphere. In a subsequent work, they copolymerized the MAA derived

from IA with styrene and butyl acrylate, which showed the same behavior as fossil-based MAA, as expected, thus reporting the first example of polymerization of biobased MAA.^[80] Avoiding expensive catalysts and corrosive alkalis are the main strengths of the work of these two research groups.

Pandey and co-workers reported in 2019 the one-pot synthesis of Co(II) formate metal organic frameworks (MOFs) together with MAA from IA, at 160 °C in water.^[81] The active catalyst would be the cobalt precursor $\text{Co}(\text{NO}_3)_2 \cdot \text{H}_2\text{O}$ which gave similar results without MOF formation. Yields of up to 90% have been claimed, which makes this process promising and should spur further investigations.

MAA can also be obtained by dehydrogenation of isobutyric acid (IBA) or dehydration of its hydroxylated analog 2-HIBA. The search for biosourced pathways toward these C4-starting materials would provide access to biobased MAA with carbon atom economy. 2-HIBA is in fact the methylated analog of lactic acid, a potential precursor of acrylic acid.

The IBA route was actually considered promising before the recent development of biobased chemistry as a precursor of MAA derived from the hydroxycarbonylation of propene.^[56] However, it never reached a commercial state because of the difficulties encountered in the last step of this process: the oxidative dehydrogenation of IBA to MAA. A conversion close to 100% is necessary because IBA and MAA have similar boiling points and chemical structure, making them difficult to separate. Two families of catalysts have been identified for this reaction, namely, iron phosphorus oxides^[82] and heteropolyacids.^[83] Acidic cesium salts of molybdo-vanado-phosphoric acids have proven to be very efficient, but the high conversion of IBA (97%) and the selectivity for MA (78%) at 350 °C are still not sufficient to make this route viable.^[84] These limitations have not hampered research in the biotechnological synthesis of IBA, as it may have other applications than MAA production. In 2011, Zhang et al. described for the first time a biosynthetic pathway to IBA from glucose using genetically engineered microorganisms (GMOs), reaching titers as high as 40 g.L⁻¹.^[85]

Since it is more convenient to separate unreacted 2-HIBA from MAA, this intermediate may have more potential than IBA for biosourced methacrylic acid. Its dehydration has been known for

years, as illustrated by a patent from Lonza dating from 1969.^[86] Since then, only limited research has been conducted, although it is expected to behave similarly to lactic acid. In the same work they did on IA decarboxylation, Pirmoradi and Kastner exemplified for the first time the dehydration of 2-HIBA in subcritical water, with a 70% isolated yield, leading them to believe that this route is probably more convenient for producing biobased MAA than the IA pathway, if a suitable green synthesis of 2-HIBA is available.^[76] Since it has been found that naturally occurring microorganisms produce polyhydroxybutyrate (PHB) via the formation of 3-hydroxybutyrate (3-HBA), recent efforts have been dedicated to stop these metabolic pathways to 3-HBA and to extend them to its 2-HIBA isomer (**Figure 7**). Evonik and Genomatica Inc. have been particularly active in this area.^[87-91] Weuster-Botz and co-workers reported titers up to 6 g.L⁻¹ in experiments conducted on a 1 L scale.^[92]

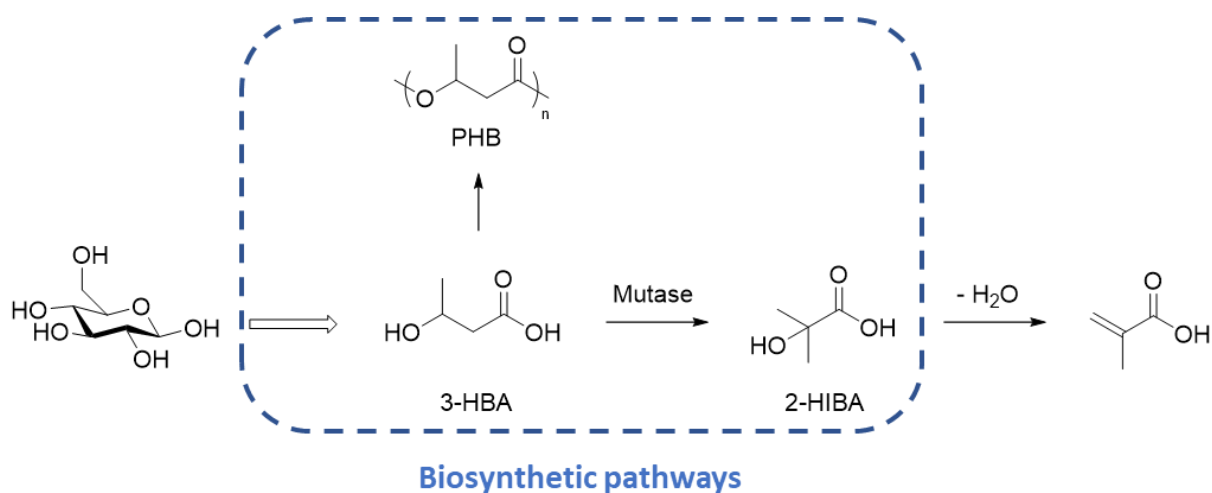


Figure 7. Bio-MAA from fermentation of 2-HIBA.

Obtaining bioisobutene has also been investigated recently. It is possible to ferment it directly or dehydrate isobutanol, an intermediate that can also be fermented.^[93] Isobutanol fermentation has only recently been reported by Atsumi et al.^[94] Highly tolerant strains are required due to the toxicity of isobutanol, which could hamper the competitiveness of this route.^[95] Nevertheless, the dehydration of isobutanol to isobutene has been patented by Gevo, a company that also claims to produce industrially bioisobutanol.^[96] The direct fermentation of isobutene by naturally occurring microorganisms was first reported by Fukuda et al. in 1984.^[97] The advantage of this process is the

low solubility of isobutene in water, allowing it to be harvested from the off-gas of the fermentation broth, which also contains CO₂ and H₂O steam. However, extensive metabolic engineering is necessary to achieve viable productivity, with the best throughput to date being 34 mg.L⁻¹.h⁻¹, whereas 2–4 g.L⁻¹.h⁻¹ would be required to be economically feasible.^[98]

Alternatively, the group of Wang reported in 2011 the synthesis of a Zn_xZr_yO_z catalyst and its use for the conversion of bioethanol to isobutene (83% of the maximum theoretical yield of 67%) in water at 450 °C.^[99] Various basic catalysts are capable of converting ethanol to acetone, while acetone is efficiently converted to isobutene using special structured acidic catalysts. The authors thus passivated ZrO₂ with ZnO to obtain a catalyst with balanced acid-base sites. Later, Román-Leshkov and coworkers used the same catalytic system to convert acetic acid to isobutene (75% of the maximum theoretical yield of 67%).^[100] Bell recently investigated the mechanism of this reaction and found that acetic acid is an intermediate in the ethanol to isobutene route, as well as a byproduct that is readily recycled (**Figure 8**).^[101] The Wang group has patented both approaches and the subsequent conversion of isobutene to MAA.^[102]

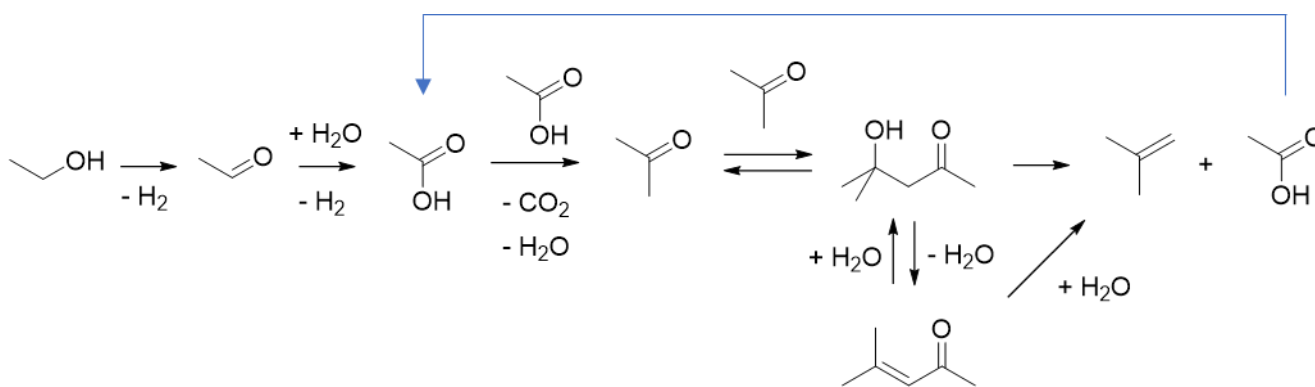


Figure 8. Isobutene from ethanol or acetic acid.^[101]

Among other possible routes to bio-MAA, its direct fermentation has been studied and several GMOs able to perform the reaction from various substrates have been patented by Genomatica,^[103,104] Lucite,^[105] or Mitsubishi.^[106] Due to the detrimental acute toxicity of MAA, this route requires robust strains, and is thus still under investigation.^[55] Propionic acid condensation with formaldehyde is

another possibility, with propionic acid fermentation being investigated in the broader context of biorefinery.^[107] Formaldehyde can theoretically be obtained from biomass gasification as it is mainly produced from methanol.^[61,108]

Overall, biosourcing of MAA is less advanced than the one of AA. The greater variety of trade routes to MAA will probably allow producers to use drop-in biobased building blocks such as ethylene derived from ethanol to obtain bio-MMA and MAA in the near future. Starting from fermentative products already available on the market, such as itaconic acid or citric acid, it would be possible to have a more direct route to bio-MAA with two green building blocks that are expected to play an important role in the future bioeconomy. The dehydration of 2-HIBA is more atom economical than the decarboxylation of IA or CA, and is also easier to achieve, as Pirmoradi and Kastner pointed out.^[76] Successful genetic engineering will however be key to produce 2-HIBA competitively. Finally, biosourcing of isobutene may not be the most straightforward route but the use of cheap substrates such as ethanol or acetic acid can promote its potential.

2.3. Itaconic Acid

As mentioned in the previous section, itaconic acid is currently produced on a 40 000 tons.year⁻¹ scale by fungal fermentation.^[67] Interest in this diacid has recently risen in academia and numerous reviews on its production and applications are available.^[65–67,109–121] Herein, we present a brief historical description of the production of IA, underlining recent promising developments, as well as its potential uses as a building-block toward various chemicals.

First discovered by Baup in 1836 as a thermal decomposition product of citric acid,^[122] itaconic acid was not produced industrially until the second half of the 20th century. Kinoshita reported in 1932 the first microorganisms able to produce IA by fermentation, *Aspergillus itaconicus*.^[123] In 1939, Calam and co-workers obtained higher productivities with *A. terreus*, a fungal strain that would later become the workhorse of IA fermentation.^[124] Pfizer was the first company to actually commercialize IA, with patents filed in the early 1940's and a production started in 1955.^[109,125] In the late 1990's,

western countries' companies (e.g., Cargill and Rhodia) were the main suppliers of IA, with a total output of 15 000 tons.year⁻¹ at 4 \$.kg⁻¹, using fermentation alone.^[66] More recently, production shifted to China with an output of 40 000 tons.year⁻¹ and a capacity of 80 000 tons.year⁻¹ at 1.7 \$.kg⁻¹.^[67] The standard process for IA production is nowadays a batch fermentation of crystallized glucose or sucrose by *A. terreus* lasting around 7 days and recovered by filtration, evaporation of a certain amount of water, and crystallization.^[109,112] The titers obtained before harvesting are in the range of 80 g.L⁻¹, and total productivity usually lies between 0.4 and 0.6 g.L⁻¹.h⁻¹.^[118] Recent research has focused on improving several aspects of this fermentation. Linko and co-workers immobilized the microorganisms on a Celite support to perform flow/continuous fermentation and increased throughput up to 1.2 g.L⁻¹.h⁻¹, thanks to the higher productivity of the strains at lower IA concentration.^[126] Other supports, such as polyurethane foams, were investigated,^[127] but flux-processing did not gather much attention so far, probably owing to the low concentration of the output stream, which can be detrimental to the recovery step. Park and co-workers suggested the use of air-lift reactors as an alternative to stirred tank reactors for the batch process, which would lower operation costs.^[128,129] Over the last decade, Kuenz and co-workers optimized the processing conditions of IA fermentation, especially pH control, to obtain titers of 160 g.L⁻¹ and a productivity of roughly 1 g.L⁻¹.h⁻¹.^[130-132] Wierckx and co-workers recently genetically modified the yeast-like *Ustilago maydis* to obtain itaconate titers of 220 g.L⁻¹, although productivity was only 0.45 g.L⁻¹.h⁻¹.^[133] Shifting from crystallized glucose to cheaper substrates has also been investigated by several groups, with published examples starting from waste streams,^[134] liquified corn starch,^[135] or lignocellulosic monosaccharides such as xylose or arabinose.^[136] However, low titers and productivities have been achieved. Using citric acid as the starting material, Yang and co-workers notably obtained high throughputs of IA (2.2 g.L⁻¹.h⁻¹) thanks to rapid fermentation (19 h) by genetically engineered *Escherichia coli*.^[137] Modest titers (42 g.L⁻¹) may nonetheless hamper the efficient harvesting of IA. Nevertheless, the cost of citric acid (0.7 \$.kg⁻¹) lies in the upper range of the one of purified glucose or sucrose (0.35–0.72 \$.kg⁻¹), so that an efficient

and productive route toward IA may be of commercial interest.^[63,67,112] Finally, alternative harvesting techniques have also been investigated, such as reactive extraction or adsorption.^[65] Crystallization is indeed a convenient process but only allows a 80% recovery of the produced IA, while adsorption is close to 100% and may have better economics.^[138] Overall, the fermentation of itaconic acid is a dynamic area of research, which has recently reduced its cost. The increase in production volumes should stem from an increase in the number applications.

IA is indeed a green chemical building block that can lead to a wide variety of derivatives and applications (**Figure 9**). IA itself can be used in adhesives or added to coatings or resins to improve their paintability.^[112] Poly(itaconic acid) obtained by vinyl polymerization of IA (covered in Section 3.2) can be used in detergents to replace phosphates that have caused eutrophication of aquatic systems.^[109] Poly(IA) has also been advocated as a potential biobased replacement of poly(acrylic acid) as superabsorbent polymer, if it proves to be more cost competitive than the various green routes from biomass to AA. IA can also be vinyl polymerized with various comonomers to yield styrene-butadiene rubber latexes, acrylate latexes, or hydrogels (e.g., by copolymerization with acrylamides or pyrrolidone).^[109,112] Polycondensation of IA with diols can lead to polyesters with applications in drug delivery, shape memory polymers, elastomers, adhesives, and coatings.^[109,115] IA can be used directly to produce polyesters bearing unsaturation in their backbone, or it can be converted into methyl succinic acid or 2-methylbutanediol to yield saturated monomers. Leitner, Klankermayer and co-workers developed in 2010 an efficient ruthenium catalytic system to successively hydrogenate and dehydrate IA into γ -butyrolactones (GBLs) and 2-methylbutanediol.^[139] More recently, Palkovits and co-workers reported the electrocatalytic conversion of IA into methylsuccinic acid directly from the fermentation broth.^[140] By taking advantage of the internal double bond of IA, it is also possible to synthesize biobased epoxy-resins.^[117] Other important vinylic monomers can be derived from IA. Biobased MAA has already been discussed (see Section 2.2). Itaconic anhydride is a versatile monomer, obtained by dehydration of IA, which can be either vinyl polymerized or copolymerized by

ring-opening with epoxides to yield polyesters. Our group recently reported a simple and efficient method to convert IA into IAnh using di-tertbutyl dicarbonate and a cheap catalyst (i.e., MgCl_2),^[141] as well as tandem synthesis of various polyesters starting from IA and converting it to IAnh.^[142] Reacting with primary amines, IAnh can lead to the widely used itaconimides, examples among others of the various heterocycles accessible from IA.^[143] Recently, Fors and co-workers reported the controlled reduction of mono-methyl itaconate into α -methylene- γ -butyrolactone (MBL), thereby paving the way for its high-scale production, which was not possible when it was obtained from tulipalin.^[144] Gowda and Chen also developed a potentially industrially relevant process for the production of another methylene butyrolactone.^[145] These biobased monomers could then be vinyl polymerized to yield high glass transition temperature (T_g) analogs of poly(methyl methacrylate) (PMMA) (see Section 3.3). Fors and co-workers described more recently the routes from IA to diesters and diols and their use in the formation of 100% itaconic acid-based polyesters.^[146]

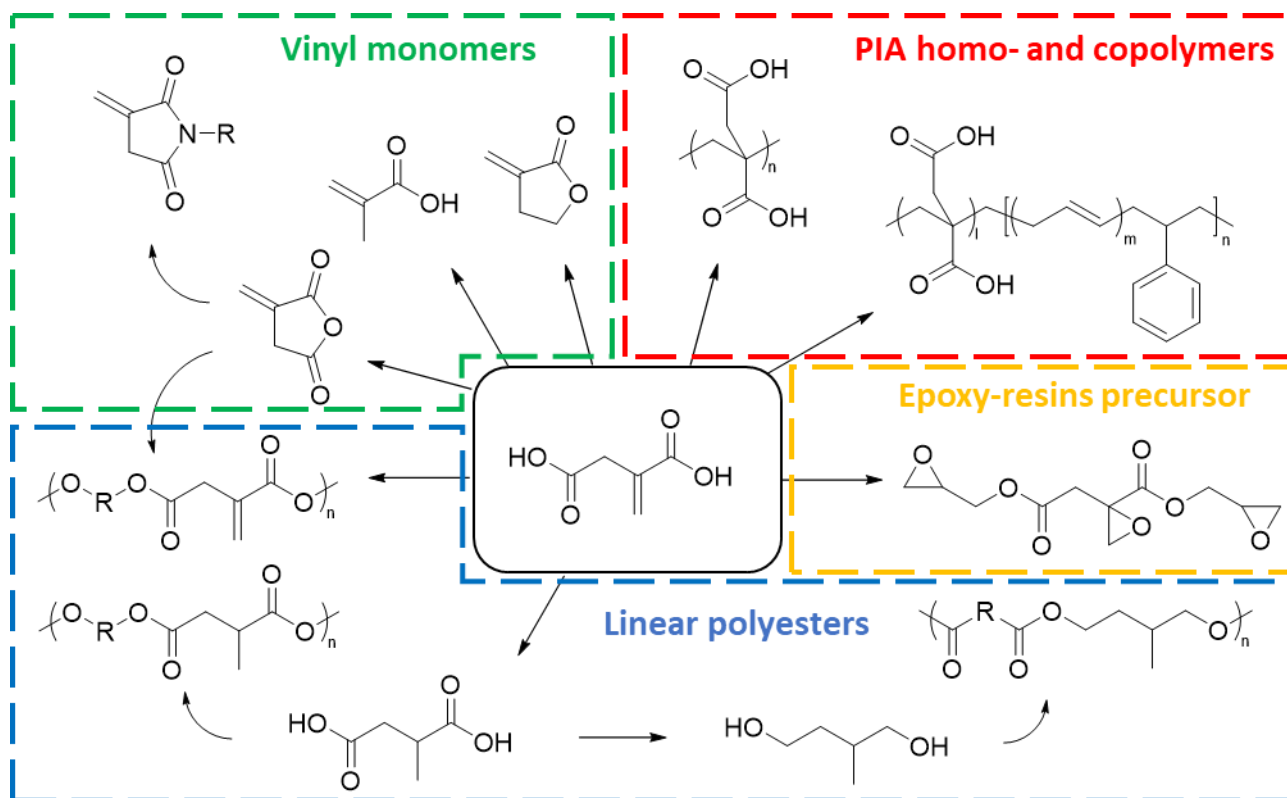


Figure 9. Possible itaconic acid transformations for polymer formation.

Itaconic acid is thus both a promising building block and a versatile monomer for biobased polymer synthesis. Since it is derived exclusively from renewable resources in a single fermentation step, it has aroused a lot of interest from academia and industry. Cost-reducing improvements are still required to make it a high-volume commodity product. Another driver for its increased production could be the wide variety of molecules accessible from this platform chemical, as exemplified by its potential uses in polyesters and polyitaconates.

2.4. α -Methylene- γ -butyrolactone and Analogs

MBL and its analogs are presented in **Figure 10a**. They can either be polymerized by their conjugated double bond or by ring-opening polymerization (ROP) to yield biodegradable polyesters. The latter process is made difficult by the stability of these 5-membered rings, although significant advances in this domain have recently been reported.^[147-151] The purpose of the present review is however the biosourcing of these monomers and their vinyl polymerization. Tulipalin A and B are naturally occurring molecules that are found in relatively high concentrations in tulips in the form of their glucose esters (Figure 10b). Kato et al. described in 2009 an efficient enzyme-catalyzed process for the recovery of tulipalin A.^[152] The same group later described a similar methodology for the less abundant tulipalin B.^[153] Although this approach is likely not convenient for high volume production of these monomers due to the high cost of feedstock and low overall mass yield (around 0.03 wt% for tulipalin B), it could pave the way for bioinspired catalytic systems for these reactions.

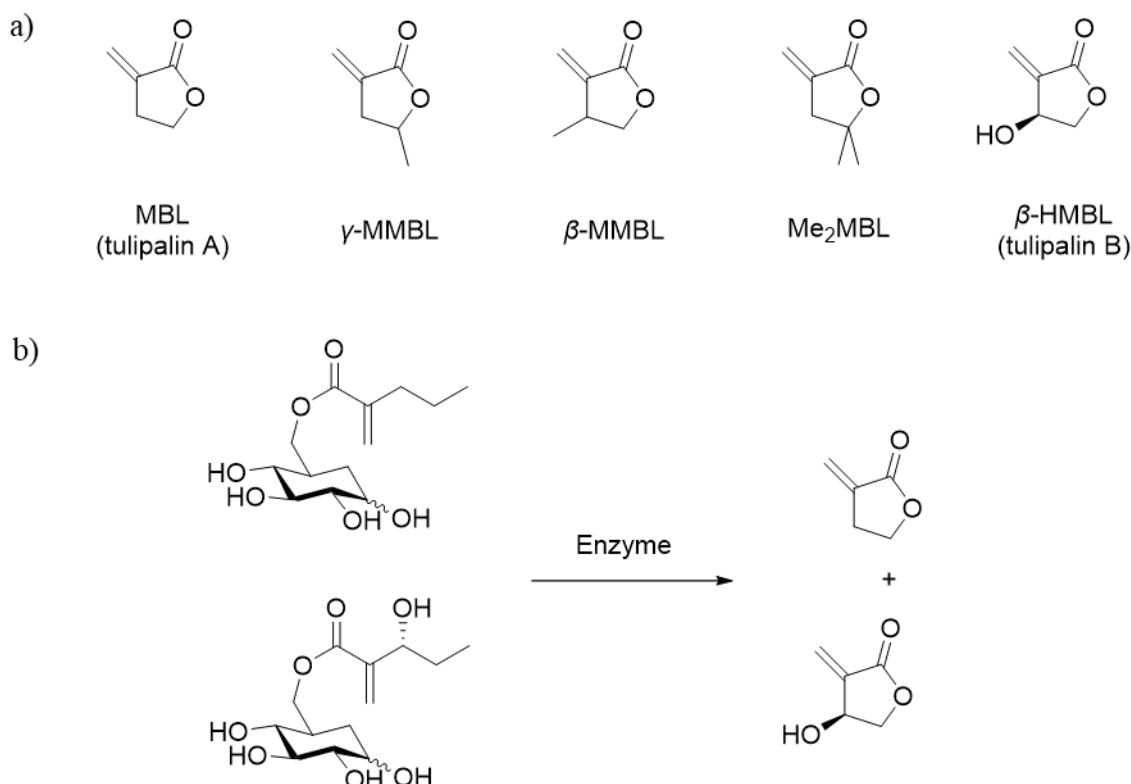


Figure 10. a) Methylene lactones covered in this section. b) Naturally occurring glucose esters of tulipalin A and B.

MBL was first extracted from *Erythronium americanum* by Cavallito and Haskell in 1946.^[154] They mentioned its high reactivity, as heating it at 70–80 °C without any initiator led to an uncharacterized polymer. Jones et al. reported the first chemical synthesis of MBL and γ -methyl- α -methylene- γ -butyrolactone (γ -MMBL) by a stoichiometric reaction between nickel carbonyl and monosubstituted acetylenic alcohols.^[155] McGrow and Morrinstown were the first to patent the synthesis and polymerization of methylene lactones in 1953.^[156] Their chemical pathway proceeded through the acylation of lactones, followed by hydrogenation and dehydration to produce the corresponding monomer (**Figure 11**). In 1975, Grieco reviewed the different routes to methylene lactones, all of which were fossil-based at the time, as GBL was mainly derived from maleic anhydride (Figure 11). Various routes to derivatives of MBL have been explored, as some of these compounds have anticancer properties useful in the pharmaceutical industry.^[157,158] This total synthesis approach is however not

applicable to the polymer industry and a direct synthetic path from biobased building blocks had to be found to produce renewable monomers.

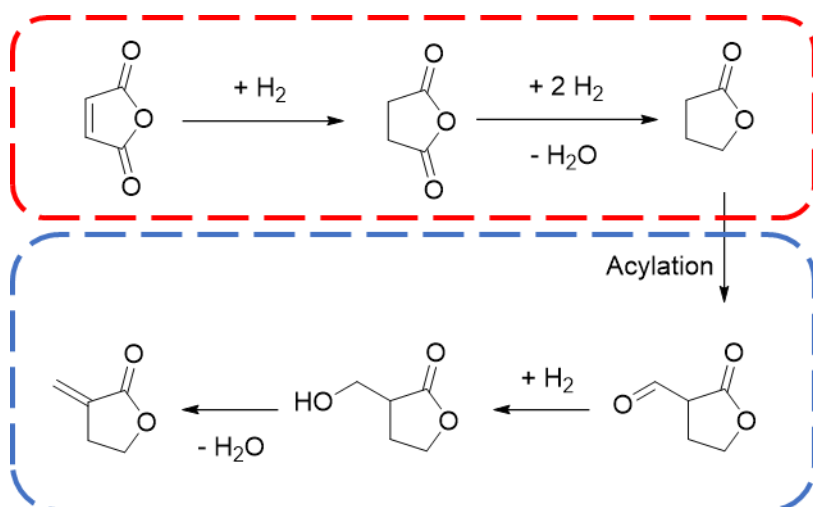


Figure 11. Fossil-based route towards GBL (red) and patent description of McGrow and Morrystown (blue).

The first mention of a biobased synthetic route to MBL is found in the work of Fetizon et al. in 1975, as they reduced dimethyl itaconate (DMI) to its corresponding diol without modification of the double bond, and subsequently oxidized it to MBL using Ag_2CO_3 supported on Celite as catalyst.^[159] Few details are given for the first step, but a 80% yield is obtained for the second one. This route was not efficient in terms of reagent use, but it has the merit of keeping the methylene moiety intact. Carlson and Oyler later prepared the enolate of DMI and reacted it with aldehydes or ketones to produce the corresponding substituted methylene butyrolactones.^[160] In 2000, Santelli and co-workers reacted itaconic anhydride with an excess of Grignard reagents or silanes and obtained the corresponding lactones with moderate yields (65%).^[161] More recently, Fors and co-workers synthesized MBL and γ,γ -dimethyl- α -methylene- γ -butyrolactone (Me_2MBL) from the β -monoester methyl itaconate.^[144] Using an excess of Grignard reagent in tetrahydrofuran (THF), they obtained Me_2MBL with a 39% isolated yield under conditions similar to those of Santelli and co-workers. By reacting methyl itaconate with 6 equivalents of reducing agent NaBH_4 in water/THF mixtures, they were able to obtain MBL with a 42% isolated yield. The use of LiBH_4 was not successful in their hands, although it had

been reported in 1992 patent from Hirabayashi and Yokota.^[162] These direct pathways from IA and its derivatives to methylene lactones are therefore promising, but lack scalability. The discovery of cheaper reducing agents combined with efficient catalysts could make them more attractive. Alternatively, IA can be converted to γ -isovalerolactone (GiVL) and further methylenated to β -methyl- α -methylene- γ -butyrolactone (β -MMBL) (**Figure 12**). Obtaining GiVL and its regioisomer α -methylbutyrolactone (AMBL) from IA was reported by Klankermayer and co-workers.^[139] GiVL and AMBL are however not easily separated and only GiVL can be methylenated to produce a reactive vinyl polymerizable lactone (dehydrogenation of AMBL preferably yields the unreactive endocyclic double bond). Thus, Gowda and Chen worked on the selective conversion of IA into GiVL. In 2014, these authors suggested a lab scale, 3-step synthesis of GiVL from methyl itaconate with a 61% yield (49% starting from IA).^[163] In 2019, they improved scalability by performing the one-pot hydrogenation of IA into GiVL in an aqueous medium, using syngas as the reductive agent and ruthenium nanoparticles as the catalyst, for a 70% yield.^[145] The Ru nanoparticles could be stabilized on Al₂O₃ and gave similar results, without loss of performance upon recycling.

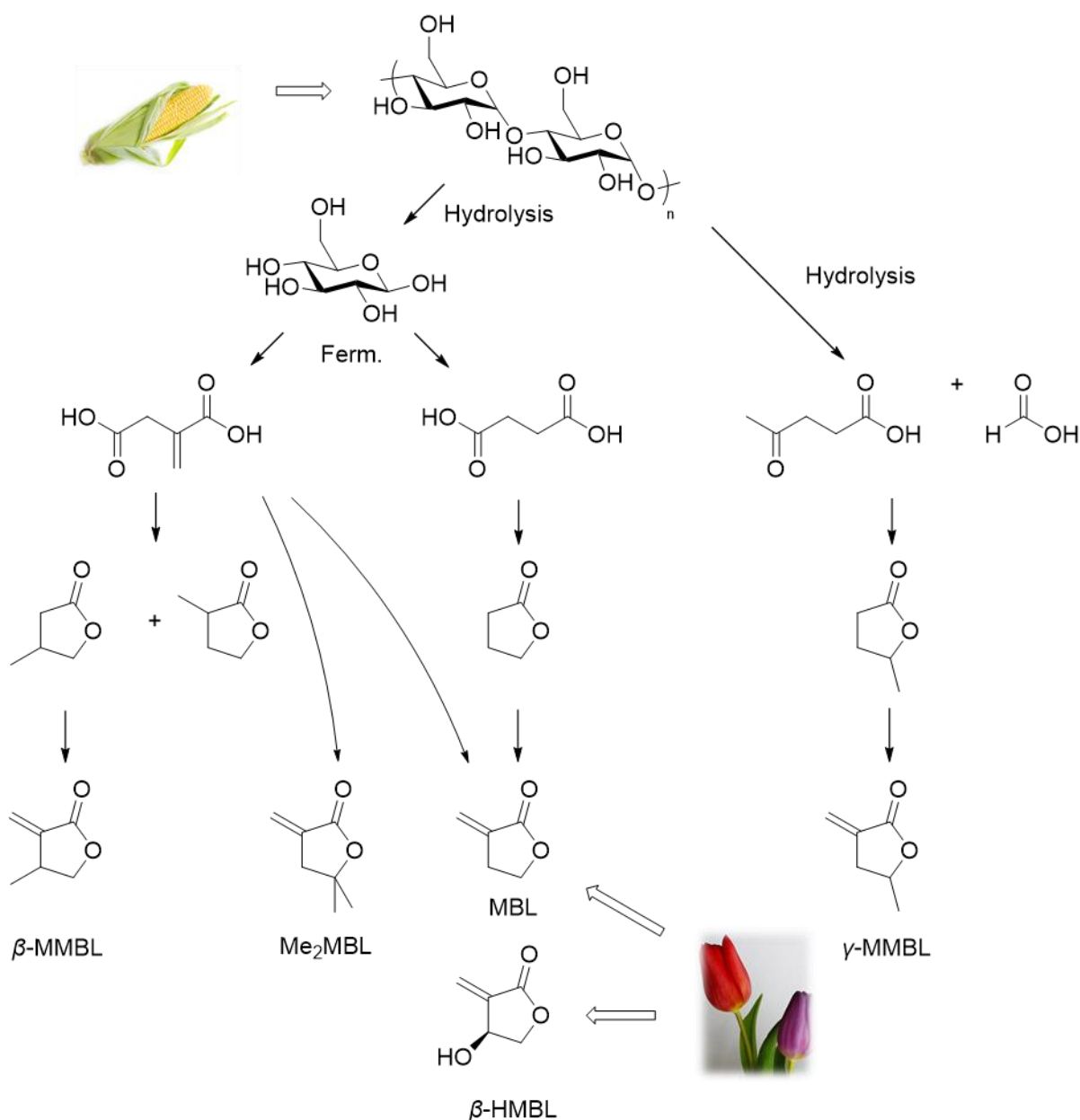


Figure 12. Routes towards biobased methylene lactones.

An alternative route to biobased synthesis of methylene butyrolactones is via the succinic acid (SA) platform (Figure 12). SA can indeed be reduced to γ -butyrolactone and further introduction of a methylene moiety on the α position leads to MBL. Succinic acid is obtained from biomass by anaerobic fermentation of various substrates, as described in recent reviews.^[164–166] It was previously obtained from hydrogenation of petro-sourced maleic acid or maleic anhydride, for a small 18 000 tons.year⁻¹ market in the 1990's,^[164] but biobased production capacities would have reached more than 64 000

tons.year⁻¹ in 2015.^[165] SA is therefore a rapidly growing biobased commodity, with a market price in the range of 2–3 \$.kg⁻¹.^[164] The main suppliers are BioAmber, Myriant, Reverdia (DSM and Roquette joint venture), and Succinity (BASF and Corbion Purac joint venture).^[165] In polymer chemistry, SA has been used in polyester synthesis as a diacid or via its reduced form 1,4-butanediol as a diol. However, its reduction can also be stopped to GBL. This process has been known for some time as succinic anhydride is an intermediate in the oil production of GBL from maleic anhydride (Figure 11). Davy McKee and Dupont commercialized this route in the 1990's, using bimetallic Cu–Cr and Cu–Zn catalysts.^[167,168] Starting from SA, initial hydrogenation to GBL is reportedly easier to control than subsequent steps to 1,4-butanediol, with pressures ranging from 50 to 300 bars, temperatures between 200 and 300 °C and yields up to 99.8% with abundant metals as catalysts.^[169] Given the technology readiness of this process, SA can thus be considered as a drop-in chemical for this route. It is therefore surprising that no reports were found on obtaining MBL from SA. One explanation could be the difficulties associated with the GBL to MBL step, which will be covered in a subsequent paragraph.

The last biobased building block for the synthesis of methylene butyrolactones is levulinic acid (LvA). Since the patented Biofine process was described in 1997,^[170] production growth has been modest, with ≈ 2700 tons.year⁻¹ in 2013 at about 5–8 \$.kg⁻¹.^[171] The main companies commercializing LvA are GFBiochemicals, Segetis, and Biofine. Unlike IA and SA, LvA is not produced by fermentation but by direct acid-catalyzed hydrolysis of polysaccharides at elevated temperature and pressure, the main coproduct being formic acid (FA). Recent reviews cover this topic in depth.^[172–174] Although avoiding the use of microorganisms can be considered an advantage, the high operation costs and small number of applications have so far prevented the low cost production of LvA. The use of homogeneous acid catalysts such as H₂SO₄ or HCl requires a recovery step, while heterogeneous catalysts have shown poor performance over time due to deactivation by the deposition of humins, polymeric byproducts generated during the process.^[173] However, the interest in LvA conversion was not hampered by these limitations. Manzer, a member of DuPont, patented in 2003 a hydrogenation of

LvA into γ -valerolactone (GVL) using pure H₂ at 55 bars, 150 °C with various heterogeneous catalysts.^[175] In a seminal work, he then published a two-step route to γ -MMBL by reacting the GVL obtained from LvA with formaldehyde in the gas phase, which led to extensive work in this field.^[176] The first step was better catalyzed by Ru/C, with yields up to 80%, while the second step was carried out by various groups 1 and 2 metal acetates. The best selectivity (99%) was obtained with barium, but this step suffered from rapid catalyst deactivation. Thereafter, much work has been dedicated to the conversion of LvA to GVL, and is reviewed elsewhere.^[177–183] Most promising studies have suggested the use of FA as a reducing agent, as it can decompose into H₂ and CO₂ under appropriate conditions. Indeed, FA is a byproduct of the hydrolysis of biomass into LvA, and its use as a co-reactant would improve the overall efficiency of the process. Shell was the first company to issue a patent regarding the use of FA with ethyl levulinate, although the addition of H₂ is still required.^[184] Horváth and co-workers then described a multistep conversion of sucrose to GVL in which sodium formate could be used as the H₂ source for the ruthenium-catalyzed LvA hydrogenation.^[185] However, a major limitation was the large excess of formate necessary. In 2009, Guo and co-workers described an efficient process for the conversion of 1:1 aqueous mixtures of LvA:FA into GVL, using a homogeneous ruthenium catalyst and high amounts of base.^[186] The same group later described improvements by immobilizing the ruthenium catalyst and avoiding the use of basic co-reactants.^[187] Also in 2009, Heeres et al. performed the one-pot Ru-catalyzed conversion of sugars into GVL with a yield of around 50 mol%, although the addition of H₂ was needed.^[188] Dumesic and co-workers later developed an integrated process for the hydrolysis of biomass into LvA and subsequent conversion into GVL over Ru/C in the same aqueous acidic medium.^[189] This approach improved H₂SO₄ recycling, since GVL is more hydrophobic than LvA and can therefore be extracted by ethyl acetate. However, it still required additional use of H₂. The group of Cao then developed a catalyst composed of gold nanoparticles stabilized on a zirconia support to promote the LvA:FA to GVL step.^[190] Performances comparable to those of the ruthenium catalysts were obtained. With the same catalyst,

they added an esterification step using *n*-butanol to obtain the corresponding formate and levulinate, and were thus able to efficiently recycle H₂SO₄ and subsequently perform the hydrogenation step.^[191] Maravelias and co-workers reported in 2012 a techno-economic evaluation of a process for converting biomass into fuels, with GVL as the major intermediate.^[192] They found out that the feedstock and the precious metal catalyst were among the main costs. Therefore, recent research has focused on the development of a cheap catalyst for LvA conversion.^[180] However, most of the reported systems required the use of molecular H₂. Notable examples using FA as a H₂ source and inexpensive catalysts are listed herein. Cao and co-workers reported in 2013 a copper-based metal oxide catalyst performing the 100% yield conversion of LvA into GVL, which stands as the most promising example to date.^[193] Fu and co-workers developed a homogeneous iron-based catalyst with similar performances but requiring an excess of FA.^[194] Varkolu et al. recently reported a Ni/SiO₂ catalyst with yields up to 90%, but the excess of FA was also a limitation of this method.^[195] Thus, the conversion of LvA has been an active area of research as most of its chemistry was not well-known until the first reports of its production from renewable resources.

As exemplified in Figure 12, the incorporation of the methylene moiety is the last step before obtaining vinyl polymerizable monomers. Surprisingly, very little work has been reported on this topic compared to the number of publications regarding their polymerization. A few years before the publication of Manzer,^[176] DuPont actually issued two patents on this transformation. Coulson et al. first described in 2001 the vapor phase reaction of GBL with formaldehyde, at 200 °C, over various basic catalysts, yielding MBL with selectivities up to 95%.^[196] The same reaction was applied by Manzer to GVL to obtain γ -MMBL,^[176] who also studied with Barteau and co-workers the deactivation/regeneration of a rubidium oxide catalyst for this transformation.^[197] The second patent mentioned milder conditions but required the use of oxalates prior to reaction with formaldehyde,^[198] a synthetic route first reported by McCurry and co-workers in 1977 for lab-scale reactions.^[199] This method was used by Gowda and Chen in their synthesis of β -MMBL from IA with a 86% yield for

these two steps.^[163] In 2015, Esposito and co-workers also developed a lab-scale protocol for the methylenation of GVL.^[200] By essentially getting rid of the oxalate step in the McCurry protocol, they used K₂CO₃ as a low-cost catalyst, paraformaldehyde as a co-reagent and 2-MeTHF as a solvent at 180 °C in an autoclave (maximum yield of 36%). Selectivities below 60% were an issue in this case, as they lead to difficult purification steps. Recently, Al-Naji et al. developed a promising stable heterogeneous catalyst (cesium-doped zeolite) for the conversion of GVL into γ -MMBL.^[201] Trioxane was selected as the formaldehyde source as it decomposes at 250 °C. This choice avoids the use of formaldehyde aqueous solutions, because water is thought to inhibit the reaction. They performed the reaction in a flow system at 300 °C and obtained selectivities of up to 90%. These encouraging results should prompt the chemical community to develop more efficient processes for obtaining biobased methylene lactones. It should be noted that formaldehyde is commonly used industrially to produce MMA from methyl propionate (Lucite process, see Section 2.2), although it is unstable and carcinogenic.^[108]

Overall, methylene lactones are promising biobased monomers. Their derivation from biomass requires more steps than acrylic, methacrylic, or itaconic acid, so that their cost limits their use as commodity chemicals for now. Future research is likely to be dedicated to finding scalable and inexpensive synthetic pathways to MBL and its analogs.

2.5. Other Biobased Lactones

Other less-studied methylene lactones from biomass have been described. Their synthesis is shortly reviewed in this section.

2.5.1. Methylene Lactide (MLA)

Among these lesser-known monomers, MLA was first reported in 1969 by Scheibelhoffer et al.^[202] These authors synthesized MLA from lactide via bromination with *N*-bromosuccinimide (NBS) and subsequent elimination of HBr with one equivalent of triethylamine (**Figure 13**). To date, there is no report of an alternative synthetic route, making this monomer difficult to access on a large scale.

Although the synthesis is not atom economical and requires toxic reagents, the final monomer is 100% biobased, as lactide is obtained by oligomerization and depolymerization under vacuum of lactic acid, which is itself derived from biomass by fermentation of carbohydrates.^[203]

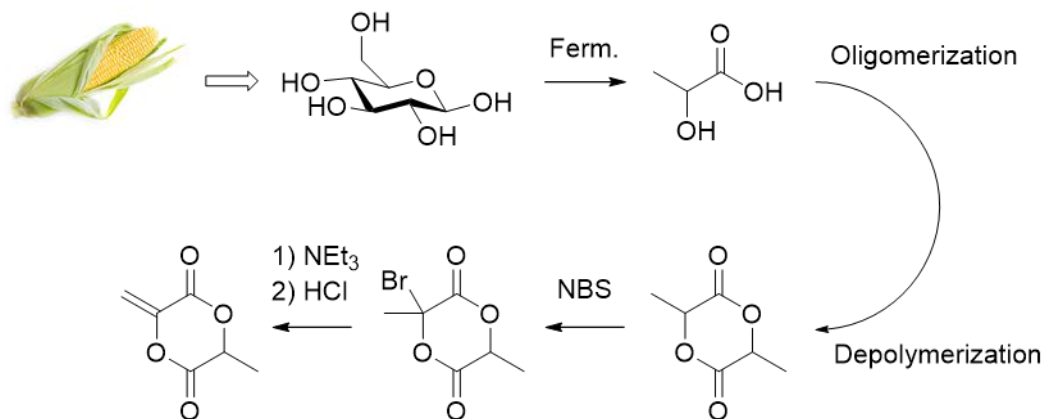


Figure 13. Synthesis of MLA.

2.5.2. β -Angelica Lactone (β -AL)

β -AL is another polar vinylic monomer derived from bioresources. Dehydration of levulinic acid leads to a mixture of α -angelica lactone (α -AL) and β -AL that can be isolated prior to further hydrogenation to GVL (**Figure 14**).^[204] The isomerization of α -AL to β -AL is catalyzed under acidic^[204] or basic^[205] conditions with moderate heating, facilitated by the conjugation of the double bond in β -AL. Enantioselective isomerization has also been reported,^[206] although the polymerization of the chiral monomer has never been described. β -AL has indeed not garnered as much attention as α -methylene lactones such as LvA-derived γ -MMBL because its endocyclic double bond is much less reactive to polymerization reactions. Nevertheless, it is easier and more direct to obtain from LvA, so that any breakthrough in its polymerization could potentially provide access to relatively cheap and biobased specialty materials.

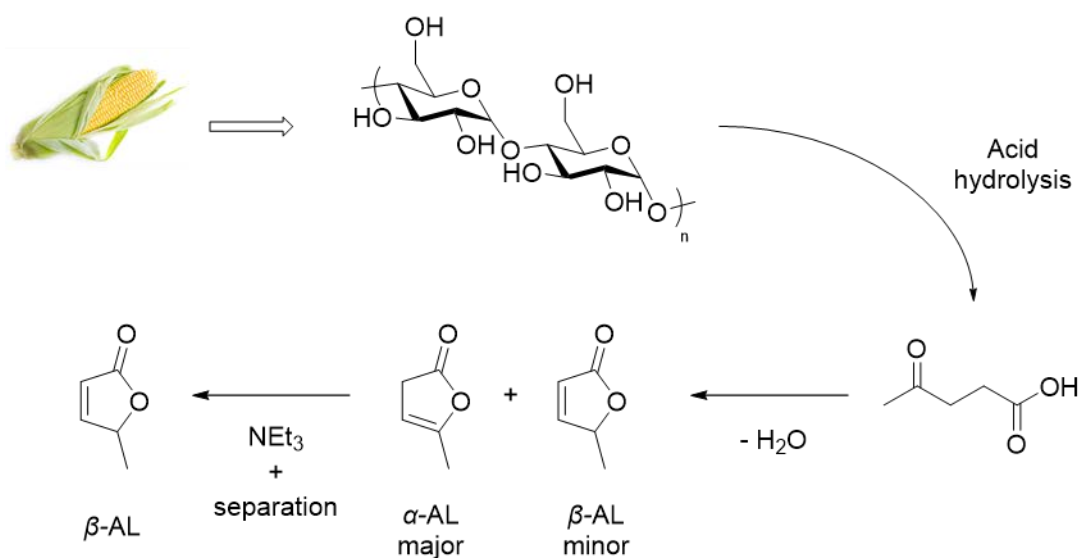


Figure 14. Production route of β -AL.

2.6. β -Substituted Acrylics

β -substituted acrylics are supposedly less reactive toward polymerization than their unsubstituted counterparts. Therefore, these compounds have been used to a lower extent as precursors for materials. However, their potential direct biosourcing as well as their original molecular structures may be of interest for various applications.

2.6.1. Cinnamic Acid

CMA and its corresponding esters are β -phenyl substituted acrylic monomers (**Figure 15**). CMA can be found in relatively high concentrations in cassia buds, and cinnamates derived from it have been used as fragrances.^[207,208] A potential larger scale route to CMA is the deamination of the amino acid, phenylalanine (PhAl).^[208] This reaction is catalyzed by the well-studied naturally occurring enzyme phenylalanine ammonia lyase.^[209] Amino acids are considered promising feedstocks in the future bioeconomy. They are usually obtained individually by fermentation means. For instance, PhAl is derived from glucose or other carbohydrate substrates by fermentation using PhAl overproducing strains of *E. coli*.^[210] A potentially cheaper route toward amino acids is to separate them from wastes produced by the agro- and biofuel industries.^[208] However, these waste streams are usually

composed of a variety of amino acids, none of which exceeds 5 wt%. Efficient fractionation technologies are thus required to render the production of individual amino acids from waste viable. Efforts in this field are highlighted by the promising process of reactive extraction. Notably, Scott and co-workers recently separated a model mixture of amino acids containing PhAl by selectively reacting them with specific enzymes (PhAl was converted to CMA by phenylalanine ammonia lyase), and further separating them by electro dialysis.^[211] Additionally, although PhAl is a primary substrate of lignin biosynthesis in plants, there is no report to date of the production of phenylalanine from lignin.^[212] Overall, CMA production from biomass is well-known and efforts are underway to make it more economically viable.

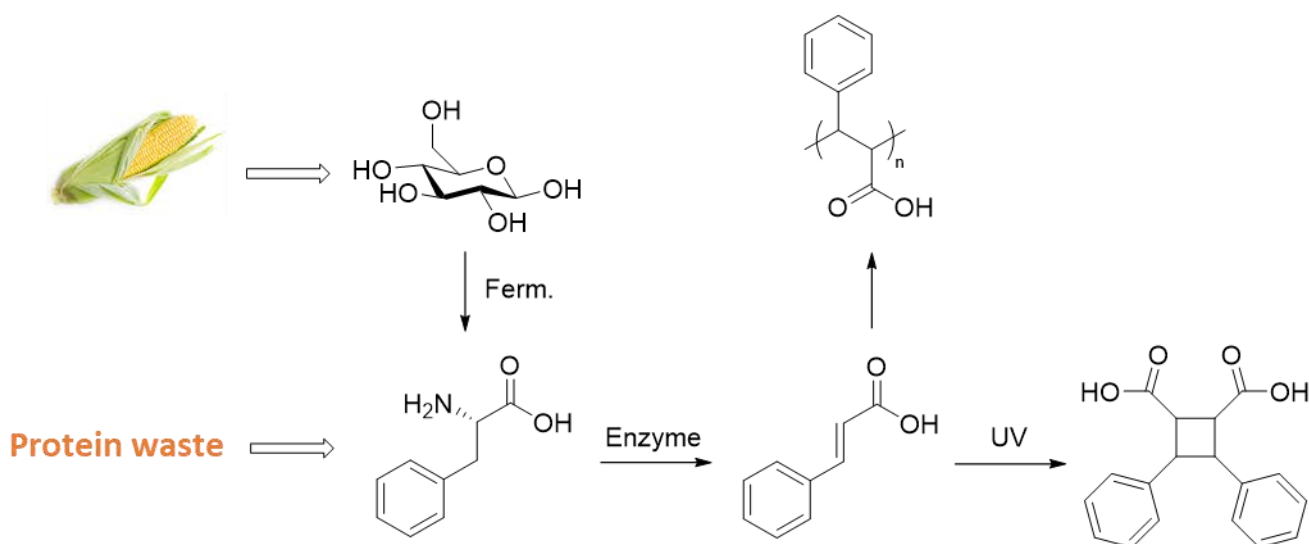


Figure 15. Production, polymerization and cyclization of cinnamic acid.

2.6.2. Fumaric Acid

FmA is an unsaturated C₄ diacid, *trans* isomer of maleic acid (**Figure 16**). Its production from renewable resources has been reviewed by several groups.^[213–218] However, it is still nowadays mainly produced from petroleum via the oxidation of benzene or *n*-butane over vanadium phosphate catalysts to yield maleic anhydride, which is subsequently hydrolyzed and isomerized at high temperature to fumaric acid.^[213] In 2014, the annual tonnage of FmA production reached 245 ktons.^[219] While some research has been devoted to enzyme-catalyzed isomerization of maleic acid under mild conditions,

biobased FmA production is only possible through the fermentation of carbohydrates. Most studied strains are naturally FmA-producing *Rhizopus arrhizus* and *Rhizopus oryzae*, two filamentous fungi. Several key points have been identified by Huang and co-workers to achieve commercialization of this process: strain improvement, morphology control, alternative substrates, process and downstream development.^[215] Genetical engineering of *E. coli* and *Saccharomyces cerevisiae* strains has been investigated, but the highest titers are obtained by naturally occurring or mutant *Rhizopus* fungi.^[218] Morphology control therefore results from the use of these filamentous fungi, which tend to agglomerate into clumps. To lower the energy requirements of the process, molding the fungi into pellets is more favorable.^[215] Glucose is the most widely studied and productive substrate so far, although fermentation of inexpensive waste streams or lignocellulosic biomass has been reported.^[220,221] During the fermentation, the pH is lowered and FmA may precipitate as it has a low solubility in water ($<10 \text{ g.L}^{-1}$). Thus, neutralizing agents such as Na_2CO_3 or CaCO_3 are required to control the pH and produce a stream of fumarate salts. Sodium salts are more soluble in water, allowing a more efficient downstream processing: the fermentation broth is filtered and the liquid stream is acidified to allow the crystallization of fumaric acid.^[222] The most productive system to date was reported by Cao and co-workers in 1996.^[223] Starting from glucose and a *Rhizopus* fungal strain, they designed an integrated process that continuously removes fumarate salts produced by adsorption on anion-exchange resins. Titrers up to 92 g.L^{-1} and productivities of $4.25 \text{ g.L}^{-1}.\text{h}^{-1}$ were obtained. Additionally, the self-cross-metathesis of acrylic acid (potentially biobased; see Section 2.1) into fumaric acid and ethylene has yet to be reported. Only acrylamides are known to undergo such cross-metathesis reactions into the corresponding fumaramides.^[224]

Efforts in the biobased production of FmA have stemmed from an increasing number of applications for this promising building block. It can be used as a food additive either directly or after hydration or amination to yield l-malic and l-aspartic acids, respectively (markets of 37 and 162 ktons.year⁻¹).^[217] In the paper and pulp industry, it is involved in Diels–Alder reactions with rosins.

Its insaturation also makes it interesting for the manufacture of unsaturated polyester resins that can be crosslinked by chemical or ultraviolet (UV) treatments.^[225,226] Notably, poly(propylene fumarate) has been involved in the manufacture of biocomposites for tissue engineering with biomedical applications.^[227] Unsaturated alkyd resins of FmA have also been used for coating applications.^[217]

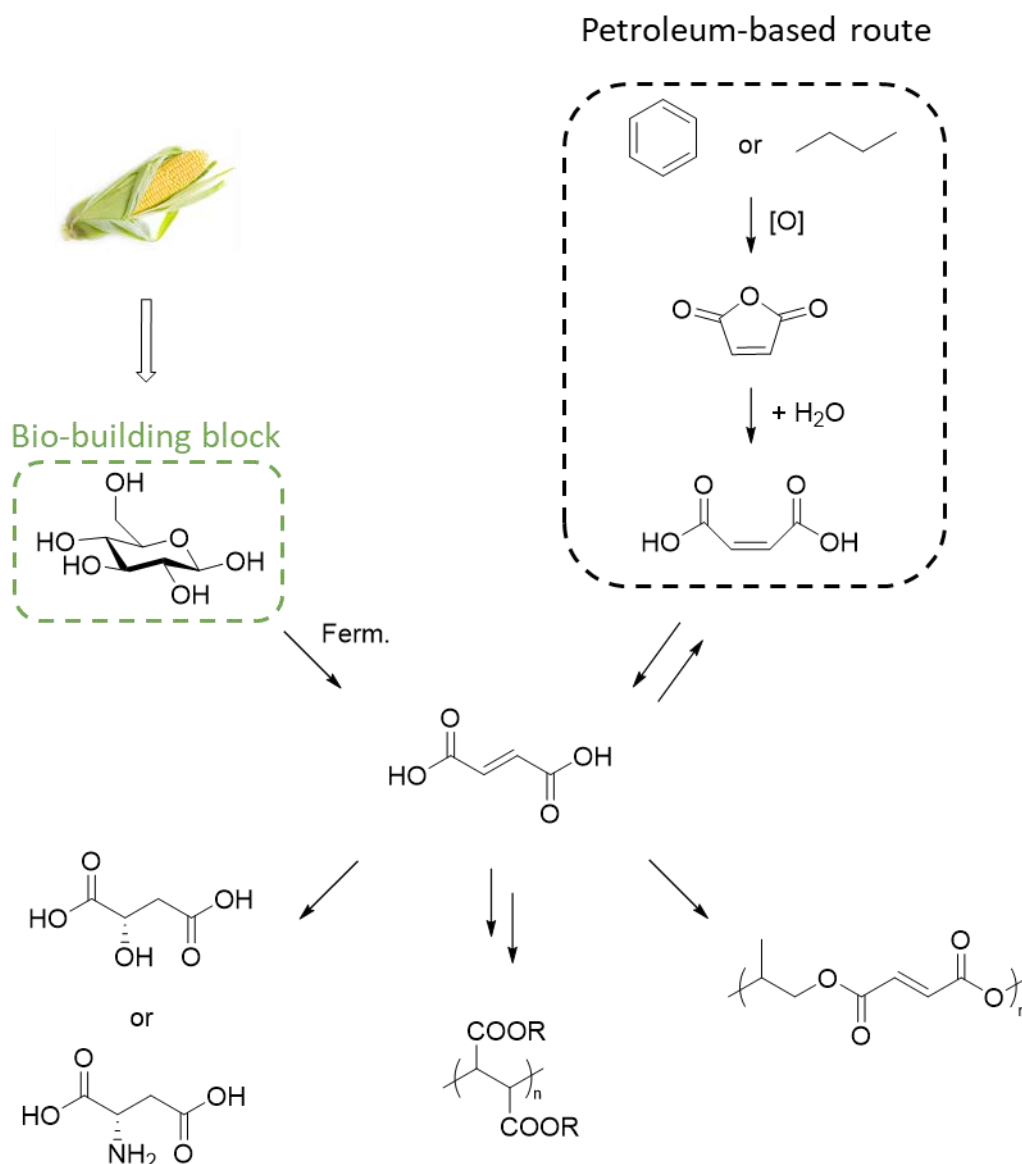


Figure 16. Production and uses of fumaric acid.

2.6.3. Muconic Acid

MuA is an acrylic analog bearing two double bonds and two carboxylic acid sites. Due to the double unsaturation, it exists in the form of three different isomers, namely, *cis,cis*-muconic acid

(ccMuA), *cis*-*trans*-muconic acid (ctMuA), and *trans,trans*muconic acid (ttMuA) (Figure 17). Its production and applications have been the object of a recent review,^[228] so this section will focus on selected examples.

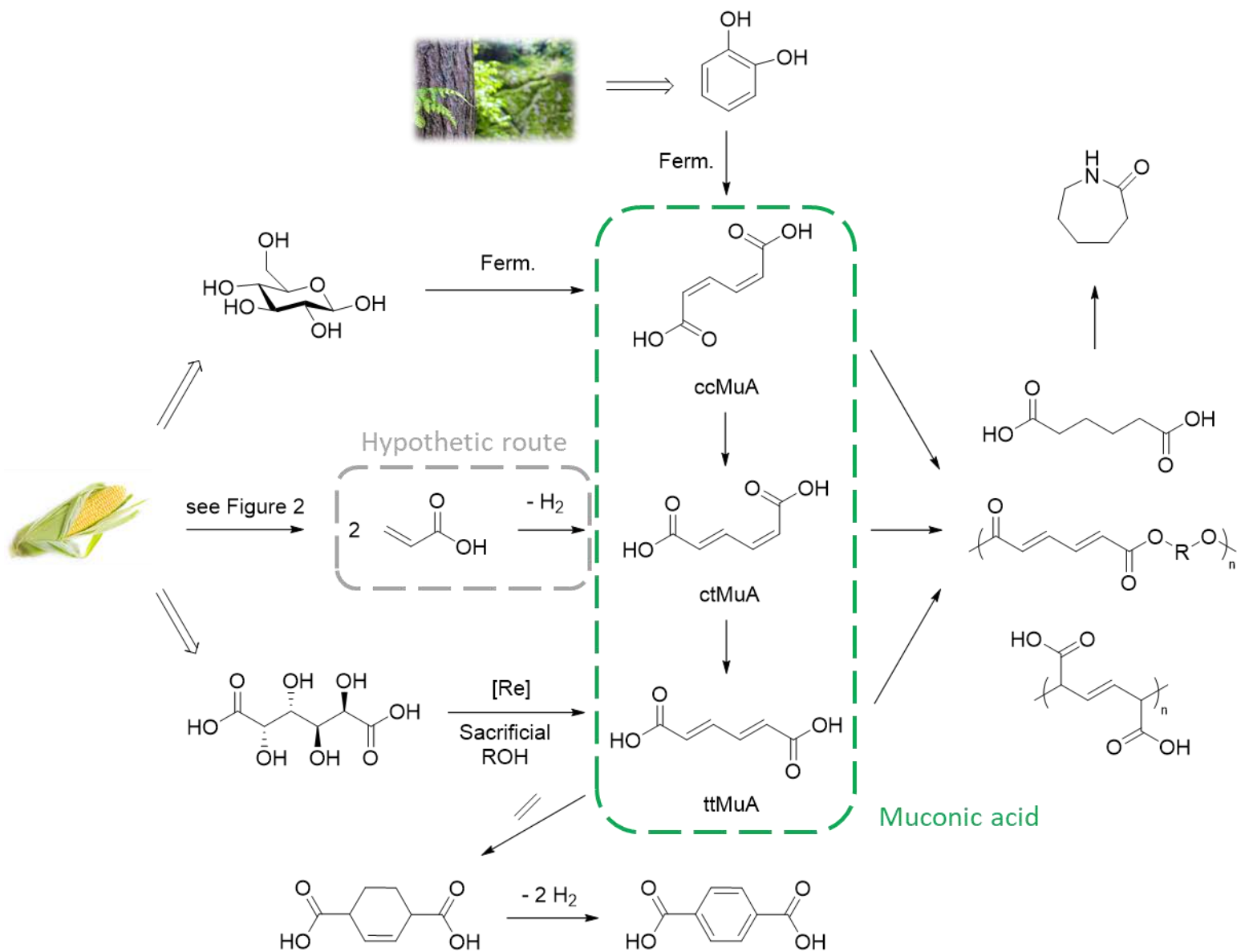


Figure 17. Muconic acid isomers production and applications.

First, isomerization reactions greatly influence the handling and potential uses of MuA. The less stable form is ccMuA, which is easily isomerized to ctMuA at room temperature under acidic conditions.^[228] Access to the more stable ttMuA is more difficult. Patents reported the use of iodine under UV light or a Pd/C catalyst to reach 80% yields in the isomerization to ttMuA.^[229,230] The low

concentrations required for these processes should however hamper their use on a higher scale.^[228] Recently, Tessonier and co-workers investigated the isomerization process in depth, heating solutions of ccMuA or ctMuA in various solvents.^[231,232] The yields were low and the reaction times long, although the addition of soluble Lewis acids permitted to obtain more competitive results. Control of the isomerization process is essential, as different routes for the production of MuA do not lead to the same isomers.

Nowadays, commercial MuA is mainly produced in its *cis,cis* form via fermentation processes (Figure 17).^[228] The *orthocleavage* of catechol by microorganisms can yield up to 100% ccMuA while the same reaction by chemical means (i.e., acids or heavy metal catalysts) is not as efficient. Other cheaper aromatic substrates, such as benzoate, have been investigated for the biosynthesis of MuA.^[233] The most promising advances are related to the production of these aromatic substrates by depolymerization of lignin. In 2015, Beckham and co-workers reported the synthesis of adipic acid from lignin via ccMuA.^[234] After investigation of various model aromatic compounds, they carried out the ccMuA production from a corn-stover derived, lignin enriched stream as the first proof of concept. In 2018, Wittman and co-workers reported titers up to 85 g.L⁻¹ for the fermentation of ccMuA from catechol by genetically engineered microorganisms.^[235] They also performed the lignin depolymerization into phenol and catechol (only 10% yield) prior to subsequent fermentation, although lower titers were obtained, probably due to the presence of contaminants in the lignin-derived stream. It should be noted that carbohydrates (corn or glucose) are required as an additional growth substrate for microorganisms producing ccMuA from aromatics. Another strategy for the biosynthesis of ccMuA is the use of glucose as the lone substrate. It takes advantage of the same kind of strains producing aromatic amino acids such as PhAl.^[233] However, productivities are still lower than those from aromatic compounds.

No direct biobased route to ctMuA has been reported so far, although Xu and co-workers have recently reported significant advances in that field.^[236] Taking advantage of a previously described

rhodium-catalyzed crosscoupling between *n*-butyl acrylate and *n*-butyl methacrylate,^[237] they developed an efficient ruthenium catalytic system for the stereoselective crosscoupling of various acrylates and methacrylates, yielding α -substituted *cis,trans* muconates. No polymerization of these compounds has been reported, so that the effect of the α -substituent on the properties of the obtained muconate is still unknown. Theoretically, the same crosscoupling involving two molecules of acrylic acid should lead to ctMuA, although no such reaction has been reported so far. The use of AA derived from renewable resources would make this route biobased as well. Finally, direct synthesis of ttMuA has been challenging. In 2013, Shiramizu and Toste reported the deoxydehydration of mucic acid, a hydrolyzed form of galactose.^[238] Catalyzed by an oxorhenium complex, this reaction however required the use of a sacrificial alcohol. Efforts in the direct synthesis of ttMuA or through the isomerization of ccMuA are thus still required.

Potentially important chemicals derived from MuA include adipic acid (3 Mtons.year⁻¹, precursor to nylon 6,6), ϵ -caprolactam (4 Mtons.year⁻¹, precursor to nylon 6), and terephthalic acid (47 Mtons.year⁻¹, precursor to PET).^[228] Notably, only ttMuA can give access to terephthalic acid due to its (*E,E*) conformation, which makes it available for a Diels–Alder reaction with ethylene. Moreover, MuA and its esters can be polymerized into materials with original properties. As a diacid, its polycondensation with diamines leads to unsaturated polyamides,^[239] while the same reaction with diols leads to unsaturated polyesters.^[240,241] The retention of the two conjugated double bonds permits to perform Diels–Alder reactions on the polyesters obtained,^[240] in addition to the usual radical crosslinking.^[242] Beckham noted slight differences depending on the isomer of MuA used for the polyester synthesis, with ttMuA yielding materials with higher T_g and strength.

2.6.4. Crotonic Acid

CrA and its corresponding esters are β -methyl substituted acrylic monomers (**Figure 18**). CrA is currently obtained by the oxidation of crotonaldehyde, which is itself derived from petroresources via the condensation of acetaldehyde.^[243] Starting from naphta, the overall yield of the process is about

30%.^[244] The *cis* isomer of CrA, also called isocrotonic acid, is less stable and is not commercially available. Obtaining CrA from bioresources has mainly been studied via three different routes: acetaldehyde production from ethanol, direct fermentation of CrA, and pyrolysis of PHB. The controlled oxidation of ethanol to acetaldehyde is probably the most suitable biobased route for the industry, as ethanol is a high tonnage renewable commodity and acetaldehyde could be used as a drop-in chemical in the current process. Recently, a 2-step process converting ethanol to CrA with a 62% overall yield has been suggested.^[245] First, acetaldehyde is obtained over a Cu or Ni catalyst on a SiO₂ support at 250 °C. Then, the conversion to CrA is catalyzed by mixed oxide of Ru, Co, and Ce in decalin at 100 °C. A continuous process using Cu/H₃PO₄ for oxidation and nano MgO for acetaldehyde condensation has also been proposed, with a lower overall yield (40%).^[246]

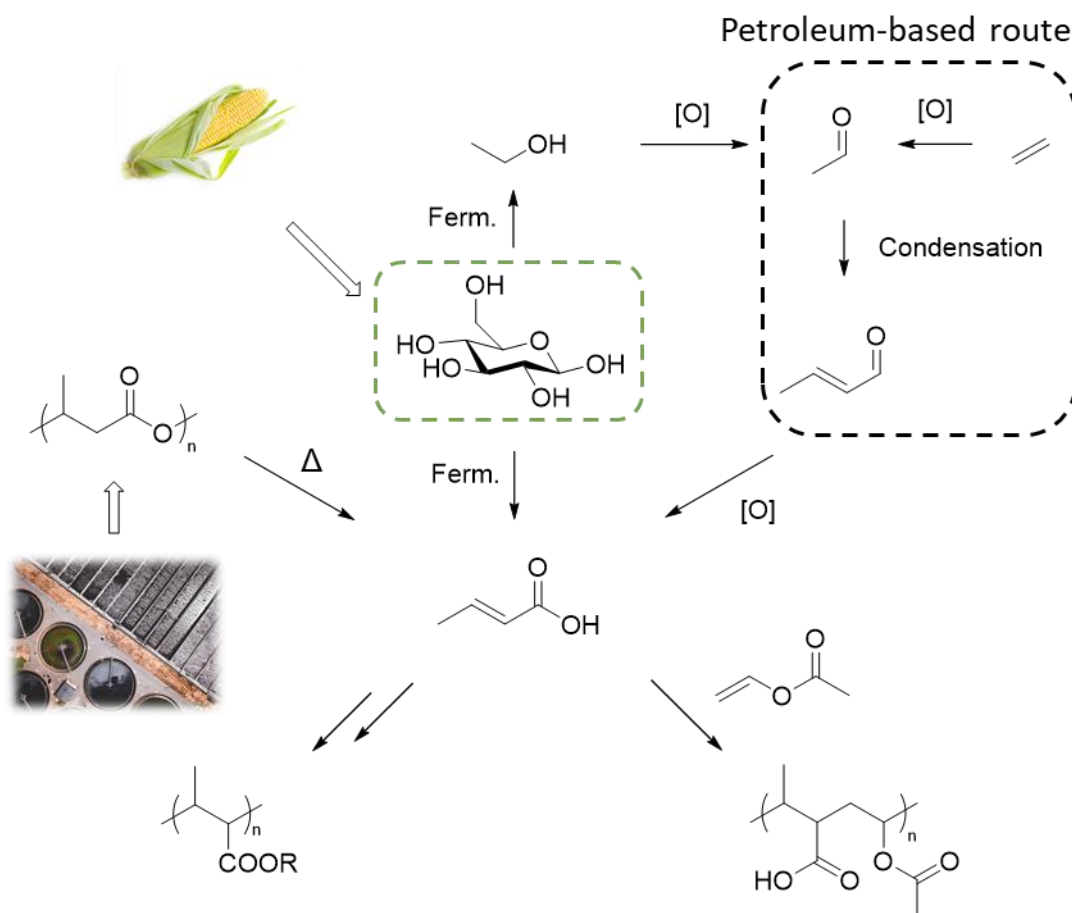


Figure 18. Production and uses of crotonic acid.

Literature on direct fermentation of crotonic acid is scarce, with only a few examples. In 2009, Insilico Biotechnology published a first patent on this process, starting from glucose.^[247] Using the same substrate, Gonzalez and co-workers engineered an *E. coli* strain to produce various fatty acids, including CrA at a titer of 200 mg.L⁻¹.^[248] Research is nowadays still dedicated to the identification of genetically engineered microorganisms suitable for CrA production.^[249,250] Quite notably, a relatively high titer of 3.2 g.L⁻¹ was obtained using glycerol as the primary substrate.^[251]

The most original approach to the biobased production of crotonic acid is the pyrolysis of PHB and other poly(hydroxyalkanoates) (PHAs). PHB, a biopolymer synthesized by various microorganisms from cheap substrates such as wastewater,^[252] can indeed be thermally degraded into CrA. This topic has been reviewed in 2006 and 2010, so that only the main contributions are highlighted in this paragraph.^[253,254] The studies on the thermal degradation of PHB were first intended to understand and optimize the processability of this biobased and biodegradable polymer. Werber and Baptist first identified crotonic acid as one of the products formed during the pyrolysis of PHB at 187 °C, slightly above its melting point.^[255] Grassie and Murray then quantified the CrA production during the pyrolysis of PHB at 500 °C (i.e., about 40%), the other products being small oligomers of PHB.^[256] They suggested a mechanism of *trans*-esterification and *cis*-elimination for the formation of the crotonate moiety during thermal degradation.^[257] The decomposition of PHB in acidic and alkaline media was also studied.^[258,259] Under basic conditions, 3-hydroxybutyrate is obtained with crotonate.^[260] The most notable advances on CrA production were however achieved by using Lewis acid catalysts during the pyrolysis of PHB. Abe and co-workers noted that the degradation of PHB was accelerated in the presence of calcium, magnesium, and sodium catalysts (loss of mass and molecular weight).^[261,262] In 2010, Ariffin et al. identified a strong increase of selectivity when using Mg(OH)₂ for the pyrolysis of PHAs, including PHB.^[263,264] With a 5 wt% catalyst loading, at 240 °C, they obtained a selectivity of 98% and a yield of 85% for crotonic acid. Since then, research has focused on process integration and the use of alternative substrates and energies. Metabolix issued a

patent encompassing the biosynthesis of PHAs by engineered microorganisms, their pyrolysis for the production of monomers including CrA (potassium, calcium, and lithium salts are cited as potential catalysts), and the subsequent metathesis of crotonates with propene to obtain acrylates and butene.^[46] Unpurified PHB from the fermentation broth was suggested as a potential raw material for CrA production.^[244,265] A mild pretreatment of PHB using a diluted NaOH solution improved the yield and purity of crotonic acid, as it presumably provides a catalyst for the reaction.^[266] Scott and coworkers suggested a thermal treatment of the unpurified PHB with methanol at 200 °C, 18 bars, yielding methyl crotonate with 60% selectivity.^[267,268] Subsequent metathesis with ethylene permitted to obtain propene and methyl acrylate. Remarkably, the techno-economic evaluation of such a process showed that methyl crotonate could be formed with a 90% purity and a presumably competitive 1.3 €·kg⁻¹ production cost.^[252] Waymouth and co-workers also showed that long chain 2-alkenoates produced from the pyrolysis of the corresponding PHAs could be metabolized by microorganisms together with methane to give PHB, which could subsequently be pyrolyzed to CrA.^[269] In an integrated process for PHA production, pyrolysis of the microbial biomass containing residual nonextractable PHAs was also performed to recover valuable crotonic acid.^[270] Alternatively, the degradation of PHAs and PHB under alkaline conditions has been reported to be substantially accelerated by microwave irradiation at moderate temperatures.^[271,272] However, the degradation of PHB in solution is not selective for CrA. Finally, it should be noted that further thermal degradation of crotonic acid is possible at high temperatures (above 300 °C), resulting in renewable propene and bio-oil.^[273–276] Overall, the bioproduction of CrA from PHB seems to have sufficient potential for the industrialization of the process.

Crotonic acid is thus a promising biobased building block. It can originally be derived rather directly from wastewater and is polymerized through its vinylic moiety, although these reactions are challenging. It should also be noted that crotonates can be converted into dimers by NHCs and thus

yield unsaturated diesters (analogous to itaconates) that could potentially be polymerized with diols to produce biodegradable polyester resins.^[277]

3. Polymerization of (Meth)Acrylic Monomers and Analogs

The vinylic monomers previously described find their most important applications in the preparation of polymeric materials. Various properties can be obtained by esterifying the corresponding acidic monomer before performing the polymerization step. The esterification step is beyond the scope of this review, but some important notions can be highlighted. On an industrial scale, esterification of (meth)acrylic monomers is usually carried out using heterogeneous catalysts at high temperatures, as illustrated by the conversion of MAA into MMA.^[54] At the laboratory scale, the direct acid-catalyzed esterification of (meth)acrylic acid is often not quantitative and thus requires a distillation step.^[278] Alternatively, acryloyl chloride or methacrylic anhydride can be reacted with the desired alcohol to quantitatively produce the corresponding (meth)acrylate.^[279–281] These reactions are convenient as they require only a simple workup, but the preparation of the reagents is not as atom economic as the direct esterification (**Figure 19**).

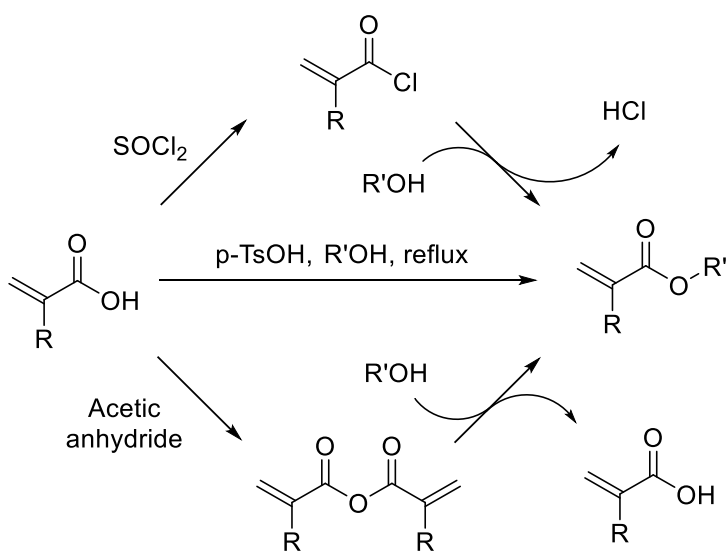


Figure 19. The various esterification routes at laboratory scale.

3.1. (Meth)Acrylates

Literature on the polymerization of acrylic acid, methacrylic acid and the various (meth)acrylates that can be derived from them is extremely rich. Long before their potential biosourcing, these monomers have been extensively studied as they provide access to a wide range of polymers with diverse properties. The aim of this section is to give a broad overview of this field. The reader is invited to consult dedicated reviews for more detailed and exhaustive analyses. Davis et al. covered the controlled polymerization of (meth)acrylates in 1994.^[282] In 2003, Webster critically reviewed the use of group transfer polymerization (GTP) with (meth)acrylates and compared it to other common polymerization techniques.^[283] Nuyken also provided a comprehensive description of the field of (meth)acrylate polymerization.^[284] More recently, Mosley described the production of acrylic plastics.^[285] In 2019, Guironnet and co-workers reviewed recent trends in catalytic polymerization, including (meth)acrylate polymerization.^[286]

The first observations of the polymerization of (meth)acrylic esters were reported in the late 1870's.^[284,285] Röhm extensively studied this topic at the beginning of the 20th century and promoted its industrialization, which led to the commercialization of PMMA in the 1930's. Since then, a wide variety of (meth)acrylic polymers has been reported, although PMMA remains the most widely studied and produced on a large scale (around 2 million tons).^[53] Different polymerization techniques have been developed and can be classified as follows: radical polymerization, which includes free radical polymerization and various reversible-deactivation radical polymerization (RDRP) techniques, such as nitroxide-mediated polymerization (NMP), atom transfer radical polymerization (ATRP), and reversible addition-fragmentation chain transfer (RAFT) polymerization, and anionic polymerization, which regroups classical anionic polymerization, GTP, coordination-type polymerization, and Lewis pair polymerization (LPP). Quite notably, cationic polymerization has never been reported for (meth)acrylic monomers as they are too electron-deficient, unlike styrenic monomers. Additionally, although most of the polymerization techniques described below apply to both acrylates and

methacrylates, they can have significantly different behaviors. In general, acrylates are more prone to transfer reactions due to the proton at the α position of the double bond. Acrylates can therefore lead to materials with higher dispersities, or even be non-polymerizable by systems that are able to polymerize methacrylates. These discrepancies are highlighted in the following section, where applicable.

3.1.1. Radical Polymerization

Free Radical Polymerization:

Free radical polymerization is employed commercially as a robust and inexpensive means to produce poly(meth)acrylates.^[285] Benzoyl peroxide and azobisisobutyronitrile (AIBN) are the most commonly used radical initiators, at temperatures up to 100 °C to ensure their thermal degradation and subsequent initiation of the polymerization process. Strict oxygen removal is necessary to avoid unwanted termination reactions with O₂. Alternatively, a redox, UV or plasma initiation can be used.^[284]

The process of free radical polymerization can be carried out in bulk, in solution, or via an emulsion. Bulk polymerization avoids the use of solvents and their subsequent removal, but attention must be paid to the solubility of the polymer in the liquid monomer. Indeed, the increase of conversion can increase the viscosity of the medium so that termination reactions are less likely, which in turn accelerates the consumption of the monomer. Known as the gel (or Tromsdorff) effect, this phenomenon is accompanied by a strong heat release and leads to a potential runaway of the reaction. Efficient mixing and heat removal systems are therefore key for a process that manufactures sheets, rods, tubes, and molding materials.^[284] Also, the use of solvents such as toluene or THF prevents the gel effect and has thus been widely applied as it allows effective control of the temperature of the medium. Most of the work described below were performed via solution polymerization, as it is suitable for research purposes. Solvent removal is usually carried out by adding a non-solvent (e.g., methanol for PMMA) to precipitate and collect the polymer formed. Finally, the radical polymerization

of (meth)acrylates can also be performed in a dispersed medium.^[287] Suspension and emulsion polymerization processes benefit from an increased concentration of monomers compared to solution polymerization, and therefore better reaction kinetics. In addition, they avoid the risk of Tromsdorff effect thanks to an efficient heat removal from the organic phase to the aqueous phase. For commercial applications, free radical polymerization in a dispersed medium may thus be preferred to bulk or solution polymerization.^[288] Emulsion polymerization has also been extensively studied in combination with reversible deactivation radical polymerization techniques such as NMP, ATRP, or RAFT.^[289] On the contrary, anionic polymerization is not possible in dispersed media as the initiators are usually sensitive to water.

Reversible-Deactivation Radical Polymerization by Organic Compounds:

The discovery of RDRP, previously called “controlled radical polymerization” techniques, is relatively recent, especially when compared to the development of anionic polymerization (see Section 3.1.2). In 1979, Rizzardo and Solomon used nitroxides to trap growing polymeric radical chains and studied the initiation mechanism of the free radical polymerization.^[290] A few years later, the same authors patented the first example of NMP, which displayed some characteristics of a living polymerization: controlled molecular weights, narrow polydispersities, and the ability to synthesize block copolymers.^[291] NMP is a powerful method that has been successfully applied to styrenic and (meth)acrylic monomers, and has recently been reviewed.^[292–294] It relies on the reversible deactivation of the growing polymer chain by a nitroxide (**Figure 20a**). The most common nitroxide is 2,2,6,6-tetramethylpiperidin-1-oxyl (TEMPO), first employed in the polymerization of styrene by the Georges group for the Xerox company,^[295,296] but also applicable to (meth)acrylates.^[294] However, the temperature of the process using TEMPO was high (150 °C), as was the polydispersity of the resulting material (higher than 1.4). Decisive improvements were obtained by Hawker and co-workers with the development of two powerful nitroxides, namely, *N*-*tert*-butyl-*N*-[1-diethylphosphono-(2,2-dimethylpropyl)] nitroxide (SG1) and 2,2,5-trimethyl-4-phenyl-3-azahexane-3-oxyl (TIPNO), which

were able to decrease the process temperature and dispersity, as well as expand the monomer scope of NMP (Figure 20b).^[297] Overall, NMP is a simple and robust polymerization technique, free of metal or sulfur traces, and is industrially applicable.^[293]

A similar RDRP mediated by organic compounds was reported in 2002 by a BASF research group.^[298] It is based on the use of 1,1-diphenylethene (DPE), which reversibly deactivates the growing polymeric chain by forming a sterically hindered and electronically stabilized free radical (Figure 20c).^[299,300] This polymerization technique has mainly been applied to MMA and is expected to be of industrial interest.

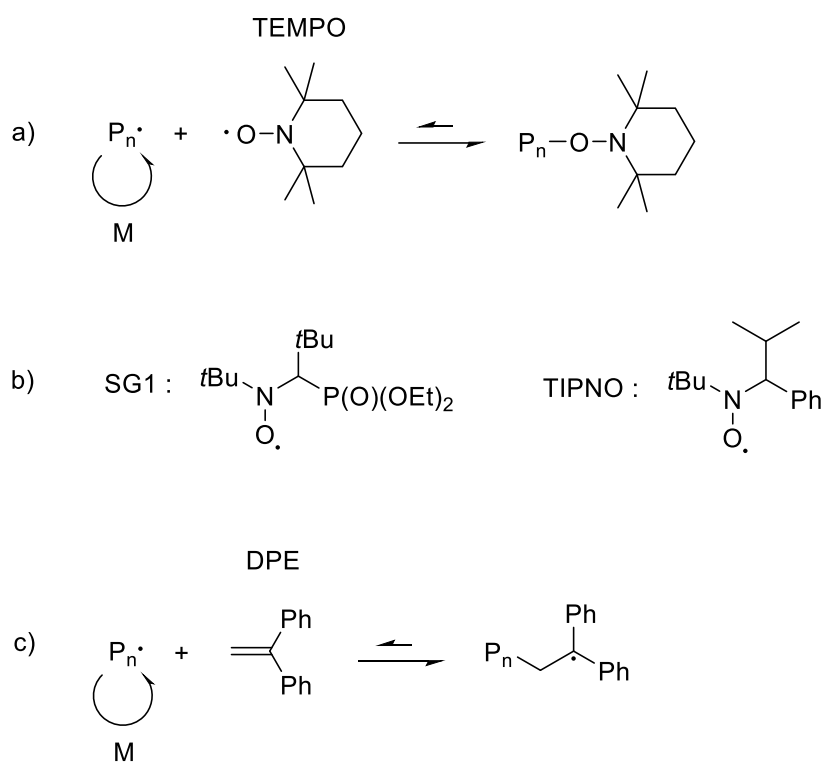


Figure 20. Reaction mechanisms of NMP and DPE-mediated radical polymerization.

Metal-Mediated Radical Polymerization: Catalytic Chain Transfer (CCT), Organometallic-Mediated Radical Polymerization (OMRP), and ATRP:

The use of metals for the controlled radical polymerization of (meth)acrylates has given rise to various polymerization techniques presented in **Figure 21**, namely CCT, OMRP, and atom transfer radical polymerization.^[301]

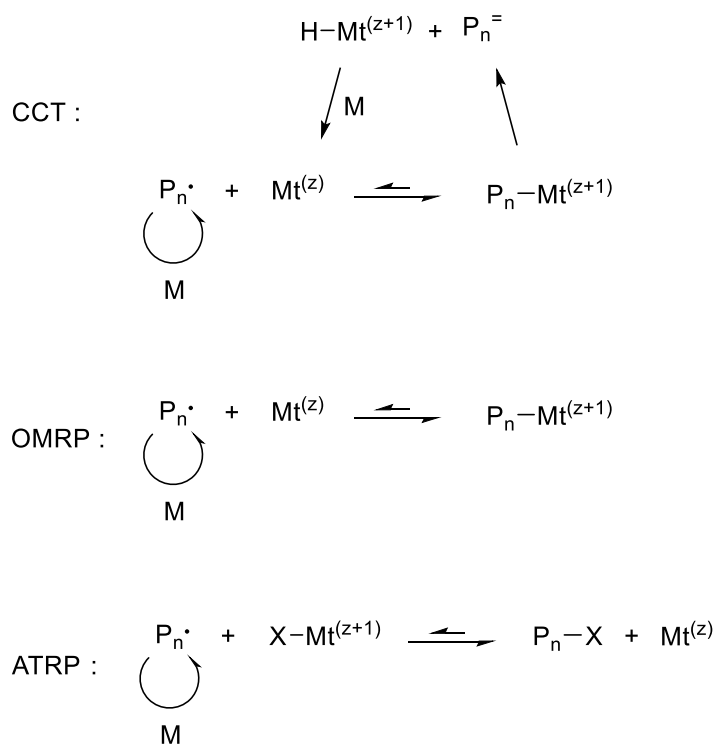


Figure 21. Reaction mechanisms of CCT, OMRP and ATRP.

CCT was first reported by Enikolopyan et al. in 1981, when they polymerized MMA with a cobalt–porphyrin catalyst.^[302] Remarkably, no metal other than cobalt has been found to promote CCT. The process is not reversible, since dissociation of the metallic center from the polymer chain results in a vinylic macromonomer (Figure 21).^[303,304] In the case of methacrylate polymerization, the vinyl macromonomer can be further used to form block copolymers with other methacrylates, or graft copolymers with styrenic or acrylic comonomers.^[304] For block copolymerization, the methacrylic macromonomer behaves as a chain-transfer agent similarly to a RAFT agent, with the advantage of being sulfur-free. However, it is not as efficient and requires low concentrations of monomer to reduce

the rate of propagation compared to chain transfer.^[304] Still, Haddleton and co-workers recently took advantage of an emulsion process to precisely prepare multiblocks of poly(methacrylates) using a macromonomer prepared by CCT.^[305]

OMRP proceeds via a mechanism similar to the one of CCT, except that the transfer of β -hydride to the metal is avoided, which allows (meth)acrylates to polymerize in a pseudoliving manner, as the deactivation of the growing species is reversible (Figure 21).^[301] The first example of OMRP was revealed by Wayland et al. in 1992, using a rhodium–porphyrin complex to polymerize acrylic acid, methyl and ethyl acrylate.^[306] A variety of other metals has subsequently proved suitable for OMRP, including cobalt, molybdenum, osmium, iron, palladium, titanium, chromium, and vanadium, although cobalt is the most studied one.^[307] As the reaction mechanism involves one organometallic compound per polymer chain as the dormant species, the amount of metal used is more important than in truly catalytic systems such as ATRP. Moreover, the final polymer contains a metal at the end of the chain, which limits the use of this polymerization technique when biocompatibility is required. OMRP is however more efficient than ATRP in the polymerization of less reactive monomers such as vinyl esters and amides, halogenated olefins, and simple alkenes.^[308]

Atom transfer radical polymerization was discovered at the same time by Wang and Matyjaszewski and Sawamoto and co-workers in 1995, when they applied it to styrene and MMA, respectively.^[309,310] Both researchers recently reviewed progresses in this field.^[311,312] Unlike CCT and OMRP, the organometallic complex is not directly covalently bound to the growing polymer chain in the ATRP process. Rather, it is present in the reaction medium in a reduced form, together with a halogencapped dormant polymeric chain. Occasionally, the metal can be oxidized by abstracting the halogen atom, yielding the active species (Figure 21). The process is thus called catalytic reversible deactivation. Various metals have been used, with a particular focus on iron due to its good biocompatibility,^[313] but the most common, efficient, and widely used is copper. Development of various types of ligands for the organometallic complex has been the subject of intensive research,

which permitted to lower catalyst loadings down to 100 ppm and expand monomer scope.^[312] Lowering the catalyst loading, however, increases the sensitivity to side reactions: various methods to regenerate the activator have thus been employed, either using chemical, electrochemical, photochemical, or mechanical means. Use of Cu⁰ in the form of powder or wire has also been studied, with two concurrent mechanisms postulated: supplemental activator and reducing agent ATRP (SARA-ATRP) and single electron transfer living radical polymerization (SET-LRP).^[312–315] Alternatively, avoiding the use of a metal catalyst has recently been proposed by photoinduced organocatalyzed ATRP.^[316] Overall, ATRP is one of the most popular polymerization techniques, as it allows the formation of block copolymers from various monomers (including (meth)acrylates) with controlled molecular weights and narrow polydispersities. In addition, the use of regeneration methods and/or oxygen scavengers allows this polymerization technique to be used in the presence of small amounts of O₂, illustrating its robustness and ease of use. One of the disadvantages of this method is however the use of copper, which can be detrimental for biological applications, even at low catalyst loadings.

RAFT Polymerization:

RAFT polymerization is one of the most recent and most efficient polymerization techniques^[317] It was first described in 1998 in a patent and a publication by Thang and co-workers.^[318,319] This area of research was reviewed on a regular basis since then.^[320–323] Hatton also recently covered its application to biobased monomers.^[24] Applied to various (meth)acrylic and styrenic monomers, RAFT polymerization exhibits living characteristics and proceeds via a degenerative transfer of growing polymer chains (**Figure 22**). Various chain transfer agents (CTAs) have been developed for RAFT polymerization, the most common being dithiobenzoates and trithiocarbonates. Depending on the monomer, careful choice of the CTA is desirable. Similar to OMRP, each polymeric chain obtained is capped with a CTA chain-end. The process is metal-free, but CTAs are usually odorous and colorful sulfur compounds. Efforts have been made to remove them

from the polymeric chain.^[324] Industrial applications of RAFT polymerization have also been hampered by the expensive synthesis of CTAs, but recent examples of large-scale commercialization of CTAs, as well as the use of the RAFT technique for specialty applications, have been described.^[325]

Finally, other degenerative transfer processes have been reported, such as iodine transfer polymerization (ITP) or organotellurium-mediated living radical polymerization (TERP), but they are less widely used.^[326,327]

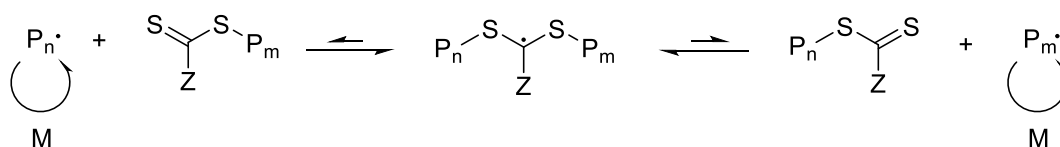


Figure 22. Reaction mechanism of RAFT polymerization.

3.1.2. Anionic Polymerizations

Classical Anionic Polymerization: Anionic polymerization was first described by Szwarc et al. in 1956, when they polymerized styrene at $-80\text{ }^\circ\text{C}$, using sodium naphthalene as an initiator.^[328] The polymerization was called “living,” as it was free of termination reactions and could therefore be used to prepare block copolymers. It was then successfully applied to (meth)acrylic monomers with a wide variety of anionic initiators, most of them being lithium alkyl derivatives.^[329,330] This process must be carried out at temperatures lower than $-40\text{ }^\circ\text{C}$, preferentially at $-78\text{ }^\circ\text{C}$ to suppress intramolecular backbiting termination reactions. It is thought to proceed via the formation of a highly reactive anionic growing polymer chain, stabilized by the electron-withdrawing ester group (**Figure 23**). Reaction rates are considerably higher than those observed for radical polymerization, and monomer conversion is usually complete within minutes. The addition of an excess of lithium salts (or other weak Lewis acids) has been found to stabilize the growing chain, thereby reducing the occurrence of side reactions and thus decreasing polydispersity. On the other hand, the addition of strong Lewis acids (such as trialkyl aluminum) has been shown to increase the polymerization rate by enhancing the electrophilicity of the monomer.^[330] A widely recognized advantage of anionic polymerization is the possibility to control

the tacticity of the polymer obtained, as a function of various parameters: initiating system, solvent, and temperature (**Figure 24**). This control on stereochemistry is even more important since it greatly influences the properties of the final material. For instance, isotactic PMMA has a T_g value of 50 °C while syndiotactic PMMA has a T_g value of 124 °C.^[331] Classical anionic polymerization suffers however from some drawbacks compared to other polymerization techniques: low temperature and highly pure monomers are mandatory, functional tolerance is low, and α -proton abstraction can occur on acrylic monomers, which results in low number average molecular weight (M_n) control.

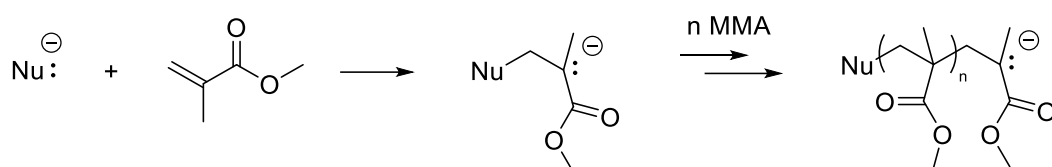


Figure 23. Reaction mechanism of anionic polymerization of MMA.

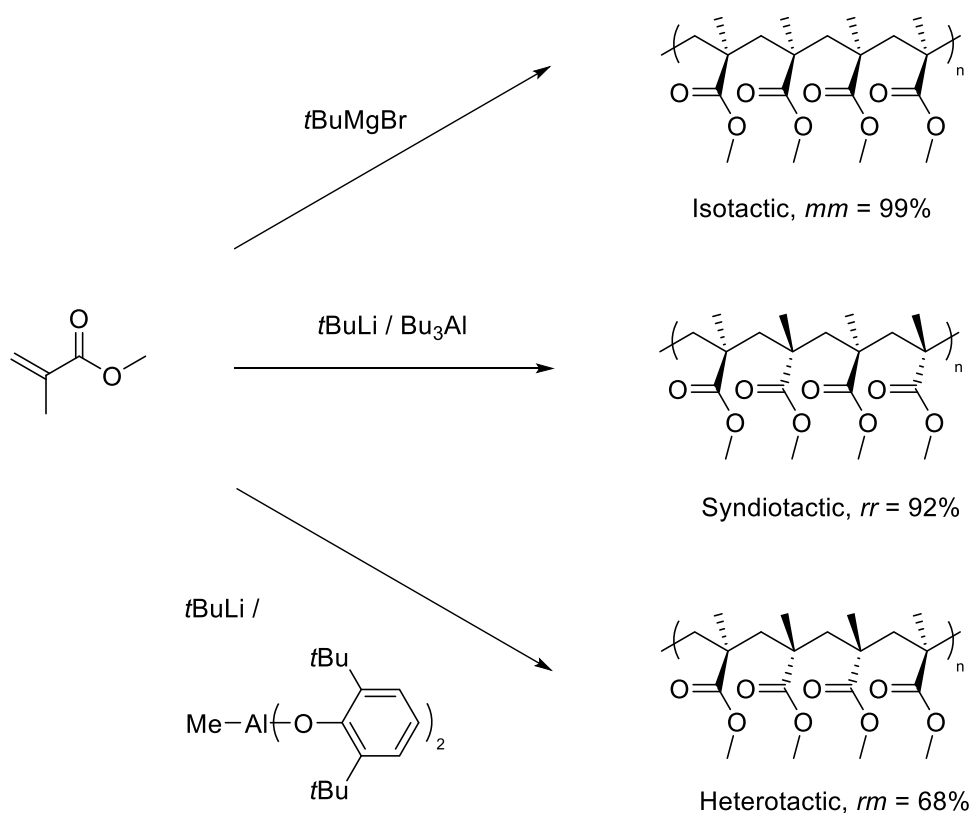


Figure 24. Stereospecific anionic polymerization of MMA in toluene at -78°C.

Group Transfer Polymerization:

GTP was first disclosed in 1983 by Webster and co-workers from a DuPont research group, as a powerful method to polymerize (meth)acrylates using organosilicon initiators.^[332] Since then, it has been widely used in industry and academia, and research advances were regularly reviewed.^[283,330,333] The process relies on the use of silyl ketene acetals (SKAs; **Figure 25**), which were supposed to attack the electrophilic monomer and transfer the silyl group intramolecularly (associative mechanism). A dissociative mechanism was later suggested. For the reaction to proceed, a Lewis base or an acid must be used with the SKA. A wide variety of functionalized SKAs, Lewis bases, and Lewis acids have been investigated. Good control over M_n , low dispersity, and the ability to form block copolymers with an extended monomer scope at room temperature are among the advantages of GTP. However, unlike anionic polymerization, it lacks stereocontrol. The high cost and instability of SKAs was also pointed out, but the recent report of the so-called “tandem-GTP” may mitigate this drawback. Indeed, Kakuchi and co-workers were able to produce the active SKA in situ from the corresponding tertiary silane and one unit of (meth)acrylic monomer, by activation with the strong Lewis acid $B(C_6F_5)_3$.^[334] Further work by the Kakuchi and Chen groups has allowed the study of various monomers, tertiary silanes and $Al(C_6F_5)_3$ as a strong Lewis acid.^[335–338]

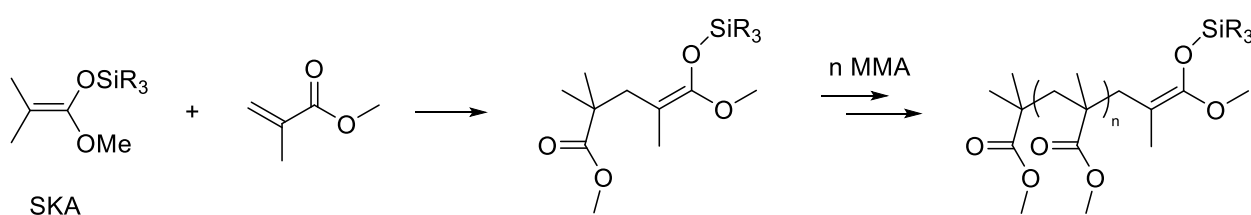


Figure 25. Simplified reaction mechanism of GTP of MMA.

Coordination-Type Polymerization:

The stereocontrolled polymerization of (meth)acrylates at or close to room temperature has so far only been reported with initiating systems composed of organometallic complexes, active through a coordination-type mechanism.^[339] At room temperature, a strong interaction between the polymer-

metallic center complex and the incoming monomer is indeed necessary to have a significant influence on the resulting tacticity. Seminal work in this field of research was published in 1992 by Yasuda et al. and Collins and Ward, on samarocene and zirconocene complexes, respectively.^[340,341] They reported the formation of syndiotactic PMMA ($rr\% = 80\%$) at 0 °C. Advances in the coordination-type polymerization of (meth)acrylates were reviewed by Chen in 2009.^[339] Notably, Inoue and co-workers used porphyrin and phenolate aluminum complexes to promote “immortal” polymerization of MMA, but no stereocontrol was reported.^[342] The coordination to the bulky organometallic complex was believed to protect the growing polymer chain from termination reactions, hence the name of “immortal” polymerization. This work can be viewed as a precursor of the LPP developed by Chen a few years later.

Organocatalyzed Polymerization and Lewis Pair Polymerization:

Avoiding the use of metals is often recommended for applications with biocompatibility requirements (although the nontoxicity of organic substitutes should be assessed). Thus, efforts were reported for the metal-free anionic polymerization of (meth)acrylates. Notably, carbanions stabilized by ammonium or phosphonium salts were able to perform such polymerizations in a living manner at room temperature.^[343–345] Recently, *N*-heterocyclic carbenes (NHCs) have attracted much attention due to their versatility and ease of synthesis.^[346] Concerning the polymerization of (meth)acrylates, they were first used in combination with SKAs in a GTP process, which Waymouth and coworkers and Taton and co-workers reported simultaneously in 2008.^[347,348] These systems produced materials with controlled M_n and narrow dispersities at room temperature. In 2012, Zhang and Chen were able to only use a sterically hindered NHC as an initiator for the polymerization of MMA at room temperature, making this process truly organocatalyzed.^[349]

Another emerging field in the polymerization of (meth)acrylates is the so-called Lewis pair polymerization, recently reviewed by the Chen group.^[333,350] The concept of frustrated Lewis pairs (FLPs) was first described by Stephan in 2008,^[351] and applied to polymerization two years later, as

Chen and co-workers described alane-based Lewis adducts with various encumbered Lewis bases as extremely active systems for the polymerization of MMA.^[352] LPP relies on the activation of the (meth)acrylic monomer by the Lewis acid and subsequent nucleophilic attack of the activated monomer by the Lewis base. Early developments were obtained with aluminum, but metal free systems were reported with boron as the Lewis acid.^[353] The classical Lewis bases are sterically hindered NHCs and phosphines, as well as newly developed *N*-heterocyclic olefins (NHOs).^[354] The LPP concept confers a good control on the polymeric structures obtained, as exemplified by recent research in this field. Chen pointed out the possibility to activate preferentially one monomer from a mixture of two acrylates to prepare block copolymers without sequential addition of the monomers.^[355] Zhang described a system for the synthesis of sequence-controlled multiblock copolymers at room temperature.^[356] However, attempts to increase the stereocontrol in LPP of (meth)acrylates at room temperature have not yet been successful.

3.2. Itaconic Acid Vinyl Polymerization

The vinyl polymerization of IA and its derivatives was reviewed in 1967 by Tate, a member of Pfizer, the largest supplier of IA at the time.^[357] The literature consisted mainly of patents, with only a few academic works on the topic. Marvel and Shepherd had previously highlighted the difficulty of homopolymerizing IA in water, obtaining only a 35% conversion of the starting material after 68 h at 50 °C in a 0.5 m HCl aqueous solution containing a potassium persulfate initiator.^[358] Tate attributed the difficulty of the IA homopolymerization to the low reactivity of its dianion form, hence the necessity to lower the pH in Marvel and Shepherd's work. An alternative and more efficient way to obtain poly(IA) is to first convert IA into IAnh or mono- or diester. Poly(IAnh) is readily hydrolyzed in water while polyitaconates can be hydrolyzed under acidic or basic conditions.^[357] More recently, the copolymerization of IA with pyrrolidones,^[359] methacrylated polyethylene glycol macromonomers,^[360] 2-hydroxyethyl methacrylate,^[361] or 2-hydroxyethyl acrylate^[362] has been reported to prepare hydrogels used in drug delivery. Xie and co-workers highlighted the potential of

star-shaped copolymers of IA and AA as glass ionomer cements for restorative dentistry.^[363] The homopolymerization of IA is still under investigation, as Bednarz et al. suggested the use of choline (a quaternary ammonium salt) to accelerate the polymerization of IA in aqueous media by activating the decomposition of the persulfate initiator as well as increasing IA solubility.^[364,365] Also, Durant's research led to the foundation of Itaconix in the early 2010's, a company commercializing poly(IA)-based detergents and chelants, while holding several patents on the topic.^[366,367]

Much like acrylic and methacrylic acid, IA can be converted into various polymerizable esters, yielding polymers with multiple properties. Herein, we review the studies related to the most common itaconates. In 1967, Tate described the polymerization of itaconates bearing methyl, ethyl, *n*-propyl, *n*-butyl, 2-ethylhexyl, and tridecyl substituents.^[357] The relatively low molecular weights obtained were attributed to the higher radical transfer to the monomer than for usual (meth)acrylates, due to the stabilizing effect of the second carbonyl moiety (**Figure 26**). Cowie later synthesized various β -monoesters of IA with a 100% selectivity and prepared the corresponding homopolymers.^[368] Various diesters of IA were prepared as well, with the T_g value of the respective polymers ranging from 144 °C (dicyclohexyl itaconate) to -85 °C (diheptyl itaconate), highlighting the great potential applicability of these materials. In 1987, Horta et al. investigated for the first time the tacticity of polyitaconates, starting from the benzyl derivative.^[369] Sato and co-workers then extended these investigations to dibutyl itaconate (DBI), and studied the influence of the temperature of radical polymerization on stereospecificity.^[370] Isotactic-enriched polymers were obtained at elevated temperatures (60% of *mm* triads at 120 °C) while a syndiotactic character was observed at low temperatures (80% of *rr* triads at -78 °C), as is observed for MMA. It is important to point out here that no successful anionic polymerization of itaconates has been performed so far, owing to the acidity of the methylene protons (the same protons that increase the transfer to the monomer in radical polymerization). Itaconimide polymerization could be initiated by *sec*-butyllithium (*sec*-BuLi), due to the methylene protons lower acidity, although only modest molecular weights and dispersities were obtained.^[371] Recent studies on

the potential group transfer polymerization of DBI failed to achieve degrees of polymerization higher than 8.^[372] Thus, RDRP techniques are the only way of precisely synthesizing itaconate polymers. Barner-Kowollik and co-workers reported in 2004 and 2006 the polymerization of itaconates by RAFT and ATRP methods.^[373,374] Satoh et al. later applied RAFT techniques to synthesize elastomeric block copolymers of itaconates (soft segment) and itaconimides (hard segment).^[375] IAnh RAFT polymerization is also possible.^[376] Recently, the group of Goto successfully used the ITP technique for itaconates.^[377] These controlled radical polymerization methods are often employed to prepare well-defined block copolymers, but it is worth mentioning that itaconates have also been randomly copolymerized with isoprene or myrcene to yield biobased elastomers with improved properties.^[378–380]

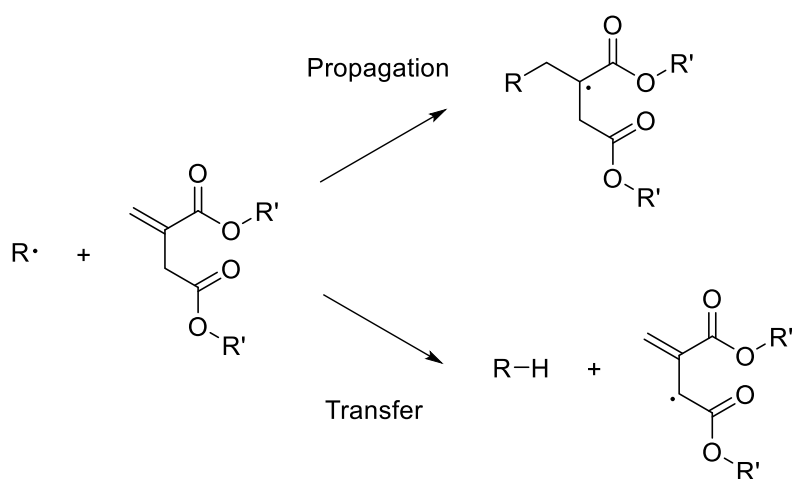


Figure 26. Propagation and transfer reactions during the polymerization of diitaconates

The vinyl polymerization of IA and its derivatives has thus been more challenging than that of its (meth)acrylic counterparts, but the high variety of properties derived from its two carboxyl groups should merit additional synthetic investigations.

3.3. α -Methylene- γ -butyrolactone and Analogs

The polymerization of methylene butyrolactones has been widely studied and led to several reviews.^[16,381–386] Interest in this field has been sparked by the potential biosourcing of these

monomers, associated with their numerous potential applications as fibers, films, low-pressure laminating resins,^[156] dental composites,^[387] tougheners,^[388] coatings,^[389] optical fibers,^[390] polymeric electrolytes,^[391] thermoplastic elastomers,^[392] superabsorbents,^[393] or pressure-sensitive adhesives.^[394] Herein, we review the polymerization of MBL, γ -MMBL, β -MMBL, and other methylene butyrolactones in successive paragraphs.

MBL polymerization:

As mentioned earlier, McGrow and Morristown were the first to patent the synthesis and vinyl polymerization of MBL and γ -MMBL in 1953.^[156] The free radical polymerization of MBL, initiated by peroxides or UV light, in solution or emulsion, gave after 12 to 24 h clear, hard transparent resins melting at 230–240 °C in the case of PMBL. More than 25 years later, Akkapeddi studied the free radical and anionic polymerization of MBL.^[395] While the radical polymerization of MBL led to slightly syndiotactic-rich polymers with a T_g of 195 °C, materials prepared by anionic means were isotactic (75% *mm*). Polymerization rates would have been slightly higher than those obtained with MMA, a widely observed feature due to the near planar conformation of the 5-membered ring. This structure allows efficient delocalization of the exocyclic double bond and thus stabilization of the propagating species. Ueda et al. later described the kinetics of the AIBN-initiated polymerization of MBL in dimethylformamide (DMF), one of the few solvents able to solubilize both monomer and polymer.^[396] The DuPont research team that developed group transfer polymerization successfully applied this process to a wide range of acrylic monomers, including MBL.^[397] By the end of the 1990's, it was also copolymerized by various techniques with acrylonitrile,^[156,398] butadiene,^[156] styrene,^[156,398–400] MMA,^[398] acrylamides,^[398] and vinyl thiophenes.^[401] In 2008, Uno et al. used MBL and comonomer poly(ethylene oxide) methyl ether methacrylate to prepare polymer electrolytes with improved thermal stability.^[391] They did so using the recently developed ATRP technique, which prompted its inventors to investigate the ATRP-initiated homopolymerization of MBL.^[402] This seminal work described a rapid polymerization in DMF, with conversions up to 90%, molecular

weights ranging from 15 000 to 60 000 g.mol⁻¹ and polydispersities of 1.1. The authors were also able to obtain block copolymers of MBL with *n*-butyl acrylate and MMA. Matyjaszewski and co-workers further illustrated the efficiency of this polymerization with various compositions and architectures.^[392,403] ATRP is now a popular technique for the preparation of block copolymers of MBL. Hillmyer and co-workers used it to prepare biobased thermoplastic elastomers by ring-opening polymerization of menthide followed by ATRP of MBL,^[404] or γ -MMBL which gave better properties for the target application as pressure-sensitive adhesives.^[394] Fors and co-workers recently produced a 100% IA-based copolymer with a similar architecture.^[146] The polyester was prepared from dimethyl succinate and 2-methyl-1,4-butanediol, and the subsequent triblock copolymers were obtained by growing PMBL at both ends of the macromonomer. Interestingly, Mosnáček and co-workers recently applied photo-ATRP to MBL with Cu loadings of 50–200 ppm, avoiding the need of deoxygenating the monomer mixture.^[405] Materials with molecular weights of 15 000 g.mol⁻¹ and dispersities of 1.2 were obtained after 6 h at room temperature. RAFT polymerization can also be employed, as illustrated by Fors, who obtained well-defined materials with MBL and Me₂BL derived from IA.^[144] Over the last decade, the Chen group issued a number of publications on MBL and γ -MMBL polymerization using various initiators and/or catalytic systems, most of them being more active for γ -MMBL. Hence, these studies are reviewed in the next paragraph. However, a notable example of MBL polymerization developed by this group is its controlled vinyl-addition/ring-opening polymerization/crosslinking (**Figure 27**).^[149] By adjusting the ratio between the homoleptic lanthanum amide catalyst and the free alcohol initiator, they were able to tune the microstructure of the material. In particular, they identified that the La-NR₂ adduct preferably leads to vinyl-addition polymerization while La-OR leads to ROP under optimal conditions. Alternatively, MBL was used to prepare superabsorbents by opening of the lactone ring after vinyl polymerization. This concept was first described by Akkapeddi in 1979, when he performed the alkaline hydrolysis of PMBL.^[395] He obtained a highly hydrophilic polymer that was, however, insoluble in water. Notably, the acidification of the medium led to complete lactone recovery.

In 2013, Mullen et al., from the Segetis company (producer of LvA), optimized the preparation of such superabsorbent materials by adding crosslinkers and 5 wt% of AA to stabilize the emulsion.^[393] After partial saponification, the resulting polymers could absorb up to 50 times their weight in water. More recently, Mosnáček and co-workers developed an alternative strategy:^[406] they first saponified 100% of the monomer to obtain sodium 4-hydroxy-2-methylenebutanoate (SHMB), and then copolymerized it with acrylamides and crosslinkers (**Figure 28**). Although the homopolymerization of SHMB is difficult due to possible back conversion to the lactone in an acidic medium, its copolymerization with acrylamides was effective. The obtained materials were able to absorb 820 times their weight in water, thanks to the complete opening of the lactone ring. The authors recently further studied the reaction conditions of this synthesis,^[407] as well as the ecotoxicological properties of the hydrogels obtained for potential cell culture applications.^[408] Hutchinson and co-workers developed a similar material from γ -MMBL.^[409] A final original example of polymerization of MBL was published by Agarwal and Kumar in 2011.^[410] They performed its initiator-free copolymerization with 2-methylene-1,3-dioxepane (MDO) at 70–120 °C, in DMF or bulk (**Figure 29**). MDO contains a nucleophilic double bond that can provide random polyester linkages to the polymer. This feature confers partial degradability to the material, along with flexibility and solubility in organic solvents for improved processability. These properties are also believed to be accessible via the controlled vinyl-addition/ROP developed by Chen and co-workers.^[149]

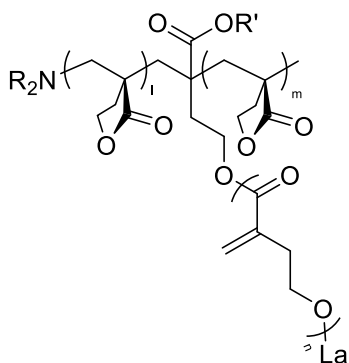


Figure 27. Potential molecular structure of a polymer of MBL obtained by vinyl addition and ROP.

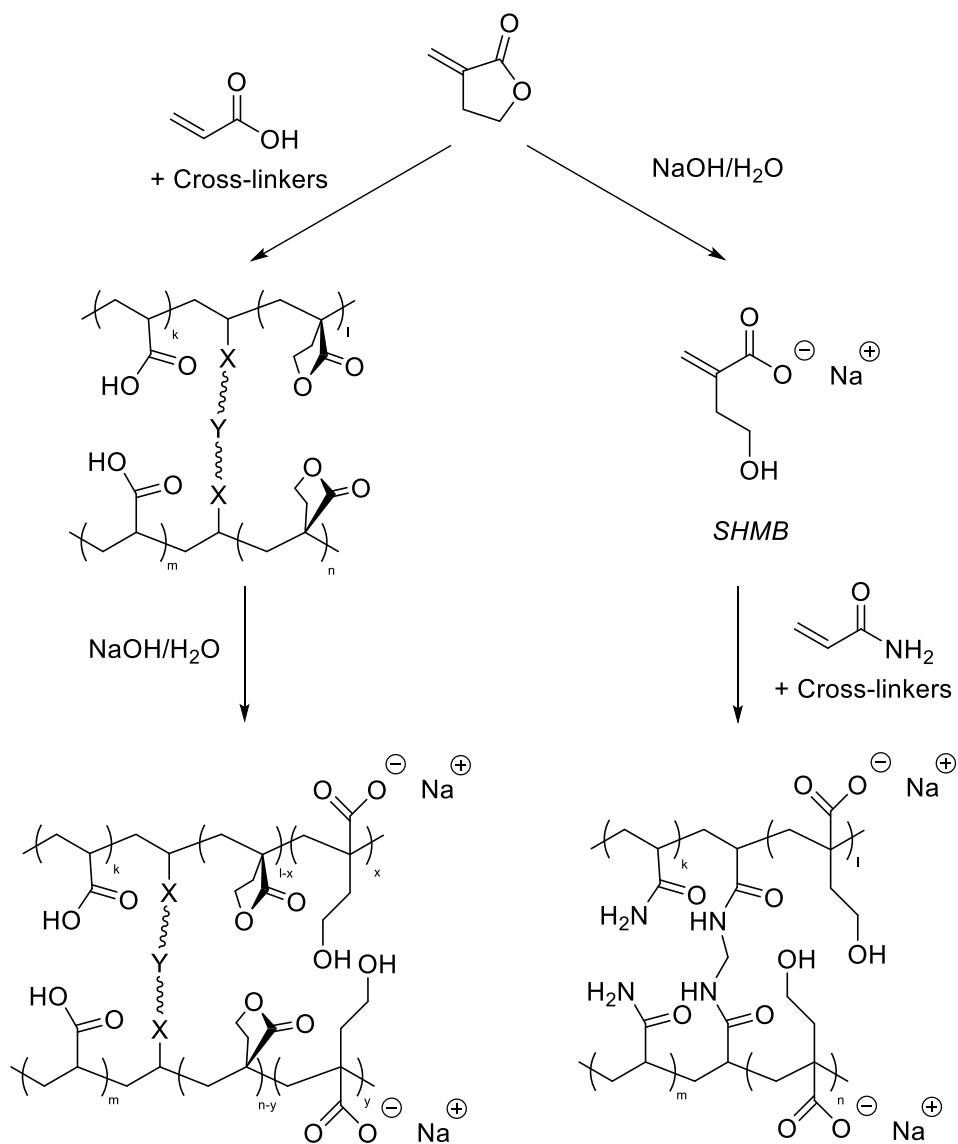


Figure 28. Two different approaches for superabsorbent synthesis.

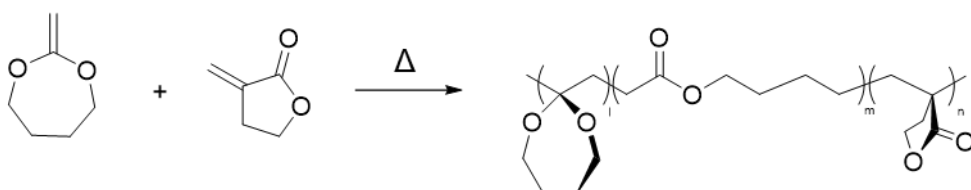


Figure 29. Temperature initiated copolymerization of MBL and MDO yielding a random copolymer.

γ -MMBL polymerization:

After its first mention by McGrow and Morrystown,^[156] γ -MMBL was only rarely studied, due to its low availability. In 1984, Stille and co-workers studied the free-radical, anionic, and group

transfer polymerizations of both racemic and enantiopure γ -MMBL.^[411] They found that all polymerization means produced a syndio-rich atactic polymer from racemic γ -MMBL ($T_g = 215\text{ }^\circ\text{C}$), while enantiopure γ -MMBL yielded a completely isotactic polymer (>99% *mm*), thanks to a suggested chain-end stereocontrol (**Figure 30**). However, chiral monomer preparation can be expensive and the synthesis of γ -MMBL developed by Manzer only produces a racemic mixture.^[176] The disclosure of a biobased route to this monomer prompted intensive research on its polymerization in recent years. By free or controlled radical polymerization, copolymers with styrene,^[412–415] MMA,^[413,416] and *n*-butyl acrylate^[414] were described, in solution or emulsion. However, most of the studies on γ -MMBL have been published by the Chen group, whose work has focused on its polymerization at room temperature (catalysts presented in **Figure 31**). In 2010, they first applied coordination-addition polymerization to γ -MMBL using highly active samarocene complexes (turnover frequency (TOF) = 3000 h⁻¹), yielding polymers with controlled molecular weights (between 17 000 and 70 000 g.mol⁻¹) and moderate dispersities (1.2 to 2.0).^[417] Sophistically engineered rare earth metal complexes could achieve even higher activities (TOF = 30 000 h⁻¹).^[418] Although they were less productive, Zrand Ti-based complexes were also able to perform the reaction with a slight syndiotactic enrichment.^[419] Anionic polymerization was also investigated, catalyzed by an aluminate complex derived from Al(C₆F₅)₃ and KH (TOF = 482 h⁻¹).^[420] GTP with suitable silyl ketene acetals gave extremely narrow distributions of polymer chain-lengths (<1.05) and exhibited good activity (TOF = 600 h⁻¹).^[421] Inspired by this work, Zhang and co-workers established that catalytic systems based on SKA and E(C₆F₅)₃ (E = Al or B) as a Lewis acid, permitted to polymerize in a living manner both γ -MMBL and MBL, thus obtaining blocks of the corresponding polymers.^[422,423] Chen and co-workers also developed FLP and classical Lewis pair (CLP) polymerization for γ -MMBL. Using the Lewis acid Al(C₆F₅)₃ and Lewis bases such as PPh₃, PMes₃, or sterically hindered NHCs, the corresponding polymer can be obtained rapidly (TOF up to 48 000 h⁻¹).^[352] Later, they developed FLPs of phosphine and borane sharing the same molecular backbone, instead of inducing frustration with sterically demanding substituents.^[424] However, the

most active catalyst in this work was a CLP that could reach TOF up to 24 000 h⁻¹. They also studied the use of amines as Lewis base, inducing transfer hydrogenation on MMA but extremely fast polymerization of γ -MMBL (TOF = 96 000 h⁻¹), yielding high molecular weights (up to 129 kg.mol⁻¹) with moderate dispersity (2.2).^[425] This work prompted several recent studies on the use of FLPs for polymerization, often highlighted by a good control of the molecular weight and dispersity of the resulting polymers.^[426-429] Finally, Zhang and Chen notably contributed to the field of organocatalysis by the development of highly active NHCs and phosphazene superbases. In 2012, they first reported that *It*Bu could convert up to 800 equivalents of γ -MMBL in less than 1 min, while it was not active for MMA.^[430] They later found that, as was observed with amines in FLPs, the NHC caused enamine or dimer formation in the presence of MMA.^[431] However, it could polymerize γ -MMBL in DMF with TOF up to 440 000 h⁻¹. Regardless of the catalyst loading, molecular weights were limited to 70–85 kg.mol⁻¹ due to internal chain transfer. This chain transfer was nevertheless not deactivating as the base formed could start another growing chain, making the process truly catalytic. Phosphazene superbases were not as active (TOF = 30 000 h⁻¹) but could yield higher chain lengths ($M_n = 135$ kg.mol⁻¹) with broader dispersities ($M_w/M_n = 2.0$ to 4.0).^[432]

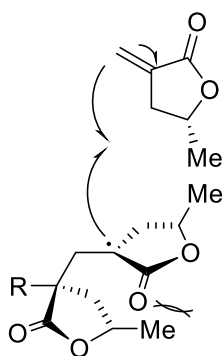


Figure 30. Chain-end stereocontrol: influence of the penultimate group on the conformation of the attacking group.

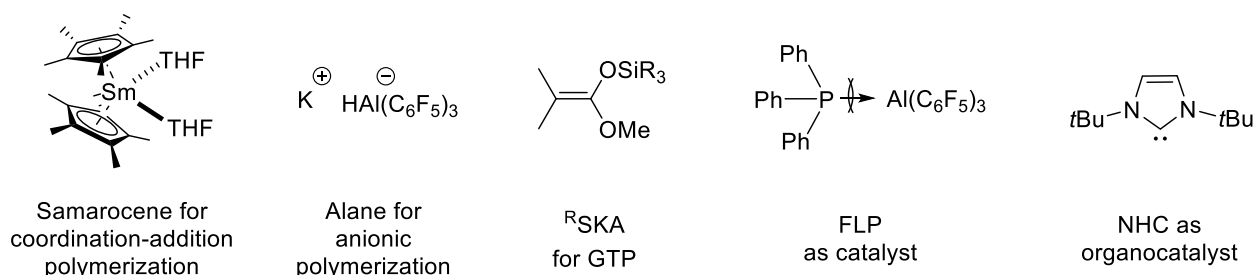


Figure 31. Catalytic systems used by the Chen group for the polymerization of γ -MMBL.

β -MMBL and other methylene butyrolactones polymerization:

Polymerization of β -MMBL was investigated to a lesser extent, although it provides some interesting features. It was first reported by Pittman and Lee in 2003, after they successfully homo- and copolymerized it with styrene by free-radical means.^[433] The resulting polymer had similar properties to those of poly(γ -MMBL) and the reaction gave similar kinetics, seemingly unaffected by the methyl group in β position. Using zirconocene catalysts, Chen et al. could prepare an isotactic poly(β -MMBL) (>99% *mm*), with an extremely high T_g of 288 °C.^[434] As in the work of Stille and co-workers,^[411] they noticed that free radical polymerization of racemic β -MMBL led to an atactic material while the free radical polymerization of enantiopure β -MMBL resulted in a fully isotactic polymer. Isotactic poly(β -MMBL) can however be obtained from racemic β -MMBL when using their zirconocene catalysts. In 2013, they also obtained *iso*-poly(β -MMBL) using homoleptic complexes of rare earth metals and thus suggested a chain-end stereocontrol that was confirmed by a density functional theory (DFT) study.^[435] Later, they applied the organocatalyst *ItBu* to the polymerization of β -MMBL on a 10 g scale, but surprisingly gave no indication on the tacticity of the final material.

Other methylene lactones have been investigated by Gowda and Chen. Vinyl-substituted MBLs were synthesized following Parrain and co-workers' procedure.^[161,436,437] Their polymerization was notably chemoselective, thanks to the high reactivity of the conjugated exocyclic double bond. However, no scalable biobased route to these monomers has been reported so far. Tang and Chen also studied the polymerization of β -HMBL (tulipalin B).^[438,439] While free radical polymerization allowed

to selectively polymerize the double bond, the use of NHCs or superbases as catalysts yielded complex structures owing to the potential conjugate Michael addition as well as the oxa-Michael addition on this polar vinyl monomer. The materials obtained were likely branched copolymers of poly(vinyl-ether lactone)s due to proton transfer with the OH group (**Figure 32**).

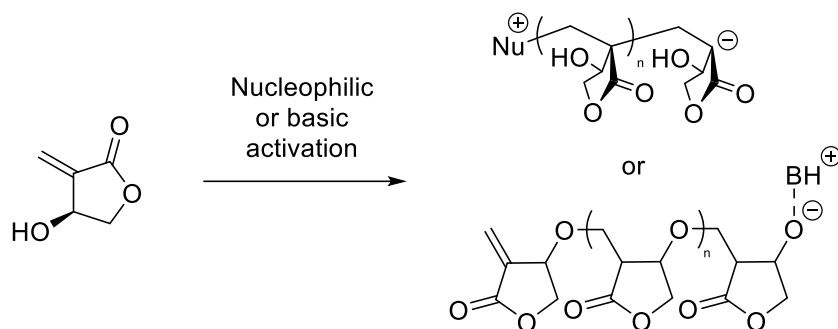


Figure 32. Two types of polymerizations that can be obtained from β -HMHL.

Over the past decade, the polymerization of methylene butyrolactones has thus been widely studied. Their obtention from biomass requires multiple steps that may be too costly to consider them as potential commodities. However, the unique properties of the resulting materials should spur their use as specialty monomers for value-added applications.

3.4. Other Biobased Lactones

3.4.1. Methylene Lactide

After describing the synthesis of MLA, Scheibelhoffer et al. also performed its free radical polymerization but only obtained low molecular weights (inferior to $1000 \text{ g}\cdot\text{mol}^{-1}$).^[202] MLA was then neglected for decades, until Jing and Hillmyer reported its use in a Diels–Alder reaction with cyclopentadiene in 2008 (**Figure 33**).^[440] The resulting monomer could be polymerized by ROP to yield PLA-type materials with improved properties (e.g., higher T_g). This seminal work prompted additional reports describing the ROP of MLA functionalized with other dienes,^[441] polyethylene glycol,^[442] thiols,^[443,444] or terminal alkenes through cross-metathesis.^[445] In 2015, Britner and Ritter investigated the free-radical vinyl-addition polymerization of MLA synthesized from L-lactide.^[446]

After only 2.5 h at 70 °C, they obtained an isotactic-rich polymer (as observed for chiral γ -MMBL and β -MMBL) with high molecular weight (up to 100 kg.mol⁻¹), moderate dispersity (2.5), and a remarkably high T_g of 244 °C. They were also able to perform the aminolysis of PMLA in DMF at room temperature, without any catalyst. This observation was attributed to a self-activation of the carbonyl groups by dipole–dipole interaction within the polymer chain. Later, the same authors published a complementary study on the kinetics of free-radical and RAFT-mediated MLA polymerization, as well as its copolymerization with styrene, MMA, and *N,N*-dimethylacrylamide.^[447] The reactivity of MLA was found to be similar to that of MMA. However, it was observed that MLA could self-initiate its polymerization in AIBN-free experiments. RAFT polymerization was surprisingly inefficient, with dispersities above 1.5 and molecular weights substantially higher than the theoretical ones, maybe owing to the singular reactivity of MLA. Chen and co-workers also studied briefly the free-radical vinyl polymerization of MLA, obtaining materials with properties similar to those reported ($M_n = 180$ kg.mol⁻¹, T_g ranging from 229 to 254 °C).^[448] Copolymers with γ -MMBL and dimethylene lactide were also prepared. Their attempts to perform the direct ROP of MLA were however unsuccessful, as the conjugated double bond is probably too reactive toward the catalysts used for this reaction.

Recently, the IBM company issued a publication and several patents on the preparation and postfunctionalization of PMLA. Boday and co-workers reported the AIBN-initiated polymerization of MLA at 60 °C in THF.^[449] After 30 h, they obtained a polymeric material ($M_n = 20$ kg.mol⁻¹, $M_w/M_n = 1.8$, $T_g = 246$ °C) that is not easily solubilized in common organic solvents. However, in a mixture of THF and alcohol, they could perform the transesterification of the polymer, catalyzed by triazabicyclodecene at 60 °C. A subsequent patent essentially covered the findings of the article, additionally mentioning the possibility of partial ring-opening of PMLA as well as the post-functionalization of the esterified form with brominated alkanes.^[450] In a 2018 patent, they described the synthesis of bottlebrush polymers either by ROP of PMLA with LA, or by transesterification of

addition of aluminum chloride complexes to successfully incorporate β -AL. The copolymer was not perfectly alternated, although it is expected when copolymerizing polar electron-rich and electron-poor comonomers. In 2020, homopolymerization of β -AL was reported for the first time by Wang and Hong.^[453] While this reaction failed under free radical, coordination-addition or group transfer polymerization conditions, the authors were able to perform it by the careful design of a Lewis pair catalytic system. The key is to avoid chain transfer to the monomer, which can occur due to the acidic proton at the γ position of β -AL (deprotonation yields an aromatic ring). A classical Lewis adduct composed of a sterically hindered aluminum complex with balanced Lewis acidity and an NHC acting as a strong Lewis base could thus catalyze the polymerization of β -AL (**Figure 34**), with a complete conversion, M_n up to $26 \text{ kg}\cdot\text{mol}^{-1}$ and M_w/M_n ranging from 1.2 to 1.8. Notably, a T_g as high as $264 \text{ }^\circ\text{C}$ was observed for this polymer, as the incorporation of the lactone ring in the polymer backbone presumably confers additional rigidity compared to analogous poly(γ -MMBL).

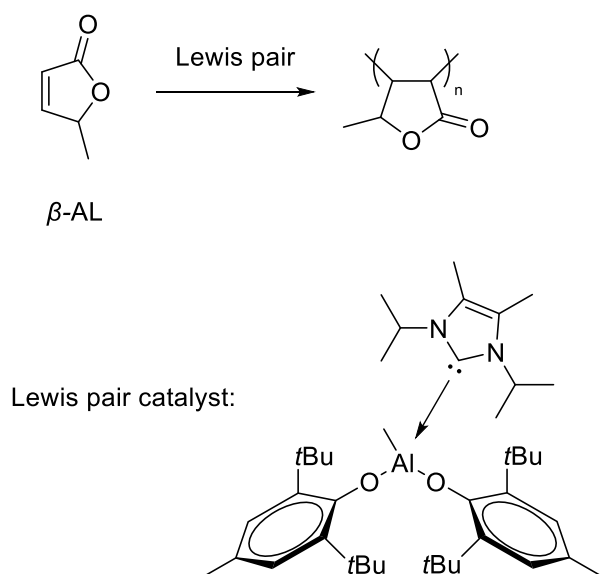


Figure 34. Polymerization of β AL by a Lewis pair catalyst.

3.5. β -Substituted Acrylics

As previously mentioned, β -substituted acrylics have been less studied than other (meth)acrylic monomers due to their lower reactivity toward polymerization. Their potential direct biosourcing has however sparked some interest for the manufacture of original and renewable materials.

3.5.1. Cinnamic Acid

The polymerization of CMA and cinnamates has been hampered by the relative stability of these monomers, owing to the stabilizing effect of the electron-donating phenyl group on the conjugated double bond. In 1955, Marvel and McCain reported the bulk free radical homopolymerization of methyl and ethyl cinnamates (MCMs and ECMs, respectively) with low conversions (<10%) and low molecular weights (2300 and 7600 g.mol⁻¹, respectively) in extremely long reaction times (1 month).^[454] To increase the reactivity of these monomers toward radical polymerization, several works have reported reactions under high pressure conditions (3000 to 5000 bars).^[455-458] For instance, ECM could be polymerized with a conversion of 99% in 23 h at $T = 100\text{ }^{\circ}\text{C}$ and $P = 5000\text{ bars}$, with $M_n = 4\ 900\text{ g.mol}^{-1}$.^[456] However, these harsh conditions hamper the large-scale use of this methodology. Due to the difficulty of homopolymerizing cinnamates, several research groups have focused on their radical copolymerization with various comonomers, including MMA,^[459,460] maleic anhydride,^[461] fumarates,^[462] methyl acrylate,^[460] acrylonitrile,^[460] or electron-donating styrene.^[460,463-468] M_n of the order of 10 000 g.mol⁻¹ could be obtained but the incorporation of cinnamates was generally low. Recently, Kamigaito and co-workers reported for the first time the use of reversible-deactivation radical polymerization techniques such as ATRP, RAFT, and NMP for the copolymerization of 1:1 mixtures of cinnamates with styrene or methyl acrylate.^[469] Conversions up to 35% could be obtained for MCM, with molecular weights in the 3000–5000 g.mol⁻¹ range and low dispersities. However, long reaction times (20 to 30 days) were still required. The same authors also obtained a slightly higher reactivity of MCM when copolymerizing it with maleic anhydride.^[470] Alternating copolymers were obtained after 13 days at 60 °C (70% conversion, $M_n = 16\text{ kg.mol}^{-1}$).

Alternatively, access to homopolymers of cinnamates may be possible using anionic polymerization techniques. In 1961, Natta and co-workers patented the use of phenylmagnesium bromide (PhMgBr) to polymerize *iso*-propyl cinnamate (*iPrCM*) at $-78\text{ }^{\circ}\text{C}$ in toluene.^[471] Graham et al. then mentioned the polymerization of *iPrCM* with fluoroenyllithium under the same conditions, but few details were given.^[472] Tsuruta et al. then used various anionic polymerization initiators such as *n*-butyllithium (*nBuLi*) or dibutylmagnesium to carry out the polymerization of *n*-alkyl cinnamates, but low yields (<15%) were obtained.^[473] In 1992, Matsumoto et al. used *sec*-BuLi as an initiator for the polymerization of *iPrCM* and *tert*-butyl cinnamate (*tBuCM*), with conversions up to 30% after 90 h at $0\text{ }^{\circ}\text{C}$.^[462] They were also able to study the thermal decomposition of these homopolymers, which starts at around $210\text{ }^{\circ}\text{C}$. In 2019, Imada et al. reported the first successful group transfer polymerization of MCM and other cinnamates, with a conversion of 89% after 14 days at $-35\text{ }^{\circ}\text{C}$, yielding a polymer with a M_n of $12\text{ kg}\cdot\text{mol}^{-1}$.^[474] Notably, $T_g = 165\text{ }^{\circ}\text{C}$ for poly(MCM), which is higher than the structural analog copolymer of methyl acrylate and styrene (around $50\text{ }^{\circ}\text{C}$). These findings highlight the importance of the density of the substituents around the polymer backbone. However, homopolymerizing cinnamates under mild conditions, with high conversions and low reaction times, remains a difficult task.

The incorporation of cinnamic acid in the pendent chain of various polymers as a photo-crosslinking agent has encountered much more success. This is due to the easily UV-catalyzed [2+2] cycloaddition of cinnamic acid on itself (Figure 15). Examples of crosslinked polymers using this methodology include cellulose,^[475,476] poly(vinyl alcohol),^[475,477,478] methacrylates,^[479–481] methacrylamides,^[482] epoxidized soybean oil,^[483] polycarbonates,^[484] dendrons,^[485] and poly(lactic acid).^[486] Notably, Ali and Srinivasan showed^[487] that radical polymerization of methacrylates with a pendent cinnamate group yields linear polymers without crosslinking owing to the low reactivity of cinnamates.^[479] Free radical crosslinking with cinnamic acid has also been reported,^[242,483] although it is less efficient than UV-catalyzed [2+2] cycloaddition.

3.5.2. Fumaric Acid

Vinyl polymerization of FmA and fumarates has been widely studied, highlighting peculiar reactivities due to their unique structure. Only radical polymerization reactions have been reported so far, with one example of unsuccessful group transfer polymerization.^[487] The first example of radical polymerization of fumarates was reported in a patent by DuPont in 1933.^[488] Initiated by benzoyl peroxide, in toluene or in bulk, the reaction was carried out with dimethyl fumarate (DMFm) and diethyl fumarate (DEFm). Later, high pressure radical polymerization of DEFm achieved full conversion and molecular weights of up to $15 \text{ kg}\cdot\text{mol}^{-1}$.^[456,489] DEFm homopolymerization was also performed using photoinitiation (γ -ray) or thermal initiation (AIBN).^[490,491] Otsu et al. were then the main contributors to this field of research for several decades, starting in 1981 with a report on the bulk homopolymerization of various dialkyl fumarates.^[492] At that time, only low conversions could be obtained, except for di-*iso*-propyl fumarate (DiPrFm) (74% after 15 h at 70 °C). These authors thoroughly examined the free radical polymerization of dialkyl fumarates in 1988 and 1995.^[493,494] Most notably, it was found that the yield and M_n value of the polymer obtained increased with the bulkiness of the substituents, a feature not observed for (meth)acrylate monomers. These observations can be explained by the extremely low rates of both propagation and termination in the polymerization of fumarates, compared to those of conventional vinylic monomers.^[495] The use of sufficiently bulky fumarates such as DiPrFm or di-*tert*-butyl fumarate (DiBuFm) effectively suppresses the termination reaction by steric hindrance around the propagating chain, resulting in a long-lived radical chain. Rod-like and comb-like polymer structures can therefore be obtained. This feature is however not observed for fumaramide analogs, supposedly due to their higher intrinsic reactivity: bulkier amide groups thus lead to lower conversions.^[496,497] Otsu et al. also reported the production of high molecular weight poly(fumaric acid) by synthesis of poly(DiBuFm) and subsequent thermal treatment that releases isobutene.^[498] In a different work, maleates, although not biobased, could be fully isomerized into the corresponding fumarates and polymerized in a one-pot procedure.^[499] Stereochemistry of the free

radical polymerization of fumarates was also studied by nuclear magnetic resonance (NMR) spectroscopy, showing a preference for the *meso* addition (around 80% of *meso* diads).^[500–502]

More recently, several research groups delved into this field. The functional group tolerance of the fumarate free radical polymerization was investigated: dl-menthol or ethyl-l-lactate fumarates were polymerized but low conversions were obtained (<10%), presumably due to the rates of side-reactions that are not negligible compared to the low rate of polymerization.^[503] The rate of polymerization of DiPrFm could be increased by an emulsion polymerization process in water.^[504] Poly(DEFm) could also be obtained in water by complexing the monomer with cyclodextrin.^[505,506] Microwave initiation also proved to be faster than thermal initiation for poly(DiPrFm) formation.^[507,508] Solid state polymerization was studied by several groups, without significant improvement over solution polymerization.^[509–511] In 2016, Matsumoto et al. reported the use of various controlled radical polymerization techniques on DiPrFm.^[512] NMP was inefficient while ATRP only led to low conversions and molecular weights, and dispersities higher than 1.3. Conversely, RAFT polymerization showed a living behavior, and block copolymers of DiPrFm and MMA or acrylates could be obtained. The same group investigated the use of various chain transfer agents such as dithiobenzoates and trithiocarbonates.^[513–515] Careful selection of the RAFT agent was essential as a balance must be found between fragmentation and re-initiation. Recently, Sato et al. developed a new route toward graft copolymers containing poly(DiPrFm) branches.^[516] They first synthesized a poly(DiPrFm) macromonomer by addition-fragmentation chain transfer and subsequently copolymerized this macromonomer with ethyl acrylate.

Thus, some challenges remain in the field of fumarate polymerization, such as the controlled synthesis of polymers with substituents less bulky than the *iso*-propyl group. However, this class of polymers has already shown interesting properties and a wide variety of applications, as they can be used as membranes,^[517] coatings,^[518] liquid crystalline polymers,^[519,520] flow improvers,^[521] detergent,^[522] and contact lenses.^[523] Recent investigations have been devoted to the characterization

of random copolymers of DiPrFm and various acrylates, as these materials exhibit promising optical properties.^[524,525]

3.5.3. Muconic Acid

Vinyl polymerization of MuA and muconates has also been explored. A few works on chloro-substituted muconates^[526,527] preceded the first report of MuA and diethyl muconate (DEMu) homopolymerizations by Bando et al. in 1977.^[528] Free radical polymerization initiated with AIBN in dimethyl sulfoxide converted only 30% of MuA and 10% of DEMu. Anionic polymerization of DEMu initiated by *n*BuLi could reach 35% conversion, while cationic initiators were inefficient for this reaction. Using infrared and NMR spectroscopy techniques, the authors identified the structure of the polymer, resulting mainly from a *trans*-1,4-addition (Figure 17). Copolymerization with styrene, acrylonitrile, and 2-vinylpyridine and the corresponding reactivity ratios were also studied in this publication. Later, a research group from DuPont illustrated the wide applicability of GTP by applying it to DEMu.^[529] Between 25 and 35 °C, materials with M_n up to 14 kg.mol⁻¹ and a dispersity of 2.4 were obtained after quantitative conversion of the monomer. Silyl polyenolates were found to provide better M_n control than SKAs, while the tacticity investigation of the resulting polymer highlighted a *meso/racemo* ratio of 2/1. Matsumoto et al. then studied in depth the radical polymerization of various muconates.^[530] They reported the radical polymerization of ccDEMu, ctDEMu, and ttDEMu, in bulk or in DMF, initiated by di-*tert*-butyl benzoyl peroxide at 120 °C. While bulk polymerization yielded high molecular weight polymers (100 to 300 kg.mol⁻¹), solution polymerization only afforded a low M_n value of 7 kg.mol⁻¹, presumably due to chain transfer to the solvent. Importantly, they quantified the amounts of *trans*-1,4-addition (84–91%), *cis*-1,4-addition (6–13%), and 1,2-addition (2–4%). The Matsumoto research group also issued numerous publications on the photopolymerization of muconates in the crystalline state.^[531,532] This topochemical reaction (i.e., the structure of the product is controlled by the crystal lattice of the reactant) was performed on various substrates in their *cis,cis* or *trans,trans* forms, and the precise design of the substituents made it possible to control the

stereochemistry of the polymers obtained.^[533,534] Itoh et al. applied these findings to prepare solid polymer electrolytes from crystalline poly(lithium muconate).^[535] In 2019, Junkers and co-workers investigated the free and controlled radical polymerization of ttDEMu and other muconates.^[536] Using the same system as Matsumoto et al.^[530] but a different solvent (anisole), they were able to reach 85–90% conversion, $M_n = 100\text{--}130 \text{ kg}\cdot\text{mol}^{-1}$ and $M_w/M_n = 1.8$ after 48 h at 120 °C. The low reactivity is probably due to the high delocalization of the radical intermediate, as well as the steric hindrance resulting from the substituent at the β position. However, the *trans,trans* isomer should be the most suitable for controlled polymerization because it is the most stable and less sterically hindered. The authors also performed the RAFT polymerization of DEMu using a trithiocarbonate and obtained materials with predictable molecular weights ranging from 1.5 to 15 $\text{kg}\cdot\text{mol}^{-1}$, and low polydispersities (1.2–1.4). They also characterized the resulting polymers by determining their Mark–Houwink coefficients as well as their glass transition temperatures (T_g values close to those of the corresponding acrylates). Overall, muconic acid is a promising acrylic analog, which has been mainly studied for its potential applications as a green precursor of high tonnage polymers such as nylon and PET. Its original structure may also lead to interesting specialty polymers.

3.5.4. Crotonic Acid

Crotonic acid and crotonates are found in the composition of various copolymers used for paints, adhesives, and coating applications.^[243] The alternated copolymer of CrA and vinyl acetate is particularly industrially important (Figure 18). It is synthesized by free radical polymerization, and an excess of the electron-poor vinyl acetate is necessary to obtain good incorporation of crotonic acid.^[537,538] Radical homopolymerization of crotonates is indeed difficult due to the lower electrophilicity of the vinylic double bond. The propagating chain is therefore more prone to termination reactions, which can be avoided to some extent by the use of bulky crotonates such as *tert*-butyl crotonate (*t*BuCr).^[537] However, only low yields (<5%) and molecular weights (<3 $\text{kg}\cdot\text{mol}^{-1}$) have been reported. Copolymerization with electron-rich monomers such as styrene is also hampered.

Acrylic acid also proved to be a rather poor comonomer.^[263] Similarly, coordination-insertion copolymerizations of methyl crotonate (MeCr) and ethyl crotonate (EtCr) with ethylene using palladium catalysts suffered from low incorporation of the crotonate monomer.^[539]

Polymerization of crotonates was in fact first mainly studied via anionic initiation. In 1961, Natta and co-workers patented the first polymerization of MeCr, *iso*-propyl crotonate (*i*PrCr) and *t*BuCr initiated by PhMgBr at $-78\text{ }^{\circ}\text{C}$ in toluene.^[471] Miller and Skogman later published the use of lithium alkyls and lithium naphthalene at $-45\text{ }^{\circ}\text{C}$ to produce poly(*t*BuCr), with conversions up to 75% in 1 h.^[540] The resulting polymer could be converted to poly(CrA) by thermal degradation at $250\text{ }^{\circ}\text{C}$. The same initiators were inefficient for the polymerization of EtCr, suggesting the importance of the steric bulk around the propagating chain to avoid termination reactions. Various anionic initiators were then reported with similar performances and limitations.^[472,541–543] CaZnEt_4 was able to polymerize *n*-alkyl crotonates to some extent (yields up to 30%).^[473] Notably, the use of 2-methylbutyllithium in THF at $-78\text{ }^{\circ}\text{C}$ for the polymerization of carefully purified *t*BuCr permitted to obtain a molecular weight of $300\text{ kg}\cdot\text{mol}^{-1}$ and a dispersity of 1.01, with 100% conversion, characteristic of a living mechanism.^[544] The behavior of the bulky crotonates is quite comparable to the one of fumarates, with propagation constants considerably lower than their methacrylate counterparts.^[545] The polymer formed had a semiflexible behavior, presumably due to the methyl group in β position and the *t*Bu ester group in α position, which restrict internal rotation. It was also found that the tacticity obtained was different than the one of the poly(*t*BuCr) synthesized with PhMgBr in toluene at $-78\text{ }^{\circ}\text{C}$.^[546] Hatada and co-workers also investigated the stereochemistry of the polycrotonates. Poly(*t*BuCr) was disyndiotactic using *t*BuLi/ Et_3Al and alternatively erythro and threo-diisotactic using PhMgBr.^[547,548] Triphenyl crotonate was threodiisotactic using a lithium complex, and had a peculiar helix conformation.^[549–551] Finally, poly(*sec*-butyl crotonate) synthesized with a lithium initiator in THF at $-78\text{ }^{\circ}\text{C}$ displayed the original behavior of having a high extensibility below its T_g .^[552]

In the late 1990's, group transfer polymerization was then applied to crotonates, and permitted to polymerize *n*-alkyl crotonates, a feature that was hardly achieved by standard anionic polymerization. Hatada and co-workers synthesized poly(MeCr) with a 85% yield at $-40\text{ }^{\circ}\text{C}$ in CH_2Cl_2 using a catalytic system composed of a silyl ketene acetal, HgI_2 , and iodotrimethylsilane.^[553] Molecular weights in the range of $10\text{ kg}\cdot\text{mol}^{-1}$ and dispersities lower than 1.3 were obtained. The authors later obtained quantitative yields by using various SKAs.^[554] The poly(MeCr) obtained were found to be disyndiotactic, and the stereocontrol depended on the bulkiness of the SKA.^[555] Other *n*-alkyl crotonates were polymerized by this method and physically characterized.^[556] Notably, the crotonates have T_g values 65 to $90\text{ }^{\circ}\text{C}$ higher than their corresponding methacrylates, due to the enhanced stiffness provided by the methyl group in the β position instead of the α position. The temperature of degradation is still sufficiently high to ensure good processability, making these polymers promising for high temperature applications. Recently, Takenaka and Abe performed the GTP of *n*-alkyl crotonates using organic superacids instead of HgI_2 , thereby avoiding the use of a highly toxic catalyst.^[557] Depending on the SKA, it is possible to control the disyndiotacticity of poly(EtCr) and this stereocontrol greatly influences the final properties of the material: $T_g = 201\text{ }^{\circ}\text{C}$ for a 92% disyndiotactic poly(EtCr) and $T_g = 82\text{ }^{\circ}\text{C}$ for a 53% disyndiotactic poly(EtCr).^[558] Finally, the Chen group applied the Lewis pair polymerization and frustrated Lewis pair polymerizations concepts to MeCr with success, obtaining quantitative conversions, high M_n (10 to $160\text{ kg}\cdot\text{mol}^{-1}$) and narrow dispersities at room temperature.^[559,560]

4. Conclusion

We have described some important advances in the synthesis of biobased (meth)acrylate monomers and the corresponding (co)polymers. Depending on the monomer, the maturity of the biobased route and the potential volume of production differ (**Figure 35**). Each vinyl moiety also has its peculiar reactivity toward anionic or radical polymerization techniques (**Figure 36**). These studies thus demonstrate that the synthesis of these compounds should make it possible to obtain new types

of innovative materials for a wide range of applications. However, renewable chemical feedstocks need to become more cost competitive with oil-based analogs as a result of advances in synthetic methods and production processes. In the authors' opinion, the increase in the market share of biobased plastics should ideally come from a decrease of the use of low-value, polluting plastics derived from petroleum (a scenario that is currently not anticipated),^[12] and an increase in the number of applications for sustainable, high-value materials derived from biomass. In this regard, policy makers can regulate the use of certain polymers or specific applications of plastics. For instance, bans on or charges for single-use bags have recently led to a rapid reduction in their use in some countries. Alternatively, financial support for biobased specialty materials could help find economically relevant solutions at the earliest stages of development. Subsidies should however be avoided for commercial processes that would not otherwise be cost competitive, such as current bio-PE production. The future of biobased polymers is undoubtedly promising, owing to the public and industrial interests in these materials. Challenges ahead will be to find truly sustainable feedstocks, synthesis paths, and applications.

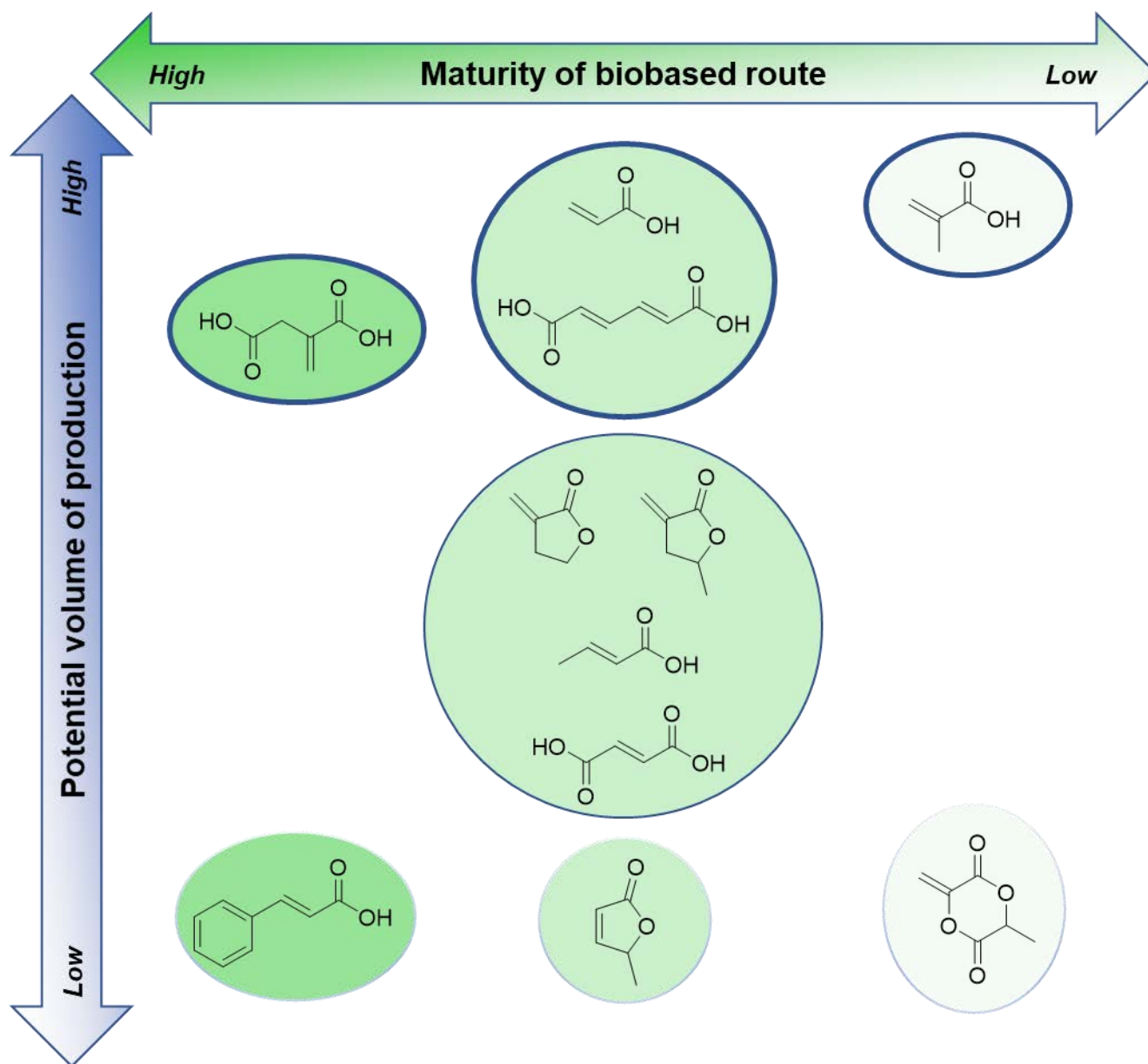


Figure 35. Current status of the production of biobased monomers presented in this review and their potential volume of production.

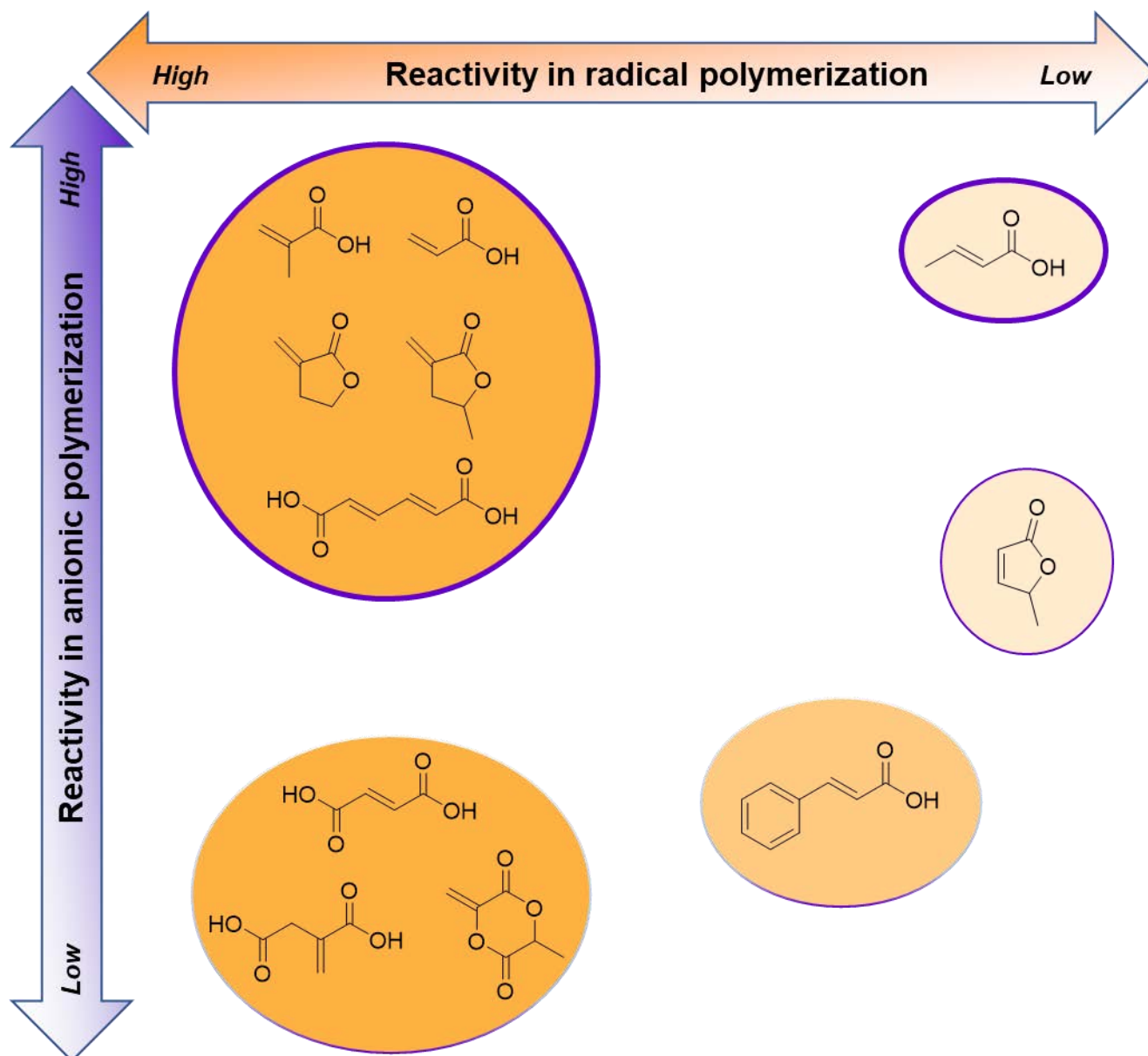


Figure 36. Relative reactivity of the monomers presented in this review.

Acknowledgements

CNRS and ENSCP are thanked for financial support. H.F. gratefully acknowledges financial support from Ecole Polytechnique (AMX) for his Ph.D. scholarship. C.M.T. is grateful to the Institut Universitaire de France.

References

- [1] *Introduction to Chemicals from Biomass* (Eds: J. H. Clark, F. E. I. Deswarte) John Wiley & Sons, Ltd., Chichester, UK **2015**.
- [2] P. Y. Dapsens, C. Mondelli, J. Perez-Ramirez, *ACS Catal.* **2012**, *2*, 1487.
- [3] P. Gallezot, *Chem. Soc. Rev.* **2012**, *41*, 1538.
- [4] F. Cherubini, A. H. Stromman, *Biofuels, Bioprod. Biorefin.* **2011**, *5*, 548.
- [5] R. A. Sheldon, *Green Chem.* **2014**, *16*, 950.
- [6] C. K. Williams, Y. Zhu, C. Romain, *Nature* **2016**, *540*, 354.
- [7] M. A. Hillmyer, *Science* **2017**, *358*, 868.
- [8] G. Lligadas, J. C. Ronda, M. Galia, V. Cadiz, *Mater. Today* **2013**, *16*, 337.
- [9] European Bioplastics, *Bioplastics, Facts and Figures*, European Bioplastics, **2014**. <https://www.european-bioplastics.org/news/publications/> (accessed: April 2020).
- [10] European Bioplastics, *Bioplastics, Facts and Figures*, European Bioplastics, **2019**. <https://www.european-bioplastics.org/news/publications/> (accessed: April 2020).
- [11] PlasticsEurope, *Plastics, the Facts*, **2015**. <https://www.plasticseurope.org/en/resources/market-data/> (accessed: April 2020).
- [12] PlasticsEurope, *Plastics, the Facts*, **2020**. <https://www.plasticseurope.org/en/resources/market-data/> (accessed: April 2020).
- [13] R. Geyer, J. R. Jambeck, K. L. Law, *Sci. Adv.* **2017**, *3*, e1700782.
- [14] R. V. Slone, *Encyclopedia of Polymer Science and Technology*, John Wiley & Sons, Inc., Hoboken, NJ **2001**. Methacrylic Ester Polymers 243.
- [15] P. F. Holmes, M. Bohrer, J. Kohn, *Prog. Polym. Sci.* **2008**, *33*, 787.
- [16] A. L. Holmberg, K. H. Reno, R. P. Wool, T. H. EppsIII, *Soft Matter* **2014**, *10*, 7405.
- [17] F. H. Isikgor, C. R. Becer, *Polym. Chem.* **2015**, *6*, 4497.
- [18] R. Palkovits, I. Delidovich, P. J. C. Hausoul, L. Deng, R. Pfitzenreuter, M. Rose, *Chem. Rev.* **2016**, *116*, 1540.
- [19] S. L. Kristufek, K. T. Wacker, Y.-Y. T. Tsao, L. Su, K. L. Wooley, *Nat. Prod. Rep.* **2017**, *34*, 433.
- [20] H. T. H. Nguyen, P. Qi, M. Rostagno, A. Feteha, S. A. Miller, *J. Mater. Chem. A* **2018**, *6*, 9298.
- [21] J. Lomege, V. Lapinte, C. Negrell, J.-J. Robin, S. Caillol, *Biomacromolecules* **2019**, *20*, 4.
- [22] S. Molina-Gutierrez, V. Ladmiral, R. Bongiovanni, S. Caillol, P. Lacroix-Desmazes, *Green Chem.* **2019**, *21*, 36.
- [23] B. M. Stadler, C. Wulf, T. Werner, S. Tin, J. G. de Vries, *ACS Catal.* **2019**, *9*, 8012.

- [24] F. Hatton, *Polym. Chem.* **2020**, *11*, 220.
- [25] K. Avasthi, A. Bohre, M. Grilc, B. Likozar, B. Saha, *Catal. Sci. Technol.* **2020**, *10*, 5411.
- [26] T. Ohara, T. Sato, N. Shimizu, G. Prescher, H. Schwind, O. Weiberg, K. Marten, H. Greim, T. D. Schaffer, P. Nandi, *Ullmann's Encyclopedia of Industrial Chemistry*, Wiley, New York **2020**.
- [27] D. Sun, Y. Yamada, S. Sato, W. Ueda, *Green Chem.* **2017**, *19*, 3186.
- [28] E. V. Makshina, J. Canadell, J. van Krieken, E. Peeters, M. Dusselier, B. F. Sels, *ChemCatChem* **2019**, *11*, 180.
- [29] S. T. Wu, Q. M. She, R. Tesser, M. D. Serio, C. H. Zhou, *Catal. Rev.* **2020**, *62*, 481.
- [30] E. de Jong, A. Higson, P. Walsh, M. Wellisch, *Biofuels, Bioprod. Biorefin.* **2012**, *6*, 606.
- [31] L. Craciun, G. P. Benn, J. Dewing, G. W. Schriver, W. J. Peer, B. Siebenhaar, U. Siegrist, *US2005/0222458A1*, **2005**.
- [32] M. A. Lilga, J. F. White, J. E. Holladay, A. H. Zacher, D. S. Muzatko, R. J. Orth, *US2007/0219391A1*, **2007**.
- [33] A. Vidra, A. Nemeth, *Period. Polytech., Chem. Eng.* **2017**, *62*, 156.
- [34] C. Jers, A. Kalantari, A. Garg, I. Mijakovic, *Front. Bioeng. Biotechnol.* **2019**, *7*, 124.
- [35] H. S. Chu, J.-H. Ahn, J. Yun, I. S. Choi, T.-W. Nam, K. M. Cho, *Metab. Eng.* **2015**, *32*, 23.
- [36] Y.-S. Ko, J. W. Kim, T. U. Chae, C. W. Song, S. Y. Lee, *ACS Synth. Biol.* **2020**, *9*, 1150.
- [37] R. Beerthuis, G. Rothenberg, N. R. Shiju, *Green Chem.* **2015**, *17*, 1341.
- [38] Y. Fan, C. Zhou, X. Zhu, *Catal. Rev.* **2009**, *51*, 293.
- [39] D. I. Collias, J. V. Lingoies, *US9926256B2*, **2018**.
- [40] M. M. Bomgardner, *Chem. Eng. News* **2020**, *98*. <https://cen.acs.org/business/biobased-chemicals/Cargill-gives-biobased-acrylicacid/98/i20> (accessed: April 2020)
- [41] J. Dubois, C. Duquenne, W. Holderich, *US2008/018313A1*, **2008**.
- [42] T. Dishisha, S.-H. Pyo, R. Hatti-Kaul, *Microb. Cell Fact.* **2015**, *14*, 200.
- [43] J. E. Mahoney, *WO2013/126375A1*, **2013**.
- [44] C. Raith, M. Pazicky, R. Paciello, R. H. Brand, M. Hartmann, K. J. Mueller-Engel, P. Zurowski, W. Fischer, *US2014/0018574A1*, **2014**.
- [45] E. W. Dunn, J. R. Lamb, A. M. LaPointe, G. W. Coates, *ACS Catal.* **2016**, *6*, 8219.
- [46] J. van Walsem, E. Anderson, J. Licata, K. A. Sparks, C. Mirley, M. S. Sivasubramanian, *WO2011/100608A1*, **2011**.
- [47] J. P. M. Sanders, J. Van Haveren, E. L. Scott, D. S. Van Es, J. Le Notre, J. Spekreijse, *US2012/0178961*, **2012**.
- [48] D. Schweitzer, K. D. Snell, *Org. Process Res. Dev.* **2015**, *19*, 715.

- [49] J. Spekrijse, J. Le Notre, J. van Haveren, E. L. Scott, J. P. M. Sanders, *Green Chem.* **2012**, *14*, 2747.
- [50] M. J. Burk, P. Pharkya, S. J. Van Dien, A. P. Burgard, C. H. Schilling, *WO 2009/045637 A2*, **2009**.
- [51] P. S. Engl, A. Tsygankov, J. De Jesus Silva, J. Lange, C. Coperet, A. Togni, A. Fedorov, *Helv. Chim. Acta* **2020**, *103*, e2000035.
- [52] S. Schofer, A. Safir, R. Vazquez, *WO 2013/082264 A1*, **2013**.
- [53] Looming Production Shutdowns and Second Dip in Operating Rates Challenge Global Methyl Methacrylate Market, IHS Markit Says, <https://www.businesswire.com/news/home/20180828005216/en/> (accessed: April 2020).
- [54] M. J. Darabi Mahboub, J.-L. Dubois, F. Cavani, M. Rostamizadeh, G. S. Patience, *Chem. Soc. Rev.* **2018**, *47*, 7703.
- [55] J. Lebeau, J. P. Efromson, M. D. Lynch, *Front. Bioeng. Biotechnol.* **2020**, *8*, 207.
- [56] W. Bauer, *Ullmann's Encyclopedia of Industrial Chemistry*, Wiley-VCH, Weinheim, Germany **2011**.
- [57] J.-L. Dubois, *US2011/0301316A1*, **2011**.
- [58] J.-L. Dubois, J. F. Crolzy, L. Campora, C. Croizy, P. Croizy, *US2011/0318515A1*, **2011**.
- [59] J.-L. Dubois, *US2011/0287991A1*, **2011**.
- [60] A. Mohsenzadeh, A. Zamani, M. J. Taherzadeh, *ChemBioEng Rev.* **2017**, *4*, 75.
- [61] V. S. Sikarwar, M. Zhao, P. Clough, J. Yao, X. Zhong, M. Z. Memon, N. Shah, E. J. Anthony, P. S. Fennell, *Energy Environ. Sci.* **2016**, *9*, 2939.
- [62] A. Galadima, O. Muraza, *J. Nat. Gas Sci. Eng.* **2015**, *25*, 303.
- [63] R. Ciriminna, F. Meneguzzo, R. Delisi, M. Pagliaro, *Chem. Cent. J.* **2017**, *11*, 22.
- [64] C. R. Soccol, L. P. S. Vandenberghe, C. Rodrigues, A. Pandey, *Food Technol. Biotechnol.* **2006**, *44*, 141.
- [65] A. I. Magalhaes, J. C. de Carvalho, J. D. C. Medina, C. R. Soccol, *Appl. Microbiol. Biotechnol.* **2017**, *101*, 1.
- [66] T. Willke, K.-D. Vorlop, *Appl. Microbiol. Biotechnol.* **2001**, *56*, 289.
- [67] J. C. De Carvalho, A. I. Magalhaes Jr., C. R. Soccol, *Chim. Oggi* **2018**, *36*, 4.
- [68] M. Carlsson, C. Habenicht, L. C. Kam, M. J. Antal Jr., N. Bian, R. J. Cunningham, M. Jones Jr., *Ind. Eng. Chem. Res.* **1994**, *33*, 1989.
- [69] J. Li, T. B. Brill, *J. Phys. Chem. A* **2001**, *105*, 10839.
- [70] D. W. Johnson, G. R. Eastham, M. Poliakoff, *WO 2011/077140 A2*, **2011**.
- [71] G. R. Eastham, D. W. Johnson, M. A. Waugh, *WO 2013/160703 A1*,

2013.

- [72] J. Le Notre, S. C. M. Witte-van Dijk, J. van Haveren, E. L. Scott, J. P. M. Sanders, *ChemSusChem* **2014**, 7, 2712.
- [73] J. E. L. Le Notre, E. L. Scott, R. L. Croes, J. Van Haveren, *US2016/0207867A1*, **2016**.
- [74] J. C. Lansing, R. E. Murray, B. R. Moser, *ACS Sustainable Chem. Eng.* **2017**, 5, 3132.
- [75] B. R. Moser, J. C. Lansing, R. E. Murray, *US2018/0105481A1*, **2018**.
- [76] M. Pirmoradi, J. R. Kastner, *ACS Sustainable Chem. Eng.* **2017**, 5, 1517.
- [77] J. Kastner, M. Pirmoradi, *US10138306B1*, **2018**.
- [78] A. Bohre, U. Novak, M. Grilc, B. Likozar, *Mol. Catal.* **2019**, 476, 110520.
- [79] A. Bohre, B. Hočevár, M. Grilc, B. Likozar, *Appl. Catal., B* **2019**, 256, 117889.
- [80] A. Bohre, M. A. Ali, M. Ocepek, M. Grilc, J. Zabret, B. Likozar, *Ind. Eng. Chem. Res.* **2019**, 58, 19825.
- [81] N. Thakur, M. D. Pandey, R. Pandey, *J. Solid State Chem.* **2019**, 280, 120987.
- [82] J.-M. M. Millet, *Catal. Rev.* **1998**, 40, 1.
- [83] M. Akimoto, Y. Tsuchida, K. Sato, E. Echigoya, *J. Catal.* **1981**, 72, 93.
- [84] K. Y. Lee, S. Oishi, H. Igarashi, M. Misono, *Catal. Today* **1997**, 33, 183.
- [85] K. Zhang, A. P. Woodruff, M. Xiong, J. Zhou, Y. K. Dhande, *ChemSusChem* **2011**, 4, 1068.
- [86] T. Volker, E. Schindelman, *US3487101A*, **1969**.
- [87] A. Marx, M. Poetter, S. Buchholz, A. May, H. Siegert, B. Alber, G. Fuchs, L. Eggeling, *US2010/0291644A1*, **2010**.
- [88] R. H. Mueller, T. Rohwerder, *US2010/0035314A1*, **2010**.
- [89] A. P. Burgard, M. J. Burk, R. E. Osterhout, P. Pharkya, *US2012/0276604A1*, **2012**.
- [90] A. Marx, M. Poetter, S. Buchholz, A. May, H. Siegert, G. Fuchs, B. Alber, L. Eggeling, *US2015/0218601A1*, **2015**.
- [91] T. Rohwerder, R. H. Muller, *Microb. Cell Fact.* **2010**, 9, 13.
- [92] T. Hoefel, E. Wittmann, L. Reinecke, D. Weuster-Botz, *Appl. Microbiol. Biotechnol.* **2010**, 88, 477.
- [93] B. N. M. van Leeuwen, A. M. van der Wulp, I. Duijnste, A. J. A. van Maris, A. J. J. Straathof, *Appl. Microbiol. Biotechnol.* **2012**, 93, 1377.
- [94] S. Atsumi, T. Hanai, J. C. Liao, *Nature* **2008**, 451, 86.
- [95] B. J. Eikmanns, B. Blombach, *Bioprocessing of Renewable Resources to Commodity Bioproducts*, John Wiley & Sons, Inc., Hoboken, NJ **2014**.
- [96] M. Peters, J. Taylor, M. M. Jenni, D. E. Henton, L. E. Manzer, *WO2011/085223A1*, **2011**.
- [97] H. Fukuda, T. Fujii, T. Ogawa, *Agric. Biol. Chem.* **1984**, 48, 1679.

- [98] J. Wilson, S. Gering, J. Pinard, R. Lucas, B. R. Briggs, *Biotechnol. Biofuels* **2018**, *11*, 234.
- [99] J. Sun, K. Zhu, F. Gao, C. Wang, J. Liu, C. H. F. Peden, Y. Wang, *J. Am. Chem. Soc.* **2011**, *133*, 11096.
- [100] A. J. Crisci, H. Dou, T. Prasomsri, Y. Roman-Leshkov, *ACS Catal.* **2014**, *4*, 4196.
- [101] J. E. Rorrer, F. D. Toste, A. T. Bell, *ACS Catal.* **2019**, *9*, 10588.
- [102] J. Sun, C. Liu, Y. Wang, K. Martin, P. Venkitasubramanian, *US2015/0218077A1*, **2015**.
- [103] A. P. Burgard, M. J. Burk, R. E. Osterhout, P. Pharkya, *US2009/0275096A1*, **2009**.
- [104] P. Pharkya, A. P. Burgard, R. E. Osterhout, M. J. Burk, J. Sun, *WO2011/031897A1*, **2011**.
- [105] G. R. Eastham, G. Stephens, A. Yiakoumetti, *US2018/0171368A1*, **2018**.
- [106] Y. Asano, E. Sato, F. Yu, W. Mizunashi, *US10570426B2*, **2020**.
- [107] A. Ekman, P. Borjesson, *J. Cleaner Prod.* **2011**, *19*, 1257.
- [108] H. R. Gerberich, G. C. Seaman, *Kirk-Othmer Encyclopedia of Chemical Technology*, John Wiley & Sons, New York **2000**, p. 1.
- [109] M. Okabe, D. Lies, S. Kanamasa, E. Y. Park, *Appl. Microbiol. Biotechnol.* **2009**, *84*, 597.
- [110] M. G. Steiger, M. L. Blumhoff, D. Mattanovich, M. Sauer, *Front. Microbiol.* **2013**, *4*, 23.
- [111] T. Klement, J. Buchs, *Bioresour. Technol.* **2013**, *135*, 422.
- [112] A. A. El-Imam, C. Du, *J. Biodiversity Bioprospect. Dev.* **2014**, *1*, 119.
- [113] A. H. Mondala, *J. Ind. Microbiol. Biotechnol.* **2015**, *42*, 487.
- [114] H. Hajian, W. M. W. Yusoff, *Curr. Res. J. Biol. Sci.* **2015**, *7*, 37.
- [115] T. Robert, S. Friebel, *Green Chem.* **2016**, *18*, 2922.
- [116] J. C. da Cruz, E. F. Camporese Servulo, A. M. de Castro, *Handbook of Bioengineering*, Elsevier, Amsterdam **2017**, pp. 291–316.
- [117] S. Kumar, S. Krishnan, S. K. Samal, S. Mohanty, S. K. Nayak, *Polym. Int.* **2017**, *66*, 1349.
- [118] R. Bafana, R. A. Pandey, *Crit. Rev. Biotechnol.* **2018**, *38*, 68.
- [119] M. Zhao, X. Lu, H. Zong, J. Li, B. Zhuge, *Biotechnol. Lett.* **2018**, *40*, 455.
- [120] A. Kuenz, S. Krull, *Appl. Microbiol. Biotechnol.* **2018**, *102*, 3901.
- [121] B.-E. Teleky, D. Vodnar, *Polymers* **2019**, *11*, 1035.
- [122] S. Baup, *Ann. Pharm.* **1836**, *19*, 29.
- [123] K. Kinoshita, *J. Chem. Soc. Jpn.* **1929**, *50*, 583.
- [124] C. T. Calam, A. E. Oxford, H. Raistrick, *Biochem. J.* **1939**, *33*, 1488.
- [125] J. H. Kane, A. C. Finaly, P. F. Amann, *US2385283*, **1945**.
- [126] H. Kautola, M. Vahvaselk, Y.-Y. Linko, P. Linko, *Biotechnol. Lett.* **1985**, *7*, 167.
- [127] N. Vassilev, A. Medina, B. Eichler-Lobermann, E. Flor-Peregrin, M. Vassileva, *Appl. Biochem. Biotechnol.* **2012**, *168*, 1311.

- [128] M. Okabe, N. Ohta, Y. S. Park, *J. Ferment. Bioeng.* **1993**, 76, 117.
- [129] Y. S. Park, M. Itida, N. Ohta, M. Okabe, *J. Ferment. Bioeng.* **1994**, 77, 329.
- [130] A. Kuenz, Y. Gallenmuller, T. Willke, K.-D. Vorlop, *Appl. Microbiol. Biotechnol.* **2012**, 96, 1209.
- [131] A. Hevekerl, A. Kuenz, K.-D. Vorlop, *Appl. Microbiol. Biotechnol.* **2014**, 98, 10005.
- [132] S. Krull, A. Hevekerl, A. Kuenz, U. Pruse, *Appl. Microbiol. Biotechnol.* **2017**, 101, 4063.
- [133] H. Hosseinpour Tehrani, J. Becker, I. Bator, K. Saur, S. Meyer, A. C. Rodrigues Loia, L. M. Blank, N. Wierckx, *Biotechnol. Biofuels* **2019**, 12, 263.
- [134] C. S. K. Reddy, R. P. Singh, *Bioresour. Technol.* **2002**, 85, 69.
- [135] X. Huang, M. Chen, X. Lu, Y. Li, X. Li, J.-J. Li, *Microb. Cell Fact.* **2014**, 13, 108.
- [136] B. C. Saha, G. J. Kennedy, N. Qureshi, M. J. Bowman, *Biotechnol. Prog.* **2017**, 33, 1059.
- [137] J. Kim, H.-M. Seo, S. K. Bhatia, H.-S. Song, J.-H. Kim, J.-M. Jeon, K.-Y. Choi, W. Kim, J.-J. Yoon, Y.-G. Kim, Y.-H. Yang, *Sci. Rep.* **2017**, 7, 39768.
- [138] A. I. Magalhaes, J. C. de Carvalho, J. F. Thoms, J. D. C. Medina, C. R. Soccol, *J. Cleaner Prod.* **2019**, 206, 336.
- [139] F. M. A. Geilen, B. Engendahl, A. Harwardt, W. Marquardt, J. Klankermayer, W. Leitner, *Angew. Chem., Int. Ed.* **2010**, 49, 5510.
- [140] F. J. Holzhauser, J. Artz, S. Palkovits, D. Kreyenschulte, J. Buchs, R. Palkovits, *Green Chem.* **2017**, 19, 2390.
- [141] C. Robert, F. de Montigny, C. M. Thomas, *ACS Catal.* **2014**, 4, 3586.
- [142] C. Robert, F. de Montigny, C. M. Thomas, *Nat. Commun.* **2011**, 2, 586.
- [143] A. M. Medway, J. Sperry, *Green Chem.* **2014**, 16, 2084.
- [144] J. T. Trotta, M. Jin, K. J. Stawiasz, Q. Michaudel, W.-L. Chen, B. P. Fors, *J. Polym. Sci., Polym. Chem.* **2017**, 55, 2730.
- [145] R. R. Gowda, E. Y.-X. Chen, *ChemSusChem* **2019**, 12, 973.
- [146] J. T. Trotta, A. Watts, A. R. Wong, A. M. LaPointe, M. A. Hillmyer, B. P. Fors, *ACS Sustainable Chem. Eng.* **2019**, 7, 2691.
- [147] J. Zhou, A. M. Schmidt, H. Ritter, *Macromolecules* **2010**, 43, 939.
- [148] M. Hong, E. Y.-X. Chen, *Macromolecules* **2014**, 47, 3614.
- [149] X. Tang, M. Hong, L. Falivene, L. Caporaso, L. Cavallo, E. Y.-X. Chen, *J. Am. Chem. Soc.* **2016**, 138, 14326.
- [150] P. Binda, Z. Barnes, D. Guthrie, R. Ford, *Open J. Polym. Chem.* **2017**, 7, 76.
- [151] M. Danko, M. Basko, S. Ďurkačova, A. Duda, J. Mosnaček, *Macromolecules* **2018**, 51, 3582.
- [152] Y. Kato, H. Yoshida, K. Shoji, Y. Sato, N. Nakajima, S. Ogita, *Tetrahedron Lett.* **2009**, 50, 4751.

- [153] T. Nomura, E. Hayashi, S. Kawakami, S. Ogita, Y. Kato, *Biosci., Biotechnol., Biochem.* **2015**, *79*, 25.
- [154] C. J. Cavallito, T. H. Haskell, *J. Am. Chem. Soc.* **1946**, *68*, 2332.
- [155] E. R. H. Jones, T. Y. Shen, M. C. Whiting, *J. Chem. Soc.* **1950**, 230.
- [156] W. J. McGraw, N. J. Morristown, *US2624723*, **1953**.
- [157] H. M. R. Hoffmann, J. Rabe, *Angew. Chem., Int. Ed. Engl.* **1985**, *24*, 94.
- [158] R. R. A. Kitson, A. Millemaggi, R. J. K. Taylor, *Angew. Chem., Int. Ed.* **2009**, *48*, 9426.
- [159] M. Fetizon, M. Golfier, J.-M. Louis, *Tetrahedron* **1975**, *31*, 171.
- [160] R. M. Carlson, A. R. Oyler, *J. Org. Chem.* **1976**, *41*, 4065.
- [161] M. Michaut, M. Santelli, J.-L. Parrain, *J. Organomet. Chem.* **2000**, *606*, 93.
- [162] T. Hirabayashi, K. Yokota, *JPH0449288A*, **1992**.
- [163] R. R. Gowda, E. Y.-X. Chen, *Org. Chem. Front.* **2014**, *1*, 230.
- [164] N. Nghiem, S. Kleff, S. Schwegmann, *Fermentation* **2017**, *3*, 26.
- [165] M. Jiang, J. Ma, M. Wu, R. Liu, L. Liang, F. Xin, W. Zhang, H. Jia, W. Dong, *Bioresour. Technol.* **2017**, *245*, 1710.
- [166] A. Maziere, P. Prinsen, A. Garcia, R. Luque, C. Len, *Biofuels, Bioprod. Biorefin.* **2017**, *11*, 908.
- [167] S. Varadarajan, D. J. Miller, *Biotechnol. Prog.* **1999**, *15*, 845.
- [168] A. Corma, S. Iborra, A. Velty, *Chem. Rev.* **2007**, *107*, 2411.
- [169] A. Cukulovic, C. V. Stevens, *Biofuels, Bioprod. Biorefin.* **2008**, *2*, 505.
- [170] S. W. Fitzpatrick, *US5608105*, **1997**.
- [171] Levulinic Acid Market Analysis and Segment Forecasts to 2020, <https://www.radiantinsights.com/research/levulinic-acid-marketanalysis-and-segment-forecasts-to-2020> (accessed: September 2014).
- [172] F. D. Pileidis, M.-M. Titirici, *ChemSusChem* **2016**, *9*, 562.
- [173] B. Girisuta, H. J. Heeres, in *Production of Platform Chemicals from Sustainable Resources* (Eds: Z. Fang, R. L. Smith, X. Qi), Springer, Singapore **2017**, pp. 143–169.
- [174] M. Hartweg, C. R. Becer, in *Green Polymer Chemistry: New Products, Processes, and Applications* (Eds: H. N. Cheng, R. A. Gross, P. B. Smith), ACS Symposium Series, American Chemical Society, Washington, DC **2018**, pp. 331–338.
- [175] L. E. Manzer, *US2003/0055270*, **2003**.
- [176] L. E. Manzer, *Appl. Catal., A* **2004**, *272*, 249.
- [177] W. R. H. Wright, R. Palkovits, *ChemSusChem* **2012**, *5*, 1657.
- [178] Z. Zhang, *ChemSusChem* **2016**, *9*, 156.

- [179] L. Prati, A. Jouve, A. Villa, in *Production of Biofuels and Chemicals with Bifunctional Catalysts* (Eds: Z. Fang, R. L. Smith, H. Li), Springer, Singapore **2017**, pp. 221–237.
- [180] S. Dutta, I. K. M. Yu, D. C. W. Tsang, Y. H. Ng, Y. S. Ok, J. Sherwood, J. H. Clark, *Chem. Eng. J.* **2019**, *372*, 992.
- [181] A. Y. Li, A. Moores, *ACS Sustainable Chem. Eng.* **2019**, *7*, 10182.
- [182] Z. Yu, X. Lu, C. Liu, Y. Han, N. Ji, *Renewable Sustainable Energy Rev.* **2019**, *112*, 140.
- [183] L. Ye, Y. Han, J. Feng, X. Lu, *Ind. Crops Prod.* **2020**, *144*, 112031.
- [184] J.-P. Lange, L. Petrus, R. J. Haan, *WO2007/099111A1*, **2007**.
- [185] H. Mehdi, V. Fabos, R. Tuba, A. Bodor, L. T. Mika, I. T. Horvath, *Top. Catal.* **2008**, *48*, 49.
- [186] L. Deng, J. Li, D.-M. Lai, Y. Fu, Q.-X. Guo, *Angew. Chem., Int. Ed.* **2009**, *48*, 6529.
- [187] L. Deng, Y. Zhao, J. Li, Y. Fu, B. Liao, Q.-X. Guo, *ChemSusChem* **2010**, *3*, 1172.
- [188] H. Heeres, R. Handana, D. Chunai, C. Borromeus Rasrendra, B. Girisuta, H. Jan Heeres, *Green Chem.* **2009**, *11*, 1247.
- [189] J. C. Serrano-Ruiz, D. J. Braden, R. M. West, J. A. Dumesic, *Appl. Catal., B* **2010**, *100*, 184.
- [190] X.-L. Du, L. He, S. Zhao, Y.-M. Liu, Y. Cao, H.-Y. He, K.-N. Fan, *Angew. Chem., Int. Ed.* **2011**, *50*, 7815.
- [191] X.-L. Du, Q.-Y. Bi, Y.-M. Liu, Y. Cao, K.-N. Fan, *ChemSusChem* **2011**, *4*, 1838.
- [192] S. Murat Sen, C. A. Henao, D. J. Braden, J. A. Dumesic, C. T. Maravelias, *Chem. Eng. Sci.* **2012**, *67*, 57.
- [193] J. Yuan, S.-S. Li, L. Yu, Y.-M. Liu, Y. Cao, H.-Y. He, K.-N. Fan, *Energy Environ. Sci.* **2013**, *6*, 3308.
- [194] M.-C. Fu, R. Shang, Z. Huang, Y. Fu, *Synlett* **2014**, *25*, 2748.
- [195] M. Varkolu, D. Raju Burri, S. R. Rao Kamaraju, S. B. Jonnalagadda, W. E. van Zyl, *Chem. Eng. Technol.* **2017**, *40*, 719.
- [196] D. R. Coulson, L. E. Manzer, N. Herron, *US6313318B1*, **2001**.
- [197] A. A. Lemonidou, L. Lopez, L. E. Manzer, M. A. Barteau, *Appl. Catal., A* **2004**, *272*, 241.
- [198] R. D. Puts, C. Brandenburg, K. R. Tarburton, *US2002/0143195*, **2002**.
- [199] G. M. Ksander, J. E. McMurry, M. Johnson, *J. Org. Chem.* **1977**, *42*, 1180.
- [200] Z. Vobecka, C. Wei, K. Tauer, D. Esposito, *Polymer* **2015**, *74*, 262.
- [201] M. Al-Naji, B. Puertolas, B. Kumru, D. Cruz, M. Baumel, B. V. K. J. Schmidt, N. V. Tarakina, J. Perez-Ramirez, *ChemSusChem* **2019**, *12*, 2628.
- [202] A. S. Scheibelhoffer, W. A. Blose, H. J. Harwood, *Polym. Prepr.* **1969**, *10*, 1375.
- [203] R. Auras, *Encyclopedia of Polymer Science and Technology*, John Wiley & Sons, Ltd., Hoboken, NJ **2010**.

- [204] J. Xin, S. Zhang, D. Yan, O. Ayodele, X. Lu, J. Wang, *Green Chem.* **2014**, *16*, 3589.
- [205] T. Hirabayashi, K. Yokota, *Polym. J.* **1982**, *14*, 789.
- [206] Y. Wu, R. P. Singh, L. Deng, *J. Am. Chem. Soc.* **2011**, *133*, 12458.
- [207] Y. Guoruoluo, H. Zhou, W. Wang, J. Zhou, H. A. Aisa, G. Yao, *Biochem. Syst. Ecol.* **2018**, *78*, 102.
- [208] F. De Schouwer, L. Claes, A. Vandekerckhove, J. Verduyck, D. E. De Vos, *ChemSusChem* **2019**, *12*, 1272.
- [209] J. D. Cui, J. Q. Qiu, X. W. Fan, S. R. Jia, Z. L. Tan, *Crit. Rev. Biotechnol.* **2014**, *34*, 258.
- [210] *Amino Acid Biosynthesis - Pathways, Regulation and Metabolic Engineering* (Ed: V. F. Wendisch), Springer, Berlin **2007**.
- [211] Y. Teng, E. L. Scott, S. C. M. Witte-van Dijk, J. P. M. Sanders, *New Biotechnol.* **2016**, *33*, 171.
- [212] A. J. Ragauskas, G. T. Beckham, M. J. Bidy, R. Chandra, F. Chen, M. F. Davis, B. H. Davison, R. A. Dixon, P. Gilna, M. Keller, P. Langan, A. K. Naskar, J. N. Saddler, T. J. Tschaplinski, G. A. Tuskan, C. E. Wyman, *Science* **2014**, *344*, 1246843.
- [213] C. A. Roa Engel, A. J. J. Straathof, T. W. Zijlmans, W. M. van Gulik, L. A. M. van der Wielen, *Appl. Microbiol. Biotechnol.* **2008**, *78*, 379.
- [214] S. T. Yang, K. Zhang, B. Zhang, H. Huang, *Comprehensive Biotechnology*, Elsevier, Amsterdam **2011**, pp. 163–177.
- [215] Q. Xu, S. Li, H. Huang, J. Wen, *Biotechnol. Adv.* **2012**, *30*, 1685.
- [216] R. K. Das, S. K. Brar, M. Verma, *Platform Chemical Biorefinery*, Elsevier, Amsterdam **2016**, pp. 133–157.
- [217] V. Martin-Dominguez, J. Estevez, F. Ojembarrena, V. Santos, M. Ladero, *Fermentation* **2018**, *4*, 33.
- [218] J. Sebastian, K. Hegde, P. Kumar, T. Rouissi, S. K. Brar, *Crit. Rev. Biotechnol.* **2019**, *39*, 817.
- [219] Fumaric Acid Market Size, Share & Trends Analysis Report By Application (Food & Beverages, Rosin Paper Sizes, Unsaturated Polyester Resins, Alkyd Resins), By Region, And Segment Forecasts, 2015–2022, www.grandviewresearch.com/industry-analysis/fumaric-acid-market/ (accessed: April 2020).
- [220] F. S. Carta, C. R. Soccol, L. P. Ramos, J. D. Fontana, *Bioresour. Technol.* **1999**, *68*, 23.
- [221] J. Rodriguez-Lopez, A. J. Sanchez, D. M. Gomez, A. Romani, J. C. Parajo, *J. Chem. Technol. Biotechnol.* **2012**, *87*, 1036.
- [222] I. C. Gangl, W. A. Weigand, F. A. Keller, *Appl. Biochem. Biotechnol.* **1990**, *24–25*, 663.
- [223] N. Cao, J. Du, C. S. Gong, G. T. Tsao, *Appl. Environ. Microb.* **1996**, *62*, 2926.
- [224] J. Streuff, K. Muniz, *J. Organomet. Chem.* **2005**, *690*, 5973.

- [225] T. Farmer, R. Castle, J. Clark, D. Macquarrie, *Int. J. Mol. Sci.* **2015**, *16*, 14912.
- [226] L. Wang, D.-G. Guo, *Materials* **2017**, *10*, 149.
- [227] A. Diez-Pascual, *Polymers* **2017**, *9*, 260.
- [228] I. Khalil, G. Quintens, T. Junkers, M. Dusselier, *Green Chem.* **2020**, *22*, 1517.
- [229] J. W. Frost, A. Miermont, D. Scheitzer, V. Bui, *US2010/0314243*, **2010**.
- [230] V. Bui, M. Kit Lau, D. MacRae, D. Schweitzer, *US2013/0030215 A1*, **2013**.
- [231] J. M. Carraher, T. Pfennig, R. G. Rao, B. H. Shanks, J.-P. Tessonier, *Green Chem.* **2017**, *19*, 3042.
- [232] J.-P. Tessonier, J. M. Carraher, T. Pfennig, B. Shanks, *US2017/0129839*, **2017**.
- [233] N.-Z. Xie, H. Liang, R.-B. Huang, P. Xu, *Biotechnol. Adv.* **2014**, *32*, 615.
- [234] D. R. Vardon, M. A. Franden, C. W. Johnson, E. M. Karp, M. T. Guarnieri, J. G. Linger, M. J. Salm, T. J. Strathmann, G. T. Beckham, *Energy Environ. Sci.* **2015**, *8*, 617.
- [235] J. Becker, M. Kuhl, M. Kohlstedt, S. Starck, C. Wittmann, *Microb. Cell Fact.* **2018**, *17*, 115.
- [236] X.-H. Hu, J. Zhang, X.-F. Yang, Y.-H. Xu, T.-P. Loh, *J. Am. Chem. Soc.* **2015**, *137*, 3169.
- [237] T. Besset, N. Kuhl, F. W. Patureau, F. Glorius, *Chem. - Eur. J.* **2011**, *17*, 7167.
- [238] M. Shiramizu, F. D. Toste, *Angew. Chem., Int. Ed.* **2013**, *52*, 12905.
- [239] H. G. Rogers, R. A. Gaudiana, J. S. Manello, R. A. Sahatjian, *J. Macromol. Sci., Chem.* **1986**, *23*, 711.
- [240] V. V. Zuev, *Mol. Cryst. Liq. Cryst.* **1995**, *265*, 111.
- [241] N. A. Rorrer, J. R. Dorgan, D. R. Vardon, C. R. Martinez, Y. Yang, G. T. Beckham, *ACS Sustainable Chem. Eng.* **2016**, *4*, 6867.
- [242] N. A. Rorrer, D. R. Vardon, J. R. Dorgan, E. J. Gjersing, G. T. Beckham, *Green Chem.* **2017**, *19*, 2812.
- [243] J. Blumenstein, J. Albert, R. P. Schulz, C. Kohlpaintner, *Ullmann's Encyclopedia of Industrial Chemistry*, Wiley-VCH, Weinheim, Germany **2015**, pp. 1–20.
- [244] M. R. Z. Mamat, H. Ariffin, M. A. Hassan, M. A. K. Mohd Zahari, *J. Cleaner Prod.* **2014**, *83*, 463.
- [245] D. Santhanaraj, M. P. Ruiz, M. R. Komarneni, T. Pham, G. Li, D. E. Resasco, J. Faria, *Angew. Chem.* **2020**, *132*, 7526.
- [246] C.-J. Yue, H.-L. Chen, L.-P. Gu, J.-W. Zheng, Y.-F. Zhuang, *Sustainable Chem. Pharm.* **2020**, *17*, 100288.
- [247] J. Schmid, K. Mauch, *WO2009/046828A1*, **2009**.
- [248] C. Dellomonaco, J. M. Clomburg, E. N. Miller, R. Gonzalez, *Nature* **2011**, *476*, 355.
- [249] D. Koch, G. Meurer, *EP2511377A1*, **2012**.

- [250] L. Wang, Z. Zong, Y. Liu, M. Zheng, D. Li, C. Wang, F. Zheng, C. Madzak, Z. Liu, *Bioresour. Technol.* **2019**, *287*, 121484.
- [251] S. Kim, S. Cheong, R. Gonzalez, *Metab. Eng.* **2016**, *36*, 90.
- [252] C. Fernandez-Dacosta, J. A. Posada, A. Ramirez, *J. Cleaner Prod.* **2016**, *137*, 942.
- [253] H. Abe, *Macromol. Biosci.* **2006**, *6*, 469.
- [254] H. Nishida, H. Ariffin, Y. Shirai, M. A. Hassan, *Biopolymers* **2010**, *19*, 370.
- [255] F. X. Werber, J. N. Baptist, *Polym. Eng. Sci.* **1964**, *4*, 245.
- [256] N. Grassie, E. J. Murray, *Polym. Degrad. Stab.* **1984**, *6*, 47.
- [257] N. Grassie, E. J. Murray, P. A. Holmes, *Polym. Degrad. Stab.* **1984**, *6*, 127.
- [258] L. X. L. Chen, J. Yu, *Macromol. Synth.* **2005**, *224*, 35.
- [259] J. Yu, D. Plackett, L. X. L. Chen, *Polym. Degrad. Stab.* **2005**, *89*, 289.
- [260] M. Kawalec, G. Adamus, P. Kurcok, M. Kowalczyk, I. Foltran, M. L. Focarete, M. Scandola, *Biomacromolecules* **2007**, *8*, 1053.
- [261] K. J. Kim, Y. Doi, H. Abe, *Polym. Degrad. Stab.* **2006**, *91*, 769.
- [262] K. J. Kim, Y. Doi, H. Abe, *Polym. Degrad. Stab.* **2008**, *93*, 776.
- [263] H. Ariffin, H. Nishida, M. A. Hassan, Y. Shirai, *Biotechnol. J.* **2010**, *5*, 484.
- [264] H. Ariffin, H. Nishida, Y. Shirai, M. A. Hassan, *Polym. Degrad. Stab.* **2010**, *95*, 1375.
- [265] C. A. Mullen, A. A. Boateng, D. Schweitzer, K. Sparks, K. D. Snell, *J. Anal. Appl. Pyrolysis* **2014**, *107*, 40.
- [266] N. F. S. M. Farid, H. Ariffin, M. R. Z. Mamat, M. A. K. Mohd Zahari, M. A. Hassan, *RSC Adv.* **2015**, *5*, 33546.
- [267] J. Spekrijse, J. Le Notre, J. P. M. Sanders, E. L. Scott, *J. Appl. Polym. Sci.* **2015**, *132*, 42462.
- [268] J. Spekrijse, J. Holgueras Ortega, J. P. M. Sanders, J. H. Bitter, E. L. Scott, *Bioresour. Technol.* **2016**, *211*, 267.
- [269] J. C. A. Flanagan, J. Myung, C. S. Criddle, R. M. Waymouth, *ChemistrySelect* **2016**, *1*, 2327.
- [270] C. Samori, A. Kiwan, C. Torri, R. Conti, P. Galletti, E. Tagliavini, *ACS Sustainable Chem. Eng.* **2019**, *7*, 10266.
- [271] J. Ramier, D. Grande, V. Langlois, E. Renard, *Polym. Degrad. Stab.* **2012**, *97*, 322.
- [272] X. Yang, K. Odelius, M. Hakkarainen, *ACS Sustainable Chem. Eng.* **2014**, *2*, 2198.
- [273] J. Wagner, R. Bransgrove, T. A. Beacham, M. J. Allen, K. Meixner, B. Drosig, V. P. Ting, C. J. Chuck, *Bioresour. Technol.* **2016**, *207*, 166.
- [274] C. Torri, T. D. O. Weme, C. Samori, A. Kiwan, D. W. F. Brillman, *Environ. Sci. Technol.* **2017**, *51*, 12683.

- [275] J. M. Clark, H. M. Pilath, A. Mittal, W. E. Michener, D. J. Robichaud, D. K. Johnson, *J. Phys. Chem. A* **2016**, *120*, 332.
- [276] Y. Li, T. J. Strathmann, *Green Chem.* **2019**, *21*, 5586.
- [277] J. C. A. Flanagan, E. J. Kang, N. I. Strong, R. M. Waymouth, *ACS Catal.* **2015**, *5*, 5328.
- [278] M. A. Drosbeke, F. E. Du Prez, *ACS Sustainable Chem. Eng.* **2019**, *7*, 11633.
- [279] T. Brotherton, J. Smith Jr., J. Lynn, *J. Org. Chem.* **1961**, *26*, 1283.
- [280] J. J. Gallagher, M. A. Hillmyer, T. M. Reineke, *ACS Sustainable Chem. Eng.* **2015**, *3*, 662.
- [281] A. Das, A. Jana, B. Maji, *Chem. Commun.* **2020**, *56*, 4284.
- [282] T. P. Davis, D. M. Haddleton, S. N. Richards, *J. Macromol. Sci., Rev. Macromol. Chem. Phys.* **1994**, *34*, 243.
- [283] O. W. Webster, *New Synthetic Methods*, Springer, Berlin **2003**, pp. 1–34.
- [284] O. Nuyken, *Handbook of Polymer Synthesis*, CRC Press, Boca Raton, FL **2004**.
- [285] A. P. Mosley, *Brydson's Plastics Materials*, Elsevier, Amsterdam **2017**, pp. 441–456.
- [286] D. J. Walsh, M. G. Hyatt, S. A. Miller, D. Guironnet, *ACS Catal.* **2019**, *9*, 11153.
- [287] P. A. Lovell, F. J. Schork, *Biomacromolecules* **2020**, *21*, 4396.
- [288] M. J. Monteiro, M. F. Cunningham, *Macromolecules* **2012**, *45*, 4939.
- [289] P. B. Zetterlund, S. C. Thickett, S. Perrier, E. Bourgeat-Lami, M. Lansalot, *Chem. Rev.* **2015**, *115*, 9745.
- [290] E. Rizzardo, D. H. Solomon, *Polym. Bull.* **1979**, *1*, 529.
- [291] D. H. Solomon, E. Rizzardo, P. Cacioli, *US4581429*, **1986**.
- [292] C. J. Hawker, A. W. Bosman, E. Harth, *Chem. Rev.* **2001**, *101*, 3661.
- [293] J. Nicolas, Y. Guilleaume, C. Lefay, D. Bertin, D. Gigmes, B. Charleux, *Prog. Polym. Sci.* **2013**, *38*, 63.
- [294] G. Moad, E. Rizzardo, in (Ed: D. Gigmes), *Nitroxide Mediated Polymerization: From Fundamentals to Applications in Materials Science*, Polymer Chemistry Series, Royal Society Of Chemistry, Cambridge **2015**, Chapter 1: The History of Nitroxide-mediated Polymerization pp. 1–44.
- [295] M. K. Georges, R. P. N. Veregin, P. M. Kazmaier, G. K. Hamer, *Macromolecules* **1993**, *26*, 2987.
- [296] M. K. Georges, R. P. N. Veregin, P. M. Kazmaier, G. K. Hamer, *US5322912*, **1994**.
- [297] D. Benoit, V. Chaplinski, R. Braslau, C. J. Hawker, *J. Am. Chem. Soc.* **1999**, *121*, 3904.
- [298] B. Raether, O. Nuyken, P. Wieland, W. Bremser, *Macromol. Synth.* **2002**, *177*, 25.
- [299] P. C. Wieland, O. Nuyken, Y. Heischkel, B. Raether, C. Strissel, in *Advances in Controlled/Living Radical Polymerization* (Ed: K. Matyjaszewski), American Chemical Society, Washington, DC **2003**, pp. 619–630.

- [300] M. Zhao, D. Chen, Y. Shi, W. Yang, Z. Fu, *Macromol. Chem. Phys.* **2013**, *214*, 1688.
- [301] F. di Lena, K. Matyjaszewski, *Prog. Polym. Sci.* **2010**, *35*, 959.
- [302] N. S. Enikolopyan, B. R. Smirnov, G. V. Ponomarev, I. M. Belgovskii, *J. Polym. Sci., Polym. Chem. Ed.* **1981**, *19*, 879.
- [303] A. Gridnev, **2000**, 14.
- [304] J. P. A. Heuts, N. M. B. Smeets, *Polym. Chem.* **2011**, *2*, 2407.
- [305] N. G. Engelis, A. Anastasaki, G. Nurumbetov, N. P. Truong, V. Nikolaou, A. Shegiwal, M. R. Whittaker, T. P. Davis, D. M. Haddleton, *Nat. Chem.* **2017**, *9*, 171.
- [306] B. B. Wayland, G. Poszmik, M. Fryd, *Organometallics* **1992**, *11*, 3534.
- [307] L. E. N. Allan, M. R. Perry, M. P. Shaver, *Prog. Polym. Sci.* **2012**, *37*, 127.
- [308] R. Poli, *Chem. - Eur. J.* **2015**, *21*, 6988.
- [309] J.-S. Wang, K. Matyjaszewski, *J. Am. Chem. Soc.* **1995**, *117*, 5614.
- [310] M. Kato, M. Kamigaito, M. Sawamoto, T. Higashimura, *Macromolecules* **1995**, *28*, 1721.
- [311] M. Ouchi, M. Sawamoto, *Macromolecules* **2017**, *50*, 2603.
- [312] T. G. Ribelli, F. Lorandi, M. Fantin, K. Matyjaszewski, *Macromol. Rapid Commun.* **2019**, *40*, 1800616.
- [313] Z. Xue, D. He, X. Xie, *Polym. Chem.* **2015**, *6*, 1660.
- [314] B. M. Rosen, V. Percec, *Chem. Rev.* **2009**, *109*, 5069.
- [315] N. Zhang, S. R. Samanta, B. M. Rosen, V. Percec, *Chem. Rev.* **2014**, *114*, 5848.
- [316] J. C. Theriot, B. G. McCarthy, C.-H. Lim, G. M. Miyake, *Macromol. Rapid Commun.* **2017**, *38*, 1700040.
- [317] K. Matyjaszewski, *Macromolecules* **2020**, *53*, 495.
- [318] T. P. Le, G. Moad, E. Rizzardo, S. H. Thang, *WO98/01478*, **1998**.
- [319] J. Chiefari, Y. K. (Bill) Chong, F. Ercole, J. Krstina, J. Jeffery, T. P. T. Le, R. T. A. Mayadunne, G. F. Meijs, C. L. Moad, G. Moad, E. Rizzardo, S. H. Thang, *Macromolecules* **1998**, *31*, 5559.
- [320] G. Moad, E. Rizzardo, S. H. Thang, *Aust. J. Chem.* **2005**, *58*, 379.
- [321] G. Moad, E. Rizzardo, S. H. Thang, *Polymer* **2008**, *49*, 1079.
- [322] G. Moad, E. Rizzardo, S. H. Thang, *Aust. J. Chem.* **2012**, *65*, 985.
- [323] S. Perrier, *Macromolecules* **2017**, *50*, 7433.
- [324] H. Willcock, R. K. O'Reilly, *Polym. Chem.* **2010**, *1*, 149.
- [325] M. Destarac, *Polym. Chem.* **2018**, *9*, 4947.
- [326] Y. Ni, L. Zhang, Z. Cheng, X. Zhu, *Polym. Chem.* **2019**, *10*, 2504.
- [327] S. Yamago, *J. Polym. Sci., Polym. Chem.* **2006**, *44*, 1.
- [328] M. Szwarc, M. Levy, R. Milkovich, *J. Am. Chem. Soc.* **1956**, *78*, 2656.

- [329] D. Baskaran, A. H. E. Muller, in *Polymer Science: A Comprehensive Reference*, Elsevier, Amsterdam **2012**, pp. 623–655.
- [330] *Anionic Polymerization: Principles, Practice, Strength, Consequences and Applications* (Eds: N. Hadjichristidis, A. Hirao), Springer Japan, Tokyo **2015**.
- [331] K. Ute, N. Miyatake, K. Hatada, *Polymer* **1995**, *36*, 1415.
- [332] O. W. Webster, W. R. Hertler, D. Y. Sogah, W. B. Farnham, T. V. RajanBabu, *J. Am. Chem. Soc.* **1983**, *105*, 5706.
- [333] M. Hong, J. Chen, E. Y.-X. Chen, *Chem. Rev.* **2018**, *118*, 10551.
- [334] K. Fuchise, S. Tsuchida, K. Takada, Y. Chen, T. Satoh, T. Kakuchi, *ACS Macro Lett.* **2014**, *3*, 1015.
- [335] Y. Chen, K. Kitano, S. Tsuchida, S. Kikuchi, K. Takada, T. Satoh, T. Kakuchi, *Polym. Chem.* **2015**, *6*, 3502.
- [336] J. Chen, E. Y.-X. Chen, *Angew. Chem., Int. Ed.* **2015**, *54*, 6842.
- [337] T. Xu, E. Y.-X. Chen, *J. Polym. Sci., Polym. Chem.* **2015**, *53*, 1895.
- [338] Y. Chen, Q. Jia, Y. Ding, S. Sato, L. Xu, C. Zang, X. Shen, T. Kakuchi, *Macromolecules* **2019**, *52*, 844.
- [339] E. Y.-X. Chen, *Chem. Rev.* **2009**, *109*, 5157.
- [340] H. Yasuda, H. Yamamoto, K. Yokota, S. Miyake, A. Nakamura, *J. Am. Chem. Soc.* **1992**, *114*, 4908.
- [341] S. Collins, D. G. Ward, *J. Am. Chem. Soc.* **1992**, *114*, 5460.
- [342] T. Adachi, H. Sugimoto, T. Aida, S. Inoue, *Macromolecules* **1993**, *26*, 1238.
- [343] M. T. Reetz, R. Ostarek, *J. Chem. Soc., Chem. Commun.* **1988**, 213.
- [344] M. T. Reetz, T. Knauf, U. Minet, C. Bingel, *Angew. Chem., Int. Ed. Engl.* **1988**, *27*, 1373.
- [345] A. P. Zagala, T. E. Hogen-Esch, *Macromolecules* **1996**, *29*, 3038.
- [346] M. Fevre, J. Pinaud, Y. Gnanou, J. Vignolle, D. Taton, *Chem. Soc. Rev.* **2013**, *42*, 2142.
- [347] M. D. Scholten, J. L. Hedrick, R. M. Waymouth, *Macromolecules* **2008**, *41*, 7399.
- [348] J. Raynaud, A. Ciolino, A. Baceiredo, M. Destarac, F. Bonnette, T. Kato, Y. Gnanou, D. Taton, *Angew. Chem.* **2008**, *120*, 5470.
- [349] Y. Zhang, E. Y.-X. Chen, *Angew. Chem., Int. Ed.* **2012**, *51*, 2465.
- [350] M. L. McGraw, E. Y.-X. Chen, *Macromolecules* **2020**, *53*, 6102.
- [351] D. W. Stephan, *Org. Biomol. Chem.* **2008**, *6*, 1535.
- [352] Y. Zhang, G. M. Miyake, E. Y.-X. Chen, *Angew. Chem., Int. Ed.* **2010**, *49*, 10158.
- [353] J. Chen, E. Y.-X. Chen, *Isr. J. Chem.* **2015**, *55*, 216.
- [354] Y.-B. Jia, Y.-B. Wang, W.-M. Ren, T. Xu, J. Wang, X.-B. Lu, *Macromolecules* **2014**, *47*, 1966.

- [355] M. L. McGraw, R. W. Clarke, E. Y.-X. Chen, *J. Am. Chem. Soc.* **2020**, *142*, 5969.
- [356] Y. Bai, H. Wang, J. He, Y. Zhang, *Angew. Chem., Int. Ed.* **2020**, *59*, 11613.
- [357] B. E. Tate, *Adv. Polym. Sci.* **1967**, *5*, 214.
- [358] C. S. Marvel, T. H. Shepherd, *J. Org. Chem.* **1959**, *24*, 599.
- [359] M. Şen, O. Guven, *Eur. Polym. J.* **2002**, *38*, 751.
- [360] T. Betancourt, J. Pardo, K. Soo, N. A. Peppas, *J. Biomed. Mater. Res.* **2010**, *93*, 175.
- [361] S. L. Tomic, S. I. Dimitrijevic, A. D. Marinkovic, S. Najman, J. M. Filipovic, *Polym. Bull.* **2009**, *63*, 837.
- [362] M. M. Babic, B. Bozic, B. D. Bozic, J. M. Filipovic, G. S. Uscumlic, S. L. Tomic, *J. Mater. Sci.* **2015**, *50*, 6208.
- [363] L. Howard, Y. Weng, D. Xie, *Dent. Mater.* **2014**, *30*, 644.
- [364] S. Bednarz, A. Błaszczyk, D. Błażejewska, D. Bogdał, *Catal. Today* **2015**, *257*, 297.
- [365] S. Bednarz, A. Wesołowska-Piętak, R. Konefał, T. Świergosz, *Eur. Polym. J.* **2018**, *106*, 63.
- [366] M. Vince, A. Augustyniak, Y. Durant, J. Shaw, *WO2015/100412A1*, **2015**.
- [367] M. Vince, A. Augustyniak, Y. Durant, J. Shaw, *US2016/194493A1*, **2016**.
- [368] J. M. G. Cowie, *Pure Appl. Chem.* **1979**, *51*, 2331.
- [369] A. Horta, I. Herández-Fuentes, L. Gargallo, D. Radić, *Makromol. Chem., Rapid Commun.* **1987**, *8*, 523.
- [370] T. Hirano, S. Tateiwa, M. Seno, T. Sato, *J. Polym. Sci., Polym. Chem.* **2000**, *38*, 2487.
- [371] H. Watanabe, A. Matsumoto, T. Otsu, *J. Polym. Sci., Polym. Chem.* **1994**, *32*, 2073.
- [372] E. Kassi, E. Loizou, L. Porcar, C. S. Patrickios, *Eur. Polym. J.* **2011**, *47*, 816.
- [373] Z. Szablan, A. A. Toy, T. P. Davis, X. Hao, M. H. Stenzel, C. Barner-Kowollik, *J. Polym. Sci., Polym. Chem.* **2004**, *42*, 2432.
- [374] Z. Szablan, A. A. Toy, A. Terrenoire, T. P. Davis, M. H. Stenzel, A. H. E. Muller, C. Barner-Kowollik, *J. Polym. Sci., Polym. Chem.* **2006**, *44*, 3692.
- [375] K. Satoh, D.-H. Lee, K. Nagai, M. Kamigaito, *Macromol. Rapid Commun.* **2014**, *35*, 161.
- [376] I. Javakhishvili, T. Kasama, K. Jankova, S. Hvilsted, *Chem. Commun.* **2013**, *49*, 4803.
- [377] K. Hu, J. Sarkar, J. Zheng, Y. H. M. Lim, A. Goto, *Macromol. Rapid Commun.* **2020**, *41*, 2000075.
- [378] R. Wang, J. Ma, X. Zhou, Z. Wang, H. Kang, L. Zhang, K. Hua, J. Kulig, *Macromolecules* **2012**, *45*, 6830.
- [379] W. Lei, X. Yang, H. Qiao, D. Shi, R. Wang, L. Zhang, *Eur. Polym. J.* **2018**, *106*, 1.
- [380] H. Yang, H. Ji, X. Zhou, W. Lei, L. Zhang, R. Wang, *Polymers* **2019**, *11*, 1897.

- [381] S. Agarwal, Q. Jin, S. Maji, in *Biobased Monomers, Polymers, and Materials* (Eds: P. B. Smith, R. A. Gross), American Chemical Society, Washington, DC **2012**, pp. 197–212.
- [382] M. J.-L. Tschan, E. Brule, P. Haquette, C. M. Thomas, *Polym. Chem.* **2012**, *3*, 836.
- [383] R. R. Gowda, E. Y.-X. Chen, *Encyclopedia of Polymer Science and Technology*, John Wiley & Sons, Inc., Hoboken, NJ **2013**.
- [384] D. D. J. Liu, E. Y.-X. Chen, *Green Chem.* **2014**, *16*, 964.
- [385] Y. Zhang, E. Y.-X. Chen, in *Selective Catalysis for Renewable Feedstocks and Chemicals* (Ed: K. M. Nicholas), Springer International Publishing, Cham **2014**, pp. 185–227.
- [386] J. Kollar, M. Danko, F. Pippig, J. Mosnaček, *Front. Chem.* **2019**, *7*, 845.
- [387] J. W. Stansbury, J. M. Antonucci, *Dent. Mater.* **1992**, *8*, 270.
- [388] C. Brandenburg, D. M. Dean, G. H. Hofmann, R. D. Puts, E. A. Flexman, K. R. Tarburton, *WO0198410*, **2001**.
- [389] C. Brandenburg, R. King, L. Oien, P. W. Uhlianuk, *WO0164793*, **2001**.
- [390] K. Sakashita, K. Iwasaka, Y. Tsukamoto, A. Aoyagi, *EP1834968A1*, **2007**.
- [391] T. Uno, S. Kawaguchi, M. Kubo, T. Itoh, *J. Power Sources* **2008**, *178*, 716.
- [392] A. Juhari, J. Mosnaček, J. A. Yoon, A. Nese, K. Koynov, T. Kowalewski, K. Matyjaszewski, *Polymer* **2010**, *51*, 4806.
- [393] B. Mullen, M. Rodwogin, F. Stollmaier, D. Yontz, C. Leibig, *Green Mater.* **2013**, *1*, 186.
- [394] K. Ding, A. John, J. Shin, Y. Lee, T. Quinn, W. B. Tolman, M. A. Hillmyer, *Biomacromolecules* **2015**, *16*, 2537.
- [395] M. K. Akkapeddi, *Macromolecules* **1979**, *12*, 546.
- [396] M. Ueda, M. Takahashi, Y. Imai, C. U. Pittman, *J. Polym. Sci., Polym. Chem. Ed.* **1982**, *20*, 2819.
- [397] D. Y. Sogah, W. R. Hertler, O. W. Webster, G. M. Cohen, *Macromolecules* **1987**, *20*, 1473.
- [398] M. K. Akkapeddi, *Polymer* **1979**, *20*, 1215.
- [399] C. Lee, H. K. Hall, *Macromolecules* **1989**, *22*, 21.
- [400] H. Koinuma, K. Sato, H. Hirai, *Makromol. Chem., Rapid Commun.* **1982**, *3*, 311.
- [401] D. L. Trumbo, *Polym. Bull.* **1991**, *26*, 271.
- [402] J. Mosnaček, K. Matyjaszewski, *Macromolecules* **2008**, *41*, 5509.
- [403] J. Mosnaček, J. A. Yoon, A. Juhari, K. Koynov, K. Matyjaszewski, *Polymer* **2009**, *50*, 2087.
- [404] J. Shin, Y. Lee, W. B. Tolman, M. A. Hillmyer, *Biomacromolecules* **2012**, *13*, 3833.
- [405] G. Zain, D. Bondarev, J. Dohaňošova, J. Mosnaček, *ChemPhotoChem* **2019**, *3*, 1138.
- [406] J. Kollar, M. Mrlik, D. Moravčikova, Z. Kronekova, T. Liptaj, I. Lacik, J. Mosnaček, *Macromolecules* **2016**, *49*, 4047.

- [407] J. Kollar, M. Mrlik, D. Moravčikova, B. Ivan, J. Mosnaček, *Eur. Polym. J.* **2019**, *115*, 99.
- [408] P. Rychter, D. Rogacz, K. Lewicka, J. Kollar, M. Kawalec, J. Mosnaček, *Adv. Polym. Technol.* **2019**, *2019*, 2947152.
- [409] S. B. Luk, J. Kollar, A. Chovancova, M. Mrlik, I. Lacik, J. Mosnaček, R. A. Hutchinson, *Polym. Chem.* **2017**, *8*, 6039.
- [410] S. Agarwal, R. Kumar, *Macromol. Chem. Phys.* **2011**, *212*, 603.
- [411] J. Suenaga, D. M. Sutherlin, J. K. Stille, *Macromolecules* **1984**, *17*, 2913.
- [412] G. Qi, M. Nolan, F. J. Schork, C. W. Jones, *J. Polym. Sci., Polym. Chem.* **2008**, *46*, 5929.
- [413] R. A. Cockburn, T. F. L. McKenna, R. A. Hutchinson, *Macromol. Chem. Phys.* **2010**, *211*, 501.
- [414] R. A. Cockburn, R. Siegmann, K. A. Payne, S. Beuermann, T. F. L. McKenna, R. A. Hutchinson, *Biomacromolecules* **2011**, *12*, 2319.
- [415] S. Xu, J. Huang, S. Xu, Y. Luo, *Polymer* **2013**, *54*, 1779.
- [416] R. A. Cockburn, T. F. L. McKenna, R. A. Hutchinson, *Macromol. React. Eng.* **2011**, *5*, 404.
- [417] G. M. Miyake, S. E. Newton, W. R. Mariott, E. Y.-X. Chen, *Dalton Trans.* **2010**, *39*, 6710.
- [418] Y. Hu, X. Xu, Y. Zhang, Y. Chen, E. Y.-X. Chen, *Macromolecules* **2010**, *43*, 9328.
- [419] R. R. Gowda, E. Y.-X. Chen, *Dalton Trans.* **2013**, *42*, 9263.
- [420] Y. Hu, L. O. Gustafson, H. Zhu, E. Y.-X. Chen, *J. Polym. Sci., Polym. Chem.* **2011**, *49*, 2008.
- [421] G. M. Miyake, Y. Zhang, E. Y.-X. Chen, *Macromolecules* **2010**, *43*, 4902.
- [422] L. Hu, J. He, Y. Zhang, E. Y.-X. Chen, *Macromolecules* **2018**, *51*, 1296.
- [423] L. Hu, W. Zhao, J. He, Y. Zhang, *Molecules* **2018**, *23*, 665.
- [424] T. Xu, E. Y.-X. Chen, *J. Am. Chem. Soc.* **2014**, *136*, 1774.
- [425] J. Chen, E. Chen, *Molecules* **2015**, *20*, 9575.
- [426] P. Xu, Y. Yao, X. Xu, *Chem. - Eur. J.* **2017**, *23*, 1263.
- [427] X. Wang, Y. Zhang, M. Hong, *Molecules* **2018**, *23*, 442.
- [428] Y. Bai, J. He, Y. Zhang, *Angew. Chem.* **2018**, *130*, 17476.
- [429] T. Yao, P. Xu, X. Xu, *Dalton Trans.* **2019**, *48*, 7743.
- [430] Y. Zhang, E. Y.-X. Chen, *Angew. Chem., Int. Ed.* **2012**, *51*, 2465.
- [431] Y. Zhang, M. Schmitt, L. Falivene, L. Caporaso, L. Cavallo, E. Y.-X. Chen, *J. Am. Chem. Soc.* **2013**, *135*, 17925.
- [432] M. Schmitt, L. Falivene, L. Caporaso, L. Cavallo, E. Y.-X. Chen, *Polym. Chem.* **2014**, *5*, 3261.
- [433] C. U. Pittman, H. Lee, *J. Polym. Sci., Polym. Chem.* **2003**, *41*, 1759.
- [434] X. Chen, L. Caporaso, L. Cavallo, E. Y.-X. Chen, *J. Am. Chem. Soc.* **2012**, *134*, 7278.
- [435] Y. Hu, X. Wang, Y. Chen, L. Caporaso, L. Cavallo, E. Y.-X. Chen, *Organometallics* **2013**, *32*, 1459.

- [436] R. R. Gowda, E. Y.-X. Chen, *ACS Macro Lett.* **2016**, *5*, 772.
- [437] R. R. Gowda, E. Y.-X. Chen, *Philos. Trans. R. Soc., A* **2017**, *375*, 20170003.
- [438] J. Tang, E. Y.-X. Chen, *Org. Chem. Front.* **2015**, *2*, 1625.
- [439] J. Tang, E. Y.-X. Chen, *Eur. Polym. J.* **2017**, *95*, 678.
- [440] F. Jing, M. A. Hillmyer, *J. Am. Chem. Soc.* **2008**, *130*, 13826.
- [441] G. L. Fiore, F. Jing, V. G. Young Jr., C. J. Cramer, M. A. Hillmyer, *Polym. Chem.* **2010**, *1*, 870.
- [442] J. A. Castillo, D. E. Borchmann, A. Y. Cheng, Y. Wang, C. Hu, A. J. Garcia, M. Weck, *Macromolecules* **2012**, *45*, 62.
- [443] T. R. Long, A. Wongrakpanich, A.-V. Do, A. K. Salem, N. B. Bowden, *Polym. Chem.* **2015**, *6*, 7188.
- [444] T. Fuoco, A. Finne-Wistrand, D. Pappalardo, *Biomacromolecules* **2016**, *17*, 1383.
- [445] F. Sinclair, M. P. Shaver, *J. Polym. Sci., Polym. Chem.* **2018**, *56*, 741.
- [446] J. Britner, H. Ritter, *Macromolecules* **2015**, *48*, 3516.
- [447] J. Britner, H. Ritter, *Beilstein J. Org. Chem.* **2016**, *12*, 2378.
- [448] G. M. Miyake, Y. Zhang, E. Y.-X. Chen, *J. Polym. Sci., Polym. Chem.* **2015**, *53*, 1523.
- [449] T. C. Mauldin, J. T. Wertz, D. J. Boday, *ACS Macro Lett.* **2016**, *5*, 544.
- [450] D. J. Boday, T. C. Mauldin, *US9260550B1*, **2016**.
- [451] B. M. Kobilka, J. Kuczynski, J. T. Porter, J. T. Wertz, *US10072121B1*, **2018**.
- [452] D. J. Boday, J. M. Garcia, J. L. Hedrick, B. M. Kobilka, J. T. Wertz, R. J. Wojtecki, *US10329380B2*, **2019**.
- [453] X. Wang, M. Hong, *Angew. Chem., Int. Ed.* **2020**, *59*, 2664.
- [454] C. S. Marvel, G. H. McCain, *J. Am. Chem. Soc.* **1953**, *75*, 3272.
- [455] R. H. Sapiro, R. P. Linstead, D. M. Newitt, *J. Chem. Soc.* **1937**, 1784. [456] W. A. Holmes-Walker, K. E. Weale, *J. Chem. Soc.* **1955**, 2295.
- [458] K. E. Weale, *Polymer* **1987**, *28*, 2151.
- [459] J. C. Bevington, F. R. Colley, J. R. Ebdon, *Polymer* **1973**, *14*, 409.
- [460] C. A. Barson, J. C. Bevington, T. N. Huckerby, *Makromol. Chem.* **1989**, *190*, 1681.
- [461] K. Fujimori, W. S. Schiller, I. E. Craven, *Makromol. Chem.* **1991**, *192*, 959.
- [462] A. Matsumoto, A. Horie, T. Otsu, *Eur. Polym. J.* **1992**, *28*, 213.
- [463] C. A. Barson, *J. Polym. Sci.* **1962**, *62*, S128.
- [464] M. Kreisel, U. Garbatski, D. H. Kohn, *J. Polym. Sci., Part A: Gen. Pap.* **1964**, *2*, 105.
- [465] C. A. Barson, M. S. Rizvi, *Eur. Polym. J.* **1970**, *6*, 241.
- [466] C. A. Barson, M. J. Turner, *Eur. Polym. J.* **1973**, *9*, 789.
- [467] C. A. Barson, M. J. Turner, *Eur. Polym. J.* **1974**, *10*, 917.

- [468] J.-I. Asakura, M. Yoshihara, H. Fujihara, Y. Matsubara, T. Maeshima, *J. Macromol. Sci., Chem.* **1983**, *19*, 311.
- [469] Y. Terao, K. Satoh, M. Kamigaito, *Biomacromolecules* **2019**, *20*, 192.
- [470] Y. Terao, S. Sugihara, K. Satoh, M. Kamigaito, *Eur. Polym. J.* **2019**, *120*, 109225.
- [471] M. Farina, G. Natta, M. Peraldo, *BE599833A*, **1961**.
- [472] R. K. Graham, J. E. Moore, J. A. Powell, *J. Appl. Polym. Sci.* **1967**, *11*, 1797.
- [473] T. Tsuruta, T. Makimoto, K. Tanabe, *Makromol. Chem.* **1968**, *114*, 182.
- [474] M. Imada, Y. Takenaka, H. Hatanaka, T. Tsuge, H. Abe, *Commun. Chem.* **2019**, *2*, 109.
- [475] L. M. Minsk, J. G. Smith, W. P. van Deusen, J. F. Wright, *J. Appl. Polym. Sci.* **1959**, *2*, 302.
- [476] M. Kamath, J. Kincaid, B. K. Mandal, *J. Appl. Polym. Sci.* **1996**, *59*, 45.
- [477] A. A. Lin, A. Reiser, *Macromolecules* **1989**, *22*, 3898.
- [478] X. Coqueret, *Macromol. Chem. Phys.* **1999**, *200*, 1567.
- [479] A. H. Ali, K. S. V. Srinivasan, *Polym. Int.* **1997**, *43*, 310.
- [480] B. Chae, S. W. Lee, M. Ree, Y. M. Jung, S. B. Kim, *Langmuir* **2003**, *19*, 687.
- [481] T. G. Kim, E. H. Jeong, S. C. Lim, S. H. Kim, G. H. Kim, S. H. Kim, H.-Y. Jeon, J. H. Youk, *Synthetic Met.* **2009**, *159*, 749.
- [482] A. Laschewsky, E. D. Rekaı, *Macromol. Rapid Commun.* **2000**, *21*, 937.
- [483] H. Esen, S. H. Kusefoglu, *J. Appl. Polym. Sci.* **2003**, *89*, 3882.
- [484] X. Hu, X. Chen, H. Cheng, X. Jing, *J. Polym. Sci., Polym. Chem.* **2009**, *47*, 161.
- [485] G.-C. Kuang, Y. Ji, X.-R. Jia, Y. Li, E.-Q. Chen, Z.-X. Zhang, Y. Wei, *Tetrahedron* **2009**, *65*, 3496.
- [486] M. Nagata, K. Inaki, *Eur. Polym. J.* **2009**, *45*, 1111.
- [487] E. Kassi, M. S. Constantinou, C. S. Patrickios, *Eur. Polym. J.* **2013**, *49*, 761.
- [488] H. Ben Dykstra, *GB389467A*, **1933**.
- [489] H. W. Starkweather, *J. Am. Chem. Soc.* **1934**, *56*, 1870.
- [490] R. H. Wiley, D. J. Parish, *J. Polym. Sci.* **1960**, *45*, 503.
- [491] W. I. Bengough, G. B. Park, R. A. Young, *Eur. Polym. J.* **1975**, *11*, 305.
- [492] T. Otsu, O. Ito, N. Toyoda, S. Mori, *Makromol. Chem., Rapid Commun.* **1981**, *2*, 725.
- [493] T. Otsu, T. Yasuhara, A. Matsumoto, *J. Macromol. Sci., Chem.* **1988**, *25*, 537.
- [494] A. Matsumoto, T. Otsu, *Macromol. Synth.* **1995**, *98*, 139.
- [495] A. Matsumoto, M. Yoshioka, T. Otsu, *J. Polym. Sci., Polym. Chem.* **1996**, *34*, 291.
- [496] T. Otsu, A. Matsumoto, K. Fukushima, *J. Chem. Soc., Chem. Commun.* **1985**, 1766.
- [497] A. Matsumoto, K. Fukushima, T. Otsu, *J. Polym. Sci., Polym. Chem.* **1991**, *29*, 1697.
- [498] T. Otsu, T. Yasuhara, K. Shiraishi, S. Mori, *Polym. Bull.* **1984**, *12*, 449.

- [499] T. Otsu, O. Ito, N. Toyoda, *J. Macromol. Sci., Chem.* **1983**, *19*, 27.
- [500] X. Wang, T. Komoto, I. Ando, T. Otsu, *Makromol. Chem.* **1988**, *189*, 1845.
- [501] M. Yoshioka, A. Matsumoto, T. Otsu, I. Ando, *Polymer* **1991**, *32*, 2741.
- [502] M. Yoshioka, A. Matsumoto, T. Otsu, *Polym. J.* **1991**, *23*, 1191.
- [503] D. Cochin, A. Laschewsky, N. Pantoustier, *Polymer* **2000**, *41*, 3895.
- [504] M. S. Cortizo, L. B. Scaffardi, J. O. Tocho, R. V. Figini, *Angew. Makromol. Chem.* **1999**, *271*, 1.
- [505] S.-W. Choi, H. Ritter, *Macromol. Rapid Commun.* **2004**, *25*, 716.
- [506] S. Choi, W. Frank, H. Ritter, *React. Funct. Polym.* **2006**, *66*, 149.
- [507] M. Susana Cortizo, *J. Appl. Polym. Sci.* **2006**, *103*, 3785.
- [508] M. S. Cortizo, S. Laurella, J. L. Alessandrini, *Radiat. Phys. Chem.* **2007**, *76*, 1140.
- [509] H. Kurosu, T. Yamada, I. Ando, K. Sato, T. Otsu, *J. Mol. Struct.* **1993**, *300*, 303.
- [510] H. Kurosu, K. Suzuki, I. Ando, T. Otsu, *J. Mol. Struct.* **1994**, *321*, 229.
- [511] M. Z. Elsabee, S. G. Ibrahim, *Polym. Test.* **2001**, *20*, 173.
- [512] A. Matsumoto, N. Maeo, E. Sato, *J. Polym. Sci., Polym. Chem.* **2016**, *54*, 2136.
- [513] K. Takada, A. Matsumoto, *J. Polym. Sci., Polym. Chem.* **2017**, *55*, 3266.
- [514] K. Takada, A. Matsumoto, *J. Polym. Sci., Polym. Chem.* **2018**, *56*, 2584.
- [515] N. Tsuji, Y. Suzuki, A. Matsumoto, *Polym. J.* **2019**, *51*, 1147.
- [516] E. Sato, N. Tamari, H. Horibe, *J. Polym. Sci., Polym. Chem.* **2019**, *57*, 2474.
- [517] S. B. Choi, A. Takahara, N. Amaya, Y. Murata, T. Kajiyama, *Polym. J.* **1989**, *21*, 433.
- [518] A. Laschewsky, D. Cochin, *Eur. Polym. J.* **1994**, *30*, 891.
- [519] K. Jahnichen, D. Voigt, D. Jehnichen, M. Ratzsch, *Macromol. Chem. Phys.* **1995**, *196*, 3323.
- [520] H.-K. Jeong, H. Kikuchi, T. Kajiyama, *Polym. J.* **1997**, *29*, 165.
- [521] H.-Y. Peng, Y.-S. Yang, G.-R. Qi, *Pet. Sci. Technol.* **2002**, *20*, 65.
- [522] S. Matsumura, H. Shigeno, T. Tanaka, *J. Am. Oil Chem. Soc.* **1993**, *70*, 659.
- [523] M. Ohnishi, T. Uno, M. Kubo, T. Itoh, *J. Polym. Sci., Polym. Chem.* **2009**, *47*, 420.
- [524] A. Matsumoto, T. Sumihara, *J. Polym. Sci., Polym. Chem.* **2017**, *55*, 288.
- [525] Y. Suzuki, T. Tsujimura, K. Funamoto, A. Matsumoto, *Polym. J.* **2019**, *51*, 1163.
- [526] M. Bezděk, K. Bouchal, J. Lokaj, H. Pivcova, F. Hrabak, *J. Polym. Sci., Polym. Chem. Ed.* **1974**, *12*, 1983.
- [527] V. Hynkova, F. Hrabak, *J. Polym. Sci., Polym. Chem. Ed.* **1976**, *14*, 1809.
- [528] Y. Bando, T. Dodou, Y. Minoura, *J. Polym. Sci., Polym. Chem. Ed.* **1977**, *15*, 1917.
- [529] W. R. Hertler, T. V. RajanBabu, D. W. Ovenall, G. S. Reddy, D. Y. Sogah, *J. Am. Chem. Soc.* **1988**, *110*, 5841.

- [530] A. Matsumoto, T. Matsumura, S. Aoki, *Macromolecules* **1996**, *29*, 423.
- [531] A. Matsumoto, T. Odani, *Macromol. Rapid Commun.* **2001**, *22*, 1195.
- [532] A. Matsumoto, *Polym. J.* **2003**, *35*, 93.
- [533] S. Nagahama, T. Tanaka, A. Matsumoto, *Angew. Chem., Int. Ed.* **2004**, *43*, 3811.
- [534] A. Matsumoto, T. Tanaka, *Mol. Cryst. Liq. Cryst.* **2005**, *440*, 215.
- [535] T. Itoh, Y. Mitsuda, T. Ebina, T. Uno, M. Kubo, *J. Power Sources* **2009**, *189*, 531.
- [536] G. Quintens, J. H. Vrijsen, P. Adriaenssens, D. Vanderzande, T. Junkers, *Polym. Chem.* **2019**, *10*, 5555.
- [537] A. Matsumoto, K. Shimizu, K. Mizuta, T. Otsu, *J. Polym. Sci., Polym. Chem.* **1994**, *32*, 1957.
- [538] I. C. McNeill, S. Ahmed, L. Memetea, *Polym. Degrad. Stab.* **1994**, *46*, 303.
- [539] M. Chen, C. Chen, *Angew. Chem., Int. Ed.* **2020**, *59*, 1206.
- [540] M. L. Miller, J. Skogman, *J. Polym. Sci., Part A: Gen. Pap.* **1964**, *2*, 4551.
- [541] T. Tsuruta, T. Makimoto, T. Miyazako, *Makromol. Chem.* **1967**, *103*, 128.
- [542] Y. Kobuke, J. Furukawa, T. Fueno, *J. Polym. Sci., Part A-1: Polym. Chem.* **1967**, *5*, 2701.
- [543] A. Matsumoto, A. Horie, T. Otsu, *Polym. J.* **1991**, *23*, 211.
- [544] T. Kitano, T. Fujimoto, M. Nagasawa, *Macromolecules* **1974**, *7*, 719.
- [545] T. Kitano, M. Mitsumura, T. Fujimoto, M. Nagasawa, *Macromolecules* **1975**, *8*, 382.
- [546] Y. Muroga, I. Noda, M. Nagasawa, *Macromolecules* **1980**, *13*, 1081.
- [547] K. Ute, T. Asada, Y. Nabeshima, K. Hatada, *Polym. Bull.* **1993**, *30*, 171.
- [548] K. Ute, T. Asada, K. Hatada, *Macromolecules* **1996**, *29*, 1904.
- [549] K. Ute, T. Asada, Y. Nabeshima, K. Hatada, *Macromolecules* **1993**, *26*, 7086.
- [550] K. Hatada, T. Kitayama, K. Ute, T. Nishiura, *Macromol. Synth.* **1995**, *89*, 465.
- [551] K. Ute, T. Asada, Y. Nabeshima, K. Hatada, *Acta Polym.* **1995**, *46*, 458.
- [552] Y. Isono, M. Kawai, T. Kazama, T. Takeuchi, *Polymer* **1994**, *35*, 441.
- [553] K. Ute, T. Tarao, K. Hatada, *Polym. J.* **1997**, *29*, 957.
- [554] K. Ute, T. Tarao, S. Hongo, H. Ohnuma, K. Hatada, T. Kitayama, *Polym. J.* **1999**, *31*, 177.
- [555] K. Ute, T. Tarao, T. Kitayama, *Polym. J.* **2005**, *37*, 578.
- [556] K. Ute, T. Tarao, S. Nakao, T. Kitayama, *Polymer* **2003**, *44*, 7869.
- [557] Y. Takenaka, H. Abe, *Macromolecules* **2019**, *52*, 4052.
- [558] M. Imada, Y. Takenaka, T. Tsuge, H. Abe, *Macromolecules* **2020**, *53*, 7759.
- [559] M. McGraw, E. Y.-X. Chen, *ACS Catal.* **2018**, *8*, 9877.
- [560] M. L. McGraw, E. Y.-X. Chen, *Tetrahedron* **2019**, *75*, 1475.

Chapter 2 – Multicatalytic Transformation of (Meth)acrylic Acids: a One-Pot Approach to Biobased Poly(meth)acrylates

Hugo Fouilloux,^a Wei Qiang,^a Carine Robert,^a Vincent Placet^b and Christophe M. Thomas^{a,*}

^aChimie ParisTech, PSL University, CNRS, Institut de Recherche de Chimie Paris, 75005 Paris, France.

E-mail: christophe.thomas@chimie-paristech.fr

^bFEMTO-ST Institute, CNRS/UFC/ENSMM/UTBM, Department of Applied Mechanics, Université de Bourgogne Franche-Comté Besançon, France.

This chapter has been published in *Angewandte Chemie International Edition*:

H. Fouilloux, W. Qiang, C. Robert, V. Placet and C. M. Thomas, *Angew. Chem. Int. Ed.* **2021**, *60*, 19374-19382.

Contributions to the publication:

H. F. and W. Q. performed the experiments. H. F., W. Q., C. R. and C. M. T. analysed the data. H. F. and C. M. T. wrote the paper. All authors discussed the results and commented on the manuscript.

Hugo Fouilloux



30/12/2021

Christophe M. Thomas



Abstract

Shifting from petrochemical feedstocks to renewable resources can address some of the environmental issues associated with petrochemical extraction and make plastics production sustainable. Therefore, there is a growing interest in selective methods for transforming abundant renewable feedstocks into monomers suitable for polymer production. Reported herein are one-pot catalytic systems, that are active, productive, and selective under mild conditions for the synthesis of copolymers from renewable materials. Each system allows for anhydride formation, alcohol acylation and/or acid esterification, as well as polymerization of the formed (meth)acrylates, providing direct access to a new library of unique poly(meth)acrylates.

Introduction

Cheap, light and versatile plastics are the dominant materials of our modern economy.^[1] The vast majority of these commodity materials are obtained from fossil fuels.^[2] In order to remedy some of the environmental challenges associated with petrochemical extraction, an alternative to fossil feedstocks involves using chemicals from renewable resources.^[3] In particular, the development of new methods for transforming biomass into resources suitable for polymer production is a critical hurdle along the path to a more sustainable chemical economy. The main challenge is then to design efficient and selective transformations of abundant, renewable, low-cost raw materials into innovative polymeric products.^[4] Catalysis is as an important tool to support a more sustainable plastics production and in this case should ideally be efficient, convenient, and versatile, using common reagents. In this regard, one-pot catalytic transformations have significant advantages over conventional multi-step syntheses such as time- and cost-savings, waste reduction and energy consumption.^[5] These synthetic schemes, which proceed through two or more consecutive catalytic steps, may serve as a versatile method in polymerization reactions, enabling the production of polymers with new structures and functions.^[6] However, the one-pot synthesis of a target (macro)molecule is not simply a linear combination of each optimized reaction.^[7] The different

catalytic systems used must be compatible with each other but also with the solvent, substrate, and reaction side products in order to obtain high activity and selectivity.^[8] A one-pot synthesis is thus not only a useful methodology to follow for the production of (macro)molecules, but also a promising green approach for polymer synthesis.^[9]

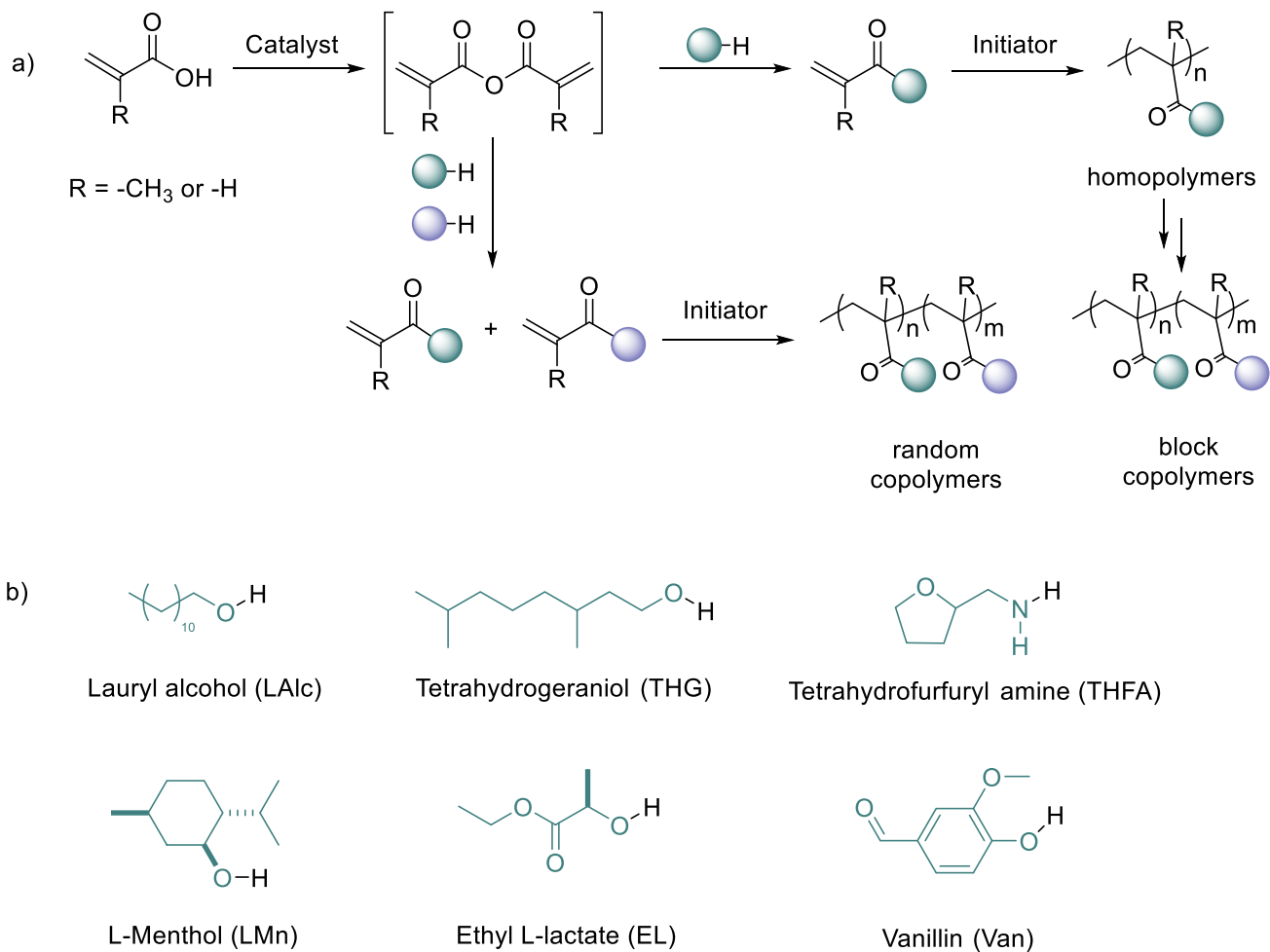
Poly(meth)acrylates are a major class of commodity plastics.^[10] Numerous studies have led to the discovery of multiple commercial applications for poly(meth)acrylates ranging from functional coatings to energy storage materials, high-performance engineering plastics and biomaterials.^[10a, 11] The diversity of pendent ester groups that can be inserted into the (meth)acrylic repeat unit is one of the features that allows poly(meth)acrylates to exhibit varied properties. Due to the vast number of alcohols that can act as precursors of (meth)acrylate ester monomers, the potential number of unique poly(meth)acrylates is large and only a small part of this extensive series of polymers has been investigated. This widely unexplored polymer library offers the possibility to identify original materials with interesting properties, particularly from renewable resources. Fully sustainable poly(meth)acrylates can nowadays theoretically be obtained by producing (meth)acrylic acid from renewable resources,^[12] efficiently coupling it with biobased alcohols,^[13] and polymerizing the resulting monomer.^[14] However, most research groups investigating the properties of biobased poly(meth)acrylates usually prepare their materials stepwise, starting from acryloyl chloride or methacrylic anhydride as these procedures require only a simple workup.^[12] Although one of the methods of choice for modifying poly(meth)acrylates properties remains copolymerization, no examples of copolymerization of (meth)acrylate derivatives from carboxylic acid precursors have yet been reported via a one-pot procedure. Herein we present a practical route to biobased poly(meth)acrylates by way of a one-pot reaction using simple commercial catalysts and we demonstrate that these requirements can be met using, *inter alia*, the synthesis of intermediate anhydride derivatives. This process provides direct access to (meth)acrylates and the corresponding (co)polymers in high yields.

Results and Discussion

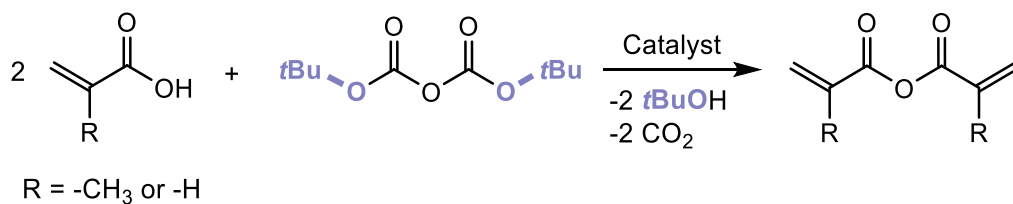
Monomer Formation Sequence

Formation of (meth)acrylic anhydrides

In order to generate (meth)acrylate monomers directly ready for copolymerization, the first objective of our one-pot approach was the synthesis of (meth)acrylic anhydrides from (meth)acrylic acids, able to act as intermediates for the synthesis of one or more esters (**Scheme 1**). This reaction is a known transformation that can only be achieved by dehydration of the starting compound under acidic conditions and at high temperature. To complete a one-pot procedure, it is therefore necessary to have an anhydride synthesis process that is efficient and produces anhydrides with a high yield. We have recently reported effective protocols for the preparation of cyclic anhydrides from the reaction of dicarboxylic acids in the presence of dialkyl dicarbonates under weak Lewis acid (LA) catalysis.^[6a, 15] Inspired by these previous results, it was envisaged that commercially available catalysts, such as magnesium chloride or triflate, could provide direct access to (meth)acrylic anhydrides with high selectivity and activity from the corresponding carboxylic acids.^[16] By reacting two equivalents of (meth)acrylic acid with di-*tert*-butyl dicarbonate (Boc₂O) and a suitable catalyst, it is indeed possible to obtain quantitatively acrylic or methacrylic anhydrides. For instance, the mild Lewis acid MgCl₂ catalyzed selectively the formation of the anhydride within 20 minutes at 30 °C (**Table 1**, entries 1&2). Magnesium triflate proved to be much slower for this reaction, reaching full conversion after 18 h (**Table 1**, entry 3). Traces of *tert*-butyl methacrylate were also observed. This by-product formation becomes even more pronounced when using strong Lewis acids (**Table S1**), as observed with La(OTf)₃ which cannot convert all the acid and only achieves 86% selectivity (**Table 1**, entry 4).



Scheme 1. a) One-pot synthesis of (meth)acrylate copolymers from biobased alcohols and (meth)acrylic anhydride. b) Biobased building block scope demonstrating generality of the methodology.

Table 1. Catalytic formation of (meth)acrylic anhydride with different catalysts.^[a]

Entry	Catalyst	Acid	Acid Conversion (Time)	Selectivity (%) ^[b]
1	MgCl ₂ (4 mol%)	Methacrylic	100% (0.33h)	>99
2	MgCl ₂ (4 mol%)	Acrylic	100% (0.33h)	>99
3	Mg(OTf) ₂ (4 mol%)	Methacrylic	100% (18h)	98
4	La(OTf) ₃ (0.5 mol%)	Methacrylic	77% (7h)	86

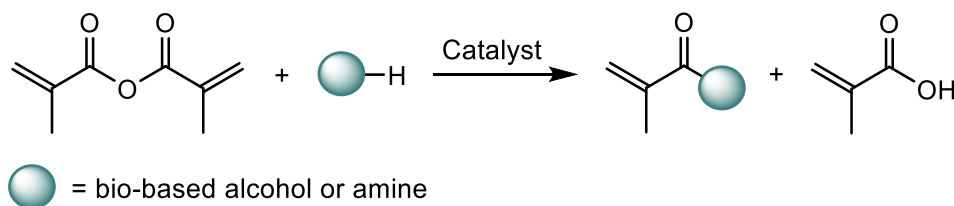
^[a] All reactions were performed under argon in acetonitrile, at T = 30°C, with [Acid] = 2 × [Boc₂O] = 3 mol/L. ^[b] Selectivity was determined by ¹H NMR spectroscopy, calculating the integral ratio of the signals of the vinylic protons of (meth)acrylic anhydride and the by-product *tert*-butyl (meth)acrylate.

Acylation with anhydrides

Encouraged by these first results, we investigated the next step of our one-pot approach: the acylation of a biobased alcohol with (meth)acrylic anhydride. We hypothesized that triflate complexes would have the potential to act as catalysts given their unique robustness and versatility,^[17] as well as their activity in the acylation of alcohol.^[18] The catalytic performances of different triflate complexes were therefore evaluated in the presence of commercially available alcohols and methacrylic anhydride. Representative results are summarized in **Table 2**.

Chapter 2

Table 2. Catalytic acylation of various alcohols/amine with different catalysts.^[a]



Entry	Catalyst	Alcohol	Time (h)	Conversion (%) ^[b]
1	Sc(OTf) ₃	Lauryl alcohol	3	100
2	Y(OTf) ₃	Lauryl alcohol	19	100
3	La(OTf) ₃	Lauryl alcohol	86	100
4	Mg(OTf) ₂	Lauryl alcohol	120	86
5	MgCl ₂	Lauryl alcohol	120	95
6	Y(OTf) ₃	Tetrahydrogeraniol	20	100
7	Y(OTf) ₃	L-menthol	39	100
8	Y(OTf) ₃	Ethyl L-lactate	72	100
9	Y(OTf) ₃	Tetrahydrofurfuryl amine	3	100
10 ^[c]	MgCl ₂	Tetrahydrogeraniol	15	100

^[a] All reactions were performed under argon in acetonitrile, at T = 40°C, with [Methacrylic Anhydride] = [Alcohol] = 1 mol/L and a catalyst loading of 2 mol%. ^[b] Conversion was determined by ¹H NMR spectroscopy, calculating the integral ratio of the signals of the vinylic protons of methacrylic anhydride and the products formed. ^[c] From the reaction mixture of the anhydride formation step. After addition of THG, T was raised to 50°C.

We first investigated the use of strong Lewis acids as catalysts, such as scandium, yttrium and lanthanum triflate: the reaction of 50 equivalents of methacrylic anhydride with lauryl alcohol was

quantitative within 3, 19 and 86 h, respectively (Table 2, entries 1–3). This trend likely reflects the influence of the metal center Lewis acidity for rare earth elements.^[19] Under the same reaction conditions, lauryl methacrylate was also obtained in the presence of mild Lewis acids such as magnesium triflate and magnesium chloride, but in lower yields (Table 2, entries 4&5). Tetrahydrogeraniol, another primary biobased alcohol, was found as reactive as lauryl alcohol using yttrium triflate (Table 2, entry 6). Secondary alcohols, such as L-menthol and ethyl L-lactate, could also be acylated (Table 2, entries 7&8), requiring a longer time than primary alcohols to give 100% of the corresponding biobased methacrylate, supposedly due to their lower nucleophilicity. This trend is confirmed by the faster acylation of amines, which are known to be better nucleophiles (Table 2, entry 9).

Finally, we were pleased to find that this acylation reaction can also be carried out from the reaction mixture of the previous anhydride formation step using MgCl_2 (Table 2, entry 10). Increasing the temperature to 50 °C in this second step even reduces the reaction time. Therefore, these results allowed us to confirm that the acylation of biobased alcohols/amine with (meth)acrylic anhydride can be carried out under mild conditions, is rapid in processing and suitable for the one-pot preparation of relevant methacrylate monomers.

Esterification of (meth)acrylic acids

We then studied the esterification of methacrylic acid using dimethyl dicarbonate (Moc_2O) and Boc_2O as coupling agents (Scheme 1). Based on the mechanism proposed by Bartoli,^[20] we assumed that the presence of a Lewis acid could cause the activation of the added dicarbonate, allowing the nucleophilic attack of the (meth)acrylic acid and ultimately leading to the formation of a mixed anhydride as a reaction intermediate (**Figure 1**). Then, the attack of a second (meth)acrylic acid generates the corresponding symmetrical anhydride, which can then react with the in situ released

alcohol (i.e., methanol) in the case of Moc_2O , or with an alcohol more nucleophilic than *t*BuOH in the case of Boc_2O , as already observed in the acylation step.

As control experiments, scandium, yttrium and lanthanum triflate derivatives were first evaluated for the esterification of methacrylic acid with Moc_2O (Table S2, entries 1–3): methyl methacrylate was the main product, with traces of dimethylcarbonate (Figure S1), as a result of the nucleophilic attack of the released methanol on the mixed anhydride intermediate or on Moc_2O itself (vide infra). As the non-sequential addition did not lead to 100% conversion of methacrylic acid into MMA with neither of the catalysts studied, sequential addition of Moc_2O was therefore performed in order to avoid the decomposition of the dicarbonate. Under these conditions, $\text{Y}(\text{OTf})_3$ was able to convert 100% of methacrylic acid into MMA within 4 h using a slight excess of Moc_2O (Table 3, entry 1). For $\text{Sc}(\text{OTf})_3$ and $\text{La}(\text{OTf})_3$ catalysts, a slightly higher excess of Moc_2O (i.e., 1.5 equivalents with respect to methacrylic acid) is necessary to obtain quantitative yields (Table S2, entries 5&6).

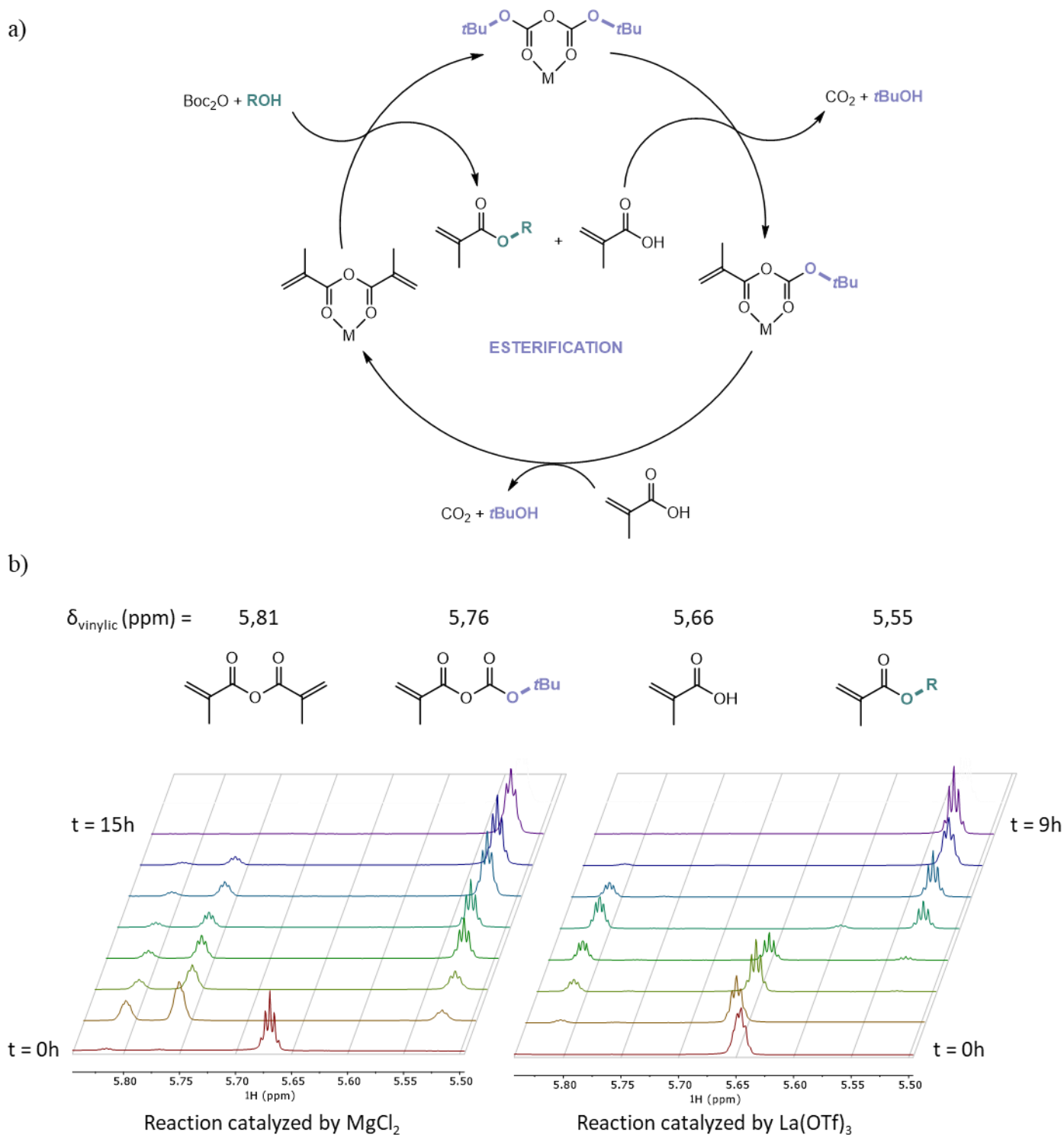
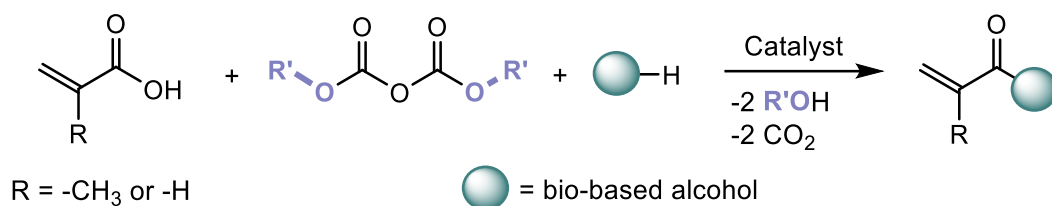


Figure 1. a) Envisaged mechanism for the esterification of methacrylic acid by an alcohol using Boc_2O , catalyzed by a metal-based complex M; b) ^1H NMR monitoring (400 MHz, CDCl_3 , 20 °C) of the reaction of methacrylic acid/tetrahydrogeraniol (1:1.2) with MgCl_2 or $\text{La}(\text{OTf})_3$, using Boc_2O .

Table 3. Catalytic esterification of methacrylic acid with different alcohols, dicarbonates and catalysts.^[a]



Entry	Roc ₂ O	Alcohol	Catalyst	Catalyst loading (mol%)	T (°C)	Completion time (h)	Selectivity for the ester ^[b] (%)
1	Moc ₂ O ^[c]	-	Y(OTf) ₃	2	40	4	>99
2	Boc ₂ O	THG	La(OTf) ₃	0.5	30	9	>99
3	Boc ₂ O	THG	MgCl ₂	4	30	15	98
4	Boc ₂ O	L-Mn	La(OTf) ₃	0.5	30	41	96
5	Boc ₂ O	EL	MgCl ₂	4	40	7	>99
7	Boc ₂ O	Vanillin	MgCl ₂	4	40	84	>99

^[a] All reactions were performed under argon in acetonitrile. [Methacrylic Acid] = 1.4 mol/L for entries 2 to 6. [Dicarbonate] = [Alcohol] = 1.2 × [Acid] for all entries. ^[b] Selectivity of the corresponding methacrylate was determined by ¹H NMR spectroscopy, calculating the integral ratio of the signals of the vinylic protons of the methacrylates involved, methacrylic acid and methacrylic anhydride. ^[c] 1.2 equivalent of Moc₂O with respect to methacrylic acid, added sequentially after the end of the first acylation step: 0.5 equivalents at t = 0, 0.25 equivalents at t = 0.5h, 0.25 equivalents at t = 1.5h, 0.2 equivalents at t = 3h.

In order to directly produce (meth)acrylates from the corresponding acid, we then investigated the use of Boc₂O as a coupling agent (Table 3, entries 2–6). Gratifyingly, esterification of methacrylic acid by primary biobased alcohols such as lauryl alcohol or THG is efficiently and selectively carried out by La(OTf)₃ and MgCl₂, within 9 and 15 h, respectively (Table 3, entries 2&3). Sc(OTf)₃ and

Y(OTf)₃ also catalyzed this reaction, although the selectivity was lower (ca. 97%, Table S3, entries 1&2). Acrylic acid is esterified under the same conditions, although it requires a longer reaction time for La(OTf)₃ than MgCl₂, with 87 and 15 h, respectively (Table S3, entries 3&4). These two catalysts are in fact quite complementary to produce a diverse library of (meth)acrylates. On the one hand, La(OTf)₃ is indeed more selective than MgCl₂ for the esterification of MAA with bulky (and less reactive) secondary alcohols such as L-menthol (Table 3, entry 4 and Table S3, entry 5). On the other hand, MgCl₂ is more functionally tolerant, as it could selectively produce methacrylates of ethyl L-lactate and vanillin (Table 3, entries 5&6). It should be noted that the use of a slight excess of alcohol and Boc₂O (ca. 1.2 × [Acid]) is mandatory to achieve complete conversion of (meth)acrylic acid, as the secondary reaction involving an alcohol attacking the activated Boc₂O to produce an unsymmetrical carbonate is observed to a small extent. Finally, although the use of amines in combination with Boc₂O is unsuitable (Table S3, entry 6), our methodology however makes it possible to obtain methacrylamides together with another methacrylate, by first the reaction of the amine with the anhydride and then esterification of the remaining acid.

To verify the mechanistic pathway during the first three steps, we performed the ¹H NMR kinetic monitoring of the esterification of methacrylic acid by tetrahydrogeraniol, in the presence of La(OTf)₃ or MgCl₂ (Table 3, entries 2&3). The nature of the resulting intermediates was assessed by examination of the vinylic and tert-butylic regions of the ¹H NMR products and hypothetical intermediates of this esterification reaction can be observed and distinguished solely by ¹H NMR spectroscopy. However, notable discrepancies are observed between the reaction catalyzed by MgCl₂ and La(OTf)₃. In the case of MgCl₂, the mixed anhydride and methacrylic anhydride are rapidly produced early in the reaction, and then gradually consumed. With La(OTf)₃, the mixed anhydride is difficult to detect, and the methacrylic anhydride is formed more slowly. These observations are consistent with the mechanism proposed by Bartoli et al, where the authors suggested that the Lewis acidity affects the reactivity of the intermediates differently. Mixed anhydride formation is probably

the fastest step when catalyzed by MgCl_2 , while methacrylic anhydride formation can be fast but slower, and alcohol acylation appears to be the rate-determining step. In the case of a stronger Lewis acid such as $\text{La}(\text{OTf})_3$, consumption of the mixed anhydride is supposedly the fastest step, which should explain why it is observed in only small amounts. However, acylation of the alcohol seems to remain the rate determining step.

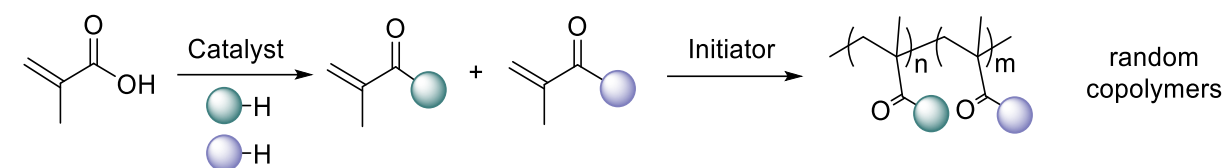
Thus, biobased (meth)acrylate monomers in solution, ready for polymerization without purification, could be obtained smoothly and quantitatively using our one-pot methodology. Starting from (meth)acrylic acid, the use of either MgCl_2 or $\text{La}(\text{OTf})_3$ provides one or several biobased (meth)acrylate(s), with excellent selectivity and a wide scope of reagents.

Polymer Formation Step

With an efficient and quantitative synthesis of (meth)acrylates in hand, we then explored the radical polymerization of the resulting monomer mixtures using 2,2'-azobis(2-methylpropionitrile) (AIBN) and various control agents. To assess the feasibility of the overall process, we conducted preliminary experiments with the rare earth triflate catalysts capable of performing the first two steps with a [catalyst]/[AIBN] ratio of 2:1 (**Table 4**, entry 1 and Table S4, entries 1–3). We first tested the copolymerization of LMA with MMA. Indeed, these copolymers could be of great interest to industry, since the resulting poly(meth)acrylate will have “soft“ (or low T_g) segments of LMA associated with “hard“ (higher T_g) segments of MMA. Remarkably, all three one-pot systems were active for the polymerization step and exhibited comparable reactivities. Also, a similar experiment using MgCl_2 for the monomer formation steps yielded comparable results (Table S4, entry 4). As a control experiment, we then performed a polymerization reaction using a clean combination of isolated methacrylates in the presence of AIBN (Table S4, entry 5). In marked contrast to what has been observed for other LA-mediated radical polymerizations of methacrylates,^[21] we noticed that direct polymerization gives poly(MMA-*co*-LMA) with a reactivity (i.e., molar masses and reaction rates) close to that obtained with one-pot systems.^[22] A conventional free radical pathway can also be suggested for these one-pot

polymerizations, as the polymers obtained with LA/AIBN were syndiotactically-enriched (rr:rm:mm = 60:40:0), such as PMMAs prepared with AIBN in the literature.^[23] In addition, increasing the catalyst loading to 5 mol% shows no significant difference (Table S4, entry 6). These results indicate that the active species formed during the (stepwise) copolymerization process might be the same species as that of the one-pot process, therefore suggesting that the coordination of a Lewis acid to the conjugate -C=O electron-withdrawing group of either an alkene or radical is not effective.^[21] This lack of effect can be attributed to the presence of a Lewis base (e.g., traces of alcohol or dimethylcarbonate), that can compete with MMA and LMA for coordination to the Lewis acid. By varying the initiator loading, we were then able to obtain copolymers of different molar masses (Table S4, entries 7–9), with increasing dispersity as the amount of AIBN decreases. Various mixtures of comonomers could be randomly copolymerized, starting from one acid and two (or more) alcohols (Table 4, entry 2), or from one alcohol and acrylic and methacrylic acids (Table 4, entry 3). These examples illustrate the wide variety of combinations possible with a one-pot system.

In order to extend the versatility of our approach, we then decided to test the reactivity of different control agents and monomer mixtures for the polymerization step.^[24] A chain transfer agent, dodecyl mercaptan (DDM), and a RAFT agent, cyanopropyl dithiobenzoate (CPDB), were thus evaluated (Table 4, entries 4–7).^[25] These control agents were efficient in controlling the homo- and copolymerization process (predictable M_n and narrow D), with various molar masses accessible depending on the loadings of chain transfer agent and initiator. The evolution of M_n^{exp} as a function of THGMA conversion was also assessed to show the control of the polymerization process using the RAFT agent (Figure S4). Overall, the radical polymerization process is efficient and not affected by the different by-products of our one-pot methodology.

Table 4. Radical polymerization of various monomer mixtures with different control agents.^[a]

Entry	M ₁	M ₂	AIBN (mol%)	Control agent (mol%)	Conv. M ₁ (%) ^[b]	Conv. M ₂ (%) ^[b]	M _n ^{exp} (g/mol) ^[c]	<i>D</i>	M _n th (g/mol) ^[d]
1	LMA	MMA	0.5	-	85	90	35 600	2.0	36 600
2	THGMA	ELMA	0.5	-	83	95	27 200	2.7	43 700
3	ELA	ELMA	0.5	-	97	99	57 500	1.7	42 000
4	LMA	MMA	0.25	DDM (4)	71	75	5 000	1.5	5 800
5	LMA	MMA	0.5	CPDB (1.5)	82	88	9 800	1.1	12 900
6	THGMA	-	1	CPDB (3)	97	-	6 200	1.2	4 900
7	THGMA	-	0.25	CPDB (0.75)	87	-	16 300	1.2	17 100

^[a] All reactions were performed under Ar, adding to the previously prepared monomer mixture in acetonitrile a solution of AIBN in toluene ($V_{\text{toluene}}/V_{\text{MeCN}} = 3$) and a control agent, and heating at $T = 70^\circ\text{C}$ for 20h. ^[b] Conversion was determined by ^1H NMR spectroscopy, calculating the integral ratio of the signals of the alkyl ester protons of the monomers and the polymers formed. ^[c] M_n^{exp} and D of polymer determined by SEC-RI in THF calibrated with polystyrene standards at 35°C . ^[d] M_n^{th} : for detailed calculations see the Supporting information.

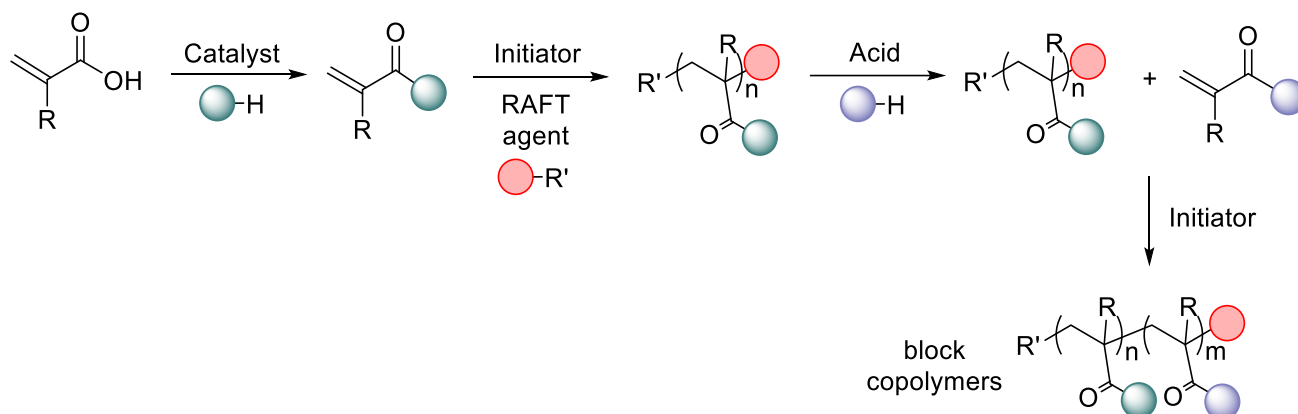
Thanks to the ability of RAFT agent-capped polymers to act as macroinitiators, we then decided to explore the one-pot synthesis of block copolymers. We envisioned that, after an initial sequence of esterification ($30\text{--}40^\circ\text{C}$) and RAFT polymerization (70°C), the reaction temperature could be reduced to $30\text{--}40^\circ\text{C}$ and new reagents could be added to perform such a sequence again. The macroinitiator

obtained upon the first sequence could then act as a RAFT agent and form block copolymers with the newly synthesized monomer (**Table 5**). This was first confirmed by the fact that the catalysts used for the initial sequence (i.e., MgCl_2 or $\text{La}(\text{OTf})_3$) were still active for a second esterification, in the same reaction mixture (Table S5). Slightly longer reaction times were required to achieve complete conversion, as the reaction medium was more diluted than under optimal conditions (Table 3). By increasing the reaction temperature again to 70 °C after adding the initiator, we then successfully obtained block copolymers. Di-block copolymers of various compositions were accessible in two sequences, depending on the RAFT agent used (Table 5). Dithioesters such as CPDB were preferred for the copolymerization of methacrylates, while trithiocarbonates such as 2-(2-cyanoprop-2-yl)-S-dodecyltrithiocarbonate (CPDTC) provided a better balance between activity and control for acrylate polymerization. If a block copolymer of methacrylate and acrylate monomers is targeted, it is mandatory to use CPDTC and start with the poly(methacrylate) block (Table 5, entries 1–4), as the poly(methacrylate) chain is a better homolytic leaving group than the poly(acrylate) chain (Table 5, entries 5&6).^[26] For the precise formation of blocks, it is crucial to attain near complete conversion of the first monomer before starting the synthesis of the second one. Depending on the monomers targeted, the catalyst must also be chosen carefully to obtain good selectivity in the esterification step. Notably, no change of molar mass was observed after the second esterification (Figures S5&S6), meaning that the macroinitiator previously formed is inactive and unaffected under the conditions of the esterification step. As already reported by Perrier, some low molar mass tailings may appear after multiple polymerization steps, due to the accumulation of dead polymer chains, initiator-derived chains or possible interactions of the multiblock copolymer with the SEC column.^[27] As in all systems based on a degenerative transfer mechanism, this can be avoided by using a higher [RAFT agent]/[initiator] ratio, as the number of living chains is dictated by the initial number of chain transfer agent. Finally, in order to determine topology and end groups of the copolymers, a diblock copolymer poly(VMA-*b*-ELMA) was characterized by MALDI-ToF-MS (Figures S7–S9). Analysis of the major

Chapter 2

isotope distributions confirmed the presence of the block copolymers with cyanopropyl and thiol end-groups.^[28]

Table 5. One-pot synthesis of various monomers and their block copolymerization.^[a]



Entry	Cat.	Control agent	M ₁	X _{M1} (%) ^[b]	M _n ^{exp} (g/mol) ^[c]	<i>D</i>	M ₂	X _{M2} (%) ^[b]	M _n ^{exp} (g/mol) ^[c]	<i>D</i>
1	La(OTf) ₃	CPDB	L-MnMA	92	8 300	1.3	THGMA	92	14 800	1.6
2 ^[d]	La(OTf) ₃	CPDB	THGMA	97	6 200	1.2	LMA	96	11 400	1.3
3 ^[e]	MgCl ₂	CPDB	VMA	96	3 800	1.1	ELMA	96	4 700	1.3
4	MgCl ₂	CPDB	VMA	86	7 400	1.4	LMA	75	13 600	1.8
5	MgCl ₂	CPDTC	THGA	90	6 900	1.2	ELA	98	10 300	1.5
6	MgCl ₂	CPDTC	ELMA	90	16 200	1.6	THGA	95	24 100	1.5

^[a] All reactions were performed under Ar, adding to the previously prepared monomer mixture in acetonitrile a solution of AIBN in toluene ($V_{\text{toluene}}/V_{\text{MeCN}} = 3$) and a control agent ($[\text{Control agent}] / [\text{AIBN}] = 5$), and heating at $T = 70^\circ\text{C}$ for 20h. Then, the reaction mixture was cooled back to 30 or 40°C (depending on the monomer) and (meth)acrylic acid, Boc₂O and the desired alcohol were introduced (same ratios as in the 1st step). Finally, after the desired amount of time, a solution of AIBN in toluene is added and the mixture is heated at $T = 70^\circ\text{C}$ for 20h. ^[b] Conversion was determined by ¹H NMR spectroscopy, calculating the integral ratio of the signals of the alkyl ester protons of the monomers and the polymers

Chapter 2

formed. ^[c] M_n^{exp} and D of polymer determined by SEC-RI in THF calibrated with polystyrene standards at 35 °C. ^[d] [Control agent] / [AIBN] = 3. ^[e] [Control agent] / [AIBN] = 12.

New homo- and copolymers synthesized by our one-pot process were then characterized by differential scanning calorimetry (DSC) and thermal gravimetric analysis (TGA) (**Tables 6 & S6**). The important range of T_g accessible confirms the wide variety of characteristics that can be obtained using our synthetic method. Starting from acrylic acid, methacrylic acid or both, coupling it with various biobased alcohols (or amines) to obtain (random or block) homo- or copolymers, the possibilities are numerous. For instance, the homopolymer of ethyl L-lactate methacrylate displays a T_g at 47 °C, while the homopolymer of tetrahydrogeraniol acrylate has a glass transition at -61 °C, due to its more flexible side chain and the less rigid nature of the polyacrylate backbone (Table 6, entries 1&2). The T_g of poly(ELMA) could either be increased or decreased by random copolymerization of ethyl L-lactate methacrylate with other suitable comonomers (Table 6, entries 4&5). Also, all of our di- and tri-block copolymers exhibited several glass transition temperatures, instead of a single T_g for fully miscible copolymers (Table 6, entries 6 to 8).^[29] Interestingly, the significant increase in the glass transition temperature of the VMA-ELMA copolymer supports the hypothesis that the T_g of these copolymers is strongly dependent on their aromatic nature (Table 6, entry 6). In addition, the double bonds in these structures can provide a functional handle for subsequent modification or cross-linking of the material. For poly(ELMA-*b*-THGA), two glass transitions were observed at -50 °C and 40 °C (Table 6, entry 7). As compared to the T_g s of poly(THGA) (-61 °C) and poly(ELMA) (47 °C) homopolymers, the small shifts indicate that the blocks of poly(THGA) and poly(ELMA) are only slightly miscible with each other. An increased thermal stability is observed for this copolymer when compared to poly(ELMA) and poly(THGA) (Figure S10). The block copolymer shows indeed a 5% weight-loss temperature of 291 °C, much higher than the ones of its respective homopolymers (248 °C and 272 °C for poly(ELMA) and poly(THGA), respectively). Such a synergy between these two blocks is noteworthy and provides better processability to the final material, as the operational window between

Chapter 2

the second glass transition temperature and the degradation temperature is expanded. The microphase separation was also confirmed for the triblock copolymer poly(ELMA-*b*-THGMA-*b*-ELMA), since two transitions are clearly observed, which are characteristic of the glass transition of the THGMA soft phase at the lower temperature (-31 °C) and the transition of the ELMA hard phase at a higher temperature (28 °C) (Table 6, entry 8).

Table 6. Thermal analyses of polymers obtained by one-pot catalysis.^[a]

Entry	Type of (co)polymer	M_n (g/mol)	T_{g1} (°C)	T_{g2} (°C)	$T_{-5\%}$ (°C)
1	poly(ELMA)	43 900	47	-	247
2	poly(THGA)	25 000	-61	-	272
3	poly(THGMA)	38 300	-27	-	214
4	poly(ELMA- <i>r</i> -MMA)	37 000	74	-	247
5	poly(ELMA- <i>r</i> -ELA)	60 300	27	-	310
6	poly(VMA- <i>b</i> -ELMA)	21 800	111	40	226
7	poly(ELMA- <i>b</i> -THGA)	24 100	40	-50	291
8	poly(ELMA- <i>b</i> -THGMA- <i>b</i> -ELMA)	22 100	28	-31	208

^[a] M_n^{exp} of polymer determined by SEC-RI in THF calibrated with polystyrene standards at 35°C. T_g of polymer determined by DSC on second heating cycle (10°C/min, N₂ flow). $T_{-5\%}$ of polymer determined by TGA (20°C/min, N₂ flow).

Remarkably, all homopolymers and random copolymers described in this study were colorless when using AIBN alone or AIBN and DDM as the initiating system. As expected, the RAFT agents used to synthesize the block copolymers imparted their color to the final material (yellow to pale

yellow for CPDTC or pink to slightly orange for CPDB at low loadings, **Figure 2**). If necessary, color removal is in principle feasible, as Perrier et al. reported an efficient method for end group modification and chain transfer agent recovery from polymethacrylates synthesized by the RAFT process.^[30]

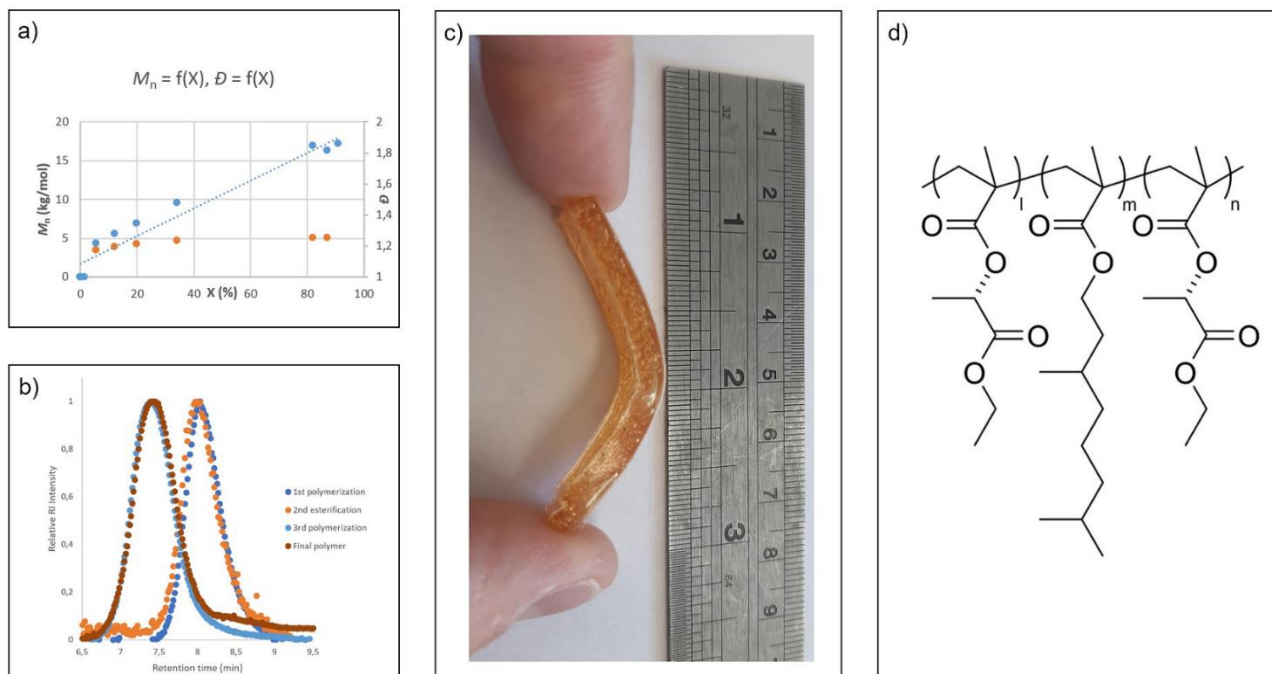


Figure 2. a) Evolution of M_n (blue dots) and D (orange dots) versus the conversion of THGMA during its one-pot synthesis and polymerization using a RAFT agent. CPDB mol% = 0.9; AIBN mol% = 0.09. $T = 70^\circ\text{C}$, for 46h. b) Evolution of the SEC-RI trace during the one-pot synthesis of the poly(ELMA-*b*-THGMA-*b*-ELMA) triblock copolymer (Table 6, entry 8), calibrated with polystyrene standards at 35°C . c) Visual representation (photo) highlighting the elastomeric character of the poly(ELMA-*b*-THGMA-*b*-ELMA) triblock copolymer (Table 6, entry 8). d) Structure of the poly(ELMA-*b*-THGMA-*b*-ELMA) triblock copolymer (Table 6, entry 8).

Finally, the environmental impact of our one-pot methodology was quickly assessed by determining the E-factor of the overall synthesis and comparing it to existing literature. For instance, Epps and co-workers reported an elegant synthesis of a block copolymer of lauryl methacrylate and vanillin methacrylate, by RAFT polymerization, via a stepwise method.^[31] Their work was highlighted

by the promising properties displayed by these new materials, but they also rightfully noted that the E-factor of their synthesis path could be improved (estimated at 500, which did not even include monomers synthesis). We could prepare a similar polymer (Table 5, entry 4) in one-pot fashion and estimated the E-factor of the overall process, including monomers synthesis, to approximately 150 (see Supporting information for detailed calculations). This dramatic decrease in mass intensity is due to the fact that workup solvents account for the major part of the total E-factor. Avoiding monomers and homopolymers isolation is therefore key for reducing the environmental impact of a synthesis path, a feature that is inherently accomplished by one-pot methodologies.

Conclusion

A new one-pot synthetic route for the production of (meth)acrylate monomers and the corresponding (co)polymers has been developed from renewable feedstocks. This approach makes it possible to directly obtain biobased materials in the form of homopolymers, or random or block copolymers, without needing to isolate and purify intermediates. In addition, these catalytic systems are remarkably robust, thus allowing the use of unpurified monomers and bench-top reaction setup. In this regard, the first steps can be performed under ambient air, although maintaining an inert atmosphere is essential for the control of the subsequent polymerization step. Ultimately, the strategy provides easy access to a set of unique macromolecular structures that can be used to meet the growing demand for new applications for commercial polymers. Our future efforts are oriented towards further study of the reaction mechanism, as well as development of catalysts that exhibit higher reactivities for the whole process.

Acknowledgements

Chimie ParisTech – PSL and CNRS are thanked for financial support. H.F. gratefully acknowledges financial support from École polytechnique (AMX) for his PhD scholarship. W.Q. acknowledges a fellowship from the CSC. Île-de-France Region is gratefully acknowledged for

financial support of 500 MHz NMR spectrometer of Chimie ParisTech in the framework of the SESAME equipment project. This project has received funding from the Bio-Based Industries Joint Undertaking under the European Union's Horizon 2020 research and innovation program under grant agreement No 744349. CMT is grateful to the Institut Universitaire de France.

References

- [1] E. MacArthur, *Science* **2017**, *358*, 843.
- [2] M. Okada, *Prog. Polym. Sci.* **2002**, *27*, 87 – 133.
- [3] a) M. A. Hillmyer, *Science* **2017**, *358*, 868 – 870; b) M. Poliakoff, P. Licence, *Nature* **2007**, *450*, 810 – 812; c) A. J. Ragauskas, C. K. Williams, B. H. Davison, G. Britovsek, J. Cairney, C. A. Eckert, W. J. Frederick, Jr., J. P. Hallett, D. J. Leak, C. L. Liotta, J. R. Mielenz, R. Murphy, R. Templer, T. Tschaplinski, *Science* **2006**, *311*, 484 – 489; d) F. Seniha Güner, Y. Yağcı, A. Tuncer Erciyes, *Prog. Polym. Sci.* **2006**, *31*, 633 – 670; e) J. F. Jenck, F. Agterberg, M. J. Droescher, *Green Chem.* **2004**, *6*, 544 – 556; f) A. Corma, S. Iborra, A. Velty, *Chem. Rev.* **2007**, *107*, 2411 – 2502; g) U. Biermann, U. T. Bornscheuer, I. Feussner, M. A. R. Meier, J. O. Metzger, *Angew. Chem. Int. Ed.* **2021**, *60*, 20144 – 20165; *Angew. Chem.* **2021**, <https://doi.org/10.1002/ange.202100778>; h) L. A. Lucia, D. S. Argyropoulos, L. Adamopoulos, A. R. Gaspar, *Can. J. Chem.* **2006**, *84*, 960 – 970.
- [4] a) P. B. Weisz, *Phys. Today* **2004**, *57*, 47 – 52; b) C. Williams, M. Hillmyer, *Polym. Rev.* **2008**, *48*, 1 – 10; c) M. J.-L. Tschan, E. Brulé, P. Haquette, C. M. Thomas, *Polym. Chem.* **2012**, *3*, 836 – 851.
- [5] a) D. E. Fogg, E. N. dos Santos, *Coord. Chem. Rev.* **2004**, *248*, 2365 – 2379; b) A. Ajamian, J. L. Gleason, *Angew. Chem. Int. Ed.* **2004**, *43*, 3754 – 3760; *Angew. Chem.* **2004**, *116*, 3842 – 3848; c) C. Robert, C. M. Thomas, *Chem. Soc. Rev.* **2013**, *42*, 9392 – 9402.
- [6] a) C. Robert, F. de Montigny, C. M. Thomas, *Nat. Commun.* **2011**, *2*, 586; b) H. Lu, J. Wang, Y. Lin, J. Cheng, *J. Am. Chem. Soc.* **2009**, *131*, 13582 – 13583; c) M. Eriksson, A. Boyer, L. Sinigoï, M. Johansson, E. Malmström, K. Hult, S. Trey, M. Martinelle, *J. Polym. Sci. Part A* **2010**, *48*, 5289 – 5297; d) C. Cheng, K. Qi, E. Khoshdel, K. L. Wooley, *J. Am. Chem. Soc.* **2006**, *128*, 6808 – 6809; e) G. Chen, D. Huynh, P. L. Felgner, Z. Guan, *J. Am. Chem. Soc.* **2006**, *128*, 4298 – 4302; f) R. B. Grubbs, C. J. Hawker, J. Dao, J. M. J. Fréchet, *Angew. Chem. Int. Ed. Engl.* **1997**, *36*, 270 – 272; *Angew. Chem.* **1997**, *109*, 261 – 264.
- [7] a) Z. Jian, S. Mecking, *Macromolecules* **2016**, *49*, 4057 – 4066; b) E.W. Dunn, G.W. Coates, *J. Am. Chem. Soc.* **2010**, *132*, 11412 – 11413; c) J.-C. Wasilke, S. J. Obrey, R. T. Baker, G. C. Bazan,

Chem. Rev. **2005**, *105*, 1001 – 1020; d) S. K. Raman, E. Brulé, M. J.-L. Tschan, C. M. Thomas, *Chem. Commun.* **2014**, *50*, 13773 – 13776; e) L. Fournier, C. Robert, S. Pourchet, A. Gonzalez, L. Williams, J. Prunet, C. M. Thomas, *Polym. Chem.* **2016**, *7*, 3700 – 3704; f) A. S. Goldman, *Science* **2006**, *312*, 257 – 261.

[8] a) S. L. Poe, M. Kobašlija, D. T. McQuade, *J. Am. Chem. Soc.* **2007**, *129*, 9216 – 9221; b) J. Zhou, *Chem. Asian J.* **2010**, *5*, 422 – 434.

[9] Y. Hayashi, *Chem. Sci.* **2016**, *7*, 866 – 880.

[10] a) P. F. Holmes, M. Bohrer, J. Kohn, *Prog. Polym. Sci.* **2008**, *33*, 787 – 796; b) O. Nuyken, in *Handbook of Polymer Synthesis* CRC Press, Boca Raton, **2004**, pp. 253 – 344; c) A. P. Mosley, in *Brydson's Plastics Materials*, Elsevier, Amsterdam, **2017**, pp. 441 – 456; d) O. W. Webster in *New Synthetic Methods*, Vol. 167, Springer, Berlin, Heidelberg, **2003**, pp. 1 – 34.

[11] a) M. J. Monteiro, M. F. Cunningham, *Macromolecules* **2012**, *45*, 4939 – 4957; b) P. B. Zetterlund, S. C. Thickett, S. Perrier, E. Bourgeat-Lami, M. Lansalot, *Chem. Rev.* **2015**, *115*, 9745 – 9800; c) M. Hong, J. Chen, E. Y.-X. Chen, *Chem. Rev.* **2018**, *118*, 10551 – 10616.

[12] H. Fouilloux, C. M. Thomas, *Macromol. Rapid Commun.* **2021**, *42*, 2000530.

[13] M. A. Droesbeke, F. E. Du Prez, *ACS Sustainable Chem. Eng.* **2019**, *7*, 11633 – 11639.

[14] a) M. F. Sainz, J. A. Souto, D. Regentova, M. K. G. Johansson, S. T. Timhagen, D. J. Irvine, P. Buijsen, C. E. Koning, R. A. Stockman, S. M. Howdle, *Polym. Chem.* **2016**, *7*, 2882 – 2887;

b) R. L. Atkinson, O. Monaghan, M. T. Elsmore, P. D. Topham, D. T. W. Toolan, M. J. Derry, V. Taresco, R. Stockman, D. De Focatiis, D. J. Irvine, S. M. Howdle, *Polym. Chem.* **2021**, *12*, 3177 – 3189.

[15] C. Robert, F. de Montigny, C. M. Thomas, *ACS Catal.* **2014**, *4*, 3586 – 3589.

[16] a) M. Carlsson, C. Habenicht, L. C. Kam, M. J. J. Antal, N. Bian, R. J. Cunningham, M. J. Jones, *Ind. Eng. Chem. Res.* **1994**, *33*, 1989 – 1996; b) J. Le Nôtre, S. C. M. Witte-van Dijk, J. van Haveren, E. L. Scott, J. P. M. Sanders, *ChemSusChem* **2014**, *7*, 2712 – 2720; c) M. Pirmoradi, J. R. Kastner, *ACS Sustainable Chem. Eng.* **2017**, *5*, 1517 – 1527; d) D.W. Johnson, G. R. Eastham, M. Poliakoff, WO 2011/077140 A2, **2011**.

[17] S. Kobayashi, M. Sugiura, H. Kitagawa, W. W.-L. Lam, *Chem. Rev.* **2002**, *102*, 2227 – 2302.

[18] a) K. Ishihara, M. Kubota, H. Kurihara, H. Yamamoto, *J. Am. Chem. Soc.* **1995**, *117*, 4413 – 4414; b) K. Ishihara, M. Kubota, H. Kurihara, H. Yamamoto, *J. Org. Chem.* **1996**, *61*, 4560 – 4567;

c) K. K. Chauhan, C. G. Frost, I. Love, D. Waite, *Synlett* **1999**, 1743 – 1744; d) P. Saravanan, V. K. Singh, *Tetrahedron Lett.* **1999**, *40*, 2611 – 2614; e) C.-T. Chen, J.-H. Kuo, C.-H. Li, N. B. Barhate, S.-W. Hon, T.-W. Li, S.-D. Chao, C.-C. Liu, Y.-C. Li, I.-H. Chang, J.-S. Lin, C.-J. Liu, Y.-C. Chou, *Org.*

- Lett.* **2001**, *3*, 3729 – 3732; f) A. Orita, C. Tanahashi, A. Kakuda, J. Otera, *J. Org. Chem.* **2001**, *66*, 8926 – 8934.
- [19] S. Fukuzumi, K. Ohkubo, *Chem. Eur. J.* **2000**, *6*, 4532 – 4535.
- [20] G. Bartoli, M. Bosco, A. Carlone, R. Dalpozzo, E. Marcantoni, P. Melchiorre, L. Sambri, *Synthesis* **2007**, 3489 – 3496.
- [21] B. B. Noble, M. L. Coote, *Adv. Phys. Org. Chem.* **2015**, *49*, 189 – 258.
- [22] a) M. Imoto, T. Otsu, Y. Harada, *Makromol. Chem.* **1963**, *65*, 180 – 193; b) S. Okuzawa, H. Hirai, S. Makishima, *J. Polym. Sci. A-1 Polym. Chem.* **1969**, *7*, 1039 – 1053; c) Y. Isobe, T. Nakano, Y. Okamoto, *J. Polym. Sci. Part A* **2001**, *39*, 1463 – 1471.
- [23] In a typical free radical polymerization, the stereoregulating effect results from a steric interaction between the incoming alkene and nearest stereocenter, but due to the conformational mobility of the chain, this effect is minimal: For example, the ratio of k_s/k_i , for methyl acrylate is 1.1 at 0 °C: a) P. Pino, U. W. Suter, *Polymer* **1976**, *17*, 977 – 995; b) T. Ando, M. Kamigaito, M. Sawamoto, *Macromolecules* **1997**, *30*, 4507 – 4510.
- [24] a) J.-F. Lutz, M. Ouchi, D. R. Liu, M. Sawamoto, *Science* **2013**, *341*, 1238149; b) T. P. Le, G. Moad, E. Rizzardo, S. H. Thang, WO98/01478, **1998**; c) J. Chiefari, Y. K. (Bill) Chong, F. Ercole, J. Krstina, J. Jeffery, T. P. T. Le, R. T. A. Mayadunne, G. F. Meijs, C. L. Moad, G. Moad, E. Rizzardo, S. H. Thang, *Macromolecules* **1998**, *31*, 5559 – 5562; d) K. Matyjaszewski, *Macromolecules* **2020**, *53*, 495 – 497; e) S. Perrier, *Macromolecules* **2017**, *50*, 7433 – 7447; f) M. Destarac, *Polym. Chem.* **2018**, *9*, 4947 – 4967.
- [25] C. Barner-Kowollik, M. Buback, B. Charleux, M. L. Coote, M. Drache, T. Fukuda, A. Goto, B. Klumperman, A. B. Lowe, J. B. Mcleary, G. Moad, M. J. Monteiro, R. D. Sanderson, M. P. Tonge, P. Vana, *J. Polym. Sci. Part A* **2006**, *44*, 5809 – 5831.
- [26] D. J. Keddie, *Chem. Soc. Rev.* **2014**, *43*, 496 – 506.
- [27] G. Gody, T. Mashmeyer, P. B. Zetterlund, S. Perrier, *Nat. Commun.* **2013**, *4*, 2505.
- [28] L. Charles, *Mass Spectrom. Rev.* **2014**, *33*, 523 – 543.
- [29] T. G. Fox, *Bull. Am. Phys. Soc.* **1956**, *1*, 123 – 135.
- [30] S. Perrier, P. Takolpuckdee, C. A. Mars, *Macromolecules* **2005**, *38*, 2033 – 2036.
- [31] A. L. Holmberg, J. F. Stanzione III, R. P. Wool, T. H. Epps III, *ACS Sustainable Chem. Eng.* **2014**, *2*, 569 – 573.

Chapter 2 – Supporting Information

Table of contents:

Methods.....	160
- Materials	160
- Measurements	160
- Representative one-pot procedure.....	161
Table S1	162
Table S2	163
Table S3	164
Table S4	165
Table S5	166
Table S6	167
Figure S1	168
Figure S2.....	169
Figure S3.....	170
Figure S4.....	171
Figure S5.....	171
Figure S6.....	172
Figure S7.....	173
Figure S8.....	174
Figure S9.....	176
Figure S10.....	177
Figure S11.....	177
Calculation of theoretical molecular weights	178
Calculation of the E-factor.....	178
Attribution of NMR signals and NMR spectra.....	180
- Monomers	180
o THGMA.....	180
o ELMA.....	185
o VMA.....	186

○ LMA.....	189
○ L-MnMA.....	190
○ THFAcm	193
- Homopolymers.....	199
○ Poly(THGA)	199
○ Poly(THGMA).....	204
○ Poly(ELMA)	207
- Random copolymers	208
○ Poly(LMA- <i>r</i> -MMA)	208
○ Poly(THGMA- <i>r</i> -ELMA)	211
○ Poly(THGMA- <i>r</i> -MMA).....	214
○ Poly(ELMA- <i>r</i> -ELA)	215
○ Poly(ELMA- <i>r</i> -MMA).....	218
- Block copolymers	221
○ Poly(THGMA- <i>b</i> -LMA)	221
○ Poly(ELMA- <i>b</i> -THGA)	223
○ Poly(L-MnMA- <i>b</i> -THGMA)	226
○ Poly(ELMA- <i>b</i> -VMA)	228
○ Poly(ELA- <i>b</i> -THGA).....	231
○ Poly(VMA- <i>b</i> -LMA).....	234
○ Poly(ELMA- <i>b</i> -THGMA- <i>b</i> -ELMA).....	238

Methods

Materials

All manipulations requiring dry atmosphere were performed under a purified argon atmosphere using standard Schlenk techniques. Solvents (acetonitrile, toluene) were freshly distilled prior to use. Deuterated solvents (chloroform-*d*, acetonitrile-*d*₃ 99.5% D, Eurisotop) were used as received. Methacrylic acid (99.5%), acrylic acid (98%) from Acros Organics, methacrylic anhydride (94%, stab. with *ca* 0.2% 2,4-dimethyl-6-tert-butylphenol), L-menthol (99%), ethyl L-lactate (99%), La(OTf)₃ (anhydrous, 99%), 1-dodecanethiol (98%), (±)-Tetrahydrofurfurylamine (97%) from Alfa Aesar, lauryl alcohol (98%), Y(OTf)₃ (97%), Sc(OTf)₃ (99%), dimethyl dicarbonate (Moc₂O, 99%), vanillin (99%) from Sigma Aldrich, Mg(OTf)₂ (98%), Zn(OTf)₂ (98%), 2-(2-Cyanoprop-2-yl)-S-dodecyltrithiocarbonate (97%), 2-Cyanoprop-2-yl-dithiobenzoate (97%) from Strem Chemicals, trifluoromethanesulfonic acid (99%), di-*tert*-butyl dicarbonate (99%) from Fluorochem, 3,7-dimethyl-1-octanol (98%) from TCI Europe were used as received. 2,2'-Azobis(isobutyronitrile) (AIBN, 98%, Sigma-Aldrich) was recrystallized from freshly distilled diethyl ether.

Measurements

NMR spectra were recorded on Bruker Avance-400 spectrometer at Chimie ParisTech. ¹H and ¹³C chemical shifts are reported in ppm versus SiMe₄ and were determined by reference to the residual solvent peaks. Assignment of signals was made from multinuclear 1D (¹H, ¹³C{¹H}) and 2D (HMQC) NMR experiments. Size exclusion chromatography (SEC) of polymers was performed in THF at 35 °C using an Agilent 1260 Infinity Series GPC (ResiPore 3 μm, 300 x 7.5 mm, 1.0 mL/min, RI (PL-GPC 220) detectors) at Chimie ParisTech. The number average molecular masses (*M*_n) and polydispersity index (*M*_w/*M*_n) of the polymers were calculated with reference to a universal calibration vs. polystyrene standards (limits *M*_w= 200 to 400,000 g/mol). Calorimetric measurements were performed using a Discovery DSC25 from TA instruments, under a nitrogen flow, calibrated with

Indium. Thermogravimetric analysis (TGA) data were obtained with a TGA55 from TA instruments, under a nitrogen flow. MALDI-TOF mass spectrometry analyses were recorded with a Axima Confidence spectrometer (Shimadzu), externally calibrated with PEG ($M_n = 2000$ g/mol).

Representative one-pot procedure

A solution of $MgCl_2$ (8.6 mg, 90 μ mol), tetrahydrogeraniol (520 μ L, 2.7 mmol), methacrylic acid (190 μ L, 2.25 mmol) and Boc_2O (630 μ L, 2.7 mmol) in freshly distilled CH_3CN (300 μ L) was stirred and heated at 30°C for 15h. The CO_2 produced is released from the reactor, while being maintained under Argon. A solution of AIBN (1.85 mg, 11.25 μ mol) in freshly distilled toluene (1.5 mL) was added under argon and the reaction mixture was stirred at 70°C for 20h. After exposure to air, the solvent was evaporated under vacuum, yielding a sticky solid. The resulting polymer was purified by dissolution in a minimum amount of CH_2Cl_2 (1.5 mL) and precipitation in MeOH (40 mL). The supernatant was removed and the obtained solid was dried under vacuum.

Table S1. Catalytic formation of (meth)acrylic anhydride with different catalysts.^[a]

Entry	Catalyst	Acid	Acid conversion (Time)	Selectivity (%) ^[b]
1	La(OTf) ₃ (0.5 mol%)	Acrylic	82% (23h)	89
2	Y(OTf) ₃ (0.5 mol%)	Methacrylic	85% (7h)	90
3	Sc(OTf) ₃ (0.5 mol%)	Methacrylic	71% (23h)	82

^[a] All reactions were performed under argon in acetonitrile, at T = 30°C, with [Acid] = 2 × [Boc₂O] = 3 mol/L. ^[b] Selectivity was determined by ¹H NMR spectroscopy, calculating the integral ratio of the signals of the vinylic protons of (meth)acrylic anhydride and the by-product *tert*-butyl (meth)acrylate.

Table S2. Catalytic esterification of methacrylic acid with dimethyldicarbonate and various catalysts.^[a]

Entry	Catalyst	Addition of Moc ₂ O ([Moc ₂ O]/[Acid])	Time (h)	Conversion of Moc ₂ O ^[b] (%)	Yield of MMA ^[c] (%)
1	Y(OTf) ₃	Non-sequential (1)	1.5	100	71
2	Sc(OTf) ₃	Non-sequential (1)	4	100	80
3	La(OTf) ₃	Non-sequential (1)	1.5	100	69
4	Y(OTf) ₃	Sequential (1.2) ^[d]	4	100	100
5	Sc(OTf) ₃	Sequential (1.5) ^[d]	7	100	100
6	La(OTf) ₃	Sequential (1.5) ^[d]	4	100	100

^[a] All reactions were performed under argon in acetonitrile, at T = 40°C, with [Methacrylic Anhydride] = [Alcohol] = 1 mol/L and a catalyst loading of 2 mol%. ^[b] Conversion of the Moc₂O was determined by ¹H NMR spectroscopy, calculating the integral ratio of the signals of the methyl protons of Moc₂O and the products formed. ^[c] Yield of the corresponding methacrylate was determined by ¹H NMR spectroscopy, calculating the integral ratio of the signals of the vinylic protons of the methacrylates involved, methacrylic acid and methacrylic anhydride. ^[d] 1.5 equivalent of Moc₂O with respect to methacrylic acid, added sequentially after the end of the first acylation step: 0.5 equivalents at t = 0, 0.5 equivalents at t = 0.5h, 0.25 equivalents at t = 1.5h, 0.25 equivalents at t = 3h.

Chapter 2

Table S3. Catalytic esterification of (meth)acrylic acid with different alcohols, dicarbonates and catalysts.^[a]

Entry	Acid	Roc ₂ O	Nucleophile	Catalyst	T (°C)	X (Time)	Selectivity for the ester ^[b] (%)
1	MAA	Boc ₂ O	THG	Sc(OTf) ₃ (0.5 mol%)	30	100% (23h)	97
2	MAA	Boc ₂ O	THG	Y(OTf) ₃ (0.5 mol%)	30	100% (15h)	97
3	AA	Boc ₂ O	THG	La(OTf) ₃ (0.5 mol%)	30	100% (87h)	>99
4	AA	Boc ₂ O	THG	MgCl ₂ (4 mol%)	30	100% (15h)	98
5	MAA	Boc ₂ O	L-Menthol	MgCl ₂ (4 mol%)	30	91% (180 h)	87
6	MAA	Boc ₂ O	THFam	MgCl ₂ (4 mol%)	40	41% (15h)	63

^[a] All reactions were performed under argon in acetonitrile. [Acid] = 1.4 mol/L and [Dicarbonate] = [Alcohol] = 1.2 × [Acid] for all entries. ^[b] Selectivity of the corresponding methacrylate was determined by ¹H NMR spectroscopy, calculating the integral ratio of the signals of the vinylic protons of the methacrylates involved, methacrylic acid and methacrylic anhydride. ^[c] 1.2 equivalent of Moc₂O with respect to methacrylic acid, added sequentially after the end of the first acylation step: 0.5 equivalents at t = 0, 0.25 equivalents at t = 0.5h, 0.25 equivalents at t = 1.5h, 0.2 equivalents at t = 3h.

Chapter 2

Table S4. Radical polymerization of an equimolar MMA-LMA mixture with different catalysts.^[a]

Entry	Catalyst	Cat. (mol%)	AIBN (mol%)	Conv. MMA (%) ^[d]	Conv. LMA (%) ^[d]	M_n^{exp} (g/mol) ^[e]	M_w/M_n
1	Sc(OTf) ₃	1	0.5	88	87	33 700	1.8
2	Y(OTf) ₃	1	0.5	90	85	35 600	2.0
3	La(OTf) ₃	1	0.5	90	84	30 300	1.9
4 ^[b]	MgCl ₂	4	0.5	86	83	37 000	2.3
5 ^[c]	-	-	0.5	90	87	35 000	2.3
6	Y(OTf) ₃	5	0.5	95	87	35 300	2.0
7	Y(OTf) ₃	1	1	96	92	21 900	1.8
8	Y(OTf) ₃	1	0.25	86	79	52 800	2.2
9	Y(OTf) ₃	1	0.125	73	70	75 900	2.3

^[a] All reactions were performed under argon, adding to the previously prepared equimolar mixture of MMA and LMA in acetonitrile a solution of AIBN in toluene ($V_{\text{toluene}}/V_{\text{MeCN}} = 3$), and heating at $T = 70^\circ\text{C}$ for 20h. All reactions gave slightly syndiotactic polymethacrylates ($[rr] = 60\text{-}65\%$, $[mr] = 40\text{-}35\%$, $[mm] = 0\%$; determined by ^{13}C NMR spectroscopy, calculating the integral ratio of the signals of the quaternary carbon of the polymer). ^[b] Reaction not performed in a one-pot fashion: LMA was prepared separately and purified in order to get rid of any trace of catalyst; it was then added to a reaction mixture that contained the same amount of commercial MMA and acetonitrile as the other reactions studied. ^[c] Conversion was determined by ^1H NMR spectroscopy, calculating the integral ratio of the signals of the methyl ester and lauryl ester protons of MMA, LMA and the copolymer formed. ^[d] M_n^{exp} of polymer determined by SEC-RI calibrated with polystyrene standards at 35°C .

Chapter 2

Table S5. Catalytic esterification of methacrylic acid with different alcohols, dicarbonates and catalysts after a first sequence of esterification-polymerization using a RAFT agent.^[a]

Entry	Acid	Dicarbonate	Alcohol	Catalyst	T (°C)	Time for full conversion (h)	Selectivity for the ester ^[b] (%)
1	MAA	Boc ₂ O	Lauryl	La(OTf) ₃ (0.5 mol%)	30	20	>99
2	AA	Boc ₂ O	THG	MgCl ₂ (4 mol%)	30	64	93
3	AA	Boc ₂ O	EL	MgCl ₂ (4 mol%)	40	14	>99
4	MAA	Boc ₂ O	Vanillin	MgCl ₂ (4 mol%)	40	134	94

^[a] All reactions were performed under argon in acetonitrile. [Acid] = 0.5 mol/L and [Dicarbonate] = [Alcohol] = 1.2 × [Acid] for all entries. ^[b] Selectivity of the corresponding methacrylate was determined by ¹H NMR spectroscopy, calculating the integral ratio of the signals of the vinylic protons of the methacrylates involved, methacrylic acid and methacrylic anhydride. ^[c] 1.2 equivalent of Moc₂O with respect to methacrylic acid, added sequentially after the end of the first acylation step: 0.5 equivalents at t = 0, 0.25 equivalents at t = 0.5h, 0.25 equivalents at t = 1.5h, 0.2 equivalents at t = 3h.

Chapter 2

Table S6. Thermal analyses of polymers obtained by one-pot catalysis.^[a]

Entry	Type of (co)polymer	M_n (g/mol)	T_{g1} (°C)	T_{g2} (°C)	$T_{-5\%}$ (°C)
1	poly(LMA- <i>r</i> -MMA)	20 000	-6	-	198
2	poly(THGMA- <i>r</i> -ELMA)	27 200	7	-	184
3	poly(THGMA- <i>r</i> -MMA)	27 600	16	-	233
4	poly(L-MnMA- <i>b</i> -THGMA)	14 800	14	86	203
5	poly(VMA- <i>b</i> -LMA)	13 600	-57	118	229
6	poly(THGA- <i>b</i> -ELA)	12 300	-55	-13	291

^[a] M_n^{exp} of polymer determined by SEC-RI calibrated with polystyrene standards at 35°C. T_g of polymer determined by DSC on second heating cycle (10°C/min, N₂ flow). $T_{-5\%}$ of polymer determined by TGA (20°C/min, N₂ flow).

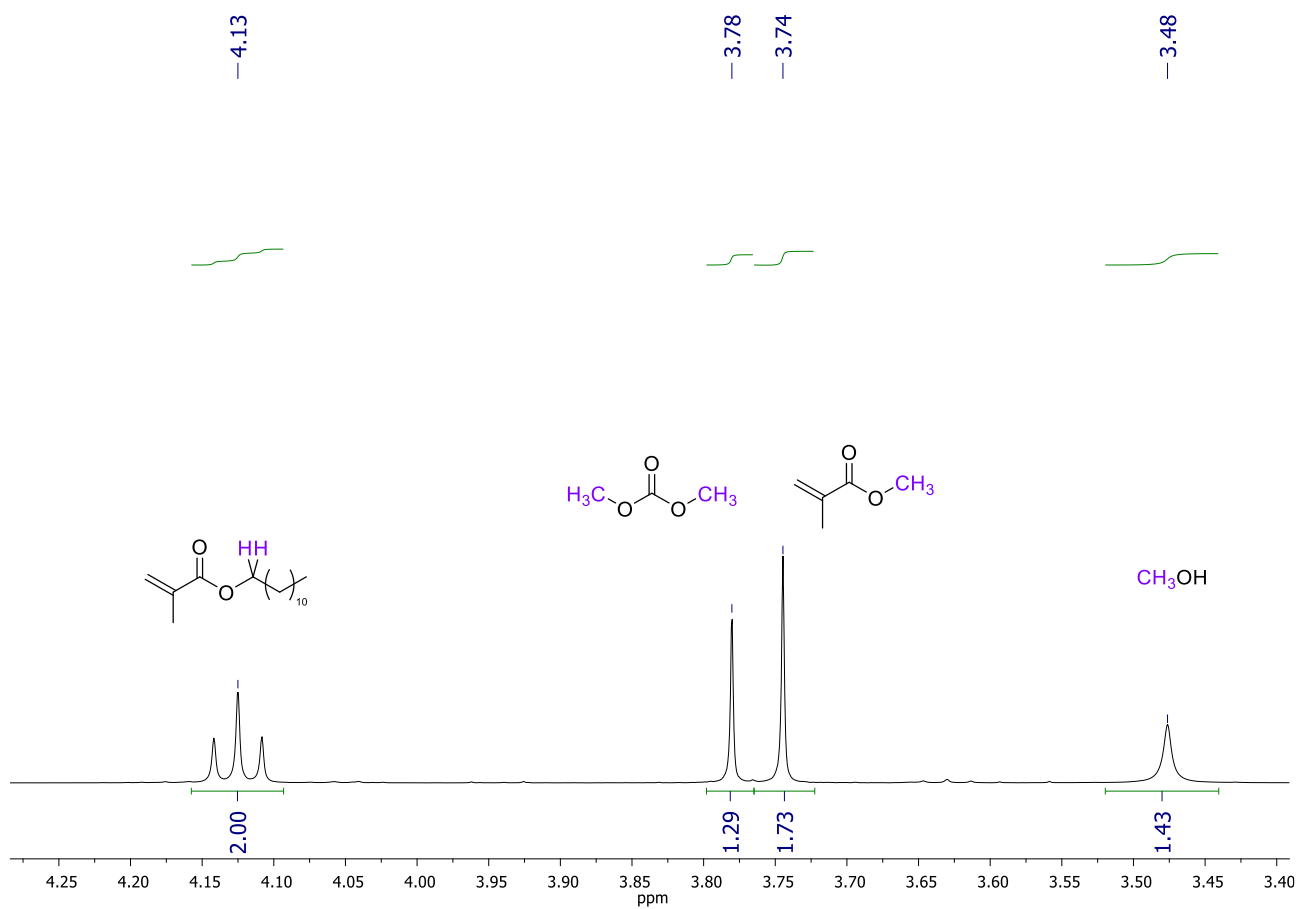


Figure S1. Alkoxy region of the ^1H NMR spectrum (400 MHz, CDCl_3 , 4.30-3.40 ppm) of the esterification of MAA with Moc_2O (1 equivalent, non-sequential), catalyzed by $\text{Y}(\text{OTf})_3$ (Table S2, entry 1).

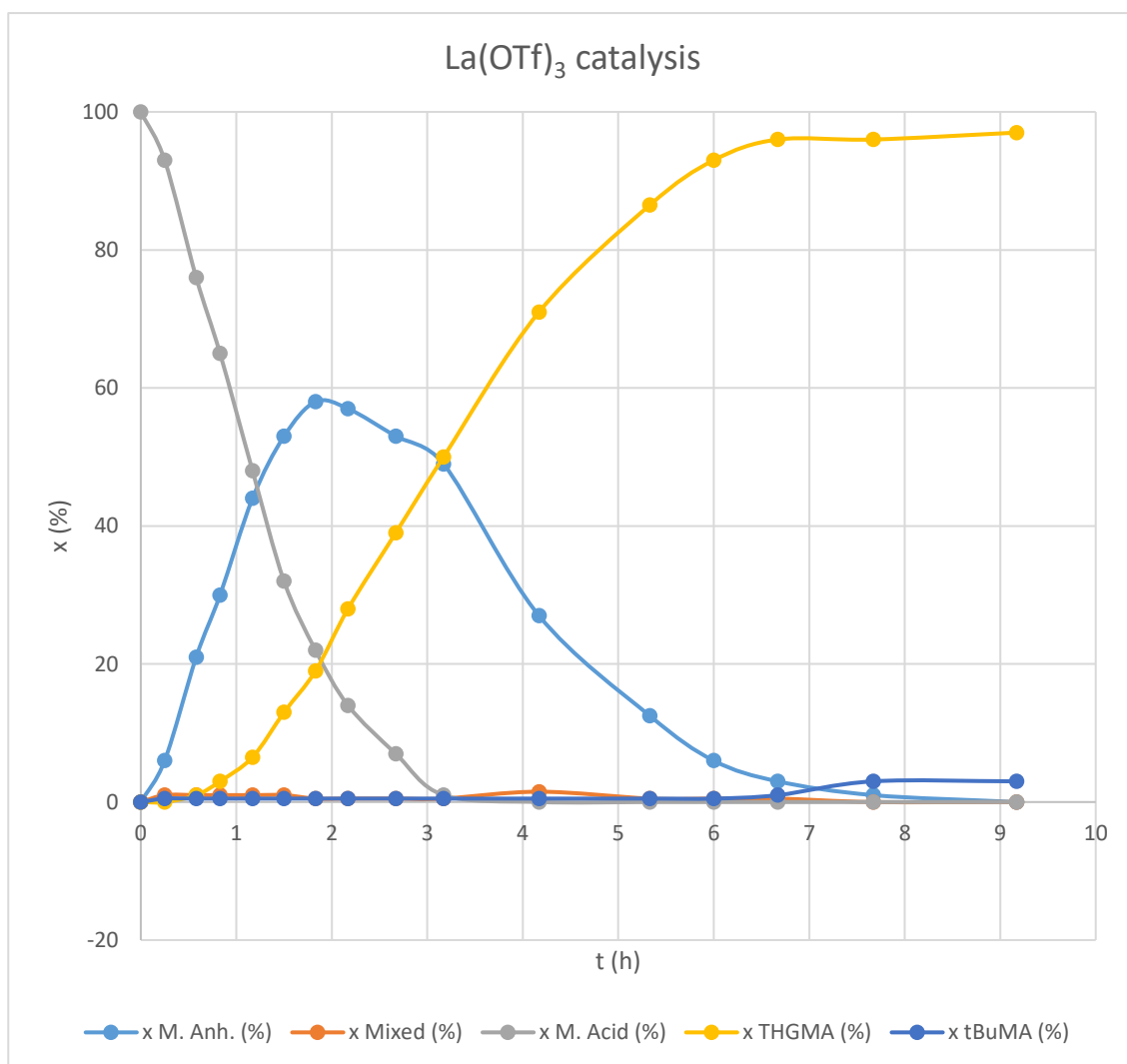


Figure S2. Evolution of the molar fraction the different vinylic reagents, products and intermediates during the esterification of MAA by THG, catalyzed by $\text{La}(\text{OTf})_3$. Molar fractions were determined by relative integration of the corresponding peaks on the ^1H NMR spectra obtained by sampling of the reaction mixture at regular intervals.

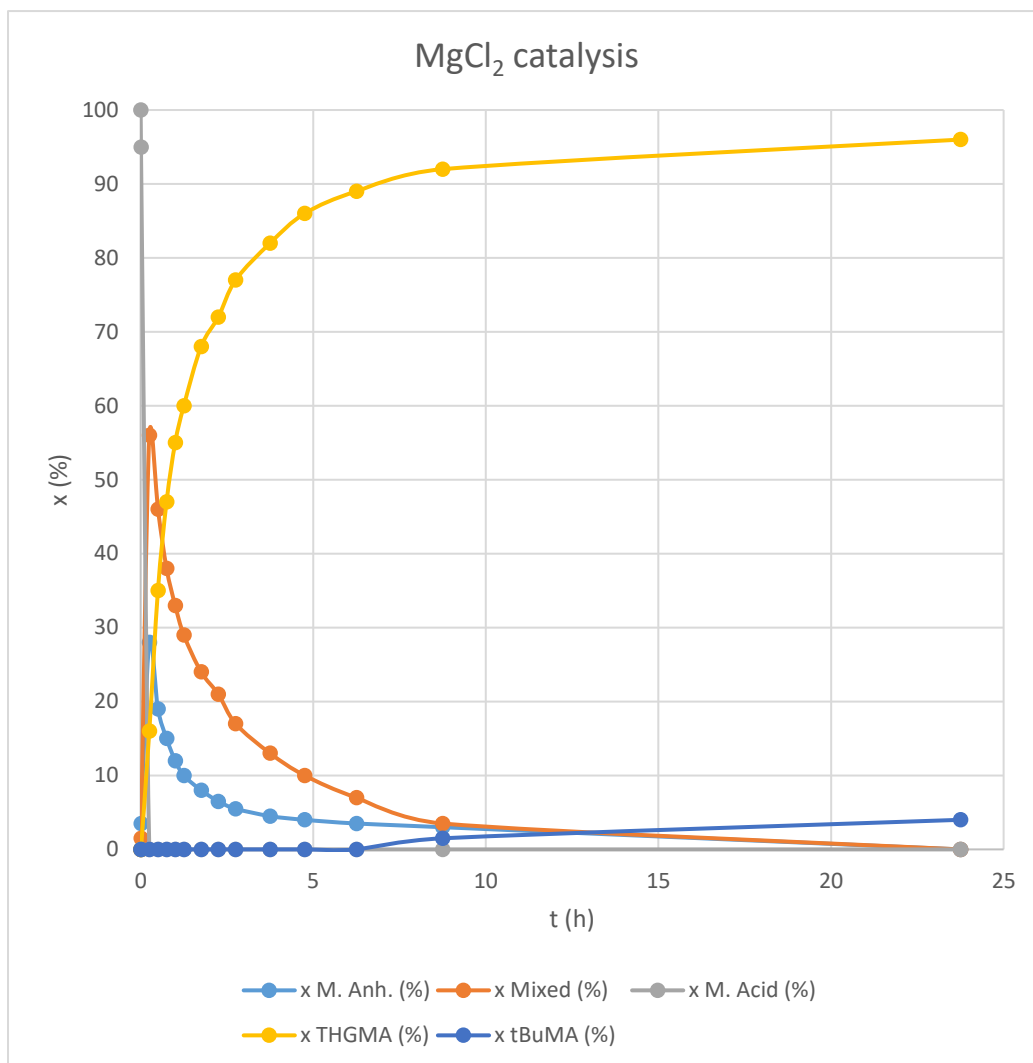


Figure S3. Evolution of the molar fraction the different vinylic reagents, products and intermediates during the esterification of MAA by THG, catalyzed by MgCl_2 . Molar fractions were determined by relative integration of the corresponding peaks on the ^1H NMR spectra obtained by sampling of the reaction mixture at regular intervals.

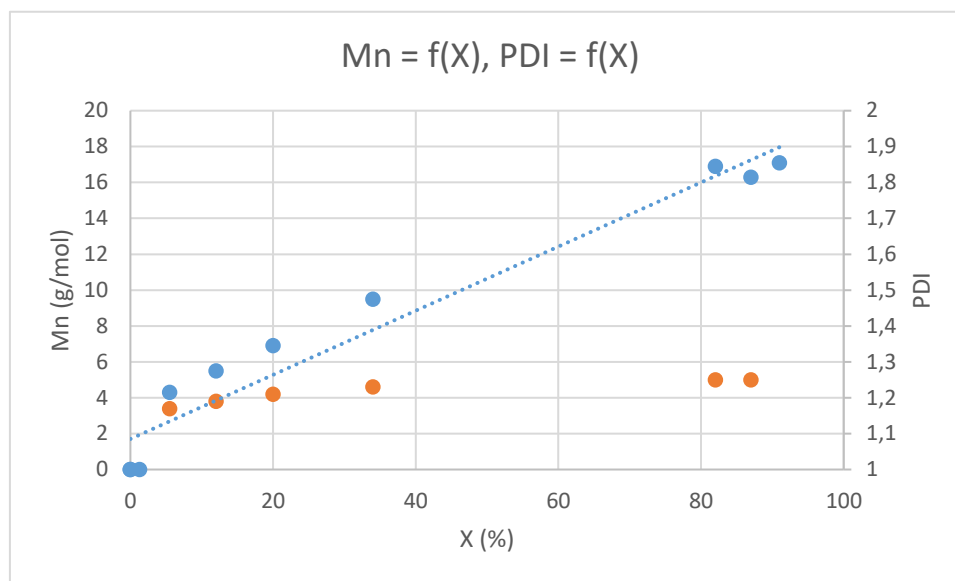


Figure S4. Evolution of M_n (blue dots) and M_w/M_n (orange dots) versus the conversion of THGMA during its one-pot synthesis and polymerization using a RAFT agent. CPDB mol% = 0.9 ; AIBN mol% = 0.09. T = 70°C, for 46h.

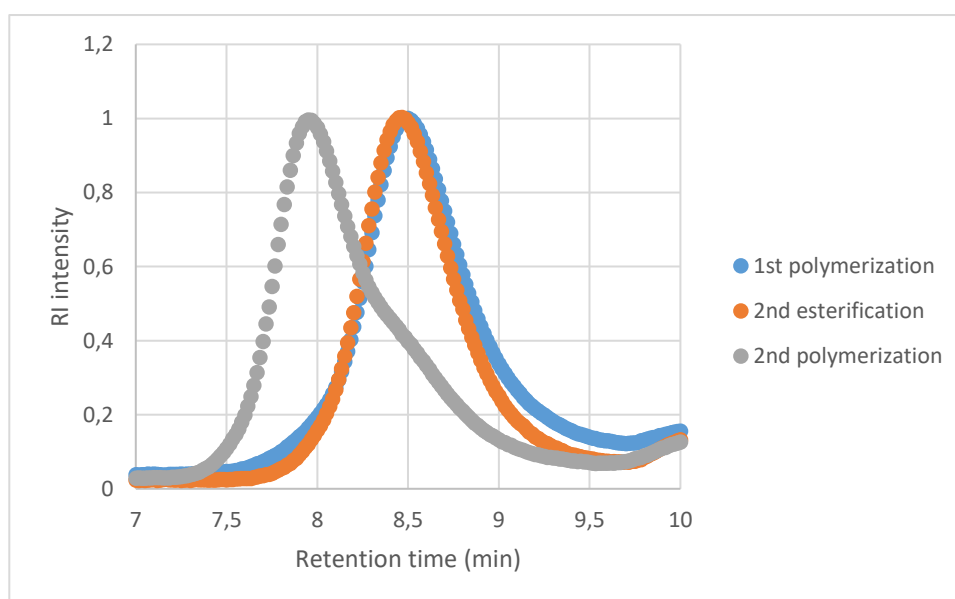


Figure S5. Evolution of the SEC-RI trace during the one-pot synthesis of a block copolymer (Table 5, entry 1), calibrated with polystyrene standards at 35°C.

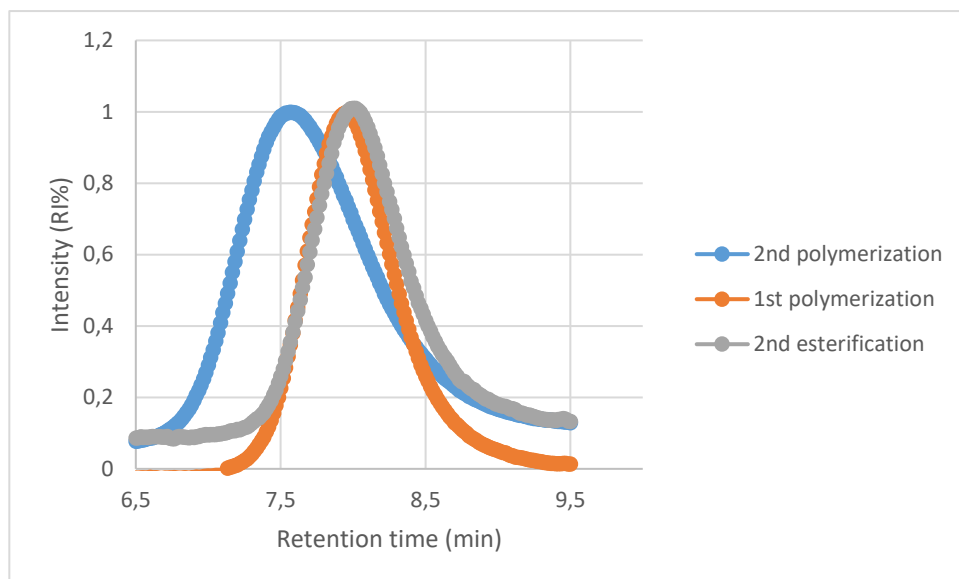


Figure S6. Evolution of the SEC-RI trace during the one-pot synthesis of a block copolymer (Table 5, entry 2), calibrated with polystyrene standards at 35°C.

MALDI-TOF mass spectrometry:

The obtention of block copolymers was further confirmed by MALDI-TOF mass spectrometry (Figure S7). Poly(VMA-*b*-ELMA) of 4 700 g/mol (determined by SEC-RI) was prepared by our methodology, using 1 mol% of AIBN and 12 mol% of CPDB (Table 5, entry 4). Each peak is separated by 186 g/mol or 220 g/mol, corresponding to the molar masses of ELMA and VMA, respectively. This observation, coupled with the fact that 96% of VMA was polymerized after the first polymerization step (determined by ^1H NMR), therefore confirms the obtention of quasi-block copolymers. Additionally, the most likely chain-end identified were the cyanopropyl and thiol moieties. The cyanopropyl group is the only initiating group present in the reaction medium (derived either from AIBN or CPDB), and is thus highly likely to be present at the beginning of each polymer chain. The thiol moiety probably comes from the degradation of the dithioester group during the MALDI-TOF analysis, as classically reported for polymethacrylates.¹ For instance, these two end-

¹L. Charles, *Mass Spectrom. Rev.* **2014**, 33, 523-543.

groups, combined with 5 units of VMA and 2 units of ELMA, give a theoretical mass of 1707,4 g/mol, in good accordance with the peak observed at 1707,1 g/mol observed during the MALDI-TOF analysis. Random copolymers obtained using DDM as chain transfer agent were also characterized by MALDI-TOF and showed good chain-end retention, as expected for the formation of more robust thioether linkages (Figures S8&S9).

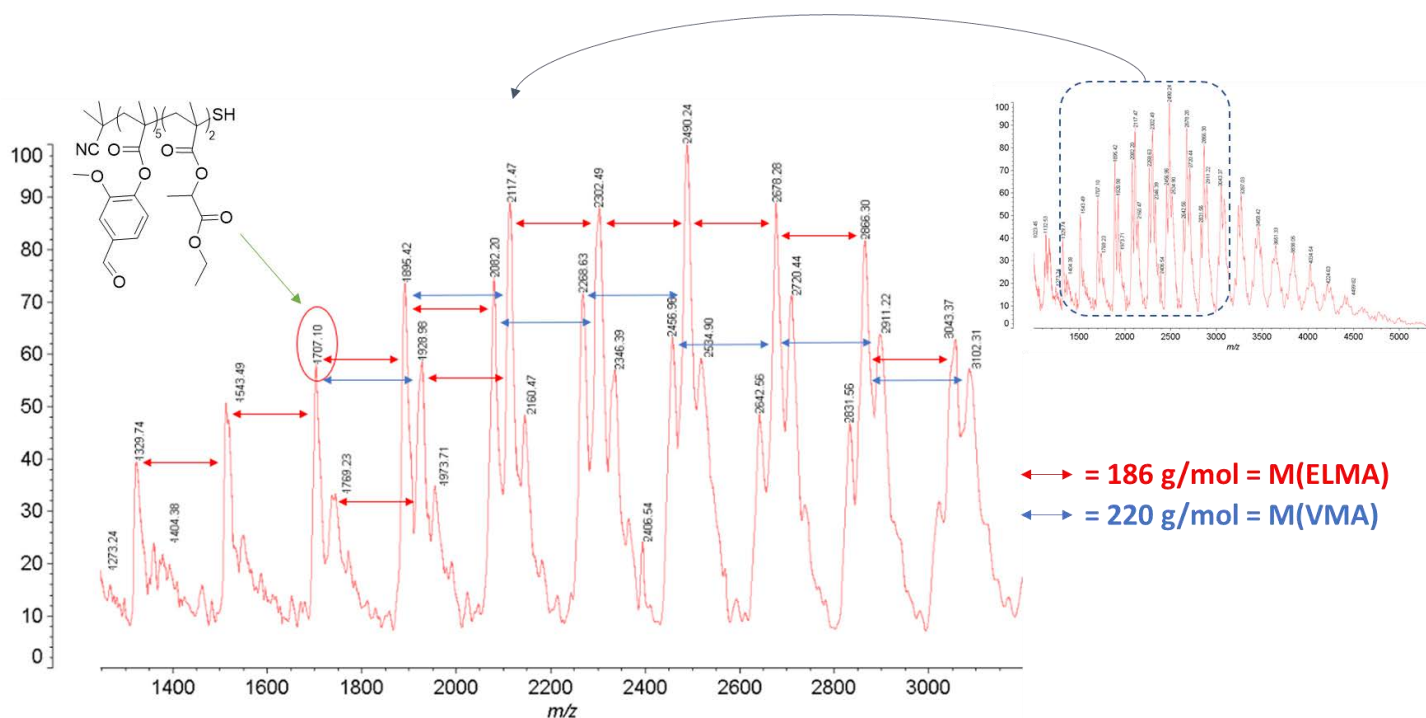


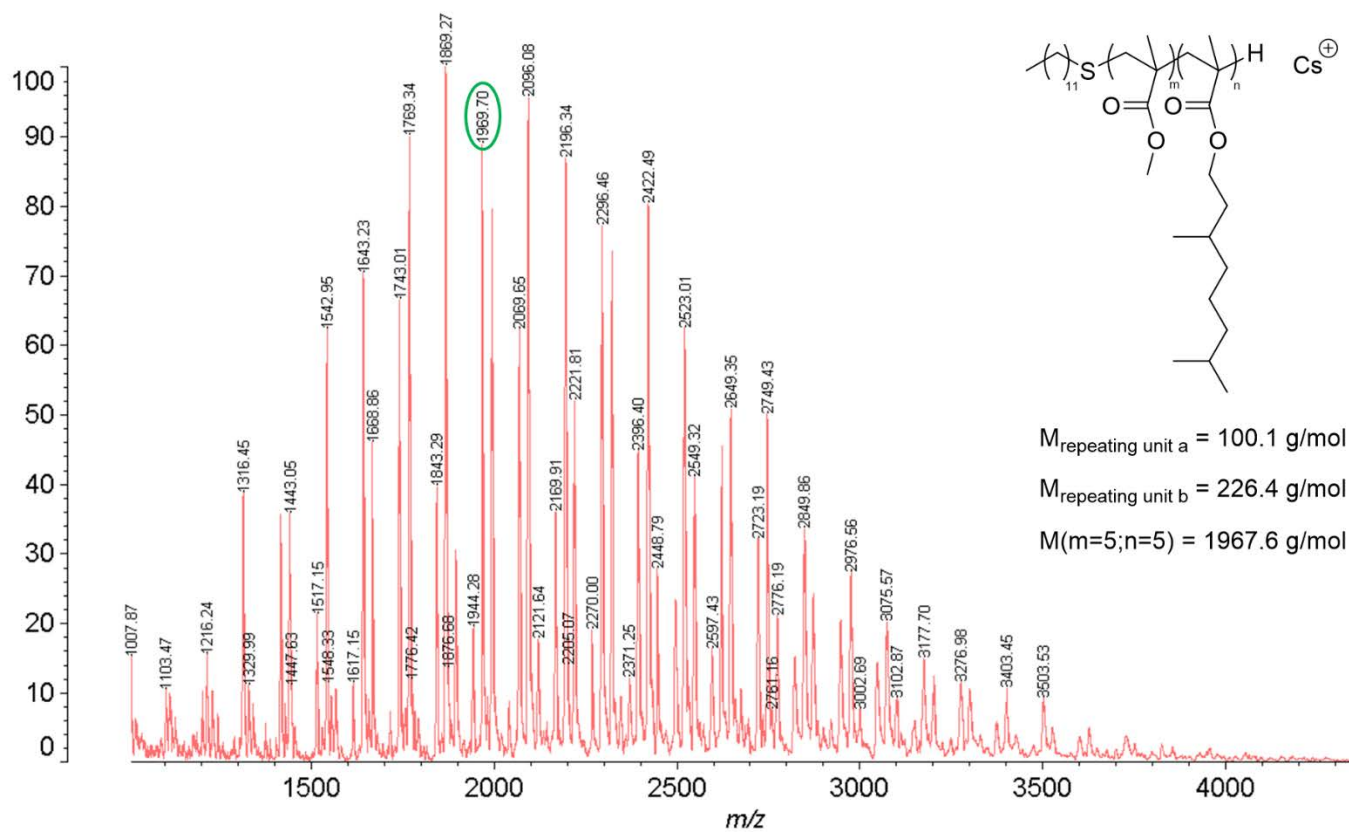
Figure S7. MALDI-TOF spectrum of poly(VMA-*b*-ELMA) synthesized in one-pot by our 4-step methodology (matrix: dithranol ; cationizing agent: cesium trifluoroacetate).

The copolymer of MMA and THGMA synthesized using DDM as control agent showed a symmetrical mass distribution and exact masses corresponding to the expected chain ends using DDM and different cationizing agents, thereby confirming the nature of the polymer obtained (Figures S7&S8). The different peaks observed are all separated by 100 or 226 g/mol, corresponding to the molecular mass of each comonomer. Hence, the number of repeating units of MMA and THGMA in the polymer chains is various and relatively independent (for instance, 1769 g/mol

Chapter 2

corresponds to 3 MMA and 5 THGMA, while 2170 g/mol corresponds to 7 MMA and 5 THGMA).

These observations seem to assess the random nature of the free radical copolymerization process.



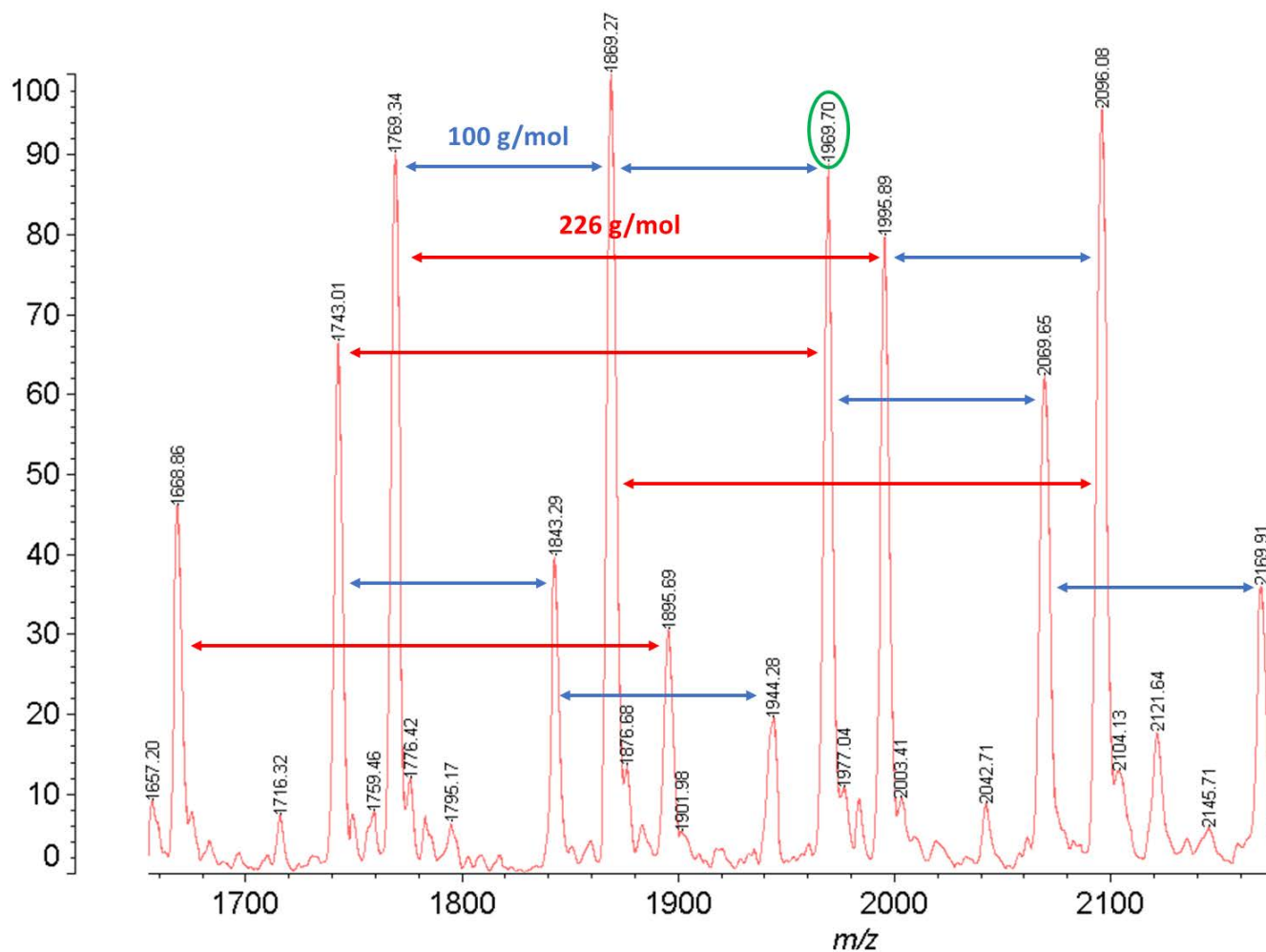


Figure S8. MALDI-TOF mass spectrum of the copolymer obtained by copolymerization of MMA and THGMA using DDM as control agent, dithranol matrix and CsTFA cationizing agent, and enlarged view of the same spectrum between 1600 and 2200 g/mol.

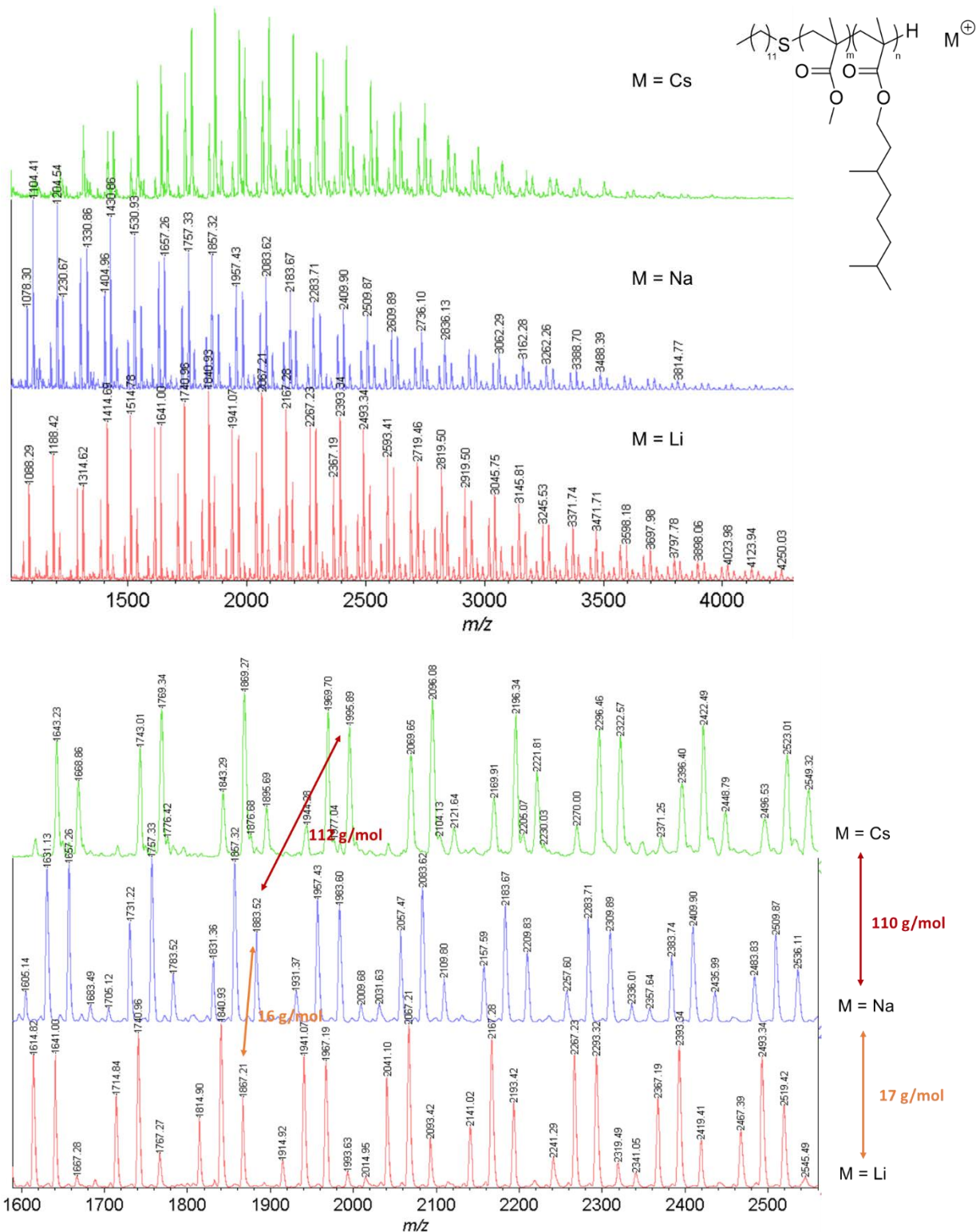


Figure S9. MALDI-TOF mass spectrum of the copolymer obtained by copolymerization of MMA and THGMA using DDM as control agent, dithranol matrix and various cationizing agents, and enlarged view of the same spectrum between 1600 and 2600 g/mol.

Thermogravimetric analysis:

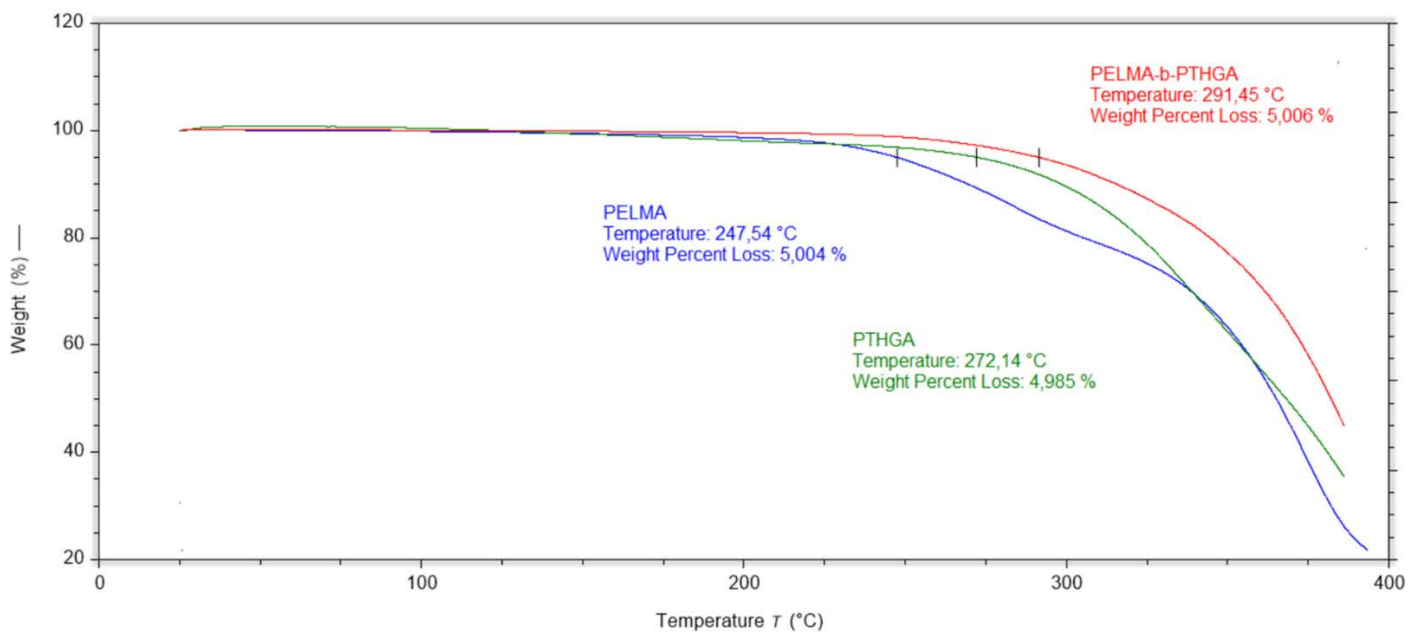


Figure S10. TGA traces of various polymers, obtained under nitrogen atmosphere, with a temperature ramp of 20°C/min from 25 to 400°C.

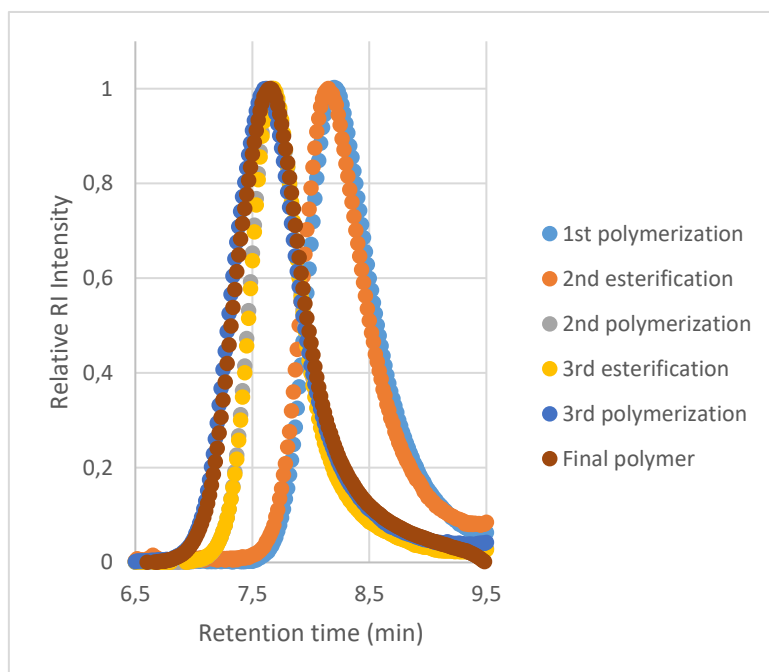


Figure S11. Evolution of the SEC-RI trace during the one-pot synthesis of a tri-block copolymer (Table 6, entry 8), calibrated with polystyrene standards at 35°C.

Calculation of theoretical molecular weights:

- Free radical polymerization:

$$M_n^{\text{th}} = \frac{100 \times \text{Conv.} \cdot M_1 \times M(M_1) + 100 \times \text{Conv.} \cdot M_2 \times M(M_2)}{2 \times f \times \text{AIBN mol\%} \times (1 - e^{-k_d \times t}) \times (1 - f_c/2)}$$

as one molecule of AIBN should initiate two polymeric chains.

- Polymerization with DDM:

$$M_n^{\text{th}} = \frac{100 \times \text{Conv.} \cdot M_1 \times M(M_1) + 100 \times \text{Conv.} \cdot M_2 \times M(M_2)}{\text{DDM mol\%} + 2 \times f \times \text{AIBN mol\%} \times (1 - e^{-k_d \times t}) \times (1 - f_c/2)}$$

- RAFT polymerization:

$$M_n^{\text{th}} = \frac{100 \times \text{Conv.} \cdot M_1 \times M(M_1) + 100 \times \text{Conv.} \cdot M_2 \times M(M_2)}{\text{RAFT mol\%} + 2 \times f \times \text{AIBN mol\%} \times (1 - e^{-k_d \times t}) \times (1 - f_c/2)} + M_{\text{RAFT}}$$

This latter formula was adapted from *Aust. J. Chem.* **2005**, 58, 379-410. The f factor represents the initiation efficiency of AIBN and is classically estimated to be 0.5. The term $e^{-k_d \times t}$ was neglected for long reaction times. The term $1 - f_c/2$ is estimated to be 1.67 for MMA and was assumed to be the same for other methacrylates. Thus, the previous formula could be used as follows:

$$M_n^{\text{th}} = \frac{100 \times \text{Conv.} \cdot M_1 \times M(M_1) + 100 \times \text{Conv.} \cdot M_2 \times M(M_2)}{\text{RAFT mol\%} + 1.67 \times \text{AIBN mol\%}} + M_{\text{RAFT}}$$

Calculation of the E-factor:

Synthesis of poly(VMA-*b*-LMA) by our one-pot methodology:

$$\text{E - factor} = \frac{\text{mass of all chemicals used (reagents, solvents, etc)}}{\text{mass of isolated product}} - 1$$

Chapter 2

$$\text{E - factor} = (m_{\text{MAA}} + m_{\text{Lauryl alcohol}} + m_{\text{Vanillin}} + m_{\text{Boc2O}} + m_{\text{MgCl}_2} + m_{\text{AIBN}} + m_{\text{CPDB}} \\ + m_{\text{MeCN}} + m_{\text{Toluene}} + m_{\text{DCM}} + m_{\text{MeOH}}) / m_{\text{poly(VMA-b-LMA)}} - 1$$

$$\text{E - factor} = (0.39 + 0.52 + 0.41 + 1.19 + 0.086 + 0.0030 + 0.010 + 0.24 + 1.73 + 5.30 \\ + 126.6) / 0.90 - 1$$

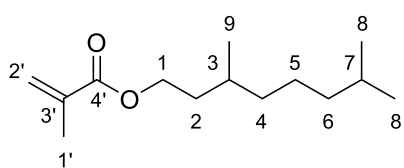
$$\text{E - factor} = 150.6$$

Chapter 2

Attribution of NMR signals and NMR spectra:

Below are listed the attributions of NMR signals of each methacrylate monomers and polymers presented in this study. NMR spectra were added when relevant, especially for determining the attribution of diastereotopic protons.

THGMA:



Group	^1H NMR (δ ppm)	$^{13}\text{C}\{^1\text{H}\}$ NMR (δ ppm)
1'	1.93	18.6
2'	6.08 ; 5.53	125.3
3'	-	136.8
4'	-	167.8
1	4.17	63.5
2	1.69 ; 1.48	35.7
3	1.57	30.2
4	1.30 ; 1.14	37.4
5	1.14	39.4
6	1.30	24.9
7	1.53	28.2
8	0.85	22.9 ; 22.8
9	0.91	19.8

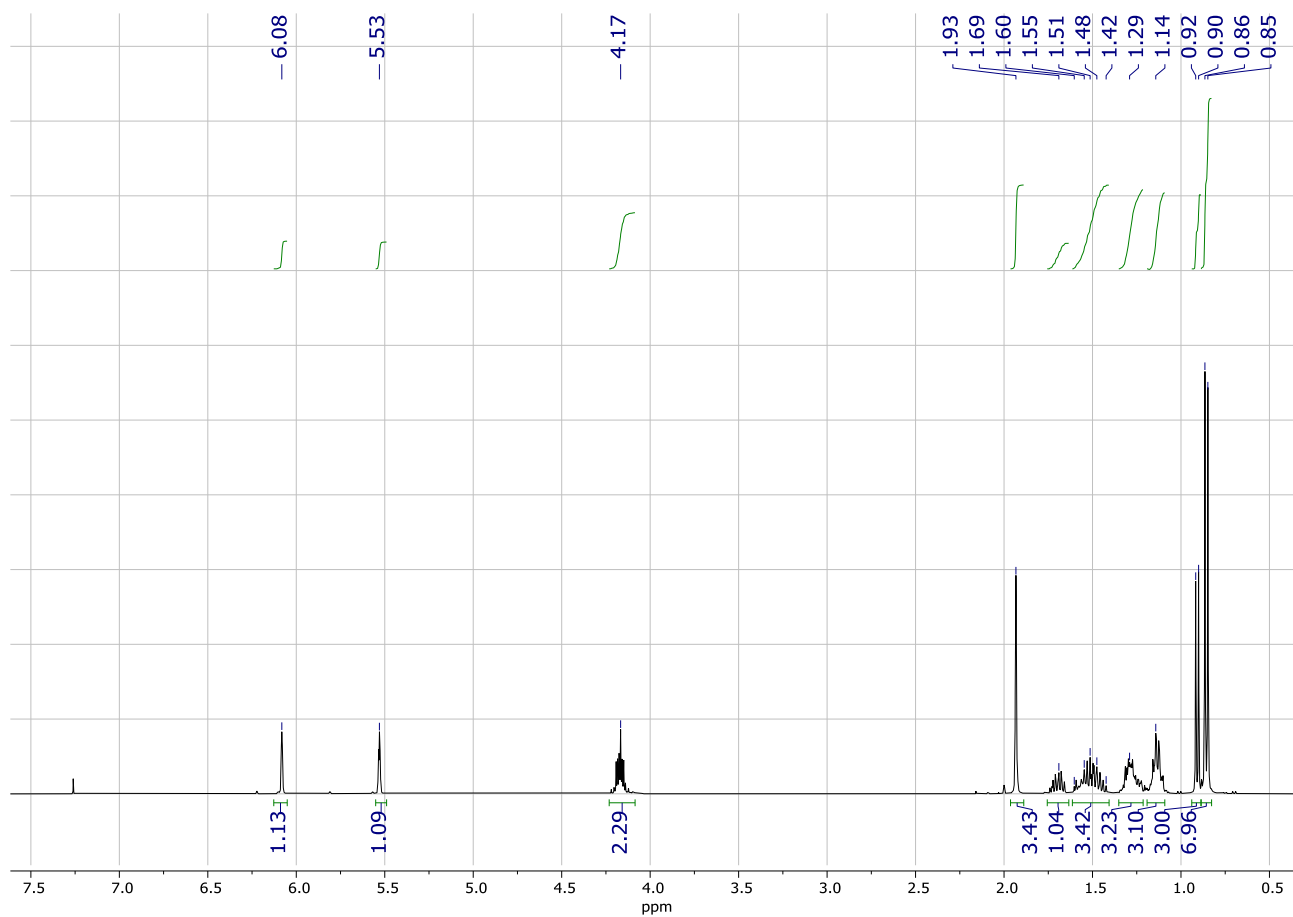


Figure S12. ^1H NMR spectrum of THGMA (CDCl_3 , 400MHz).

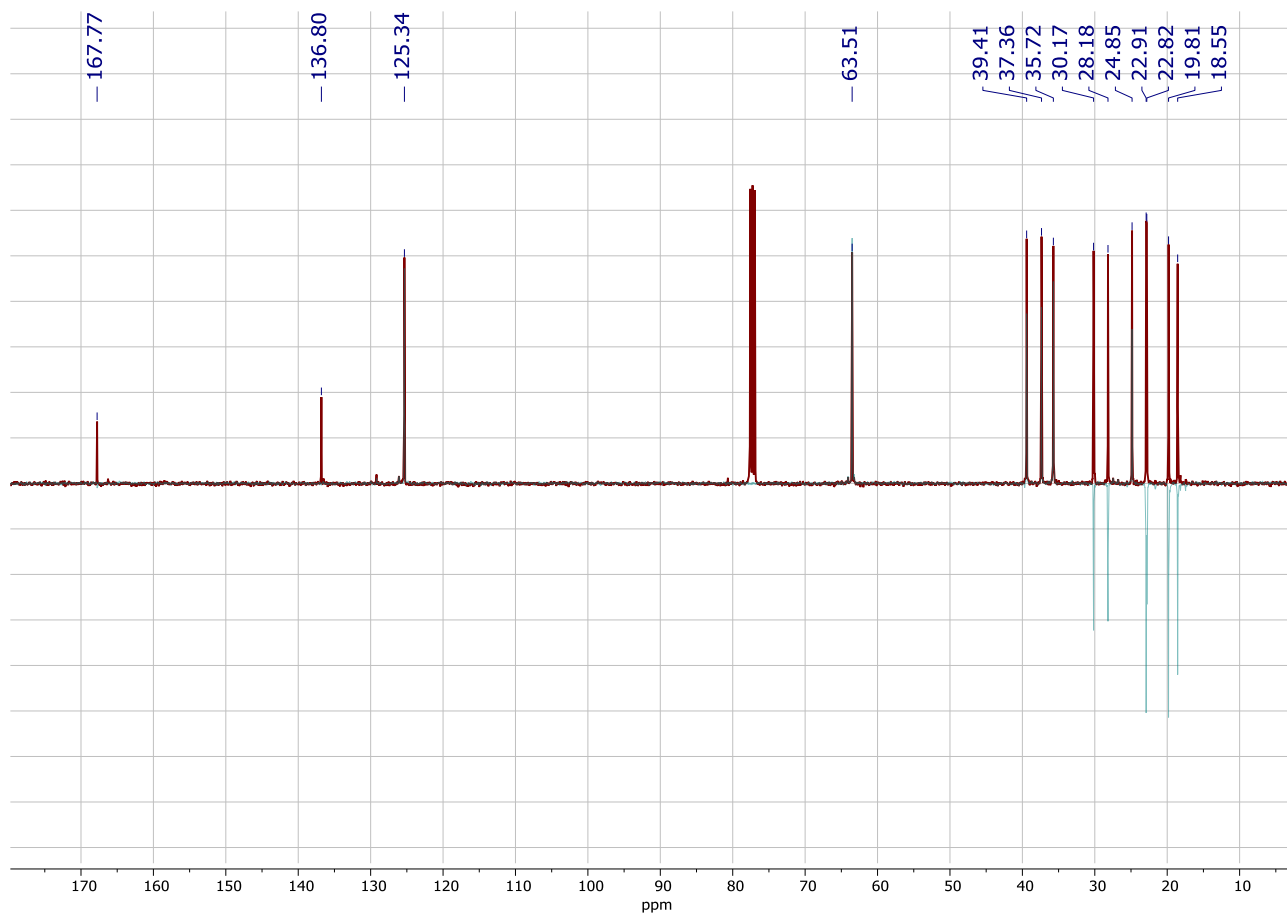


Figure S13. ¹³C (red) and DEPT (green) NMR spectra of THGMA (CDCl₃, 100MHz).

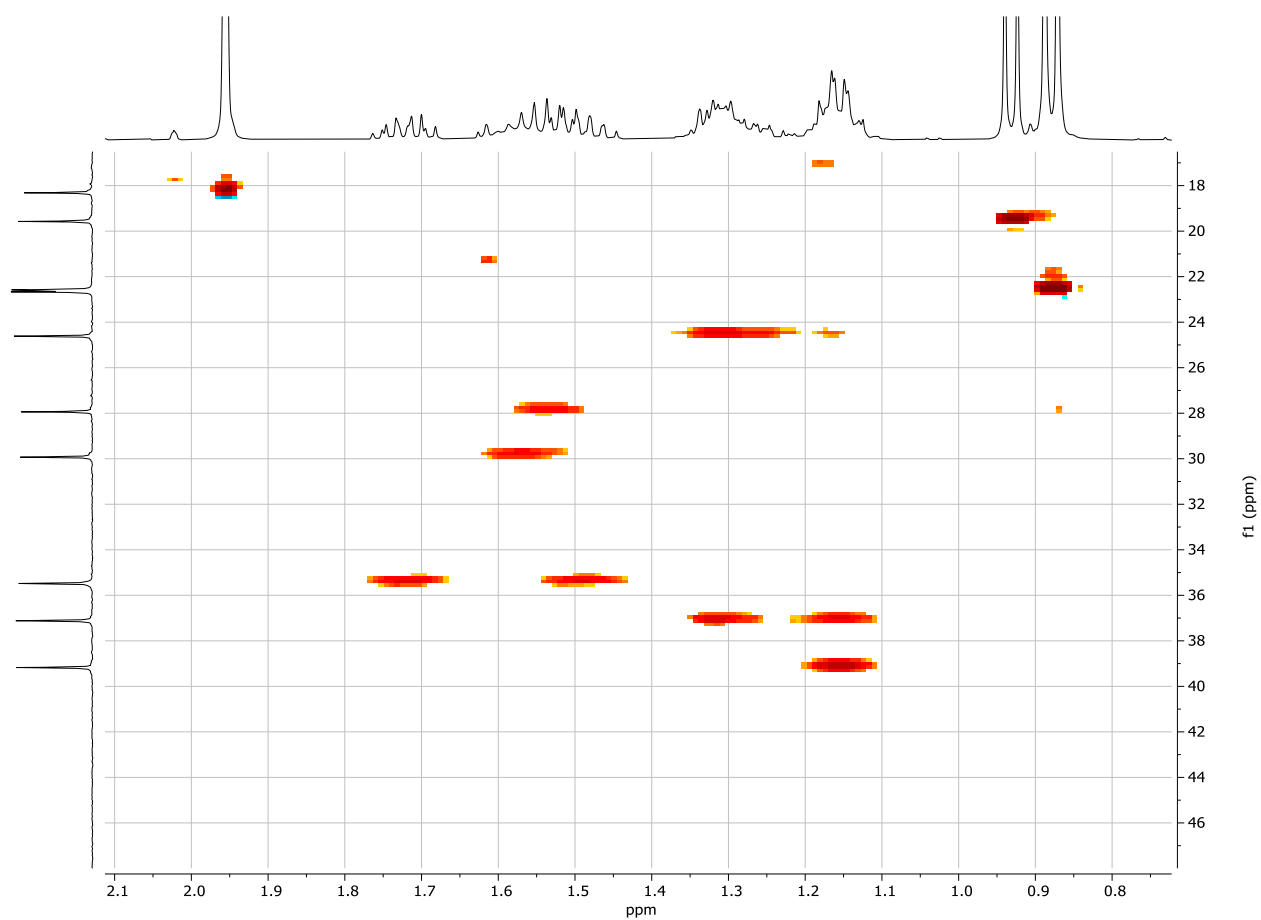


Figure S14. Enlarged view of the HSQC NMR spectrum of THGMA (CDCl_3 , 400MHz).

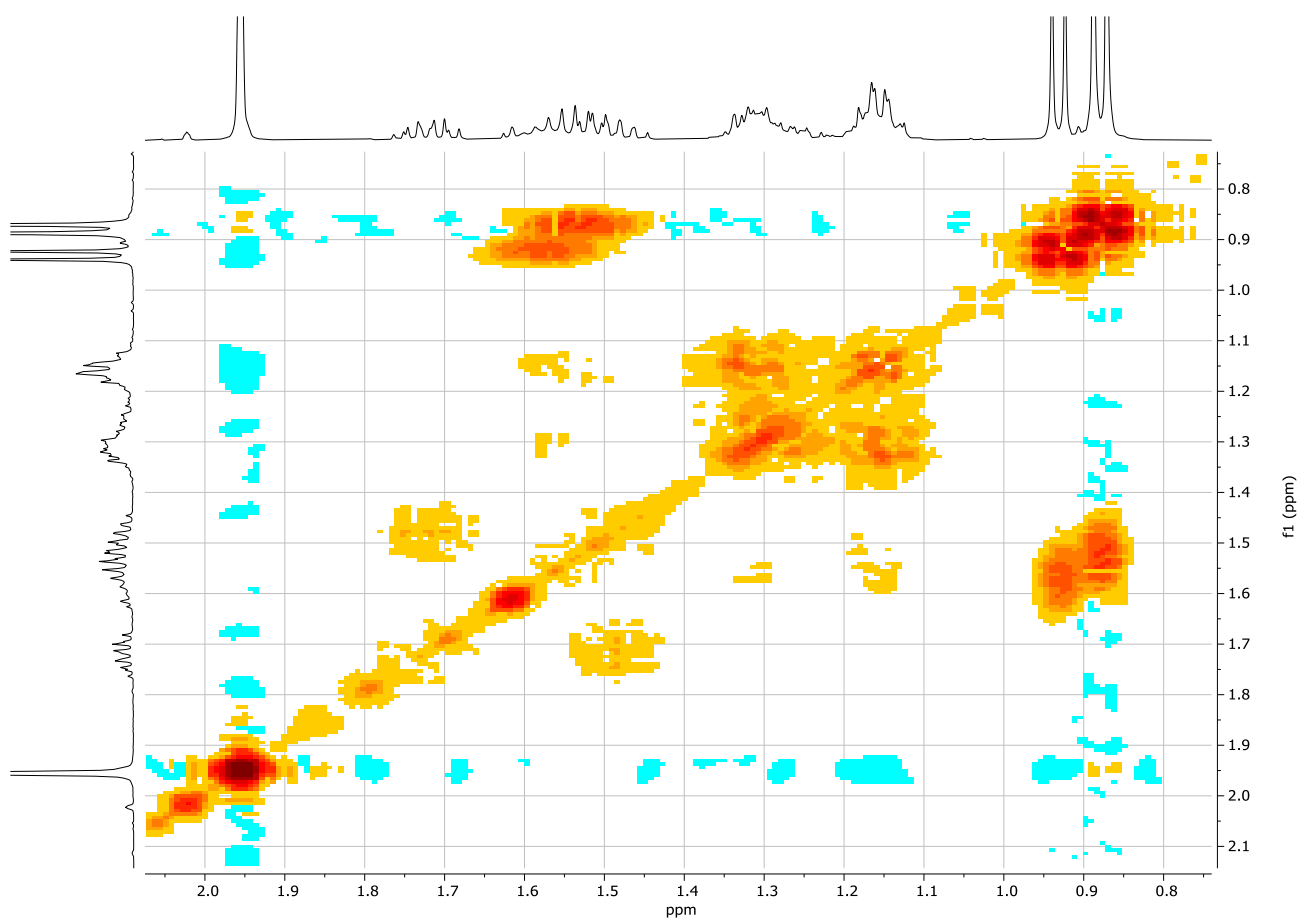
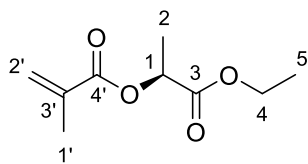


Figure S15. Enlarged view of the COSY NMR spectrum of THGMA (CDCl₃, 400MHz).

Chapter 2

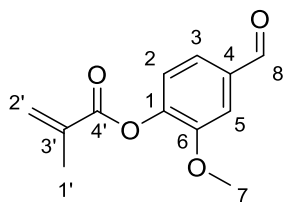
ELMA:



Group	^1H NMR (δ ppm)	$^{13}\text{C}\{^1\text{H}\}$ NMR (δ ppm)
1'	1.90	18.1
2'	6.13 ; 5.56	126.3
3'	-	135.6
4'	-	166.6
1	5.04	68.9
2	1.47	16.9
3	-	170.8
4	4.14	61.3
5	1.20	14.04

Chapter 2

VMA:



Group	¹ H NMR (δ ppm)	¹³ C{ ¹ H} NMR (δ ppm)
1'	2.07	18.5
2'	6.38 ; 5.79	128.1
3'	-	135.3
4'	-	164.9
1	-	152.3
2	7.25	123.6
3	7.49	124.9
4	-	128.1
5	7.49	110.9
6	-	145.4
7	3.89	56.3
8	9.95	191.2

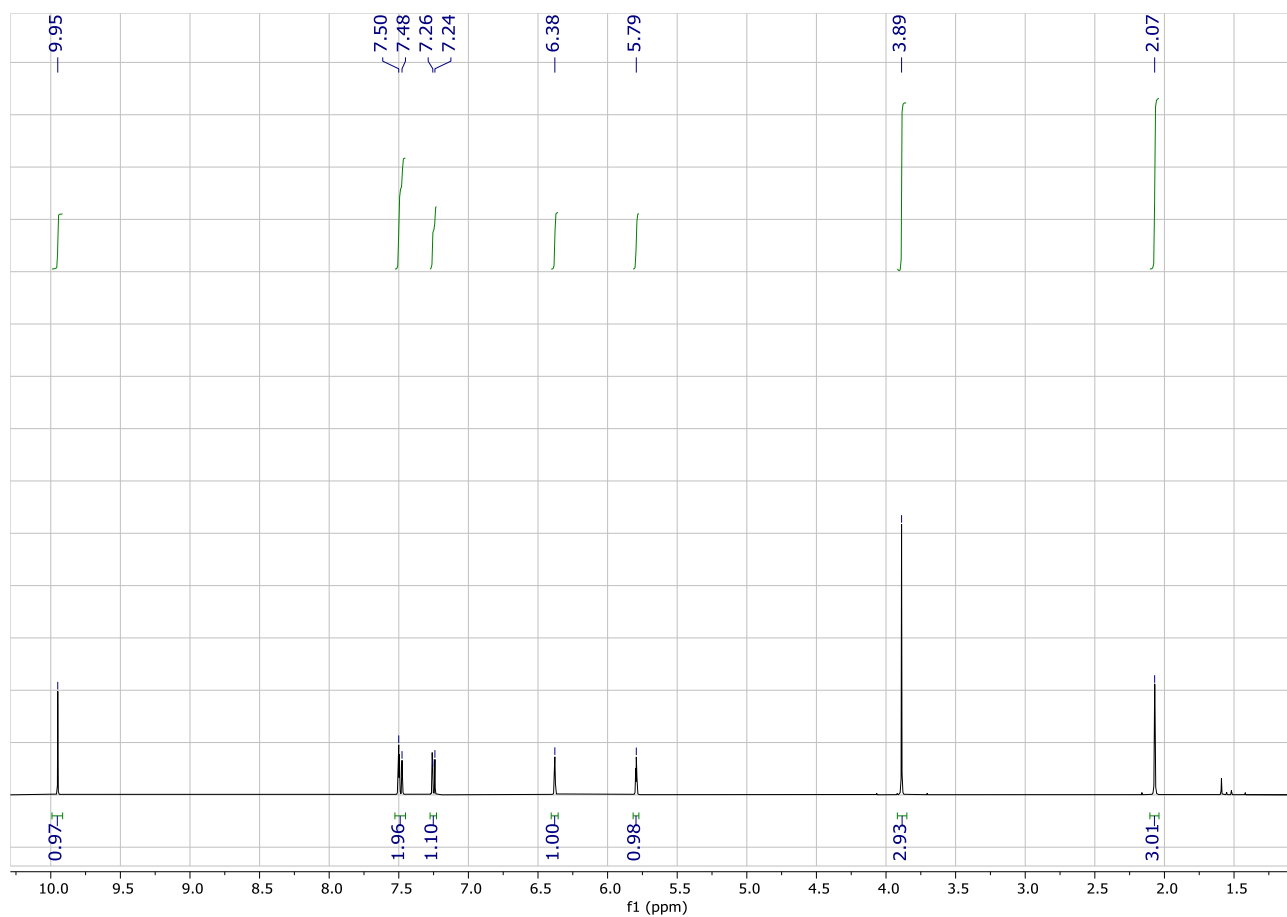


Figure S16. ^1H NMR spectrum of VMA (CDCl_3 , 400MHz).

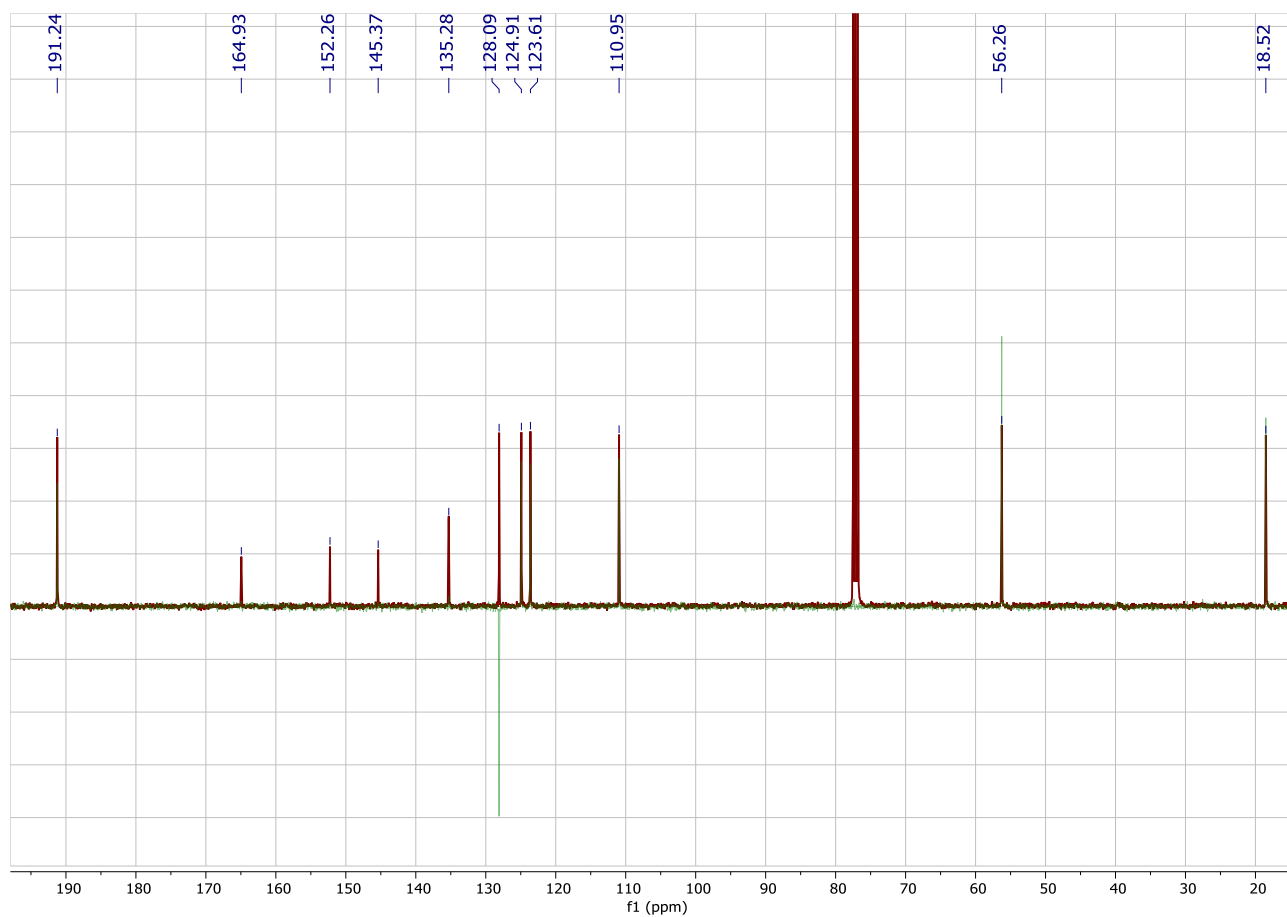
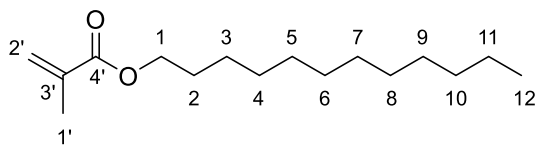


Figure S17. ¹³C (red) and DEPT (green) NMR spectra of VMA (CDCl₃, 100MHz).

Chapter 2

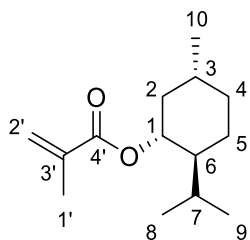
LMA:



Group	^1H NMR (δ ppm)	$^{13}\text{C}\{^1\text{H}\}$ NMR (δ ppm)
1'	1.92	18.4
2'	6.08 ; 5.53	125.2
3'	-	136.7
4'	-	167.7
1	4.12	65.0
2	1.65	32.0
3		
4		
5		
6		
7	Broad signal at 1.24	8 peaks between 29.8 and 22.8
8		
9		
10		
11		
12	0.86	14.1

Chapter 2

L-MnMA:



Group	^1H NMR (δ ppm)	$^{13}\text{C}\{^1\text{H}\}$ NMR (δ ppm)
1'	1.92	18.5
2'	6.06 ; 5.50	124.9
3'	-	137.0
4'	-	167.1
1	4.72	74.6
2	2.02 ; 1.04	41.0
3	1.47	31.5
4	1.68 ; 0.96	34.4
5	1.68 ; 1.06	23.8
6	1.43	47.3
7	1.86	26.7
8	0.90	22.1
9	0.88	20.9
10	0.76	16.6

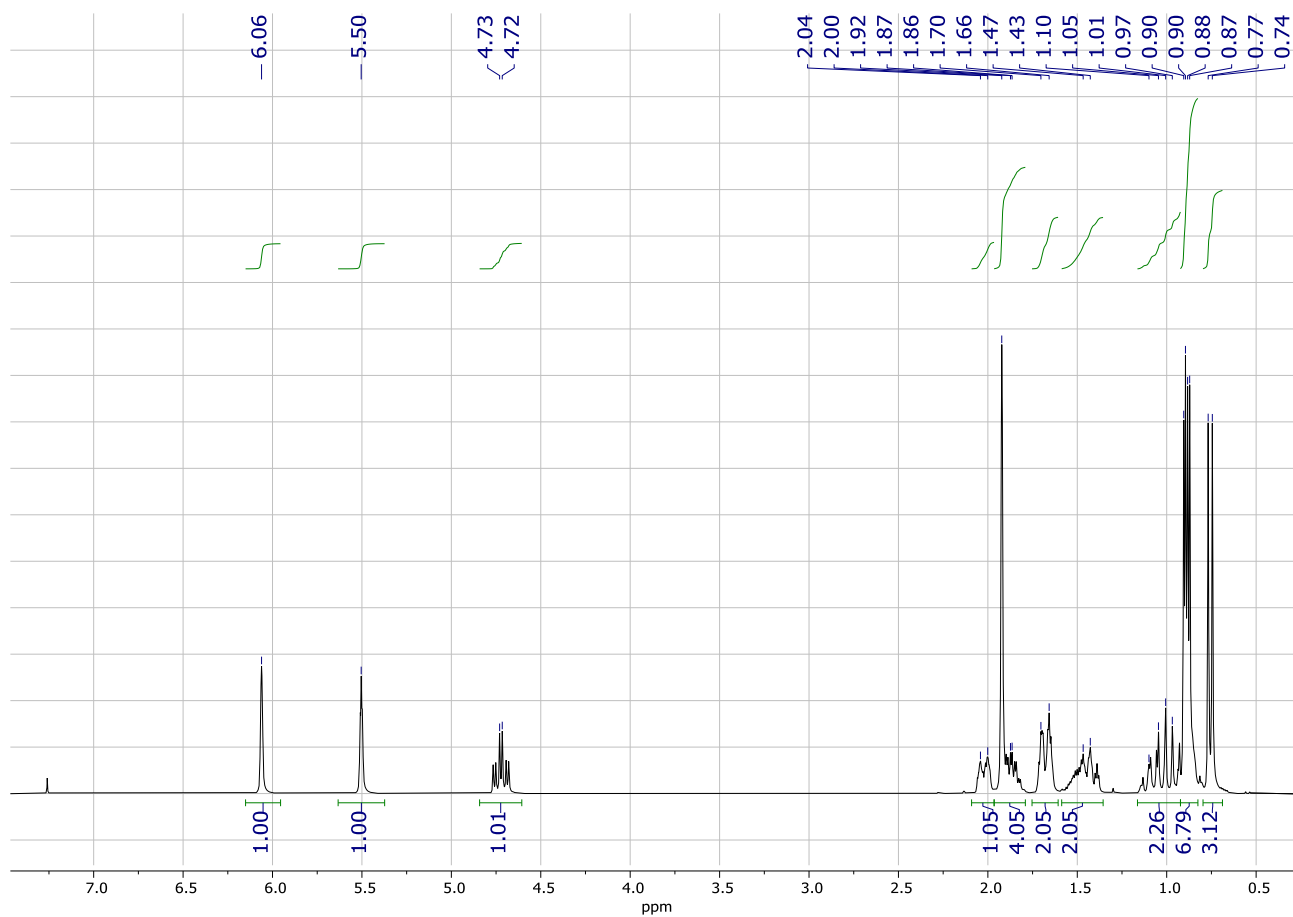


Figure S18. ^1H NMR spectrum of L-MnMA (CDCl_3 , 400MHz).

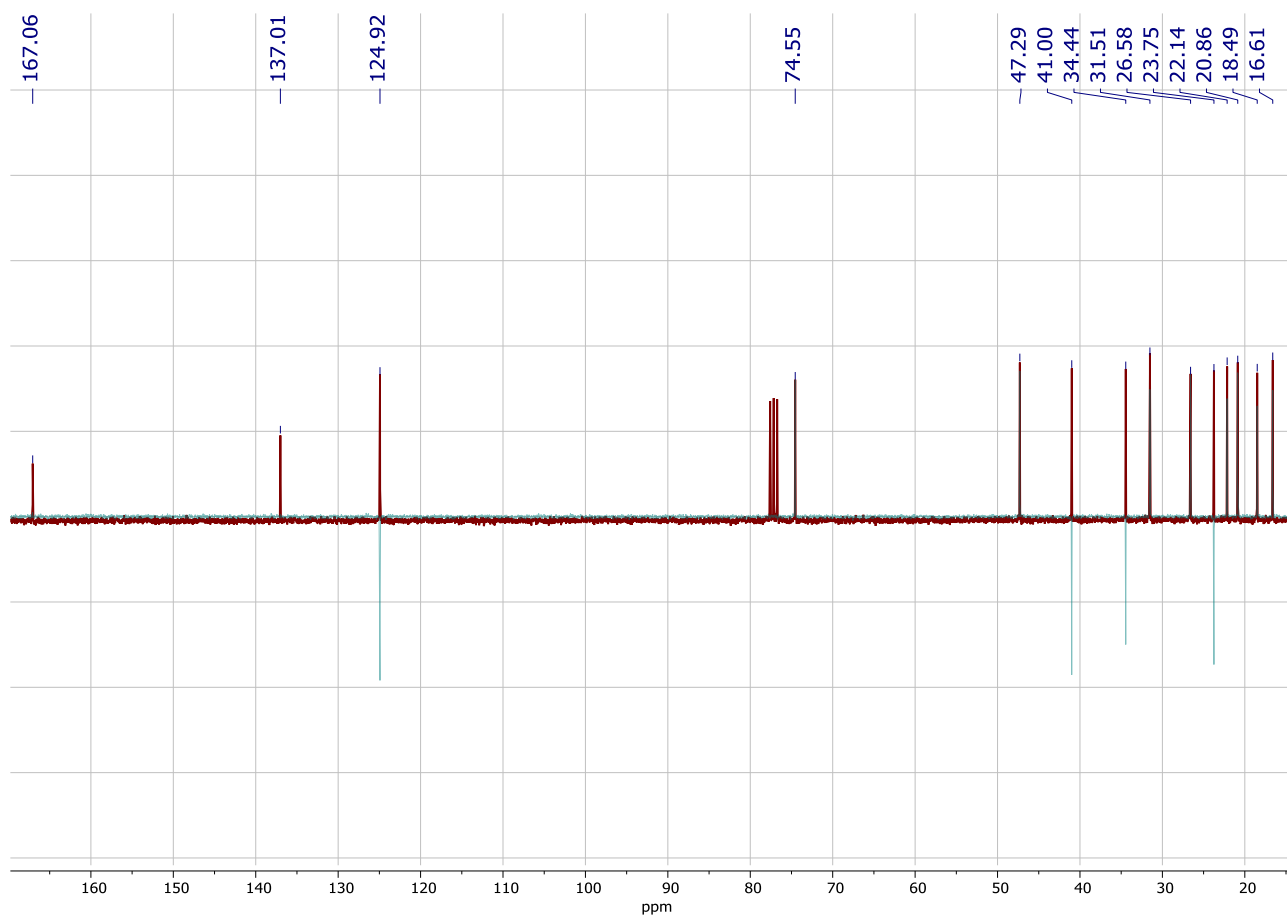
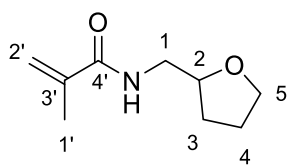


Figure S19. ^{13}C (red) and DEPT (green) NMR spectra of L-MnMA (CDCl_3 , 100MHz).

Chapter 2

THFMAcm:



Group	^1H NMR (δ ppm)	$^{13}\text{C}\{^1\text{H}\}$ NMR (δ ppm)
Amido	6.18	-
1'	1.97	18.8
2'	5.70 ; 5.33	119.7
3'	-	140.5
4'	-	168.9
1	3.65 ; 3.21	43.4
2	4.00	77.9
3	2.00 ; 1.56	28.8
4	1.89	26.0
5	3.85 ; 3.75	68.3

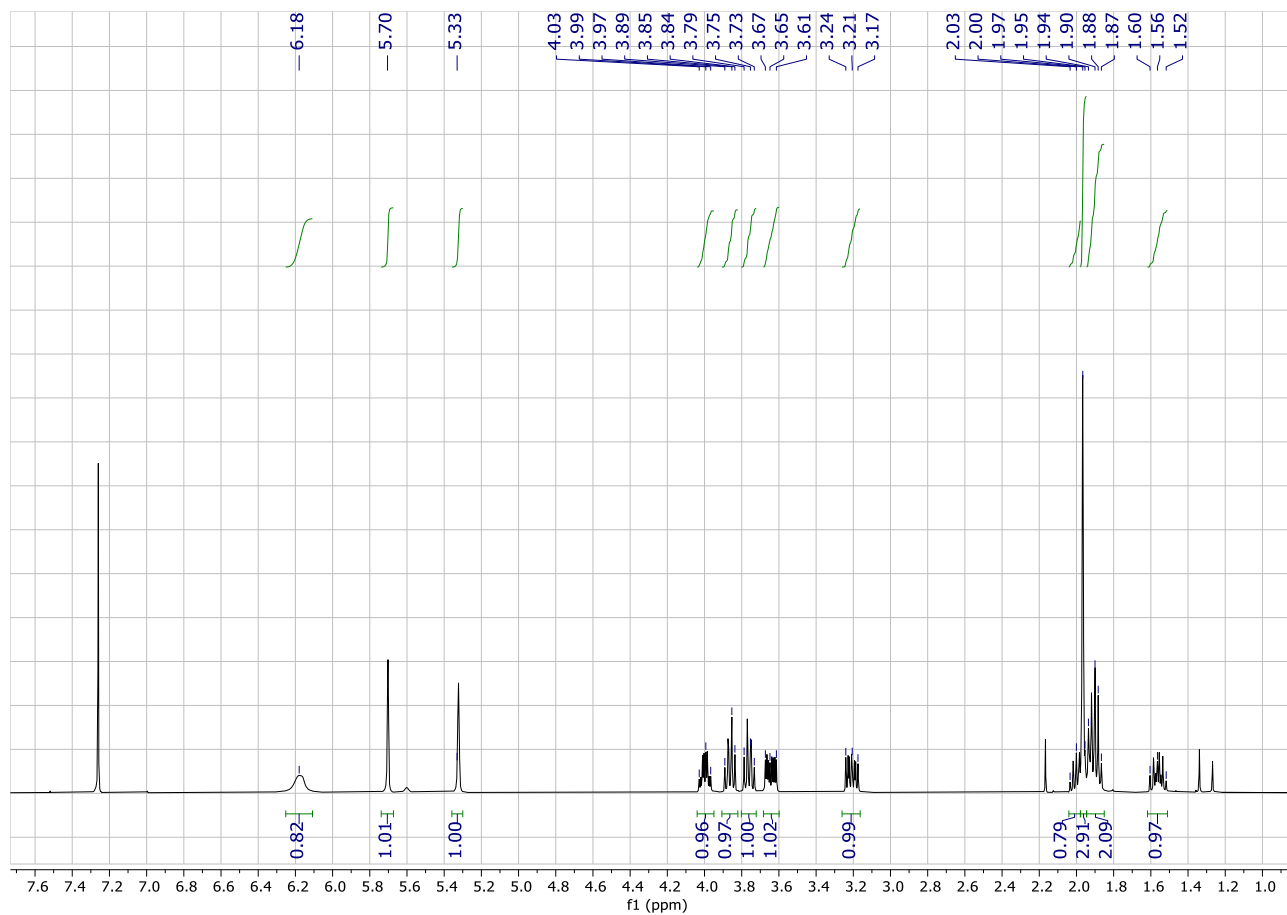


Figure S20. ^1H NMR spectrum of THFMAcm (CDCl_3 , 400MHz).

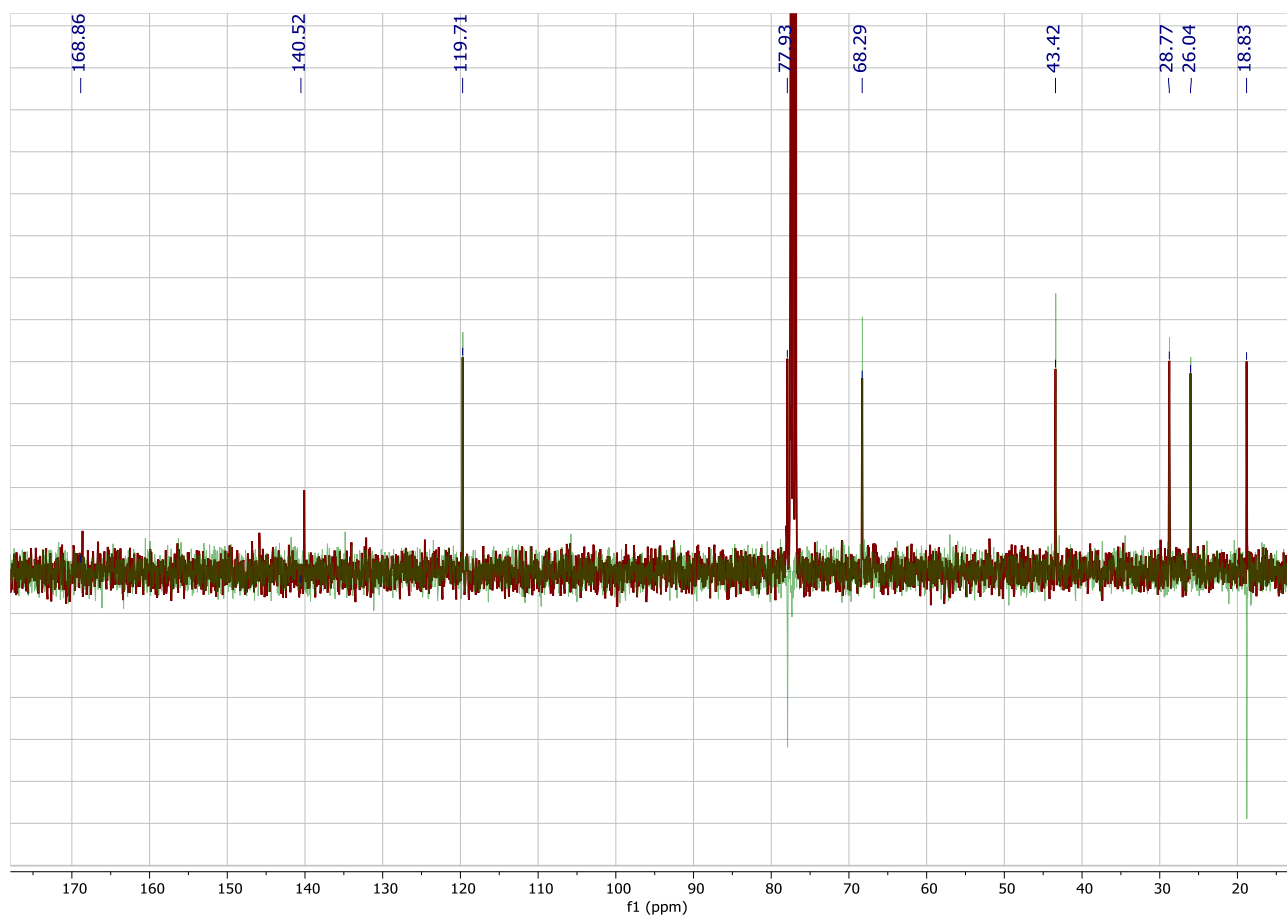


Figure S21. ¹³C (red) and DEPT (green) NMR spectra of THFMAcm (CDCl₃, 100MHz).

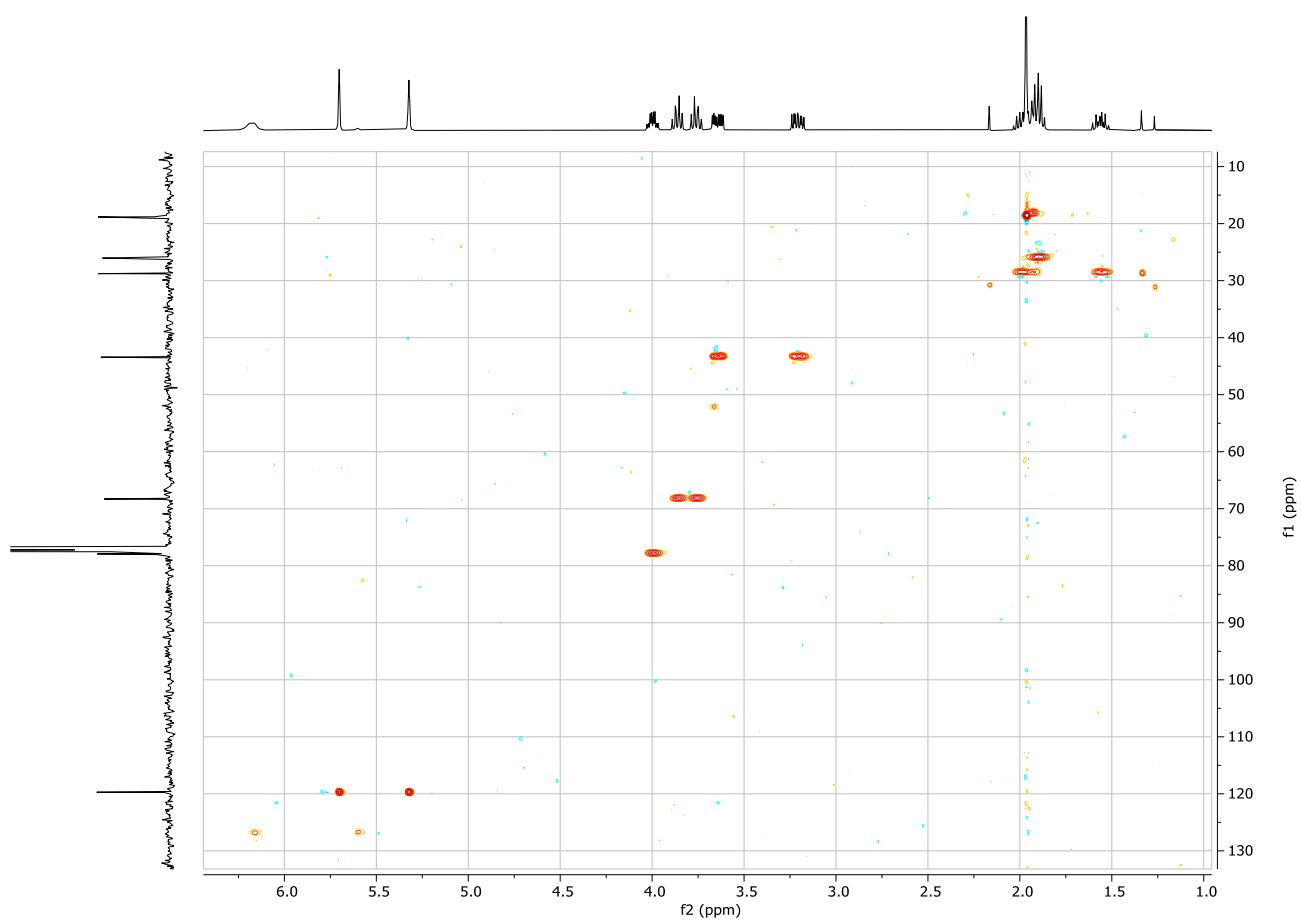


Figure S22. Enlarged view of the HSQC NMR spectrum of THFMAcm (CDCl₃, 400MHz).

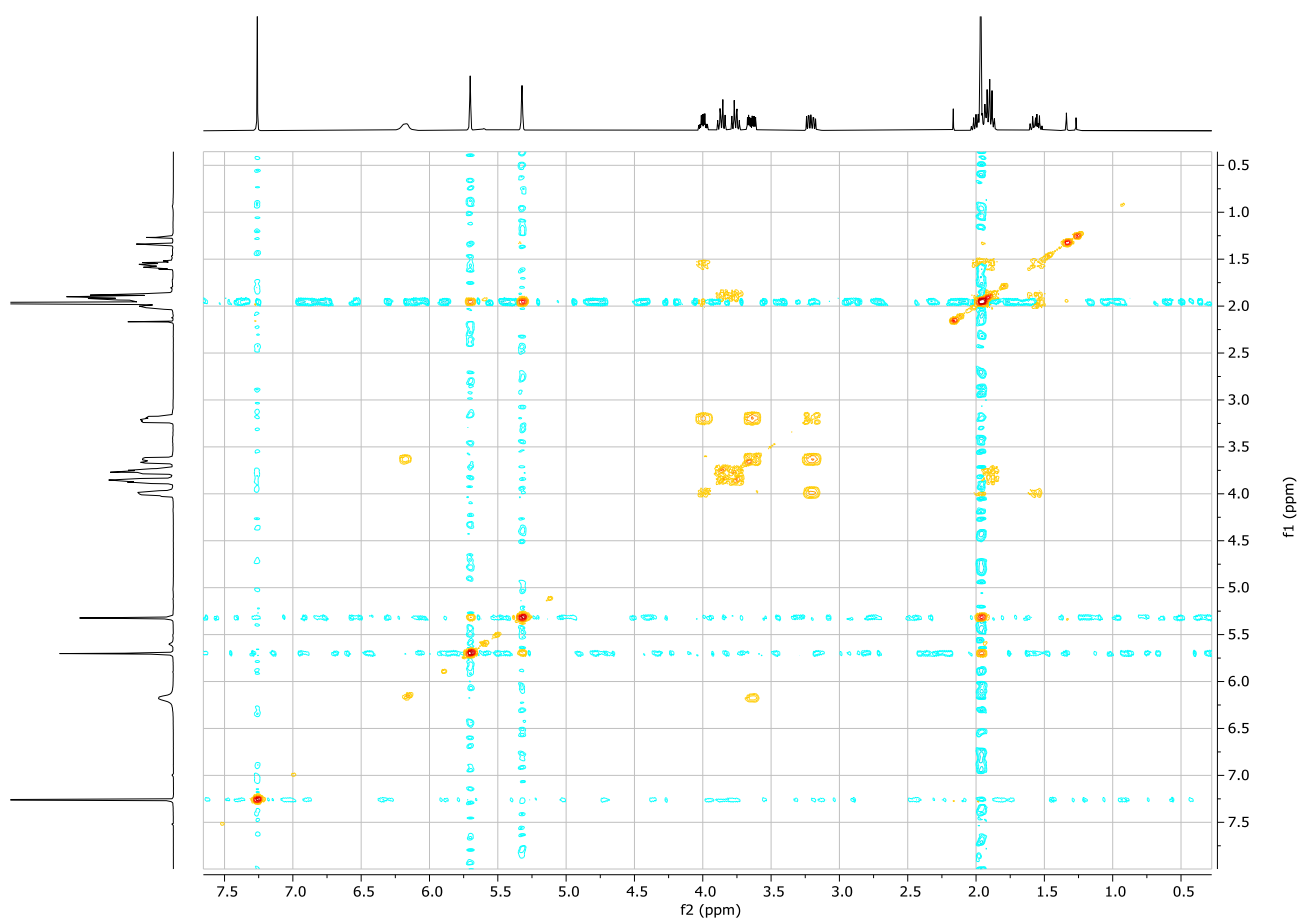


Figure S23. COSY NMR spectrum of THFMAcm (CDCl_3 , 400MHz).

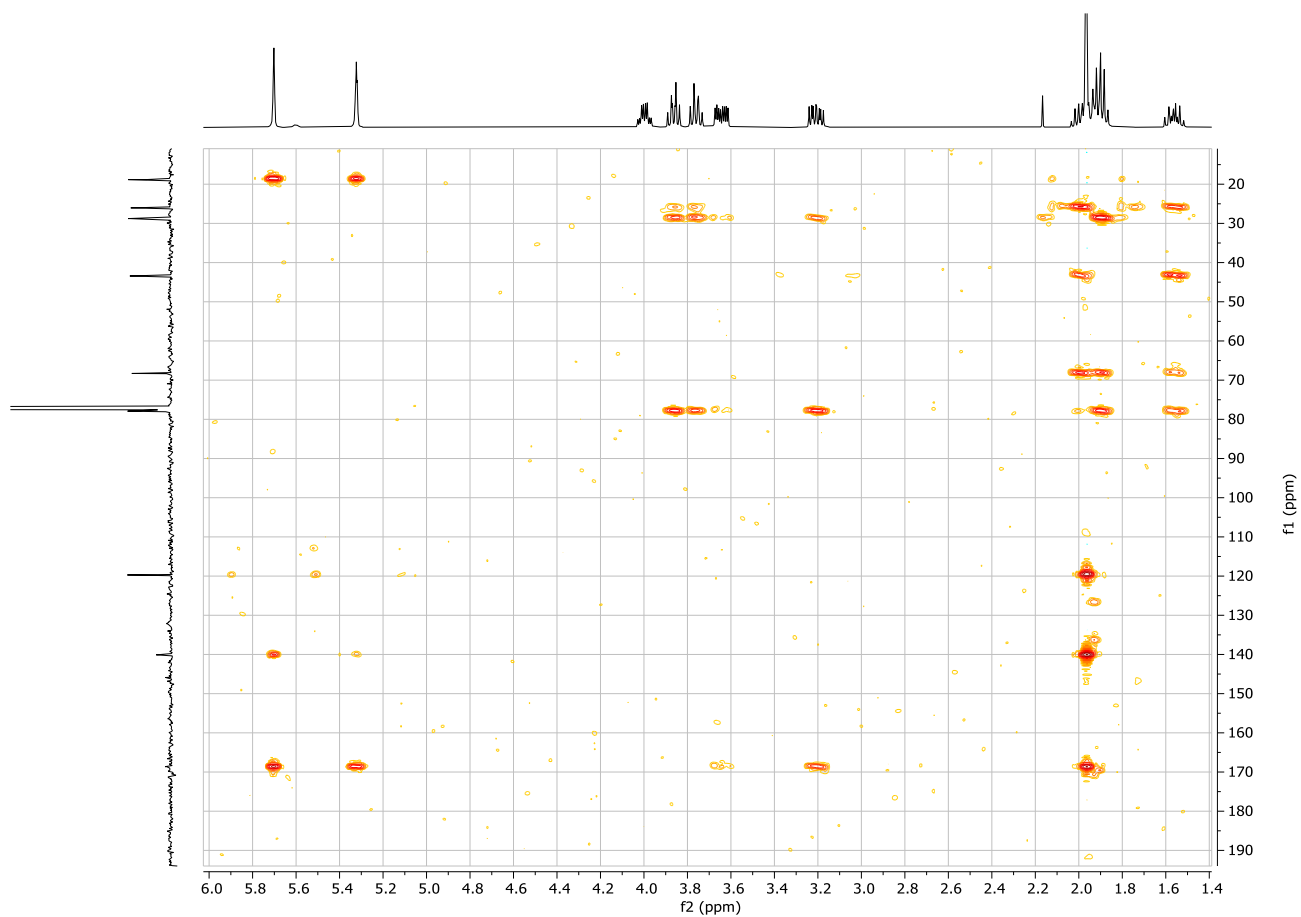
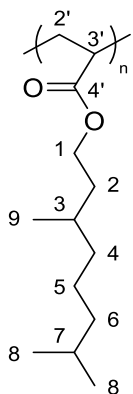


Figure S24. Enlarged view of the HMBC NMR spectrum of THFMAcm (CDCl₃, 400MHz).

Chapter 2

Poly(THGA):



Group	^1H NMR (δ ppm)	$^{13}\text{C}\{^1\text{H}\}$ NMR (δ ppm)
2'	2.26	41.6
3'	1.87	35.7
4'	-	174.5
1	4.04	63.4
2	1.62 ; 1.42	35.7
3	1.52	30.2
4	1.30 ; 1.13	37.4
5	1.13	39.4
6	1.30	24.8
7	1.52	28.1
8	0.86	22.9
9	0.88	19.6

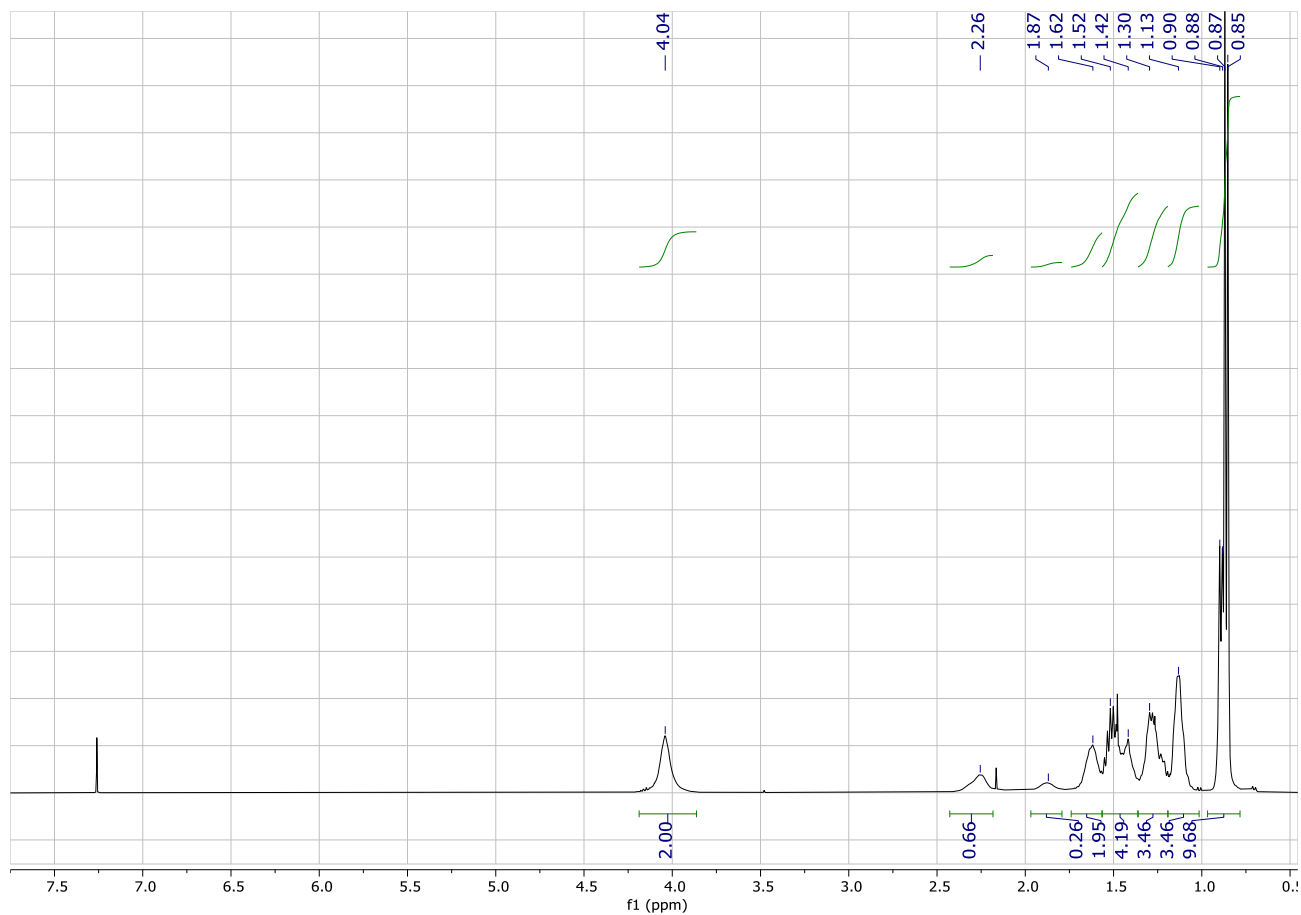


Figure S25. ^1H NMR spectrum of poly(THGA) (CDCl_3 , 400MHz).

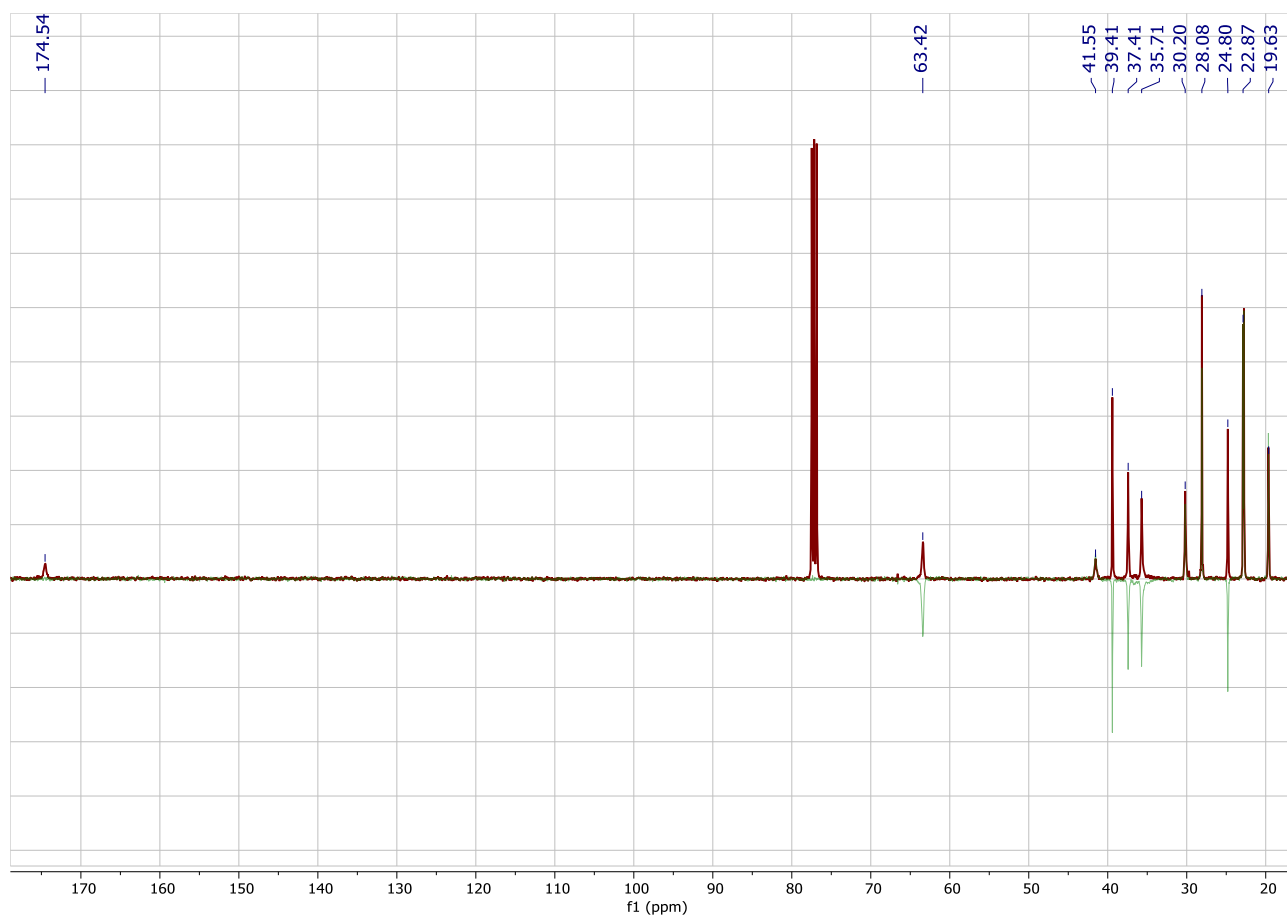


Figure S26. ¹³C (red) and DEPT (green) NMR spectra of poly(THGA) (CDCl₃, 100MHz).

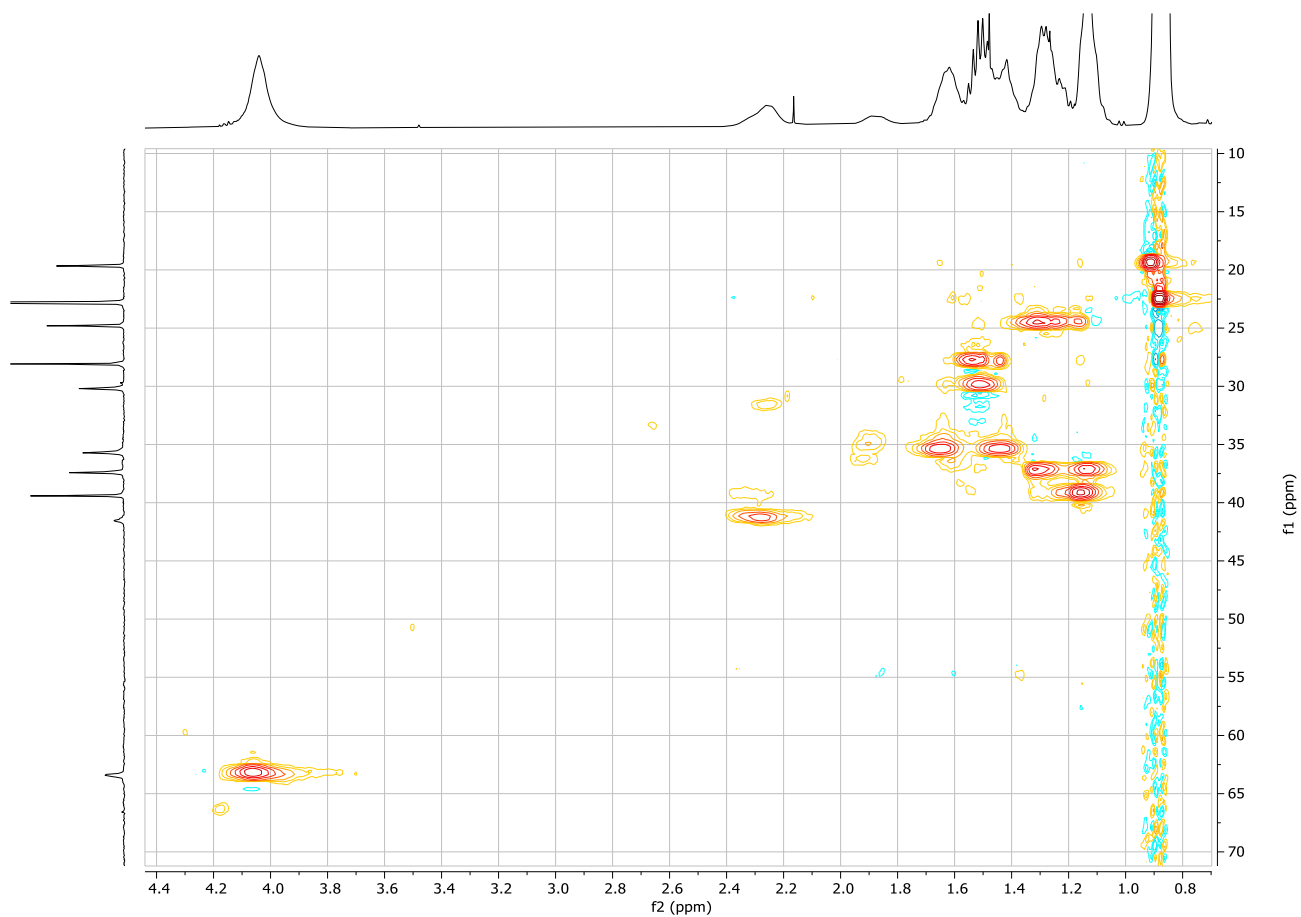


Figure S27. Enlarged view of the HSQC NMR spectrum of poly(THGA) (CDCl_3 , 400MHz).

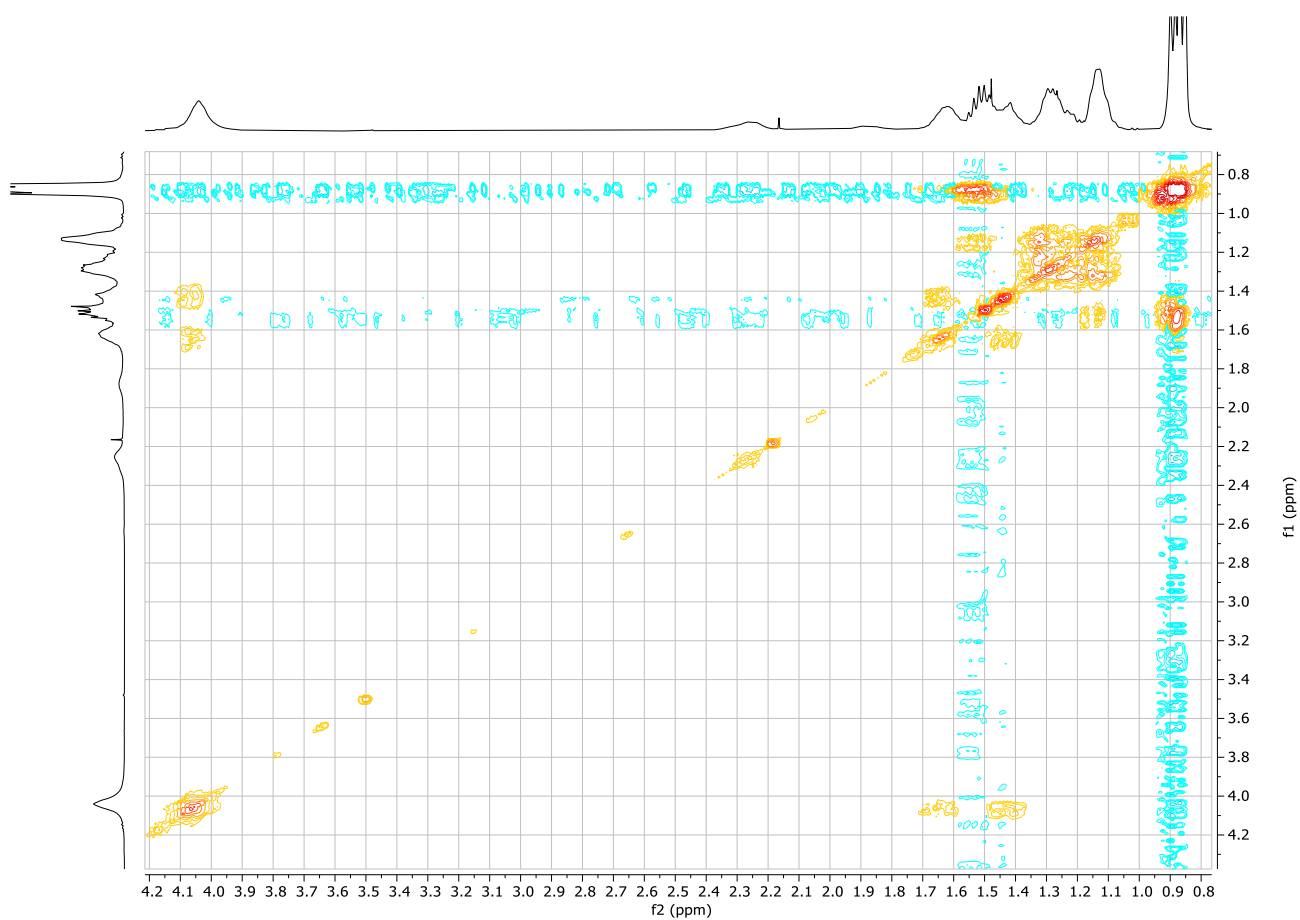
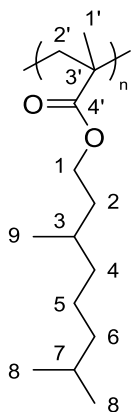


Figure S28. Enlarged view of the COSY NMR spectrum of poly(THGA) (CDCl_3 , 400MHz).

Chapter 2

Poly(THGMA):



Group	¹ H NMR (δ ppm)	¹³ C{ ¹ H} NMR (δ ppm)
1'	0.9 for <i>rr</i> , 1.0 for <i>mr</i> , 1.2 for <i>mm</i>	16.7 for <i>rr</i> , 18.5 for <i>mr</i> , 21.0 for <i>mm</i>
2'	Broad signal between 2.05 and 1.71	Broad signal between 55.0 and 52.0
3'	-	44.9 for <i>rr</i> , 45.3 for <i>mr</i> , 45.7 for <i>mm</i>
4'	-	Between 178.0z and 176.8
1	3.95	63.6
2	1.63 ; 1.42	35.2
3	1.53	30.1
4	1.30 ; 1.15	37.3
5	1.15	39.4
6	1.30	24.8
7	1.53	28.1
8	0.86	22.8
9	0.86	19.6

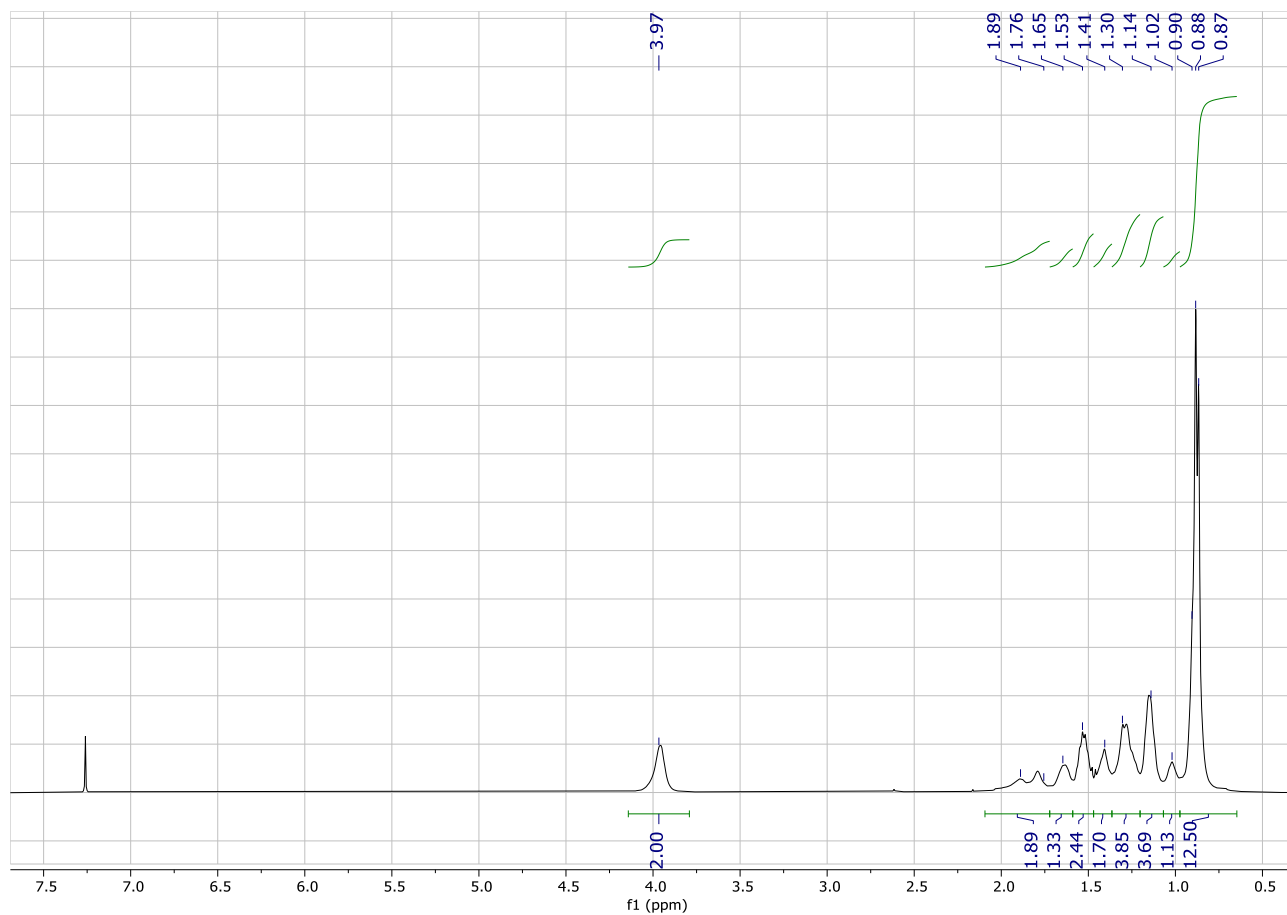


Figure S29. ^1H NMR spectrum of poly(THGMA) (CDCl_3 , 400MHz).

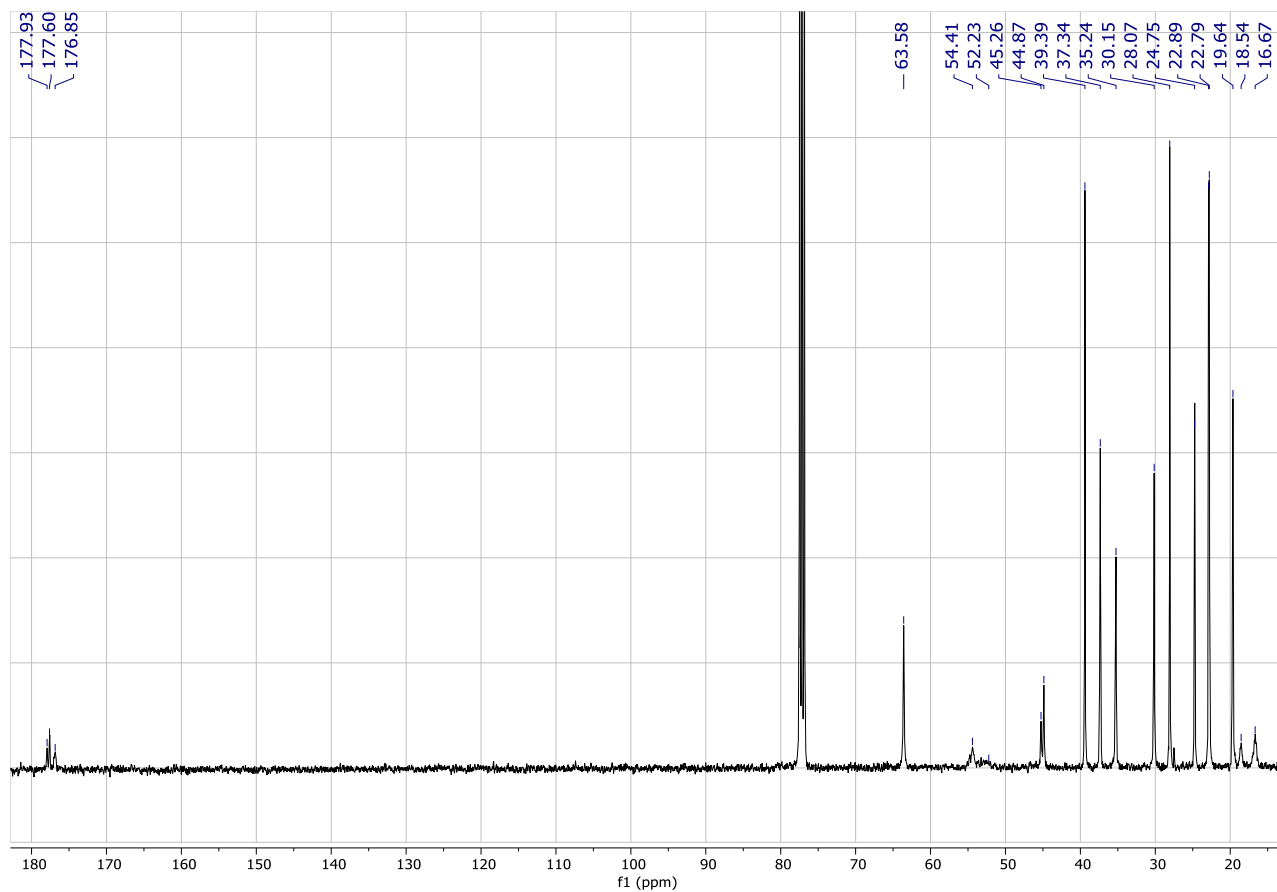
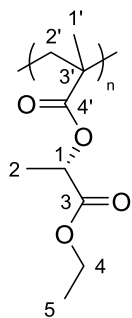


Figure S30. ^{13}C NMR spectrum of poly(THGMA) (CDCl_3 , 100MHz).

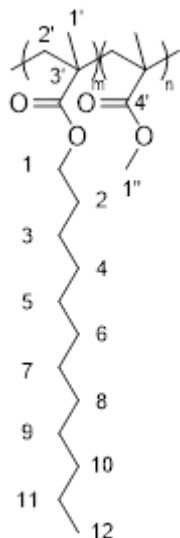
Poly(ELMA):



Group	^1H NMR (δ ppm)	$^{13}\text{C}\{^1\text{H}\}$ NMR (δ ppm)
1'	Between 1.20 and 1.00	Between 19.8 and 17.5
2'	Between 2.17 and 1.84	53.5
3'	-	Between 45.7 and 45.2
4'	-	Between 177.6 and 170.5
1	4.93	69.5
2	1.46	17.1
3	-	170.5
4	4.15	61.2
5	1.25	14.2

Chapter 2

Poly(LMA-*r*-MMA):



Group	^1H NMR (δ ppm)	$^{13}\text{C}\{^1\text{H}\}$ NMR (δ ppm)
1'	0.9 for <i>rr</i> , 1.0 for <i>mr</i> , 1.2 for <i>mm</i>	16.7 for <i>rr</i> , 18.8 for <i>mr</i> , 21.0 for <i>mm</i>
2'	Broad signal between 2.00 and 1.75	Broad signal between 55.0 and 52.0
3'	-	44.8 for <i>rr</i> , 45.1 for <i>mr</i> , 45.7 for <i>mm</i>
4'	-	Signals between 178.2 and 176.8
1	3.91	65.2
2	1.60	32.1
3		
4		
5		
6		
7	Broad signal at 1.26	8 peaks between 29.8 and 22.8
8		
9		
10		
11		
12	0.87	14.3
1''	3.57	51.8

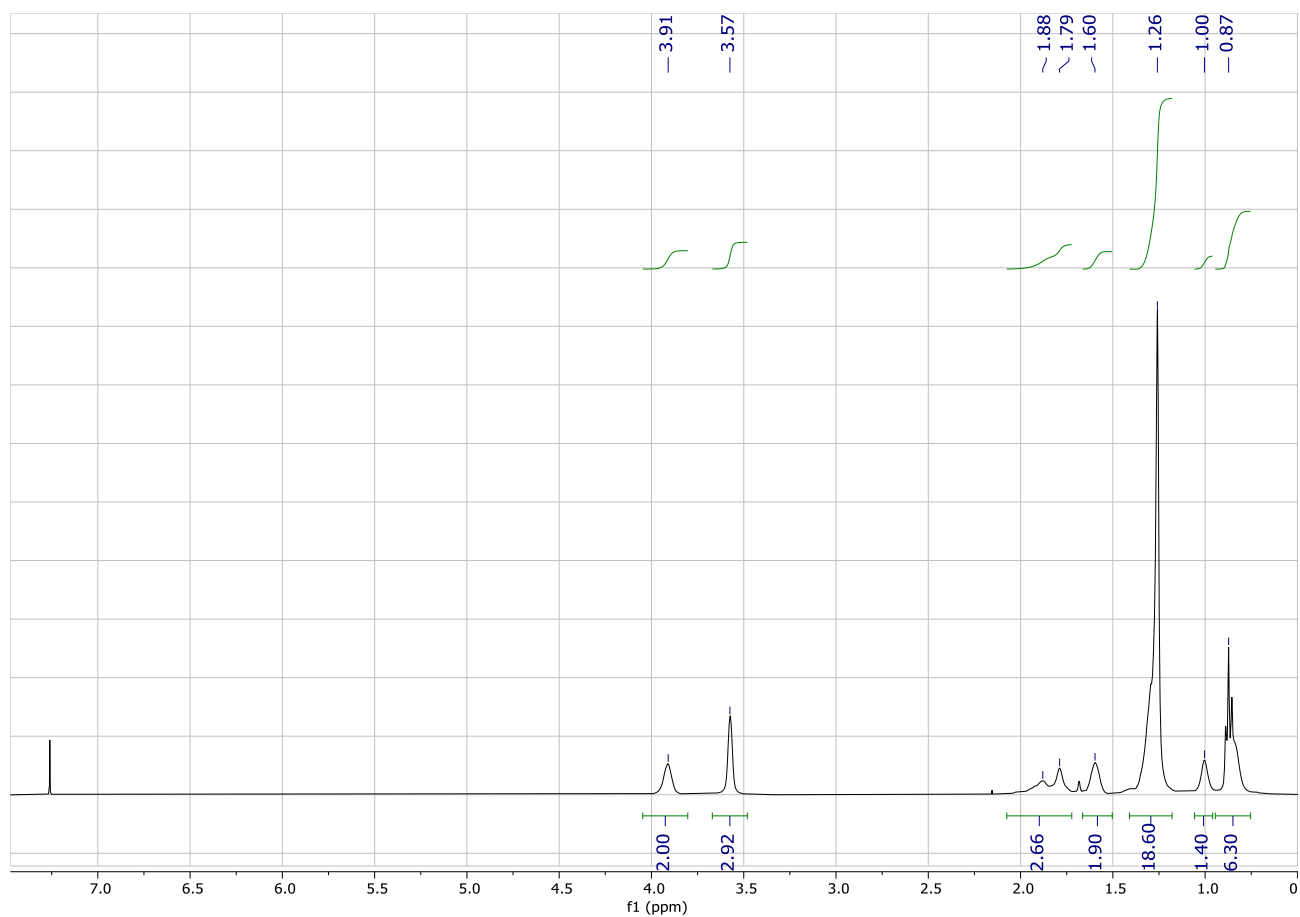


Figure S31. ^1H NMR spectrum of poly(LMA-*r*-MMA) (CDCl_3 , 400MHz).

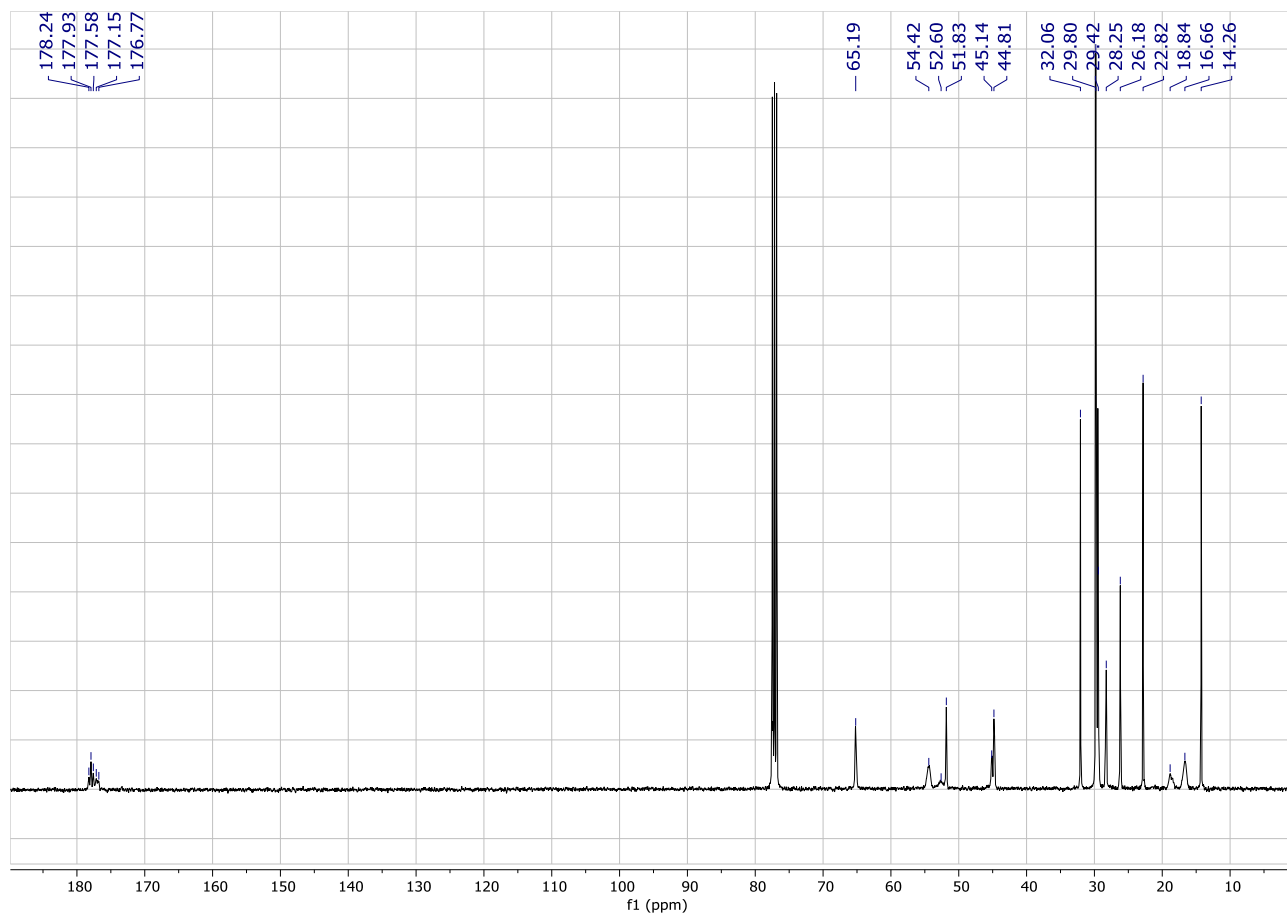
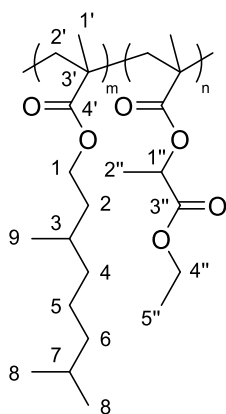


Figure S32. ^{13}C NMR spectrum of poly(LMA-*r*-MMA) (CDCl_3 , 100MHz).

Chapter 2

Poly(THGMA-*r*-ELMA):



Group	^1H NMR (δ ppm)	$^{13}\text{C}\{^1\text{H}\}$ NMR (δ ppm)
1'	Between 1.20 and 1.00	Between 19.8 and 17.5
2'	Between 2.17 and 1.84	54.4
3'	-	45.2
4'	-	Between 178.5 and 175.7
1	3.97	63.7
2	1.63 ; 1.42	35.2
3	1.53	30.2
4	1.30 ; 1.15	37.3
5	1.15	39.4
6	1.30	24.7
7	1.53	28.1
8	0.86	22.9
9	0.86	19.6
1''	4.94	69.5
2''	1.46	17.1
3''	-	170.5
4''	4.18	61.2
5''	1.25	14.3

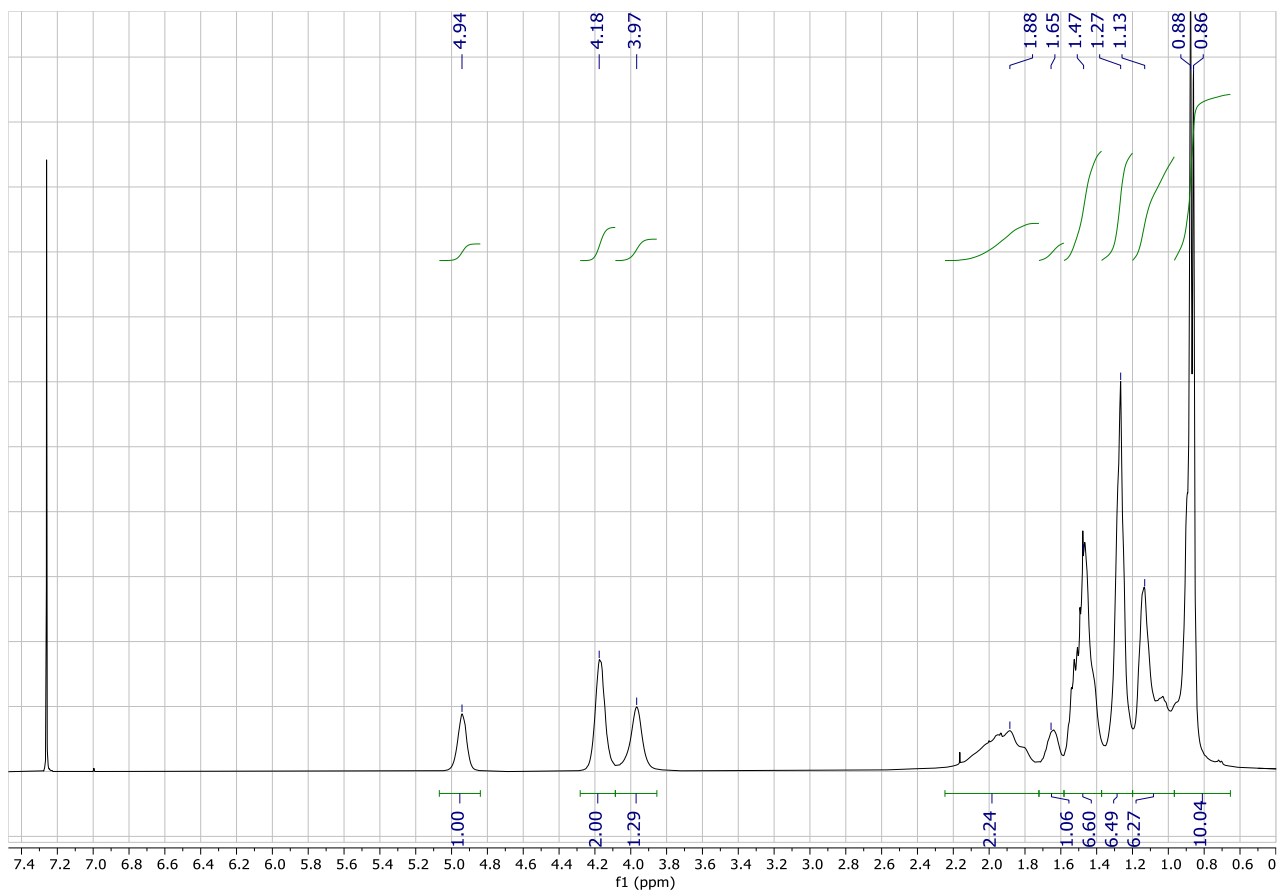


Figure S33. ^1H NMR spectrum of poly(THGMA-*r*-ELMA) (CDCl_3 , 400MHz).

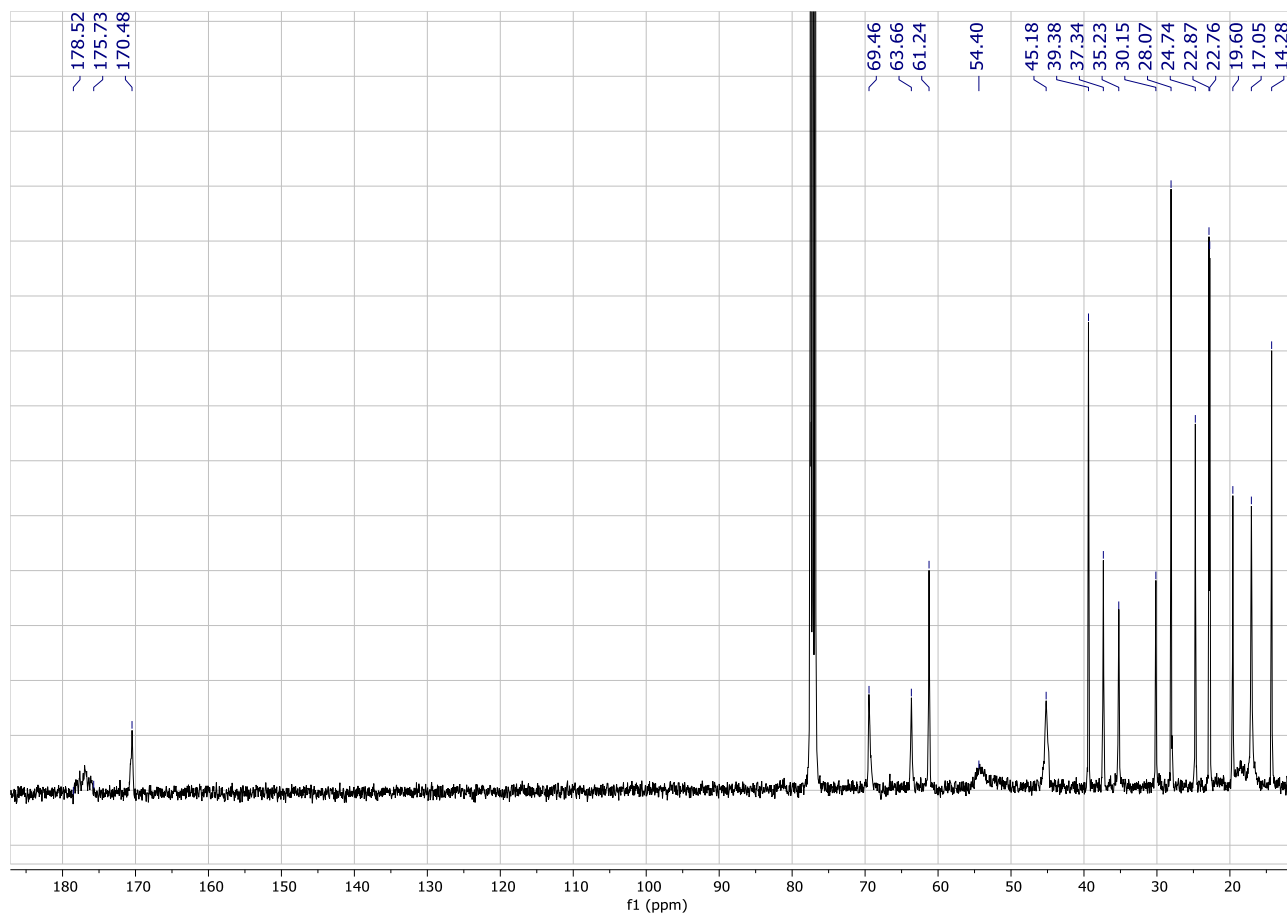
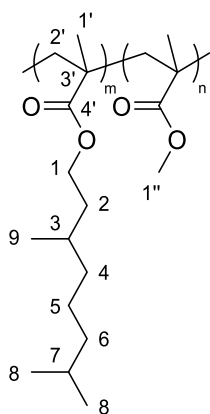


Figure S34. ^{13}C NMR spectrum of poly(THGMA-*r*-ELMA) (CDCl_3 , 100MHz).

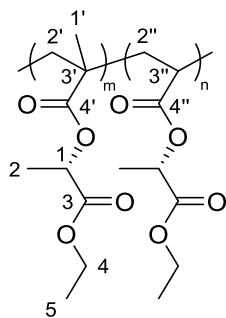
Poly(THGMA-*r*-MMA):



Group	¹ H NMR (δ ppm)	¹³ C{ ¹ H} NMR (δ ppm)
1'	Between 1.20 and 1.00	Between 19.8 and 16.6
2'	Between 2.17 and 1.79	54.4
3'	-	45.2
4'	-	Between 178.6 and 176.2
1	3.97	63.7
2	1.63 ; 1.42	35.2
3	1.53	30.1
4	1.30 ; 1.15	37.3
5	1.15	39.4
6	1.30	24.7
7	1.53	28.1
8	0.86	22.8
9	0.86	19.6
1''	3.58	51.8

Chapter 2

Poly(ELMA-*r*-ELA):



Group	^1H NMR (δ ppm)	$^{13}\text{C}\{^1\text{H}\}$ NMR (δ ppm)
1'	Between 1.20 and 1.00	Between 23.8 and 19.1
2'	Between 2.17 and 1.84	51.3
3'	-	Between 45.7 and 45.1
4'	-	Between 177.7 and 173.6
2''	2.52	37.7
3''	2.00	28.0
4''	-	Between 177.7 and 173.6
1	4.94	69.0
2	1.46	16.9
3	-	170.5
4	4.16	61.2
5	1.25	14.3

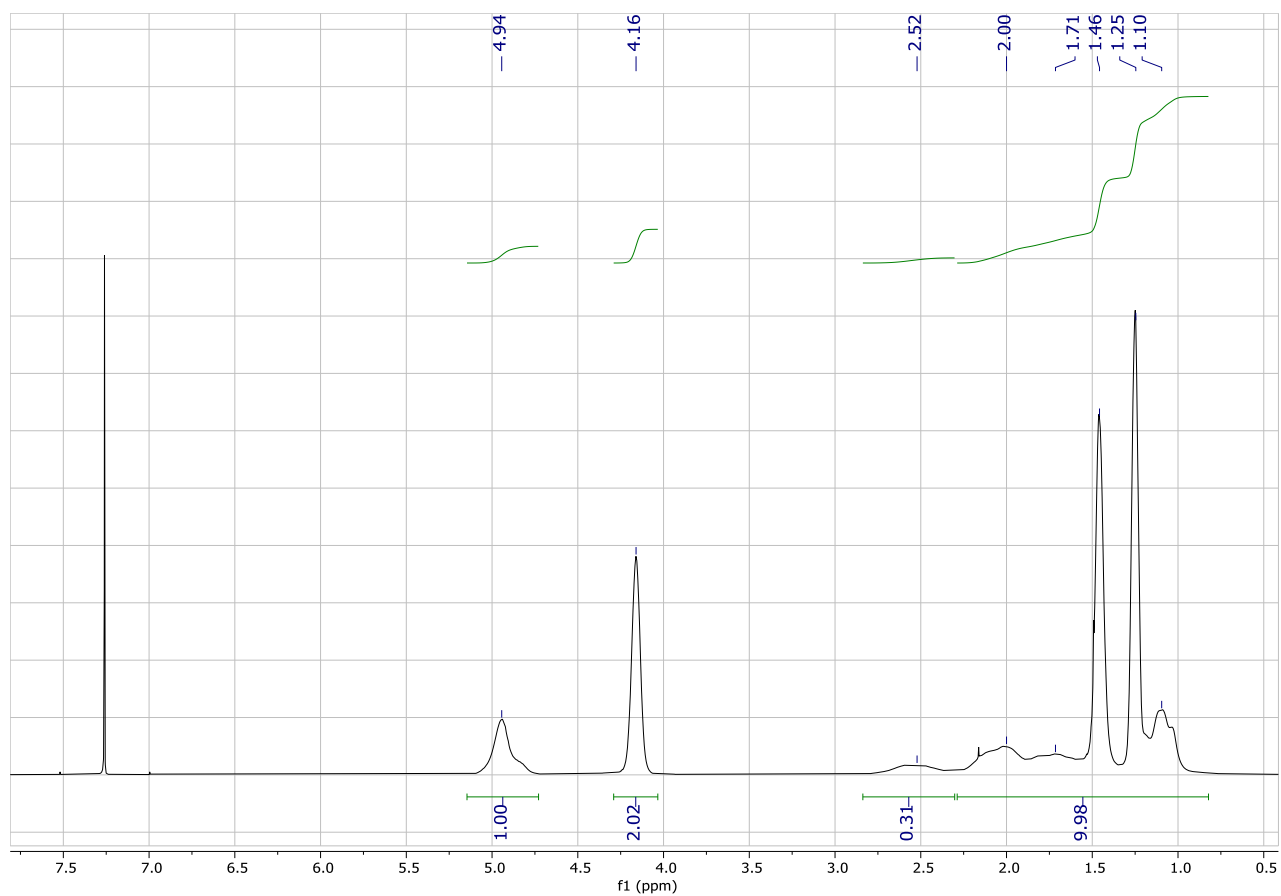


Figure S35. ^1H NMR spectrum of poly(ELMA-*r*-ELA) (CDCl_3 , 400MHz).

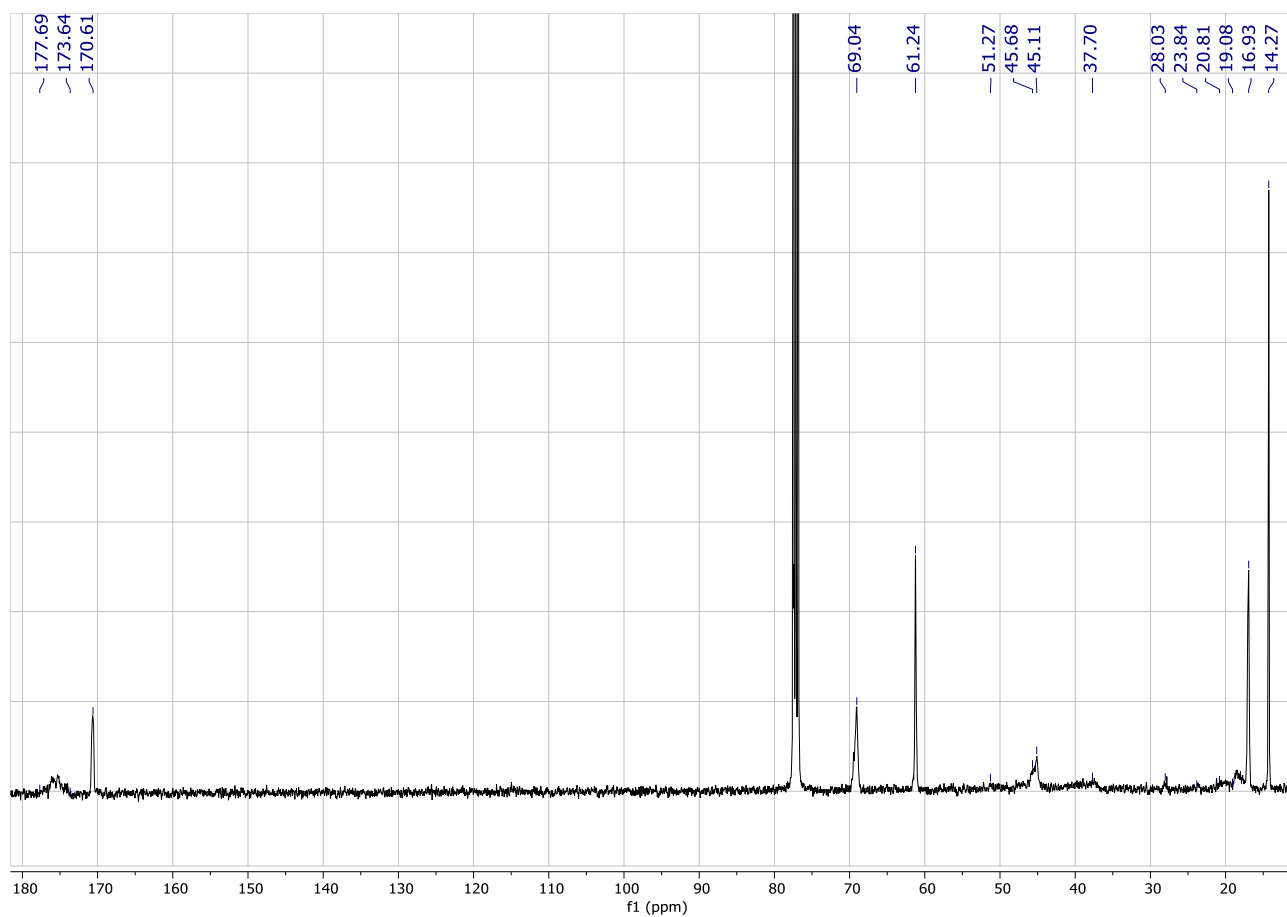
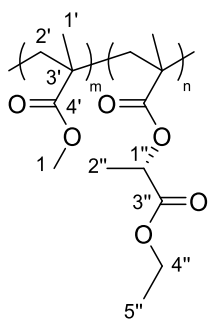


Figure S36. ^{13}C NMR spectrum of poly(ELMA-*r*-ELA) (CDCl_3 , 100MHz).

Chapter 2

Poly(ELMA-*r*-MMA):



Group	^1H NMR (δ ppm)	$^{13}\text{C}\{^1\text{H}\}$ NMR (δ ppm)
1'	Between 1.20 and 0.80	Between 19.8 and 17.5
2'	Between 2.17 and 1.80	Broad signal between 55.0 and 50.0
3'	-	Between 45.7 and 44.5
4'	-	Between 178.7 and 175.7
1	3.60	51.9
1''	4.96	69.4
2''	1.48	17.0
3''	-	170.5
4''	4.19	61.3
5''	1.28	14.3

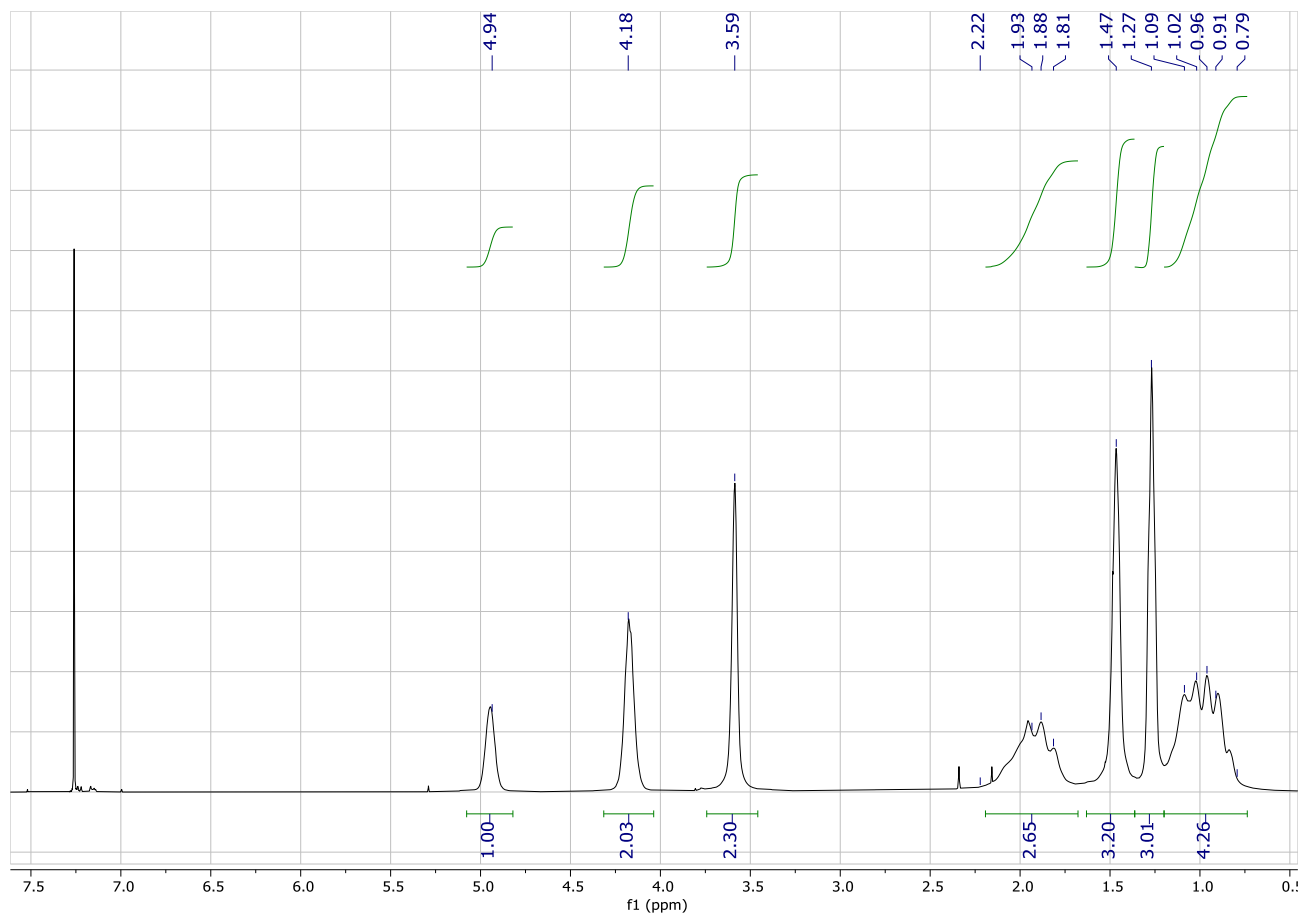


Figure S37. ^1H NMR spectrum of poly(ELMA-*r*-MMA) (CDCl_3 , 400MHz).

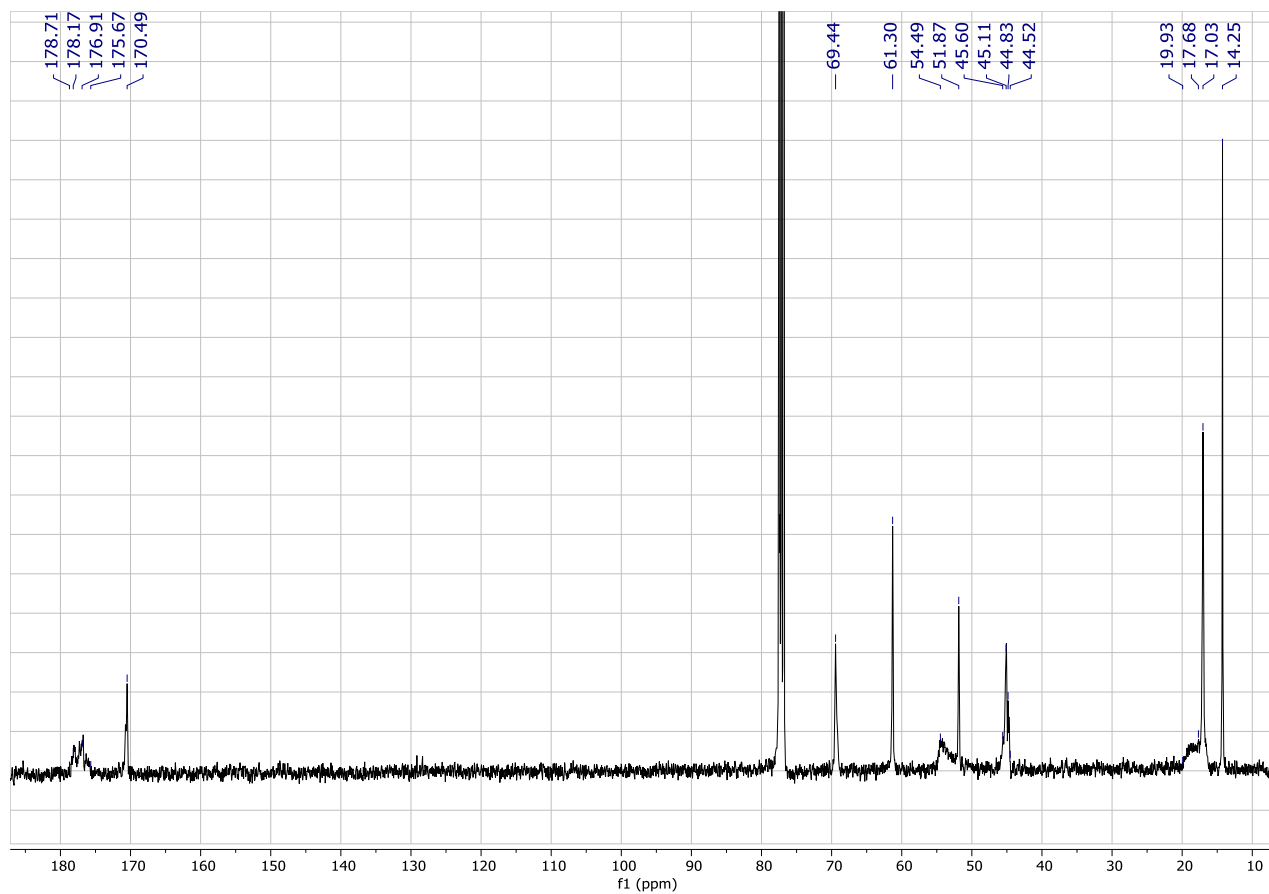
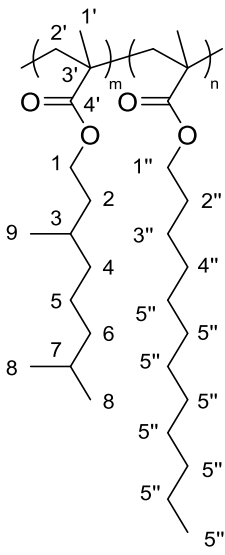


Figure S38. ^{13}C NMR spectrum of poly(ELMA-*r*-MMA) (CDCl_3 , 100MHz).

Poly(THGMA-*b*-LMA):

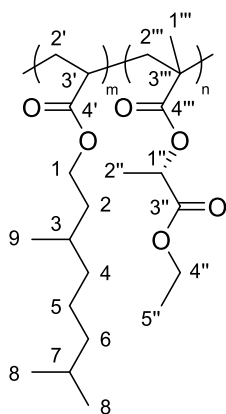


Chapter 2

Group	^1H NMR (δ ppm)	$^{13}\text{C}\{^1\text{H}\}$ NMR (δ ppm)
1'	0.9 for <i>rr</i> , 1.0 for <i>mr</i> , 1.2 for <i>mm</i>	16.7 for <i>rr</i> , 18.8 for <i>mr</i> , 21.0 for <i>mm</i>
2'	Broad signal between 2.00 and 1.75	Broad signal between 55.0 and 52.0
3'	-	44.8 for <i>rr</i> , 45.1 for <i>mr</i> , 45.7 for <i>mm</i>
4'	-	Signals between 178.2 and 176.8
1	3.98	63.6
2	1.63 ; 1.42	35.2
3	1.53	30.1
4	1.30 ; 1.15	37.3
5	1.15	39.4
6	1.30	24.7
7	1.53	28.1
8	0.86	22.8
9	0.86	19.6
1''	3.93	65.2
2''	1.60	32.1
3''		
4''		
5''		
6''		
7''	Broad signal at 1.27	8 peaks between 29.8 and 22.8
8''		
9''		
10''		
11''		
12''	0.87	14.3

Chapter 2

Poly(ELMA-*b*-THGA):



Group	^1H NMR (δ ppm)	$^{13}\text{C}\{^1\text{H}\}$ NMR (δ ppm)
2'	2.26	41.6
3'	1.87	35.7
4'	-	174.6
1'''	Between 1.20 and 1.00	Between 23.8 and 19.1
2'''	Between 2.17 and 1.84	Broad peak at 51.3
3'''	-	Between 45.9 and 45.3
4'''	-	Between 177.4 and 174.6
1	4.04	63.4
2	1.62 ; 1.42	35.7
3	1.52	30.2
4	1.30 ; 1.13	37.4
5	1.13	39.4
6	1.30	24.8
7	1.52	28.1
8	0.86	22.9
9	0.88	19.6
1''	4.94	69.5
2''	1.48	17.0
3''	-	170.5
4''	4.16	61.2
5''	1.26	14.3

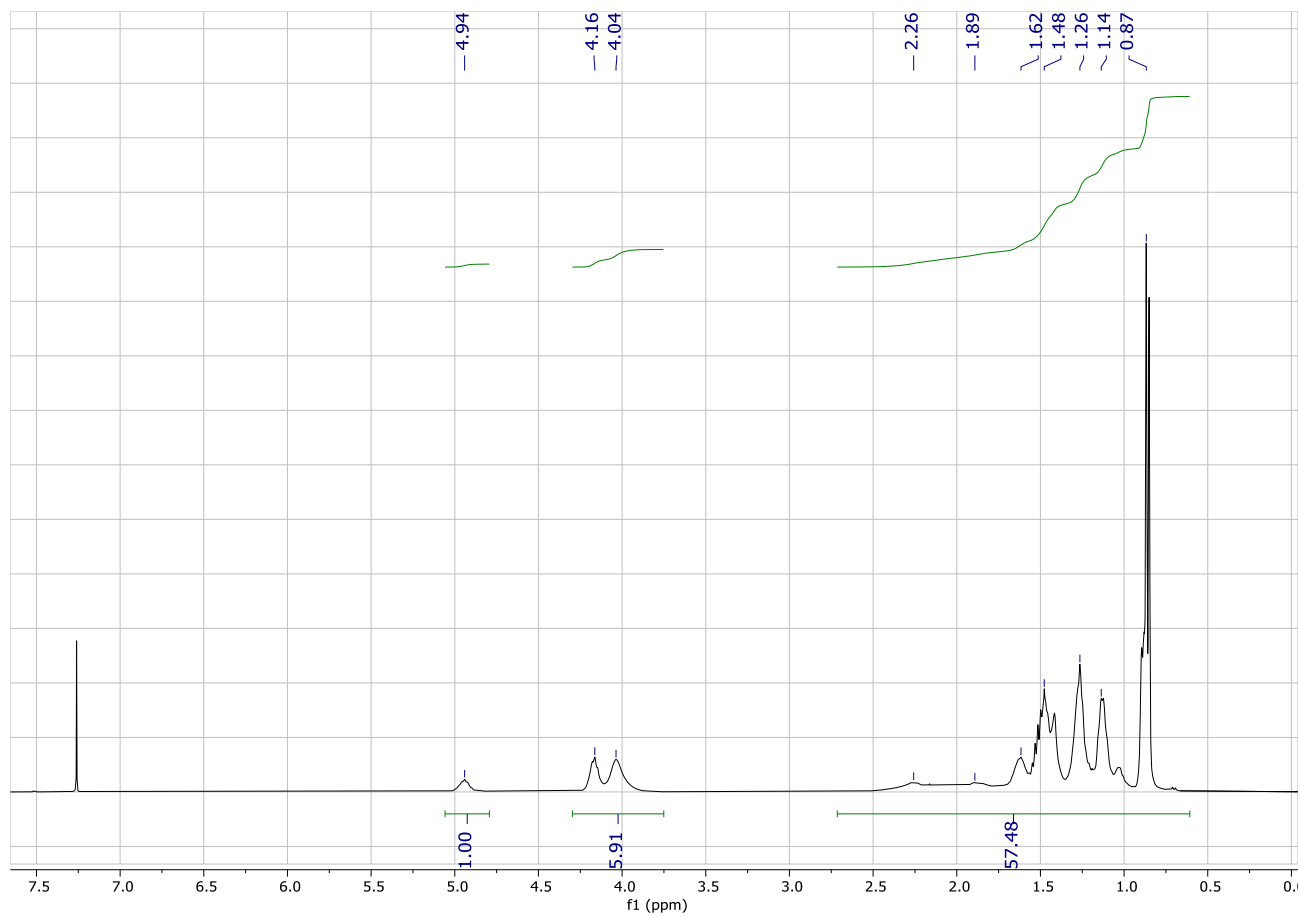


Figure S39. ^1H NMR spectrum of poly(ELMA-*b*-THGA) (CDCl_3 , 400MHz).

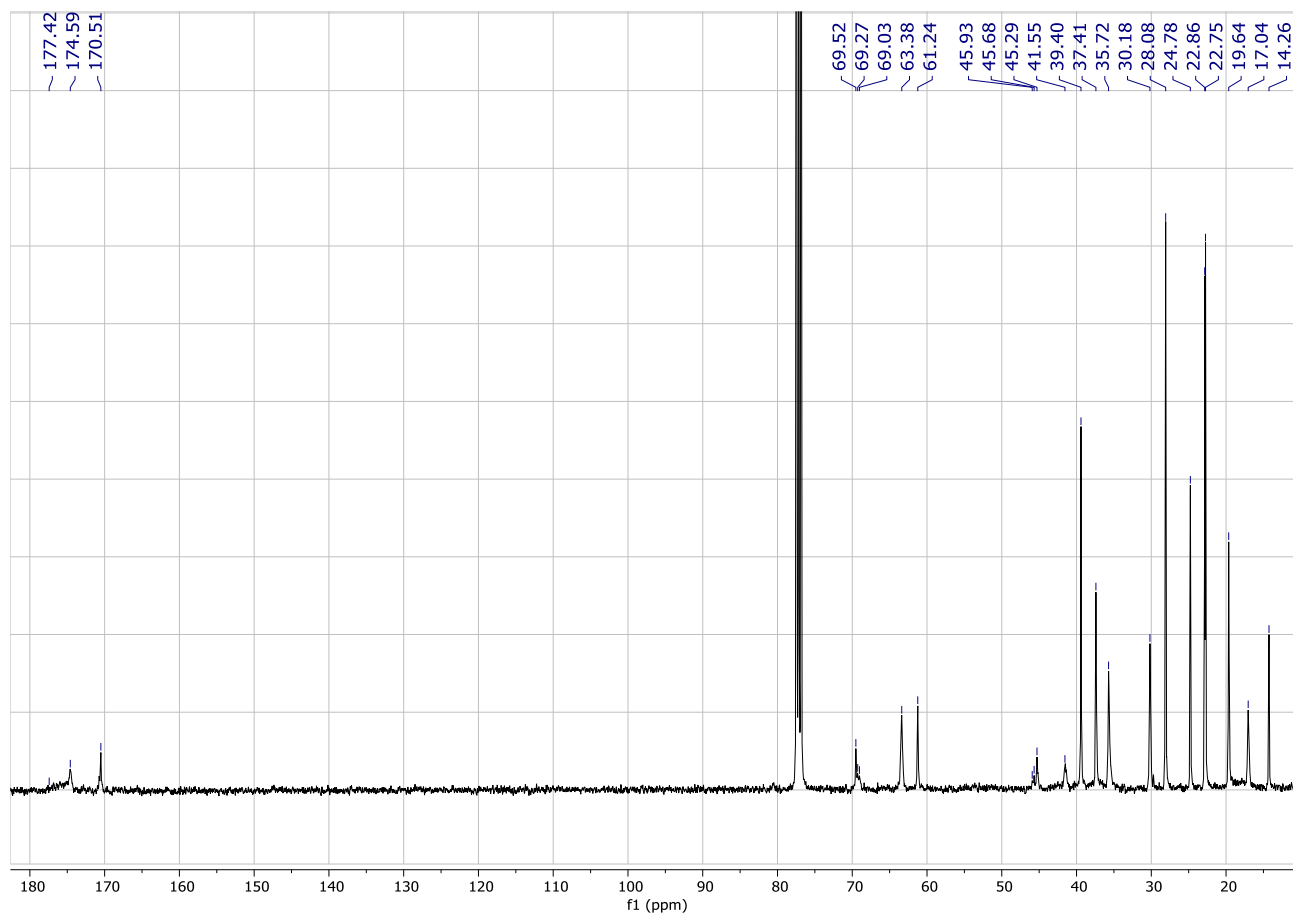
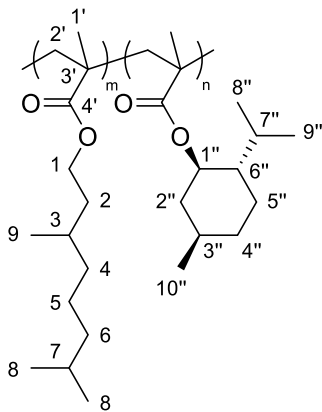


Figure S40. ^{13}C NMR spectrum of poly(ELMA-*b*-THGA) (CDCl_3 , 100MHz).

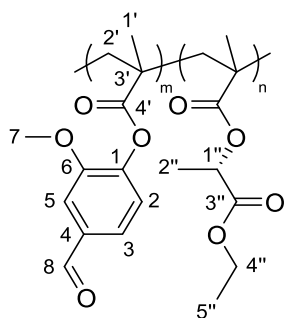
Poly(L-MnMA-*b*-THGMA):



Chapter 2

Group	^1H NMR (δ ppm)	$^{13}\text{C}\{^1\text{H}\}$ NMR (δ ppm)
1'	Between 1.20 and 0.90	Between 21.0 and 17.9
2'	Broad signal between 2.3 and 1.7	Broad signal between 55.0 and 52.0
3'	-	Between 46.2 and 44.8
4'	-	Between 178.5 and 176.1
1	3.95	63.6
2	1.63 ; 1.42	35.2
3	1.53	30.1
4	1.30 ; 1.15	37.3
5	1.15	39.4
6	1.30	24.7
7	1.53	28.0
8	0.86	22.8
9	0.86	19.6
1''	4.41	75.8
2''	2.02 ; 1.04	40.0
3''	1.47	31.5
4''	1.68 ; 0.96	34.4
5''	1.68 ; 1.06	22.9
6''	1.43	47.3
7''	1.86	25.5
8''	0.90	22.3
9''	0.88	21.6
10''	0.66	15.9

Poly(ELMA-*b*-VMA):



Group	^1H NMR (δ ppm)	$^{13}\text{C}\{^1\text{H}\}$ NMR (δ ppm)
1'	Between 1.20 and 1.00	Between 20.0 and 17.9
2'	Between 2.60 and 1.84	Broad peak between 55.8 and 50.0
3'	-	Between 46.3 and 45.2
4'	-	Between 176.9 and 174.8
1	-	151.9
2	7.31	123.3
3	7.39	124.4
4	-	135.1
5	7.39	111.0
6	-	144.5
7	3.73	55.8
8	9.86	190.9
1''	4.94	69.5
2''	1.48	17.0
3''	-	170.5
4''	4.16	61.2
5''	1.27	14.2

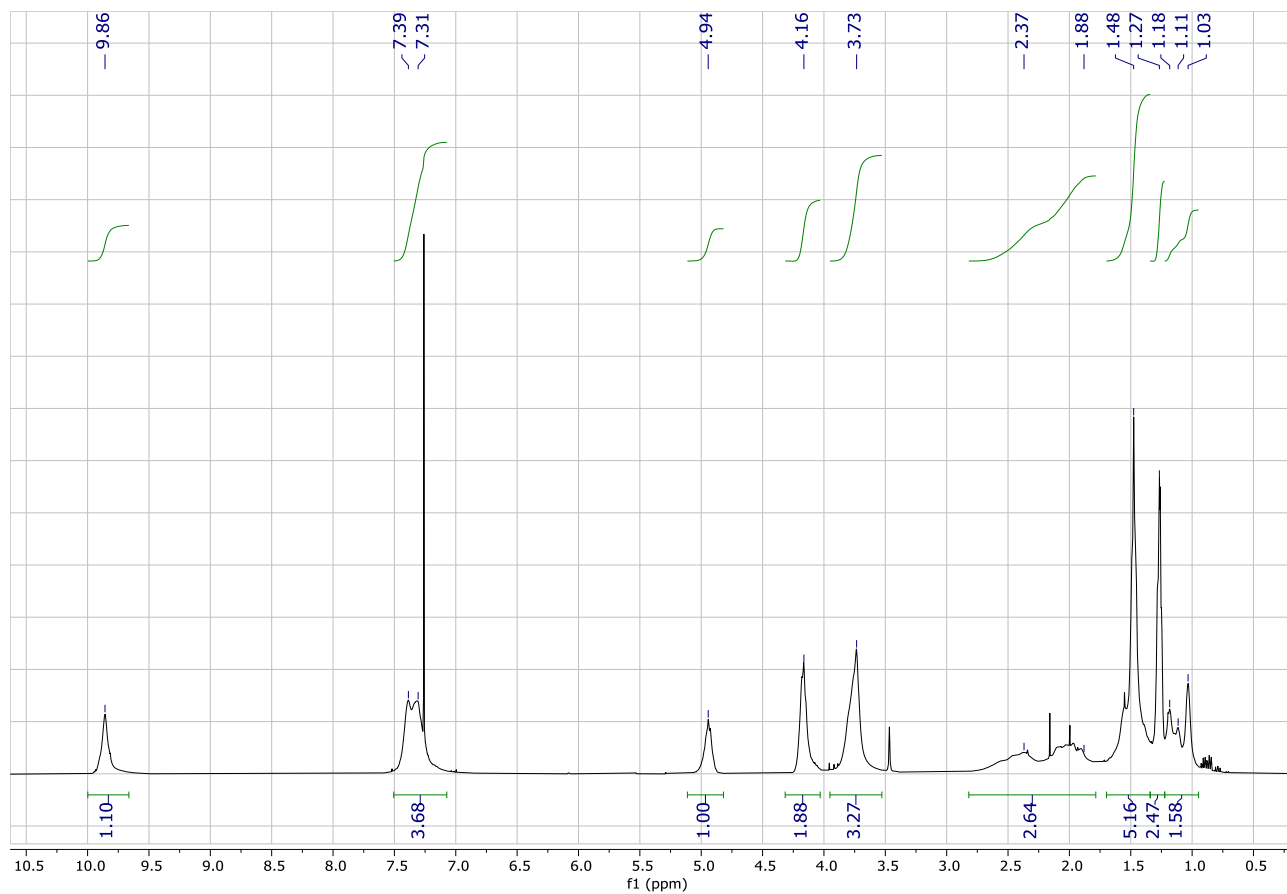


Figure S41. ^1H NMR spectrum of poly(ELMA-*b*-VMA) (CDCl_3 , 400MHz).

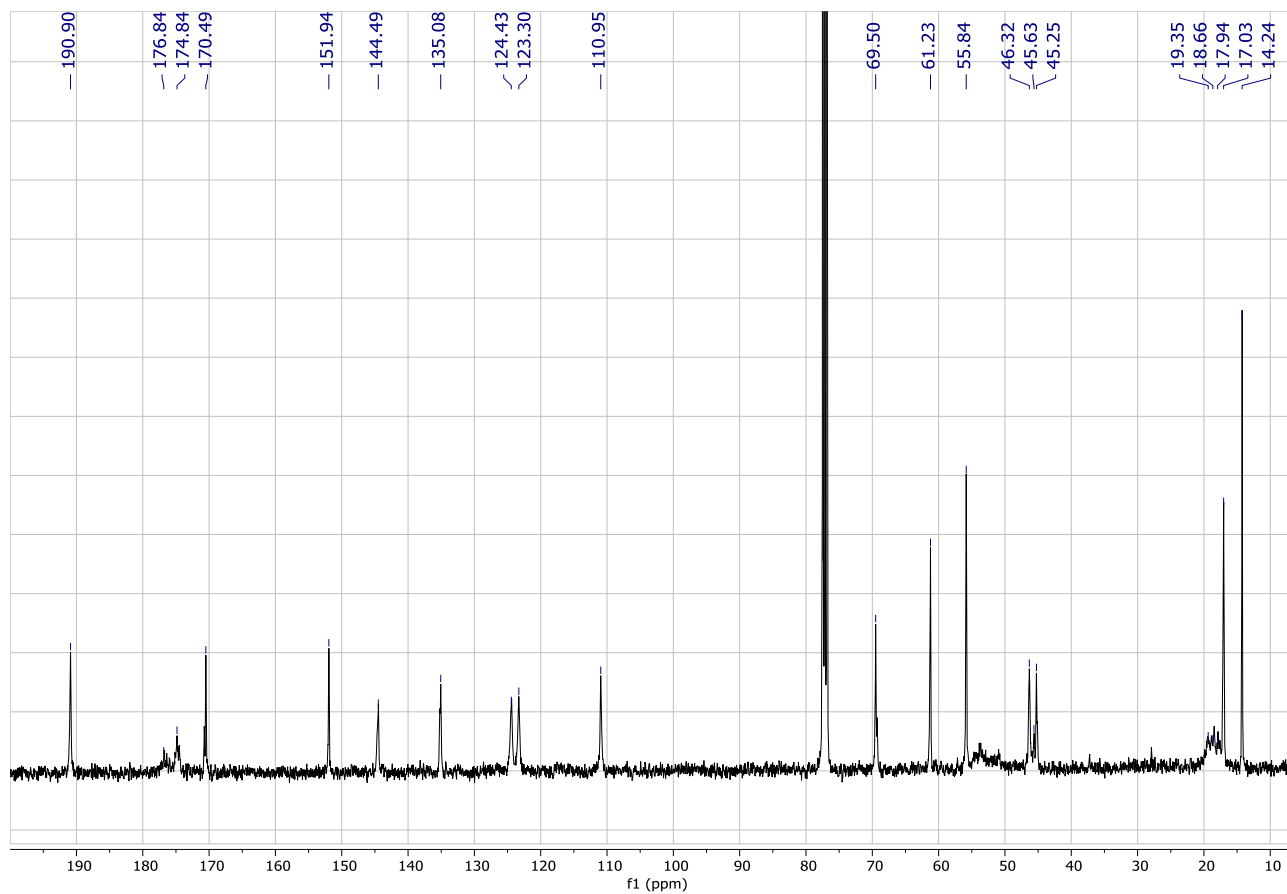
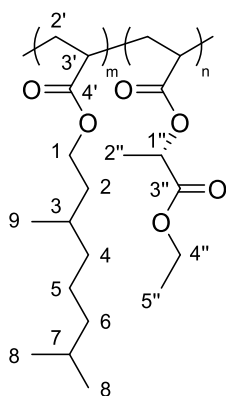


Figure S42. ^{13}C NMR spectrum of poly(ELMA-*b*-VMA) (CDCl_3 , 100MHz).

Poly(ELA-*b*-THGA):



Group	^1H NMR (δ ppm)	$^{13}\text{C}\{^1\text{H}\}$ NMR (δ ppm)
2'	Between 2.71 and 2.17	Between 41.5 and 40.3
3'	2.04	35.7
4'	-	Between 174.6 and 174.1
1	4.04	63.4
2	1.62 ; 1.42	35.7
3	1.52	30.2
4	1.30 ; 1.13	37.4
5	1.13	39.4
6	1.30	24.8
7	1.52	28.1
8	0.86	22.8
9	0.89	19.6
1''	4.98	68.9
2''	1.44	16.9
3''	-	170.6
4''	4.16	61.2
5''	1.23	14.3

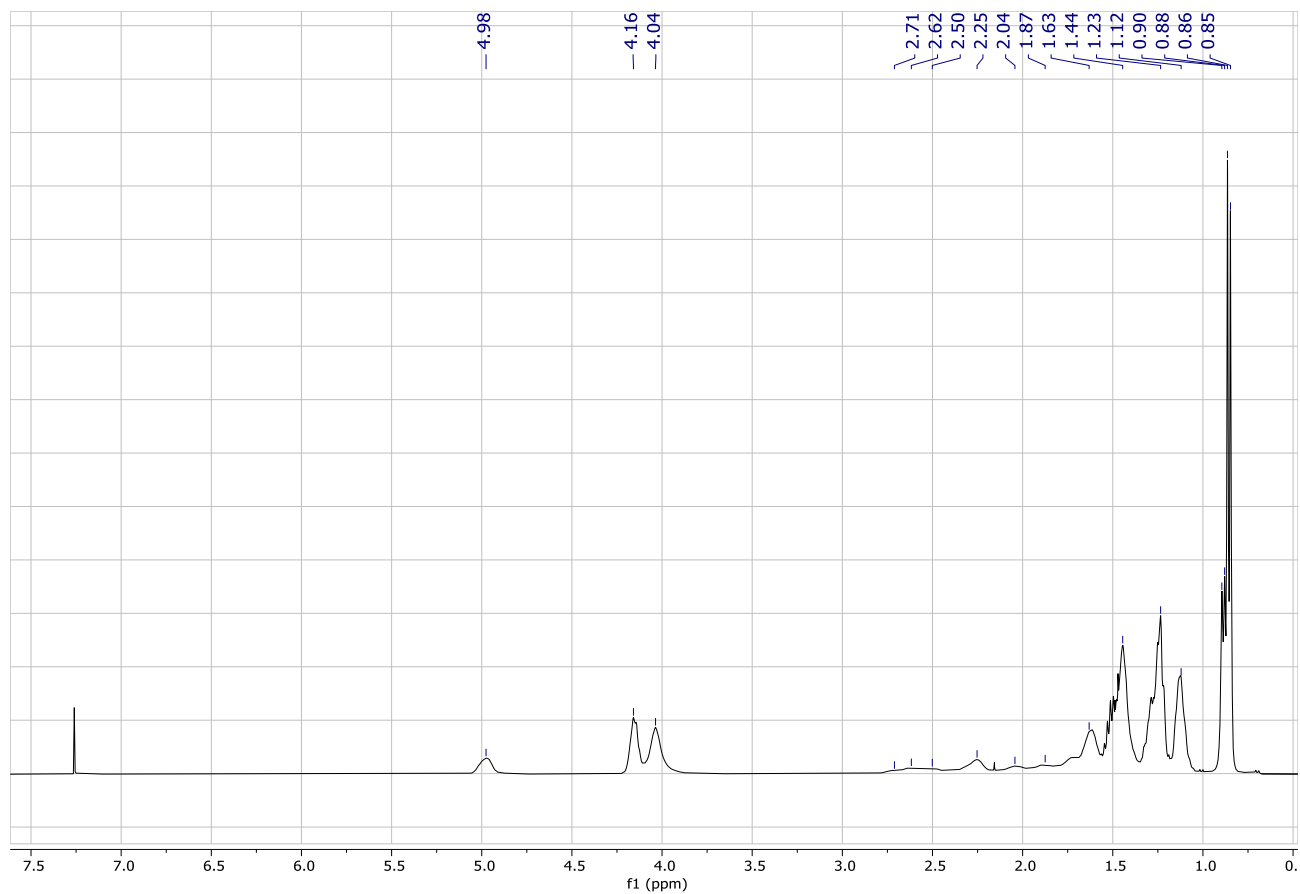


Figure S43. ^1H NMR spectrum of poly(ELA-*b*-THGA) (CDCl_3 , 400MHz).

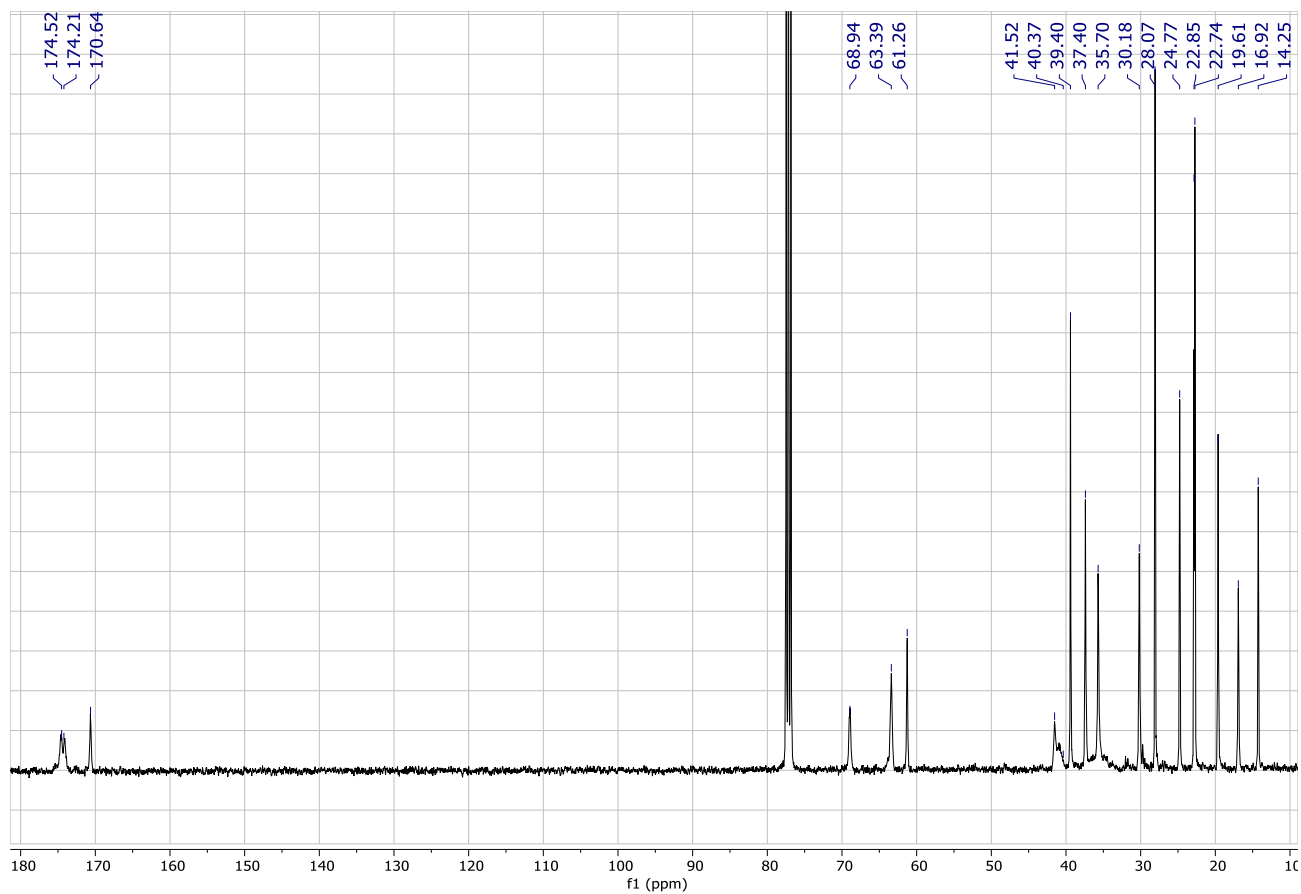
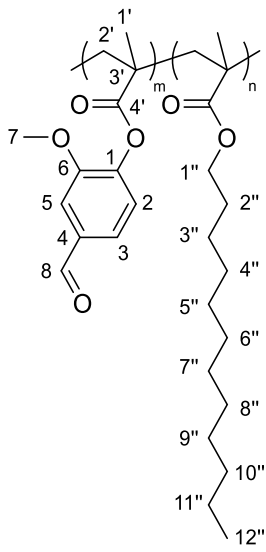


Figure S44. ^{13}C NMR spectrum of poly(ELA-*b*-THGA) (CDCl_3 , 100MHz).

Poly(VMA-*b*-LMA):



Chapter 2

Group	^1H NMR (δ ppm)	$^{13}\text{C}\{^1\text{H}\}$ NMR (δ ppm)
1'	Between 1.20 and 1.00	Between 21.0 and 16.0
2'	Between 2.60 and 1.84	Broad peak between 55.8 and 50.0
3'	-	Between 46.4 and 44.8
4'	-	Between 178.1 and 173.6
1	-	151.9
2	7.31	123.3
3	7.40	124.4
4	-	135.1
5	7.40	111.0
6	-	144.5
7	3.74	55.9
8	Between 9.93 and 9.85	190.9
1''	3.91	65.2
2''	1.61	32.1
3''		
4''		
5''		
6''		
7''	Broad signal at 1.25	8 peaks between 29.8 and 22.8
8''		
9''		
10''		
11''		
12''	0.87	14.3

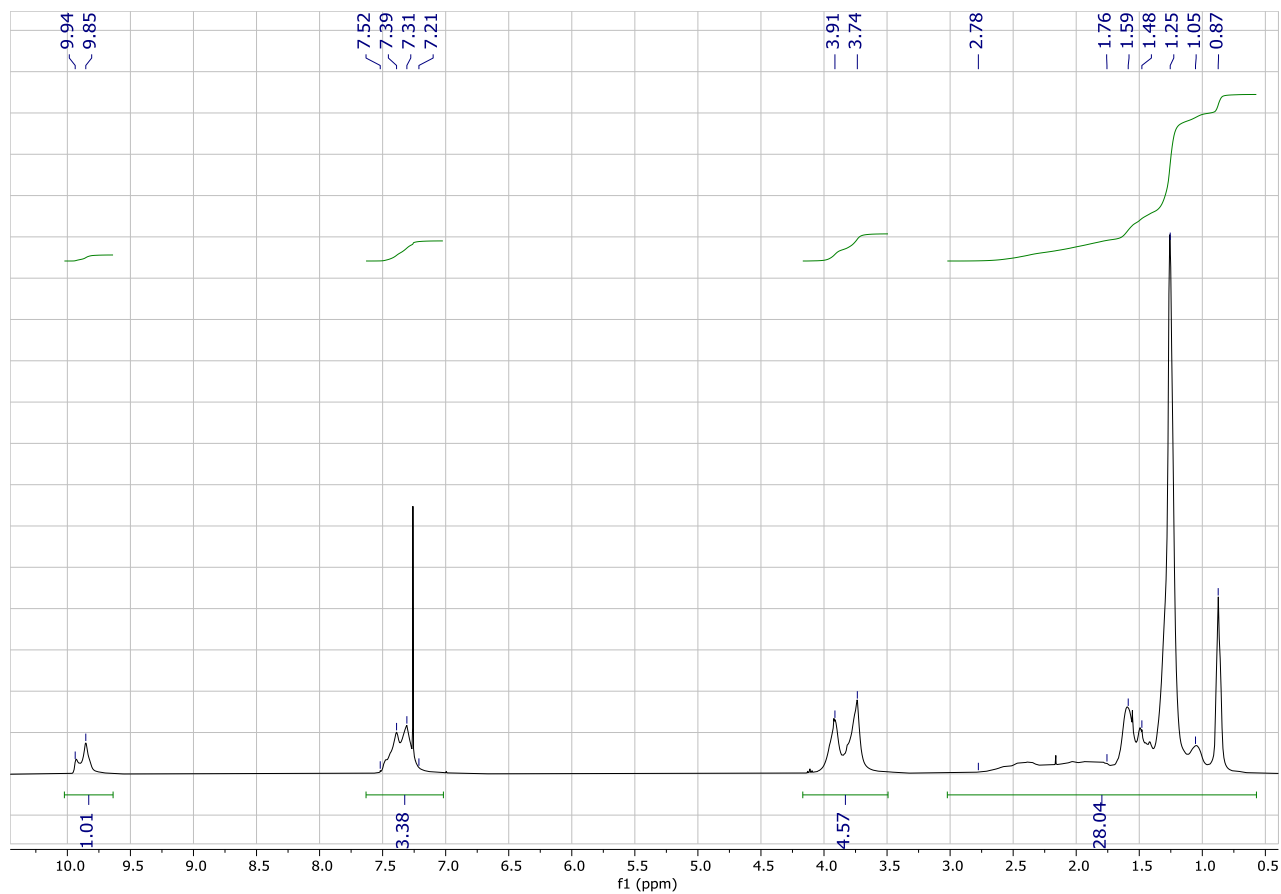


Figure S45. ^1H NMR spectrum of poly(VMA-*b*-LMA) (CDCl_3 , 400MHz).

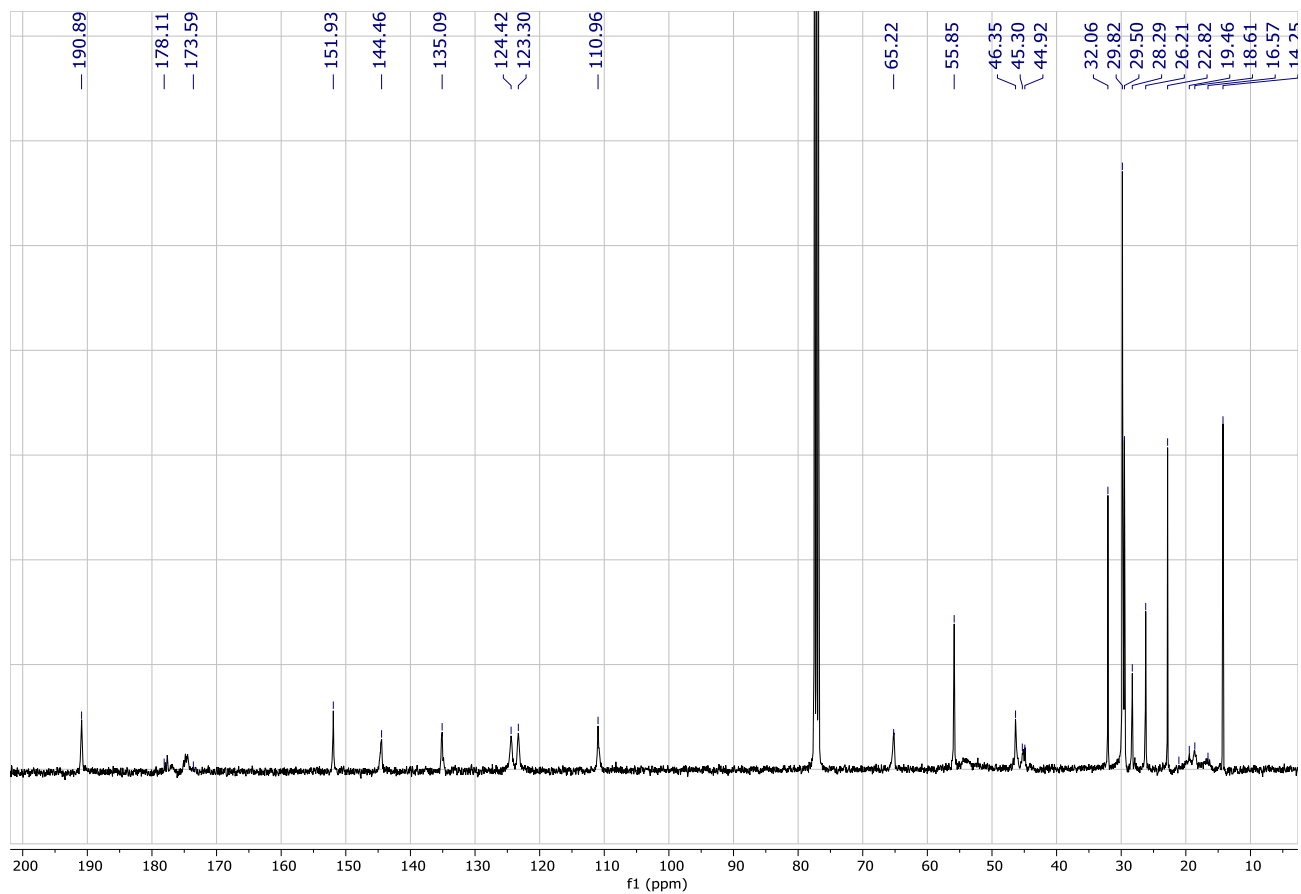
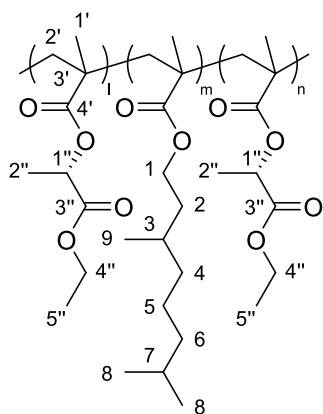


Figure S46. ^{13}C NMR spectrum of poly(VMA-*b*-LMA) (CDCl_3 , 100MHz).

Chapter 2

Poly(ELMA-*b*-THGMA-*b*-ELMA):



Group	^1H NMR (δ ppm)	$^{13}\text{C}\{^1\text{H}\}$ NMR (δ ppm)
1'	Between 1.20 and 1.00	Between 19.6 and 17.9
2'	Between 2.17 and 1.84	54.3
3'	-	45.2
4'	-	Between 177.9 and 175.9
1	3.94	63.6
2	1.63 ; 1.42	35.2
3	1.53	30.2
4	1.30 ; 1.15	37.3
5	1.15	39.4
6	1.30	24.7
7	1.53	28.1
8	0.86	22.9
9	0.86	19.6
1''	4.94	69.5
2''	1.46	17.0
3''	-	170.5
4''	4.16	61.2
5''	1.25	14.3

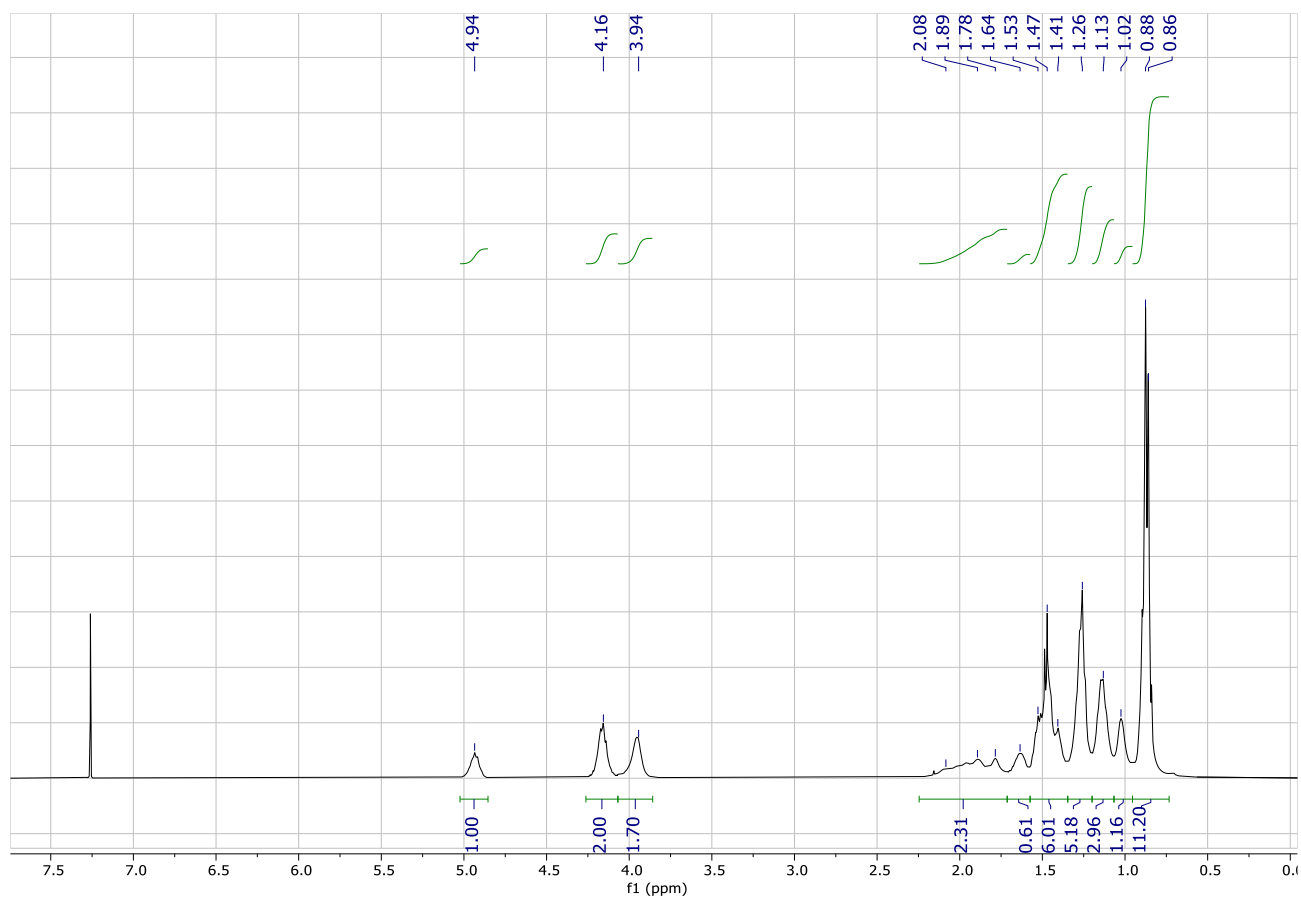


Figure S47. ^1H NMR spectrum of poly(ELMA-*b*-THGMA-*b*-ELMA) (CDCl_3 , 400MHz).

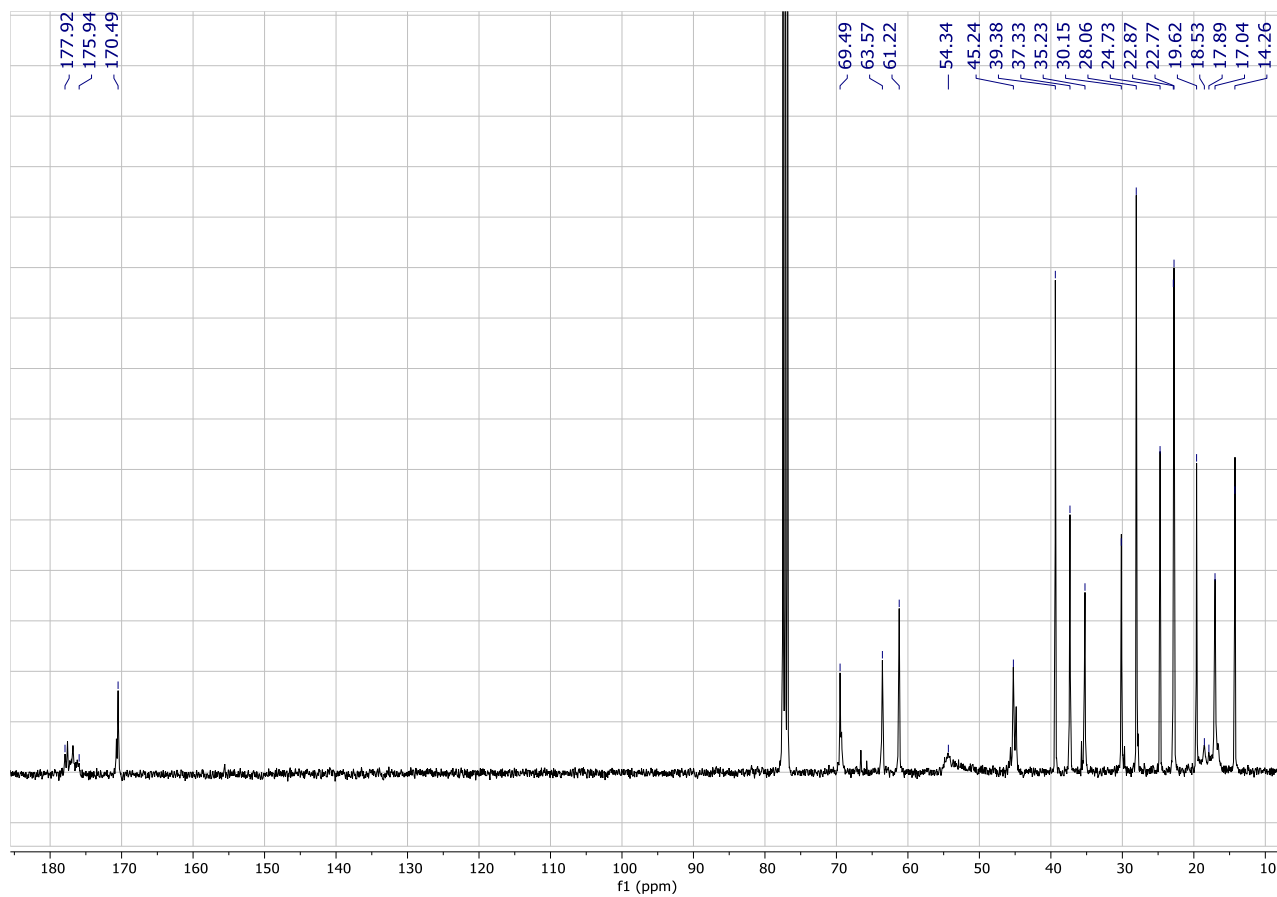


Figure S48. ^{13}C NMR spectrum of poly(ELMA-*b*-THGMA-*b*-ELMA) (CDCl_3 , 100MHz).

Chapter 3 – Ambient Temperature Polymerization of MMA mediated by Ate Complexes

Hugo Fouilloux,^a and Christophe M. Thomas^{a,*}

^a Chimie ParisTech, PSL University, CNRS, Institut de Recherche de Chimie Paris, 75005 Paris, France.

E-mail: christophe.thomas@chimie-paristech.fr

This chapter has been accepted for publication in *ChemCatChem*:

H. Fouilloux, C. M. Thomas, *ChemCatChem* **2021**, DOI: 10.1002/cctc.202101673.

Contributions to the publication:

H. F. performed the experiments. H. F and C. M. T. analysed the data and wrote the paper

Hugo Fouilloux



30/12/2021

Christophe M. Thomas



Abstract

Finding catalysts that are both robust and highly active at room temperature can often be considered as a daunting challenge. Yet, these features are desirable for polymer synthesis as they allow to produce materials of interest easily and sustainably. Herein we report the use of commercial reagents to form *in situ* “ate” complexes, which were found to be highly active in the room temperature anionic polymerization of methyl methacrylate. Also of particular interest is their ability to polymerize *rac*-lactide, and even form block copolymers of poly(methylmethacrylate) and poly(lactic acid).

Introduction

Poly(methylmethacrylate) (PMMA) is a transparent thermoplastic with a high chemical stability and weather resistance.^[1] This polymer is widely used as a substitute for inorganic glass, because it shows high impact strength, is lightweight, shatter-resistant, and exhibits favorable processing conditions.^[2–4] PMMA can be obtained by either radical or anionic polymerization.^[5] While radical polymerization techniques are generally preferred as cheap and robust methods to prepare acrylic materials, only anionic polymerization can provide of stereoregular PMMA in short reaction times.^[6,7] Classical anionic polymerization is usually carried out at low temperature (between -40 and -78 °C), and while several new room temperature polymerization techniques have emerged (*e.g.*, group transfer polymerization and Lewis pair polymerization), they often require the tedious synthesis of highly reactive catalysts. Because of this reactivity, preparing and isolating such catalysts can turn out to be a challenge. Therefore, the use of inexpensive, easily accessible complexes exhibiting high activities under mild reaction conditions would be desirable. With these observations in mind, we decided to investigate the anionic polymerization of MMA at room temperature, initiated by “ate” complexes formed *in situ* from commercially available reagents.

A metalate or “ate” complex can be defined as a salt formed from the stoichiometric reaction of a Lewis base and a Lewis acid in which the acidic moiety formally increases its valency and becomes

anionic.^[8] The first example of an alkali-metal ate complex, NaZnEt_3 , was synthesized by Wanklyn in 1858.^[9] The term “ate” was coined by Wittig in 1951 after he isolated the first magnesiate LiMgPh_3 .^[10] In solution, ate complexes occur either as contacted ion pair (CIP) or as solvent-separated ion pair (SSIP).^[11] They are usually prepared by two distinct strategies: homoleptic complexes are generally obtained by salt metathesis, while heteroleptic complexes are more often produced *via* co-complexation. Metalate complexes, especially magnesiates^[12–14] and zincates,^[15–17] have given rise during the last decades to several versatile catalytic systems. Their unique diversity makes them useful for a variety of organic reactions. For these reactions, they exhibit higher stability than their organolithium counterparts close to room temperature, while they are usually more reactive than the metal complexes they are derived from.^[18] Good functional tolerance and regioselectivity are also among their notable features. Several excellent reviews cover the wide variety of “ate” complexes already described in the literature.^[11,18–20]

Only few examples of MMA polymerization initiated by “ate” complexes have been reported. The three most notable examples feature magnesiate,^[21,22] yttriumate^[23] and cuprate complexes.^[24] Lin and coworkers described lithium and sodium magnesiate heteroleptic complexes bearing bisphenolate ligands. At -30°C in toluene, they polymerized MMA with a 95% isospecificity. However, M_n were not controlled.^[21] Sherrington also reported sodium and potassium magnesiates containing a ferrocene cation.^[22] The resulting polymerizations were not controlled but the polymers were slightly syndiotactic even at room temperature in THF (84% of $[rr]$). Ihara *et al.* then described lithium/yttrium “ate” complexes formed *in situ* from YCl_3 , $n\text{BuLi}$ and various secondary amines, that were found to promote living polymerization of MMA at -78°C .^[23] Interestingly, mechanistic studies clearly evidenced the initiation of the polymerization reaction by the amido group (even in heteroleptic complexes containing both amido and alkyl ligands). Equally impressive results were reported by Kawaguchi and coworkers, using a mixture of CuI and 2 equivalents of MeLi as catalysts.^[24] The

polymerization of various (meth)acrylates proceeded quantitatively at 0°C in THF, yielding materials with narrow dispersities, although initiator efficiency was only of 5% (M_n not controlled).

In our search for new polymerization catalysts, we recently focused our efforts on investigating the catalytic activity of different metalate complexes.^[25-27] Herein, we describe the use of hetero-bimetallic complexes and their catalytic activities for the polymerization of methyl methacrylate and *rac*-lactide. These catalytic systems exhibit high activity yet controlled behavior for the polymerization of MMA and could even form the block copolymer PMMA-*b*-PLA.

Results and Discussion

Our attention was first drawn to the synthesis of simple lithium-magnesiates complexes $\text{LiMg}[\text{N}(\text{TMS})_2]_2\text{R}$ (with R = alkyl group) from commercially available $\text{Mg}[\text{N}(\text{TMS})_2]_2$ and the corresponding organolithium reagents. Such complexes have already been isolated and fully characterized,^[28,29] but their reactivity for polymerization reactions have not been investigated. Also, as demonstrated by Sherrington, the lithium amide derived from hexamethyldisilazane exhibits lower nucleophilicity for MMA polymerization than other common lithium amides, and thus higher stability at room temperature.^[30] Considering the observations of Ihara and coworkers using simple yttriumates,^[23] a cheaper and more useful ambient temperature alternative can be expected by simply mixing LiR and $\text{Mg}[\text{N}(\text{TMS})_2]_2$.

The reaction of *n*BuLi with $\text{Mg}[\text{N}(\text{TMS})_2]_2$ was first studied in a J-Young NMR tube in THF-*d*₈, and gave rise to a Schlenk equilibrium presented in Figure 1.^[31] The proton signals of the starting materials all disappeared, leading to three new products: the expected $\text{LiMg}[\text{N}(\text{TMS})_2]_2\text{nBu}$ (signal of TMS at -0.02 ppm, signal of Mg-CH₂-R at -0.62 ppm), and the products of the Schlenk equilibrium $\text{Mg}[\text{N}(\text{TMS})_2]_4\text{Li}_2$ (signal of TMS at -0.17 ppm) and $\text{Mg}(\text{nBu})_2$ (signal of Mg-CH₂-R at -0.68 ppm, as confirmed by the ¹H NMR of commercial $\text{Mg}(\text{nBu})_2$).

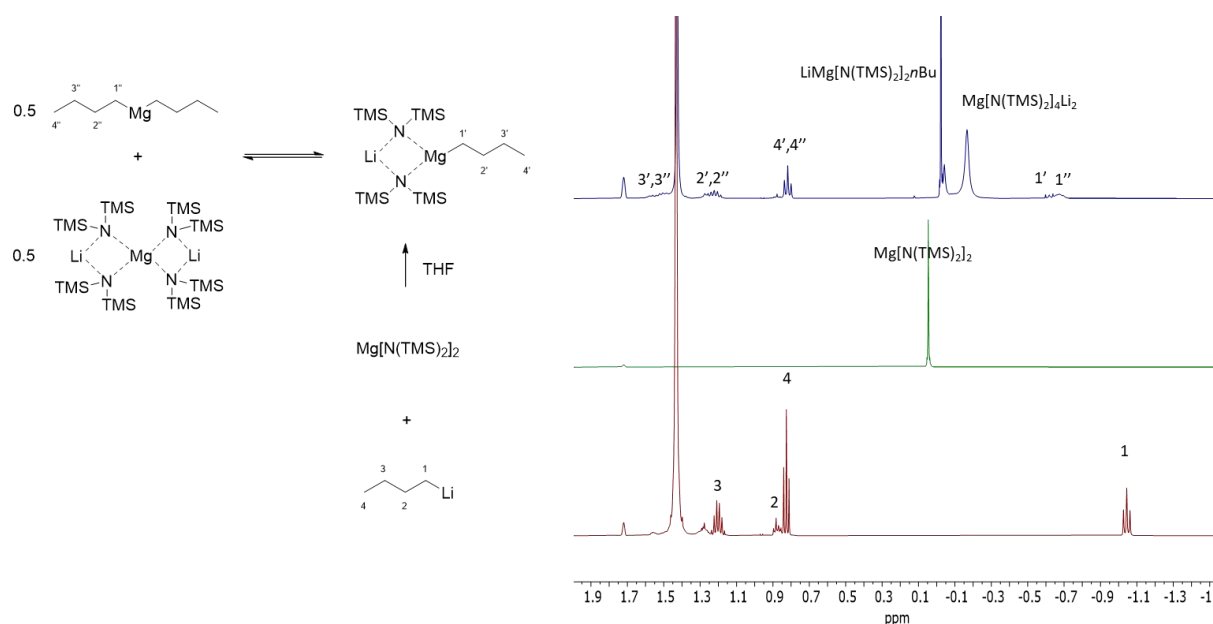


Figure 1. ^1H NMR spectra of $\text{Mg}[\text{N}(\text{TMS})_2]_2$, $n\text{BuLi}$ and the products resulting from their reaction in $\text{THF-}d_8$ (400 MHz).

Addition of 20 equivalents of MMA at room temperature to this mixture confirmed the signal attribution and provided valuable information on the reactivity of each magnesium species (Figure 2). First, the monomer is quantitatively converted into the corresponding oligomers. The spectrum features the $-\text{CH}_3$ resonances of PMMA at δ 0.84 ppm and δ 1.11 ppm. Then, while $\text{Mg}[\text{N}(\text{TMS})_2]_4\text{Li}_2$ (at δ -0.17 ppm) seems to remain largely unaffected, the signal at δ -0.02 ppm ($\text{LiMg}[\text{N}(\text{TMS})_2]_2n\text{Bu}$) is shifted to 0.03 and 0.01 ppm, due to initiation of MMA polymerization and thus formation of a N-C bond that slightly shifts the TMS signal. Alkyl resonances in the -0.6 ppm region have also disappeared, supposedly due to side reactions involving highly reactive Mg-alkyl bonds.

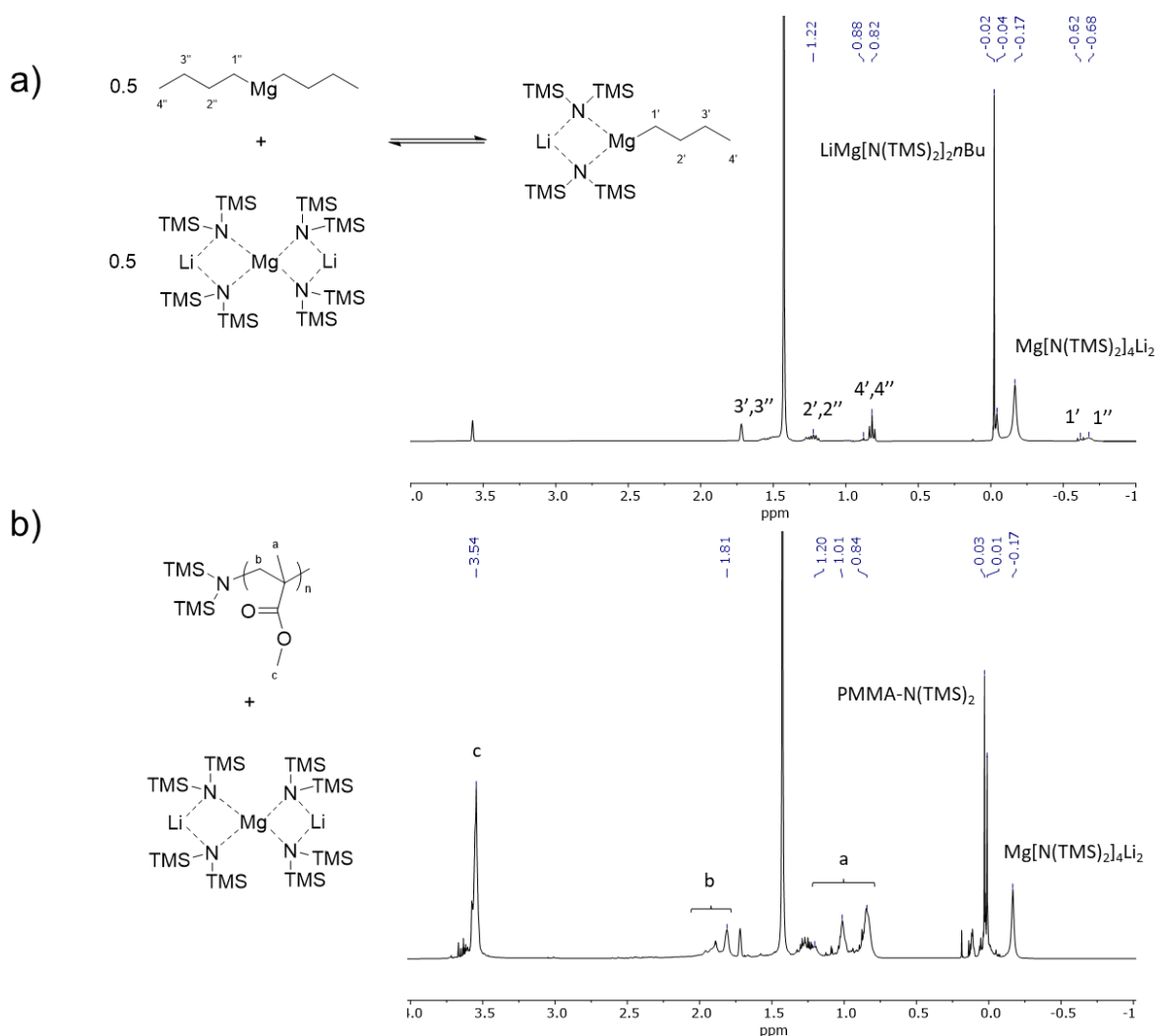
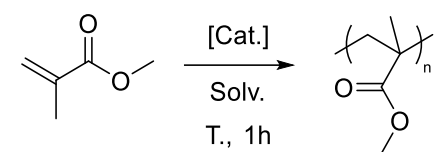


Figure 2. ^1H NMR spectra of $\text{LiMg}[\text{N}(\text{TMS})_2]_2n\text{Bu}$ in a Schlenk equilibrium before (a) and after (b) addition of 20 equivalents of MMA.

When performing the complex synthesis in $\text{toluene-}d_8$, no Schlenk equilibrium is observed and the expected ate species is quantitatively produced, as reported by Hill (Figure S1).^[29] However, addition of MMA to this catalyst in toluene led to an uncontrolled polymerization process and a multimodal molar mass distribution (*vide infra*). The first encouraging result in THF thus prompted us to investigate systematically the performances of this system in Schlenk reactors, at room temperature in THF (Table 1).

Chapter 3

Table 1. Anionic polymerization of MMA with various initiating systems and conditions.^[a]



Entry	Cat.	Solv.	T (°C)	[MMA]/[Cat.]	Conv. (%)	M_n^{th} (g/mol) ^[b]	M_n^{NMR} (g/mol) ^[c]	M_n^{exp} (g/mol) ^[d]	\bar{D}
1	[Mg] + RLi	THF	25	100	90	9 000	5 900	7 600	1.58
2	[Mg]	THF	25	100	1	-	-	-	-
3	RLi	THF	25	100	1	-	-	-	-
4	[Mg] + RLi	THF	25	50	99	5 000	3 800	4 200	2.02
5	[Mg] + RLi	THF	25	200	83	16 600	10 300	12 200	1.65
6 ^[e]	[Mg] + RLi	THF	25	100	91	9 100	6 800	6 400	1.57
7	[Mg] + RLi	Tol.	25	100	74	7 400	4 900	4 600	3.64
8	[Mg] + RLi	Tol.	-30	200	75	15 000	19 200	27 900	4.38
9 ^[f]	[Mg] + RLi	THF	-30	200	5	1 000	540 000	48 000	2.08
10	[Mg] + RLi	THF	50	200	73	14 600	9 300	10 800	1.56

^[a] [Mg] = Mg[N(TMS)₂]₂ for all entries. RLi = *n*BuLi for all entries except entries 2 and 6. All reactions were performed under argon in a glovebox at room temperature. [MMA] = 1 mol/L. Time of reaction: 1h (stopped by addition of MeOH). ^[b] M_n^{th} = Eq. of MMA × M(MMA) × Conv. ^[c] M_n^{NMR} determined by relative integration of the methyl group of MMA (at 1.14, 0.95 and 0.77 ppm) with respect to the trimethylsilyl protons of the initiator at 0.04 ppm. ^[d] M_n^{exp} and \bar{D} of polymer determined by refractive index - size exclusion chromatography calibrated with polystyrene standards in THF at 35°C. ^[e] RLi = *t*BuLi. ^[f] Solution stopped stirring after 20 minutes due to high viscosity.

Interestingly, $\text{LiMg}[\text{N}(\text{TMS})_2]_2n\text{Bu}$ can convert 90% of MMA at room temperature (Table 1, entry 1) while its two precursors $\text{Mg}[\text{N}(\text{TMS})_2]_2$ and $n\text{BuLi}$ cannot (Table 1, entries 2&3), presumably hampered by quick initiator destruction or too easy backbiting termination reactions.^[6] $\text{Mg}(n\text{Bu})_2$ gave the same result as $\text{Mg}[\text{N}(\text{TMS})_2]_2$ and $n\text{BuLi}$ under these reaction conditions. An examination of the ^1H and ^{13}C NMR spectra of the PMMA obtained after purification (Figures 3&S2) confirmed the fact that anionic polymerization is initiated by an amido ligand of the magnesiate complex, as observed by Ihara and coworkers in the case of yttriumate.^[23] Thanks to this chain end identification, proton NMR spectroscopy can be used for the quantitative analysis of the average molecular weight of the PMMA obtained, which is of the same magnitude as M_n^{th} (obtained from monomer conversion) and M_n^{exp} (obtained from SEC).

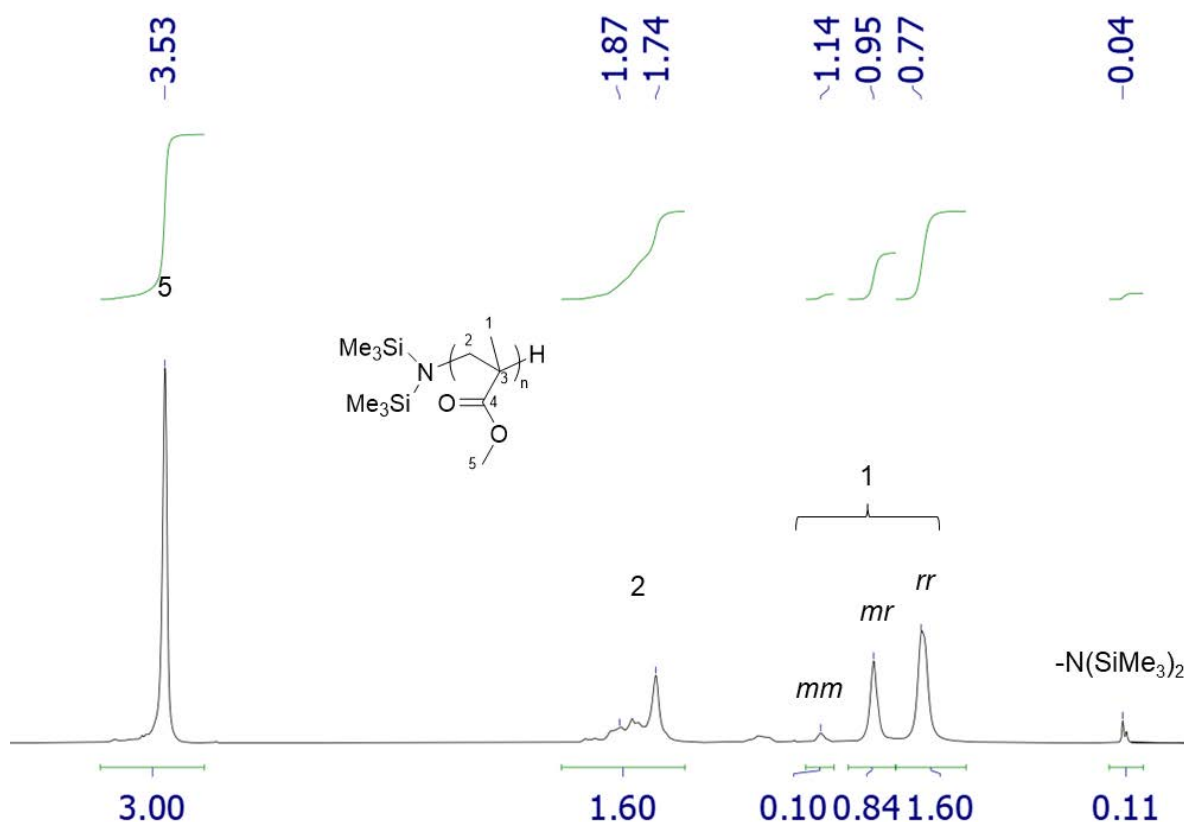


Figure 3. ^1H NMR spectrum after purification of PMMA obtained by polymerization initiated by $\text{LiMg}[\text{N}(\text{TMS})_2]_2n\text{Bu}$ at room temperature (Table 1, entry 5). $M_n^{\text{NMR}} = 16\,900$ g/mol for the purified

polymer, presumably due to small oligomers loss during the precipitation in cold methanol (see Experimental section).

Depending on the initiator loading used, various M_n were accessible (Table 1, entries 4&5), which exemplifies the rather good control on molecular weight obtained with our initiating system. Using another organolithium reagent (namely *t*BuLi, Table 1, entry 6), no significant difference in the final polymer was observed, probably due to the innocent behavior of the alkyl ligand of the magnesiate complex in the polymerization process. This surprising feature (alkyl anions are generally more nucleophilic than amido ones) may be explained by the hetero-bimetallic nature of the initiating system, with both amido groups acting as bridging ligands between the Mg and Li centers, while the alkyl moiety is mainly chelating the magnesium center.

The peculiarity of our initiating system was further exemplified by several control experiments. Using toluene as the solvent led to uncontrolled polymerization with a broad multimodal molecular weight distribution (Table 1, entry 7). This observation can be ascribed to the higher reactivity induced by the lower stabilizing effect of toluene when compared to THF. Lowering the temperature to -30 °C in toluene or THF did not permit to increase the control on the M_n obtained (Table 1, entries 8&9), as the M_n^{exp} did not match the M_n^{th} . This behavior can be attributed to the presumably slower initiation by the bulky N(TMS)₂ at -30 °C than at room temperature, while propagation steps remained fast: consequently, high molecular weights are quickly obtained. At 50°C, results are similar to those obtained at room temperature in THF (Table 1, entry 10).

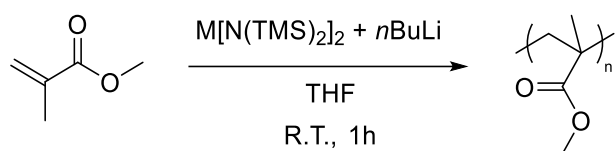
Heterobimetallic LiMg(HMDS)₂*n*Bu did not show tangible stereocontrol on the resulting PMMA, as the triad distribution obtained at room temperature in THF remained largely atactic ($mm = 4\%$, $mr = 32\%$, $rr = 64\%$). Lowering the temperature to -30°C increased the syndiotacticity ($mm = 1\%$, $mr = 18\%$, $rr = 81\%$), while using toluene afforded PMMA with higher isotactic content ($mm = 40\%$,

Chapter 3

$mr = 47\%$, $rr = 13\%$), but poor control on the polymerization process under these conditions prevent their extensive use (Table 1).

The influence of the metallic center was also studied and demonstrated the potential of alkaline earth metals for these polymerization reactions (Table 2). Indeed, calcium gave similar results to those obtained with magnesium (Table 2, entries 1&2). A slight influence of the calcium metal center was observed on tacticity ($mm = 11\%$, $mr = 33\%$, $rr = 56\%$). Zinc and iron were also tested but lacked proper control on the polymerization process (Table 2, entries 3&4). The calcium precursor is however not commercial, so that $\text{Mg}[\text{N}(\text{TMS})_2]_2$ was preferred for the remainder of this study.

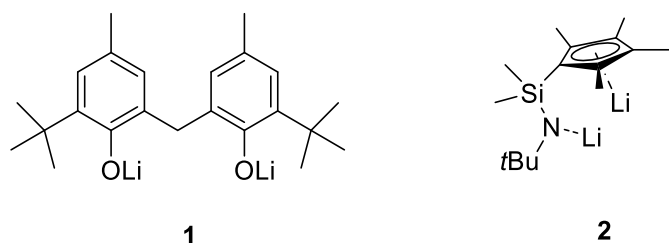
Table 2. Anionic polymerization of MMA with various metallic centers.^[a]



Entry	Metal	Conv. (%)	M_n^{th} (g/mol) ^[b]	M_n^{NMR} (g/mol) ^[c]	M_n^{exp} (g/mol) ^[d]	\bar{D}
1	Mg	83	16 600	10 300	12 200	1.65
2	Ca	72	14 400	9 500	12 900	1.68
3	Zn	14	2 800	12 400	15 100	1.61
4	Fe	22	4 400	23 600	11 700	1.56

^[a] All reactions were performed under argon in a glovebox at room temperature. $[\text{MMA}] = 1 \text{ mol/L}$, 200 equivalent with respect to the catalyst ($[\text{MMA}]/[\text{Cat}] = 200$). Time of reaction: 1h (stopped by addition of MeOH). $\text{Ca}[\text{N}(\text{TMS})_2]_2$ and $\text{Fe}[\text{N}(\text{TMS})_2]_2$ were prepared as THF bis-adduct (see Supporting Information). ^[b] $M_n^{\text{th}} = \text{Eq. of MMA} \times M(\text{MMA}) \times \text{Conv.}$ ^[c] M_n^{NMR} determined by relative integration of the methyl group of MMA (at 1.14, 0.95 and 0.77 ppm) with respect to the trimethylsilyl protons of the initiator at 0.04 ppm. ^[d] M_n^{exp} and \bar{D} of polymer determined by refractive index - size exclusion chromatography calibrated with polystyrene standards in THF at 35°C.

In an attempt to increase the stability of the catalytic active species, two ancillary ligands were then investigated as potential partners to the $\text{Mg}[\text{N}(\text{TMS})_2]_2$ precursor (see Scheme 2). Ligand **1** was obtained *in situ* from the corresponding bisphenol and 2 equivalents of $n\text{BuLi}$.^[25] Its reaction with $\text{Mg}[\text{N}(\text{TMS})_2]_2$ in $\text{THF-}d_8$ seemed to give rise to the expected Schlenk equilibrium (Figure S3).



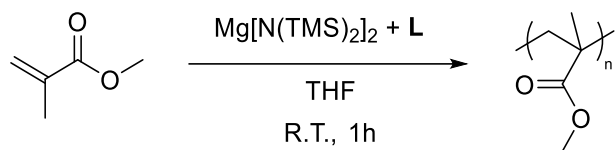
Scheme 2. Ligands used in combination with $\text{Mg}[\text{N}(\text{TMS})_2]_2$ for MMA polymerization.

Notably, the protons of the methylene bridge are equivalent in the free phenol and bis(lithium) forms but appear as two distinct doublets ($J_{H-H} = 13.4$ Hz, characteristic of geminal protons) upon addition of $\text{Mg}[\text{N}(\text{TMS})_2]_2$, probably due to a conformational adaptation of the ligand around the magnesium center. Two broad signals are also observed in the region of the trimethylsilyl protons (one at -0.02 ppm, the other at -0.16 ppm), which is similar to the Schlenk equilibrium observed with $\text{LiMg}[\text{N}(\text{TMS})_2]_2n\text{Bu}$. Remarkably, ligand **2** seemed to lead to only one main product when reacted with $\text{Mg}[\text{N}(\text{TMS})_2]_2$, supposedly due to higher steric hindrance around the Mg center, which would prevent the formation of the homoleptic complex bearing two ligands **2** (Figure S4).

The two catalytic systems were then tested for the room temperature anionic polymerization of MMA (Table 3). Surprisingly, the magnesiate complex obtained from **1** and $\text{Mg}[\text{N}(\text{TMS})_2]_2$ was less efficient in converting MMA than $\text{LiMg}[\text{N}(\text{TMS})_2]_2n\text{Bu}$ (Table 3, entries 1&2). Also noteworthy is the fact that despite having a Schlenk equilibrium in solution, M_n^{exp} is very close to M_n^{th} , which means that half of the amido groups actually initiated the polymerization process (one per magnesium atom). It can be hypothesized that the Schlenk equilibrium is displaced during the reaction with MMA. The

Chapter 3

use of ligand **2** with $\text{Mg}[\text{N}(\text{TMS})_2]_2$ permitted to convert quantitatively 100 equivalents of MMA, but its productivity decreased when using 200 equivalents (Table 3, entries 3&4).^[32]

Table 3. Anionic polymerization of MMA with two ancillary ligands **L**.^[a]

Entry	Ligand L	[MMA]/[Cat.]	Conv. (%)	M_n^{th} (g/mol) ^[b]	M_n^{NMR} (g/mol) ^[c]	M_n^{exp} (g/mol) ^[d]	\bar{D}
1	1	100	82	8 200	5 700	8 800	1.60
2	1	200	53	10 600	9 000	11 600	1.62
3	2	100	98	9 800	7 200	7 800	1.65
4	2	200	82	16 400	10 700	10 800	1.61

^[a] All reactions were performed under argon in a glovebox at room temperature. [MMA] = 1 mol/L. Time of reaction: 1h (stopped by addition of MeOH). ^[b] $M_n^{\text{th}} = \text{Eq. of MMA} \times \text{M(MMA)} \times \text{Conv.}$ ^[c] M_n^{NMR} determined by relative integration of the methyl group of MMA (at 1.14, 0.95 and 0.77 ppm) with respect to the trimethylsilyl protons of the initiator at 0.04 ppm. ^[d] M_n^{exp} and \bar{D} of polymer determined by refractive index - size exclusion chromatography calibrated with polystyrene standards in THF at 35°C.

Finally, to illustrate the versatility of our system, $\text{LiMg}[\text{N}(\text{TMS})_2]_2n\text{Bu}$ was used to initiate the ring-opening polymerization of *rac*-lactide. At room temperature, in THF (0.5 mol/L), the catalyst formed *in situ* could convert 88% of the 100 equivalents of *rac*-lactide it was reacted with within 5 hours. A monomodal distribution of molar masses was obtained, and the M_n value increased linearly with conversion (Figure S5), confirming the control on the polymerization process. The polymer obtained was essentially atactic ($P_m = 0.43$, determined from the methine region of the homonuclear CH_3 -decoupled ^1H NMR spectrum). We then hypothesized that the enolate formed during the polymerization of MMA could also initiate the ring-opening polymerization of *rac*-lactide. First, anionic polymerization of 50 equivalents of MMA was initiated by *in situ* formed

Chapter 3

LiMg[N(TMS)₂]₂nBu in THF at room temperature. Then, *rac*-lactide was added to the reaction solution at room temperature and the resulting PMMA macroinitiator was found to be remarkably efficient for *rac*-lactide polymerization, as already 96% of monomers were converted after 1h (Figure 4, enolates and alkoxides are indeed known to be more efficient than amido groups for initiating ring-opening polymerization of lactones).^[33] The formation of a block copolymer of PMMA and PLA was further confirmed by size exclusion chromatography (Figure 4): the monomodal distribution was shifted to higher molar masses after addition of *rac*-lactide. As already observed by Mehrkhodavandi,^[33b] differential scanning calorimetry of our copolymer revealed only one glass transition at 46°C, corresponding to the PLA block.

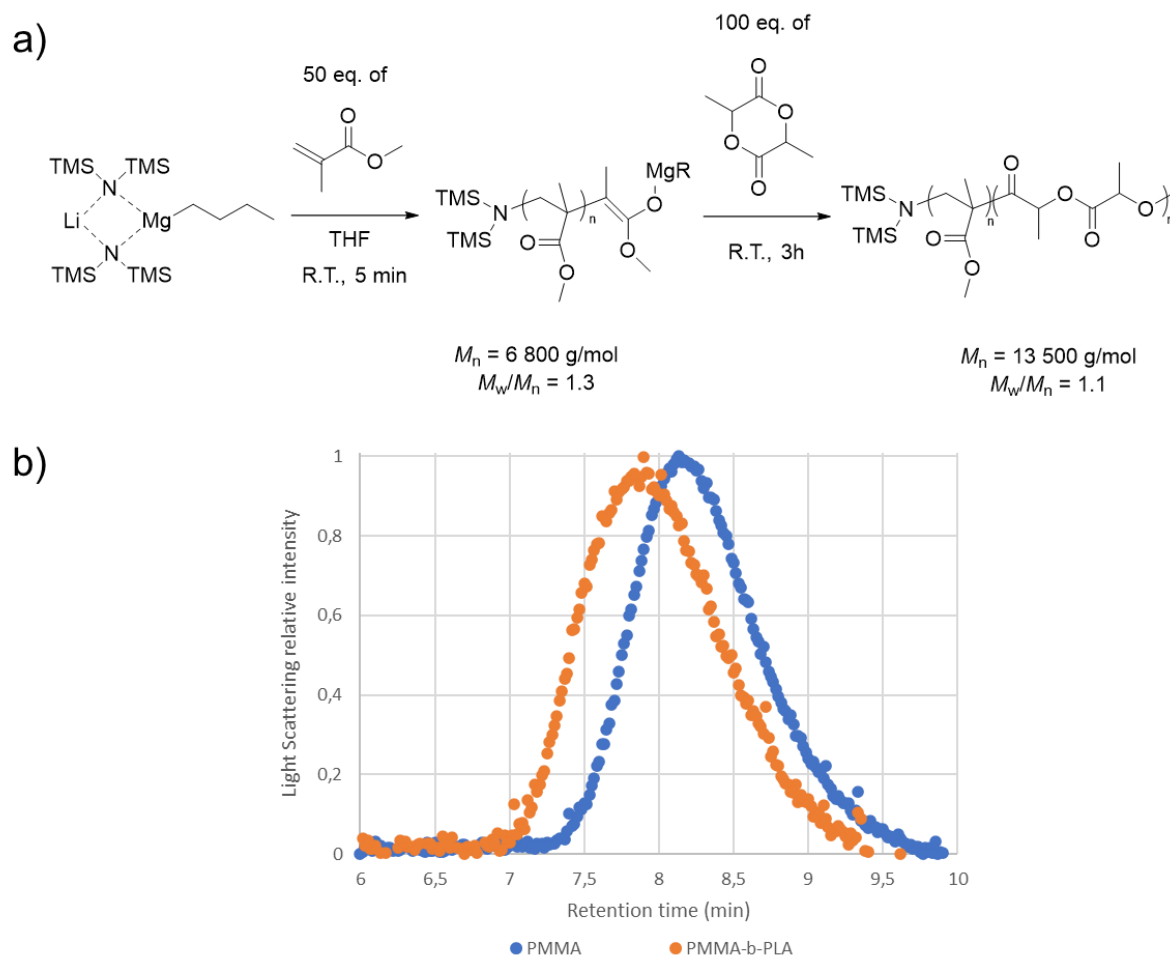


Figure 4. Scheme of the PMMA-*b*-PLA block polymer synthesis (a) and comparison of the SEC-LS traces before and after addition of *rac*-lactide (b).

Conclusion

A simple methodology for the polymerization of MMA at room temperature has been developed. By taking advantage of the stability and high activity of the ate complexes formed *in situ* from commercial reagents, it is possible to prepare polymers of controlled molar masses within minutes. Our investigations showed that the temperature, solvent, metal center and ligand chosen all have an impact on the reactivity of the catalytic system. Promising results were obtained at room temperature in THF, using a magnesiate complex bearing simple ligands. Notably, this catalyst also initiated the ring-opening polymerization of *rac*-lactide, and block copolymers of PMMA and PLA were even accessible using this unprecedented methodology. Our future efforts will be oriented towards the polymerization of other biobased monomers, as well as further study of the reaction mechanism.

Experimental section

Materials and methods

All manipulations requiring dry atmosphere were performed under a purified argon atmosphere using standard Schlenk techniques in a glovebox. Solvents for synthesis (toluene, THF) were freshly distilled from Na/benzophenone under argon and degassed thoroughly by freeze-thaw-vacuum cycles prior to use. Deuterated chloroform (99.5% D, Eurisotop) was used as received. THF-*d*₈ (99.5% D, Eurisotop) and toluene-*d*₈ (99.5% D, Eurisotop) were freshly distilled from Na/benzophenone under argon and degassed thoroughly by freeze-thaw-vacuum cycles prior to use. Methylmethacrylate (99%) from Sigma-Aldrich was dried over CaH₂ and distilled twice before being degassed thoroughly by freeze-thaw-vacuum cycles. *rac*-Lactide from Corbion Purac was purified by recrystallization in dry isopropanol and toluene followed by sublimation and was stored in the glovebox prior to use. *n*BuLi (2.0 mol/L solution in cyclohexane) and *t*BuLi (2.56 mol/L solution in heptane) from Sigma-Aldrich were titrated using diphenylacetic acid (99%, Sigma-Aldrich, recrystallized from toluene) in dry THF

and used as received. $\text{Mg}[\text{N}(\text{TMS})_2]_2$ (97%, Sigma-Aldrich) was recrystallized from dry toluene. 2,2'-Methylenebis(6-*tert*-butyl-4-methylphenol) (99%, TCI Chemicals) was recrystallized from boiling *n*-hexane and washed twice with cold *n*-pentane. The constrained geometry ligand **2** was prepared as previously reported in the literature.^[34]

Measurements

NMR spectra were recorded on Bruker Avance-400 and Avance-Neo 500 spectrometers at Chimie ParisTech. ^1H and ^{13}C chemical shifts are reported in ppm versus SiMe_4 and were determined by reference to the residual solvent peaks for ^1H and ^{13}C NMR. Assignment of signals was made from multinuclear 1D (^1H , $^{13}\text{C}\{^1\text{H}\}$) and 2D (COSY, HMQC, HMBC) NMR experiments. Size exclusion chromatography (SEC) of polymers was performed in THF at 35 °C using an Agilent 1260 Infinity Series GPC (ResiPore 3 μm , 300 x 7.5 mm, 1.0 mL/min, RI (PL-GPC 220) and Light scattering detectors) at Chimie ParisTech. When using the RI detector, the number average molecular masses (M_n) and polydispersity index (\mathcal{D}) of the polymers were calculated with reference to a universal calibration vs. polystyrene standards (limits $M_w = 200$ to 400,000 g/mol). Calorimetric measurements were performed using a Discovery DSC25 from TA instruments, under a nitrogen flow, calibrated with Indium.

MMA polymerization procedure

Inside the glovebox, a stock solution of the desired catalyst in the selected dry solvent is prepared (*e.g.* 4 mL of dry THF is added to $\text{Mg}[\text{N}(\text{TMS})_2]_2$, 34.5 mg, 100 μmol , then put into a freezer for 15 minutes. A precise volume of a 2.0 mol/L *n*BuLi solution in cyclohexane, 50 μL , 100 μmol , is then added dropwise and allowed to stabilize for 30 minutes at room temperature). A precise amount of this stock solution is added to a dry Schlenk tube (*e.g.* 380 μL , 9.4 μmol , for a 1 mol% catalyst loading) and some dry THF is added to reach 0.84 mL. MMA, 100 μL , 940 μmol is then added quickly at room temperature. When the desired time of reaction is reached, small drops of methanol are added

to stop the propagation. Volatiles (solvent and unreacted MMA) are evaporated under vacuum. The final polymer was purified by dissolving it in the minimum amount of CH_2Cl_2 and precipitation in cold MeOH. As it was observed that this purification method led to the loss of smaller oligomers, M_n and D were estimated on the crude polymer mixture, unless stated otherwise.

PMMA-*b*-PLA synthesis

Inside the glovebox, a stock solution of the desired catalyst in the selected dry solvent is prepared (see MMA polymerization procedure). A precise amount of MMA is first added to a dry Schlenk tube (*e.g.* 25 mg, 250 μmol) and some dry THF is added to reach 0.3 mL. A precise amount of the stock solution (*e.g.* 200 μL for 5 μmol of catalyst) is then added quickly at room temperature. After 5 minutes of reaction, a small aliquot is taken for NMR and SEC characterizations. Then, a solution of *rac*-lactide (72 mg, 500 μmol) in dry THF (0.5 mL) is added to the reaction mixture and stirred at room temperature. When the desired time of reaction is reached, the reaction medium is exposed to air to stop the propagation. Volatiles (solvent and unreacted MMA) are evaporated under vacuum. The final polymer was purified by dissolving it in the minimum amount of CH_2Cl_2 and precipitation in cold Et_2O /pentane (1:1 solution).

Acknowledgements

Chimie ParisTech – PSL and CNRS are thanked for financial support. H.F. acknowledges financial support from École polytechnique (AMX) for his PhD scholarship. Île-de-France Region is gratefully acknowledged for financial support of 500 MHz NMR spectrometer of Chimie ParisTech in the framework of the SESAME equipment project (n°16016326). CMT is grateful to the Institut Universitaire de France.

References

- [1] U. Ali, K. J. Bt. A. Karim, N. A. Buang, *Polym. Rev.* **2015**, *55*, 678–705.
- [2] M. Zuber, S. Tabasum, T. Jamil, M. Shahid, R. Hussain, K. S. Feras, K. P. Bhatti, *J. Appl. Polym. Sci.* **2014**, *131*, 39806.
- [3] X. Liu, J. Krücker, G. Zheng, D. W. Schubert, *ACS Appl. Mater. Inter.* **2013**, *5*, 8857–8860.
- [4] Y. Hwang, Y. Je, D. Farrar, J. E. West, S. M. Yu, W. Moon, *Polymer* **2011**, *52*, 2723–2728.
- [5] See for instance: a) H. Fouilloux, C. M. Thomas, *Macromol. Rapid Commun.* 2021, *42*, 2000530. b) H. Fouilloux, W. Qiang, C. Robert, V. Placet, C. M. Thomas, *Angew. Chem., Int. Ed.* 2021, *60*, 19374–19382. [6] D. Baskaran, A. H. E. Müller, in *Polymer Science: A Comprehensive Reference*, Elsevier, **2012**, pp. 623–655.
- [7] N. Hadjichristidis, A. Hiraio, Eds., *Anionic Polymerization: Principles, Practice, Strength, Consequences and Applications*, Springer Japan, Tokyo, **2015**.
- [8] G. Wittig, *Angew. Chem.* **1958**, *70*, 65–71.
- [9] J. A. Wanklyn, *Ann. Chem. Pharm.* **1858**, *108*, 67–79.
- [10] G. Wittig, F. J. Meyer, G. Lange, *Justus Liebigs Ann. Chem.* **1951**, *571*, 167–201.
- [11] R. E. Mulvey, S. D. Robertson, in *Organo-Di-Metallic Compounds (or Reagents)* (Ed.: Z. Xi), Springer International Publishing, Cham, **2013**, pp. 129–158.
- [12] T. Iida, T. Wada, K. Tomimoto, T. Mase, *Tetrahedron Lett.* **2001**, *42*, 4841.
- [13] A. Inoue, K. Kitagawa, H. Shinokubo, K. Oshima, *J. Org. Chem.* **2001**, *66*, 4333.
- [14] S. Dumouchel, F. Mongin, F. Trécourt, G. Quéguigner, *Tetrahedron* **2003**, *59*, 8629.
- [15] M. Uchiyama, T. Furuyama, M. Kobayashi, Y. Matsumoto, K. Tanaka, *J. Am. Chem. Soc.* **2006**, *128*, 8404.
- [16] T. Furuyama, M. Yonehara, S. Arimoto, M. Kobayashi, Y. Matsumoto, M. Uchiyama, *Chem. Eur. J.* **2008**, *14*, 10348.
- [17] N. T. T. Chau, M. Meyer, S. Komagawa, F. Chevallier, Y. Fort, M. Uchiyama, F. Mongin, P. C. Gros, *Chem. Eur. J.* **2010**, *16*, 12425.
- [18] R. E. Mulvey, S. D. Robertson, in *Alkaline-Earth Metal Compounds* (Ed.: S. Harder), Springer Berlin Heidelberg, Berlin, Heidelberg, **2013**, pp. 103–139.
- [19] A. J. Martínez-Martínez, C. T. O'Hara, in *Advances in Organometallic Chemistry*, Elsevier, **2016**, pp. 1–46.
- [20] D. Tilly, F. Chevallier, F. Mongin, P. C. Gros, *Chem. Rev.* **2014**, *114*, 1207–1257.
- [21] C.-C. Lin, M.-L. Hsueh, B.-T. Ko, T. Athar, T.-M. Wu, S.-F. Hsu, *Organometallics* **2006**, *25*, 4144–4149.

- [22] G. W. Honeyman, A. R. Kennedy, R. E. Mulvey, D. C. Sherrington, *Organometallics* **2004**, *23*, 1197–1199.
- [23] E. Ihara, N. Omura, T. Itoh, K. Inoue, *J. Organomet. Chem.* **2007**, *692*, 698–704.
- [24] S. Kawaguchi, E. Nomura, K. Ito, *Polym. J.* **1998**, *30*, 546–551.
- [25] J. Char, E. Brulé, P. C. Gros, M.-N. Rager, V. Guérineau, C. M. Thomas, *J. Organomet. Chem.* **2015**, *796*, 47–52.
- [26] J. Char, O. G. Kulyk, E. Brulé, F. de Montigny, V. Guérineau, T. Roisnel, M. J.-L. Tschan, C. M. Thomas, *C. R. Chimie* **2016**, *19*, 167-172.
- [27] C. Robert, T. E. Schmid, V. Richard, P. Haquette, S. K. Raman, M.-N. Rager, R. M. Gauvin, Y. Morin, X. Trivelli, V. Guérineau, I. del Rosal, L. Maron, C. M. Thomas, *J. Am. Chem. Soc.* **2017**, *139*, 6217–6225.
- [28] P. C. Andrikopoulos, D. R. Armstrong, A. R. Kennedy, R. E. Mulvey, C. T. O'Hara, R. B. Rowlings, S. Weatherstone, *Inorg. Chim. Acta* **2007**, *360*, 1370–1375.
- [29] D. J. Liptrot, M. S. Hill, M. F. Mahon, *Chem. Eur. J.* **2014**, *20*, 9871–9874.
- [30] S. A. Couper, R. E. Mulvey, D. C. Sherrington, *Eur. Polym. J.* **1998**, *34*, 1877–1887.
- [31] L. J. Bole, N. R. Judge, E. Hevia, *Angew. Chem. Int. Ed.* **2021**, *60*, 7626–7631.
- [32] B. Lian, C. M. Thomas, C. Navarro, J.-F. Carpentier, *Organometallics* **2007**, *26*, 187–195.
- [33] a) M. J.-L. Tschan, R. M. Gauvin, C. M. Thomas, *Chem. Soc. Rev.* **2021**, *50*, 13587-13608. b) H.-J. Jung, I. Yu, K. Nyamayaro, P. Mehrkhodavandi, *ACS Catal.* **2020**, *10*, 6488–6496.
- [34] Stevens, J. C.; Timmers, F. J.; Rosen, G.; Knight, G. W.; Lai, S. Y. (Dow Chemical Co.) *Eur. Pat. App.*, EP 0416815 A2, 1991.

Chapter 3 – Supporting Information

Table of contents:

Figure S1	261
Figure S2	262
Figure S3	263
Figure S4	263
Figure S5	264
NMR characterization data of catalysts and polymers	265

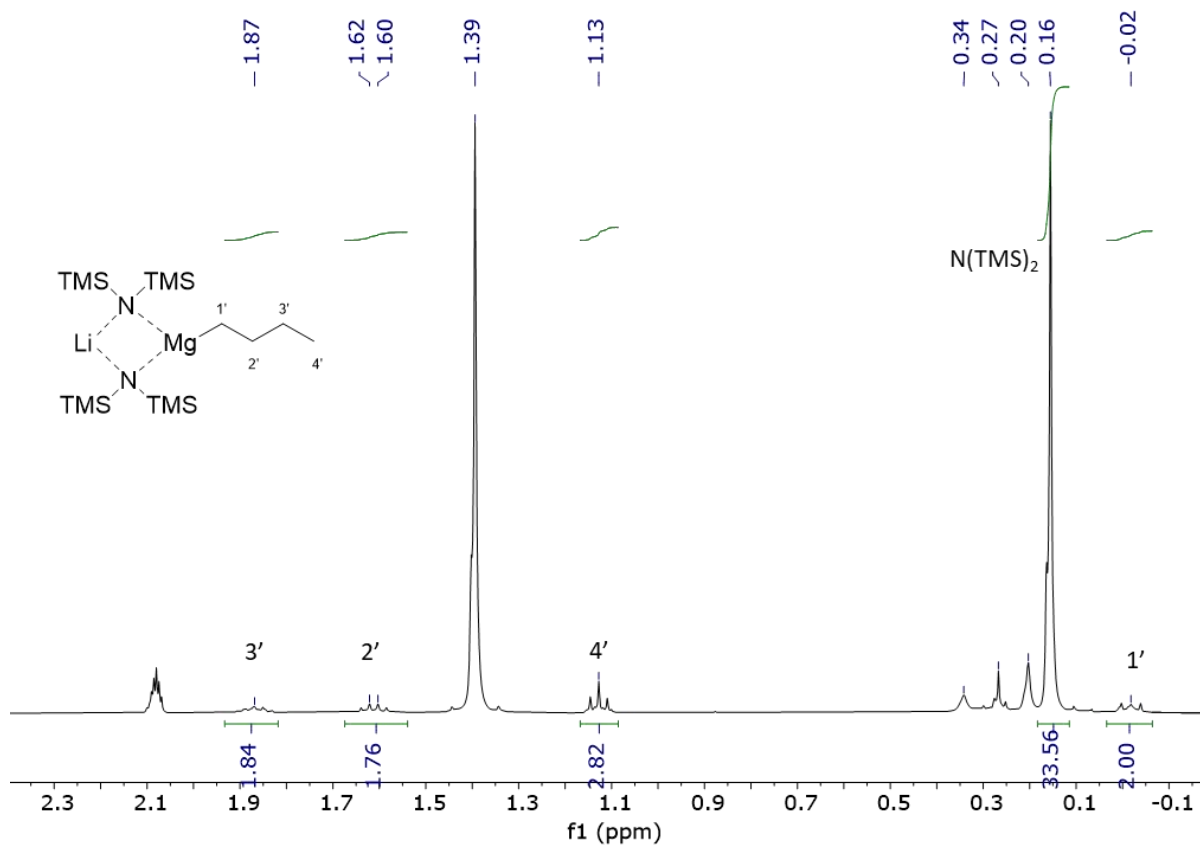


Figure S1. ^1H NMR spectrum of $\text{LiMg}(\text{N}(\text{TMS})_2)_2n\text{Bu}$ in $\text{toluene-}d_8$ (400 MHz).

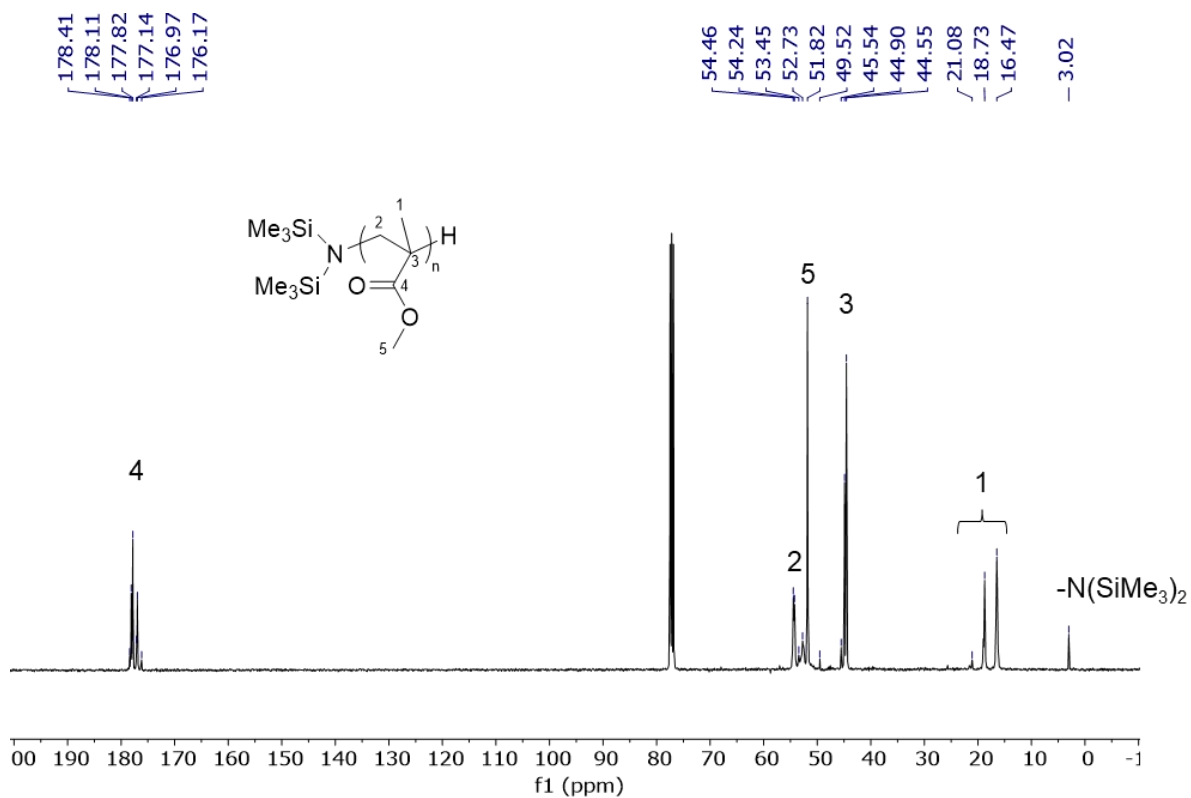


Figure S2. ^{13}C NMR spectrum after purification of PMMA obtained by polymerization initiated by $\text{LiMg}(\text{HMDS})_2n\text{Bu}$ at room temperature (Table 1, entry 5).

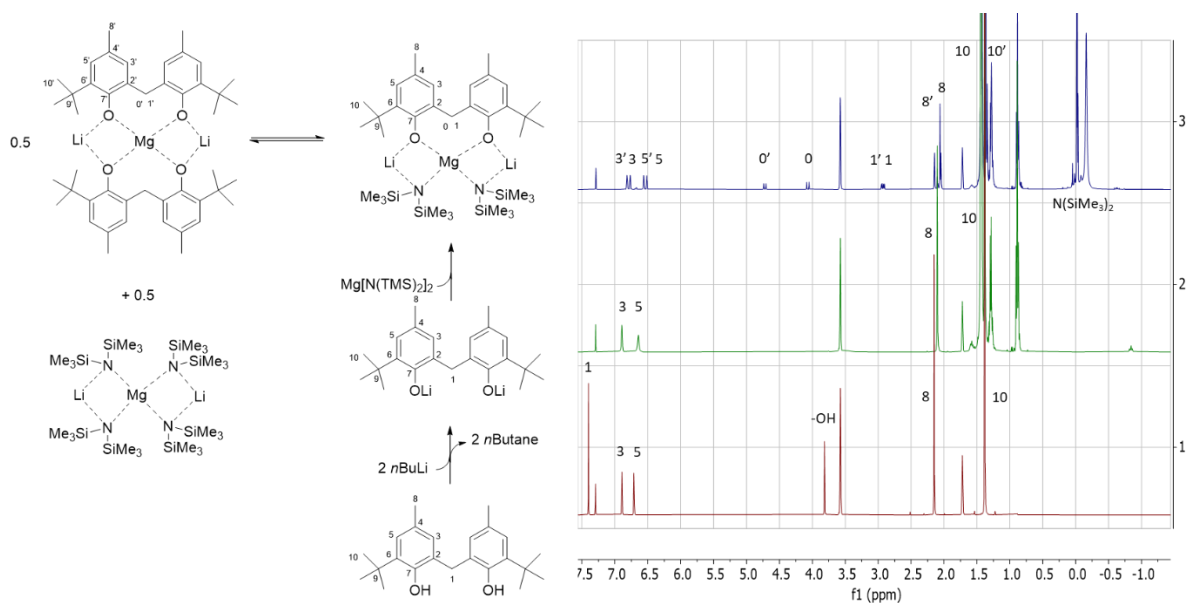


Figure S3. ^1H NMR spectrum ($\text{THF-}d_8$, 400 MHz) evolution of the methylene-bridged bis(aryloxo) ligand after addition of 2 $n\text{BuLi}$ and $\text{Mg}[\text{N}(\text{TMS})_2]_2$, and the hypothesized structures observed.

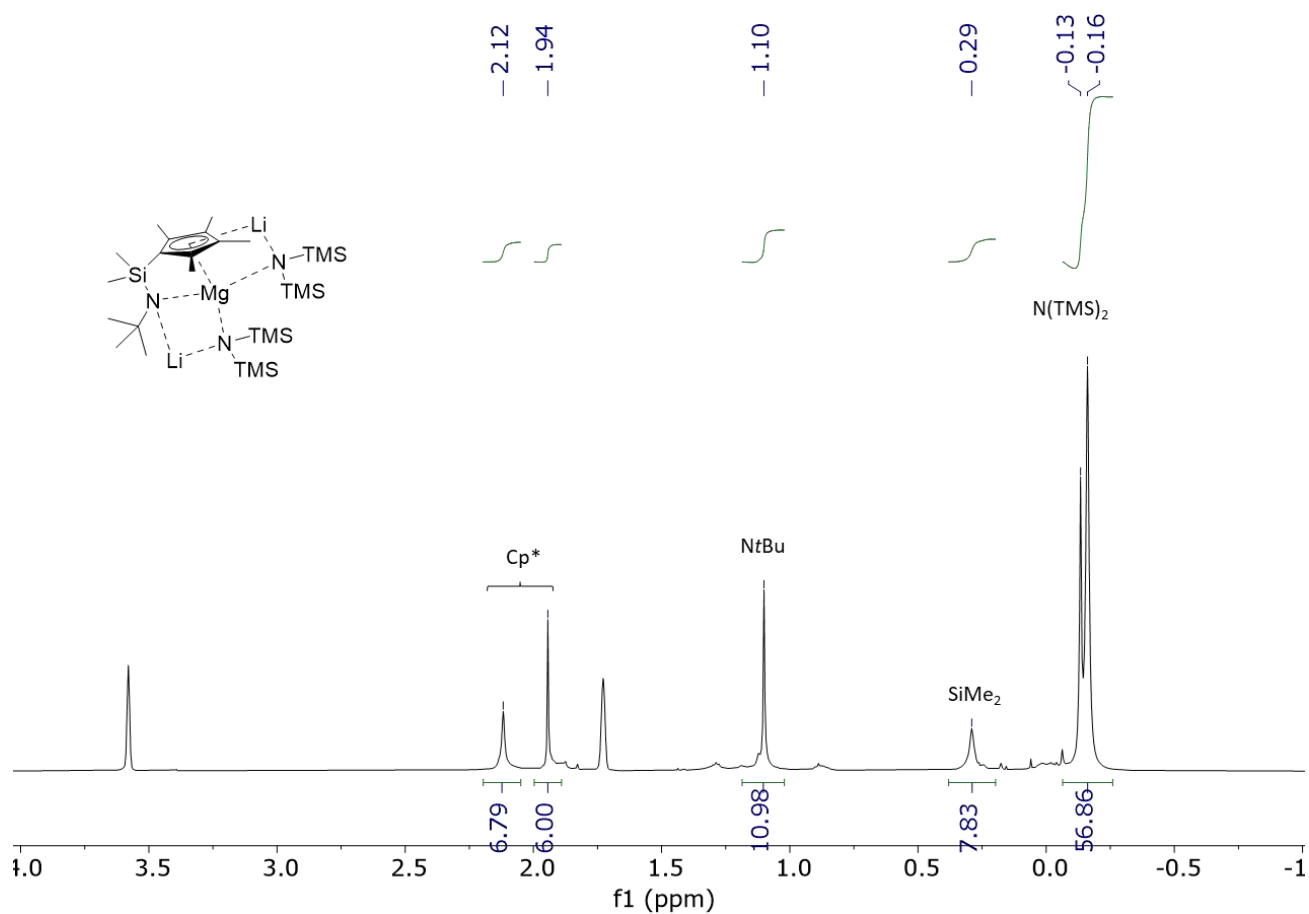


Figure S4. ^1H NMR spectrum ($\text{THF-}d_8$, 400 MHz) of the product formed by reacting $\text{Mg}[\text{N}(\text{TMS})_2]_2$ and ligand **2**.

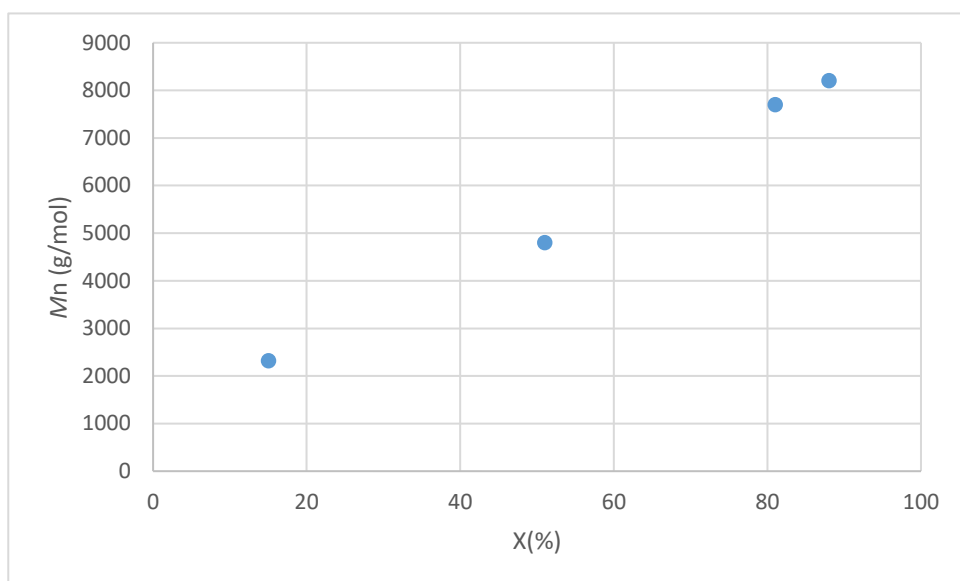
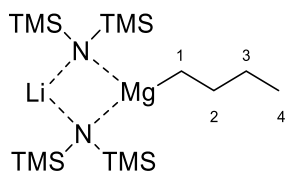


Figure S5. Evolution of the M_n value (corrected by the Mark Houwink factor for PLA : 0.58) as a function of monomer conversion during the polymerization of *rac*-lactide by $\text{LiMg}(\text{N}(\text{TMS})_2)_2n\text{Bu}$ formed *in situ*.

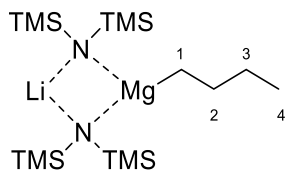
NMR characterization data of catalysts and polymers

LiMg[N(TMS)₂]₂*n*Bu in THF-*d*₈



Group	¹ H NMR (δ ppm)	¹³ C{ ¹ H} NMR (δ ppm)
1	-0.62	8.2
2	1.22	32.5
3	1.56	34.0
4	0.88	14.8
-N(TMS) ₂	-0.02	6.6

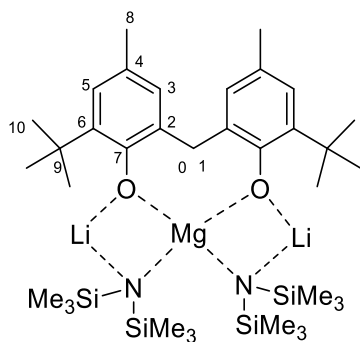
LiMg[N(TMS)₂]₂*n*Bu in toluene-*d*₈



Group	¹ H NMR (δ ppm)
1	-0.02
2	1.61
3	1.87
4	1.13
-N(TMS) ₂	0.16

Chapter 3

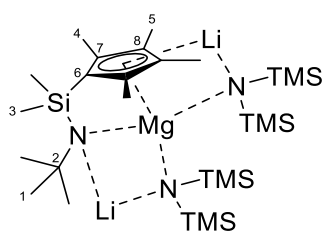
Mg[N(TMS)₂]₂ + **1** in THF-*d*₈



Group	¹ H NMR (δ ppm)	¹³ C{ ¹ H} NMR (δ ppm)
0	4.07	35.3
1	2.92	35.3
2	-	129.0
3	6.77	124.0
4	-	132.2
5	6.52	117.2
6	-	135.9
7	-	160.6
8	2.06	21.4
9	-	34.3
10	1.36	30.7
-N(TMS) ₂	-0.02	6.5

Chapter 3

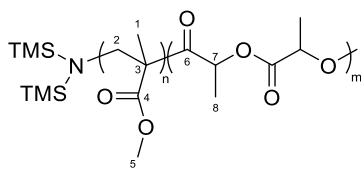
Mg[N(TMS)₂]₂ + **2** in THF-*d*₈



Group	¹ H NMR (δ ppm)	¹³ C{ ¹ H} NMR (δ ppm)
1	1.10	37.9
2	-	51.3
3	0.29	8.8
4	1.94	12.0
5	2.12	15.0
6	-	116.2
7	-	114.0
8	-	108.8
-N(TMS) ₂	-0.13 ; -0.16	5.9 ; 5.7

Chapter 3

PMMA-*b*-PLA in CDCl₃



Group	¹ H NMR (δ ppm)	¹³ C{ ¹ H} NMR (δ ppm)
1	1.20 ; 1.04 ; 0.87	20.0 to 18.8
2	1.99 to 1.83	54.5
3	-	45.0 ; 44.7
4	-	178.2 ; 177.9
5	3.61	51.9
6	-	169.8 to 169.2
7	5.26 to 5.14	69.5 to 69.1
8	1.61 to 1.54	16.9 to 16.7
-N(TMS) ₂	0.13 ; 0.12	3.2

Chapter 4 – Highly Efficient Synthesis of Poly(silylether)s: Access to Degradable Polymers from Renewable Resources

Hugo Fouilloux,^a Marie-Noelle Rager,^a Pablo Ríos,^b Salvador Conejero^{b,*} & Christophe M.

Thomas^{a,*}

^a Chimie ParisTech, PSL University, CNRS, Institut de Recherche de Chimie Paris, 75005 Paris, France.

E-mail: christophe.thomas@chimie-paristech.fr

^b Instituto de Investigaciones Químicas (IIQ), Departamento de Química Inorgánica, Centro de Innovación en Química Avanzada (ORFEO-CINCA), CSIC and Universidad de Sevilla, Avda. Américo Vespucio 49, 41092 Sevilla, Spain

This chapter has been accepted for publication in *Angewandte Chemie International Edition*:

H. Fouilloux, M.-N. Rager, P. Ríos, S. Conejero, C. M. Thomas, *Angew. Chem. Int. Ed.* **2021**, DOI: 10.1002/anie.202113443.

Contributions to the publication:

H. F. and P. R. performed the experiments. H. F. and M.-N. R. performed the NMR analysis. H. F., S. C. and C. M. T. analyzed the data and wrote the paper. All authors discussed the results and commented on the manuscript.

Hugo Fouilloux



30/12/2021

Christophe M. Thomas



Abstract

The design of new materials with tunable properties and intrinsic recyclability, derived from biomass under mild conditions, stands as a gold standard in polymer chemistry. Reported herein are platinum complexes which catalyze the formation of poly(silylether)s (PSEs) at low catalyst loadings. These polymers are directly obtained from dual-functional biobased building blocks such as 5-hydroxymethylfurfural (HMF) or vanillin, coupled with various dihydrosilanes. Access to different types of copolymer architectures (statistical or alternating) is highlighted by several synthetic strategies. The materials obtained were then characterized as low T_g materials (ranging from -60 to 29°C), stable upon heating ($T_{5\%}$ up to 301°C) and resistant towards uncatalyzed methanolysis. Additionally, quantitative chemical recycling of several PSEs could be triggered by acid-catalyzed hydrolysis or methanolysis. These results emphasize the interest of biobased poly(silylether)s as sustainable materials with high recycling potential.

Introduction

Fossil feedstocks, especially crude oil, represent the most important raw materials for the chemical industry.^[1] For almost half a century, however, various oil crises have affected the global crude oil market and have coincided with the emergence of alternative raw materials such as biomass.^[2] As such, the development of new methods for converting biomass into resources suitable for polymer production is a crucial hurdle on the road to a more sustainable chemical economy. Although nearly all polymers can be prepared from renewable feedstocks, the main challenge remains to design efficient and selective transformations of abundant, renewable and inexpensive feedstocks into innovative polymers.^[3] The disposal of plastics, which are generally designed to be robust and durable, is also a 21st century environmental challenge. Indeed, the amount of plastic waste residing either in landfills or in the natural environment exceeds all living biomass. Recycling processes have the potential to facilitate the transition of economies to a greener and more sustainable model. Unlike

mechanical recycling, chemical recycling preserves the quality of the recycled product, allowing depolymerization into monomer or conversion into other useful chemicals.^[4] It is therefore important to design and synthesize polymers that can be degraded under mild conditions, directly into their own starting materials.

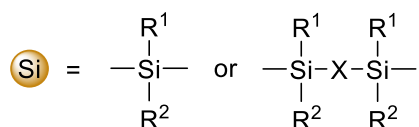
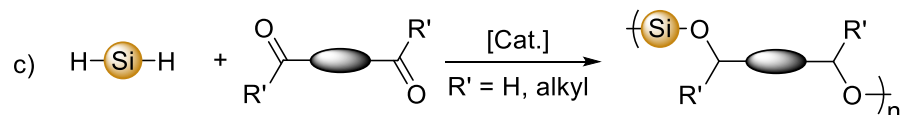
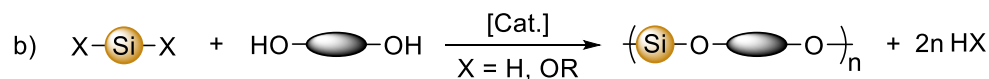
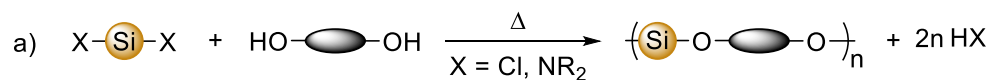
Poly(silylether)s are an intriguing class of polymers, due to the Si-O-C linkage of their backbone. This peculiar linkage confers a certain degradability to these materials, as the Si-O-C bonds are sensitive to acidic and basic hydrolysis or alcoholysis.^[5] Robust materials can however be obtained using bulky substituents around the silylether bond. Poly(silylether)s have therefore been considered for various applications in the aerospace industry,^[6] as CO₂-philic^[7] or enantioselective membranes,^[8] for the preparation of dielectric^[9] or fluorescent materials,^[10] as reprocessable thermosets^[11] or as drug carriers.^[12] Although their degradation in various media is often reported, these polymers are not considered as biodegradable, because only few microorganisms in the environment metabolize silicon. The impact of silicon-containing polymers on the environment is in fact rarely studied.^[13] The metabolites of hydrolytic cleavage of silyl ethers, (*i.e.*, alcohols and silanols, and ultimately SiO₂), are, however, considered rather benign. To the best of our knowledge, the chemical recycling of PSEs has never been reported.

The synthesis of PSEs was first envisioned *via* the polycondensation of diols with dichlorosilanes, yielding HCl as the only by-product (Figure 1a).^[14] Although the availability of dichlorosilanes obtained *via* the Rochow process is an advantage,^[15] this approach remains inefficient for accessing high molar mass polymers.^[12e,16] Another popular route to obtain poly(silylether)s is the polycondensation of diols with diaminosilanes, usually *via* a melt polymerization process (Figure 1a).^[6,17] However, in addition to the high temperatures, this procedure requires the preparation of diaminosilane from the corresponding dichlorosilane.^[18] Dialkoxysilanes have also been investigated as comonomers in combination with diols for PSEs synthesis (Figure 1b).^[14] Lithium, sodium and potassium salts, as well as Brønsted acids, catalyze this reaction that generates volatile alcohols as by-

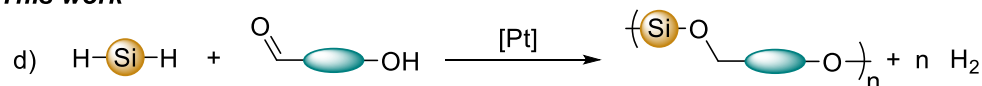
products.^[17b,19] Although noteworthy improvements were realized with dihydrosilanes and different comonomers to produce PSEs of various architectures, use of renewable materials by this approach is rare (Figures 1b & 1c).^[5,8,10a,20] In this regard, promising results were obtained by copolymerizing dihydrosilanes with difunctional hydroxyaldehyde monomers (Figure 1d). This method seems particularly relevant for the conversion of platform molecules derived from bioresources, such as 5-hydroxymethylfurfural, in a few steps.^[21]

In this work, we investigated the polycondensation of dihydrosilanes with renewable hydroxyaldehydes, seeking to address the following challenges: 1) achieve copolymerization with highly active catalysts at low loadings (ppm range) under mild conditions; 2) extend the scope of comonomers using platform molecules easily accessible from biomass such as vanillin, and less activated silanes such as dialkylsilanes (diphenylsilane is usually preferred as it is more reactive); 3) set the ground for studying the chemical recyclability of PSEs, by investigating the degradation of these polymers under different conditions. Indeed, varying the chemical environments around the Si-O-C linkages by controlled copolymerization should allow modulating different physicochemical properties, including degradability. To achieve these tasks, the highly reactive $B(C_6F_5)_3$ is not sufficiently tolerant to various functional groups,^[5b,20t] such as furan rings,^[21b] or ethers.^[22] In contrast, platinum-based complexes that are widely used in the silicon-based polymer industry (including the well-known Karstedt's catalyst for hydrosilylation reactions),^[23] have never been applied to the synthesis of poly(silylether)s. Unlike other types of already used catalysts, these Pt-based complexes are generally much more robust and tolerant, and therefore suitable for bioresource functionalization. Taking into account recent developments in our laboratories, namely the catalytic synthesis of renewable polymers,^[24] and the development of well-defined platinum complexes for catalytic applications,^[25] we set out to jointly capitalize^[25] on these advances to make poly(silylether)s by polycondensation of dihydrosilanes with biosourced hydroxyaldehydes. Here we describe the initial results of our studies.

Previous works



This work



- ✓ **Highly active catalysts at low loadings**
- ✓ **Various hydrosilanes and biobased hydroxyaldehydes**
- ✓ **Chemical recycling *via* acid-catalyzed hydrolysis or methanolysis**

Figure 1. Various synthetic strategies for poly(silylether)s preparation and the methodology developed in this work.

Results and Discussion

Our attention was drawn to the two different Pt^{II} complexes whose structures are presented in Figure 2. [Pt]_{tBu} has previously been reported,^[25a] while [Pt]_{Me} synthesis is described in the Supporting Information (Figures S1 to S6). The former complex is a bulky cyclometalated precursor which can be converted into a non-cyclometalated active species upon oxidative addition of dihydrosilanes, such as Et₂SiH₂,^[25e,26] whereas [Pt]_{Me} has less sterically hindered *N*-heterocyclic carbene (NHC) ligands and a more stable platinum-silicon bond that is less easily displaced in the presence of excess of Et₂SiH₂.^[27] Therefore, a different reactivity can be expected for these two complexes.

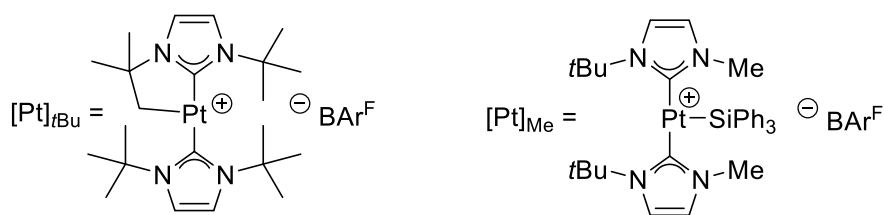
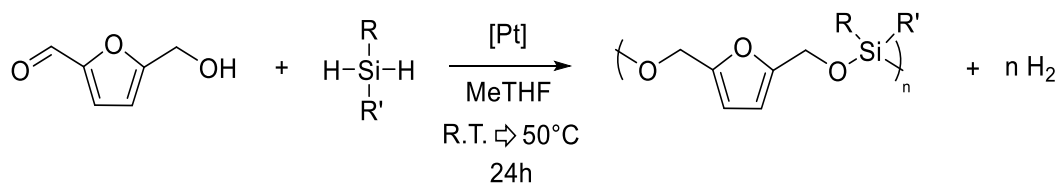


Figure 2. Structures of the Pt^{II} complexes used in this study.

The first results obtained for the polymerization of HMF with various dihydrosilanes are presented in Table 1. The solvent, methyl tetrahydrofuran (MeTHF), was selected as a green alternative to tetrahydrofuran (THF). THF has also already been observed to bind reversibly to the platinum atom of our catalyst,^[25d] thereby slowing down the rates of reaction. The coordination of the bulkier MeTHF is more difficult, so that the [Pt] catalyst is more reactive in that solvent. The reaction medium was kept at room temperature for 20h and heated to 50°C under static vacuum for 4 additional hours. Under these mild conditions, a catalytic loading of 500 ppm of [Pt]_{Me} was found to be sufficient to catalyze the copolymerization of HMF with MePhSiH₂ and achieve satisfying molar masses and isolated yields (Table 1, entry 1). The expected poly(silylether) was characterized by NMR and FT-IR spectroscopies (Figure 3). Notably, the complete disappearance of the aldehyde (9.56 ppm in ¹H NMR, 1670 cm⁻¹ in FT-IR) and alcohol (2.74 ppm in ¹H NMR, 3360 cm⁻¹ in FT-IR) functions of HMF and of the Si-H (4.37 ppm in ¹H NMR, 2130 cm⁻¹ in FT-IR) function of MePhSiH₂ were observed. In addition, the final polymer exhibits a symmetric structure confirmed by the appearance of a single peak for the furanic protons at 6.22 ppm in ¹H NMR and the formation of the Si-O-C linkage is observed at around 1200 cm⁻¹ in FT-IR.^[21a] The protons in α of the oxygen-silicon bond are diastereotopic, as confirmed by the two doublets observed at 4.78 and 4.73 ppm (see Supporting Information for detailed characterization data). The use of Ph₂SiH₂ or Et₂SiH₂ as comonomers with HMF yielded polymers with similar chain lengths (Table 1, entries 2&3). The slight decrease in the isolated yield of poly(HMF-*co*-Et₂SiH₂) was attributed to the assumed higher solubility of this polymer in cold pentane, the solvent used to precipitate the final product. Remarkably, [Pt]_{tBu} was also efficient in catalyzing

the formation of these HMF-containing PSEs, but a higher catalyst loading was required to achieve molar masses in the 20 kg/mol range (Table 1, entry 4). Increasing the reaction time to 48h led to polymer chains of similar molar masses (Table S1, entry 1). At 0.1 mol%, the highly reactive [Pt]_{Me} gave materials with higher molar masses but broader dispersities (Table S1, entry 2). As a control experiment, the Karstedt's catalyst was found to be ineffective for the synthesis of PSE: using conditions similar to those described in Table 1, entry 1, the solution quickly turned from colorless to orange to black, presumably due to catalyst degradation; the resulting polymer, analyzed by size exclusion chromatography, exhibited a bimodal distribution and a high polydispersity, presumably from undesirable crosslinking ($M_n^{\text{exp}} = 59.7 \text{ kg/mol}$, $D = 5.3$). At lower Karstedt's catalyst loading (50 ppm), the molar mass of the product obtained remained below 500 g/mol. These observations show that catalyst design and metal stabilization are essential to obtain a controlled catalytic activity in the synthesis of poly(silylether)s.

Table 1. Catalytic synthesis of HMF-containing PSEs with different Pt(II) catalysts.^[a]

Entry	Catalyst	Silane	Isolated yield	M_n^{exp} (g/mol) ^[b]	M_w^{exp} (g/mol)	D
1	[Pt] _{Me} (500 ppm)	MePhSiH ₂	90%	15 900	49 700	3.1
2	[Pt] _{Me} (500 ppm)	Ph ₂ SiH ₂	95%	16 600	57 500	3.5
3	[Pt] _{Me} (500 ppm)	Et ₂ SiH ₂	57%	13 200	45 700	3.5
4	[Pt] _{tBu} (0.1 mol%)	MePhSiH ₂	77%	20 200	47 300	2.3

^[a] All reactions were performed under argon, with [HMF] = [Dihydrosilane] = 2 mol/L. ^[b] M_n^{exp} , M_w^{exp} and D of polymer determined by light scattering size exclusion chromatography in THF at 35°C. Light scattering was preferred to refractive index as it has been reported to be more accurate in the determination of molecular weights of PSEs.^[20] Refractive index data are also available in Table S1.

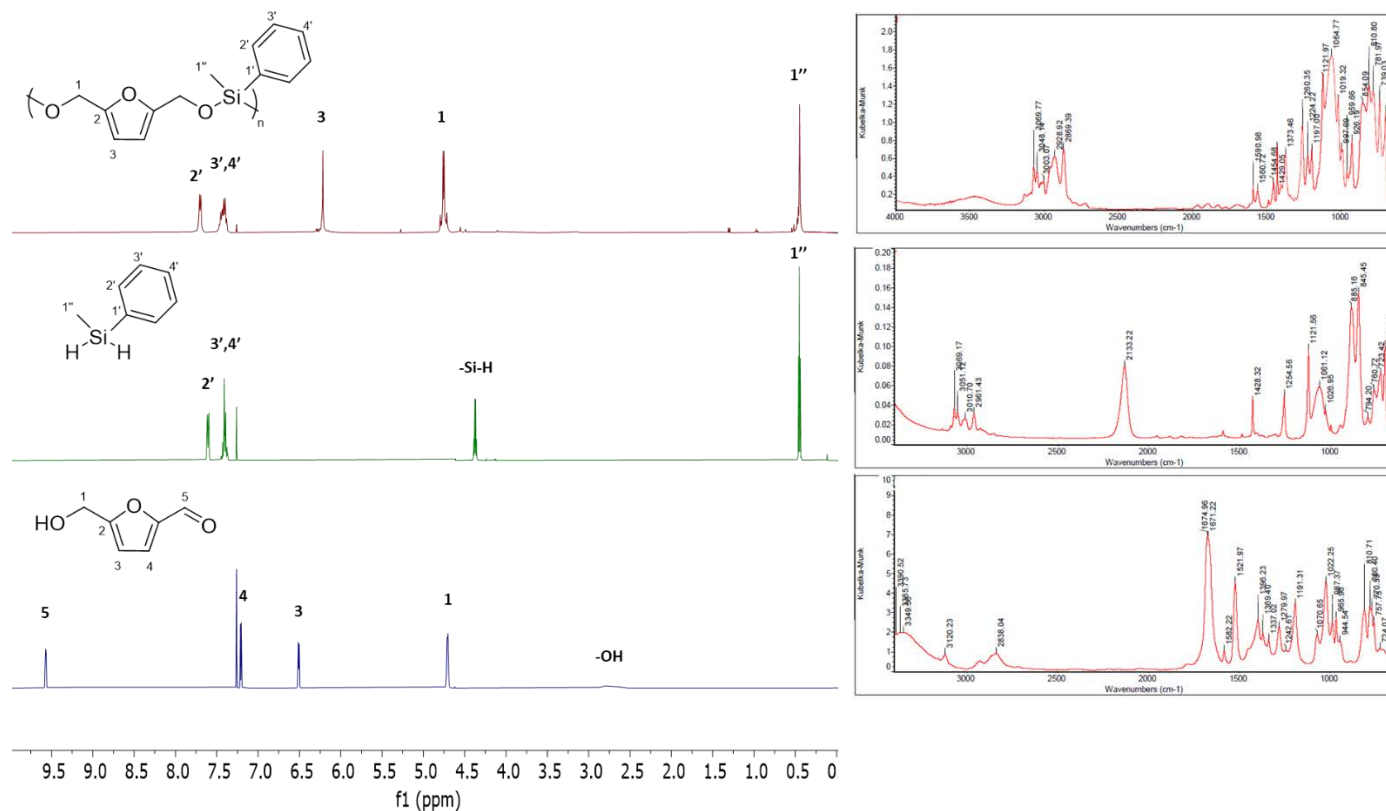
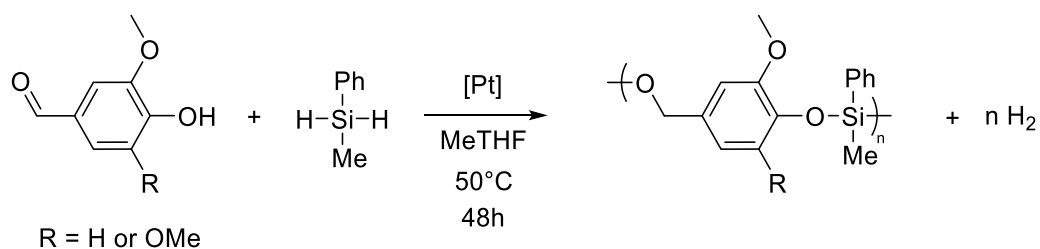


Figure 3. ¹H NMR spectra and FT-IR spectra of poly(HMF-co-MePhSiH₂), MePhSiH₂ and HMF (from top to bottom).

The reactivity of the two Pt^{II} complexes was then evaluated by investigating the synthesis of PSEs starting from other biobased hydroxyaldehydes. Vanillin and syringaldehyde are considered promising green building blocks derived from second generation biomass, since they can be obtained from lignin depolymerization.^[28] In particular vanillin is the only biosourced aromatic derivative, available on an industrial scale. However, neither of these two compounds has so far been used without further chemical modification to produce PSEs. We present in Table 2 the first poly(silylether)s formed directly from these two comonomers. As they were found to be less reactive than HMF under similar conditions, the reaction media were kept at 50°C for 48h during the corresponding polymerizations (static vacuum after 5h). Assuming an outer-sphere ionic reaction mechanism involving the nucleophilic addition of the alcohol on the coordinated dihydrosilane (σ -SiH complex of platinum),^[25d,25f,29] this different reactivity can be explained by the lower nucleophilicity of the

phenolic moiety compared to the primary alcohol moiety of HMF. Under these conditions, [Pt]_{Me} produced only small oligomers (Table 2, entries 1&2) while [Pt]_{tBu} afforded the expected polymers in good yields (Table 2, entries 3&4). Remarkably, the reaction with vanillin gave higher molar mass PSEs, presumably due to its lower steric hindrance around the phenolic proton (only one methoxy substituent in *ortho* position vs two for syringaldehyde). NMR and FT-IR spectroscopies confirmed the structures of the polymers obtained (Supporting Information). Since the repeating unit of the formed polymer is not symmetric (unlike the HMF-containing PSEs), the obtained silyl ether linkages can exhibit "head-to-head" (HH), "head-to-tail" (HT) and "tail-to-tail" (TT) regioselectivity, as shown in Figure 4. The regioselectivity of the polymerization can be approximated using ²⁹Si NMR and ¹H-²⁹Si HMBC NMR spectroscopy data, thus allowing the proportion of "head-to-tail" linkages to be determined. In the vanillin-based PSE, HT linkages account for approximately 50% of the silyl ether linkages, as expected for a statistical distribution with similar reactivities of the phenol and aldehyde moieties. However, the syringaldehyde-based PSE has a proportion of "head-to-tail" linkages of about 64% (Figure S7): this observation can be explained by the high steric hindrance around the phenolic protons, which makes "head-to-head" linkages with four methoxy groups around the silicon atom less favorable than in the case of vanillin.

Table 2. Catalytic synthesis of PhMeSiH₂-containing PSEs with different Pt(II) catalysts.^[a]



Chapter 4

Entry	Catalyst	Hydroxyaldehyde	Isolated yield	M_n^{exp} (g/mol) ^[b]	M_w^{exp} (g/mol)	\bar{D}
1	[Pt] _{Me} (500 ppm)	Vanillin	74%	515	780	1.5
2	[Pt] _{Me} (0.1 mol%)	Vanillin	70%	430	650	1.5
3	[Pt] _{tBu} (0.1 mol%)	Vanillin	77%	6 000	29 800	5.0
4	[Pt] _{tBu} (0.1 mol%)	Syringaldehyde	90%	3 800	6 200	1.7

^[a] All reactions were performed under argon, with [Hydroxyaldehyde] = [MePhSiH₂] = 2 mol/L. ^[b] M_n^{exp} , M_w^{exp} and \bar{D} of polymer determined by light scattering size exclusion chromatography in THF at 35°C. Light scattering was preferred to refractive index as it has been reported to be more accurate in the determination of molecular weights of PSEs.^[20] Refractive index data are also available in Table S1.

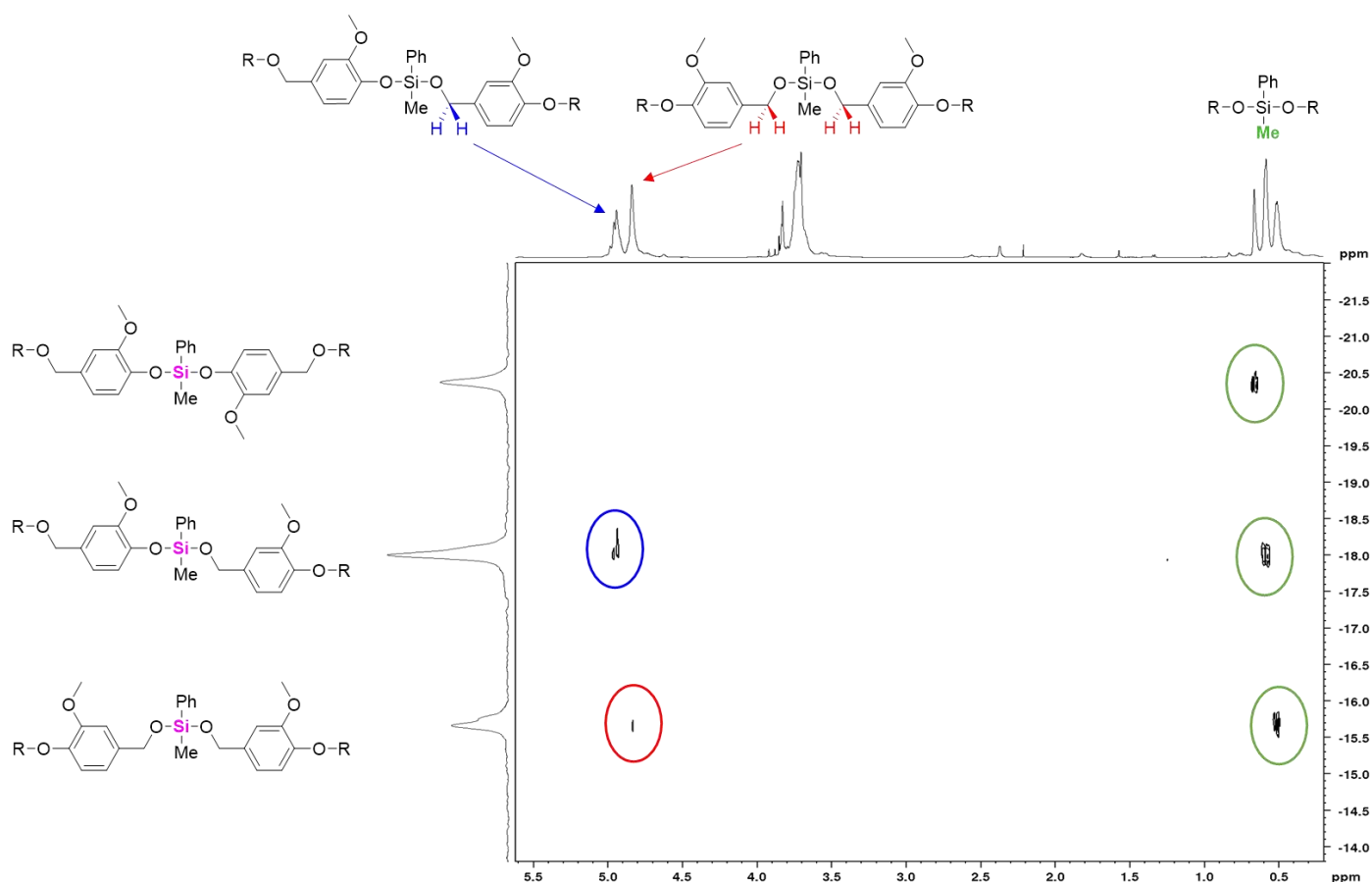


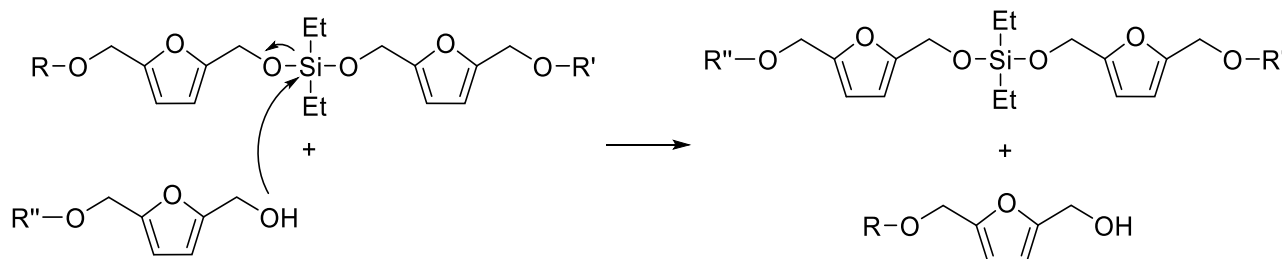
Figure 4. ¹H-²⁹Si HMBC NMR spectrum of poly(Vanillin-*co*-MePhSiH₂) (CDCl₃, 500 MHz).

The versatility of our catalysts was then illustrated by preparing D-isosorbide-based PSEs. D-Isosorbide is a biobased diol derived from glucose, frequently used in polymer architectures to impart rigidity to the resulting materials,^[30] with only one example of its use in PSE synthesis.^[20n] In contrast to what was observed with phenolic monomers, [Pt]_{Me} was much more efficient than [Pt]_{tBu} for the polymerization of this secondary diol (Table S1, entries 12&13): the polymer obtained with [Pt]_{Me} had a molar mass in the 15 kg/mol range, while only oligomers could be produced with [Pt]_{tBu}. NMR spectroscopy confirmed the formation of poly(D-isosorbide-*co*-PhMeSiH₂) (Supporting Information).

To further expand the number of macromolecular architectures accessible for PSEs, we investigated the possible formation of statistical, block or alternating copolymers. Statistical copolymers can be obtained in a similar manner as homopolymers, starting from a mixture of various dihydrosilanes. For instance, the direct copolymerization of 1 equivalent of HMF with 0.5 equivalent of Et₂SiH₂ and 0.5 equivalent of MePhSiH₂ under conditions similar to the ones described in Table 1 (500 ppm of [Pt]_{Me} catalyst, MeTHF, 20h at room temperature and 4h at 50°C under static vacuum) gave the expected statistical copolymer ($M_n = 19\,000$ g/mol and $D = 2.5$, see Supporting Information for additional characterization data). This method allows to easily tune thermal and degradability properties of the materials, as they strongly depend on the nature of the hydrosilane used (*vide infra*).

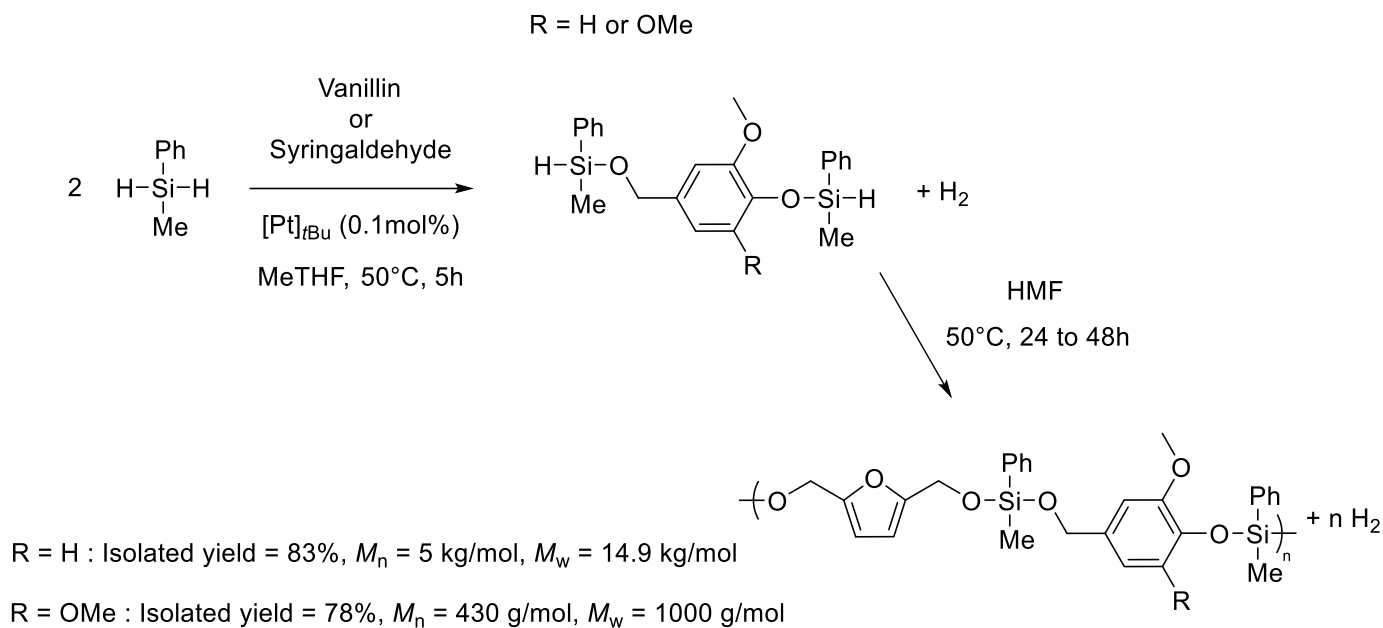
We then sought to obtain block copolymers by sequential addition of different silanes. First, HMF and Et₂SiH₂ were polymerized under conditions similar to the ones described in Table 1: the resulting crude poly(HMF-*co*-Et₂SiH₂) had a molar mass of 24 700 g/mol ($D = 2.6$). In the same reaction mixture, without any intermediate purification, HMF and MePhSiH₂ were then added and subjected to the same conditions as step 1. The polymer was finally purified and characterized by size exclusion chromatography: a monomodal distribution was obtained, with $M_n = 9\,000$ g/mol and $D = 2.0$. The formation of a lower molar mass polymer than after step 1 was unexpected and suggested the occurrence of redistribution reactions between the polymer backbone and the free HMF, as described in Scheme 1. The copolymer would then undergo a loss of molar mass, and its structure could be close

to random. This hypothesis was confirmed by the fact that NMR and FT-IR spectra were identical to those of the statistical copolymer, and both products had similar glass transition temperatures (*vide infra*). These observations seem to confirm that the platinum complexes used catalyze redistribution reactions that prevent the formation of sequence-controlled PSEs with HMF.



Scheme 1. Suggested redistribution reaction leading to randomization of the polymer structure.

To obtain alternating copoly(silylether)s, bi-functional monomers were prepared by reacting 1 equivalent of vanillin or syringaldehyde with 2 equivalents of MePhSiH₂ (Scheme 2). [Pt]_{Me} could not selectively produce the expected monomers, as it presumably catalyzed the reaction of R-O-Si-H moieties with the unreacted aldehyde or phenol groups. On the contrary, [Pt]_{tBu} was selective in the formation of the expected bis-silyl ethers, within 5h at 50°C in MeTHF. The products were fully characterized by NMR and FT-IR spectroscopies: notably, two different signals for the Si-H and Si atoms were observed in both ¹H and ²⁹Si NMR spectra; moreover, the Si-H bond stretching band could be identified at 2100 cm⁻¹ in FT-IR (Figures S46 to S53). Interestingly, these bis-silyl ethers could then be engaged in a one-pot polymerization sequence with 1 equivalent of HMF, without any intermediate purification, to yield alternating copolymers: after 24h at 50°C (under static vacuum), poly(vanillin-*alt*-HMF-*co*-MePhSiH₂) with a molar mass of 5 000 g/mol could be obtained in high yield (83%). The syringaldehyde-based bis-silyl ether was found to be less reactive, due to its higher steric hindrance, thus giving oligomers after 48h at 50°C under static vacuum.



Scheme 2. Reaction sequence leading to alternated copolymers.

The copolymers obtained were also characterized by differential scanning calorimetry (DSC) and thermogravimetric analysis (TGA). The results are presented in Table 3. As commonly observed in the literature, the glass transition temperature of PSEs is strongly dependent on the nature of the dihydrosilane precursor. For instance, Ph_2SiH_2 provides aromaticity and stiffness around the silicon atom, which results in a higher T_g for its copolymer with HMF than the one obtained with Et_2SiH_2 and the same comonomer (Table 3, entries 1&2). The glass transition temperature of poly(HMF-*co*- MePhSiH_2) is in between the two previous copolymers at -15°C (Table 3, entry 3). Fine tuning of the T_g is also attainable by mixing different dihydrosilanes, as shown in the preparation of poly(HMF-*co*- MePhSiH_2 -*ran*- Et_2SiH_2) (Table 3, entries 4&5). Using the same dihydrosilane but a different hydroxyaldehyde, it is possible to study the influence of the latter comonomer. Vanillin and syringaldehyde increased the T_g of their copolymer with MePhSiH_2 when compared to HMF, from -15 to nearly 10°C (Table 3, entries 6&7). The alternating copolymers prepared using HMF and vanillin or syringaldehyde surprisingly yielded materials with glass transitions close to the ones of poly(HMF-*co*- MePhSiH_2) (Table 3, entries 9&10). Thus, it is clearly demonstrated that the control of the T_g of the PSEs obtained occurs mainly by the type and proportion of the different dihydrosilanes used, and

depends in a more limited way on the type of hydroxyaldehyde. These observations underline the importance of having a catalytic system capable of copolymerizing various dihydrosilanes, from Ph_2SiH_2 to Et_2SiH_2 .

Thermogravimetric analysis also showed the influence of comonomers on the thermal stability of the final material. HMF-based PSEs were relatively stable upon heating, with $T_{-5\%}$ values ranging from 270 to 301°C, depending on the dihydrosilane comonomer (Table 3, entries 1-3). The $T_{-5\%}$ of the various PSEs obtained was also dependent on the hydroxyaldehyde used, with higher thermal stability in the following order: HMF > vanillin > syringaldehyde. These observations are somewhat surprising, but caution should be exercised drawing any conclusions given the variety of molar masses obtained for these materials.

Table 3. Thermal analyses of PSEs obtained in this study.^[a]

Entry	Type of copolymer	M_n (g/mol)	D	T_g (°C)	$T_{-5\%}$ (°C)
1	poly(HMF- <i>co</i> -Ph ₂ SiH ₂)	7 300	2.1	7	301
2	poly(HMF- <i>co</i> -Et ₂ SiH ₂)	13 200	3.5	-60	280
3	poly(HMF- <i>co</i> -MePhSiH ₂)	15 900	3.1	-15	270
4 ^[b]	poly(HMF- <i>co</i> -MePhSiH ₂ - <i>r</i> -Et ₂ SiH ₂)	9 000	2.0	-46	272
5 ^[c]	poly(HMF- <i>co</i> -MePhSiH ₂ - <i>r</i> -Et ₂ SiH ₂)	19 000	2.5	-40	281
6	poly(Vanillin- <i>co</i> -MePhSiH ₂)	6 000	5.0	7	245
7	poly(Syringaldehyde- <i>co</i> -MePhSiH ₂)	3 800	1.7	7	215
8 ^[d]	poly(Vanillin- <i>co</i> -Ph ₂ SiH ₂)	32 000	4.7	29	208
9	poly(Vanillin- <i>alt</i> -HMF- <i>co</i> -MePhSiH ₂)	5 000	3.0	-21	237
10	poly(Syringaldehyde- <i>alt</i> -HMF- <i>co</i> - MePhSiH ₂)	430	2.2	-15	210

^[a] M_n^{exp} of polymer determined by light scattering size exclusion chromatography in THF at 35°C. T_g of polymer determined by DSC on second heating cycle (10°C/min, N₂ flow). $T_{-5\%}$ of polymer determined by TGA (20°C/min, N₂ flow). ^[b] Copolymer obtained by addition of HMF and MePhSiH₂ on the previously formed poly(HMF-*co*-Et₂SiH₂). ^[c] Copolymer obtained by reaction between 2 HMF and 1 MePhSiH₂ and 1 Et₂SiH₂. ^[d] Copolymer obtained under conditions similar to the ones described in Table 2, using a 0.4 mol% [Pt]_{tBu} catalyst loading.

Finally, the degradability and potential recyclability of our PSEs were investigated. The most common protocols for studying the degradation of poly(silylether)s consist in dissolving the polymer in an organic solvent (usually THF) and adding a nucleophilic agent (methanol or a solution of HCl/H₂O) under mild heating.^[5a,5c,12a,20r,21a,31] We thus adapted those protocols and first investigated

the degradation of lignin-based PSEs such as poly(syringaldehyde-*co*-MePhSiH₂), poly(vanillin-*co*-MePhSiH₂) and poly(vanillin-*co*-Ph₂SiH₂) (Figure S8 and Table S2). Remarkably, all three polymers were fairly stable towards acid hydrolysis, with relative M_w losses of around 25% for vanillin-based copolymers and only 5% for poly(syringaldehyde-*co*-MePhSiH₂) after 24h at 30°C. The higher stability of the syringaldehyde-based PSE was attributed to the higher steric bulk around the silicon atom, thanks to the two methoxy substituents in *ortho* position of the silyl ether linkage. The uncatalyzed methanolysis of these polymers also evidenced the influence of the dihydrosilane precursor, as poly(vanillin-*co*-MePhSiH₂) suffered a 70% M_w loss while poly(vanillin-*co*-Ph₂SiH₂) remained largely unaffected (7% M_w loss). These observations are consistent with the ones of Paulasaari and Weber, who prepared a similar PSE from terephthalaldehyde and tetramethyldisiloxane, and reported its sensitivity towards methanolysis.^[5a] As observed in the thermal studies, the degradation properties of our PSEs thus seem to be dependent on both the hydroxyaldehyde and the dihydrosilane precursors used, with a higher stability conferred by bulky comonomers.

HMF-based poly(silylether)s were also studied and their remarkably clean degradation properties highlight their potential chemical recyclability. Poly(HMF-*co*-Ph₂SiH₂), poly(HMF-*co*-Et₂SiH₂) and poly(HMF-*co*-MePhSiH₂) were all subjected to methanolysis and acid hydrolysis conditions (Figures 5 & S9). Surprisingly, these three polymers were relatively stable towards uncatalyzed methanolysis (between 15 and 30% M_w loss after 24h at 30°C).

When compared to poly(vanillin-*co*-MePhSiH₂), these results suggest the importance of electronic effects of the electron-withdrawing aromatic ring which can destabilize the silyl ether bond in the lignin-based polymers. However, HMF-based PSEs were found to be strongly degraded by acid hydrolysis (Figures 5 & S10). Remarkably, poly(HMF-*co*-MePhSiH₂) lost nearly 100% of its molar mass within 17h, and produced quantitatively 2,5-bis(hydroxymethyl)furan and the corresponding silanediol (Scheme 3). Similarly, acid catalyzed methanolysis of poly(HMF-*co*-MePhSiH₂) or poly(vanillin-*co*-MePhSiH₂) permitted to obtain cleanly the corresponding diol (2,5-

bis(hydroxymethyl)furan or 4-hydroxy-3-methoxy-benzenemethanol) with a presumably small oligomers mixture of polysiloxanes (Figures S11 to S14).

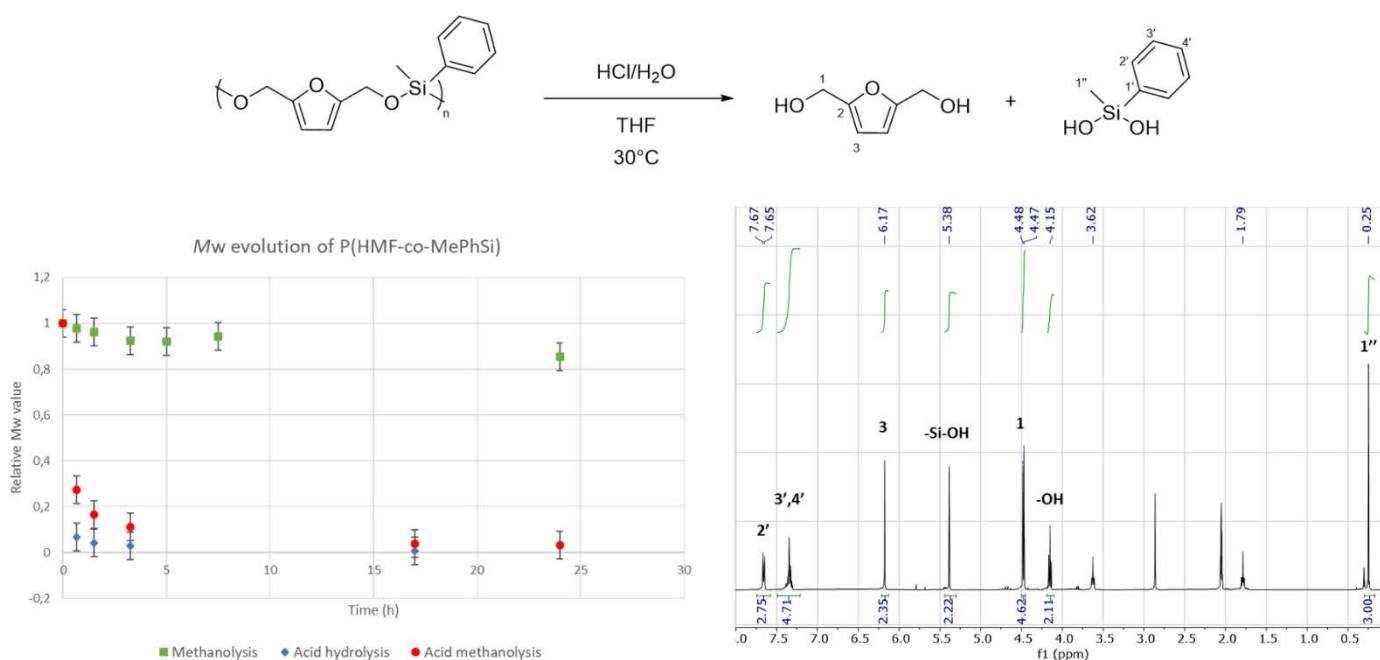
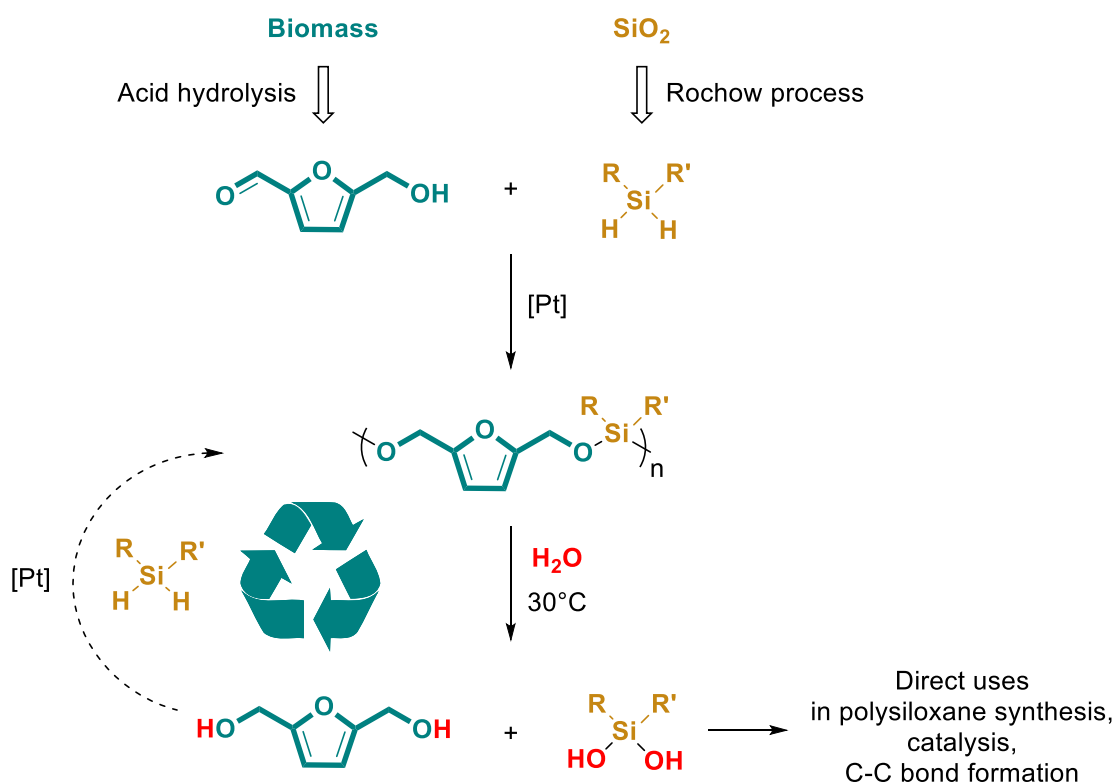


Figure 5. Degradation study of poly(HMF-co-MePhSiH₂) showing the reaction conditions (up), the evolution of the relative M_w of the polymer over time, depending on the reaction conditions (bottom left), and the ¹H NMR spectrum of the crude of the acid hydrolysis of poly(HMF-co-MePhSiH₂) after 17h (Acetone-*d*₆, 400 MHz) (bottom right).

These results suggest a relative robustness of partially biobased poly(silylether)s when used in solvent-free and Brønsted acid-free environments. Additionally, their chemical recycling can easily be triggered by dissolving the polymer in an organic solvent and subjecting it to a Brønsted acid-catalyzed methanolysis or hydrolysis. In particular, while the diol can be directly isolated and reused in polymer preparation,^[32] silanediols have found applications as polysiloxane precursors,^[33] organocatalysts of various reactions including C-H bond activation and cyclic carbonate synthesis from CO₂ and various epoxides,^[34] or as cross-coupling partners for carbon-carbon bond formation.^[35] This recycling

strategy, coupled with the direct biosourcing of hydroxyaldehydes from biomass, highlights the potential of PSEs as truly sustainable polymers.



Scheme 3. Chemical recyclability of poly(silylether)s.

Conclusion

A highly efficient synthesis of poly(silylether)s from hydroxyaldehydes, derived from biomass in few steps, has been developed. Catalyzed by low loadings of Pt^{II} complexes under mild conditions, this synthetic pathway allowed the formation of various homo- and copolymers thanks to the variety of starting hydroxyaldehydes as well as dihydrosilanes used. The influence of the comonomers on the properties of the final polymers could be exemplified: *T_g* values ranging from -60 to 29°C were obtained, poly(syringaldehyde-*co*-MePhSiH₂) was resistant to acid hydrolysis while poly(HMF-*co*-MePhSiH₂) could be quantitatively converted to the corresponding diol and silanediol under the same conditions. The acid-catalyzed methanolysis or hydrolysis of HMF-based PSEs were even highlighted as promising routes to chemically recycle the starting polymers. These results underline the potential

of robust, yet degradable polymers as sustainable materials of the future which can be derived from renewable resources and are designed to be recycled when subject to the right stimulus. Our future efforts are oriented towards the rationalization of the Pt^{II} complexes catalytic activity, as well as on the purification and reuse of comonomers from the chemical degradation reaction.

Acknowledgements

Chimie ParisTech – PSL and CNRS are thanked for financial support. H.F. acknowledges financial support from École polytechnique (AMX) for his PhD scholarship. Île-de-France Region is gratefully acknowledged for financial support of 500 MHz NMR spectrometer of Chimie ParisTech in the framework of the SESAME equipment project (n°16016326). Financial support (FEDER contribution) from the Ministerio de Ciencia e Innovación (projects PID2019-109312GB-I00 and RED2018-102387-T) and Junta de Andalucía (project P20_00513) are gratefully acknowledged. CMT is grateful to the Institut Universitaire de France.

References

- [1] H. Fouilloux, C. M. Thomas, *Macromol. Rapid Commun.* **2021**, *42*, 2000530.
- [2] a) M. A. Hillmyer, *Science* **2017**, *358*, 868-870; b) M. Poliakoff, P. Licence, *Nature* **2007**, *450*, 810-812; c) A. J. Ragauskas, C. K. Williams, B. H. Davison, G. Britovsek, J. Cairney, C. A. Eckert, W. J. Frederick Jr., J. P. Hallett, D. J. Leak, C. L. Liotta, J. R. Mielenz, R. Murphy, R. Templer, T. Tschaplinski, *Science* **2006**, *311*, 484–489; d) F. Seniha Güner, Y. Yağcı, A. Tuncer Erciyes, *Prog. Polym. Sci.* **2006**, *31*, 633–670; e) J. F. Jenck, F. Agterberg, M. J. Droescher, *Green Chem.* **2004**, *6*, 544-556; f) A. Corma, S. Iborra, A. Velty, *Chem. Rev.* **2007**, *107*, 2411–2502; g) J. H. Clark, F. E. I. Deswarte in *Introduction to chemicals from biomass*, John Wiley & Sons, Ltd, Chichester, West Sussex, United Kingdom, **2015**; h) P. Y. Dapsens, C. Mondellu, J. Pérez- Ramírez, *ACS Catal.* **2012**, *2*, 1487-1499; i) P. Gallezot, *Chem. Soc. Rev.* **2012**, *41*, 1538-1558; j) F. Cherubini, A. H. Strømman, *Biofuels, Bioprod. Bioref.* **2011**, *5*, 548–561; k) R. A. Sheldon, *Green Chem.* **2014**, *16*, 950–963.
- [3] a) P. B. Weisz, *Phys. Today* **2004**, *57*, 47-52; b) C. Williams, M. Hillmyer, *Polymer Revs.* **2008**, *48*, 1-10; c) M. J.-L. Tschan, E. Brule, P. Haquette, C. M. Thomas. *Polym. Chem.* **2012**, *3*, 836-851.

- [4] a) M. Hong, E. Y.-X. Chen, *Green Chem.* **2017**, *19*, 3692–3706; b) G. W. Coates, Y. D. Y. L. Getzler, *Nat. Rev. Mater.* **2020**, DOI 10.1038/s41578-020-0190-4.
- [5] a) J. K. Paulasaari, W. P. Weber, *Macromolecules* **1998**, *31*, 7105–7107; b) J. Cella, S. Rubinsztajn, *Macromolecules* **2008**, *41*, 6965–6971 ; c) C. Cheng, A. Watts, M. A. Hillmyer, J. F. Hartwig, *Angew. Chem.* **2016**, *128*, 12051–12055.
- [6] J. E. Curry, J. D. Byrd, *J. Appl. Polym. Sci.* **1965**, *9*, 295–311.
- [7] Y. Zhang, Z. Zhu, Z. Bai, W. Jiang, F. Liu, J. Tang, *RSC Adv.* **2017**, *7*, 16616–16622.
- [8] a) Y. Li, M. Seino, Y. Kawakami, *Macromolecules* **2000**, *33*, 5311–5314; b) X.-Q. Wang, X.-Y. Zhai, B. Wu, Y.-Q. Bai, Y.-G. Zhou, *ACS Macro Lett.* **2020**, *9*, 969–973.
- [9] X. Chen, L. Fang, X. Chen, J. Zhou, J. Wang, J. Sun, Q. Fang, *ACS Sustain. Chem. Eng.* **2018**, *6*, 13518–13523.
- [10] a) J. M. Mabry, J. K. Paulasaari, W. P. Weber, *Polymer* **2000**, *41*, 4423–4428; b) Yun, Seung-Beom, Park, Young Tae, *B. Kor. Chem. Soc.* **2008**, *29*, 2373–2378; c) Jung, In-Kyung, Park, Young Tae, *B. Kor. Chem. Soc.* **2011**, *32*, 1303–1309; d) Jung, Eun Ae, Park, Young Tae, *B. Kor. Chem. Soc.* **2012**, *33*, 2031–2036.
- [11] S. Gao, Y. Liu, S. Feng, Z. Lu, *J. Mater. Chem. A* **2019**, *7*, 17498-17504.
- [12] a) M. Wang, Q. Zhang, K. L. Wooley, *Biomacromolecules* **2001**, *2*, 1206–1213; b) M. C. Parrott, J. C. Luft, J. D. Byrne, J. H. Fain, M. E. Napier, J. M. DeSimone, *J. Am. Chem. Soc.* **2010**, *132*, 17928–17932; c) T. Ware, A. R. Jennings, Z. S. Bassampour, D. Simon, D. Y. Son, W. Voit, *RSC Adv.* **2014**, *4*, 39991–40002; d) Y. Wang, S. Fan, D. Xiao, F. Xie, W. Li, W. Zhong, X. Zhou, *Cancers* **2019**, *11*, 957; e) C. M. Bunton, Z. M. Bassampour, J. M. Boothby, A. N. Smith, J. V. Rose, D. M. Nguyen, T. H. Ware, K. G. Csaky, A. R. Lippert, N. V. Tsarevsky, D. Y. Son, *Macromolecules* **2020**, *53*, 9890–9900.
- [13] C. Rücker, K. Kümmerer, *Chem. Rev.* **2015**, *115*, 466–524.
- [14] R. MacFarlane, E. S. Yankura, *Synthesis of Regulated Structure Polyphenylether Siloxane Block Copolymers.*, United States Rubber Co Naugatuck CT Chemical Div., **1963**.
- [15] Y. Kawakami, Y. Li, *Des. Monomers and Polym.* **2000**, *3*, 399–419.
- [16] a) C. E. Carraher Jr, G. H. Klimiuk, *J. Polym. Sci. A1* **1970**, *8*, 973–978; b) K. Nagaoka, H. Naruse, I. Shinohara, M. Watanabe, *J. Polym. Sci. Pol. Lett.* **1984**, *22*, 659–663; c) D.-J. Liaw, B.-Y. Liaw, *J. Polym. Sci. A1* **1999**, *37*, 4591–4595; d) A. M. Issam, M. Haris, *J. Inorg. Organomet. P.* **2009**, *19*, 454–458; e) K. Drake, I. Mukherjee, K. Mirza, H.-F. Ji, Y. Wei, *Macromolecules* **2011**, *44*, 4107–4115; f) K. Drake, I. Mukherjee, K. Mirza, H.-F. Ji, J.-C. Bradley, Y. Wei, *Macromolecules* **2013**, *46*, 4370–4377; g) I. A. Mohammed, S. Shahabuddin, R. Khanam, R. Saidur, *Polímeros* **2018**, *28*, 406–412.

- [17] a) L. W. Breed, R. L. Elliott, *Synthesis of Elastomers Containing Si-N Bonds in the Main Chain.*, Midwest Research Institute, **1963**; b) W. R. Dunnivant, R. A. Markle, P. B. Stickney, J. E. Curry, J. D. Byrd, *J. Polym. Sci. A-1 Polym. Chem.* **1967**, *5*, 707–724; c) W. R. Dunnivant, R. A. Markle, R. G. Sinclair, P. B. Stickney, J. E. Curry, J. D. Byrd, *Macromolecules* **1968**, *1*, 249–254.
- [18] a) M. Padmanaban, M.-A. Kakimoto, Y. Imai, *J. Polym. Sci. A1* **1990**, *28*, 2997–3005; b) S. A. Nye, S. A. Swint, *J. Polym. Sci. A1* **1994**, *32*, 131–138; c) Y. Nagasaki, F. Matsukura, M. Kato, H. Aoki, T. Tokuda, *Macromolecules* **1996**, *29*, 5859–5863; d) Y. Liu, I. Imae, A. Makishima, Y. Kawakami, *Sci. Technol. Adv. Mat.* **2003**, *4*, 27–34.
- [19] E. Sahmetlioglu, H. T. H. Nguyen, O. Nsengiyumva, E. Göktürk, S. A. Miller, *ACS Macro Lett.* **2016**, *5*, 466–470.
- [20] a) J. M. Mabry, M. K. Runyon, W. P. Weber, *Macromolecules* **2001**, *34*, 7264–7268; b) J. M. Mabry, M. K. Runyon, W. P. Weber, *Macromolecules* **2002**, *35*, 2207–2211; c) Y. Li, Y. Kawakami, *Macromolecules* **1999**, *32*, 3540–3542; d) Y. Li, Y. Kawakami, *Macromolecules* **1999**, *32*, 6871–6873; e) A. Purkayastha, J. B. Baruah, *Appl. Organomet. Chem.* **2000**, *14*, 477–483; f) P. N. Reddy, B. P. S. Chauhan, T. Hayashi, M. Tanaka, *Chem. Lett.* **2000**, *29*, 250–251; g) G. Lázaro, M. Iglesias, F. J. Fernández-Alvarez, S. Miguel, J. J. Pérez-Torrente, L. A. Oro, *ChemCatChem* **2013**, *5*, 1133–1141; h) G. Lázaro, F. J. Fernández-Alvarez, M. Iglesias, C. Horna, E. Vispe, R. Sancho, F. J. Lahoz, M. Iglesias, J. J. Pérez-Torrente, L. A. Oro, *Catal. Sci. Technol.* **2014**, *4*, 62–70; i) M. Zhao, W. Xie, C. Cui, *Chem. Eur. J.* **2014**, *20*, 9259–9262; j) C. Lichtenberg, M. Adelhardt, M. Wörle, T. Büttner, K. Meyer, H. Grützmacher, *Organometallics* **2015**, *34*, 3079–3089; k) C. Lichtenberg, L. Viciu, M. Adelhardt, J. Sutter, K. Meyer, B. de Bruin, H. Grützmacher, *Angew. Chem. Int. Ed.* **2015**, *54*, 5766–5771; l) C. Li, X. Hua, Z. Mou, X. Liu, D. Cui, *Macromol. Rapid Commun.* **2017**, *5*; m) S. Vijjamarri, V. K. Chidara, G. Du, *ACS Omega* **2017**, *2*, 582–591; n) S. Vijjamarri, M. Hull, E. Kolodka, G. Du, *ChemSusChem* **2018**, *11*, 2881–2888; o) X.-Y. Zhai, S.-B. Hu, L. Shi, Y.-G. Zhou, *Organometallics* **2018**, *37*, 2342–2347; p) X.-Y. Zhai, X.-Q. Wang, Y.-X. Ding, Y.-G. Zhou, *Chinese Chem. Lett.* **2020**, *31*, 1197–1200; q) X.-Y. Zhai, X.-Q. Wang, Y.-G. Zhou, *Eur. Polym. J.* **2020**, *134*, 109832; r) C. S. Sample, S.-H. Lee, M. W. Bates, J. M. Ren, J. Lawrence, V. Lensch, J. A. Gerbec, C. M. Bates, S. Li, C. J. Hawker, *Macromolecules* **2019**, *52*, 1993–1999; s) A. F. Schneider, E. Laidley, M. A. Brook, *Macromol. Chem. Phys.* **2019**, 1800575; t) Y. Tao, J. Zhou, L. Fang, Y. Wang, X. Chen, X. Chen, J. Hou, J. Sun, Q. Fang, *ACS Sustain. Chem. Eng.* **2019**, *7*, 7304–7311; u) L. J. Morris, M. S. Hill, M. F. Mahon, I. Manners, F. S. McMenamy, G. R. Whittell, *Chem. Eur. J.* **2020**, *13*.
- [21] a) S. Vijjamarri, S. Streed, E. M. Serum, M. P. Sibi, G. Du, *ACS Sustain. Chem. Eng.* **2018**, *6*, 2491–2497; b) C. Li, L. Wang, M. Wang, B. Liu, X. Liu, D. Cui, *Angew. Chem. Int. Ed.* **2019**, *58*, 11434–11438.

- [22] a) J. Zhang, Y. Chen, M. A. Brook, *ACS Sustain. Chem. Eng.* **2014**, *2*, 1983–1991; b) E. Feghali, G. Carrot, P. Thuéry, C. Genre, T. Cantat, *Energ. Environ. Sci.* **2015**, *8*, 2734–2743; c) L. L. Adduci, M. P. McLaughlin, T. A. Bender, J. J. Becker, M. R. Gagné, *Angew. Chem. Int. Ed.* **2014**, *53*, 1646–1649; d) J. Zhang, S. Park, S. Chang, *Angew. Chem. Int. Ed.* **2017**, *56*, 13757–13761.
- [23] a) L. N. Lewis, J. Stein, Y. Gao, R. E. Colborn, G. Hutchins, *Platin. Met. Rev.* **1997**, *41*, 66–75; b) R. Yu. Lukin, A. M. Kuchkaev, A. V. Sukhov, G. E. Bektukhamedov, D. G. Yakhvarov, *Polymers* **2020**, *12*, 2174.
- [24] a) C. Robert, F. de Montigny, C. M. Thomas, *Nat. Commun.* **2011**, *2*, 1–6; b) S. K. Raman, E. Brulé, M. J.-L. Tschan, C. M. Thomas, *Chem. Commun.* **2014**, *50*, 13773–13776; c) C. Robert, T. E. Schmid, V. Richard, P. Haquette, S. K. Raman, M.-N. Rager, R. M. Gauvin, Y. Morin, X. Trivelli, V. Guérineau, I. del Rosal, L. Maron, C. M. Thomas, *J. Am. Chem. Soc.* **2017**, *139*, 6217–6225; d) J. Kiriratnikom, C. Robert, V. Guérineau, V. Venditto, C. M. Thomas, *Front. Chem.* **2019**, *7*, 301; e) P. Marin, M. J.-L. Tschan, F. Isnard, C. Robert, P. Haquette, X. Trivelli, L.-M. Chamoreau, V. Guérineau, I. del Rosal, L. Maron, V. Venditto, C. M. Thomas, *Angew. Chem. Int. Ed.* **2019**, *58*, 12585–12589; f) D. Zhang, Y. Zhang, Y. Fan, M.-N. Rager, V. Guérineau, L. Bouteiller, M.-H. Li, C. M. Thomas, *Macromolecules* **2019**, *52*, 2719–2724; g) H. Fouilloux, W. Qiang, C. Robert, V. Placet, C. M. Thomas, *Angew. Chem. Int. Ed.* **2021**, *60*, 19374–19382.
- [25] a) O. Rivada-Wheelaghan, B. Donnadieu, C. Maya, S. Conejero, *Chem. Eur. J.* **2010**, *16*, 10323–10326; b) M. Roselló-Merino, J. López-Serrano, S. Conejero, *J. Am. Chem. Soc.* **2013**, *135*, 10910–10913; c) M. Roselló-Merino, R. J. Rama, J. Díez, S. Conejero, *Chem. Commun.* **2016**, *52*, 8389–8392; d) S. Conejero, P. Ríos, M. Roselló-Merino, O. Rivada-Wheelaghan, J. Borge, J. López-Serrano, *Chem. Commun.* **2018**, *54*, 619–622; e) P. Ríos, J. Díez, J. López-Serrano, A. Rodríguez, S. Conejero, *Chem. Eur. J.* **2016**, *22*, 16791–16795; f) P. Ríos, H. Fouilloux, P. Vidossich, J. Díez, A. Lledós, S. Conejero, *Angew. Chem. Int. Ed.* **2018**, *57*, 3217–3221.
- [26] M. Lersch, M. Tilset, *Chem. Rev.* **2005**, *105*, 2471–2526.
- [27] A. Sevy, E. Tieu, M. D. Morse, *J. Chem. Phys.* **2018**, *149*, 174307.
- [28] M. P. Pandey, C. S. Kim, *Chem. Eng. Technol.* **2011**, *34*, 29–41.
- [29] a) X. L. Luo, R. H. Crabtree, *J. Am. Chem. Soc.* **1989**, *111*, 2527–2535; b) M. Iglesias, F. J. Fernández-Alvarez, L. A. Oro, *Coordin. Chem. Rev.* **2019**, *386*, 240–266.
- [30] D. J. Saxon, A. M. Luke, H. Sajjad, W. B. Tolman, T. M. Reineke, *Prog. Polym. Sci.* **2020**, *101*, 101196.
- [31] Y. Li, Y. Kawakami, *Macromolecules* **1999**, *32*, 8768–8773.
- [32] L. Guillaume, A. Marshall, N. Niessen, P. Ni, R. M. Gauvin, C. M. Thomas, *Green Chem.* **2021**, *23*, 6931–6935.

- [33] M. Jeon, J. Han, J. Park, *ACS Catal.* **2012**, *2*, 1539–1549.
- [34] a) A. G. Schafer, J. M. Wieting, A. E. Mattson, *Org. Lett.* **2011**, *13*, 5228–5231; b) A. M. Hardman-Baldwin, A. E. Mattson, *ChemSusChem* **2014**, *7*, 3275–3278.
- [35] K. Hirabayashi, A. Mori, J. Kawashima, M. Suguro, Y. Nishihara, T. Hiyama, *J. Org. Chem.* **2000**, *65*, 5342–5349.

Chapter 4 – Supporting Information

Table of contents:

Methods.....	294
Materials	294
Measurements	294
Synthesis of [Pt] _{Me} and Figures S1 to S6	295
Polymerization procedure	302
Degradation procedure.....	302
Recycling procedure	303
Table S1	304
Table S2	304
Figure S7: ²⁹ Si NMR spectra of lignin-based polymers	306
Figures S8 & S9: degradation studies of polymers.....	307
Figures S10 to S14: recycling studies of polymers.....	308
NMR and IR characterization data of PSEs.....	313
- poly(HMF- <i>co</i> -MePhSiH ₂)	313
- poly(HMF- <i>co</i> -Ph ₂ SiH ₂)	316
- poly(HMF- <i>co</i> -Et ₂ SiH ₂).....	319
- poly(Vanillin- <i>co</i> -Ph ₂ SiH ₂).....	322
- poly(Vanillin- <i>co</i> -MePhSiH ₂).....	325
- poly(Vanillin- <i>co</i> -Et ₂ SiH ₂).....	328
- poly(Syringaldehyde- <i>co</i> -MePhSiH ₂).....	331
- poly(Isosorbide- <i>co</i> -MePhSiH ₂)	334
- MePhSiH-Vanillin-MePhSiH monomer.....	337
- MePhSiH-Syringaldehyde-MePhSiH monomer.....	340
- poly(Vanillin- <i>alt</i> -HMF- <i>co</i> -MePhSiH ₂)	343
- poly(Syringaldehyde- <i>alt</i> -HMF- <i>co</i> -MePhSiH ₂)	347
- poly(HMF- <i>co</i> -MePhSiH ₂ - <i>r</i> -Et ₂ SiH ₂).....	351

Methods

Materials

All manipulations requiring dry atmosphere were performed under a purified argon atmosphere using standard Schlenk techniques or in a glovebox. Solvents for synthesis (toluene, THF, Et₂O, *n*-pentane, MeTHF) were freshly distilled from Na/benzophenone under argon and degassed thoroughly by freeze-thaw-vacuum cycles prior to use. Deuterated chloroform (99.5% D, Eurisotop) was used as received. Triphenylsilane was purchased from Sigma-Aldrich and used as received. *Tert*-butylimidazol,² [H(OEt₂)] [BArF]³ and complex [PtMe₂(cod)]⁴ were prepared according to procedures previously described in the literature. HMF (98%) from BLDpharm was recrystallized from freshly distilled Et₂O and dried under vacuum prior to introduction in the glovebox, as reported in existing literature.⁵ Vanillin (98%) from TCI Europe was sublimated at 50°C under vacuum prior to introduction in the glovebox. Syringaldehyde (98%) from TCI Europe was recrystallized from toluene, washed twice with *n*-pentane and dried under vacuum prior to introduction in the glovebox. Ph₂SiH₂, MePhSiH₂ and Et₂SiH₂ from Fluorochem were distilled and degassed prior to introduction in the glovebox.

Measurements

NMR spectra were recorded on Bruker Avance-400 and Avance-Neo 500 spectrometers at Chimie ParisTech. ¹H, ¹³C and ²⁹Si chemical shifts are reported in ppm versus SiMe₄ and were determined by reference to the residual solvent peaks for ¹H and ¹³C NMR and to the chemical shift of TMS (0ppm) used as external reference for ²⁹Si NMR. Assignment of signals was made from multinuclear 1D (¹H, ¹³C{¹H}) and 2D (COSY, HMQC, HMBC) NMR experiments. Elemental

² R. E. Cowley, R. P. Bontchev, E. N. Duesler, J. M. Smith, *Inorg. Chem.* **2006**, *45*, 9771–9779.

³ M. Brookhart, B. Grant, A. F. Volpe, *Organometallics* **1992**, *11*, 3920–3922.

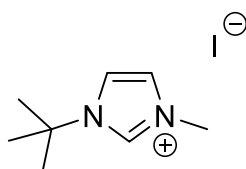
⁴ R. Bassan, K. H. Bryars, L. Judd, A. W. G. Platt, P. G. Pringle, *Inorg. Chim. Acta* **1986**, *121*, L41–42.

⁵ K. I. Galkin, E. A. Krivodaeva, L. V. Romashov, S. S. Zalesskiy, V. V. Kachala, J. V. Burykina, V. P. Ananikov, *Angew. Chem.* **2016**, *128*, 8478–8482.

analysis was carried out with a LECO TruSpec CHN elementary analyzer. Diffuse reflectance Fourier transform infrared measurements were carried out on a Thermo Fisher Nicolet IS 20 FT-IR spectrometer equipped with a Harrick Praying Mantis device. Size exclusion chromatography (SEC) of polymers was performed in THF at 35 °C using an Agilent 1260 Infinity Series GPC (ResiPore 3 μm , 300 x 7.5 mm, 1.0 mL/min, RI (PL-GPC 220) and Light scattering detectors) at Chimie ParisTech. When using the RI detector, the number average molecular masses (M_n) and polydispersity index (\mathcal{D}) of the polymers were calculated with reference to a universal calibration vs. polystyrene standards (limits $M_w = 200$ to 400,000 g/mol). Calorimetric measurements were performed using a Discovery DSC25 from TA instruments, under a nitrogen flow, calibrated with Indium. Thermogravimetric analysis (TGA) data were obtained with a TGA55 from TA instruments, under a nitrogen flow.

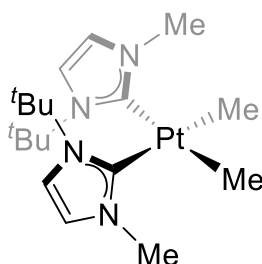
Synthesis of [Pt]_{Me}

Synthesis and characterization of 1-(*tert*-butyl)-3-(*iso*-propyl)-1*H*-imidazolium iodide, **tBuMe·HI**



2 g (16 mmol) of 1-(*tert*-butyl)-1*H*-imidazol and 1.3 mL of methyl iodide (2.28 g, 8.5 mmol) were dissolved in a J. Young flask, under argon, in 10 mL of toluene and sealed. The mixture was heated at 100 °C for 18 h, cooled down and the resulting white solid was filtered off and washed with diethyl ether (3 x 10 mL) and THF (10 mL). 3.86 g (90 % yield) of an analytically pure white solid was obtained. NMR spectroscopic data was identical to that reported previously.⁶

⁶ R. Corberán, M. Sanaú, E. Peris, *Organometallics* **2006**, 25, 4002–4008.

Synthesis and characterization of complex *cis*-[Pt(CH₃)₂(I^tBuMe)₂].

1-(*tert*-butyl)-3-(methyl)-1*H*-imidazolium iodide, I^tBuMe·HI (0.8 g, 3.0 mmol) and ^tBuOK (0.37 g, 3.3 mmol) were mixed in a J. Young flask and suspended, under argon at – 30 °C, in 7 mL of dry THF. The mixture was stirred for 10 min at this temperature and for 2h at rt. Thereafter, the mixture was cooled to – 30 °C and a solution of complex [Pt(CH₃)₂(cod)] (0.5 g, 1.5 mmol) in 3 mL of THF was added slowly via cannula. The mixture was left to reach rt and stirred for 1h. The solvent was then removed under vacuum and the residue was suspended in 10 mL of pentane. Pentane was then evaporated and complex *cis*-[Pt(CH₃)₂(I^tBuMe)₂] was extracted with 10 + 5 mL of toluene, filtering it via cannula. The solvent was removed under vacuum yielding a viscous oil. Pentane (10 mL) was added and the suspension was vigorously stirred until a white precipitate appears. The solid was filtered off yielding a white solid. 0.47 g (62 % yield) of complex *cis*-[Pt(CH₃)₂(I^tBuMe)₂] were obtained.

¹H-NMR (400 MHz, C₆D₆, 298 K): δ 6.49 (br, z, 2H, =CH), 6.22 (br, 2H, =CH), 3.93 (s, 3H, N-CH₃), 1.53 (s, 18H, C(CH₃)₃), 0.79 (s+d, *J*_{Pt,H} = 63 Hz, 6H, Pt-CH₃).

¹³C{¹H}-NMR (100 MHz, C₆D₆, 298 K): δ 189.2 (s + d, ¹*J*_{Pt,C} = 846, Hz Pt=C), 119.0 (s + d, ³*J*_{Pt,C} = 20 Hz, =CH), 116.5 (s + d, ³*J*_{Pt,C} = 26 Hz, =CH), 57.1 (C(CH₃)₃), 38.31 (s + d, ³*J*_{Pt,C} = 47 Hz, N-CH₃), 30.1 (C(CH₃)₃), –9.5 (s + d, ¹*J*_{Pt,C} = 580 Hz, Pt-CH₃).

Elem. Anal. Calcd. for C₁₈H₃₄N₄Pt: C, 43.10; H, 6.83; N, 11.17. Found: C, 42.9; H, 6.2; N, 11.1.

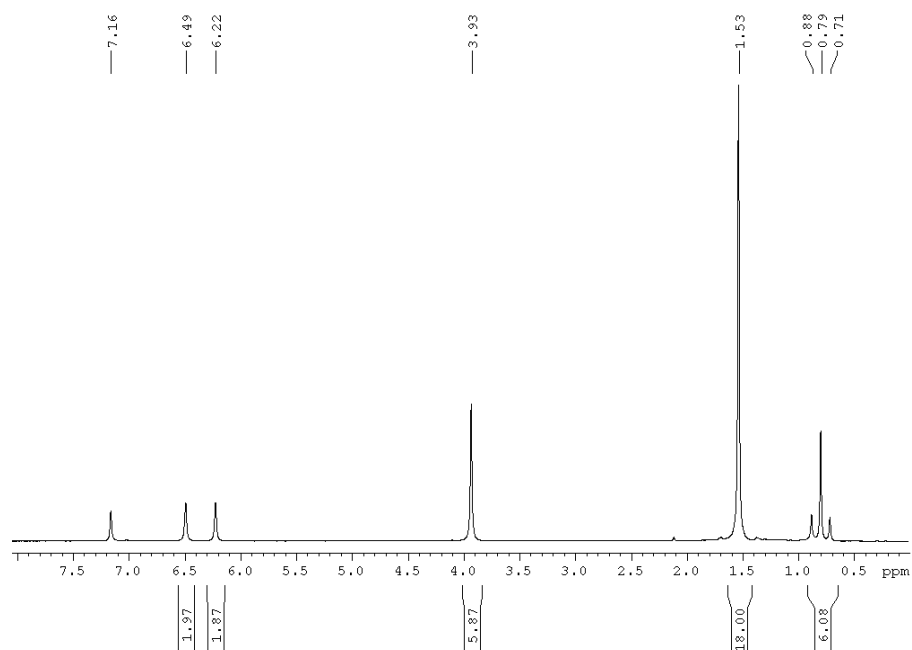


Figure S1. ^1H NMR spectrum of *cis*-[Pt(CH₃)₂(I'BuMe)₂] (C₆D₆, 400 MHz).

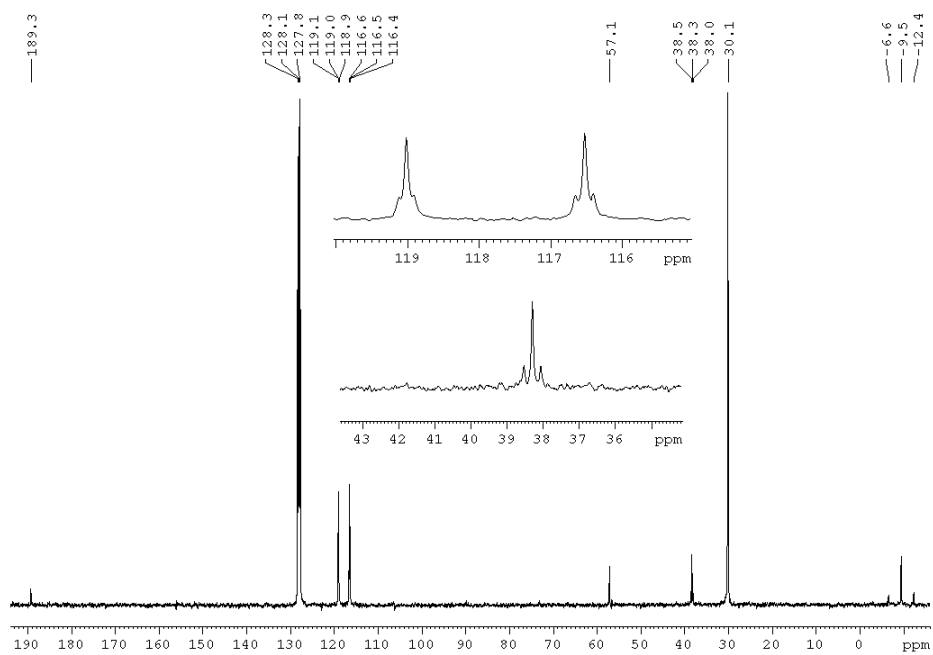
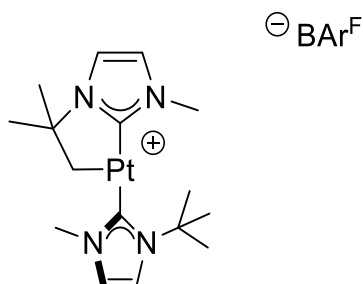


Figure S2. $^{13}\text{C}\{^1\text{H}\}$ NMR spectrum of *cis*-[Pt(CH₃)₂(I'BuMe)₂] (C₆D₆, 100 MHz).

Synthesis and characterization of complex $[\text{Pt}(\text{I}^t\text{BuMe})'(\text{I}^t\text{BuMe})][\text{BAr}^{\text{F}}]$.



Complex *cis*- $[\text{Pt}(\text{CH}_3)_2(\text{I}^t\text{BuMe})_2]$ (260 mg, 0.52 mmol) and $\text{H}(\text{OEt}_2)_2 \cdot \text{BAr}^{\text{F}}$ (525 mg, 0.52 mmol) were dissolved in 5 mL of CH_2Cl_2 , under argon, at -78°C . After 5 minutes, the cold bath was removed allowing the flask to reach room temperature. After 30 minutes, the solvent was evaporated under vacuum. The resulting yellow solid was washed twice with 12 mL of pentane, re-dissolved in CH_2Cl_2 (6 mL) and evaporated under vacuum in order to remove the remaining diethyl ether. This last process (dissolution/evaporation in CH_2Cl_2) was repeated leading to a pale yellow thin powder that was dried under vacuum for 2h yielding complex $[\text{Pt}(\text{I}^t\text{BuMe})(\text{I}^t\text{BuMe})][\text{BAr}^{\text{F}}]$ (606 mg, 88% yield). Complex $[\text{Pt}(\text{I}^t\text{BuMe})(\text{I}^t\text{BuMe})][\text{BAr}^{\text{F}}]$ can be stored in a glove-box or under an inert atmosphere indefinitely.

$^1\text{H-NMR}$ (400 MHz, CD_2Cl_2 , 298 K): δ 7.76 (br, 8H, $\text{H}_{ortho}\text{-BAr}^{\text{F}}$), 7.60 (br, 4H, $\text{H}_{para}\text{-BAr}^{\text{F}}$), 7.18 and 6.99 (d, $^3J_{\text{H,H}} = 1.9$ Hz, 1H each, =CH), 6.93-6.90 (br, 2H, =CH), 4.04 and 3.67 (s, 3H each, N- CH_3), 2.60 (s+d, $^2J_{\text{Pt,H}} = 105$ Hz, 2H, Pt- CH_2), 1.81 (s, 9H, $(\text{CH}_3)_3$), 1.47 (s, 6H, 2 CH_3).

$^{13}\text{C}\{^1\text{H}\}\text{-NMR}$ (100 MHz, CD_2Cl_2 , 298 K): δ 174.9 and 170.8 (Pt=C), 162.2 (q, $J_{\text{C,B}} = 50$ Hz, $\text{C}_{ipso}\text{-BAr}^{\text{F}}$), 135.2 (br, $\text{C}_{ortho}\text{-BAr}^{\text{F}}$), 129.2 (br q, $J_{\text{C,F}} = 31$ Hz, $\text{C}_{meta}\text{-BAr}^{\text{F}}$), 124.9 (q, $J_{\text{C,F}} = 272$ Hz, $\text{CF}_3\text{-BAr}^{\text{F}}$), 122.9 (s+d, $^3J_{\text{Pt,C}} = 26$ Hz, =CH), 122.3 (s+d, $^3J_{\text{Pt,C}} = 32$ Hz, =CH), 119.9 (s+d, $^3J_{\text{Pt,C}} = 38$ Hz, =CH), 117.9 (br, $\text{C}_{para}\text{-BAr}^{\text{F}}$), 116.0 (s+d, $^3J_{\text{Pt,C}} = 58$ Hz, =CH), 65.4 (s+d, $^3J_{\text{Pt,C}} = 40$ Hz, $\underline{\text{C}}(\text{CH}_3)_3$), 59.5 ($\underline{\text{C}}(\text{CH}_3)_3$), 39.3 (s+d, $^3J_{\text{Pt,C}} = 34$ Hz, N- CH_3), 37.1 (N- CH_3), 31.2 ($\text{C}(\underline{\text{C}}\text{H}_3)_3$), 30.2 (s+d, $^3J_{\text{Pt,C}} = 50$ Hz, 2 CH_3), 20.5 (s+d, $^1J_{\text{Pt,C}} = 880$ Hz, Pt- CH_2).

Elem. Anal. Calcd. for $\text{C}_{48}\text{H}_{39}\text{BF}_{24}\text{N}_4\text{Pt}$: C, 43.23; H, 2.95; N, 4.20. Found: C, 42.8; H, 3.2; N, 4.1.

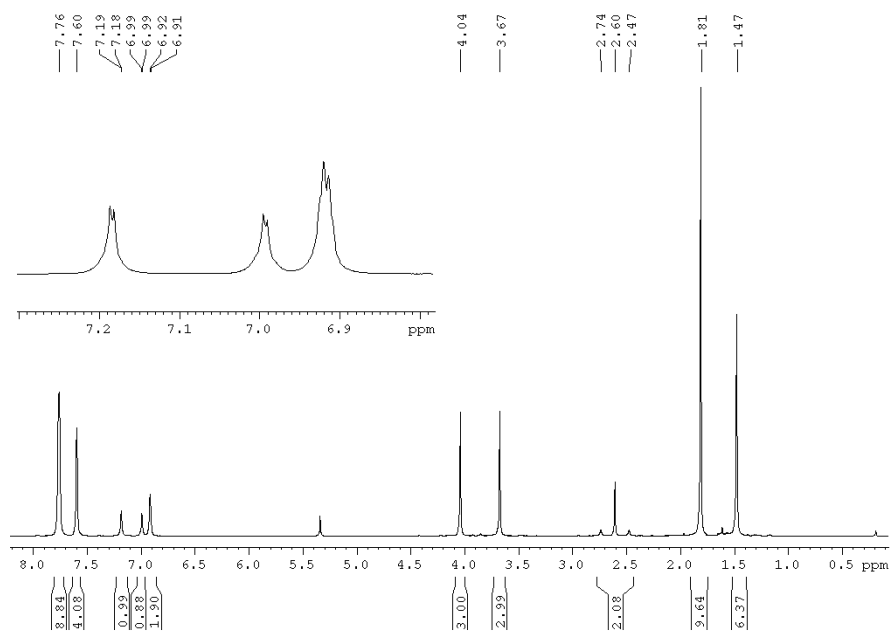


Figure S3. ¹H NMR spectrum of [Pt(I'BuMe)'(I'BuMe)][BAR^F] (CD₂Cl₂, 400 MHz).

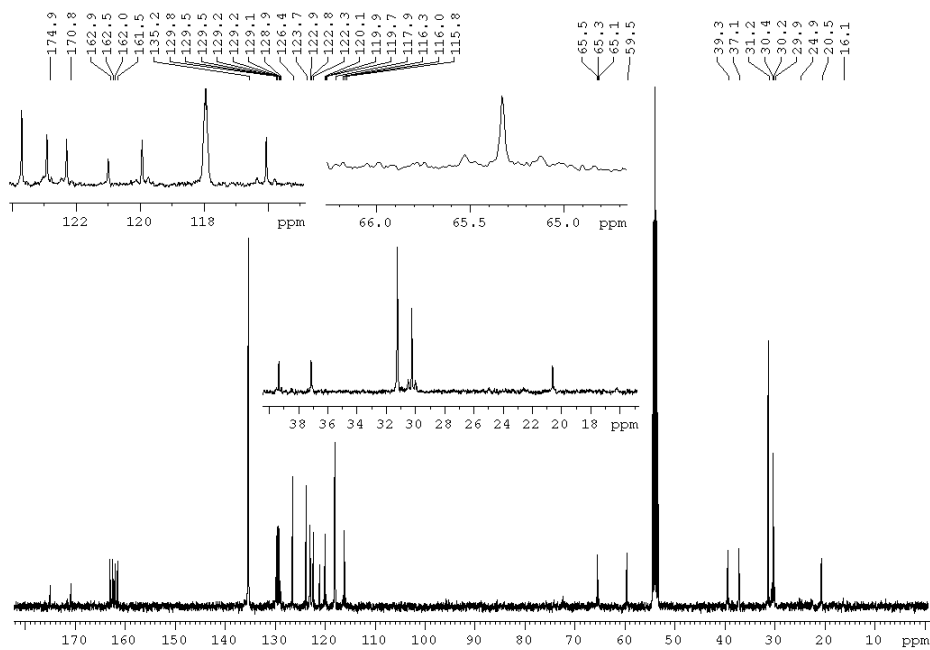
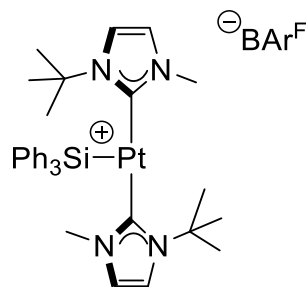


Figure S4. ¹³C{¹H} NMR spectrum of [Pt(I'BuMe)'(I'BuMe)][BAR^F] (CD₂Cl₂, 100 MHz).

Synthesis and characterization of complex [Pt(SiPh₃)(I'BuMe)₂][BAr^F], ([Pt]_{Me}).

Complex [Pt(I'BuMe')(I'BuMe)][BAr^F] (200 mg, 0.15 mmol) and Ph₃SiH (50 mg, 0.19 mmol) were dissolved in CH₂Cl₂ (5 mL) under argon, and the mixture was stirred for 2 h at rt. Evaporation of the solvent and washing with dry pentane (2 x 5 mL) yielded complex [Pt]_{Me} as a bright yellow solid (190 mg, 79% yield).



¹H-NMR (400 MHz, CD₂Cl₂, 298 K): δ 7.72 (br, 8H, H_{ortho}-BAr^F), 7.56 (br, 4H, H_{para}-BAr^F), 7.35-7.28 (m, 9H, Ph), 7.22-7.17 (m, 6H, Ph), 7.15 (d, ³J_{H,H} = 2.1 Hz, 2H, =CH), 6.63 (d, ³J_{H,H} = 2.1 Hz, 2H, =CH), 3.25 (s, 6H, N-CH₃), 1.84 (s, 18 H, C(CH₃)₃).

¹³C{¹H}-NMR (100 MHz, CD₂Cl₂, 298 K): δ 176.9 (Pt=C), 162.2 (q, J_{C,B} = 50 Hz, C_{ipso}-BAr^F), 137.5 (C_{ipso}-Ph), 136.5 (Ph), 135.3 (br, C_{ortho}-BAr^F), 129.8 and 127.8 (Ph), 129.4 (br q, J_{C,F} = 31 Hz, C_{meta}-BAr^F), 125.1 (q, J_{C,F} = 272 Hz, CF₃-BAr^F), 122.3 and 120.7 (s+d, =CH), 117.9 (br, C_{para}-BAr^F), 59.7 (C(CH₃)₃), 39.9 (N-CH₃), 33.3 (C(CH₃)₃).

Elem. Anal. Calcd. for C₆₆H₅₅BF₂₄N₄PtSi: C, 49.73; H, 3.48; N, 3.51. Found: C, 50.1; H, 3.7; N, 3.4.

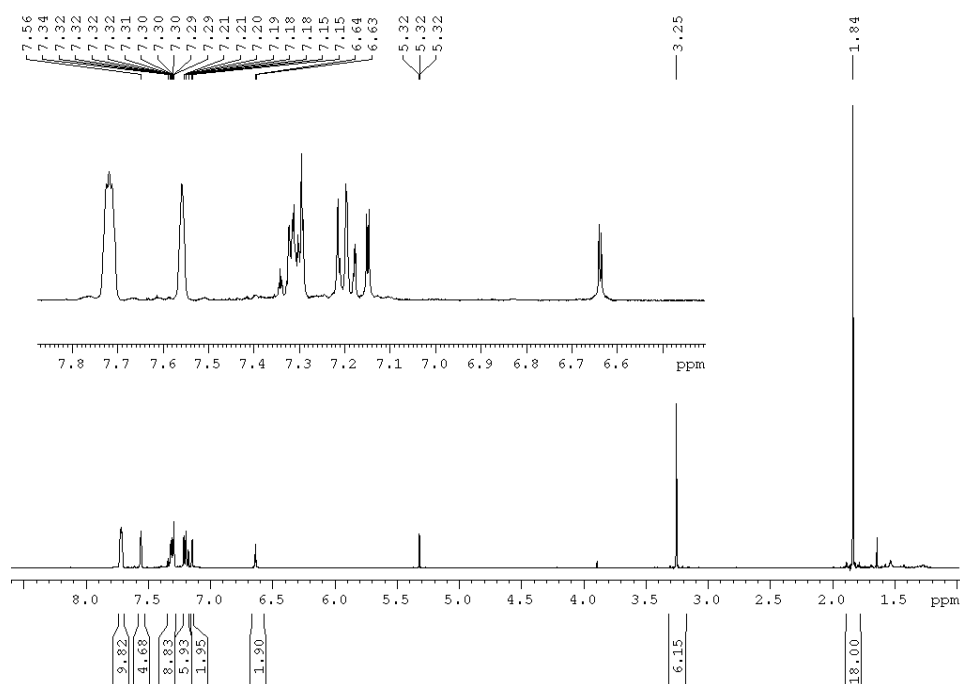


Figure S5. ¹H NMR spectrum of [Pt(SiPh₃)(I'BuMe)₂][BAR^F], ([Pt]_{Me}) (CD₂Cl₂, 400 MHz).

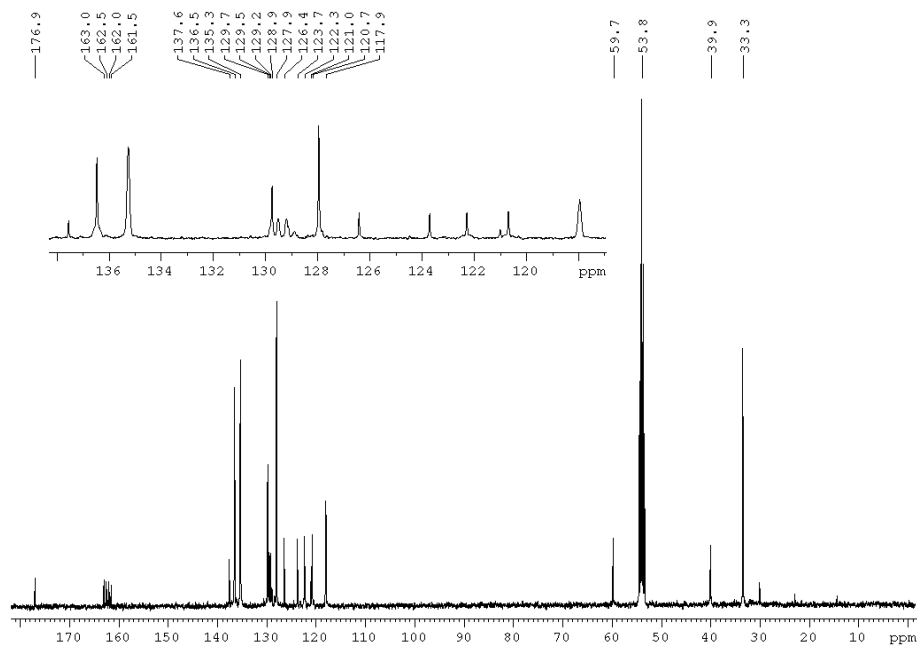


Figure S6. ¹³C{¹H} NMR spectrum of [Pt(SiPh₃)(I'BuMe)₂][BAR^F], ([Pt]_{Me}) (CD₂Cl₂, 100 MHz).

Polymerization procedure

Inside the glovebox, a stock solution of the desired Pt(II) catalyst (*e.g.* [Pt]_{Me}, 5.4 mg, 3.39 μmol) in the selected dry solvent (*e.g.* MeTHF, 900 μL) is prepared. A precise amount of this stock solution is added to a dry Schlenk tube (*e.g.* 150 μL for a 500 ppm catalyst loading) and some dry solvent is added to reach the desired concentration (*e.g.* 150 μL for [MePhSiH₂] = 2 mol/L). A precise amount of the selected silane is then added (*e.g.* MePhSiH₂, 138.6 mg, 1.134 mmol) and the solution is stirred for 1 minute at room temperature. Then, a precise amount of the desired hydroxyaldehyde (*e.g.* HMF, 143 mg, 1.134 mmol) is weighed and added to the Schlenk tube, stirred at room temperature for 20h. The H₂ produced is released from the reactor, while being maintained under Argon (most of the H₂ evolution is observed at the onset of the reaction). A slight increase of viscosity is also generally observed. Then, the reaction medium is put under static vacuum and heated to 50°C for 4 additional hours. After this 24h total reaction time, the Schlenk tube is cooled down in an ice bath and the reaction medium is exposed to air. Solvent is removed under vacuum, yielding a colorless sticky paste. A minimal amount of dichloromethane (*e.g.* 300 μL) is added to completely dissolve the crude product. This solution is then added dropwise to a solution of pentane at -10°C (*e.g.* 20 mL), which precipitates the polymer. The supernatant was removed and the obtained solid was dried under vacuum.

Degradation procedure

Under atmospheric conditions, 20 mg of the desired polymers are added to a dry Schlenk tube and dissolved in 2.0 mL of HPLC-grade THF. The desired nucleophilic degrading agent is then added, and the solution is stirred at 30°C for 24h. Small aliquots are regularly taken, dried under vacuum and analyzed by SEC-RI. Refractive index was preferred to light scattering in that case, because light scattering requires precise concentration of purified polymers to be accurate. The results are all presented in relative loss of M_w , which makes up for the inaccuracy of the RI method due to calibration with polystyrene standards.

Nucleophilic degrading agents:

Methanolysis: 0.5 mL of MeOH; Acid hydrolysis: 40 μ L of a HCl/H₂O solution (pH = 2); Acid methanolysis: 40 μ L of a (HCl/Et₂O)/MeOH solution (pH = 2).

Recycling procedure

Same as the degradation procedure.

Nucleophilic recycling agents:

Acid hydrolysis: 40 μ L of a HCl/H₂O solution (pH = 2); Acid methanolysis: 200 μ L of a (HCl/Et₂O)/MeOH solution (pH = 2) for poly(HMF-*co*-MePhSiH₂), 500 μ L of a (HCl/Et₂O)/MeOH solution (pH = 2) for poly(Vanillin-*co*-MePhSiH₂).

Table S1. Catalytic synthesis of HMF-containing PSEs with different Pt(II) catalysts.^[a]

Entry	Catalyst	Hydroxyaldehyde or diol	Silane	Isolated yield	M_n^{LS} (g/mol) ^[b]	\bar{D}	M_n^{RI} (g/mol) ^[c]	\bar{D}
1 ^[d]	[Pt] _{Me} (500 ppm)	HMF	MePhSiH ₂	87%	20 100	3.6	17 700	3.8
2	[Pt] _{Me} (0.1 mol%)	HMF	MePhSiH ₂	94%	36 300	7.5	21 300	7.3
3	[Pt] _{Me} (500 ppm)	HMF	MePhSiH ₂	90%	15 900	3.1	12 000	3.6
4	[Pt] _{Me} (500 ppm)	HMF	Ph ₂ SiH ₂	95%	16 600	3.5	7 900	3.7
5	[Pt] _{Me} (500 ppm)	HMF	Et ₂ SiH ₂	57%	13 200	3.5	15 300	3.6
6	[Pt] _{<i>t</i>Bu} (500 ppm)	HMF	MePhSiH ₂	70%	700	2.6	800	2.1
7	[Pt] _{<i>t</i>Bu} (0.1 mol%)	HMF	MePhSiH ₂	77%	20 200	2.3	1 300	1.8
8	[Pt] _{Me} (500 ppm)	Vanillin	MePhSiH ₂	74%	515	1.5	720	1.4

9	[Pt] _{Me} (500 ppm)	Syringaldehyde	MePhSiH ₂	81%	500	1.4	730	1.4
10	[Pt] _{tBu} (0.1 mol%)	Vanillin	MePhSiH ₂	77%	6 000	5.0	5 000	5.9
11	[Pt] _{tBu} (0.1 mol%)	Syringaldehyde	MePhSiH ₂	90%	3 800	1.7	1 900	2.1
12	[Pt] _{Me} (500 ppm)	D-Isosorbide	MePhSiH ₂	77%	14 400	2.9	2 300	5.1
13	[Pt] _{tBu} (0.1 mol%)	D-Isosorbide	MePhSiH ₂	88%	700	2.3	1 100	1.7

^[a] All reactions were performed under argon, with [Hydroxyaldehyde or diol] = [Disilane] = 2 mol/L. ^[b] M_n^{exp} and D of polymer determined by light scattering size exclusion chromatography in THF at 35°C. ^[c] M_n^{exp} and D of polymer determined by refractive index size exclusion chromatography in THF calibrated with polystyrene standards at 35°C. ^[d] Total time of reaction for this entry is 48h : 40h under argon atmosphere at room temperature, then 8h under static vacuum at 50°C.

Table S2. Molar mass of each polymer sample used for degradation study.

Entry	Polymer	M_w^{LS} (g/mol) ^[a]	D	M_w^{RI} (g/mol) ^[b]	D
1	poly(syringaldehyde- <i>co</i> -MePhSiH ₂)	6 200	1.7	4 100	2.1
2	poly(vanillin- <i>co</i> -MePhSiH ₂)	29 800	5.0	29 500	5.9
3	poly(vanillin- <i>co</i> -Ph ₂ SiH ₂)	151 000	4.7	36 600	10.2
4	poly(HMF- <i>co</i> -Ph ₂ SiH ₂)	57 500	3.5	28 900	3.7
5	poly(HMF- <i>co</i> -Et ₂ SiH ₂)	18 200	1.9	33 200	1.9
6	poly(HMF- <i>co</i> -MePhSiH ₂)	29 600	2.2	34 400	2.4

^[a] M_w^{exp} and D of polymer determined by light scattering size exclusion chromatography in THF at 35°C. ^[b] M_w^{exp} and D of polymer determined by refractive index size exclusion chromatography in THF calibrated with polystyrene standards at 35°C.

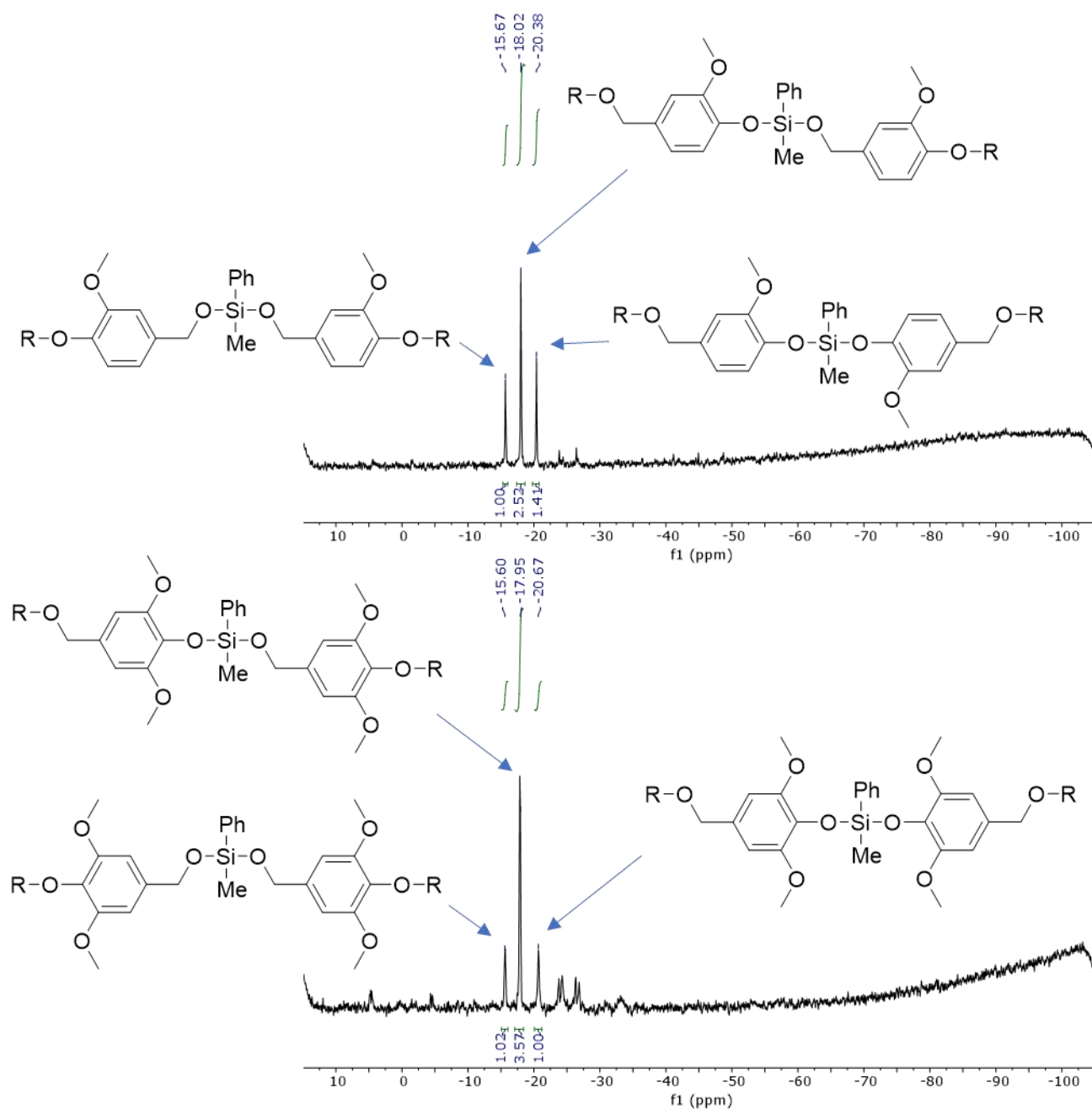


Figure S7. ^{29}Si NMR spectra of poly(Vanillin-co-MePhSiH₂) and poly(Syringaldehyde-co-MePhSiH₂) (CDCl₃, 99 MHz).

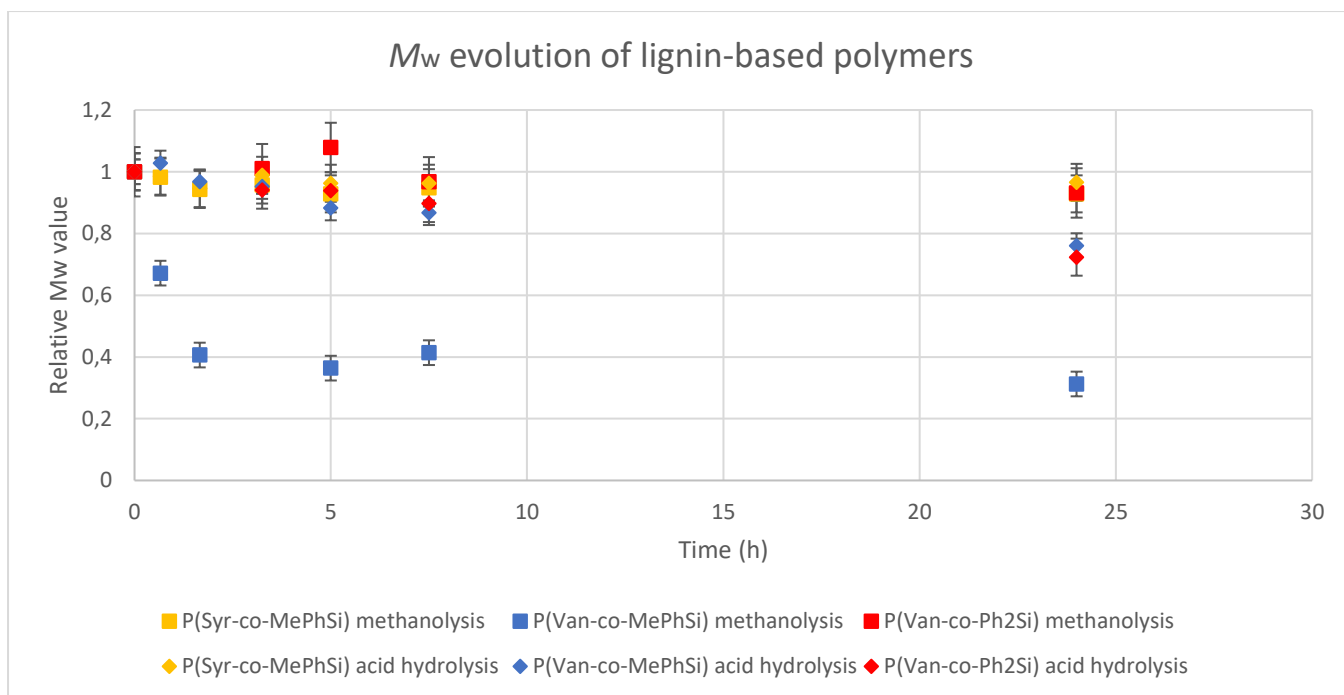


Figure S8. Degradation study of lignin-based PSEs showing the evolution of the relative M_w of the polymers over time, depending on the reaction conditions.

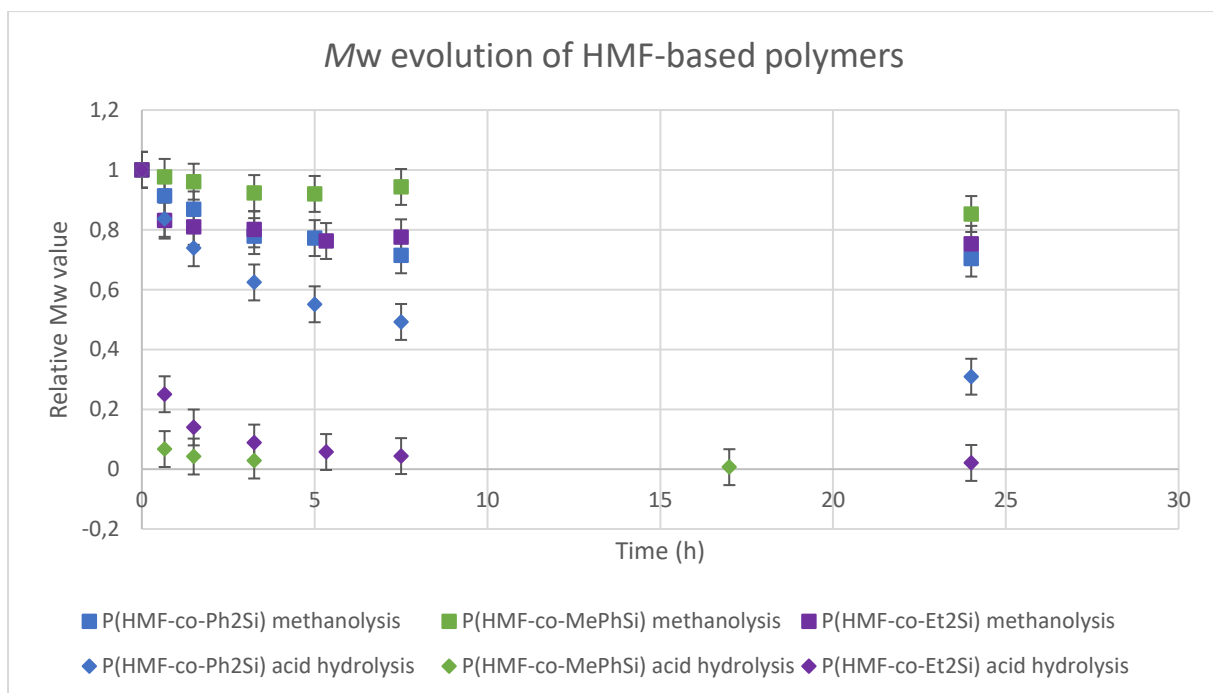


Figure S9. Degradation study of HMF-based PSEs showing the evolution of the relative M_w of the polymers over time, depending on the reaction conditions.

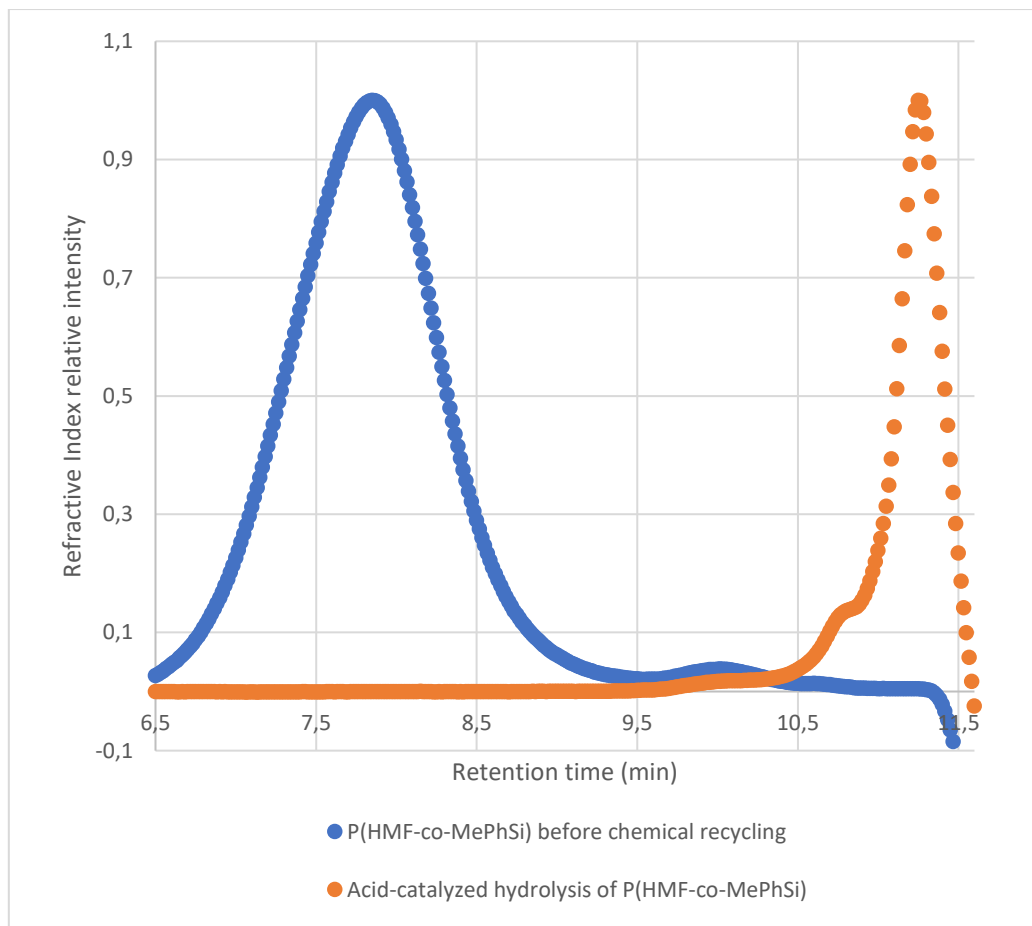


Figure S10. SEC-RI traces before and after the acid-catalyzed hydrolysis of poly(HMF-*co*-MePhSiH₂).

Chapter 4

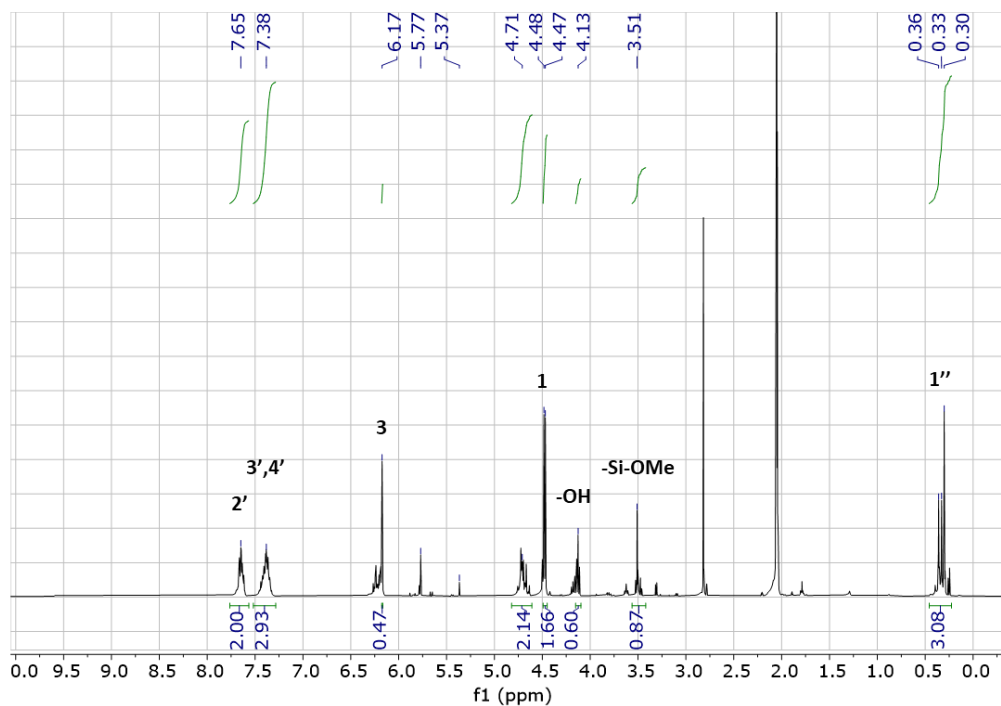
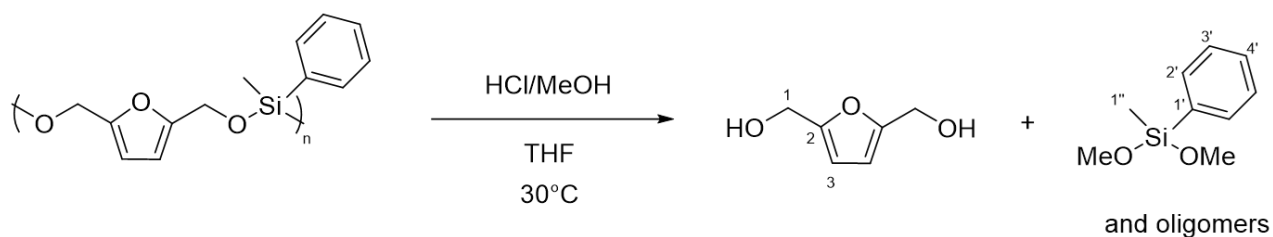


Figure S11. Scheme of the acid-catalyzed methanolysis of poly(HMF-coMePhSiH₂) and ¹H NMR spectrum of the crude after 7h at 30°C in THF (Acetone-*d*₆, 400 MHz).

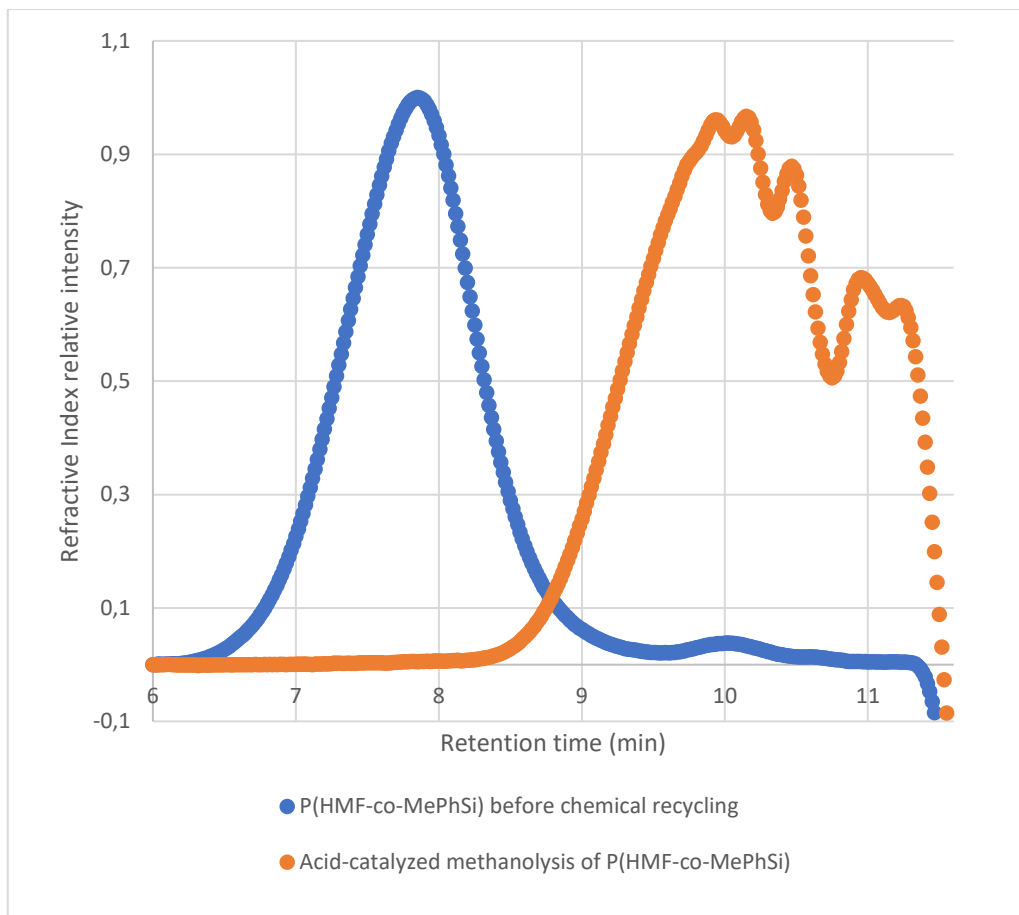


Figure S12. SEC-RI traces before and after the acid-catalyzed methanolysis of poly(HMF-*co*-MePhSiH₂).

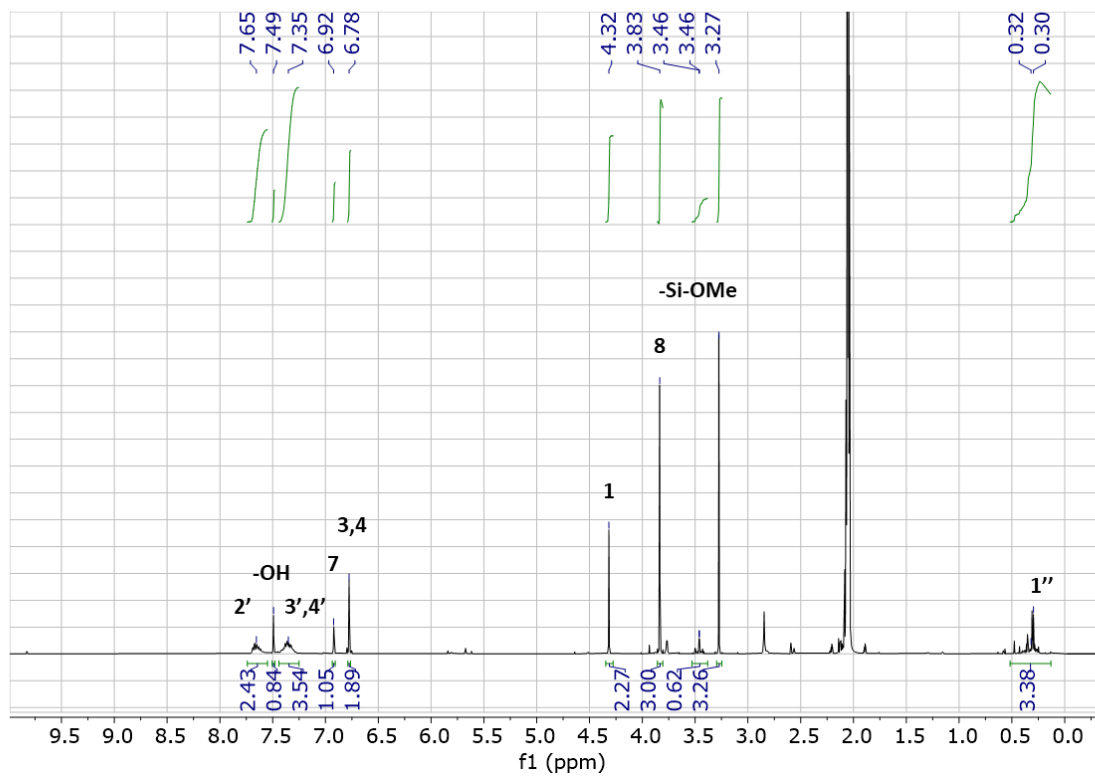
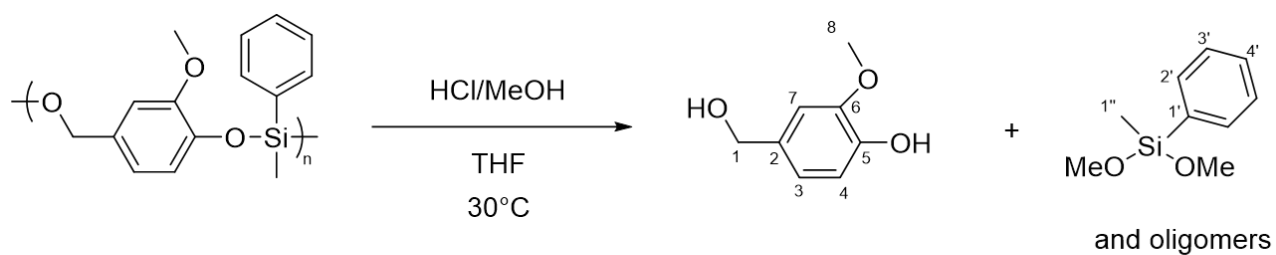


Figure S13. Scheme of the acid-catalyzed methanolysis of poly(Vanillin-coMePhSiH₂) and ¹H NMR spectrum of the crude after 14h at 30°C in THF (Acetone-*d*₆, 400 MHz).

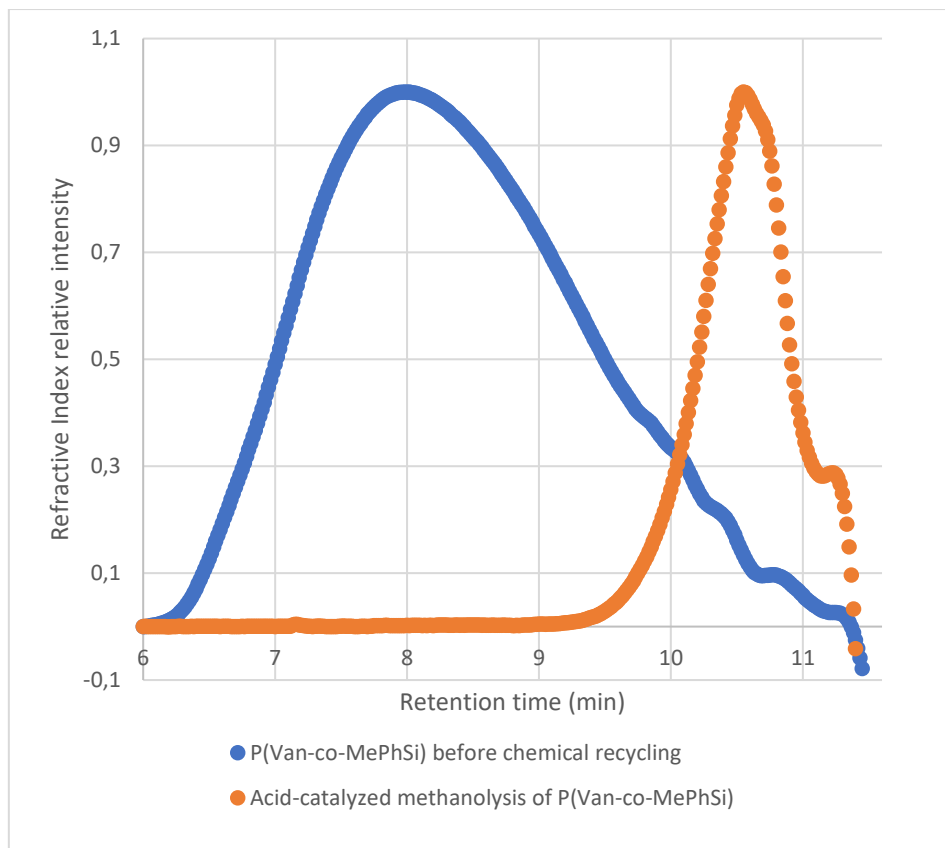
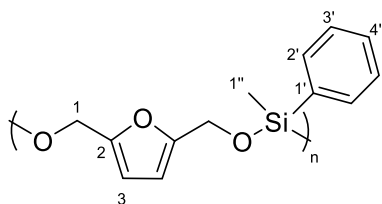


Figure S14. SEC-RI traces before and after the acid-catalyzed methanolysis of poly(Vanillin-*co*-MePhSiH₂).

NMR and IR characterization data of PSEs

Poly(HMF-co-MePhSiH₂):

Group	¹ H NMR (δ ppm)	¹³ C{ ¹ H} NMR (δ ppm)	²⁹ Si{ ¹ H} NMR (δ ppm)
1	4.78, 4.73	57.6	-
2	-	153.3	-
3	6.22	108.8	-
1'	-	133.7	-
2'	7.70	134.2	-
3'	7.48, 7.38	127.9	-
4'	7.48, 7.38	130.3	-
1''	0.45	-3.95	-
Si	-	-	-14.73

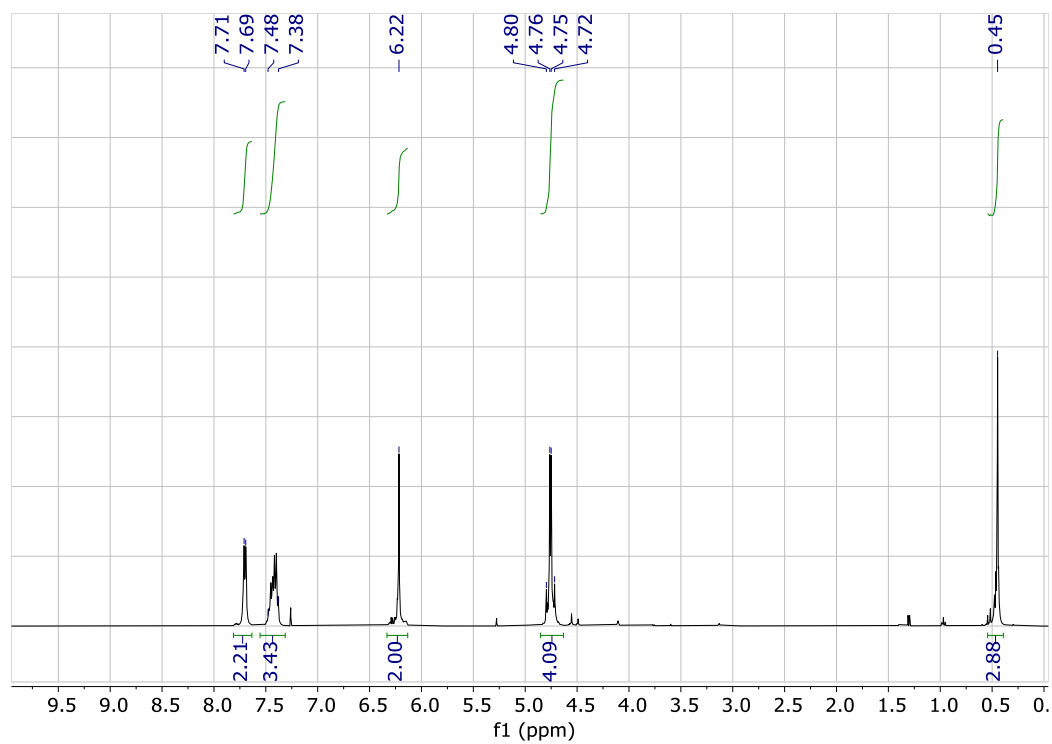


Figure S15. ^1H NMR spectrum of poly(HMF-co-MePhSiH₂) (CDCl₃, 400 MHz).

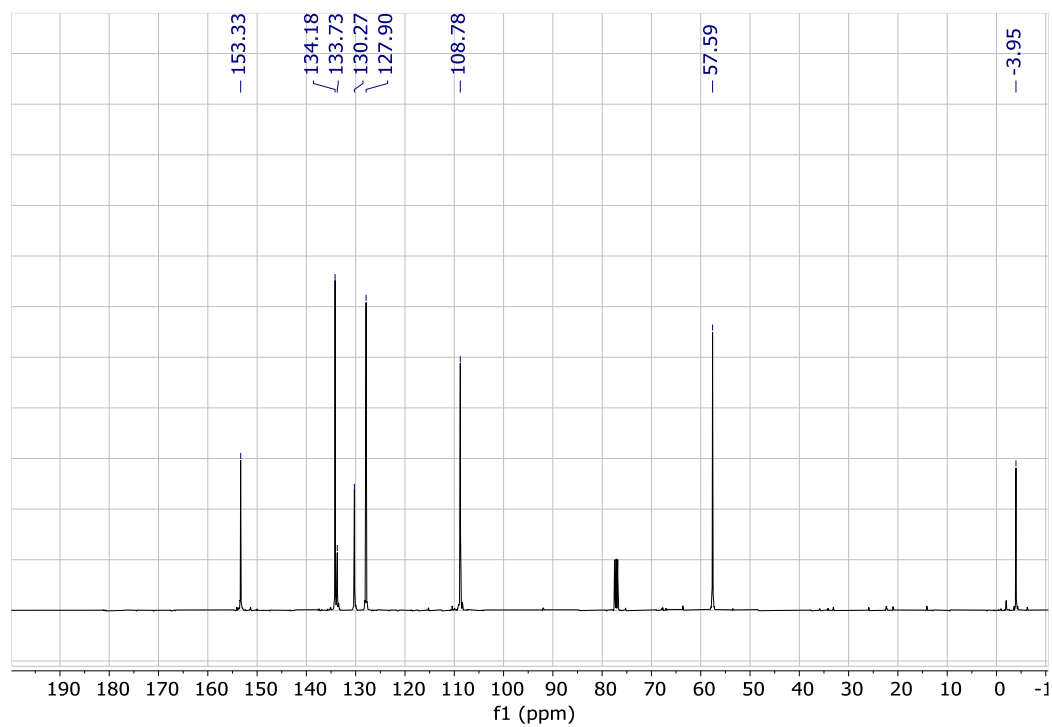


Figure S16. $^{13}\text{C}\{^1\text{H}\}$ NMR spectrum of poly(HMF-co-MePhSiH₂) (CDCl₃, 100 MHz).

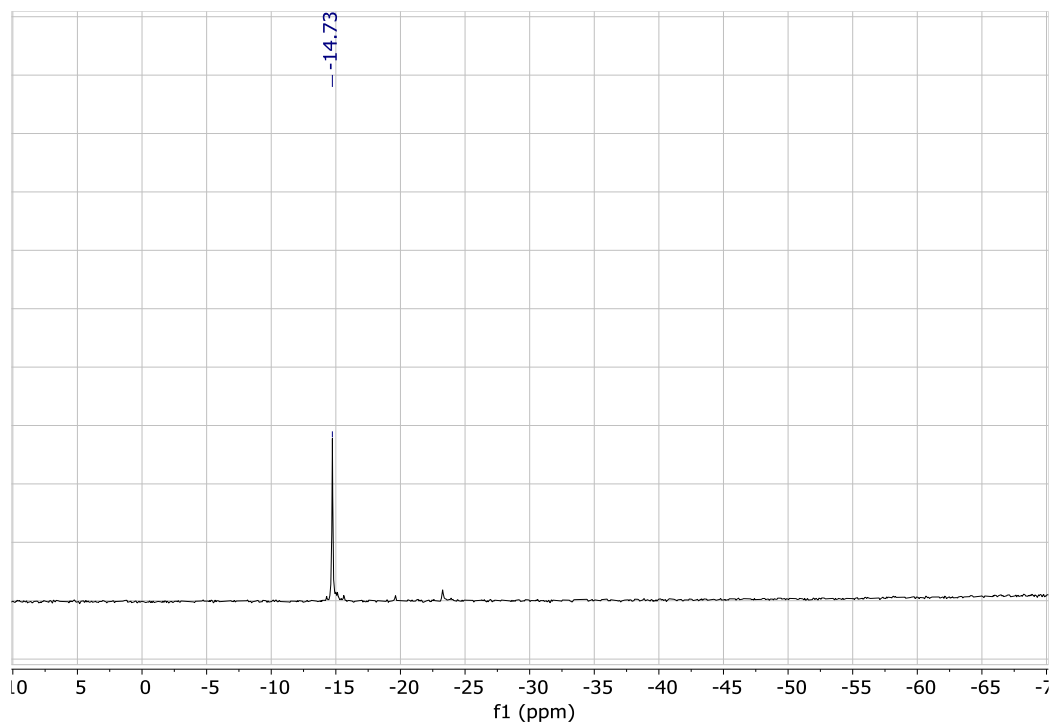


Figure S17. ^{29}Si NMR spectrum of poly(HMF-*co*-MePhSiH₂) (CDCl₃, 99 MHz).

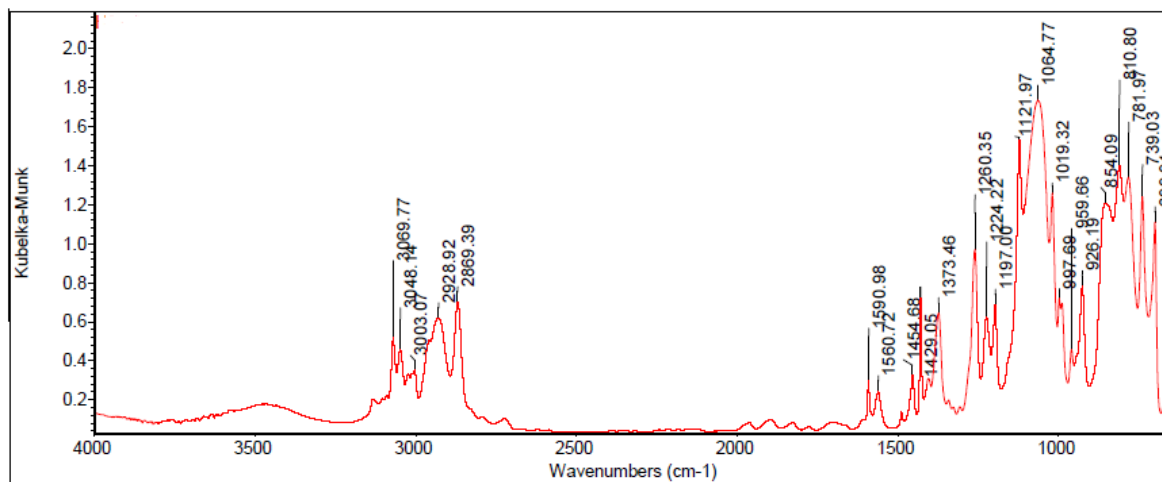
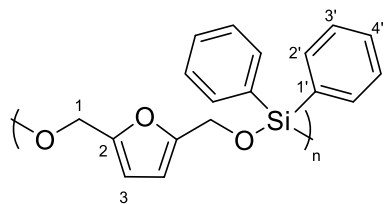


Figure S18. FT-IR spectrum of poly(HMF-*co*-MePhSiH₂).

Chapter 4

Poly(HMF-co-Ph₂SiH₂):



Group	¹ H NMR (δ ppm)	¹³ C{ ¹ H} NMR (δ ppm)	²⁹ Si{ ¹ H} NMR (δ ppm)
1	4.76	58.0	-
2	-	153.3	-
3	6.13	108.8	-
1'	-	132.1	-
2'	7.73	135.1	-
3'	7.36	127.9	-
4'	7.36	130.5	-
Si	-	-	-29.70

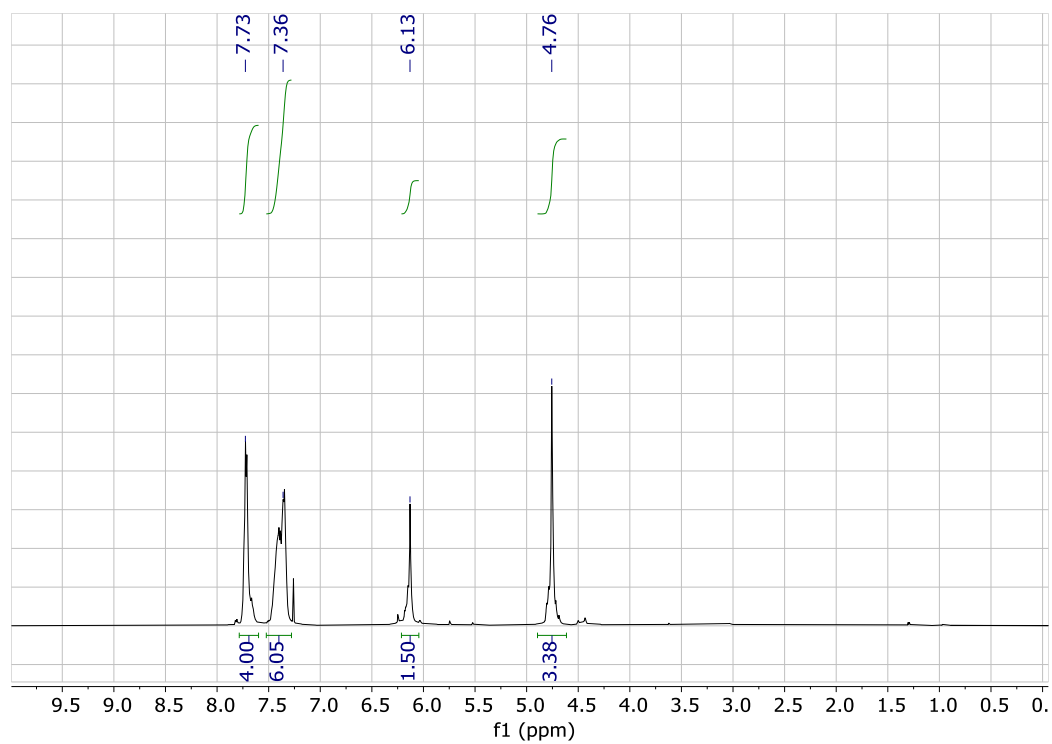


Figure S19. ^1H NMR spectrum of poly(HMF-co- Ph_2SiH_2) (CDCl_3 , 400 MHz).

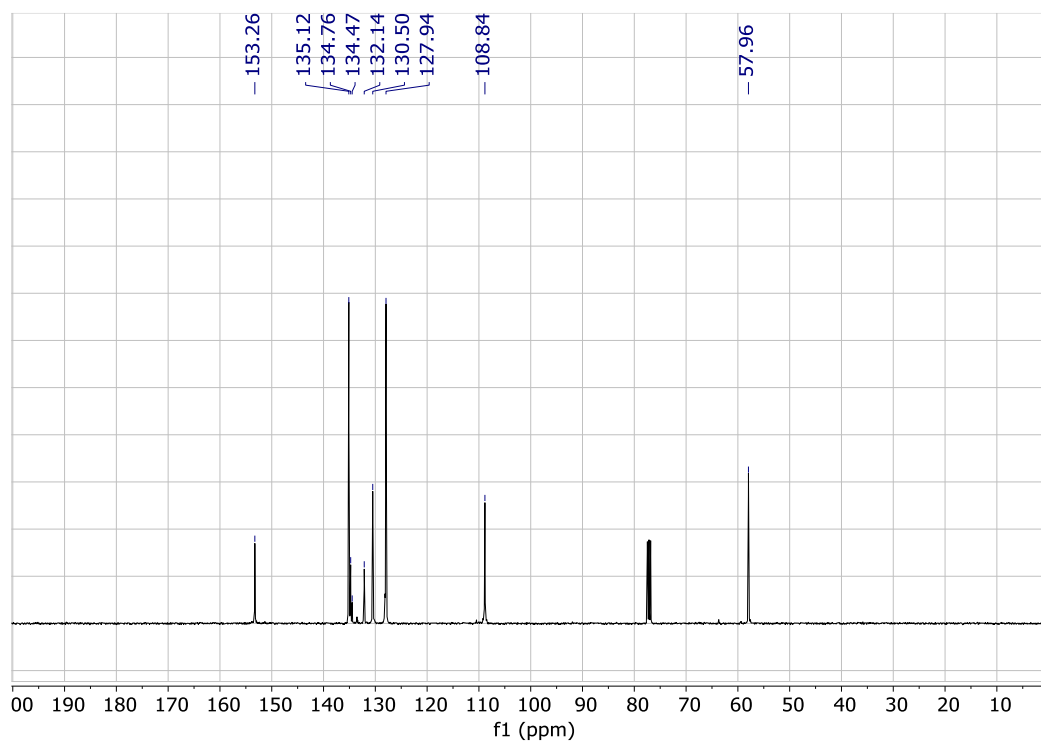


Figure S20. ^{13}C $\{^1\text{H}\}$ NMR spectrum of poly(HMF-co- Ph_2SiH_2) (CDCl_3 , 100 MHz).

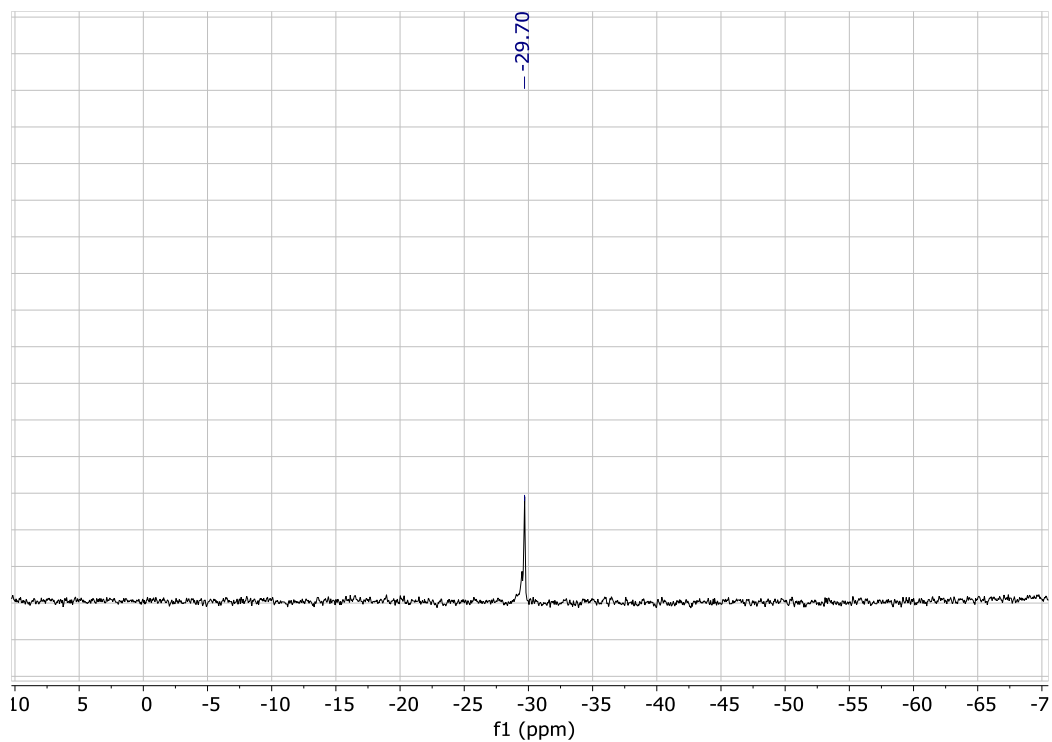


Figure S21. ^{29}Si NMR spectrum of poly(HMF-*co*- Ph_2SiH_2) (CDCl_3 , 99 MHz).

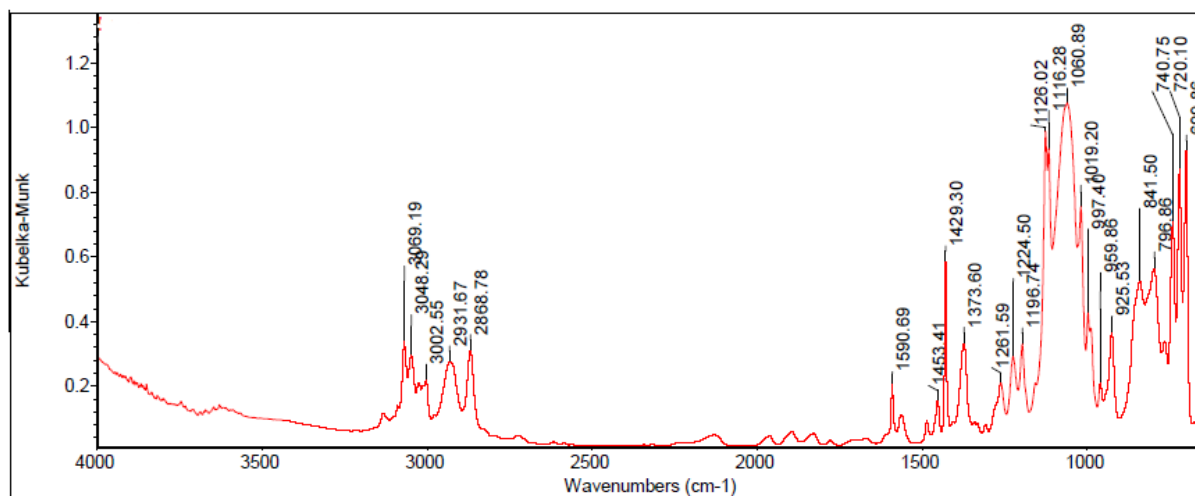
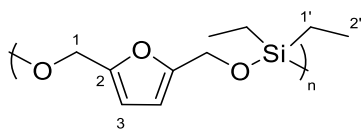


Figure S22. FT-IR spectrum of poly(HMF-*co*- Ph_2SiH_2).

Chapter 4

Poly(HMF-*co*-Et₂SiH₂):



Group	¹ H NMR (δ ppm)	¹³ C{ ¹ H} NMR (δ ppm)	²⁹ Si{ ¹ H} NMR (δ ppm)
1	4.66	57.4	-
2	-	153.7	-
3	6.19	108.5	-
1'	0.64	3.9	-
2'	0.94	6.4	-
Si	-	-	-1.31

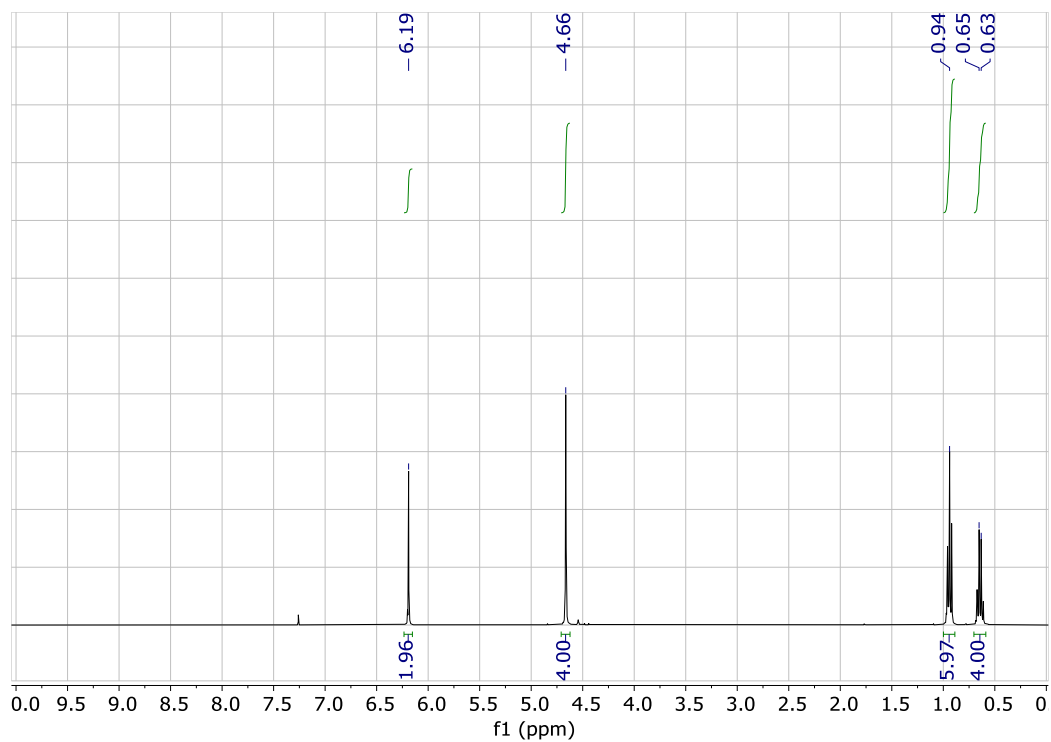


Figure S23. ¹H NMR spectrum of poly(HMF-*co*-Et₂SiH₂) (CDCl₃, 400 MHz).

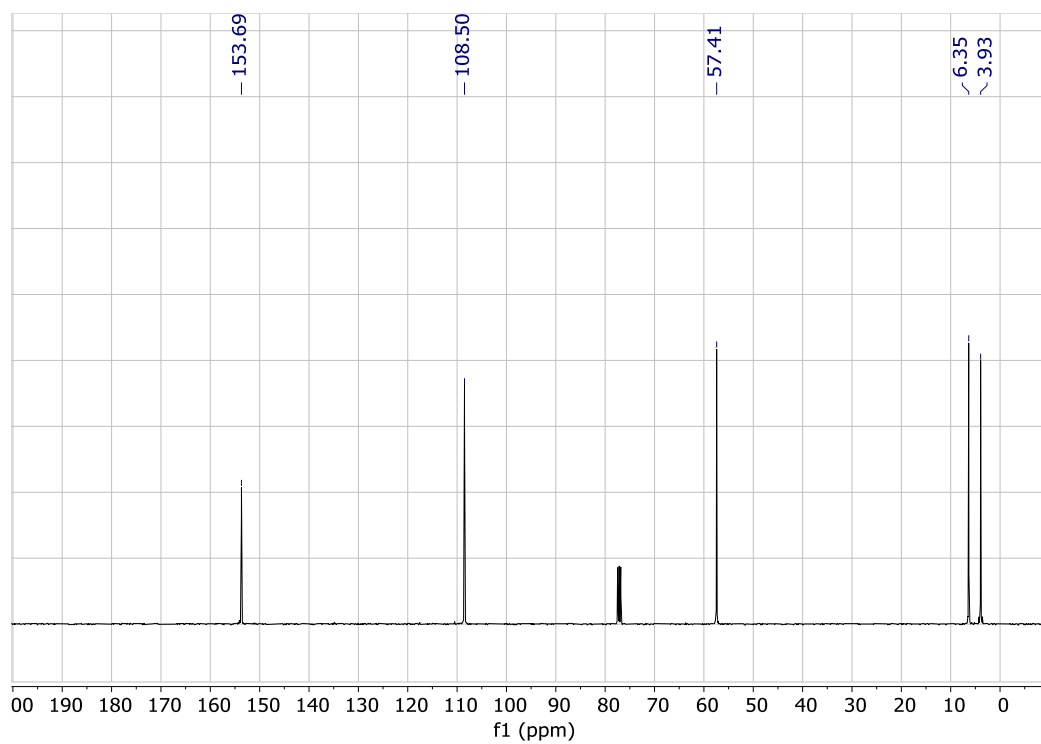


Figure S24. $^{13}\text{C}\{^1\text{H}\}$ NMR spectrum of poly(HMF-*co*-Et₂SiH₂) (CDCl₃, 100 MHz).

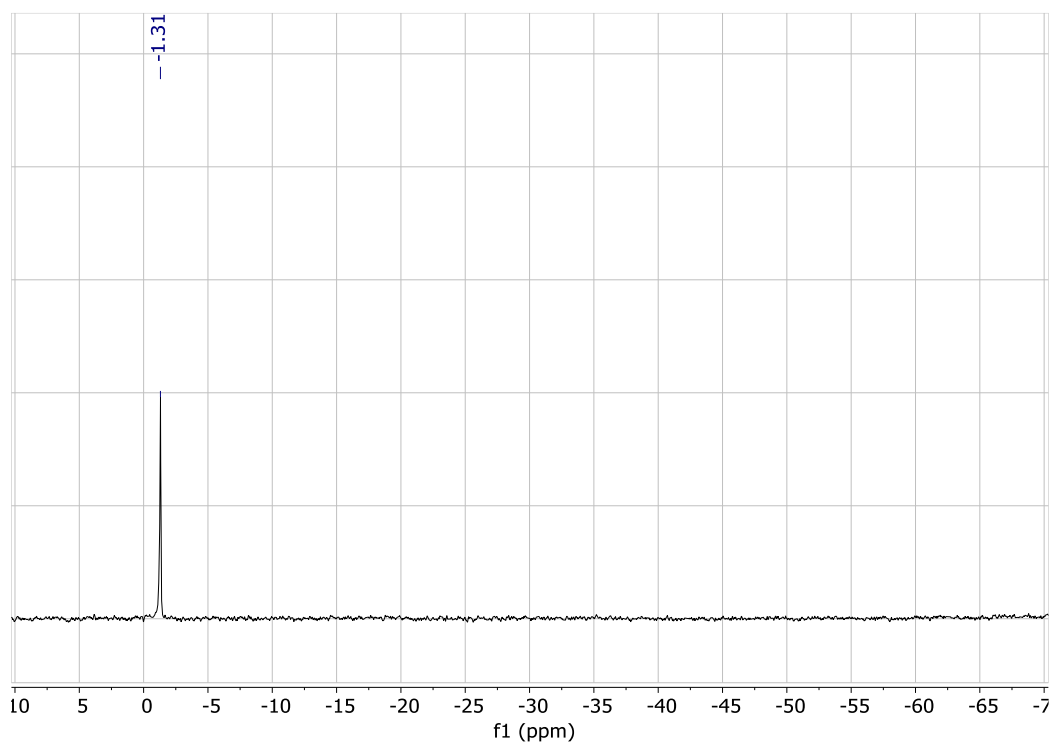


Figure S25. ^{29}Si NMR spectrum of poly(HMF-*co*-Et₂SiH₂) (CDCl₃, 99 MHz).

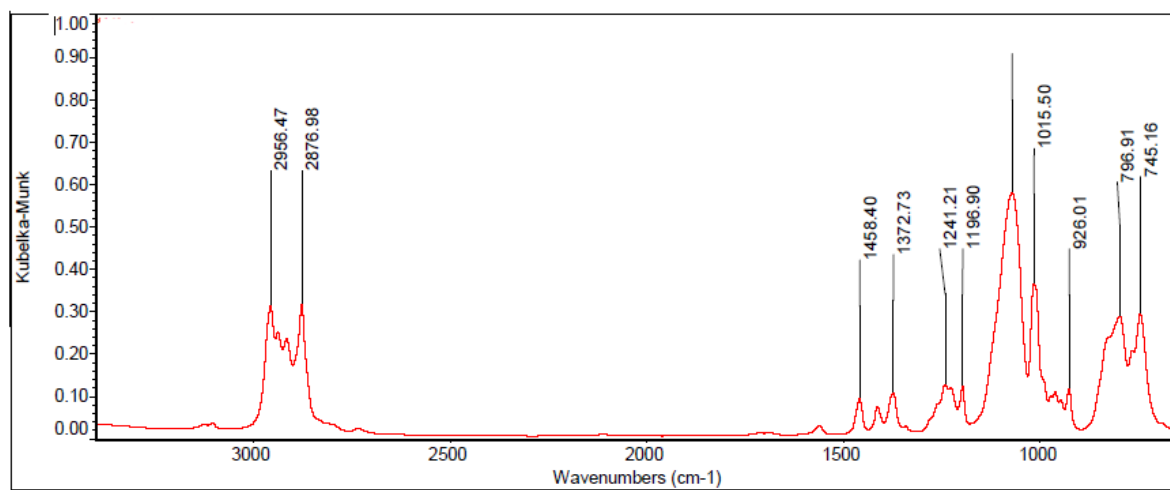
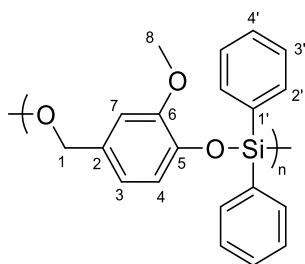


Figure S26. FT-IR spectrum of poly(HMF-*co*-Et₂SiH₂).

Poly(Vanillin-*co*-Ph₂SiH₂):

Group	¹ H NMR (δ ppm)	¹³ C{ ¹ H} NMR (δ ppm)	²⁹ Si{ ¹ H} NMR (δ ppm)
1	4.85 (HT), 4.73 (TT)	65.3 (HT), 65.1 (TT)	-
2	-	135.1	-
3	6.76	119.4	-
4	6.89	119.9	-
5	-	144.0	-
6	-	150.1	-
7	6.89, 6.76	111.2	-
8	3.51	55.4	-
1'	-	132.6	-
2'	7.69	134.6	-
3'	7.37	127.8	-
4'	7.37	130.4	-
Si	-	-	-30.51 (TT), -33.93 (HT), -37.63 (HH)

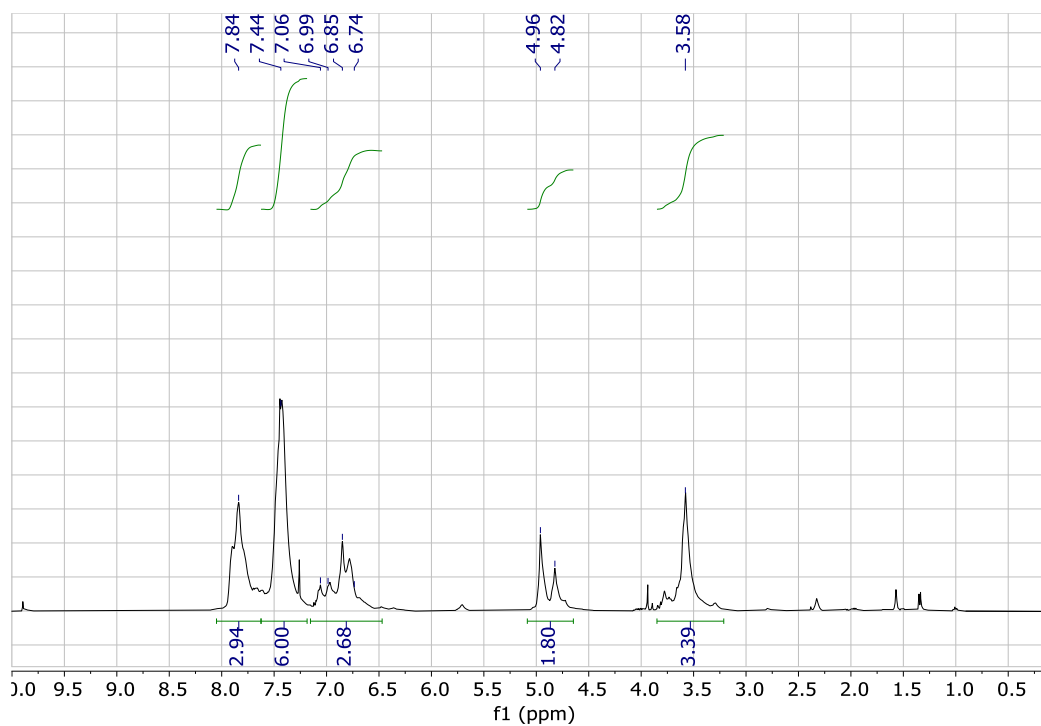


Figure S27. ¹H NMR spectrum of poly(Vanillin-*co*-Ph₂SiH₂) (CDCl₃, 400 MHz).

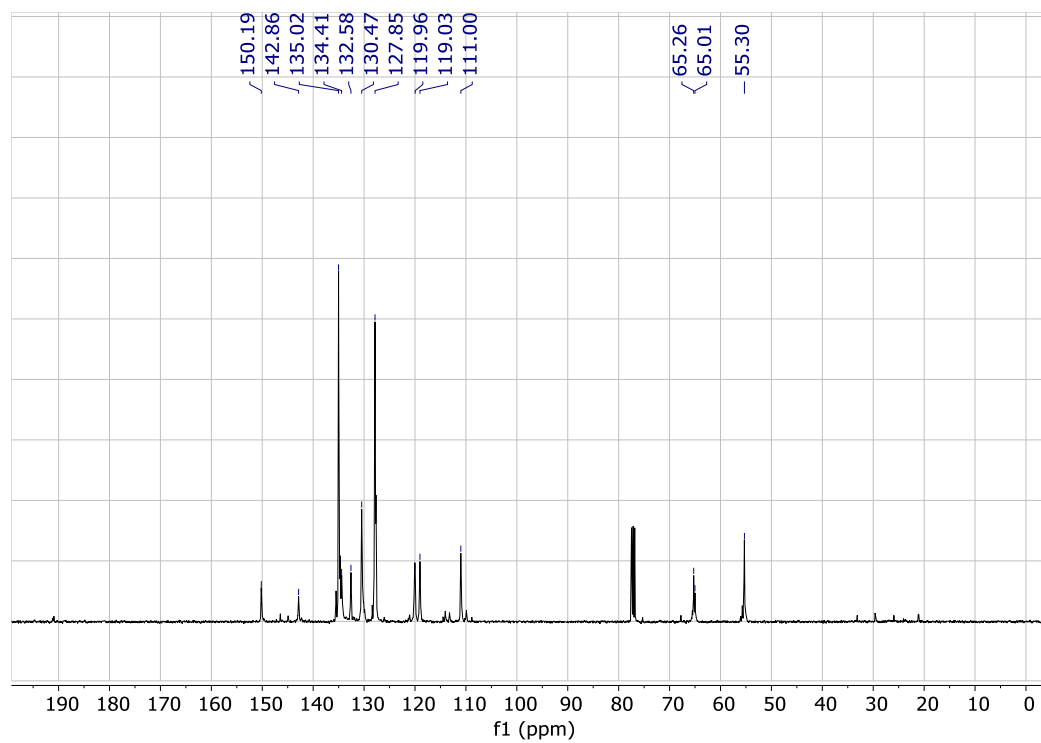


Figure S28. ¹³C {¹H} NMR spectrum of poly(Vanillin-*co*-Ph₂SiH₂) (CDCl₃, 100 MHz).

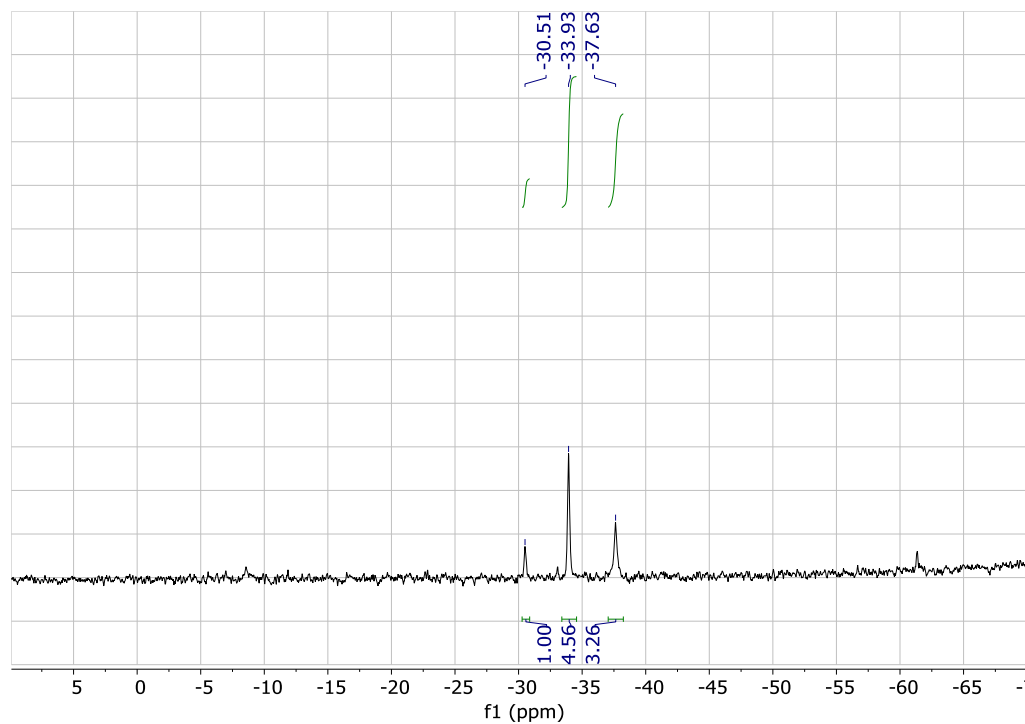


Figure S29. ^{29}Si NMR spectrum of poly(Vanillin-*co*- Ph_2SiH_2) (CDCl_3 , 99 MHz).

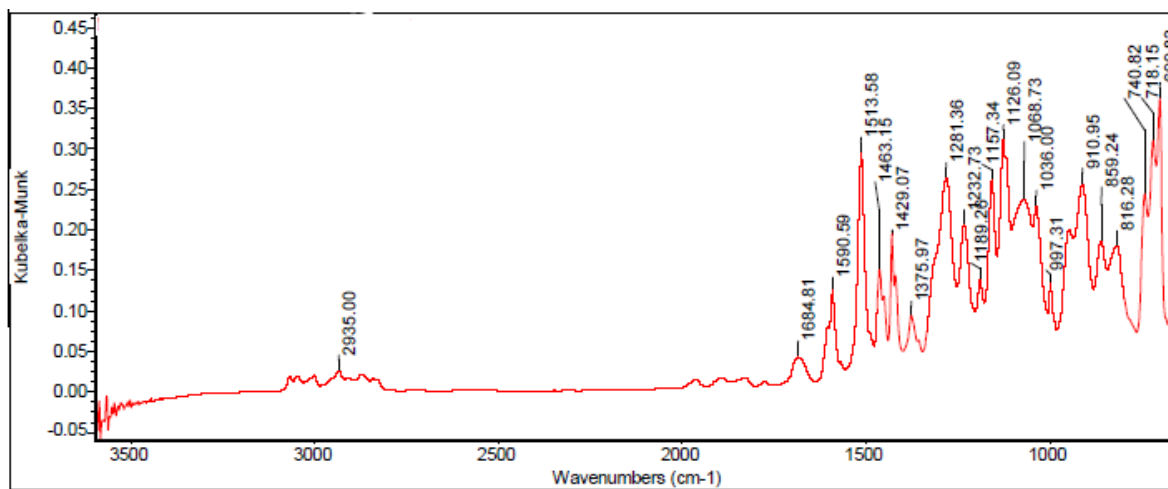
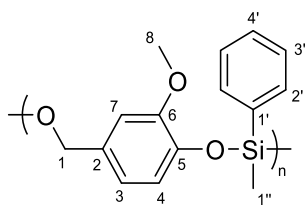


Figure S30. FT-IR spectrum of poly(Vanillin-*co*- Ph_2SiH_2).

Chapter 4

Poly(Vanillin-*co*-MePhSiH₂):



Group	¹ H NMR (δ ppm)	¹³ C{ ¹ H} NMR (δ ppm)	²⁹ Si{ ¹ H} NMR (δ ppm)
1	4.93 (HT), 4.82 (TT)	65.0 (HT), 64.8 (TT)	-
2	-	130.4	-
3	6.95; 6.82	120.4; 120.1	-
4	6.95; 6.82	119.2	-
5	-	143.0	-
6	-	150.2	-
7	7.09; 7.01	111.0	-
8	3.70	55.4	-
1'	-	132.6	-
2'	7.83	134.2; 134.1; 134.0	-
3'	7.45	128.0; 127.9; 127.7	-
4'	7.45	134.3	-
1''	0.65 (HH), 0.57 (HT), 0.49 (TT)	-3.36 (HH), -3.55(HT), -3.90 (TT)	-
Si	-	-	-15.67 (TT), - 18.02 (HT), -20.38 (HH)

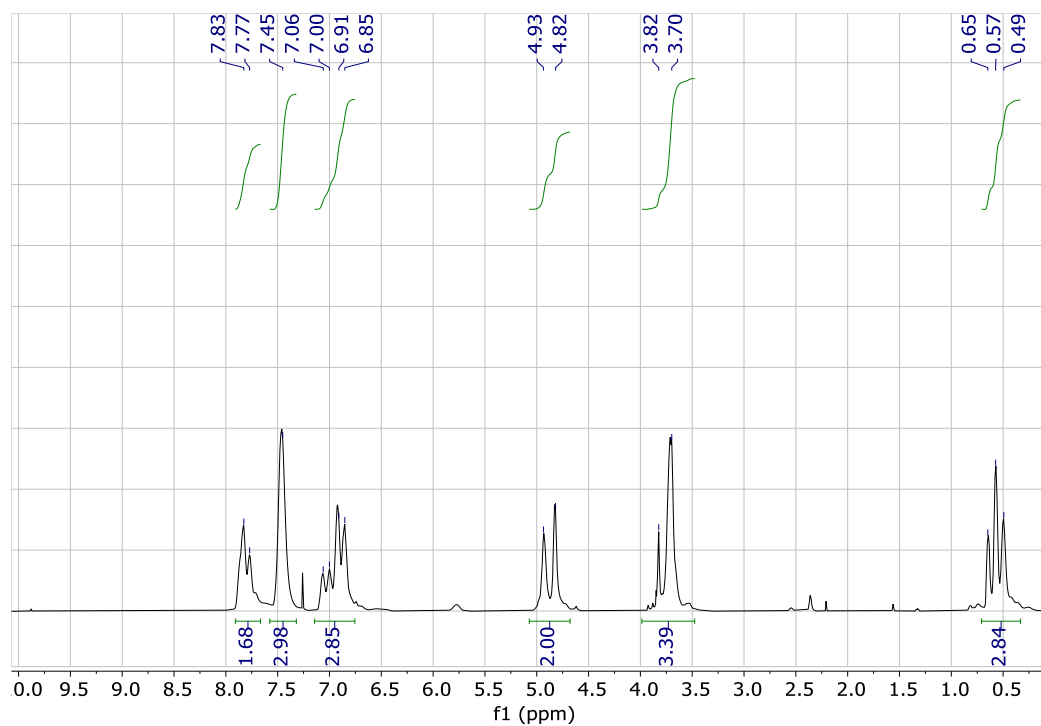


Figure S31. ^1H NMR spectrum of poly(Vanillin-*co*-MePhSiH₂) (CDCl₃, 400 MHz).

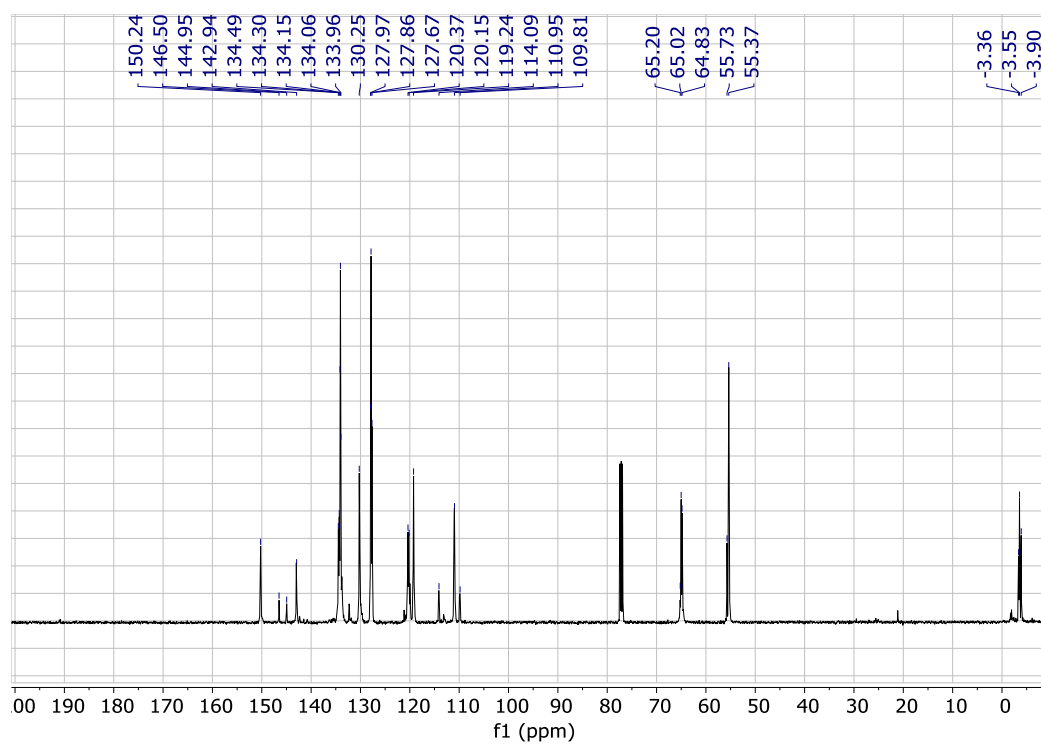


Figure S32. $^{13}\text{C}\{^1\text{H}\}$ NMR spectrum of poly(Vanillin-*co*-MePhSiH₂) (CDCl₃, 100 MHz).

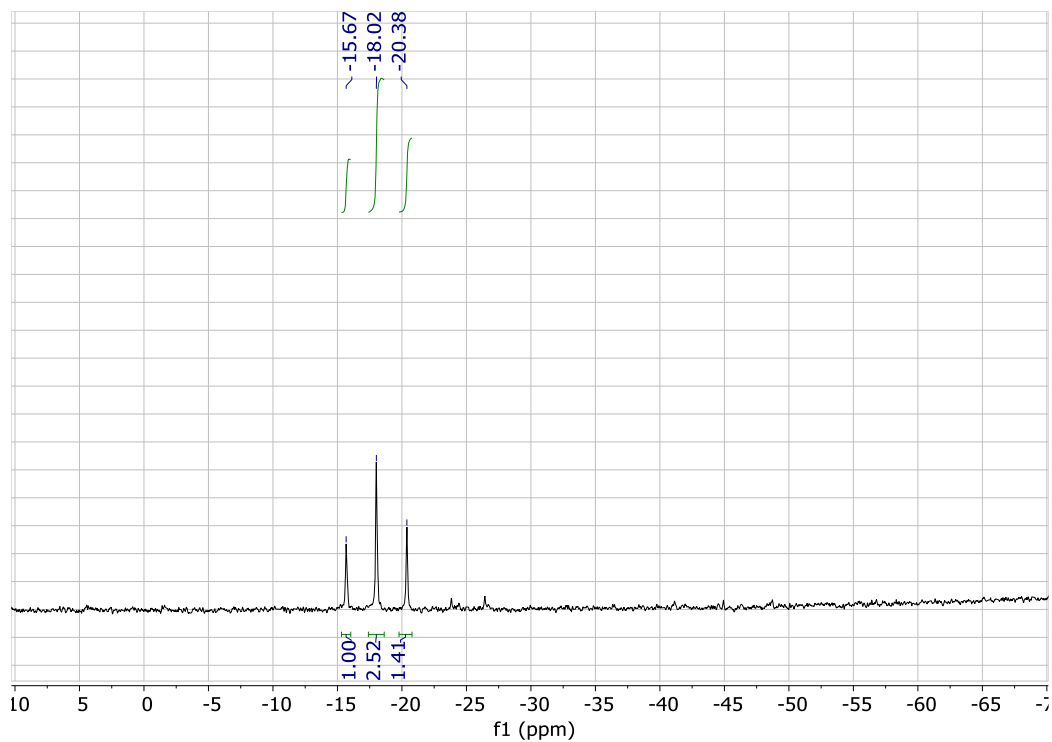


Figure S33. ^{29}Si NMR spectrum of poly(Vanillin-*co*-MePhSiH₂) (CDCl₃, 99 MHz).

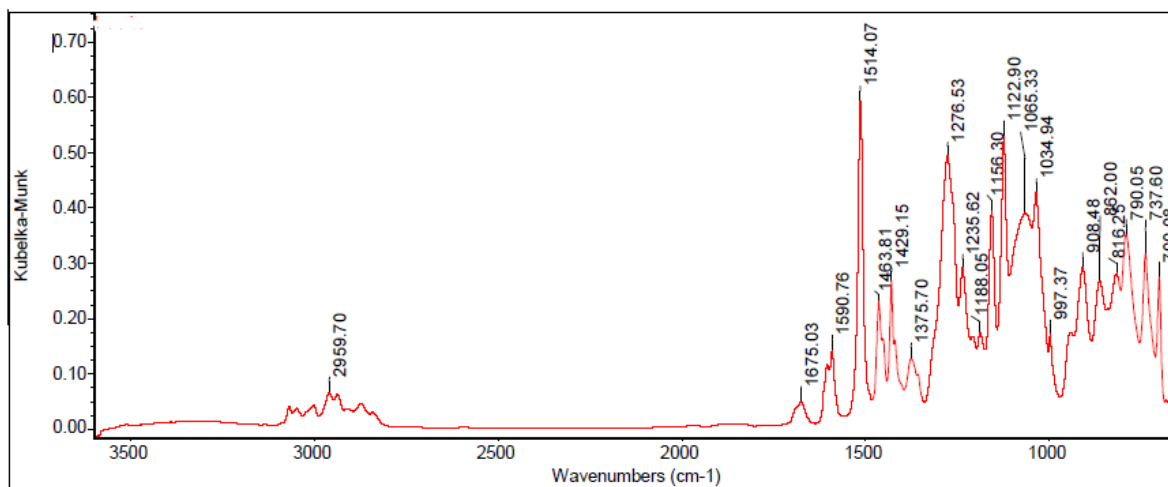
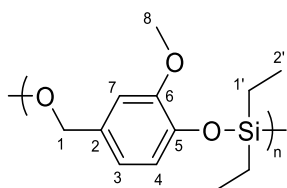


Figure S34. FT-IR spectrum of poly(Vanillin-*co*-MePhSiH₂).

Chapter 4

Poly(Vanillin-*co*-Et₂SiH₂):



Group	¹ H NMR (δ ppm)	¹³ C{ ¹ H} NMR (δ ppm)	²⁹ Si{ ¹ H} NMR (δ ppm)
1	4.84 (HT), 4.71 (TT)	64.7 (HT), 64.5 (TT)	-
2	-	134.8	-
3	6.95; 6.87	119.0	-
4	6.79; 6.75	120.5, 120.3	-
5	-	150.6	-
6	-	143.2	-
7	6.95; 6.87	110.8, 110.7	-
8	3.78; 3.76	55.6	-
1'	0.84 (HH), 0.77 (HT), 0.70 (TT)	5.0 (HH), 4.6 (HT), 4.2 (TT)	-
2'	1.00	6.6 (TT), 6.5 (HT), 6.3(HH)	-
Si	-	-	-2.56 (TT), -4.35 (HT), -6.03 (HH)

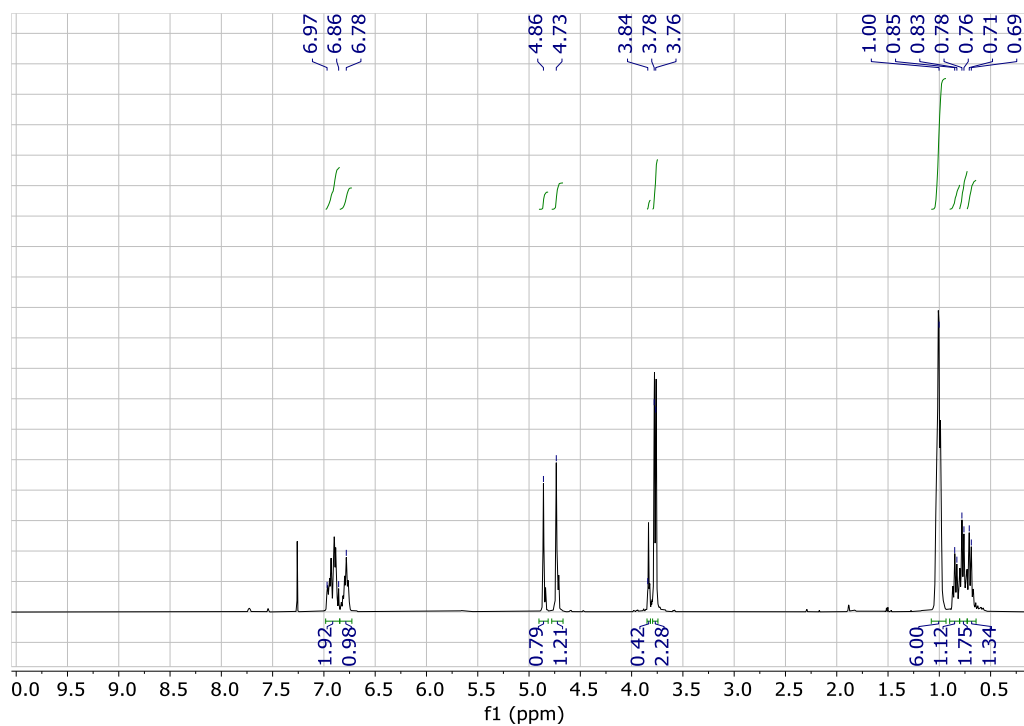


Figure S35. ^1H NMR spectrum of poly(Vanillin-*co*-Et₂SiH₂) (CDCl₃, 400 MHz).

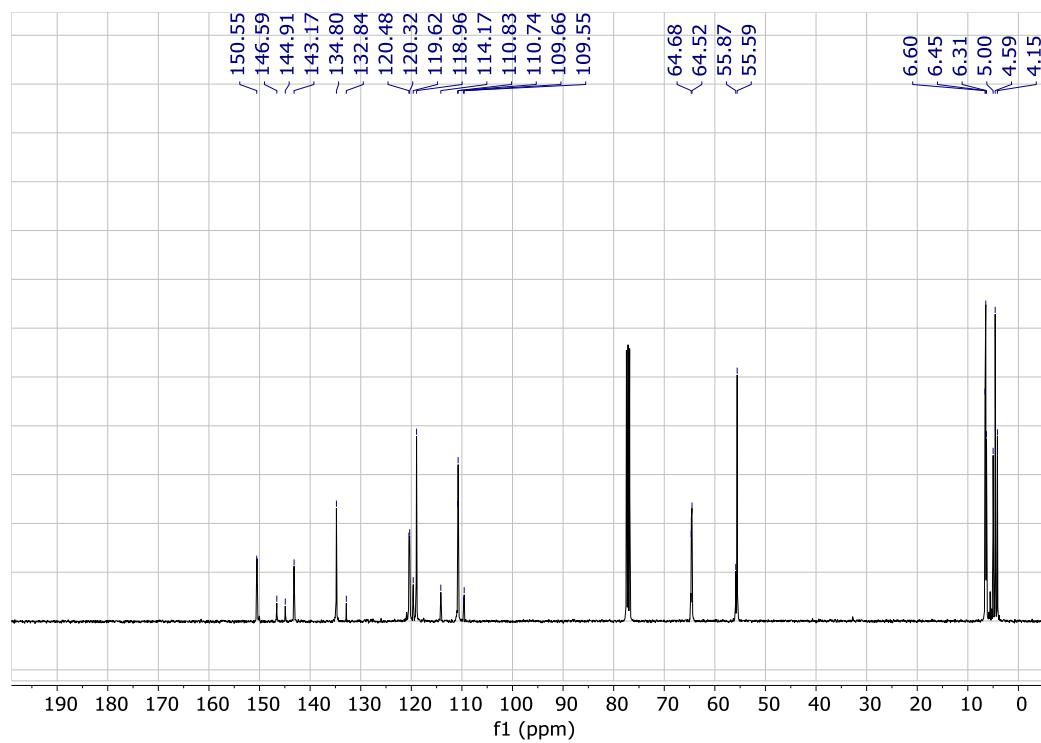


Figure S36. $^{13}\text{C}\{^1\text{H}\}$ NMR spectrum of poly(Vanillin-*co*-Et₂SiH₂) (CDCl₃, 100 MHz).

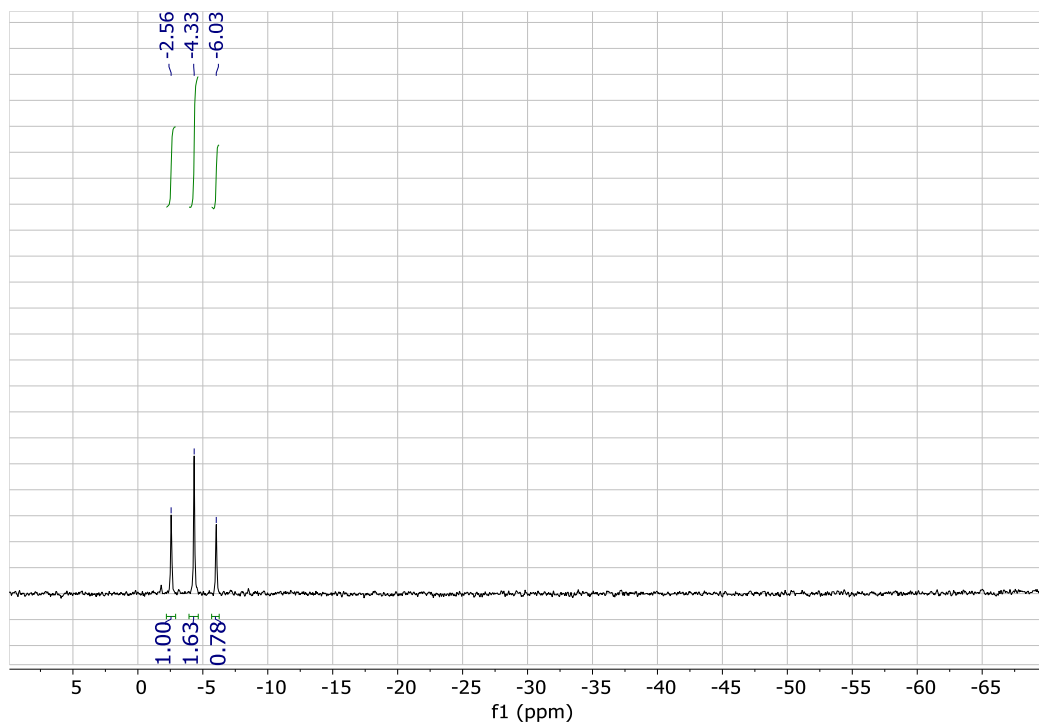


Figure S37. ^{29}Si NMR spectrum of poly(Vanillin-*co*- Et_2SiH_2) (CDCl_3 , 99 MHz).

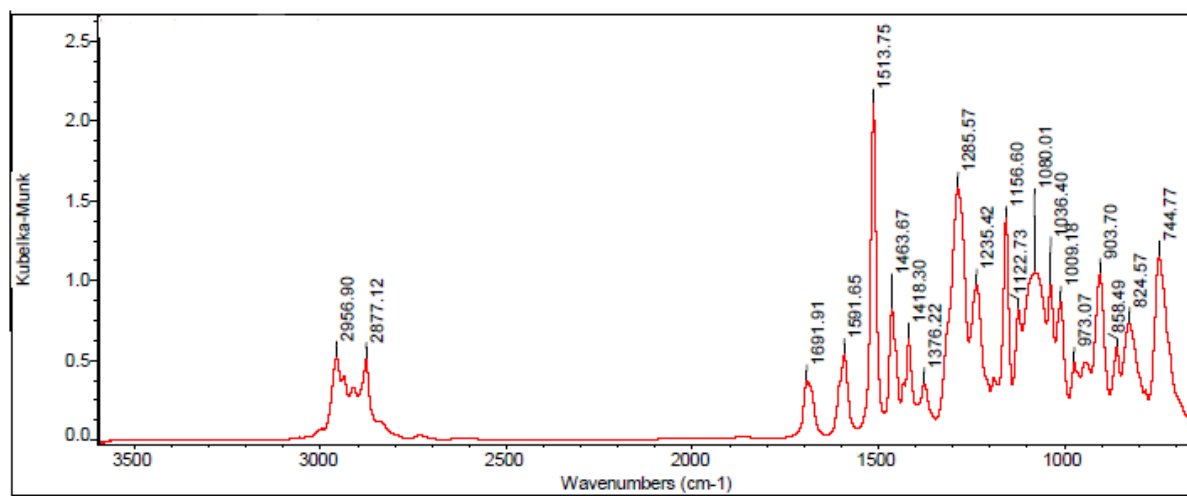
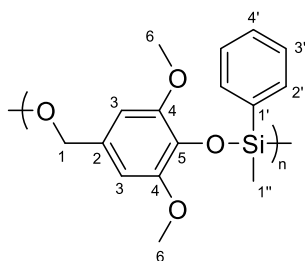


Figure S38. FT-IR spectrum of poly(Vanillin-*co*- Et_2SiH_2).

Chapter 4

Poly(Syringaldehyde-*co*-MePhSiH₂):



Group	¹ H NMR (δ ppm)	¹³ C{ ¹ H} NMR (δ ppm)	²⁹ Si{ ¹ H} NMR (δ ppm)
1	4.95 (HT), 4.81 (TT)	65.1	-
2	-	130.4	-
3	6.61, 6.56	103.7, 103.6	-
4	-	150.7	-
5	-	146.8	-
6	3.83, 3.73, f3.63	56.0, 55.6	-
1'	-	133.8	-
2'	7.86	134.0	-
3'	7.44	127.8, 127.5, 127.1	-
4'	7.44	130.2, 129.8, 129.3	-
1''	0.56	-2.82, -3.62, -4.02	-
Si	-	-	-15.60 (TT), -17.95 (HT), -20.67 (HH)

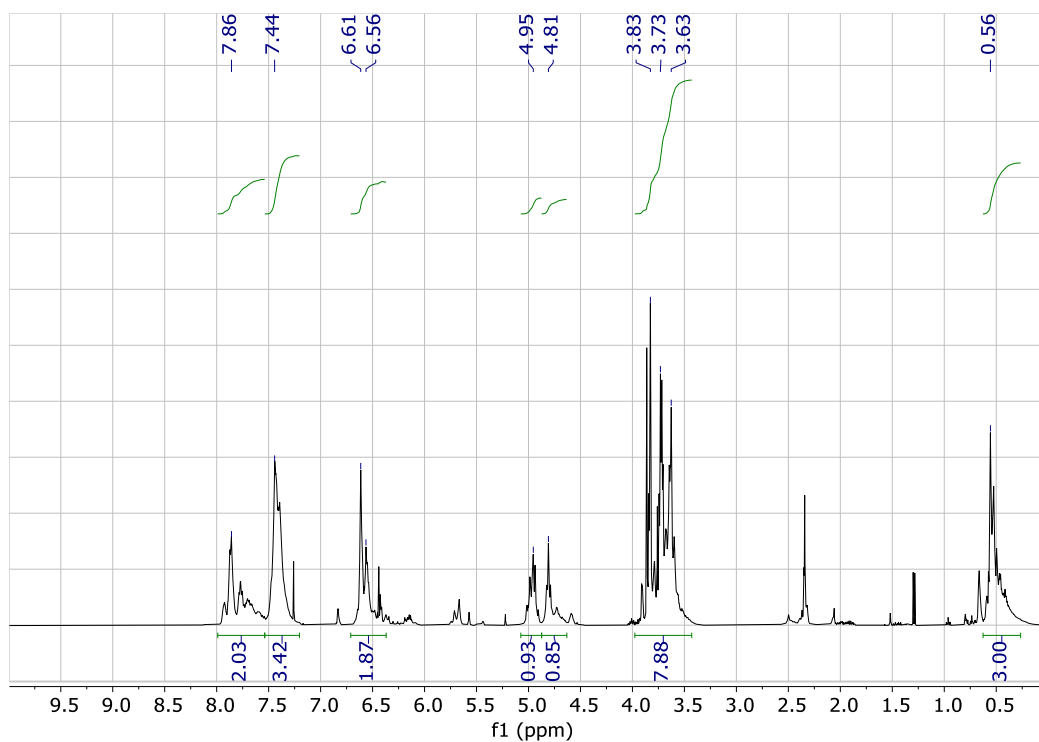


Figure S39. ^1H NMR spectrum of poly(Syringaldehyde-co-MePhSiH₂) (CDCl₃, 400 MHz).

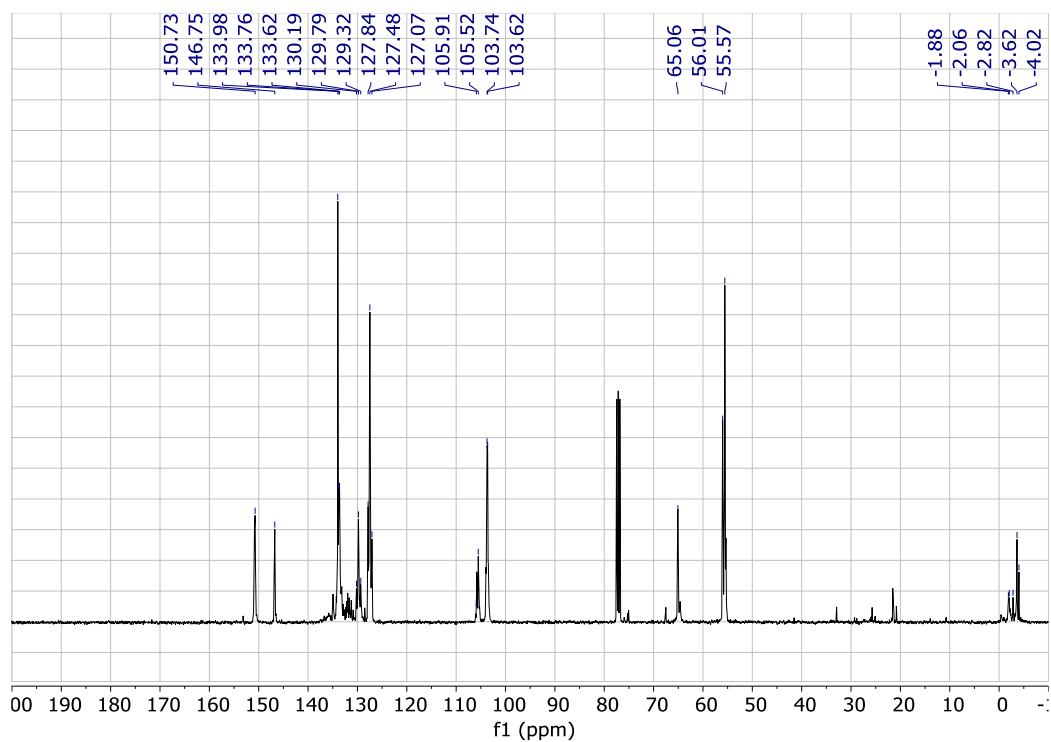


Figure S40. $^{13}\text{C}\{^1\text{H}\}$ NMR spectrum of poly(Syringaldehyde-co-MePhSiH₂) (CDCl₃, 100 MHz).

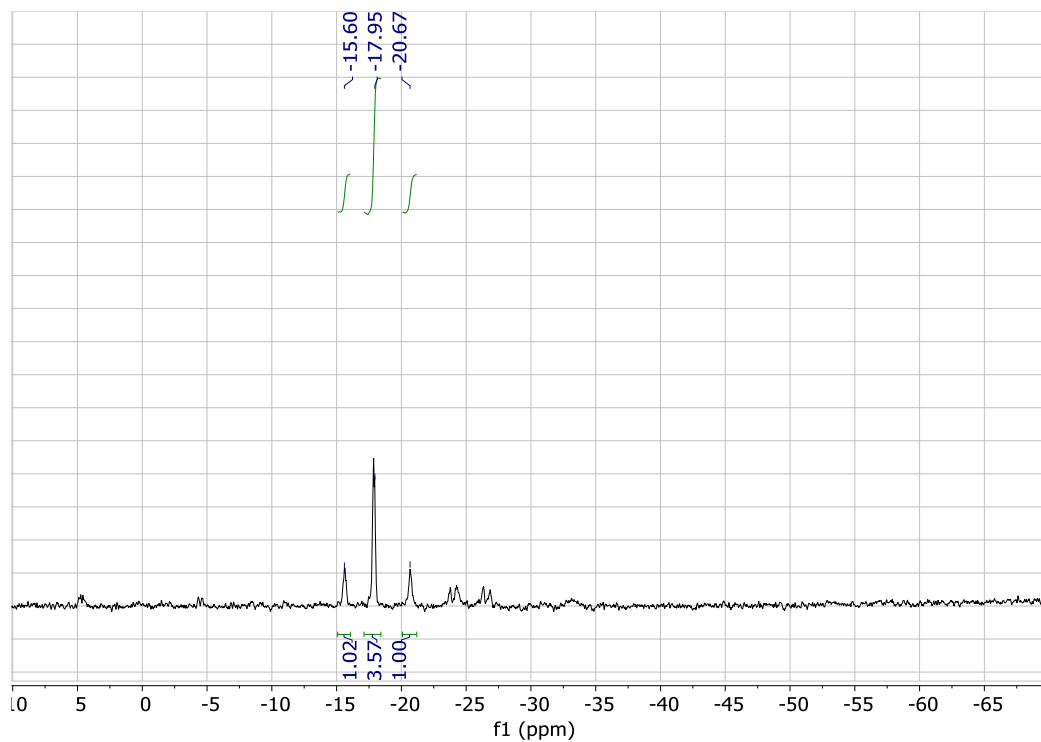


Figure S41. ^{29}Si NMR spectrum of poly(Syringaldehyde-*co*-MePhSiH₂) (CDCl₃, 99 MHz).

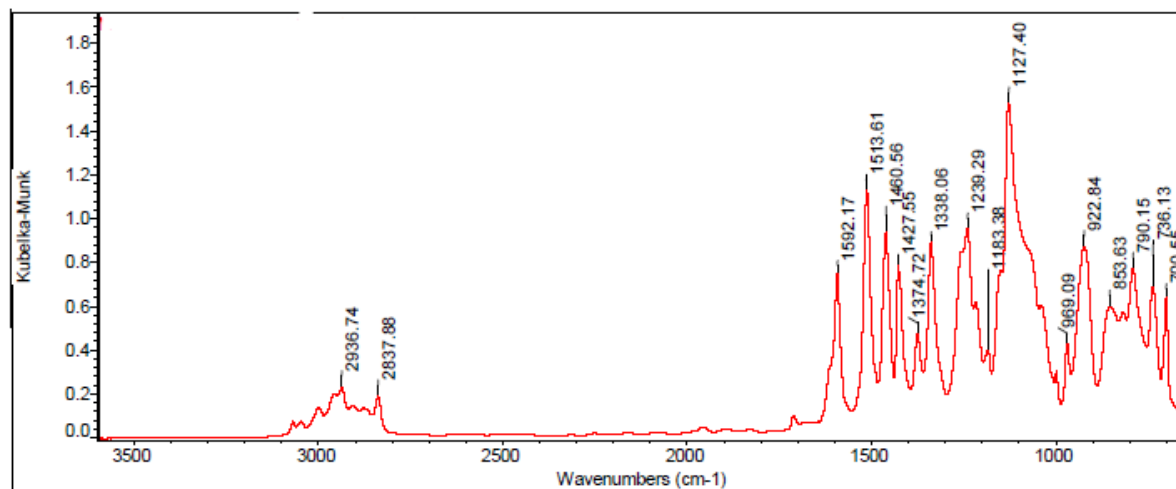
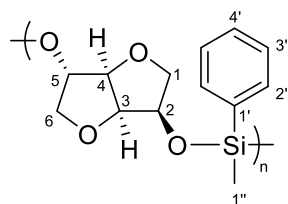


Figure S42. FT-IR spectrum of poly(Syringaldehyde-*co*-MePhSiH₂).

Poly(D-Isosorbide-*co*-MePhSiH₂):

Group	¹ H NMR (δ ppm)	¹³ C{ ¹ H} NMR (δ ppm)	²⁹ Si{ ¹ H} NMR (δ ppm)
1	3.79, 3.49	71.3	-
2	4.69 to 4.23	73.2	-
3	4.69 to 4.23	81.5	-
4	4.69 to 4.23	87.8	-
5	4.69 to 4.23	77.3	-
6	3.87, 3.79	75.7	-
1'	-	133.5	-
2'	7.65 to 7.53	134.0 to 133.8	-
3'	7.42 to 7.31	128.0 to 127.9	-
4'	7.42 to 7.31	130.4	-
1''	0.46, 0.29	-2.6, -3.6	-
Si	-	-	-15.06 to -16.81

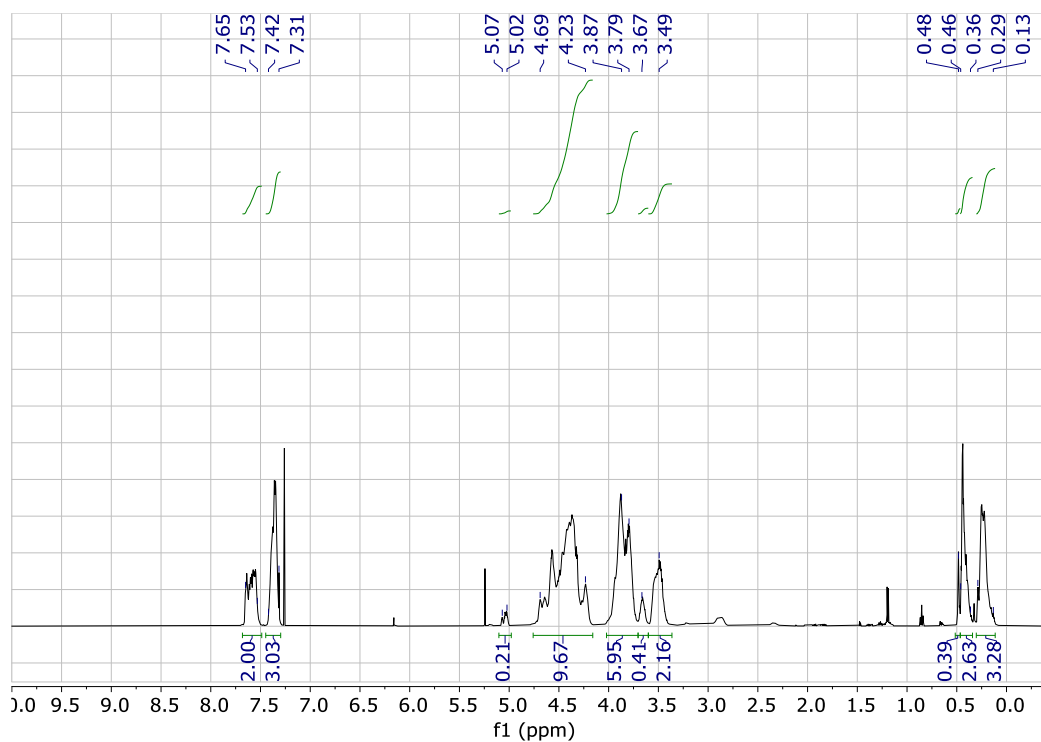


Figure S43. ^1H NMR spectrum of poly(D-Isosorbide-*co*-MePhSiH₂) (CDCl₃, 400 MHz).

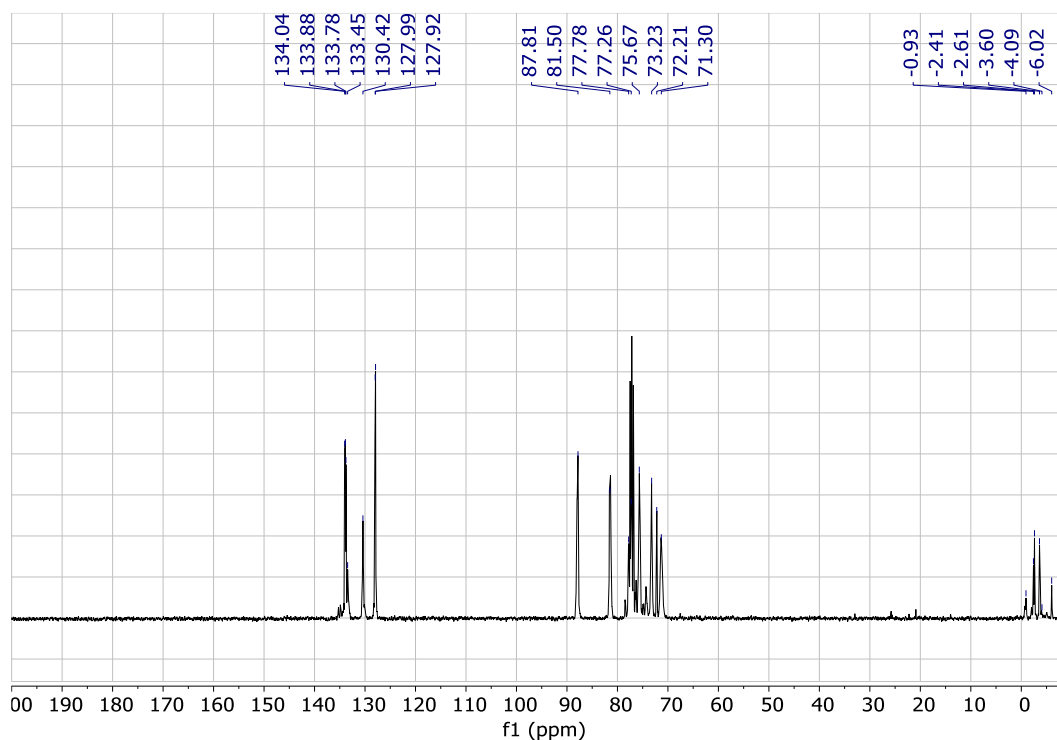


Figure S44. $^{13}\text{C}\{^1\text{H}\}$ NMR spectrum of poly(D-Isosorbide-*co*-MePhSiH₂) (CDCl₃, 100 MHz).

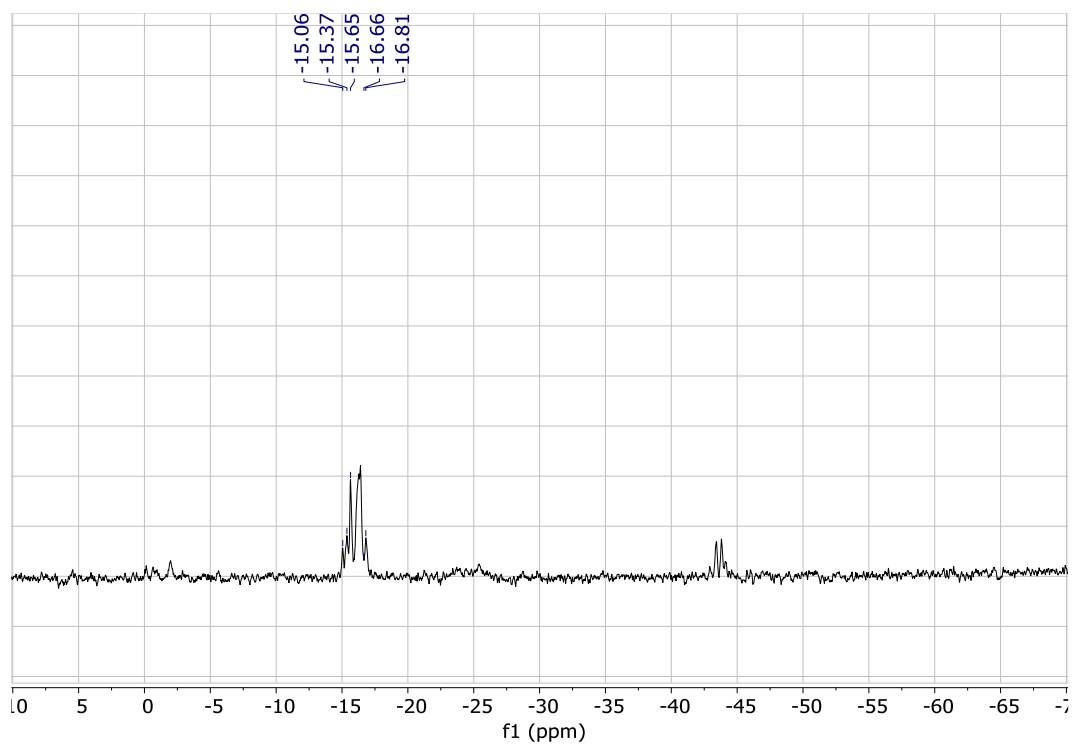
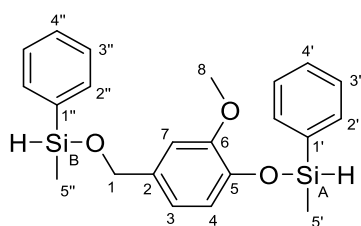


Figure S45. ^{29}Si NMR spectrum of poly(D-Isosorbide-*co*-MePhSiH₂) (CDCl₃, 99 MHz).

Chapter 4

MePhSiH-Vanillin-MePhSiH monomer :



Group	^1H NMR (δ ppm)	$^{13}\text{C}\{^1\text{H}\}$ NMR (δ ppm)	$^{29}\text{Si}\{^1\text{H}\}$ NMR (δ ppm)
1	4.85	66.5	-
2	-	134.1	-
3	6.90	119.6	-
4	7.06	120.0	-
5	-	144.0	-
6	-	150.2	-
7	6.98	111.2	-
8	3.86	55.4	-
1'	-	135.8	-
2'	7.85	134.0	-
3'	7.58, 7.51	128.0	-
4'	7.58, 7.51	130.2	-
5'	0.75	-2.01	-
1''	-	135.6	-
2''	7.79	133.8	-
3''	7.58, 7.51	127.9	-
4''	7.58, 7.51	130.1	-

Chapter 4

5''	0.65	-2.62	-
Si _A	5.53	-	-2.60
Si _B	5.30	-	-1.03

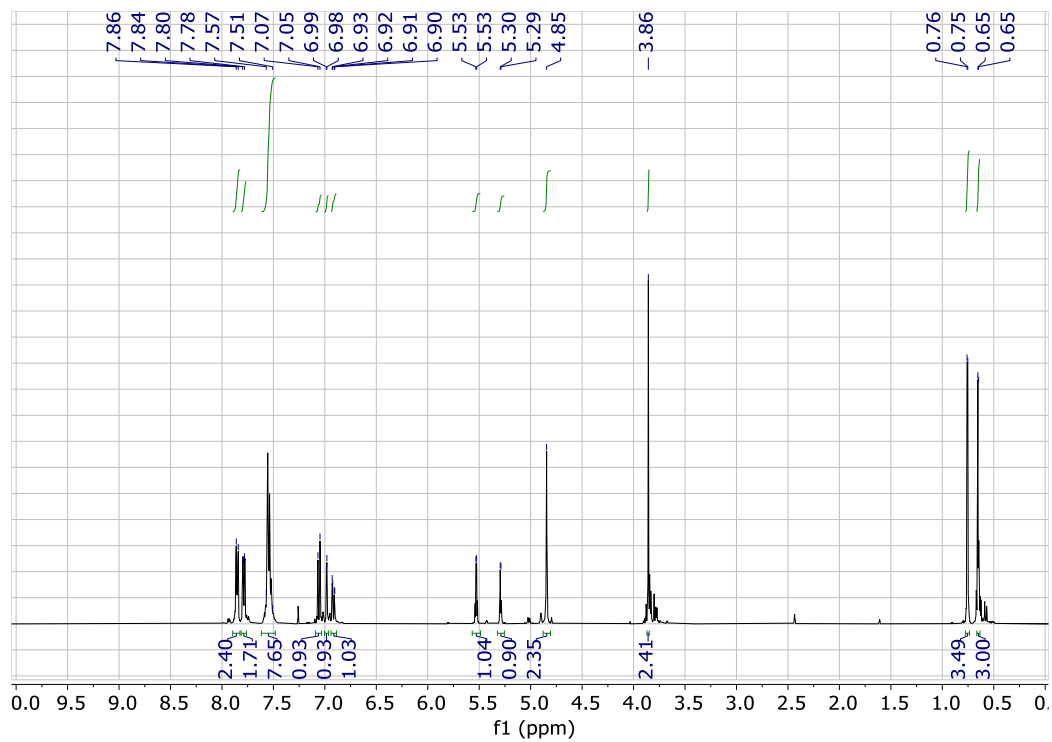


Figure S46. ¹H NMR spectrum of MePhSiH-Vanillin-MePhSiH monomer (CDCl₃, 400 MHz).

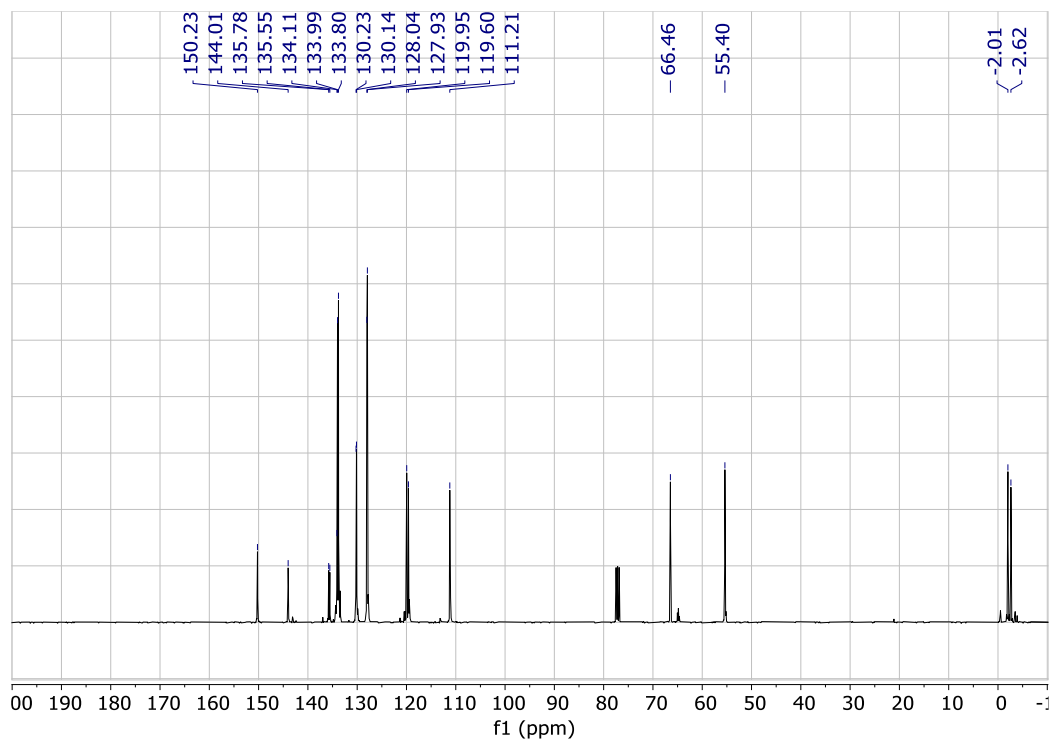


Figure S47. $^{13}\text{C}\{^1\text{H}\}$ NMR spectrum of MePhSiH-Vanillin-MePhSiH monomer (CDCl_3 , 100 MHz).

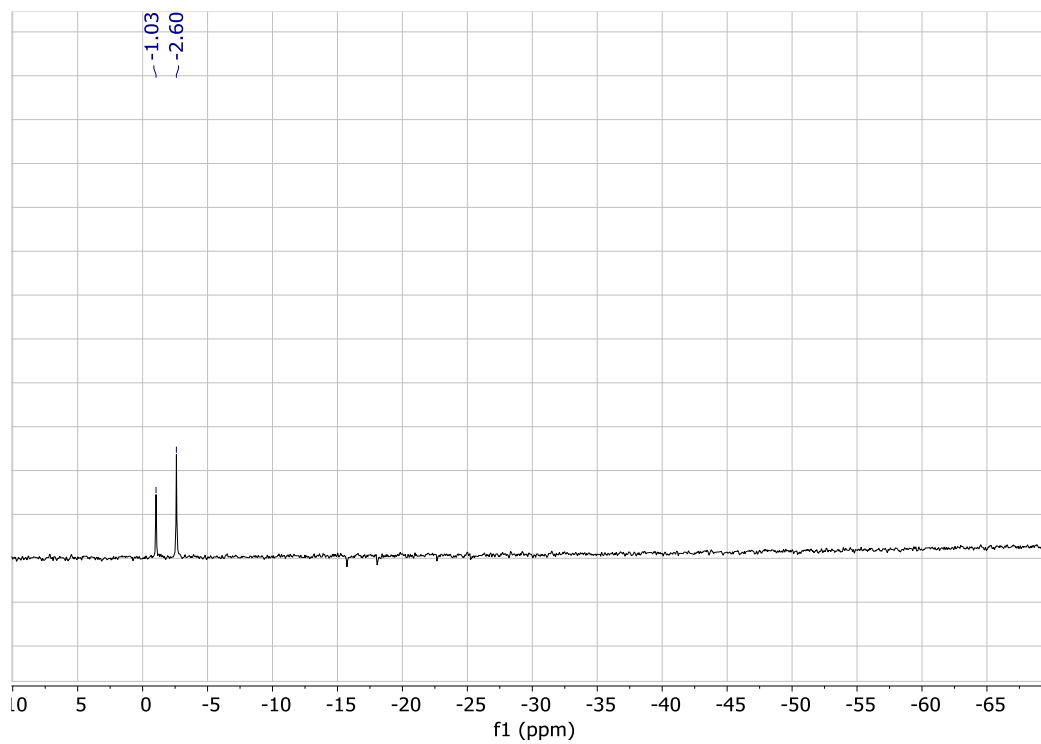


Figure S48. $^{29}\text{Si}\{^1\text{H}\}$ NMR spectrum MePhSiH-Vanillin-MePhSiH monomer (CDCl_3 , 99 MHz).

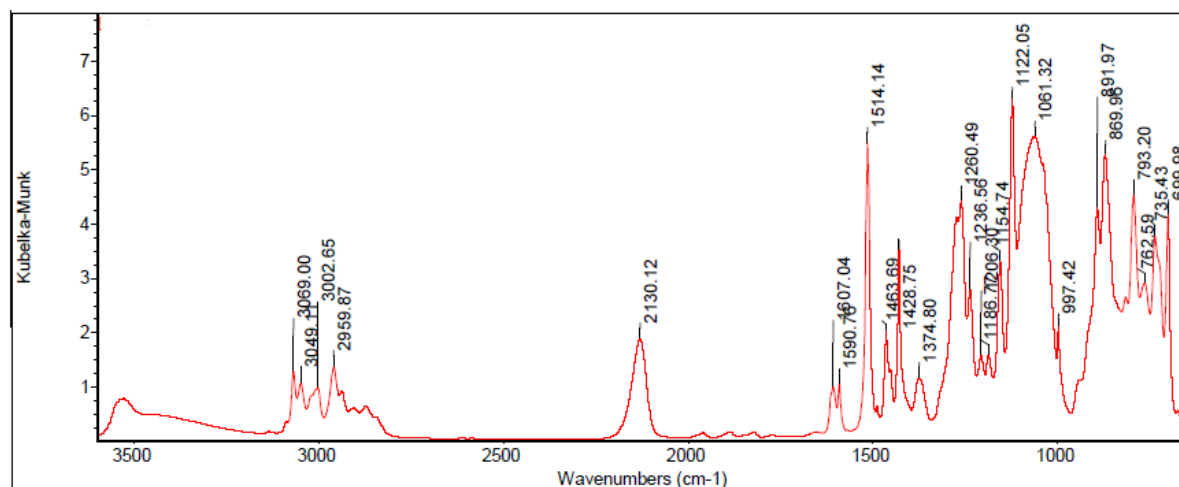
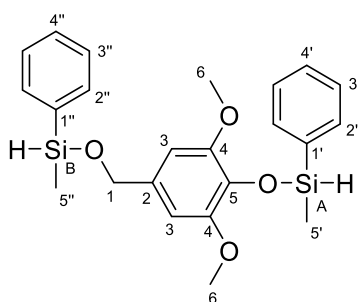


Figure S49. FT-IR spectrum of MePhSiH-Vanillin-MePhSiH monomer.

MePhSiH-Syringaldehyde-MePhSiH monomer :



Group	^1H NMR (δ ppm)	$^{13}\text{C}\{^1\text{H}\}$ NMR (δ ppm)	$^{29}\text{Si}\{^1\text{H}\}$ NMR (δ ppm)
1	4.81	66.8	-
2	-	133.1	-
3	6.62	104.1	-
4	-	150.9	-
5	-	133.2	-
6	3.83	55.8	-
1'	-	136.3	-

Chapter 4

2'	7.87	134.0	-
3'	7.51	128.0	-
4'	7.51	130.2	-
5'	0.71	-1.84	-
1''	-	135.5	-
2''	7.75	133.8	-
3''	7.51	127.7	-
4''	7.51	129.8	-
5''	0.63	-2.69	-
Si _A	5.47	-	-1.64
Si _B	5.26	-	-0.84

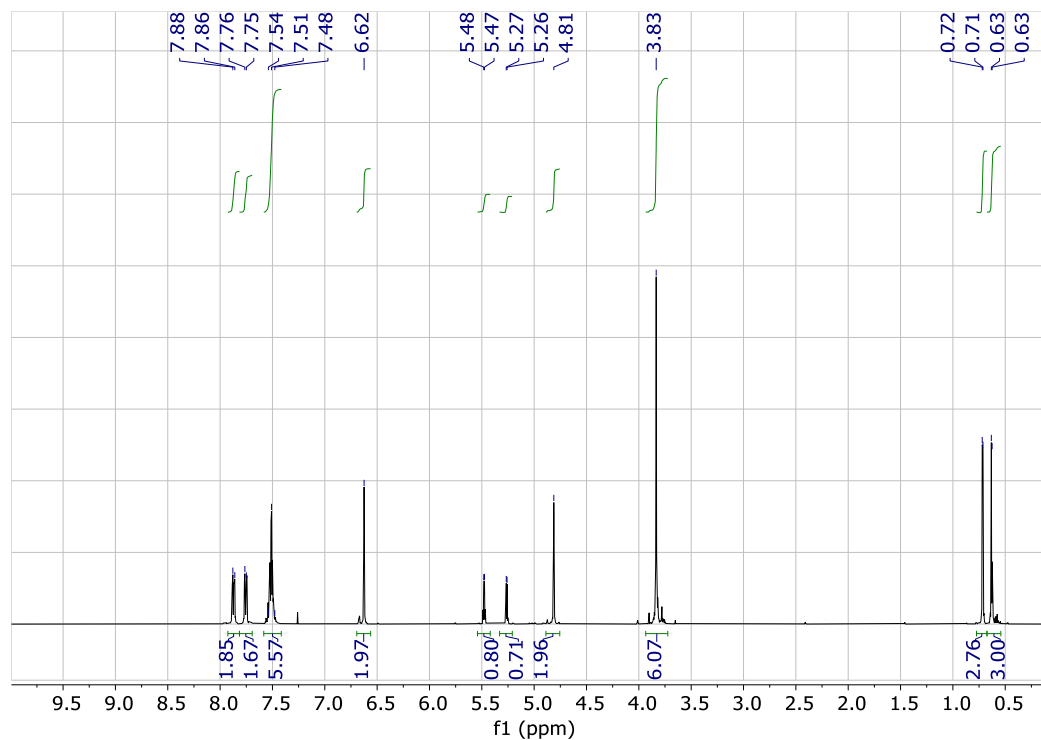


Figure S50. ¹H NMR spectrum of MePhSiH-Syringaldehyde-MePhSiH monomer (CDCl₃, 400 MHz).

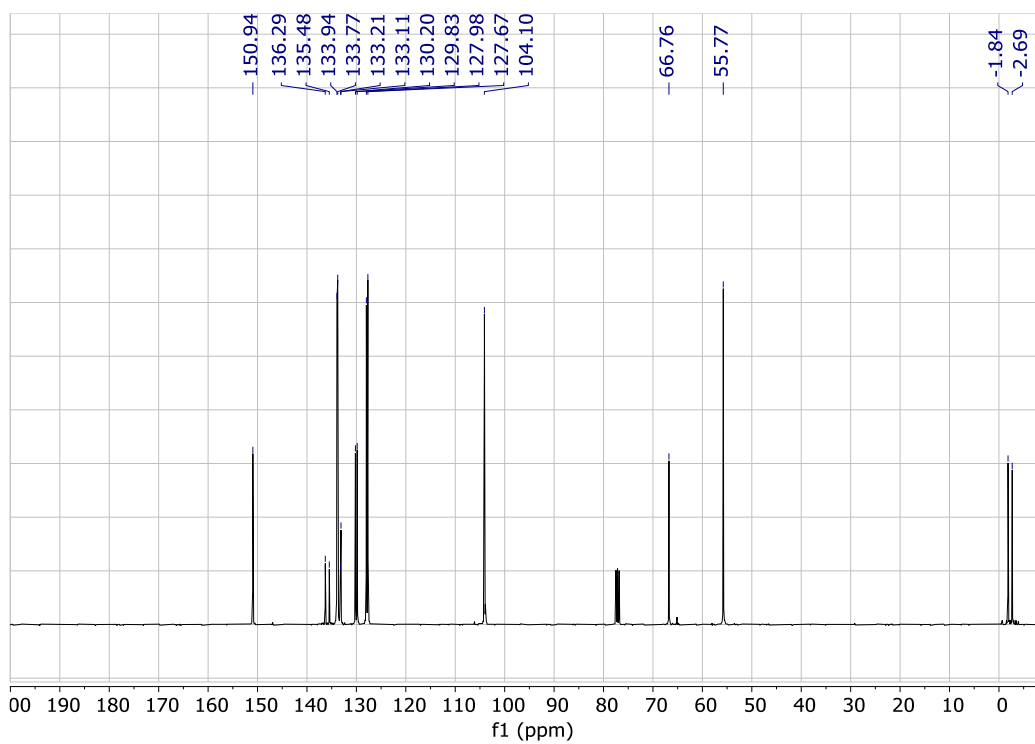


Figure S51. $^{13}\text{C}\{^1\text{H}\}$ NMR spectrum of MePhSiH-Syringaldehyde-MePhSiH monomer (CDCl_3 , 100 MHz).

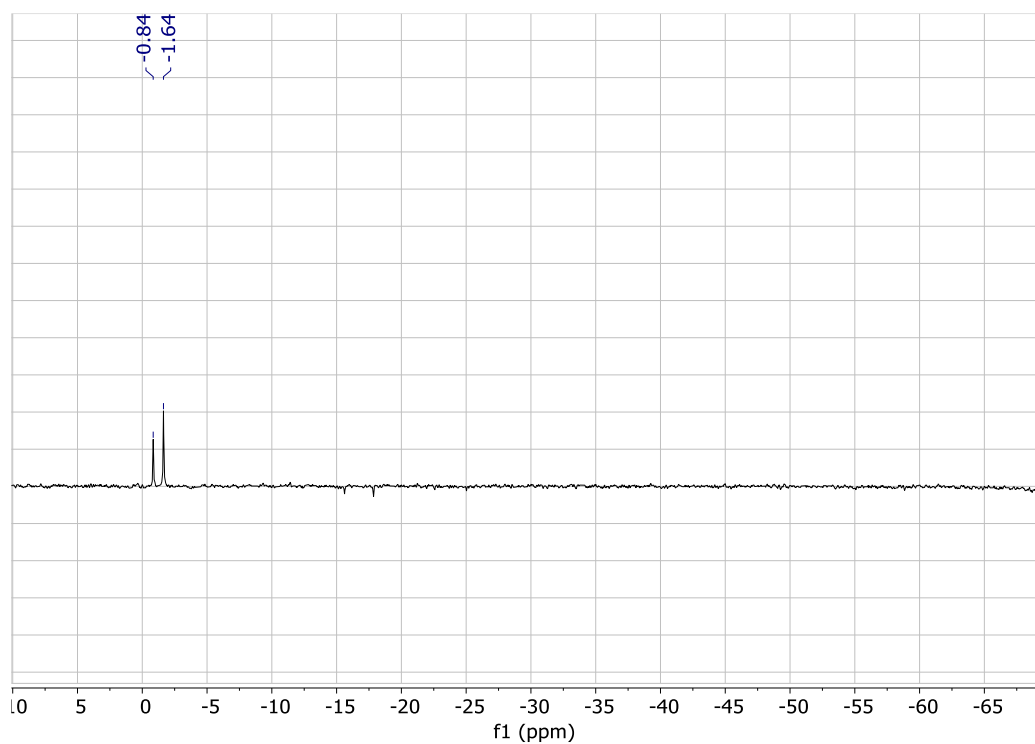


Figure S52. ^{29}Si NMR spectrum MePhSiH- Syringaldehyde-MePhSiH monomer (CDCl_3 , 99 MHz).

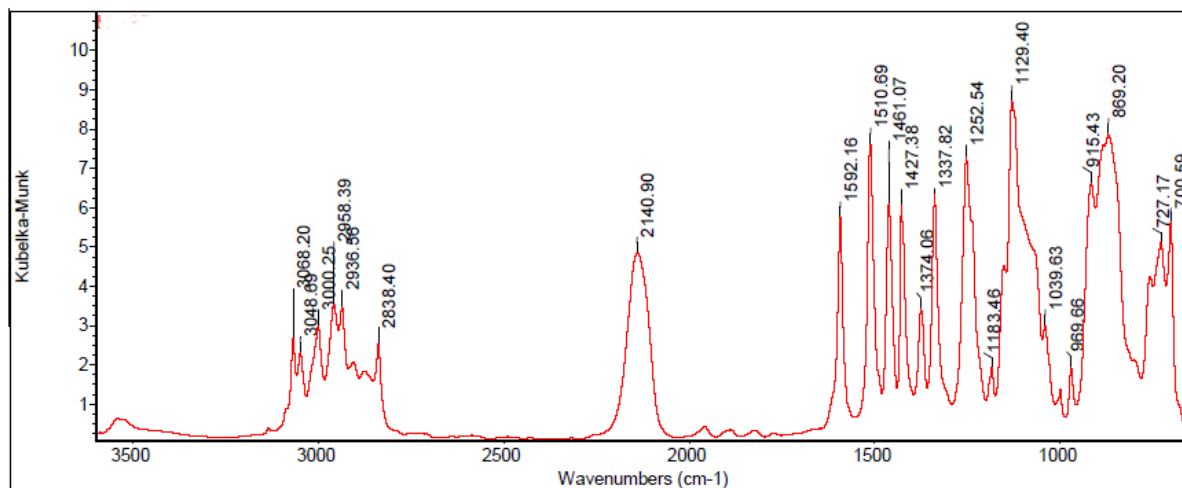
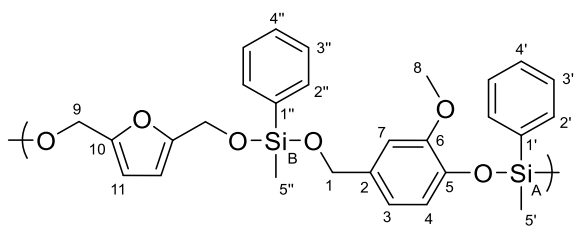


Figure S53. FT-IR spectrum of MePhSiH-Syringaldehyde-MePhSiH monomer.

Poly(Vanillin-*alt*-HMF-*co*-MePhSiH₂):



Group	¹ H NMR (δ ppm)	¹³ C{ ¹ H} NMR (δ ppm)	²⁹ Si{ ¹ H} NMR (δ ppm)
1	4.86	64.9	-
2	-	134.1	-
3	6.96	119.9	-
4	6.96	120.2	-
5	-	145.0	-
6	-	150.2	-
7	6.96	109.9	-
8	3.86	55.7, 55.3	-
9	4.79	57.5	-

Chapter 4

10	-	153.3	-
11	6.25	108.7	-
1'	-	135.8	-
2'	7.74	134.1	-
3'	7.49	127.9	-
4'	7.49	130.2	-
5'	0.62	-4.03	-
1''	-	135.6	-
2''	7.74	134.1	-
3''	7.49	127.9	-
4''	7.49	130.2	-
5''	0.52	-4.03	-
Si _A	-	-	-14.65
Si _B	-	-	-15.25

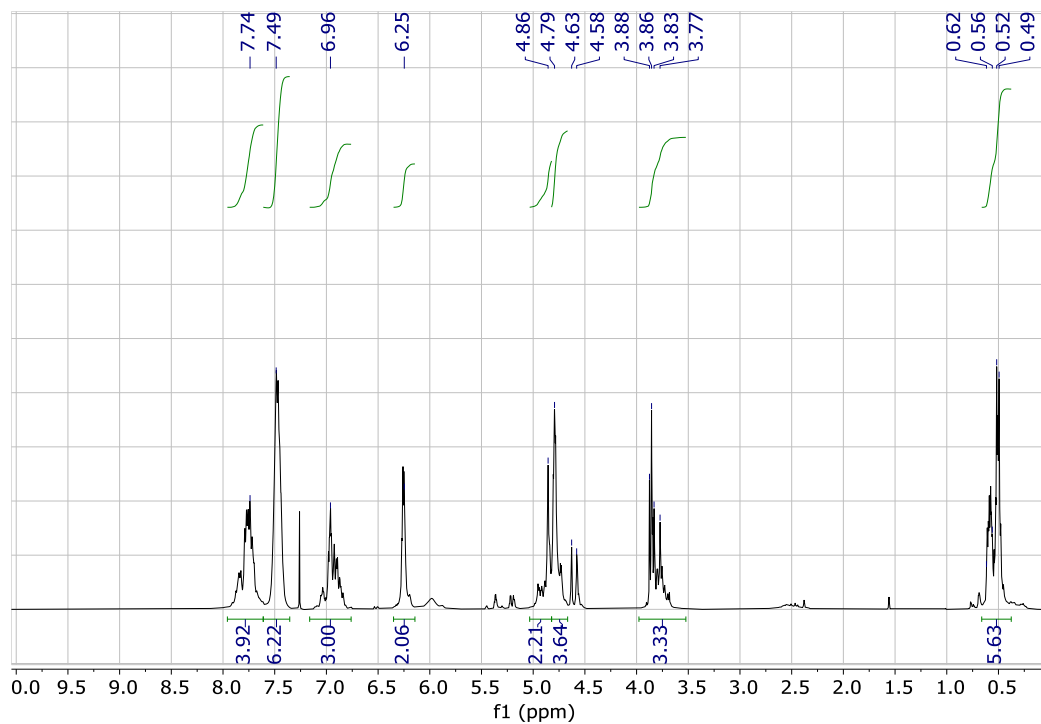


Figure S54. ^1H NMR spectrum of poly(Vanillin-*alt*-HMF-*co*-MePhSiH₂) (CDCl₃, 400 MHz).

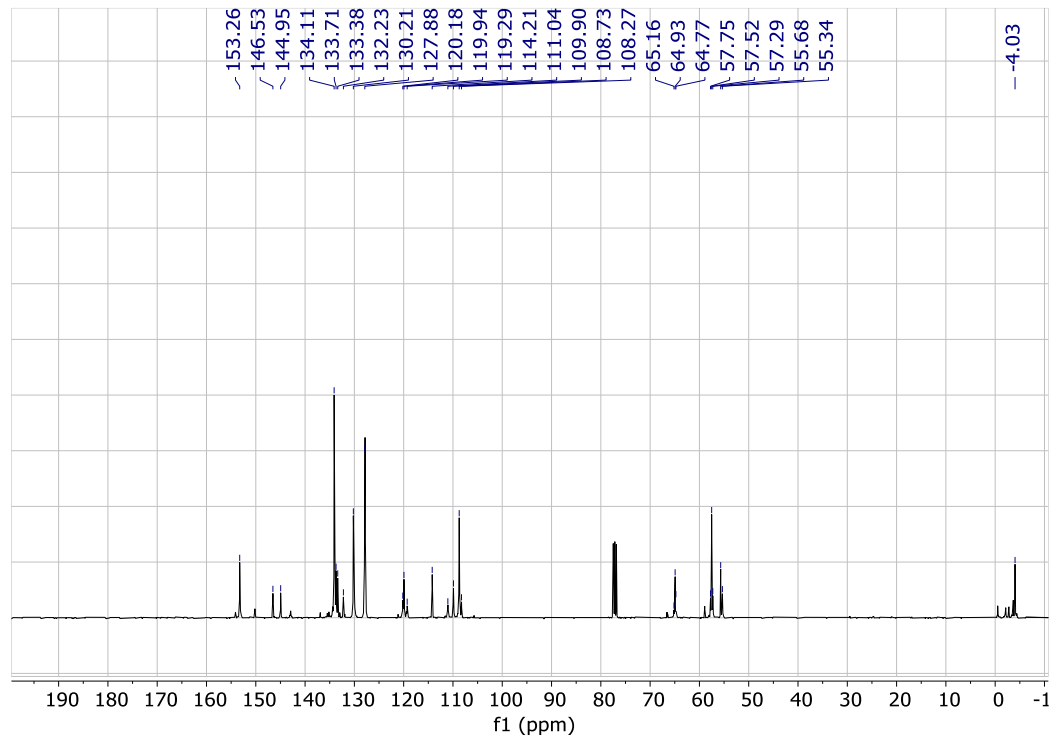


Figure S55. ^{13}C $\{^1\text{H}\}$ NMR spectrum of poly(Vanillin-*alt*-HMF-*co*-MePhSiH₂) (CDCl₃, 100 MHz).

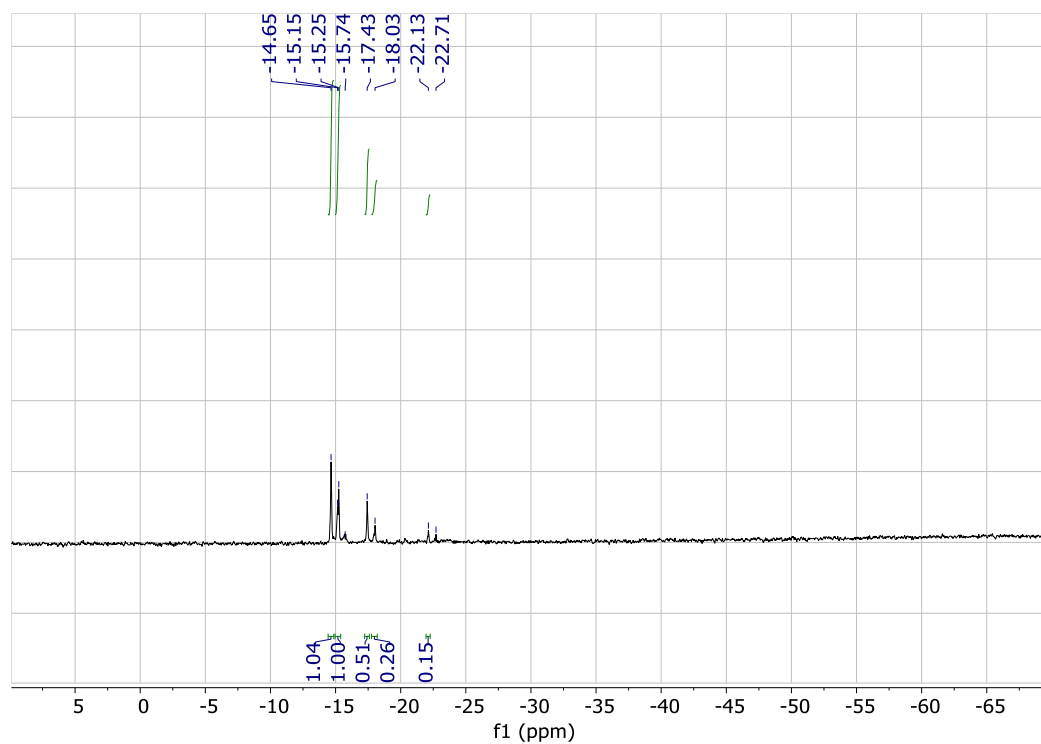


Figure S56. ^{29}Si NMR spectrum poly(Vanillin-*alt*-HMF-*co*-MePhSiH₂) (CDCl_3 , 99 MHz).

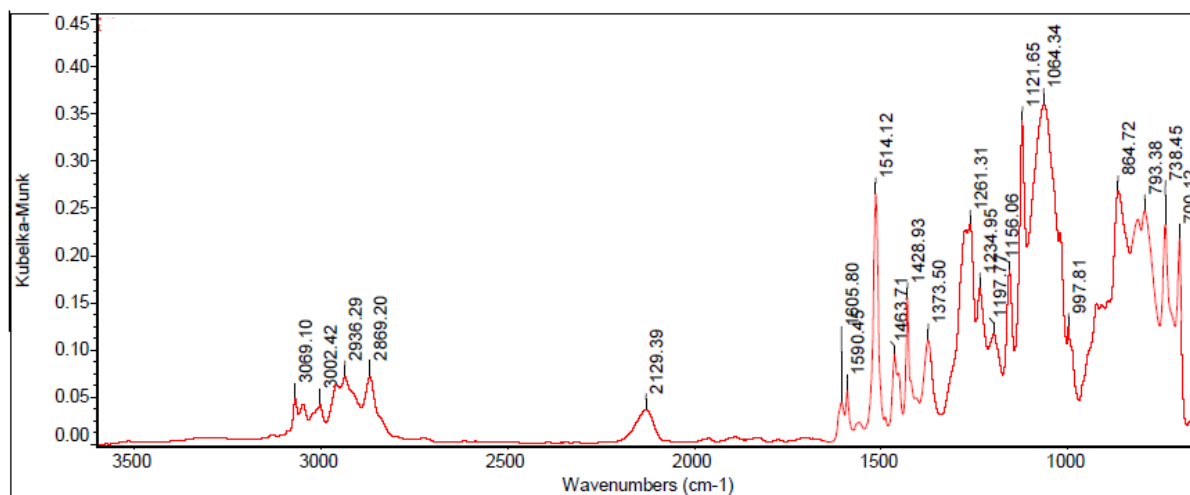
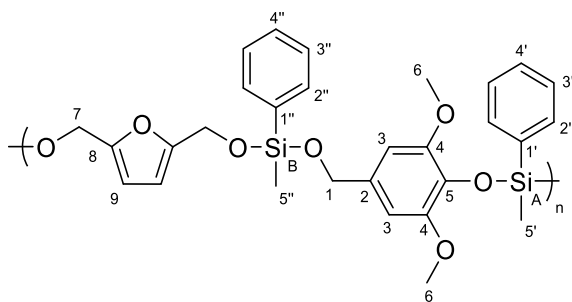


Figure S57. FT-IR spectrum of poly(Vanillin-*alt*-HMF-*co*-MePhSiH₂).

Poly(Syringaldehyde-*alt*-HMF-*co*-MePhSiH₂):



Group	¹ H NMR (δ ppm)	¹³ C{ ¹ H} NMR (δ ppm)	²⁹ Si{ ¹ H} NMR (δ ppm)
1	4.81	65.1	-
2	-	133.3	-
3	6.61	103.7	-
4	-	150.9	-
5	-	146.9	-
6	3.84	56.1	-
7	4.74	57.4	-
8	-	153.2	-
9	6.21	108.7	-
1'	-	133.8	-
2'	7.71	134.0	-
3'	7.42	127.8	-
4'	7.42	130.2	-
5'	0.48	-4.12	-
1''	-	133.6	-
2''	7.71	134.0	-

Chapter 4

3''	7.42	127.8	-
4''	7.42	130.2	-
5''	0.44	-4.12	-
Si _A	-	-	-14.74
Si _B	-	-	-15.21

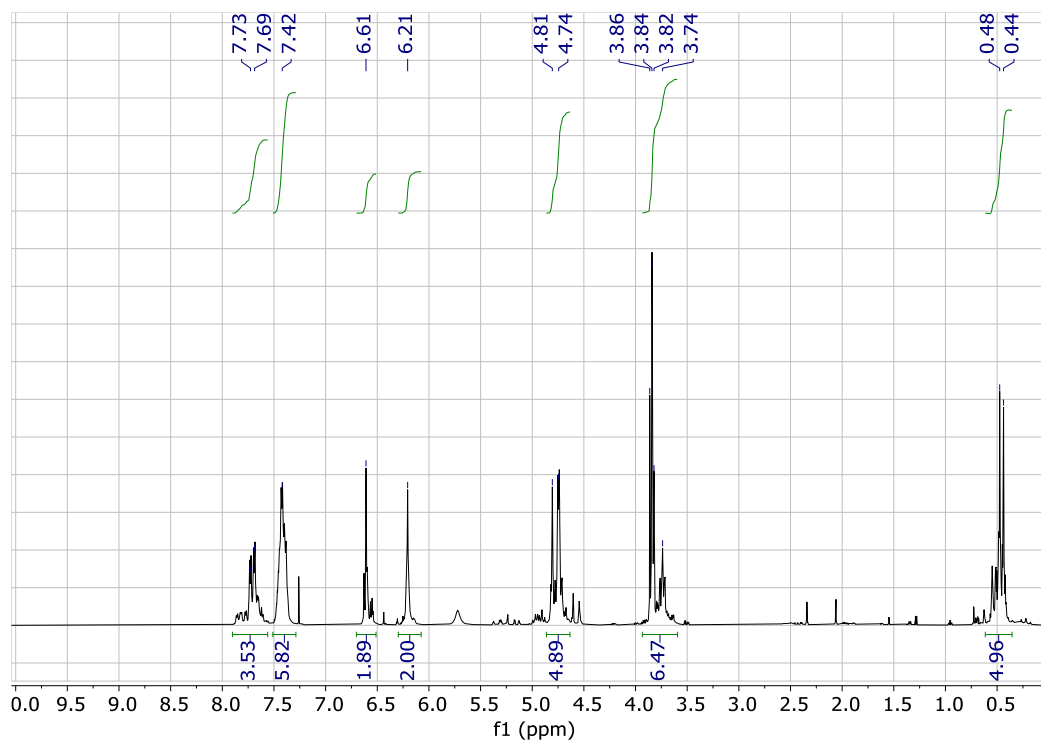


Figure S58. ¹H NMR spectrum of poly(Syringaldehyde-*alt*-HMF-*co*-MePhSiH₂) (CDCl₃, 400 MHz).

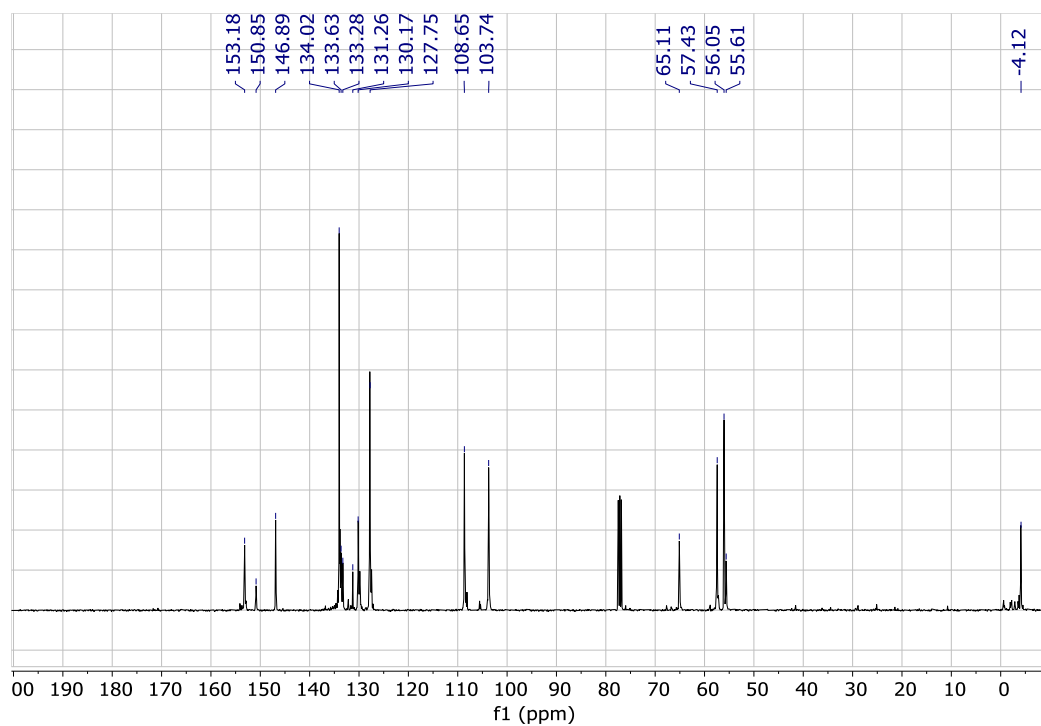


Figure S59. $^{13}\text{C}\{^1\text{H}\}$ NMR spectrum of poly(Syringaldehyde-*alt*-HMF-*co*-MePhSiH₂) (CDCl₃, 100 MHz).

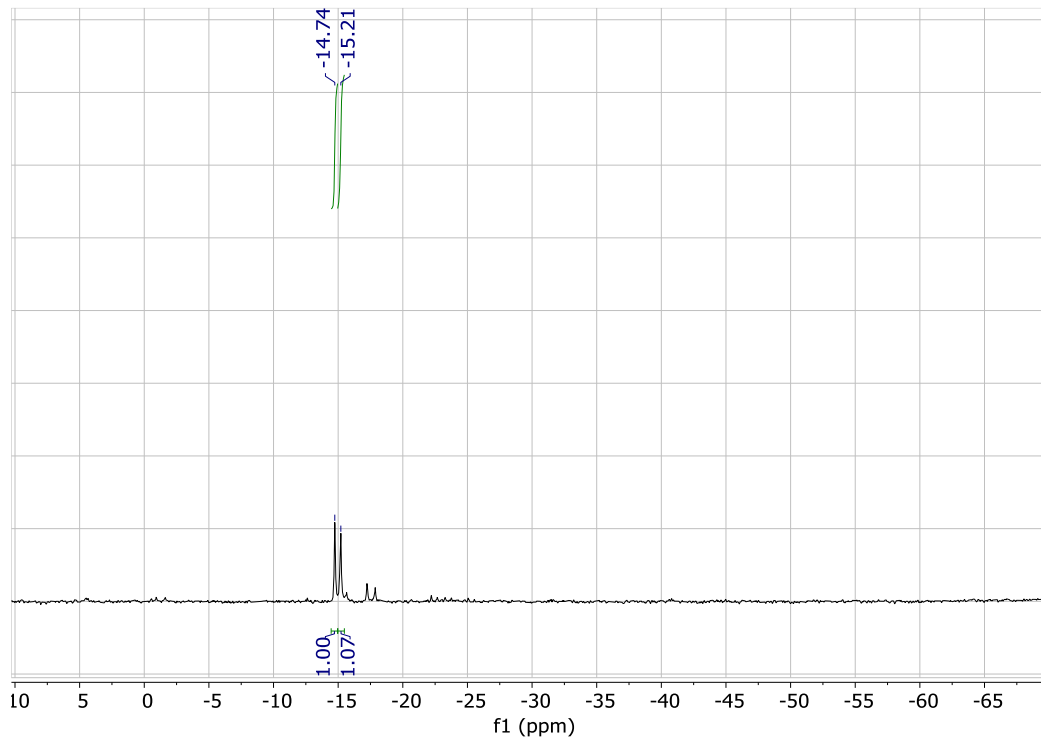


Figure S60. ^{29}Si NMR spectrum poly(Syringaldehyde-*alt*-HMF-*co*-MePhSiH₂) (CDCl₃, 99 MHz).

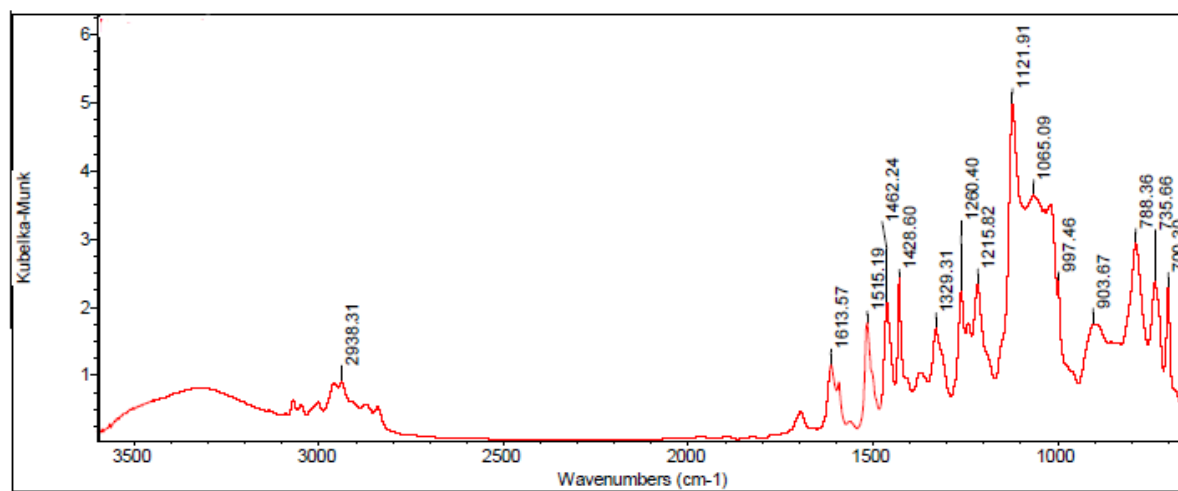
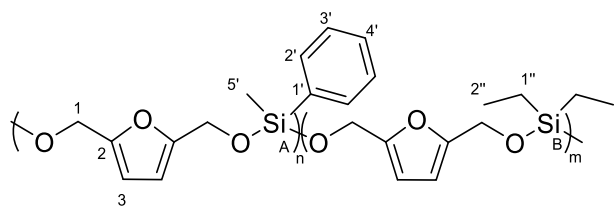


Figure S61. FT-IR spectrum of poly(Syringaldehyde-*alt*-HMF-*co*-MePhSiH₂).

Poly(HMF-*co*-MePhSiH₂-*r*-Et₂SiH₂):

Group	¹ H NMR (δ ppm)	¹³ C{ ¹ H} NMR (δ ppm)	²⁹ Si{ ¹ H} NMR (δ ppm)
1	4.69	57.6, 57.4	-
2	-	153.7, 153.3	-
3	6.21, 6.18	108.8, 108.5	-
1'	-	133.8	-
2'	7.65	134.2	-
3'	7.40, 7.36	127.9	-
4'	7.40, 7.36	130.3	-
5'	0.39	-4.0	-
1''	0.67	3.9	-
2''	0.97	6.3	-
Si _A	-	-	-14.78
Si _B	-	-	-1.26

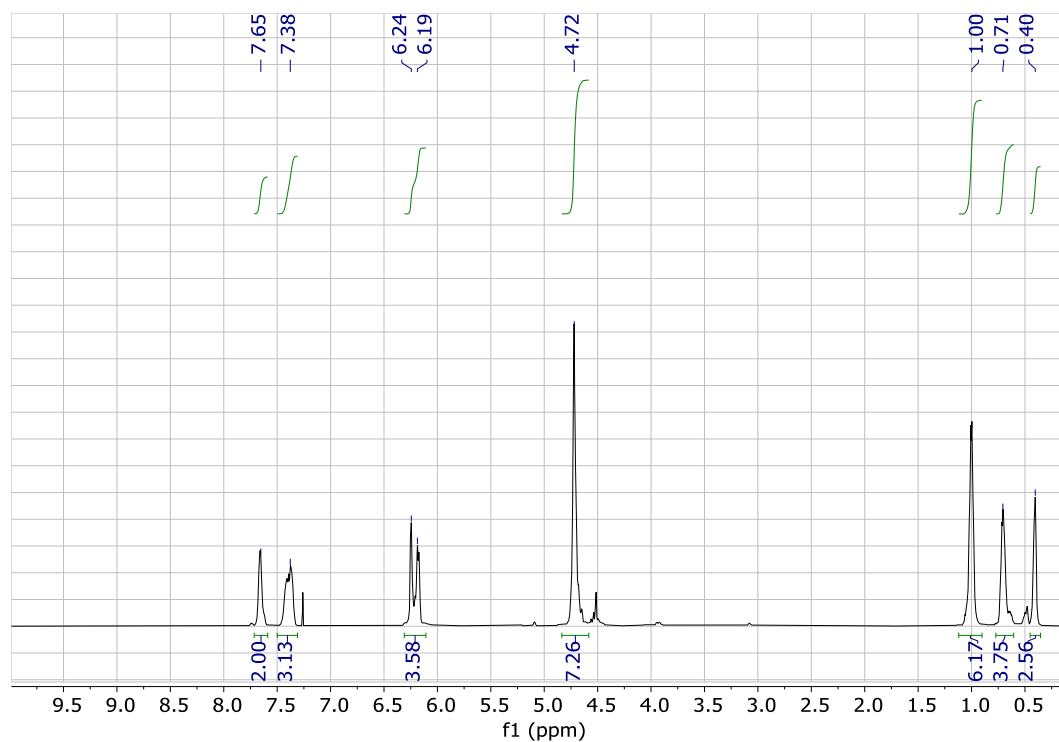


Figure S62. ¹H NMR spectrum of poly(HMF-*co*-MePhSiH₂) (Table 4, entry 4) (CDCl₃, 400 MHz).

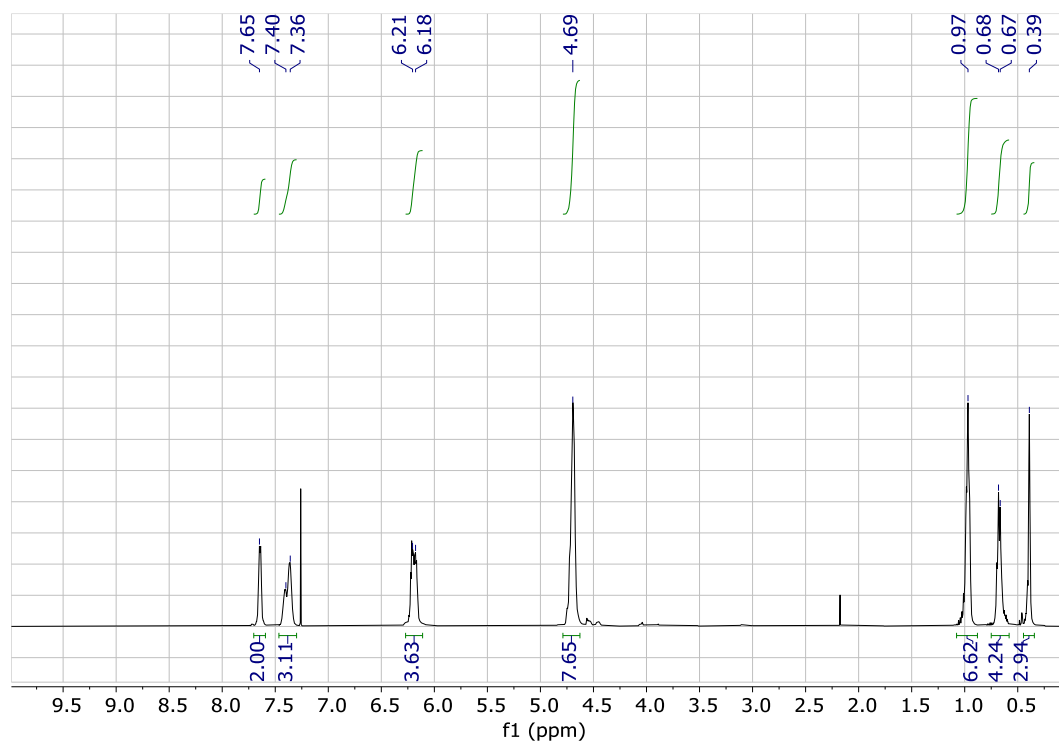


Figure S63. ¹H NMR spectrum of poly(HMF-*co*-MePhSiH₂) (Table 4, entry 5) (CDCl₃, 400 MHz).

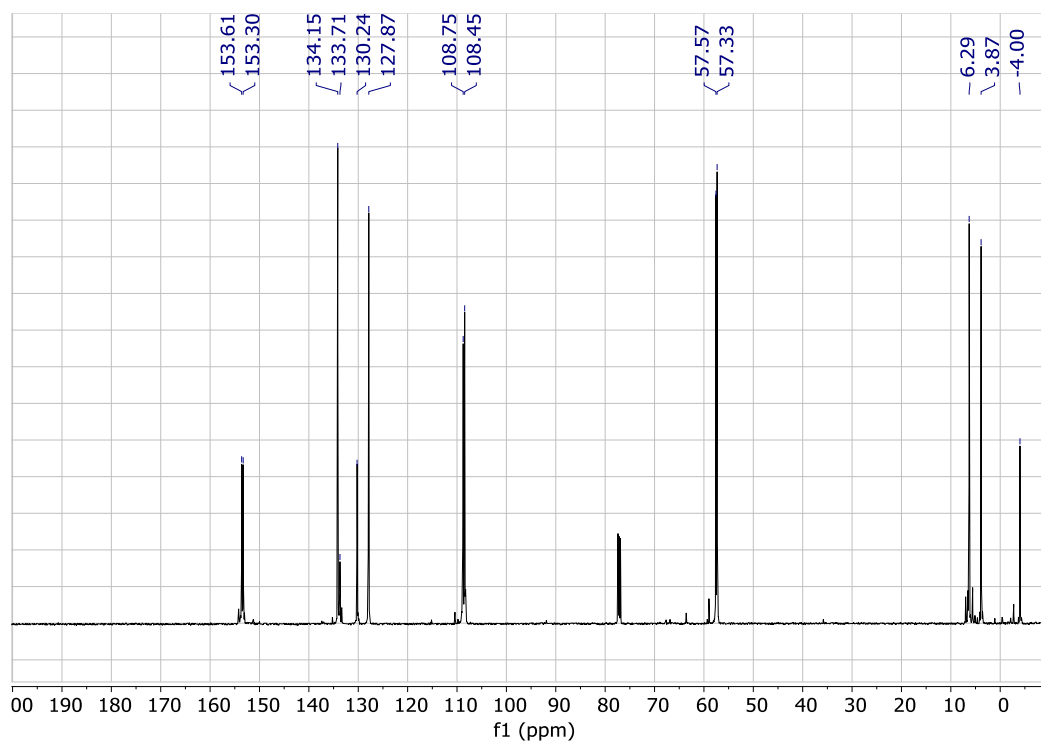


Figure S64. $^{13}\text{C}\{^1\text{H}\}$ NMR spectrum of poly(HMF-*co*-MePhSiH₂) (Table 4, entry 4) (CDCl₃, 100 MHz).

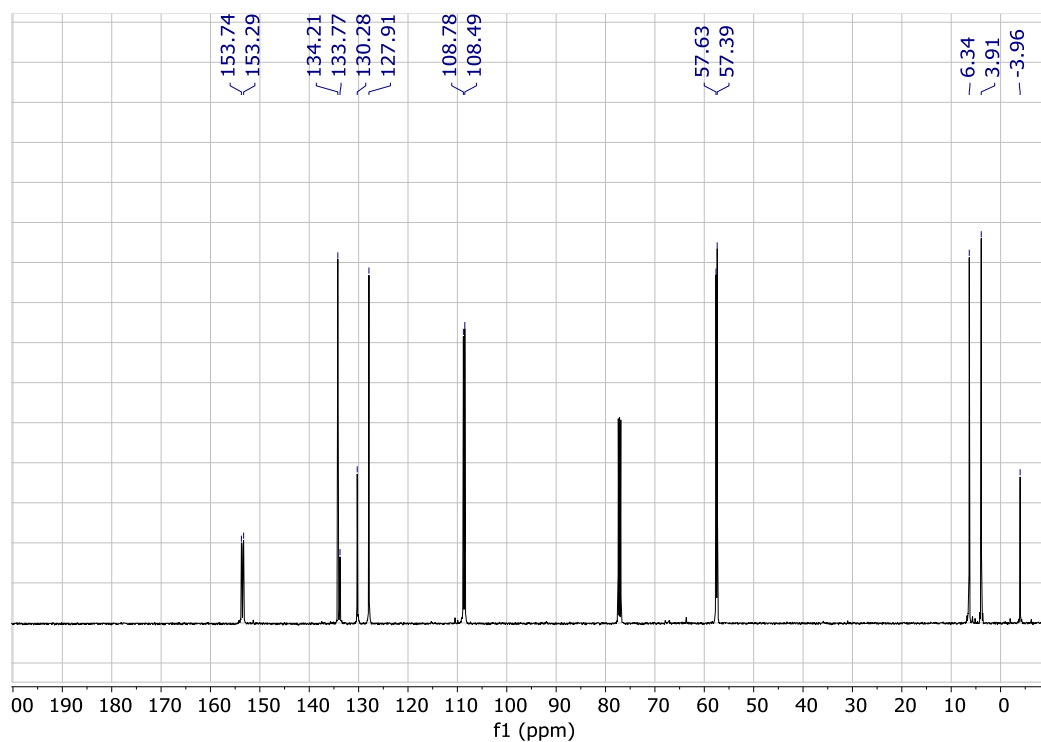


Figure S65. $^{13}\text{C}\{^1\text{H}\}$ NMR spectrum of poly(HMF-*co*-MePhSiH₂) (Table 4, entry 5) (CDCl₃, 100 MHz).

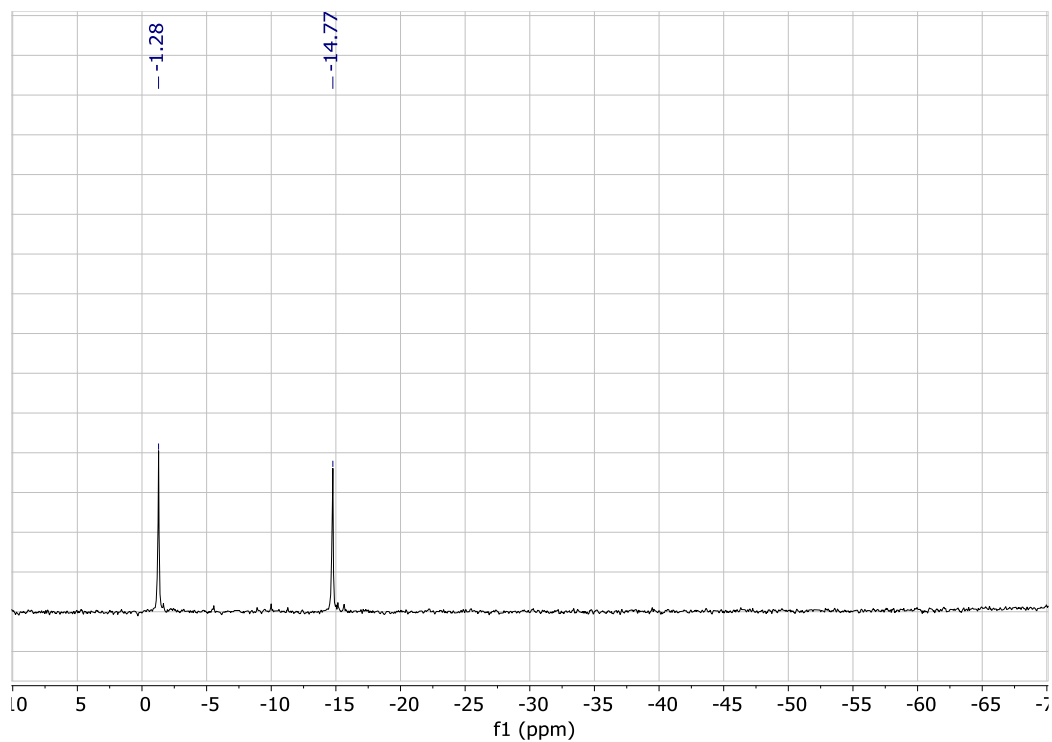


Figure S66. ^{29}Si NMR spectrum of poly(HMF-*co*-MePhSiH₂) (Table 4, entry 4) (CDCl_3 , 99 MHz).

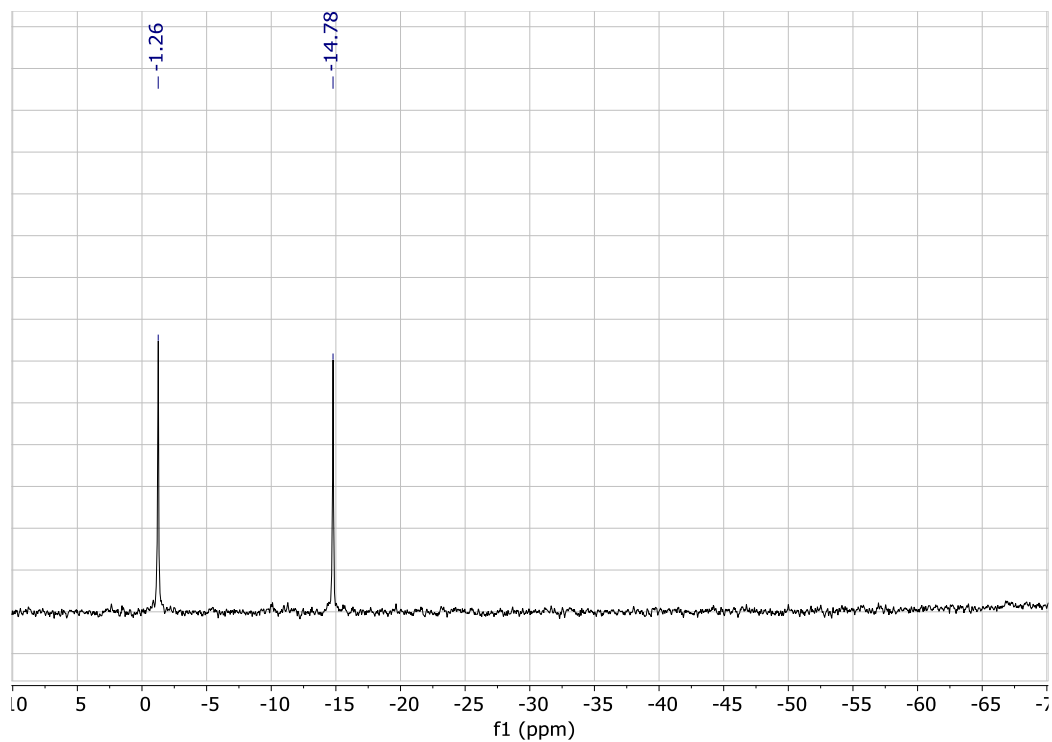


Figure S67. ^{29}Si NMR spectrum of poly(HMF-*co*-MePhSiH₂) (Table 4, entry 5) (CDCl_3 , 99 MHz).

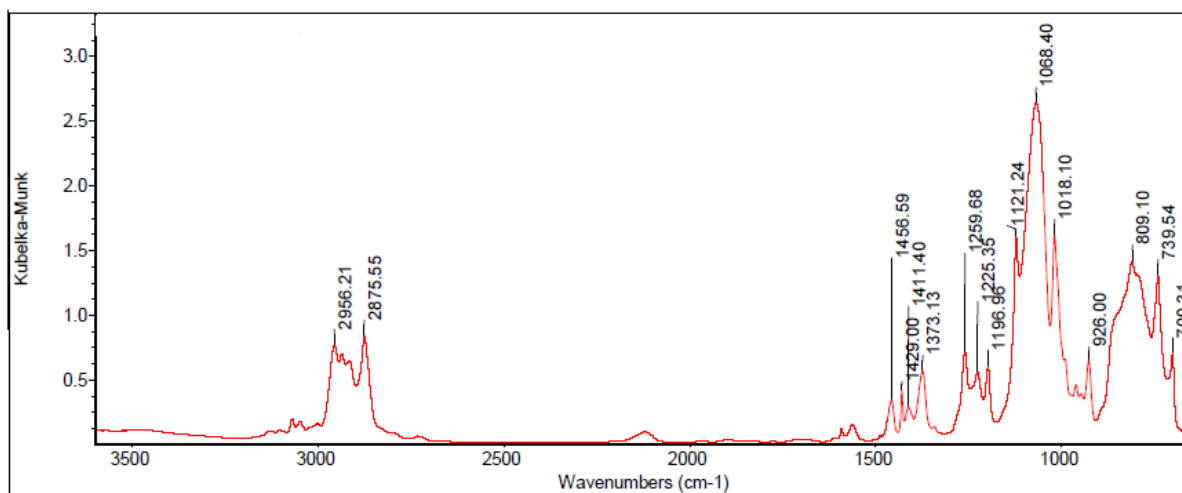


Figure S68. FT-IR spectrum of poly(HMF-co-MePhSiH₂) (Table 4, entry 4).

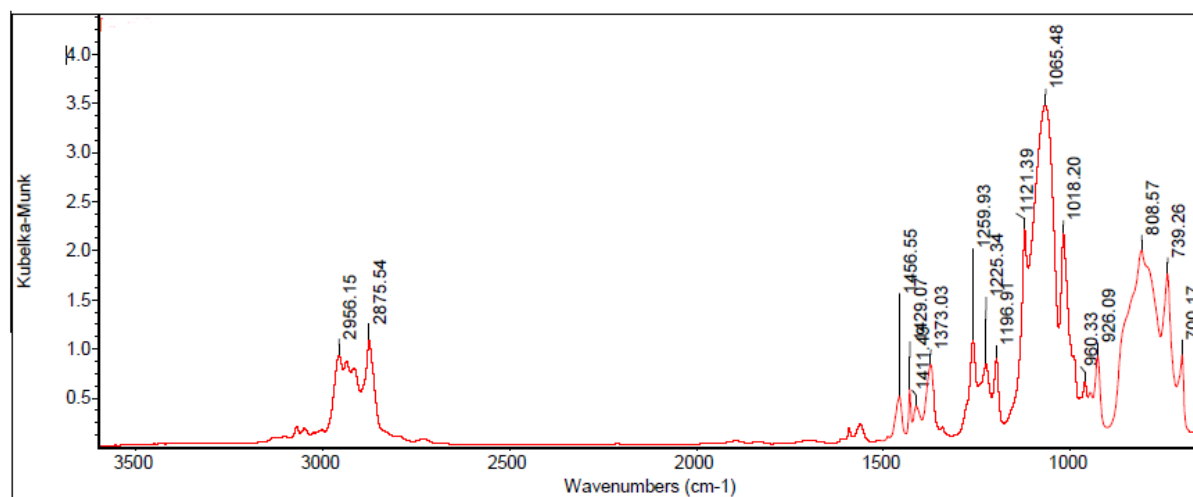


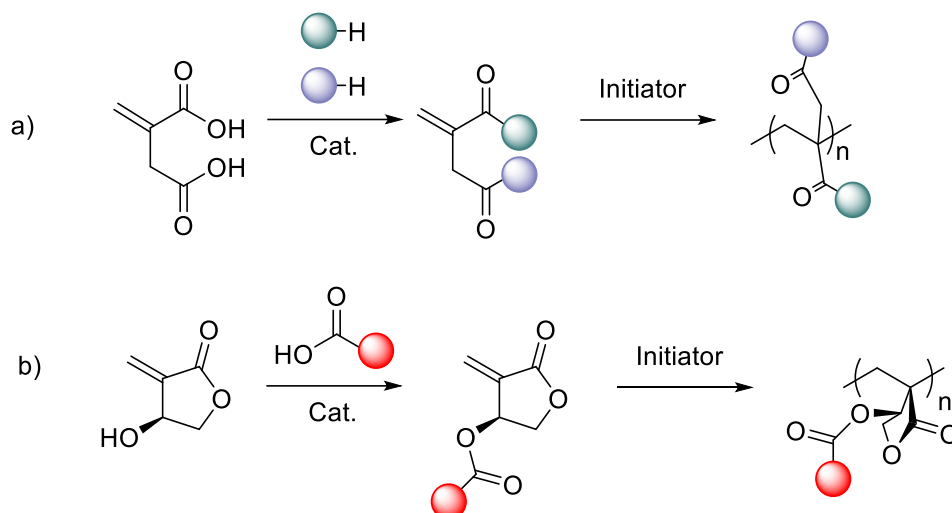
Figure S69. FT-IR spectrum of poly(HMF-co-MePhSiH₂) (Table 4, entry 5).

Conclusion and Perspectives

The design of new synthetic methods for producing biobased and recyclable polymers has been a long-standing challenge. Chapter 1 of this manuscript has highlighted the extent of research efforts by academia and industry to obtain acrylic monomers from renewable resources. The major monomer of this class, MMA, is however still industrially produced from petroleum feedstocks. So far, the most promising route towards biobased MMA is the decarboxylation of itaconic acid, readily obtained by fermentation of saccharides. Intensifying efforts on this route is probably the easiest way to obtain industrially relevant biobased PMMA. For specific applications where original properties and biosourcing of the material are more important than its cost, it may be more relevant to develop new materials from methylene butyrolactones, itaconic, or crotonic acids. A good complement to our state of the art can be found in a recent publication by Miller, Allais *et al.*, which reviewed the various biobased alcohols used to prepare original poly(meth)acrylates.^[1]

The one-pot approach to biobased poly(methacrylate)s that we presented in chapter 2 offers a method for the expeditious and eco-friendly synthesis of innovative materials. The use of cheap and commercial catalyst, MgCl₂, as well as the possibility of obtaining block copolymers in one-pot, is of particular interest to research groups working in the field of materials characterization. By limiting the number of purification steps to only one, and requiring only bench-top reaction conditions, this method can theoretically be used by inexperienced chemists for rapid materials synthesis and properties screening. Although our work has focused on acrylate and methacrylate chemistry, other monomers suitable for radical vinyl polymerization should be accessible *via* a similar method. Coupling itaconic acid with various biobased alcohols could be of particular interest, while β -hydroxy methylene butyrolactone could be combined with biobased monoacids such as levulinic acid in order to explore new materials (see Scheme 1).

Conclusion and perspectives

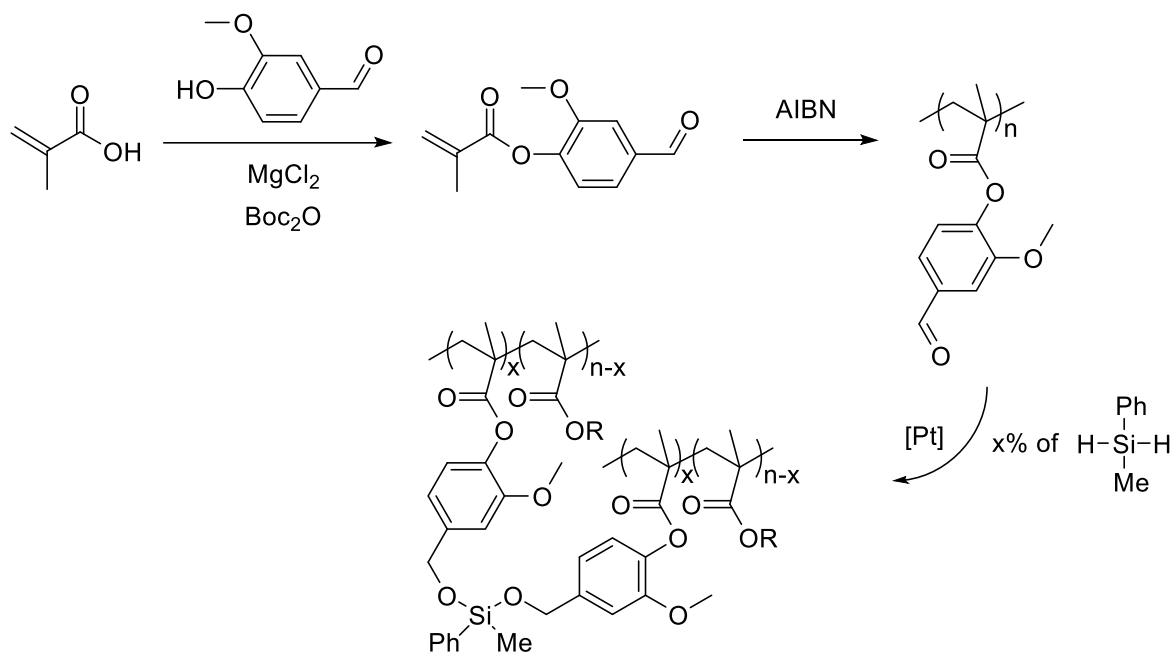


Scheme 1. Possible one-pot synthesis of (a) poly(itaconate)s or of (b) polymers derived from β -HMBL and a biobased acid.

The preparation of PMMA by anionic polymerization at room temperature has shown promising features in chapter 3. The potential of metalate complexes as catalysts for polymerization reactions under mild conditions is fully demonstrated. However, the lack of stereocontrol on the resulting polymer is detrimental, since anionic polymerization is usually used to prepare stereoregular polymers. The design of ligands having a sufficiently strong interaction with the metal center of the catalyst could increase this stereocontrol. Our methodology also permitted to prepare a block copolymer of PMMA and PLA. Taking advantage of the ability of our system to initiate both vinyl polymerization and ring-opening polymerization should allow to expend the scope of materials accessible *via* this method.

Finally, the synthesis of poly(silylether)s from renewable resources has shed new light on this relatively unknown class of polymers. Our contribution highlights for the first time their potential for chemical recycling, as we could degrade them down to the monomer level. The next challenge for these polymers would be to separate and reuse the monomers obtained from acid hydrolysis or methanolysis. Due to the cost of the silicon-based monomers and the low T_g s of the materials obtained, the use of the silyl ether linkage may be more appropriate in the pendant chain of a high T_g -polymer

(see Scheme 2):^[2] it would allow the cross-linking of the material while allowing it to be reprocessed when subjected to an acidic environment.



Scheme 2. Potentially reprocessable thermoset thanks to silylether cross-links.

In conclusion, new sustainable polymers have been prepared using innovative and environmental-friendly synthetic methods, which may be used to discover the high-performance materials of tomorrow.

References

- [1] C. Veith, F. Diot-Néant, S. A. Miller, F. Allais, *Polym. Chem.* **2020**, *11*, 7452–7470.
 [2] S. Gao, *J. Mater. Chem. A* **2019**, *7*, 17498–17504.

RÉSUMÉ

L'industrie des polymères fait aujourd'hui face à deux principaux défis : 1) réduire son empreinte sur l'environnement en produisant des matériaux réutilisables, recyclables, ou biodégradables ; 2) sortir de sa dépendance à l'industrie pétrolière en extrayant ses matières premières de ressources renouvelables. Le travail présenté dans ce manuscrit s'attaque à ces deux défis en étudiant la préparation de nouveaux polymères recyclables à partir de monomères issus de la biomasse. Des méthodes de synthèse respectueuses de l'environnement ont été développées, avec une attention toute particulière à la réduction de la production de déchets en évitant des étapes de purification intermédiaires. Des catalyseurs hautement actifs ont été préparés à partir de produits commerciaux, ce qui a permis un accès rapide à des matériaux originaux. Enfin, de nouveaux polymères recyclables chimiquement ont été préparés et caractérisés, illustrant ainsi leur potentiel.

MOTS CLÉS

Polymères, biosourcé, recyclable, catalyse.

ABSTRACT

The polymer industry is nowadays facing two main challenges: 1) reduce its impact on environment by designing reusable, recyclable, or biodegradable materials; 2) decrease its reliance on the petroleum industry by shifting towards biobased and renewable feedstocks. The work presented in this manuscript has tackled both challenges by investigating the preparation of novel recyclable polymers from renewable resources. First, eco-friendly synthesis methods have been developed, with a particular focus on reducing waste generation by avoiding intermediate purification steps. Preparation of highly active catalysts from commercial reagents has also permitted to rapidly obtain original materials. Finally, new chemically recyclable polymers have been synthesized and characterized as high potential materials.

KEYWORDS

Polymers, biobased, recyclable, catalysis.